An Investigation of T Cell Immunity and the HIV Reservoir During Primary HIV Infection: Implications for Cure Strategies



Dr Genevieve Elizabeth Martin

St Peter's College

University of Oxford

Submitted in partial fulfillment of the requirements for the degree of

Doctor of Philosophy in Clinical Medicine

Trinity Term 2018

Abstract

This work focuses on aspects of T cell immunity during the early stages of human immunodeficiency virus (HIV) infection, termed primary infection. Individuals who commence antiretroviral therapy (ART) during primary infection may have preserved immune function, making them a target group for curative strategies.

The efficacy of HIV cure interventions are assessed by stopping ART and measuring how long it takes until plasma viraemia recurs. Here, the normal dynamics of this viral rebound in treated and untreated primary infection were characterised, showing that transient control of viral replication is not uncommon at this time.

The prospect of HIV cure is heavily reliant on an immune response to eliminate the virus - but such responses become rapidly dysfunctional. During primary infection, changes in T cell activation, memory distribution and the expression of immune checkpoint receptors (which are associated with a type of T cell dysfunction termed exhaustion) occurred. Not all of the demonstrated perturbations in these had normalised following a year of ART which is started during primary infection.

This work then turns to the HIV reservoir itself; this is the pool of cells in which the virus persists during long-term therapy and which is the barrier to HIV cure. A longitudinal analysis showed that the size of this reservoir is determined during primary infection where it is linked with aspects of the T cell response measured above. A final chapter shows that CD32, a proposed marker of the reservoir, does not appear to mark cells that comprise the reservoir as specifically as originally reported.

Overall this work highlights some of the barriers to current HIV cure strategies and contributes to a body of knowledge which may in the future inform rational design of targeted therapeutic interventions.

Word count: 42441 words

Original research publications resulting from my DPhil research*:

Martin GE*, Pace M*, Thornhill JP* *et al.* CD32 expressing CD4 T cells are phenotypically diverse and can contain proviral HIV DNA. *Frontiers in Immunology*, **8**(928) (2018).

Martin GE, Gossez M, Williams JP *et al.* Post-treatment control or treated controllers? Viral remission in treated and untreated primary HIV infection. *AIDS*, **31**, pp. 477–484 (2017)

Hoffmann M*, Pantazis N*, Martin GE*, *et al.* Exhaustion of Activated CD8 T cells Predicts Disease Progression in Primary HIV-1 Infection. *PLoS Pathogens*, **2**(7), e1005661 (2016).

Review and general readership publications:

Martin GE & Frater J Post-treatment and spontaneous HIV control. *Current Opinions in HIV/AIDS*, **13**(5), pp. 402-407 (2018)

Martin GE, Alcami J, Spano JP & Ross AL. Converging roads: the latest science from the 2017 IAS HIV Cure and Cancer Forum. *Journal of Virus Eradication*, **3** e1-e6 (2017).

Martin GE, Pace M & Frater J. Hidden menace: the key to curing HIV lies in eradicating the reservoir of viruses residing in quiescent immune cells. *The Scientist*, **29** 34-39 (2015).

Submitted manuscripts:

Gossez M, Martin GE, Pace M, *et al.* Virological remission after antiretroviral therapy interruption in female African HIV seroconverters. [In Press]

Thornhill, JP*, Martin GE*, Pace M*, *et al.* CD32 expressing CD4 T cells in gut-associated lymphoid tissue have an activated, T-follicular helper cell phenotype and do not associate with HIV reservoir. [Submitted]

*indicates co-first authorship

Acknowledgements

I would like to express my gratitude to Professor John Frater for his encouragement and supervision throughout this project. Thank you, John, for allowing me to test my own hypotheses - and for pulling me back on track at times. I would also like to extend my sincere thanks to Dr Chris Willberg for his advice and patience, in particular with my multitudinous technical questions. Both John and Chris, my supervisors, have taught me by example what it means to be a diligent and honest scientist. In some very Australian words: *"We must think critically, and not just about the ideas of others. Be hard on your beliefs. Take them out onto the verandah and beat them with a cricket bat. Be intellectually rigorous."*[1]; John and Chris have both encouraged and helped me to do this from the beginning. I am extremely grateful for the opportunities they have given me to develop skills I will take forward into my career, and for all of the discussions and diversions along the way.

Thank you to the participants of SPARTAC and HEATHER - their commitment to be part of this research is integral to its success. I would particularly like to recognize the role of the clinical staff at the HEATHER trial sites with whom I have worked closely on the collation of data for this study. I am grateful for their assistance and patience with my repeated data requests. Throughout my DPhil I have been fortunate enough to work with members of the study teams of both these trials whose specific contributions are acknowledged in the following section. The names of the SPARTAC trial investigators, and the CHERUB (Collaborative HIV Eradication of Reservoirs: UK BRC) collaboration steering committee are listed in Appendix A.

This work has been a truly collaborative effort, and there are many people who have contributed experiments, ideas and advice to this thesis.

I am extremely grateful to everybody at the Peter Medawar Building for making coming to work every day such an enjoyable experience. I have worked particularly closely with Dr Matthew Pace during my time in Oxford; I extend my thanks to

[1] Minchin, Tim; from an occasional address given at the University of Western Australia in September 2013

him for teaching me in the lab, for becoming my experimental sounding board, for his patience with the CD32 story - and for all of the cake. The support of Mathew Jones, John Thornhill and Morgane Gossez, my student contemporaries, was absolutely indispensable. I am grateful for their practical assistance, but most importantly for their friendship. As someone was instrumental in the success of this project, I would like to recognise Jodi Meyerowitz who helped track down so much of the clinical data - and always approached this with enthusiasm. For technical advice and for helping me to learn new techniques thanks to Helen Brown, Nicola Robinson, Dr Chan Phetsouphanh, Dr Ellen Leitman and Dr Emily Adland. I would also like to extend my thanks to Natalia Olejniczak, Emily Hopkins and Dr James Williams who performed qPCR assays that were included in this work. Thanks also to Professor Kholoud Porter and Dr Wolfgang Stöhr (both Medical Research Council, London) who provided advice on the analyses performed in Chapter 2. For statistical advice and ideas I am indebted to Dr Jacob Hurst and Dr Freya Shearer who gave me the confidence to learn to try things myself - I understand my data all the better for it. Thank you to Dr Nicholas Grayson for helpful comments on a draft of the introduction. Finally, thank you to other members of the Frater group and my office for your camaraderie and conversation over the past four years: Dr Masa Mori, Dr Lyle Murray, Dr Lucia Parolini, Dr Hannah Roberts, Debbie Cross and Reena D'Souza.

I would like to extend my sincere thanks to Professor Nicholas Haining and Debattama Sen for embarking on an exciting project together with us and for hosting me in Boston. I learnt so much from my discussions with Deb about T cell immunology and many other things; I look forward to our ongoing collaboration.

For thought-provoking discussions in the course of my studies, I would like to express my appreciation to the following people: Professor Rodney Phillips, Professor Paul Klenerman, Professor Philip Goulder, Professor Ellie Barnes, Professor Lucy Dorrell, Dr Leo Swadling, Professor Sarah Fidler, Professor Damian Purcell, Professor Anthony Kelleher and Professor Sharon Lewin. Your generosity with your ideas has helped me to shape my own ideas into this work.

For sparking my interest in the immune system and encouraging me from then on special thanks to Karen Lampman. I also would not have embarked upon these studies were it not for the ongoing mentorship of Professor Suzanne Crowe and the research experience I had as part of her lab during my undergraduate degree - and would like to extend my gratitude to her.

Beyond my work there a number of people without whom this thesis wouldn't exist. To everybody who made Oxford my home: all those at 26 Western Road (Alex, Jamie, Simon, Nick, Tamara, Greg, Lucian, Claudia, Neil JB and other roadents past and present), Emma, Mandy, Katie, Ben, Geoff, Freya, Alex, Elise, Jaime, Alexis, Morgane, Leo, Matt as well as everybody at the Oxford University Australian Rules Football Club. Thank you for the good conversations, the adventures and your friendship. I am extremely grateful to Amber and Sarah for always making me smile and sticking with me despite the distance. I must acknowledge everybody at Zappis and the Missing Bean for fuelling my daily routine. And for making it such a welcoming community and place to live, I am grateful to all of the staff at St Peter's College.

Finishing this thesis would not have been possible without the support of the oldest friends I have - Eleanor, Charlotte and Harry; I am looking forward to spending more time with you in the coming years. And finally, for inspiring and listening, Mum and Dad - you have never wavered in your support and I cannot thank you enough.

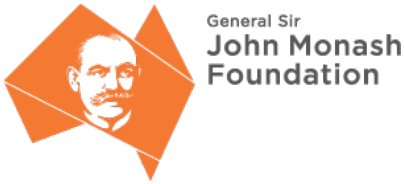
Funding statement

The SPARTAC trial was funded by the Wellcome Trust. Funding for HEATHER comes from the Medical Research Council, Oxford National Institute of Health Research and British HIV Association.





My time in Oxford was funded by a John Monash Scholarship (General Sir John Monash Foundation, Australia), a Clarendon Scholarship and a Nuffield Department of Medicine Prize studentship (both University of Oxford).







Contributions to this thesis

The work presented in this thesis is predominantly mine, but some of the experiments were performed with the assistance of others. For all work presented I designed the experiments, conducted most of the assays and performed the data analysis. I prepared all of the figures and tables presented in this work, and wrote the initial draft of all of the text. Contributions by others are listed below.

Chapter 5

- Dr Matthew Pace performed the majority of experiments pertaining to the phenotype of CD32 expressing CD4 T cells in healthy individuals, the HIV DNA quantification in sorted populations and measured cell-associated unspliced RNA;
- Dr Chan Phetsouphanh assisted with the sorting protocols.

Other specific experimental contributions are listed below:

- Collation and management of SPARTAC clinical trial data was performed by the Medical Research Council Clinical Trials Unit (MRC CTU);
- Recruitment of patients and collection of data from clinical sites for HEATHER was performed by the following individuals:
  - Chelsea and Westminster Hospital (London): Dr Nneka Nwokolo, Sathya Visvendra, Rhian Bull and Gabriele Pasluostaite;
  - St Mary's Hospital (London): Professor Sarah Fidler, Dr John Thornhill, Kristin Kuldanek, Heather Lewis and Rebecca Hall;
  - St Thomas' Hospital (London): Dr Julie Fox, Dr Julianne Lwanga and Teresa Solano.
- I performed the majority of flow cytometry experiments presented in this work. Additional flow cytometry assays in Chapter 2 were performed by Morgane Gossez and Jodi Meyerowitz;

- ELIspot assays in Chapter 2 were performed by Nicola Robinson, Helen Brown and myself. Reagents for the assays using clade C peptides were supplied by Professor Phillip Goulder;
- Tetramer staining in Chapter 3 was performed by Debattama Sen as part of an ongoing collaboration between our group and the group of Professor Nicholas Haining (Dana Faber Cancer Institute, Broad Institute and Harvard University, Boston, US);
- The measurement of sPD-1 and sTim-3 in plasma was conducted by Final Honours School (FHS) student Eva Zilber, whose project I co-supervised in 2017-2018;
- The measurement of total HIV DNA was performed by Helen Brown, Nicola Robinson, Dr James Williams, Morgane Gossez and myself.

Contents

List of Figures **xxi**

List of Tables **xxv**

List of Abbreviations and Terms **xxvii**

1 Introduction **1**

1.1 Human immunodeficiency virus (HIV) 2

1.1.1 Viral structure and replication 3

1.2 T cells and the immune response 5

1.3 Primary HIV infection 8

1.4 T cell function and dysfunction during HIV infection 9

1.4.1 The development of T cell functions during the course of HIV infection 10

1.4.2 T cell exhaustion and immune checkpoint receptors 13

1.5 The HIV reservoir 19

1.5.1 Immune checkpoint receptor expression is related to HIV reservoir size 23

1.6 Post-treatment and spontaneous viral control 24

1.6.1 Post-treatment control is distinct from spontaneous control . 24

1.6.2 Reservoir size, viral blips and virological control 25

1.6.3 How common is post-treatment control? 27

1.6.4 Post-treatment control as a model for HIV cure 28

1.7 HIV curative strategies 28

1.7.1 Viral remission, rather than eradication, as a model for HIV cure 29

1.7.2 Major approaches towards the development of an HIV cure . 30

1.7.3 The central role of anti-HIV immunity in developing HIV curative interventions – moving beyond “kick and kill” . . . 32

1.8 Conclusion 36

2 The impact of antiretroviral therapy initiated during primary HIV infection on viral remission following treatment interruption 37
2.1 Context . . . 38
2.2 Aims . . . 39
2.3 Hypothesis . . . 39
2.4 Results . . . 40
2.4.1 Participants and study design . . . 40
2.4.2 Transient control of viraemia (remission) is evident in untreated primary HIV infection . . . 41
2.4.3 Duration of remission in treated and untreated controllers . 43
2.4.4 Controllers have more favourable baseline clinical characteristics than non-controllers . . . 46
2.4.5 Spontaneous controllers have lower baseline VL than those who received >12 weeks ART . . . 46
2.4.6 Similar demographics and immunological characteristics in ART-receiving and spontaneous controllers . . . 49
2.4.7 Comparison of the frequency of post-treatment remission and control in the literature . . . 49
2.5 Discussion . . . 50
2.5.1 Spontaneous remission . . . 51
2.5.2 Comparing post-treatment and spontaneous remission . . . 52
2.5.3 Measuring post-treatment control and remission . . . 53
2.5.4 Limitations of this work . . . 55
2.5.5 Implications for treatment interruption trial design . . . 56
2.6 Conclusion . . . 57

3 Characterisation of activation and T cell immune checkpoint receptor expression during treated primary HIV infection 59
3.1 Context . . . 60
3.2 Aims . . . 61
3.3 Hypothesis . . . 62
3.4 Results . . . 62
3.4.1 Clinical characteristics of the HEATHER cohort . . . 62
3.4.2 Immunologic changes during primary HIV infection . . . 65
3.4.3 Biomarkers of T cell exhaustion . . . 72
3.4.4 Incomplete resolution of immune parameters following ART initiated during primary HIV infection . . . 78
3.4.5 Immunologic changes during primary HIV infection are linked to markers of clinical progression . . . 86

3.5 Discussion . . . 89
3.5.1 T cell differentiation . . . 90
3.5.2 T cell activation and Tim-3 expression . . . 93
3.5.3 ICR expression and co-expression . . . 96
3.5.4 Partial but incomplete restoration of T cell parameters with early initiation of ART . . . 98
3.5.5 CD39 as a biomarker of T cell exhaustion . . . 98
3.5.6 Soluble immune checkpoint receptors . . . 100
3.5.7 Strengths and limitations of this work . . . 103
3.6 Conclusion . . . 103
3.6.1 Next steps . . . 104

4 The relationship between T cells and the CD4 T cell HIV reservoir during treated primary HIV infection 107
4.1 Context . . . 108
4.2 Aims . . . 109
4.3 Hypothesis . . . 109
4.4 Results . . . 110
4.4.1 HIV reservoir size following 1 year of ART is closely related to pre-ART reservoir size . . . 110
4.4.2 Reservoir size is related to HLA class I alleles . . . 110
4.4.3 Immunological and clinical variables associated with HIV reservoir size are highly correlated . . . 112
4.4.4 Reservoir size at baseline is related to CD8 T cell activation and memory expansion . . . 114
4.4.5 Reservoir size at baseline is the best predictor of reservoir size once stabilised on ART . . . 117
4.4.6 Immunological variables at 1 year do not have a statistically independent relationship with HIV reservoir size . . . 118
4.5 Discussion . . . 120
4.5.1 Proviral burden is set during early infection . . . 120
4.5.2 Limitations of viral load during as a predictor of reservoir size 121
4.5.3 Activation, ICR expression and memory expansion . . . 123
4.5.4 Model selection - advantages and disadvantages . . . 125
4.5.5 Strengths and limitations of this work . . . 126
4.6 Conclusion . . . 128

5 CD32 as a marker of an enriched CD4 T cell HIV reservoir during treated primary HIV infection 129

5.1 Context . . . 130
5.2 Aims . . . 131
5.3 Hypothesis . . . 131
5.4 Results . . . 131
5.4.1 Depletion of CD32 expressing CD4 T cells by negative bead selection due to the expression of non-T cell markers . . . 131
5.4.2 CD32 expressing CD3+CD4+ cells differ in their expression of immune checkpoint receptors and memory phenotype . . . 135
5.4.3 $CD32^{high}$ CD3+CD4+ T cells are activated and express high levels of HIV co-receptors . . . 136
5.4.4 HIV DNA in CD32 expressing CD3+CD4+ cell subsets . . . 136
5.4.5 The frequency of CD32 expressing CD3+CD4+ cells is not related to the overall size of the HIV reservoir . . . 138
5.4.6 $CD32^{high}$CD4+ events are doublets which pass through a doublet exclusion gate . . . 142
5.5 Discussion . . . 142
5.5.1 Other studies of CD32 and the HIV reservoir have excluded the $CD32^{high}$ population . . . 144
5.5.2 The existence of B/T cell doublets can explain the observed phenotype of $CD32^{high}$ events . . . 145
5.5.3 Failure to reproduce a marked enrichment of HIV DNA in CD32-expressing cells . . . 147
5.5.4 Associations of CD32-expression on CD4 T cells with activation and transcription . . . 148
5.5.5 Lessons learnt and implications for future studies of markers of an enriched HIV reservoir . . . 150
5.6 Conclusion . . . 151

6 General discussion and conclusions 153

6.1 Early ART for curative interventions . . . 155
6.2 Shifting the goalposts for HIV cure . . . 158
6.3 Future directions . . . 160
6.4 Conclusion . . . 161

7 Materials and Methods **163**
7.1 Ethics Statement . . . 164
7.2 Clinical cohorts . . . 165
7.2.1 SPARTAC . . . 165
7.2.2 HEATHER . . . 166
7.3 Media and buffer composition . . . 168
7.4 General techniques for working with *ex vivo* samples . . . 169
7.4.1 Cryopreservation of blood components . . . 169
7.4.2 Thawing and handling of primary cells . . . 169
7.4.3 T cell isolation . . . 170
7.5 Flow cytometry . . . 170
7.5.1 Surface staining . . . 170
7.5.2 Intracellular staining . . . 176
7.5.3 Acquisition of flow cytometry data . . . 177
7.5.4 Analysis of flow cytometry data . . . 178
7.5.5 Technical considerations . . . 178
7.6 Cell sorting . . . 179
7.6.1 Sorting of CD32 expressing CD4 T cells . . . 179
7.6.2 Staining of HIV-specific CD8 T cells . . . 180
7.7 HLA typing . . . 182
7.7.1 DNA extraction . . . 182
7.7.2 HLA typing by sequence specific primers . . . 182
7.8 CD8 ELISpot assays . . . 182
7.9 ELISA . . . 184
7.10 HIV reservoir quantification . . . 185
7.10.1 Nucleic acid extraction . . . 185
7.10.2 Total HIV DNA quantification . . . 185
7.10.3 Cell-associated unspliced RNA quantification . . . 186
7.11 Determination of viral clade . . . 189
7.12 Statistical analyses . . . 189
7.12.1 Missing data . . . 189
7.12.2 Group comparisons . . . 191
7.12.3 Correlative analyses . . . 191
7.12.4 Survival analyses . . . 191
7.12.5 Principle component analysis . . . 191
7.12.6 Regression analyses . . . 192

References **193**

Appendices

A Study committees **229**
A.1 SPARTAC trial investigators 229
A.2 CHERUB Steering Committee 230

B Additional figures and tables **231**

C HIV-1 *gag* overlapping peptide sequences **261**

D Publications **267**

List of Figures

1.1 Overview of HIV structure and replication 4
1.2 Phenotypic markers used to define T cell memory subsets 7
1.3 Dynamics of viral load, CD4 count and CD8 T cell activation during the natural history of HIV infection 9
1.4 Immune checkpoint receptors and their ligands 14
1.5 Heterogeneous distribution of the HIV reservoir 21
1.6 Potential strategies to augment anti-HIV immunity as part of HIV curative interventions 32

2.1 Individuals eligible for inclusion in analysis of viral remission 40
2.2 Viral load dynamics observed in SPARTAC 42
2.3 Baseline clinical variables of controllers and non-controllers 47
2.4 Estimates of post-treatment control and remission frequency in the literature 50

3.1 Changes in immunological and virological parameters following ART initiation in the HEATHER cohort 64
3.2 Relationship between baseline VL and method of diagnosing PHI . 65
3.3 T cell memory expansion and activation during PHI 67
3.4 ICR expression on T cell memory subsets during PHI 68
3.5 Increases in ICR expression during PHI 69
3.6 Memory phenotype and PD-1 expression on tetramer-specific CD8 T cells during PHI 71
3.7 Inter-individual variation in CD39 expression 73
3.8 Soluble PD-1 and Tim-3 during PHI 76
3.9 Immune parameters are incompletely resolved following 1 year of ART 77
3.10 Changes in T cell memory subsets following 1 year of ART 79
3.11 Subsets of CD8 T cells expressing combinations of the transcription factors T-bet and Eomes 81
3.12 Co-expression of CD38, Tim-3 and PD-1 remains elevated on CD8 T cells following 1 year of ART 83
3.13 Co-expression of ICRs remains elevated following 1 year of ART . . 84

3.14 Immunological changes during PHI correlate with measures of clinical progression 87
3.15 Additional relationships between immunological changes during PHI 88

4.1 Relationship between total HIV DNA measured at baseline and 1 year 110
4.2 Relationship between HLA class I alleles and HIV reservoir size . . 111
4.3 Correlations between clinical/immunological variables and HIV reservoir size 113
4.4 Stages of analysis to look at reservoir size 114
4.5 Boosted regression tree models to assess predictors of reservoir size 115
4.6 Model for factors which influence reservoir size in treated PHI . . . 119

5.1 Depletion of diverse populations of CD32 expressing CD4 T cells by negative bead selection due to the expression of non-T cell markers 132
5.2 Characterisation of T cell receptor and immunoglobulin expression on $CD32^{high}$CD3+CD4+ T cells 134
5.3 Further characterisation of CD32 expressing CD3+CD4+ cells . . . 137
5.4 HIV DNA quantification in sorted CD32 expressing CD3+CD4+ T cell populations 139
5.5 The frequency of CD32-expressing CD3+CD4+ cells does not correlate with the size of the HIV reservoir 140
5.6 Imaging cytometry of $CD32^{high}$ CD4+CD3+ cells 143

6.1 Shrinking therapeutic window for HIV curative interventions 158

B.1 Representative gating of CD4 and CD8 T cells 232
B.2 Representative gating for tetramer stains 234
B.3 Persistently high PD-1 expression on HIV-specific CD8 T cells with and without ART 235
B.4 Memory expansion of HIV-specific CD8 T cells with and without ART 240
B.5 Complete data for co-expression analysis presented in Figure 3.12 . 241
B.6 Complete data for CD8 T cell co-expression analysis presented in Figure 3.13 242
B.7 Complete data for CD4 T cell co-expression analysis presented in Figure 3.13 243
B.8 Missing immunological and clinical data in HEATHER 252
B.9 CD14+CD32+ CD3+CD4+ cells have forward and side scatter characteristics which fall outside a conservative lymphocyte gate . . 253
B.10 CD32 expressing CD4 T cells from whole, fresh blood have a similar phenotype to those from cryopreserved PBMCs 254
B.11 Doublet exclusion strategy as used in phenotyping experiments . . . 255

B.12 Representative gating for sorts of CD3+CD4+ T cells based on CD32 expression 257
B.13 Low cell input results in overestimation of HIV and albumin DNA by qPCR 258

List of Tables

1.1 Reported associations between T cell immune checkpoint receptor expression and disease progression 16

2.1 Characteristics of controllers identified in SPARTAC 45
2.2 Baseline immunological and virological characteristics of non-controllers and controllers 48
2.3 Baseline immune checkpoint receptor and activation marker expression on CD4 and CD8 T cells in controllers 51

3.1 Baseline clinical parameters for individuals in the HEATHER cohort 63

4.1 LASSO outputs for regression of immunological/clinical variables with reservoir size 118

7.1 Definition of primary HIV infection in SPARTAC and HEATHER . 167
7.2 Media and buffer composition 168
7.3 Flow cytometry panels used for surface staining experiments 173
7.4 Antibodies used for flow cytometry experiments 175
7.5 Flow cytometry panels used for intracellular staining experiments . 177
7.7 Flow cytometry panels used for cell sorting experiments 180
7.8 MHC Class I/peptide multimers 181
7.9 ELISA kits used 184
7.10 Primers and probes used for HIV DNA quantification by qPCR . . 187
7.11 Primers and probes used for CA-usRNA quanitifcation by qPCR . . 190

B.1 Summary data for comparisons presented in Figure 3.5 233
B.2 Summary data for comparisons presented in Figure 3.7 237
B.3 Summary data for correlations presented in Figure 3.8 238
B.4 Summary data for comparisons presented in Figure 3.9 239
B.5 Correlations of immunological variables following 1 year of ART with baseline clinical variables 246
B.6 Summary data for comparisons presented in Figure 3.14 250
B.7 Multivariable regression for CD8 T cell CD38 expression and EM phenotype 251

B.8 Demographic and clinical characteristics of participants included in clinical studies 256
B.9 qPCR detection of HIV DNA for CD3+CD4+ T cell populations sorted based on CD32 expression directly from PBMCs 259
B.10 Cox proportional hazard models of time to viral rebound 260

C.1 Subtype C *gag* overlapping peptide sequences 262
C.2 Subtype B *gag* overlapping peptide sequences 265

List of Abbreviations and Terms

Acronyms

ACD	acid-citrate-dextrose
ACK	ammonium-chloride-potassium
AIDS	acquired immunodeficiency syndrome
alloSCT	allogenic stem cell transplant
ALP	alkaline phosphatase
APC	allophycocyanin
APC	antigen presenting cell
ART	antiretroviral therapy
BCIP	5-bromo-4-chloro-3-indoly phosphate
BHQ-1	Black Hole Quencher 1
bNAb	broadly-neutralising antibody
BRT	boosted regression tree
BSA	bovine serum albumin
BV	brilliant violet
CA-usRNA	cell associated unspliced RNA
CAR	chimeric antigen receptor
CD	cluster of differentiation
cDNA	complementary DNA
CM	central memory
CMV	cytomegalovirus
ConA	concanavalin A
CRF	circulating recombinant form
CRP	C-reactive protein
CTL	cytotoxic T lymphocyte
CV	coefficient of variation
DMSO	dimethyl sulfoxide
DNA	deoxyribonucleic acid
DNAse	deoxyribonuclease
dNTPs	deoxyribonucleotide triphosphates
DTT	dithiothreitol

EBV	Epstein-Barr virus
EDSC	estimated date of seroconversion
EDTA	ethylenediaminetetraacetic acid
ELISA	enzyme linked immunosorbent assay
ELISpot	enzyme linked immunospot
EM	effector memory
FACS	fluorescence activated cell sorting
FAM	fluorescein amidite
FBS	fetal bovine serum
FDR	false discovery rate
FITC	fluorescein isothiocyanate
FMO	fluorescence minus one
GALT	gut-associated lymphoid tissue
GWAS	genome-wide association study
HBV	hepatitis B virus
HCV	hepatitis C virus
HDACi	histone deacetylase inhibitor
HEATHER	HIV Reservoir Targeting with Early Antiretroviral Therapy
HIV	human immunodeficiency virus
HLA	human leukocyte antigen
ICR	immune checkpoint receptor
IFN-α	interferon-α
IFN-γ	interferon-γ
Ig	immunoglobulin
IQR	interquartile range
LASSO	least absolute shrinkage and selection operator
LCMV	lymphocytic chroriomeningitis virus
LLD	lower limit of detection
LRA	latency reversing agent
LTR	long terminal repeat
MHC	major histocompatibility complex
MRC CTU	Medical Research Council Clinical Trials Unit
MSM	men who have sex with men
MSW	men who have sex with women
NBT	nitro-blue tetrazolium chloride
NK	natural killer
NNRTI	non-nucleoside reverse transcriptase inhibitor
NRTI	nucleoside reverse transcriptase inhibitor
OD	optical density

OLPs	overlapping peptides
PAMP	pathogen associated molecular pattern
PBA	PBS/BSA/(sodium) azide buffer
PBMC	peripheral blood mononuclear cell
PBS	phosphate buffered saline
PCA	principle component analysis
PCR	polymerase chain reaction
PCR-SSP	polymerase chain reaction by sequence specific primers
PE	phycoerythrin
PerCP	peridinin chlorophyll protein complex
PHA	phytohaemagglutinin
PKC	protein kinase C
qPCR	quantitative polymerase chain reaction
RITA	recent incident test algorithm
RNA	ribonucleic acid
RT	reverse transcriptase
SD	standard deviation
SFU	spot forming units
SIV	simian immunodeficiency virus
SNP	single nucleotide polymorphism
SPARTAC	Short Pulse Antiretroviral Therapy at HIV Seroconversion
$\mathbf{T_{EMRA}}$	effector memory with re-expression of CD45RA
$\mathbf{T_{SCM}}$	stem-cell memory T
TCR	T cell receptor
TFH	T-follicular helper
TI	treatment interruption
TLR	toll-like receptor
TM	transitional memory

Immune checkpoint receptors

CD39	ectonucleoside triphosphate diphosphohydrolase-1
CTLA-4	cytotoxic T lymphocyte antigen 4
Lag-3	lymphocyte-activation gene 3
PD-1	programmed death cell protein 1
sPD-1	soluble PD-1
sTim-3	soluble Tim-3
TIGIT	T cell immunoreceptor with immunoglobulin and ITIM domains
Tim-3	T cell immunoglobulin and mucin-domain containing protein 3

CD antigens and signalling molecules

CCR5	a chemokine receptor; HIV entry co-receptor
CCR7	a chemokine receptor; CD197
CD11b	subunit of integrin CR3; expressed on myeloid and NK cells
CD123	IL-3 receptor α chain
CD14	lipopolysaccharide/lipopolysaccharide binding protein complex receptor; expressed on myeloid cells
CD15	a trisaccharide expressed on glycolipids and cell-surface glycoproteins; expressed on neutrophils, eosinophils and monocytes
CD16	Fc-γ receptor III; expressed on NK, neutrophils and macrophages
CD19	B cell lineage marker; immunoglobulin superfamily
CD2	a surface adhesion molecule; expressed on T cells and NK cells
CD20	B cell lineage marker
CD235a	glycophorin A; expressed on erythroid cells
CD27	co-stimulatory molecule from TNF superfamily
CD3	T cell co-receptor, component of the TCR complex]
CD32	low-affinity Fc receptor; FCγII; expressed on myeloid cells, granulocytes and B cells
CD36	a platelet adhesion molecule
CD38	cyclic ADP ribose hydrolase; cellular activation marker
CD4	co-receptor for MHC class II
CD45RA	an isoform of CD45 (leucocyte common antigen)
CD56	isoform of neural cell adhesion molecule (NCAM); expressed on NK cells
CD69	transmembrane C-type lectin protein; cellular activation marker
CD8	co-receptor for MHC class I
CD95	first apoptosis signal receptor (FasR); death receptor
CEACAM-1	carcinoembryonic antigen-related cell adhesion molecule 1
CXCR4	a chemokine receptor; HIV entry co-receptor
CXCR5	a chemokine receptor which facilitates T cell migration into B cell zones in lymph nodes; CD185
HLA-DR	receptor for MHC class II; cellular activation marker
PVR	poliovirus receptor

Transcription factors

Bcl6	transcription factor involved in the differentiation of T-follicular helper cells
Eomes	eomesdermin
T-bet	T-box transcription factor

1

Introduction

Contents

1.1 Human immunodeficiency virus (HIV) 2
1.1.1 Viral structure and replication 3
1.2 T cells and the immune response 5
1.3 Primary HIV infection 8
1.4 T cell function and dysfunction during HIV infection . 9
1.4.1 The development of T cell functions during the course of HIV infection 10
1.4.2 T cell exhaustion and immune checkpoint receptors . . . 13
1.5 The HIV reservoir 19
1.5.1 Immune checkpoint receptor expression is related to HIV reservoir size 23
1.6 Post-treatment and spontaneous viral control 24
1.6.1 Post-treatment control is distinct from spontaneous control 24
1.6.2 Reservoir size, viral blips and virological control 25
1.6.3 How common is post-treatment control? 27
1.6.4 Post-treatment control as a model for HIV cure 28
1.7 HIV curative strategies 28
1.7.1 Viral remission, rather than eradication, as a model for HIV cure 29
1.7.2 Major approaches towards the development of an HIV cure 30
1.7.3 The central role of anti-HIV immunity in developing HIV curative interventions – moving beyond “kick and kill” . 32
1.8 Conclusion 36

1.1 Human immunodeficiency virus (HIV)

In the early 1980s, human immunodeficiency virus (HIV) was identified as the causative agent of immunodeficiency described amongst men who have sex with men in the United States [1–3]. This acquired immunodeficiency syndrome (AIDS) is now recognised as the consequence of CD4 T cell decline which occurs during untreated infection with this virus. It is characterised by the development of opportunistic infections (such as cryptococcal meningitis and pneumocystis pneumonia), as well as specific cancers [4]. The development of effective medications against HIV has transformed the prognosis of this infection; for those with access to therapy, HIV infection is no longer a terminal diagnosis. Despite this progress, a cure remains elusive and treatment is required for life.

Antiretroviral therapy (ART) as a treatment for HIV infection is one of the greatest therapeutic successes of modern medicine [5]. The identification of a long-lived viral reservoir (section 1.5) dampened early hopes that ART itself may be curative [6–8]. These drugs, however, are able to effectively suppress viral replication, preventing the onset of AIDS and converting HIV infection into a manageable chronic disease. Despite effective viral suppression, individuals with treated HIV infection are still at an increased risk of a number of non-AIDS co-morbidities, which appear to have be linked to chronic inflammation [4, 9]. There are now a large number of licensed agents which target various stages of the HIV replication cycle (section 1.1.1). Innovation in ART development has improved the safety profile of antiretroviral agents and reduced the pill burden associated with therapy [4]. ART is taken as a combination of three of these drugs, although with the high-efficacy of newer integrase inhibitors some two-drug regimens are now being trialled [10, 11]. The last few years have also seen some important developments in the way that ART is used, with recognition that earlier initiation is associated with better clinical outcomes [12] and that ART-induced viral suppression

prevents onwards transmission of the virus [13, 14]. Furthermore, antiretroviral agents are now used to prevent HIV acquisition following or prior to viral exposure (post-exposure prophylaxis (PEP) and pre-exposure prophylaxis (PrEP))[15–17].

With over 35 million people worldwide living with HIV infection [18], effective prevention and treatment remain key public health priorities. HIV can be transmitted sexually, via blood products or from mother to child during childbirth; effective prevention strategies have been developed to target all of these transmission routes [4]. The epidemiology of HIV infection is complex, with distinct geographic regions and populations disproportionately affected. These key population groups include people who inject drugs, sex workers, men who have sex with men, transgender people and, in some parts of the world, women [18]. Nearly 1 million deaths per year still occur globally as a result of HIV infection [18]. In large part, this is because access to ART and other clinical care remains limited for many people living with HIV. The current Joint United Nations Programme on HIV/AIDS (UNAIDS) goal (termed 90-90-90) is that by 2020 90% of individuals living with HIV will know their diagnosis, 90% of these will be receiving ART and 90% of these will have virologic suppression [19]. These population health measures to target the HIV epidemic globally are complemented by efforts to better understand the virus itself and host response, with the aim of developing preventative vaccines and curative strategies.

1.1.1 Viral structure and replication

HIV is an enveloped retrovirus with a single-stranded ribonucleic acid (RNA) genome. There are two species, HIV-1 and HIV-2, which differ in their virulence [21]; unless otherwise specified the term HIV will be used throughout this thesis to refer to HIV-1, the predominant species globally [21]. The virion is composed of two copies of this genome within a protein capsid which, along with several enzymes and other regulatory and accessory proteins, are contained with a host-derived membrane (Figure 1.1 A) [4, 22]. The 9.7 kB genome encodes the major genes *gag* (structural proteins), *pol* (the enzymes protease, integrase and reverse transcriptase [RT]), *env* (the envelope glycoproteins gp120 and gp41) (Figure 1.1 B)

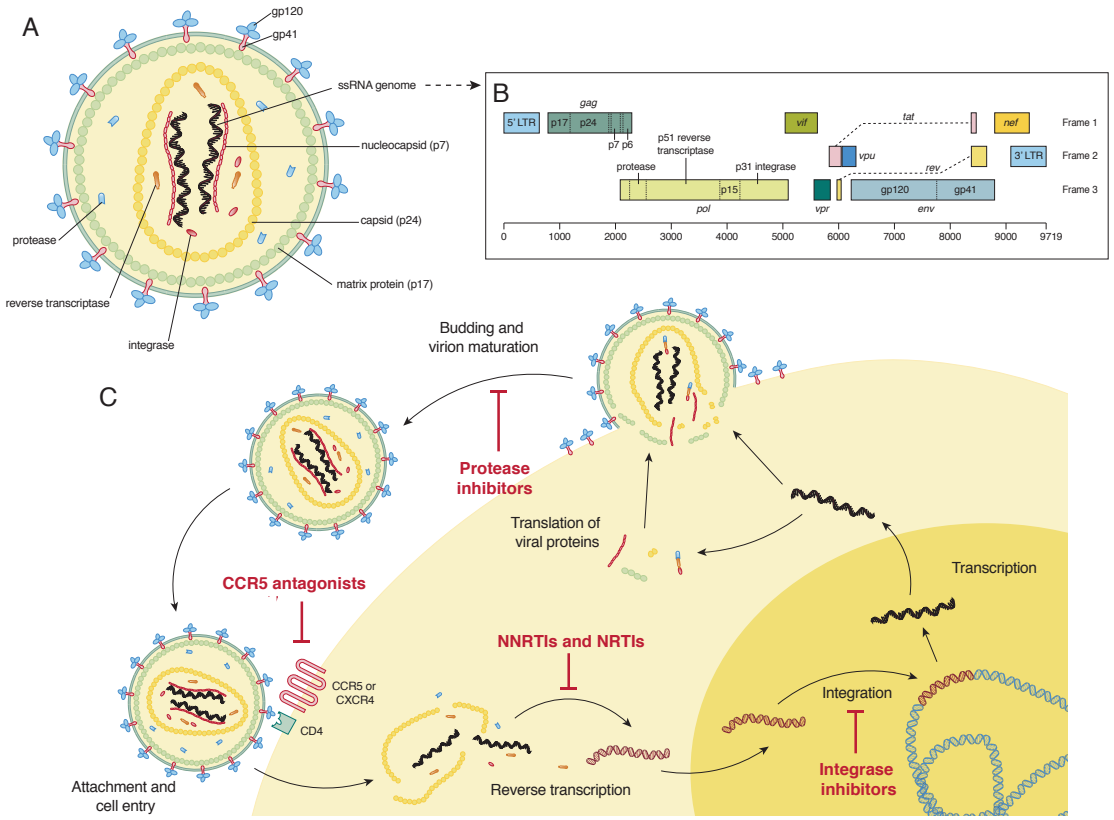


Figure 1.1: Overview of HIV structure and replication. (A) Simplified structure of the HIV virus. (B) The HIV genome showing major viral proteins in three reading frames are shown. Numbering and reading frames are based on the reference genome HXB2 [20]. (C) Simplified replication cycle of the HIV virus. Major antiretroviral drug classes are shown in red with bars to indicate the aspect of viral replication they target. Abbreviations: NNRTI, non-nucleoside reverse transcriptase inhibitor; NRTI, nucleoside reverse transcriptase inhibitor; LTR, long terminal repeat.

along with those of other viral proteins [20]. The replication cycle of HIV has been well-characterised and is summarised in Figure 1.1 C. In brief, the virus attaches to target cells via the interaction of the gp120/gp41 complex with CD4 and one of the co-receptors CCR5 or CXCR4, facilitating membrane fusion and viral entry. The tropism of the virus is limited to those cells which express CD4 on their surface: CD4 T cells, macrophages, monocytes and some dendritic cells [4]. Following viral uncoating, the viral genome is reverse transcribed and imported into the nucleus where integration of viral deoxyribonucleic acid (DNA) into the host-cell genome occurs; it is this integrated proviral DNA that is the barrier to HIV cure (discussed further in section 1.5). Transcription and nuclear export of viral mRNA occur with

the involvement of the regulatory proteins Tat and Rev. Translation of viral proteins occurs in the cell cytoplasm: Gag and Pol are translated as a polyprotein from unspliced mRNA, whilst various mRNA spliceforms code for other viral proteins [23]. Viral proteins and mRNA traffic to the cell membrane where viral assembly and budding off of the viral particle occur. Viral maturation (including the cleavage of the Gag/Pol polyprotein by the viral protease) occurs following budding to result in the formation of a mature virion (Figure 1.1 C) [22].

1.2 T cells and the immune response

The immune response to infectious or cancerous stimuli is a coordinated effort involving numerous cell types, soluble signalling molecules (cytokines) and anatomic compartments. The human immune system is often divided into two parts: the innate and adaptive immune systems. The innate immune system involves cells which sense structures that are common to many pathogens (pathogen associated molecular patterns; PAMPs); these include macrophages, dendritic cells and natural killer (NK) cells. The innate immune system has an important role not only in directly targeting pathogens, but also activating the adaptive immune response [24]. The adaptive immune system is characterised by the recognition of molecular sequences (antigens) which are highly specific to an individual pathogen. Increasingly, with the identification of cells with both innate and adaptive features [25–27], this division is becoming less clear. Adaptive immunity comprises B cells, which produce antibodies, and T cells, which have cytotoxic and co-stimulatory functions; both of these responses are characterised by the formation of immunologic memory meaning that repeated exposure to the same antigen will result in a more robust response. Whilst often described separately, these two systems operate in an interdependent way [28].

T cells comprise two major subtypes with differential expression of the T cell receptor (TCR) co-receptors CD4 and CD8 [29], both of which show enormous functional complexity. In the simplest description of their differential function, CD8 T cells (also known as cytotoxic T lymphocytes, CTL) are directly cytotoxic and

have several mechanisms to lyse target (infected or cancerous) cells including release of cytotoxic granules (containing granzymes and perforin) and Fas (CD95)/Fas ligand interactions [29, 30]. CD4 (helper) T cells play important roles in directing other aspects of the immune response and comprise several functional subsets (reviewed in [31]).

Each T cell possesses a TCR with unique antigenic specificity which is generated as a result of genetic recombination during its development. The existence of highly variable TCRs ensures that, for any given antigen, it is highly probable that there is a specific T cell which can bind it [32]. Following deletion of T cells with specificities against host-derived antigens (to prevent autoimmunity), the naïve T cell pool is poised to react to any potential pathogenic sequences [32]. T cells recognise fragments of antigens (epitopes) presented in major histocompatibility complex (MHC) molecules. MHC class I are expressed widely on all nucleated cells and present a "sample" of peptides produced by that cell to CD8 T cells [29]; this provides surveillance for cancerous or virally infected cells. MHC class II is only expressed on professional antigen presenting cells (APCs) which present antigen to CD4 T cells [33]. These interactions take place primarily in secondary lymphoid tissues such as the lymph node and spleen. In the absence of co-stimulation, T cell binding of a cognate epitope presented on an MHC molecule is insufficient for initial activation of T cells and the generation of maximal effector responses. Sometimes referred to as the "second signal", this co-stimulation comes from the interaction of receptors on the T cell surface with co-stimulatory molecules on the APC surface [34]. Co-inhibitory pathways, which have an opposite role, are discussed in section 1.4.2.

Following T cell activation the development of effector functions (such as cytokine production, cytolytic potential, proliferation and memory formation) occurs. In the presence of antigen (and appropriate co-stimulation) these effector functions develop as cells progress from naïve to terminally differentiated. Much of what we understand about T cell fate has come from murine studies because of challenges in the ability to track human T cell fate *in vivo* [38]. In a resolving infection, in mice, T cell development progresses from naïve through effector to long-lived memory cells

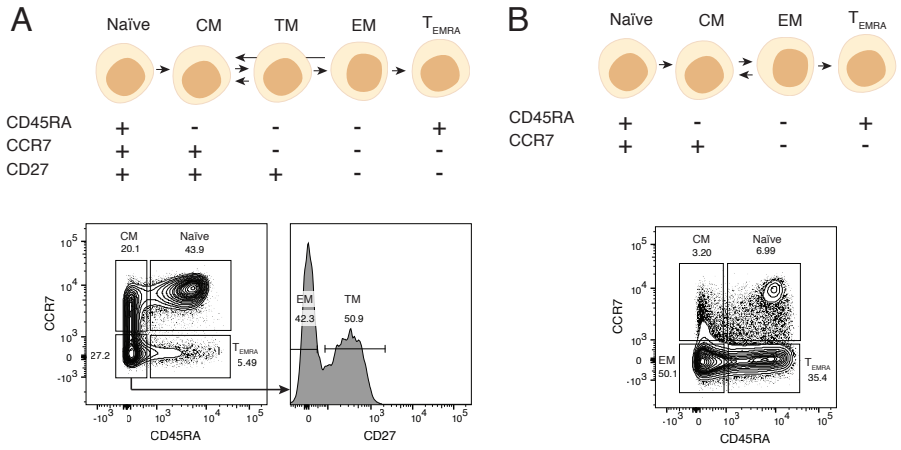


Figure 1.2: Phenotypic markers used to define T cell memory subsets in this work. Combinations of surface markers and representative flow cytometry gating are shown for CD4 T cells (A) and CD8 T cells (B). The division of CD4 T cells is performed using CD45RA, CCR7 and CD27 [35] and is commonly used in the HIV latency literature [36]. For CD8 T cells, this is based on CD45RA and CCR7 [37]. The ontogeny of these subsets *in vivo* is incompletely understood; arrows mark likely developmental relationships between these.

(reviewed in [38–40]). Phenotypic, transcriptomic and epigenetic studies support the notion that, in humans, these subsets are similarly related [41, 42]. Recent work using deuterium labelled water tracked developing CD8 T cells in response to yellow fever virus vaccination [42]. This work demonstrated that long lived memory cells arise at the same time as rapid effector memory expansion [42] which may be consistent with the developmental progression described in mice. This model is complicated by the identification of long-lived memory populations with naïve like features in both mice and humans [43, 44]. The ontogeny of effector and memory T cell subsets *in vivo* is an area of ongoing study.

Both CD4 and CD8 T cells are commonly divided into subsets of increasing differentiation status based on the expression of CD45 isoforms and other surface markers. The loss of CD45RA and reciprocal expression of CD45RO was one of the earliest described distinctions between naïve and memory T cells [45]. Further division into memory subsets was subsequently described with CCR7 [37, 46], CD27 and CD28 [35, 47–50]. There is functional and phenotypic heterogeneity within these subsets [41, 51, 52] making these divisions somewhat limited. Furthermore, the division of effector and memory subsets based on these markers may not overlap

with the functional changes that occur in the transition from naïve to effector and memory cells [51]. These subsets are, nevertheless, a useful framework for studying bulk T cell populations *ex vivo*. Figure 1.2 shows the schema that is used throughout this work. Interestingly, persistent viral infections differ in the memory phenotype of their viral-specific CD8 T cells [37, 41, 51], suggesting distinct T cell qualities induced by each infection.

1.3 Primary HIV infection

Early HIV infection is associated with a rapid increase in the number of viral copies detectable in the blood (termed the viral load) to high levels, approximately 10^7 copies/mL [53–55]. At the same time there is a depletion in the number of CD4 T cells (referred to as the CD4 count). This high viral load (VL) peaks around 2-3 weeks following infection and returns to a lower level, accompanied by a partial recovery of the CD4 count in the peripheral circulation. Following this acute phase, the VL reaches a steady state called the set point [53–56]. Without treatment the VL, and CD4 count, remain steady for a variable number of years before an eventual increase in VL and decline in CD4 count mark the onset of AIDS (Figure 1.3).

This period of early infection is a dynamic phase with widespread activation and apoptosis of innate and adaptive cells, occurring with the production of acute phase proteins and inflammatory cytokines (reviewed in [57]). In many, but not all, infected individuals, this is associated with a febrile illness termed acute retroviral syndrome [58]. Increasingly, it is understood that events at this time can have an important impact on HIV pathogenesis and disease outcome. As an example, a marked depletion of CD4 T cells (particularly Th17 cells) in the gut mucosa occurs during early HIV infection [59–62]. This Th17 depletion is thought to be an important contributor to persistent immune activation and inflammation once ART is established (reviewed in [9]).

The early stages of HIV infection can be divided based on the evolution of antibody responses to the virus. Initial staging proposed by Fiebig *et al.* divides

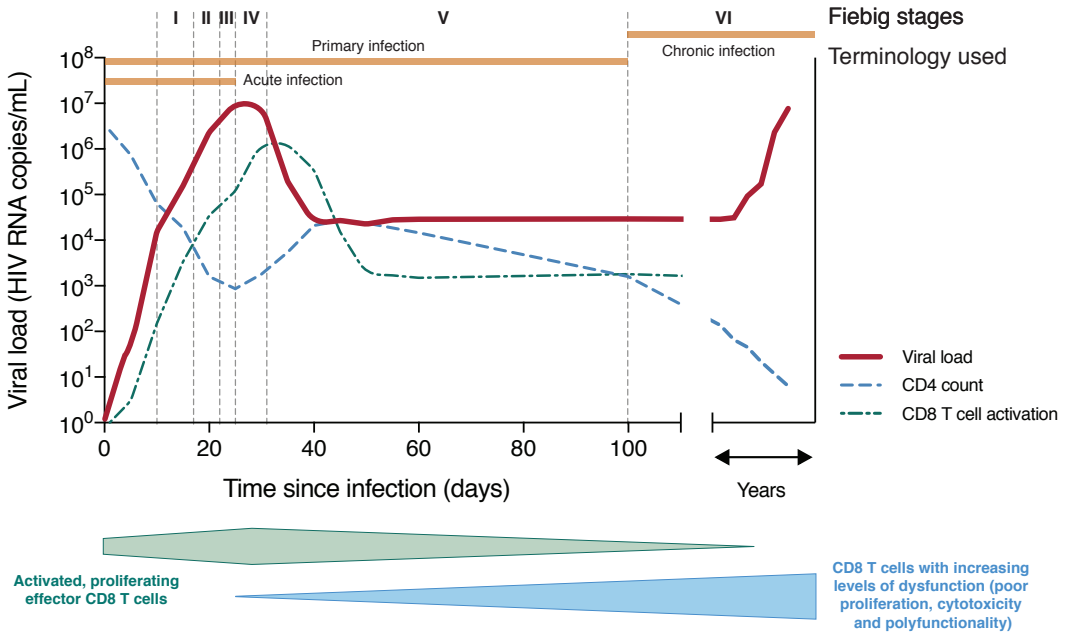


Figure 1.3: Dynamics of viral load, CD4 count and CD8 T cell activation during the natural history of HIV infection. CD8 T cells refer to HIV-specific CD8 T cells, although these changes are also observed in the bulk T cell pool. The terminology used in this work is overlaid over the corresponding Fiebig stages [56, 63].

the infection into six stages [56, 63] using the sequential gains in diagnostic test positivity that occur (detection of nucleic acids, p24 antigen and antibodies against viral proteins). Whilst modern diagnostic tests are more sensitive and may no longer correspond to the Fiebig stages [64], this staging system has utility as a framework to allow for the comparison of studies of acute infection. There is substantial variation in the terminology used to describe the early stages of HIV infection. Throughout this work, the term primary HIV infection (PHI) will be used to refer to the first 6 months following infection, reserving the term acute for the period of time prior to peak viraemia. These terms are shown alongside the corresponding Fiebig stages in Figure 1.3.

1.4 T cell function and dysfunction during HIV infection

The role of T cells, particularly CD8 (cytotoxic) T cells, in the immune response against HIV is well-established. In simian immunodeficiency virus (SIV) infection,

the depletion of CD8 T cells results in high level viral replication [65–70] indicating a role for CD8 T cells in controlling the virus. In humans, this is supported by strong epidemiological evidence from genome-wide association studies (GWAS) linking disease progression to the human leukocyte antigen (HLA) class I locus [71, 72], and subsequent identification that particular HLA alleles are associated with disease control or progression [73]. Further evidence comes from the existence of rare individuals who are able to spontaneously control HIV infection through particularly strong anti-HIV CD8 T cell responses (discussed in section 1.6.1). Finally, the development of immune escape mutations which are no longer recognised by CD8 T cells have been well described ([74–76], reviewed in [77]) and provide evidence of selection pressure imposed by CD8 T cells. T cell responses against HIV, however, are not sufficient to eradicate the virus and, in the vast majority of individuals, do not prevent progression to AIDS. This inability for the immune system to control HIV is due, at least in part, to the development of dysfunctional HIV-specific T cell responses.

1.4.1 The development of T cell functions during the course of HIV infection

A characteristic of early HIV infection is the induction of large numbers of activated HIV-specific T cells. There is evidence that this CD8 T cell expansion coincides with the decrease in VL following its peak (Figure 1.3)[76, 78–81] and is correlated with subsequent VL set point [82–84], suggesting a role for CD8 T cells in controlling this viral expansion.

Recent work, which has been able to more precisely characterise the immune response at these very early stages of infection, has shown that activated, antigen specific T cells show a peak in number with or shortly after the VL peaks [85–87]. The magnitude of this response settles down to a lower level, in a way that mirrors the viral load dynamic (Figure 1.3) [88, 89]. The "set point" activation level appears to be established during primary infection [85, 90], and has been associated with subsequent disease progression in untreated individuals [90–93]. There is

evidence that these activated, effector CD8 T cells play a role in controlling viral replication: if ART is not initiated at peak viraemia, these CD8 responses correlate with subsequent VL set point [85]. Similarly, if ART is started at peak viraemia the magnitude of this response is linked to reduction in VL and subsequent HIV DNA levels [86]. Some studies suggest this immune activation appears to occur largely in HIV-specific CD8 T cells [85, 86], although there is disagreement in the literature about the extent of bystander activation [88, 94, 95].

With the induction of such extensive T cell activation, why is viral control not maintained? In HIV infection it appears that features considered to be part of an optimal T cell response (including memory formation, cytotoxicity and production of multiple cytokines, or polyfunctionality) do not develop contemporaneously and may not all occur. T cell functions do not fully mature until peak viraemia, and features of T cell dysfunction also appear at this time. Prior to peak viraemia (Fiebig stages I and II) there is rapid induction of activated (HLA-DR/CD38 positive), proliferating CD8 T cells (Ki-67^{high}Bcl-2^{low})[85, 86]. The acquisition of cytolytic potential, however, does not occur fully until VL peaks [85, 86]. At this same stage, CD8 T cells already show evidence of metabolic dysfunction, reduced expression of the IL-7 receptor [85, 86] (which is critical for memory formation [96]), and are pro-apoptotic [85, 86]. This functional phenotype is similar to what has been observed in later stages of primary infection [87, 97], where poor memory development has been linked to lack of viral control [97]. In acute infection, the early rapid development of short-lived effector cells can in part explain the initial efficacy but ultimate failure of CD8 T cells to control HIV replication.

Further dysfunction develops during the progression from primary to chronic infection [88, 97–100], most notably with the subsequent loss of cytotoxicity. CD8 T cells during untreated chronic infection proliferate poorly, have low cytotoxic potential (measured by perforin expression) and activity, and low polyfunctionality [88, 98, 99, 101–107] - consistent with a process known as T cell exhaustion (discussed in section 1.4.2). This CD8 dynamic, with initial expansion of activated effectors, but subsequent paucity of effector functions is depicted in Figure 1.3

The benefits of earlier ART initiation for CD4 count recovery and reduced mortality are now well-established [12, 108–111]. It could be hypothesised that earlier initiation of ART could also preserve T cell effector function. Indeed, there is evidence that ART initiation during PHI is associated with partial conservation of effector CD8 numbers, proliferation and polyfunctionality [98, 112–115] as well as lower T cell activation in some [108, 116] but not all studies [117]. There are, however, relatively few studies that directly compare the timing of ART initiation between primary and chronic infection.

Initiation of ART before peak viraemia appears to preserve the memory potential of CD8 T cells but also abrogates the development of effector functions [86] and breadth of the response [81]. Demonstrating how effector functions are impacted, when ART is initiated at peak viraemia the pool of activated, proliferating CD8 T cells plays a role in reducing subsequent VL and HIV DNA levels, but this is not seen if ART is started before VL peaks [86]. The notion that treatment initiation prior to VL peak may prevent the development of some CD8 effector functions is supported by data from a recent treatment interruption (TI) trial performed with individuals treated in Fiebig I[118]. In this group, CD8 T cell responses were related to the magnitude of VL upon viral rebound when measured at the time of rebound, but not before, [118] suggesting these had not fully developed in the period of initial (pre-ART) viraemia.

Due to their dysfunction and/or depletion, CD4 T cell responses also contribute to the failure to control viral replication (reviewed in [119, 120]). HIV-specific CD4 T cell responses have been detected during acute infection, but are already impaired by later stages of PHI [81]. CD4 T cells during untreated infection also show defects in proliferation [98, 121], and there is some evidence of a benefit of ART initiation during acute or primary HIV infection in preserving T helper responses [81, 98, 113, 114].

Overall, it appears that there is considerable temporal overlap in the development of CD8 T cell function and dysfunction (Figure 1.3). With substantial evidence that ART initiation even at the earliest stages of infection does not completely preserve

a functional T cell response, it appears unlikely that ART alone will sufficiently preserve CD8 T cell function to use as part of an HIV curative strategy (section 1.7).

1.4.2 T cell exhaustion and immune checkpoint receptors

T cell exhaustion is used to described a cellular state characterised by a loss of effector functions that develops in settings of chronic antigen persistence, such as chronic viral infections and cancer. In murine lymphocytic chroriomeningitis virus (LCMV) models, where exhaustion has been well-characterised, persistent infection is associated with a progressive loss of effector functions. Ongoing antigenic stimulation is considered to be a major driver of this process, although a role for the inflammatory milieu has also been proposed (reviewed in [122]). CD8 T cell exhaustion has been found to occur particularly in the absence of CD4 T cell help [123, 124], an observation of clear relevance in the context of HIV infection.

T cell exhaustion is associated with the expression of co-inhibitory receptors (or immune checkpoint receptors; ICRs) on the cell surface. Many of these are analogous to the co-stimulatory receptors required for T cell activation but provide inhibitory rather than activating signals. These ICRs have an important role in modulating the immune response during an acute infection, but appear to limit the efficacy of this response if infection persists. The discovery that the blockade of programmed death cell protein 1 (PD-1; CD279) signalling could restore CD8 T cell functionality [125] has led to substantial research to identify and characterise the roles of other co-inhibitory molecules. Numerous ICRs have since been described, many of which share ligands with co-stimulatory receptors. This thesis will include the study of a number of ICRs from discrete signalling pathways which are summarised in Figure 1.4. T cell exhaustion is of significant clinical interest because of the success of monoclonal antibodies targeting ICR signalling pathways, including PD-1 and its ligands, as cancer therapeutics (reviewed in [126]). Clinically, the resulting augmentation of immune responses from these drugs has resulted in high remission rates, and similar approaches are being considered for HIV infection (section 1.7.3).

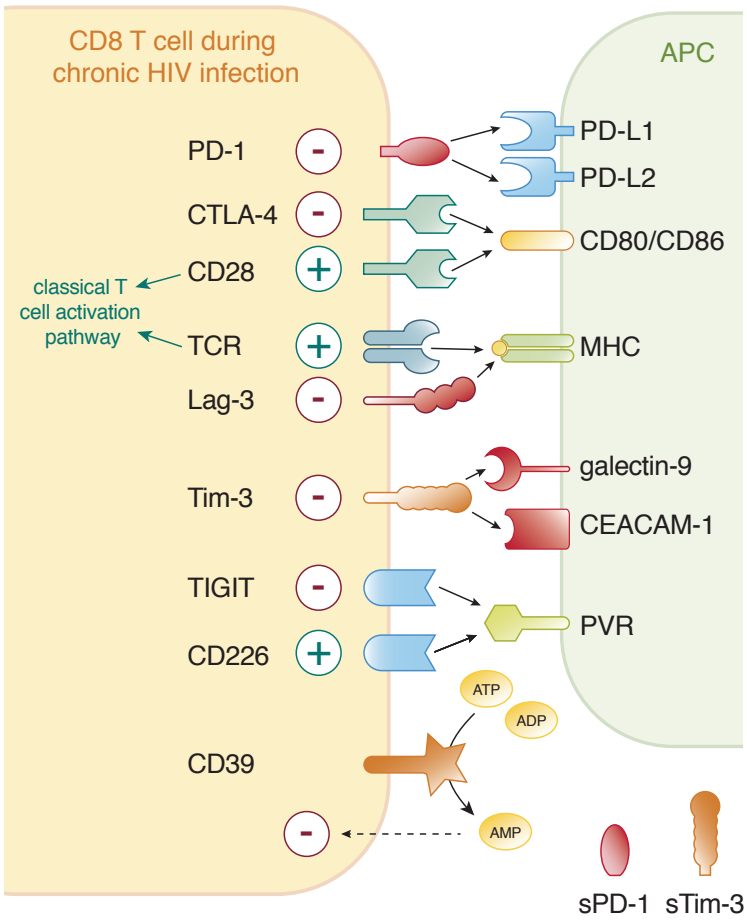


Figure 1.4: Immune checkpoint receptors (ICRs) on CD8 T cells and their corresponding ligands. Other key signalling molecules in T cell activation, which interact with these ICR pathways are also shown. (+) indicates an activating signal and (-) an inhibitory signal. Programmed death cell protein 1 (PD-1) interacts with PD-1 ligands 1 and 2 (PD-L1 and PD-L2); signalling through this pathways has potent inhibitory actions [122]. Cytotoxic T lymphocyte antigen 4 (CTLA-4) shares its ligands CD80 and CD86 with the important co-stimulatory molecule CD28, which provides the "second signal" to ensure T cell response to antigen presentation. Lymphocyte activation gene 3 (Lag-3) interacts with major histocompatibility complex (MHC) class II on the surface of antigen presenting cells (APCs); this shared pathway with the T cell receptor (TCR) highlights the relatedness of co-inhibitory signalling to T cell stimulatory processes. Several ligands for T cell immunoglobulin and mucin domain–containing molecule 3 (Tim-3) have been identified, notably galectin-9 and carcinoembryonic antigen-related cell adhesion molecule 1 (CEACAM-1) [126, 127]. T cell immunoreceptor with immunoglobulin and ITIM domains (TIGIT) shares the poliovirus receptor (PVR; CD155) with the activating receptor CD226 [128]. CD39 is an ectonuclease which does not exert its co-inhibitory actions via receptor-ligand interactions but rather facilitates the catalysis of extracellular adenosine tri/diphosphate (ATP/ADP) to adenosine monophosphate. This is subsequently converted by CD73 to adenosine, which has directly immunoregulatory activity [129]. Soluble forms of PD-1 (sPD-1) and Tim-3 (sTim-3) exist, although their interactions with these signalling pathways in HIV infection remains poorly characterised. Adapted from [130].

Elevation in the expression of multiple ICRs on T cells has been described during primary and chronic HIV infection [127, 131–138], where they have been associated in untreated individuals with CD4 count, VL and clinical progression in many (Table 1.1), but not all studies [139]. During chronic HIV infection, CD8 T cells expressing ICRs including PD-1, Tim-3, TIGIT and Lag-3 have been shown to have functional defects reflecting exhaustion such as impaired cytokine production [127, 132, 136, 137], proliferation [131, 140] and cytotoxic potential and/or degranulation [133, 136, 141]. These functions having been shown to improve with *ex vivo* blockade of these ICR pathways [127, 131–133, 136, 141–143], demonstrating that during HIV infection these pathways are involved in mediating T cell dysfunction.

In murine models, co-expression of ICRs has been shown to mark cells with higher degrees of exhaustion, and blockade of multiple pathways further improves CD8 T cell function [144]. This has also been observed during HIV infection where HIV-specific CD8 T cells upregulate ICR co-expression [145–147]; this is associated with more dysfunction than single expression of these markers [136, 146, 147].

There is considerable evidence for the role of antigen in driving this process during HIV infection. Consistent correlations have been shown in cohort studies between VL and CD8 T cell expression of PD-1 and other ICRs (Table 1.1), suggesting a key role for persistent antigen in driving this process. Supporting this, PD-1, TIGIT and CD39 have all been shown to be expressed at higher levels on HIV-specific CD8 T cells compared with Epstein-Barr virus (EBV)- or cytomegalovirus (CMV)-specific cells from the same individual [129, 131, 132, 137, 142, 148, 156, 157]. In the case of PD-1, immunologic controllers with persistent viral replication (viraemic controllers) have been demonstrated to express higher levels than controllers with undetectable viraemia (elite controllers) [135]. Furthermore within an individual, PD-1 expression on CD8 T cells has been shown to mirror fluctuations in VL [132, 148, 156], as well as decrease on HIV-specific T cells following viral escape from their cognate epitope [99, 148, 157].

In addition to the phenotypic differences detailed above, exhausted T cells in murine models have been shown to have transcriptomic [158, 159], metabolic

	CD8 T cells	CD4 T cells
PD-1	*VL*: CHI [131–133, 148, 149] and PHI [134, 135]. *CD4 count*: CHI [131, 133] and PHI [134]. *CD4 decline*: PHI [134]	*VL*: CHI [131, 140, 149, 150] and mixed cohort [151]*. *CD4 count*: CHI [131, 150], PHI [135] and mixed cohort [151]*.
Lag-3	*VL*: CHI [152] and PHI [134]. *CD4 count*: CHI [143]. *CD4 decline*: PHI [134]	*VL*: CHI [143]. *CD4 count*: CHI [143].
Tim-3	*CD4 count*: CHI [127]	*VL*: CHI [127] and PHI [127].
TIGIT	*CD4 count*: CHI [136, 137].	
CD39	*VL*: CHI [129, 153]. *CD4 count*: CHI [153]. *Mortality*: CHI with TB co-infection [153].	
CTLA-4		*VL*: CHI [154, 155]*. *CD4 count*: CHI [154]*

Table 1.1: Reported associations between T cell immune checkpoint receptor expression and disease progression. Unless specified, results are for ICRs measured on bulk CD4 or CD8 T cells in untreated individuals during primary or chronic HIV infection; * on HIV-specific T cells. Abbreviations: CHI, chronic HIV infection; PHI, primary HIV infection; VL, viral load.

[159, 160] and epigenetic [161] features that are distinct from effector T cells - providing evidence that T cell exhaustion represents a distinct functional state or cell fate. Stability in exhaustion-associated epigenetic changes have been shown following successful, albeit temporary, re-invigoration of T cell responses with PD-1 blockade, suggesting inflexibility in cell fate once exhaustion has developed [162]. Further supporting this is the observation that resistance to PD-1 blockade in lung cancer models can develop with the upregulation of another ICR, Tim-3, on cells which have bound anti-PD-1 antibodies [163]. The demethylation around the *PDCD1* (PD-1 encoding gene) locus observed in murine models of exhaustion has also been observed in HIV-specific T cells during chronic HIV infection [164, 165]. Interestingly, this demethylation can already be observed during PHI and does not revert following virological suppression with ART initiated during chronic infection [165], suggesting limited functional potential of these cells.

Certain transcription factors have been implicated in the fate of exhausted CD8 T cells including the T-box transcription factors, T-bet and eomesodermin (Eomes)

[166, 167]. T-bet and Eomes operate in concert in the development of effector T cell functions. In T cell exhaustion, a change in the expression pattern of these occurs where two subsets of cells have been described with reciprocal expression of these markers. In murine models, T-bet^{high}Eomes^{dim} are responsive to PD-1 blockade [168]. With further antigenic stimulation these cells give rise to T-bet^{dim}Eomes^{high} cells which express higher levels of PD-1 [167], and do not respond to PD-1 blockade [168]. The functional significance of these transcription factor subsets has been studied in HIV infection where HIV-specific CD8 T cells were shown to be mostly T-bet^{dim}Eomes^{high} and have poor polyfunctionality and high ICR co-expression [169]. Furthermore, CD8 T cells expressing TIGIT and CD39 have been shown to have a T-bet^{dim}Eomes^{high} phenotype [129, 137], consistent with functional exhaustion. T-bet and Eomes are not the only transcription factors implicated in exhausted cell fate; the transcription factor TCF-1 is necessary for CD8 regenerative capacity in chronic viral infections [170–172]. Levels of TCF-1 have been recently found to be elevated in HIV-specific T cells from elite controllers, and correlate with viral control [173]. Future work will need to determine if CD8 T cell fate can be targeted therapeutically in HIV-infected individuals to improve the functional capacity of these cells. Other transcription factors associated with exhaustion, including IRF-4 and NFAT [174, 175], are yet to be studied in the context of HIV infection.

Functional exhaustion also occurs in CD4 T cells and is associated with ICR expression. Whilst there is some overlap in exhaustion pathways observed between CD4 and CD8 T cells, aspects of CD4 T cell exhaustion appear distinct [151, 154, 176]. As an example, CTLA-4 appears to function as a marker of exhaustion on CD4, but not CD8, T cells [154]. As in the CD8 compartment, upregulation of ICRs including PD-1 and CTLA-4, and ICR co-expression, occurs on HIV-specific CD4 T cells during untreated HIV infection [154, 155, 177], where it is associated with functional defects which are partially recoverable via blockade of the receptor [145, 151, 154, 155, 177].

It is important to note than ICR expression does not always equate to functional exhaustion. The role of PD-1 up-regulation as a consequence of cellular activation

is well-recognised [178]. Indeed, PD-1 expression is observed on CD8 T cells from healthy individuals, where it is not associated with functional deficits or an exhaustion-associated transcriptional state [179]. Even in the context of chronic viral infections, PD-1 does not always mark functional exhaustion [180, 181]. Recent work in hepatitis B (HBV) infection identified that HBV-specific T cell responses derived from PD-1 expressing cells were protective against flares following treatment discontinuation [181]. This is likely also applicable to other ICRs. In one study comparing ICR expression between HIV elite controllers and chronic progressors, co-expression of the ICRs CD160 and 2B4 was increased in controllers and marked cells with higher perforin expression [138], suggesting increased cytotoxicity. Consistent with this, several ICRs (including 2B4) have been shown to have activating, as well as inhibitory roles [34, 182].

During HIV infection the expression of a number of ICRs has been linked, either through correlation or co-expression, with markers of T cell activation such as CD38 and HLA-DR [127, 129, 133–135, 137, 147–149, 153, 156, 171]. Some differences in ICR expression patterns between primary and chronic infection have also been noted [97, 136, 139, 146], suggesting there may be functional differences in these receptors at different stages of infection. In one study, PD-1 was associated with poor CD8 proliferation during chronic, but not primary infection [140] and may be a marker of activation, rather than exhaustion, at this early stage.

It is becoming increasingly recognised that there is significant heterogeneity within exhausted and ICR expressing T cell populations [170–172]. It is likely that the balance of stimulatory and inhibitory receptors, as well as the context of their expression, influence cellular functionality. The role of ICRs, and the relevance of T cell activation during primary HIV infection remains incompletely characterised and is an important area for future research.

1.5 The HIV reservoir

During long-term suppressive ART, integrated proviral HIV DNA persists in a pool of cells known as the HIV reservoir. Upon treatment cessation, recrudescent infection occurs in almost all individuals - arising from this reservoir. Theoretically, elimination of the HIV reservoir would be curative, and reduction in reservoir size has been a significant target of HIV cure research (section 1.7). The HIV reservoir is considered to consist predominantly of CD4 T cells although other infectable cell types, particularly myeloid cells, may also contribute (reviewed in [183]). Evidence from SIV models suggest that the HIV reservoir is established in the initial days after infection [184, 185]. This reservoir is maintained over long periods of time by homoeostatic proliferation of memory CD4 T cells [36, 186–189] and possible replenishment via low-level ongoing viral replication [190] (although this remains controversial [191, 192]). The decay in reservoir size is so slow that ART alone will not be able to reduce reservoir size sufficiently to cure HIV [193–197].

When the HIV reservoir was first identified as a barrier to HIV cure [6–8], it was thought that only resting cells would be able to facilitate latent, rather than productive infection [6, 7, 198]. There is now evidence that activated cells during sustained ART may contribute to the reservoir [199–201] and that even with strong cellular activation, latency can be maintained [202]. Strictly, virological latency refers to complete transcriptional silence of a provirus. It is now clear that the production of viral products during HIV represents a spectrum with some cells capable of producing mRNA or viral proteins in the absence of infectious virus [186, 203, 204] - and that these may influence anti-HIV immunity [204, 205]. Here, the term reservoir will be used to refer to all cells during suppressive ART from which rebound viraemia could arise including those which may be activated or producing some viral products (that is, not restricted to those with true latent infection). This intentionally broad definition reflects the functional goal of HIV cure research (an absence of rebound viraemia upon ART cessation) and the increasing understanding of heterogeneity within the reservoir. There is clear

evidence that ART initiation during PHI is associated with a smaller reservoir size when compared with chronic infection [36, 116, 117, 206–212], an observation that may be linked to the development of post-treatment control (section 1.6.2). This is also one key reason why early ART initiation is considered to be important in HIV curative strategies (section 1.7).

Numerous assays have been developed to measure the HIV reservoir. The aim of curative interventions has been to reduce reservoir size such that viral rebound is prevented upon ART cessation. As such, the "gold-standard" measure of HIV reservoir size is the time to rebound viraemia following TI; the measurement of time to viral rebound is the focus of Chapter 2. With practical limitations and safety concerns around TI protocols (discussed in section 2.5.5), surrogate measures of reservoir size are used. The advantages and limitations of these were recently reviewed in [213], and there is considerable disagreement over which measures are most appropriate [214, 215]. Broadly, polymerase chain reaction (PCR) based assays are used to measure persistent HIV DNA (either all HIV DNA, termed total HIV DNA, or only integrated forms) or RNA - these will overestimate the size of the reservoir as the vast majority of proviral DNA is not replication competent [7, 188, 202, 216–218]. Other assays aim to stimulate viral production and measure infectious virions, viral proteins and/or transcripts induced. Conceptually these are closer to a "true" reservoir, but these generally require larger numbers of cells and all are limited by the inability of single or recurrent rounds of T cell activation to stimulate out all infectious virus [202]. Studies that have compared different reservoir measures side by side have shown differing degrees of concordance [211, 219]. Of note, the only reservoir measures which have been shown to be associated with time viral rebound following TI are HIV DNA [220–223] and cell-associated unspliced RNA (CA-usRNA) [224, 225]. This is likely, in part, because they are high-throughput assays well suited to cohort studies, but does confirm the validity of these measures. Furthermore, the proportion of intact/defective proviruses has been shown to be similar between individuals who experience prolonged viral control

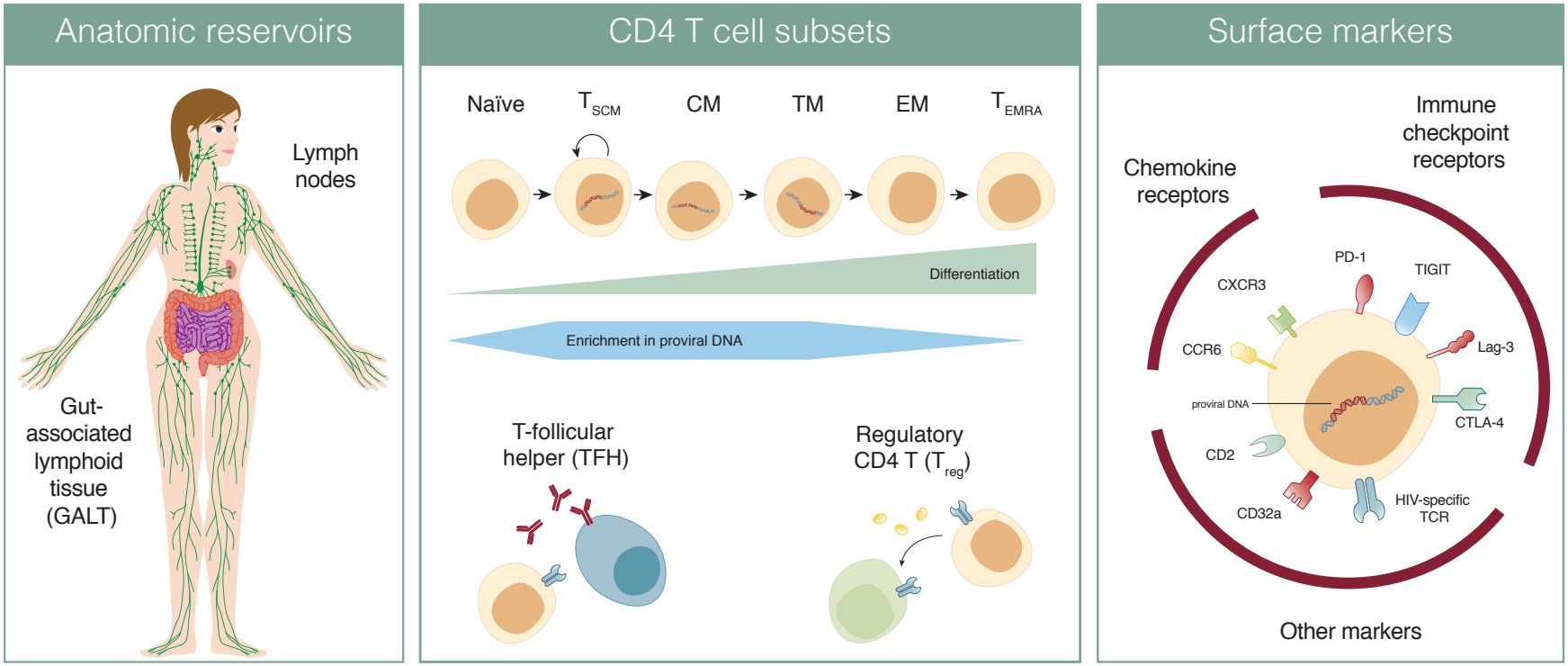


Figure 1.5: Heterogeneous distribution of the HIV reservoir with variation in anatomical and cellular compartments. Lymphoid tissue, including gut-associated lymphoid tissue and lymph nodes are major anatomical reservoirs[227–233]. Important cellular reservoirs include CD4 T cells of intermediate differentiation stages (stem-cell memory (T_{SCM}), central memory (CM) and transitional memory (TM) subsets) [36, 206, 210, 231, 234–236]. Enrichment of proviral DNA has also been observed in follicular helper (TFH) [230, 237] and regulatory (T_{reg}) CD4 T cells [238, 239]. HIV-specific CD4 T cells [240], those expressing immune checkpoint receptors [36, 241, 242], chemokine receptors [243], CD2 [244] and CD32a [245] are also enriched.

following TI and those who rebound rapidly [226], suggesting the total HIV DNA may be a good surrogate of the replication competent reservoir size.

The HIV reservoir is heterogeneously distributed throughout anatomical and cellular sites (Figure 1.5). It is well recognised that HIV replicates predominantly in lymphoid tissues, and both the lymph nodes and gut associated lymphoid tissue (GALT) are major anatomical reservoirs for persistent HIV RNA and DNA during ART [227–233]. They are also sanctuary sites as limited ART penetration [246], and immune privilege (see below) may allow for ongoing viral replication. Due to the challenges of obtaining tissue samples from certain anatomical sites, the ability to study anatomical HIV reservoirs during HIV infection is limited. Recent work in SIV-infected rhesus macaques has suggested that >98% of viral nucleic acid during ART is found within lymphoid tissues [247] - supporting the central role of these sites. Several other tissues, including the brain, have also been identified as sites of HIV persistence (reviewed in [248]) but controversy remains over their contribution [249] and further study is needed.

A number of CD4 subsets have been found to preferentially comprise the reservoir. Notably, memory CD4 T cells, particularly central memory (CM) and transitional memory (TM) cells represent the major HIV reservoir in the periphery [36, 206, 231, 234, 235]; these have also been shown to be the major site of replicating virus in untreated individuals [250, 251]. This may differ in GALT, where higher latent infection has been observed in the more differentiated effector memory (EM) CD4 T cells [206, 231]. Another functional CD4 T cell subset of particular interest are T-follicular helper (TFH) cells which are largely resident in B cell follicles in lymph nodes, and are preferentially infected by HIV and enriched for replication competent proviral DNA [230, 237, 250, 252]. As the B cell follicle is an immune privileged site (that is, limited entry of CD8 T cells allows evasion of immune responses) [253], this subset represents an important cellular reservoir [254]. Other functional CD4 subsets that may serve as HIV reservoirs include regulatory T (T_{reg}) cells [238, 239] and stem cell memory T (T_{SCM}) cells [210, 236] (Figure 1.5).

Given the rarity of latent infection, the identification of surface markers which could uniquely distinguish between infected and uninfected cells has been a significant goal of HIV cure research. Such markers could allow for easier study of the HIV reservoir, by enriching for cells of interest, or be therapeutically targeted as part of a curative strategy. A number of surface markers have been shown to mark an enriched HIV reservoir in sorted CD4 T cell populations (Figure 1.5), including several ICRs (section 1.5.1), CCR6, CXCR3 [243], CD2 [244] and CD32a (the focus of Chapter 5) [245]. In general, however, these enrichments are modest and none uniquely mark latently infected cells.

1.5.1 Immune checkpoint receptor expression is related to HIV reservoir size

Several lines of evidence link ICR expression to the HIV reservoir. During PHI the expression of PD-1, Tim-3 and Lag-3 has been shown to predict subsequent time to viral rebound (considered the "gold standard" of reservoir size) following 48 weeks of ART and subsequent TI [255]. Notably, in this study these ICRs did not predict viral rebound when measured at the time of TI, when reservoir size (total HIV DNA) predicted viral rebound in the same cohort [220]. The expression of several ICRs including PD-1, TIGIT, Tim-3 and Lag-3 on CD4 T cells also correlate with reservoir size [136, 229, 242, 255, 256]. Prior to the initiation of ART, HIV DNA or RNA has been found preferentially in CD4 T cells expressing PD-1, TIGIT and CTLA-4 [149, 250, 257], suggesting these cells may be preferentially infected or upregulate ICRs following infection. Importantly, these relationships persist on ART with demonstrated enrichments of HIV DNA in cells expressing CTLA-4, PD-1, TIGIT and Lag-3 from treated individuals [36, 230, 241, 242].

These observations, demonstrate an association rather than a causative role for ICRs in the formation of the reservoir. It is plausible, however, that ICR pathways could influence HIV reservoir size. With an important role in controlling early viral replication (section 1.4.1), exhaustion of HIV-specific T cells may be associated with higher seeding or slower decay of HIV reservoir size on ART, although this

has not been directly demonstrated. CD4 T cells which are activated [258–260] and HIV-specific [240] are more likely to be infected by the virus; given that HIV-specific T cells have higher ICR expression (section 1.4.2), and that markers of activation are commonly co-expressed or correlated with ICRs [36, 127, 133–135, 147–149, 153, 156], preferential infection of cells which express ICRs could also explain this relationship.

There is some evidence that ICRs play a mechanistic role in the establishment or the maintenance of latent infection. Using an *in vitro* model of latency establishment, Evans *et al.* recently demonstrated that blocking PD-1 reduced the level of latent infection observed [261]. Several further case studies of HIV-infected individuals treated with monoclonal antibodies against PD-1 or CTLA-4 for malignancies suggest a role for these markers in maintaining latency *in vivo*. Administration of these drugs was followed by modest increases in cell-associated RNA [261, 262] and HIV-specific T cell responses [263–265], suggesting a degree of latency reversal. This has further heightened the interest in the potential use of these agents as part of HIV curative strategies (section 1.7).

1.6 Post-treatment and spontaneous viral control

Recent years have seen reports of individuals living with HIV who are able to control viral replication after stopping ART. Whereas spontaneous (elite) controllers who maintain undetectable viraemia have been recognised from early in the HIV epidemic, such ART-induced control is a relatively new and unexpected phenotype. Of particular interest in the development of HIV cure strategies, understanding the mechanisms driving this "post-treatment control" (PTC) may inform interventions to induce long-term virological remission.

1.6.1 Post-treatment control is distinct from spontaneous control

Studies of extreme phenotypes of HIV control have improved our understanding of HIV pathogenesis. Reports of HIV control prior to ART, here termed "spontaneous

control", have included both control of viral replication (e.g. elite controllers) or an absence of CD4 count decline (e.g. long-term non-progressors). Sustained spontaneous control of viral replication is rare - occurring in less than 1% of infected individuals [266] - and has been associated with strong anti-HIV immunity, evidenced particularly by associations with certain class I HLA alleles (such as B*57 and B*27) and strong HIV-specific CD8 T cell responses. ([101], reviewed in [267, 268]).

There is significant evidence that PTC is mechanistically distinct from spontaneous control. While PTC is still rare amongst individuals who undergo TI, the estimated frequency appears to be substantially higher than that of spontaneous control [269–272]. Furthermore, PTC appears to be more frequent amongst individuals who initiate ART during PHI [223, 269–273], and who have a longer duration of therapy prior to TI [270, 274]. PTCs have also been reported to have a small viral reservoir [223, 269, 271] (discussed in section 1.6.2). Together, this suggests a role for ART in inducing a control phenotype in some individuals who would otherwise have not been able to control viral replication. Importantly, the strong HIV-specific CD8 T cell responses observed in elite controllers have not been seen in descriptions of PTC [269, 271] – suggesting that the underlying mechanisms are not related to classical HLA class I mediated CD8 T cell control. While the small numbers of PTC cohorts and case studies limit the power of analyses to identify associations with HLA class I, PTCs do not appear to be more likely than the broader population to possess protective alleles including B*57 and B*27 [269, 271, 275]. In one of the earliest characterised PTC cohorts (VISCONTI) controllers were reported to have over-representation of HLA B*35 which is associated with rapid HIV progression [271, 276], although this has not been consistently observed in other cohorts [275, 277].

1.6.2 Reservoir size, viral blips and virological control

A small HIV reservoir has been consistently linked to PTC. Initial evidence was from case studies of individuals with very low HIV reservoirs either due to allogenic stem cell transplantation (alloSCT) [278, 279] or extremely early ART initiation [280, 281]

who have experienced subsequent periods of PTC. Further evidence comes from the consistent observation that PTCs [223, 226, 269, 271] and individuals with remission [277] have smaller HIV reservoir size (measured by HIV DNA) than non-controllers. Reservoir size measured by HIV DNA has also shown to be predictive of time to viral rebound [220]. Further, a large analysis of the CASCADE cohort aimed to identify factors associated with post-TI control in individuals treated during PHI [274]. They identified that a shorter interval between seroconversion and ART start, and a longer duration on ART, were both associated with viral control following TI [274]. While reservoir size itself was not measured, these are both factors that could conceivably be acting by limiting initial reservoir size.

Two additional case-studies describe individuals with extremely low (or undetectable) viral reservoir size who, following a period of viral remission, experience eventual viral rebound [282, 283]. One of these individuals had undergone alloSCT [283], and the other initiated ART at a very early stage following pre-exposure prophylaxis (PrEP) [282]. Viral rebound in these individuals occurred at 288 and 225 days respectively, a time period remarkably similar to the duration of viral remission experienced by one of the Boston patients [279]. What is becoming clear, is that whilst low-reservoir size is a common feature of post-TI virological control, it is not on its own sufficient to confer this phenotype.

While the mechanisms driving PTC are not known, studies of loss of spontaneous control can add to our understanding. A study of >1000 spontaneous controllers in the COHORE database explored factors that predicted loss of virological control [284]. They demonstrated that viral blips were predictive of subsequent loss of control [284], a factor that was also shown to predict loss of control following TI in CASCADE [274]. When compared with spontaneous controllers who experience viral blips, those who maintain consistently undetectable viral loads have been recently shown to have lower reservoir size and T cell activation levels [285], suggesting that tighter control is associated with lower immune activation. This distinction between "leaky" and strict virological control may also have utility in the study of PTC. Indeed, viral blips have been recently shown to predict ART resumption

in PTCs from the VISCONTI cohort [286]. It is possible in both models that immune activation may play a role in the loss of virological control, although this has not been explored in the context of PTC.

1.6.3 How common is post-treatment control?

One of the challenges of studying viral control following TI is variation in the definitions and terminology used. As the number of reports of potential PTC increase, the need for a consistently applied definition becomes critical. Studies to identify post-treatment controllers have differed in the thresholds used to define an undetectable viral load (VL), the duration of ART prior to interruption, whether or not viral blips are acceptable, and the duration of control [224, 269, 272, 274, 275, 287, 288]. This has parallels with the study of spontaneous viral control, where significant heterogeneity has been identified in both the terminology and clinical parameters used to identify controllers [289], which have been shown to lead to substantial variation in the estimated frequency of elite control [290]. In general, I propose that the term PTC be reserved for the extreme of this type of viral control – that is long-standing, sustained viral suppression (e.g. >5 years) to below the limit of detection of current best assays (e.g. 20 copies/mL). Such a definition would allow for robust mechanistic studies. For those not fulfilling this extreme phenotype, the term "remission" can be used describe shorter periods of control, the duration of which should also be made explicit; this is the terminology that will be used throughout this work. The term remission also has utility as, drawing upon its meaning in the context of malignancy, it reflects the ongoing risk of viral rebound [291].

In the VISCONTI cohort the estimated frequency of sustained PTC was 15% [271, 292]. Other studies of early treated infection have estimated the frequency of individuals who controlled viral replication for >12 months following TI to be lower, ranging from 0 to 9% [269, 270, 272, 274, 275, 287]. Potential explanations for this variation include differences in the timing of ART initiation, the duration of ART prior to TI and the denominator used to calculate the frequency. The frequency of PTC when ART is commenced during PHI has been reported to be higher

than that observed following TI when ART is commenced during chronic infection [223, 288], although there have been few studies that directly compare this. A recent description of PTC following treated chronic infection (for at least 6 months) estimated a frequency of 4% [293], within the range of that observed for PHI.

1.6.4 Post-treatment control as a model for HIV cure

A key question that remains unanswered is whether transient remission is a step towards durable PTC, or merely a delay in viral rebound, reflecting normal inter-individual variation. Many HIV cure studies use delayed time to viral rebound as a gold standard of efficacy [294–298]. This approach assumes that remission is a step towards PTC – and that progressive prolongation of the duration of remission will result in a PTC phenotype. There is, however, currently insufficient evidence that remission and durable PTC are mediated via the same processes.

The study of PTC and the measurement of time to viral rebound following TI present a number of challenges for researchers. These will be further discussed in Chapter 2, which aims to quantify viral remission in treated and untreated PHI in the context of how we evaluate HIV cure trials.

1.7 HIV curative strategies

The persistence of the HIV is ubiquitous and the infection has long been considered incurable. Indeed, the absence of any individuals who can spontaneously clear the virus distinguishes HIV from hepatitis C virus (HCV) - another chronic viral infection for which curative interventions are now widely successful [299, 300]. In 2009, it was announced that Timothy Ray Brown (the Berlin patient) had been cured of HIV following two alloSCTs for acute myeloid leukaemia [278]. The donor had a mutation in the CCR5 gene (CCR5Δ32), making the engrafted T cells resistant to infection with R5 tropic viral strains [278]. Since that time, Timothy Ray Brown has not taken ART and no evidence of residual virus has been found [301]. This unusual case sparked a high level of interest in the prospect of curative interventions

for HIV which could be employed on a wider scale. Whilst transplantation will not be appropriate for all individuals living with HIV, this case suggests some features which may be required for a successful HIV cure. These include prevention of further viral seeding, a substantial reduction of HIV reservoir size and strong anti-reservoir immune responses (which, in the case of the Berlin patient, was evidenced by graft versus host disease [278]). In the decade since, research towards an HIV cure has not resulted in the development of any strategies with therapeutic efficacy. This research has, however, furthered understanding of the challenges in designing a cure for HIV and uncovered significant complexity in the barriers to reservoir eradication.

Parallels have been drawn between efforts to eradicate HIV with those to cure cancer [302] - and several therapeutic approaches initially developed for cancer are being explored in the context of HIV infection. Indeed, these two clinical entities share a number of features, including the presence of low-level residual disease and a limited or dysfunctional immune response. One key difference, however, is that the long-term clinical outcomes for individuals treated with ART is significantly better than for most malignancies. For HIV cure efforts, this means that the level of acceptable toxicity from any intervention is substantially lower than that for cancer therapeutics. Consideration of the safety and feasibility of putative cure interventions is critical as the field moves forward.

1.7.1 Viral remission, rather than eradication, as a model for HIV cure

A number of case studies of TI in individuals with extremely low reservoirs have now been reported [118, 279, 281, 282, 303]. These include individuals with extremely early ART initiation through rapid diagnosis [118], alloSCT [279], acquisition whilst taking PrEP [282] or perinatal infection [281, 303]. Whilst viral rebound in these situations may be delayed, viraemia returns. It is now becoming clear that reduction in HIV reservoir size to very low or undetectable levels is not, in itself, sufficient to induce HIV cure.

This observation reflects our understanding that latently infected cells are found in a number of anatomical and cellular compartments - and that theoretically even a single intact provirus could be a source of recrudescent infection. Any therapeutic approach to eradicate the HIV reservoir would need to be efficacious in all of these sites and cells - a seemingly impossible task. In contrast to a "sterilising" concept of cure, where all virus would be eliminated from the body, models of HIV cure have instead focused on the idea of a "functional" cure. That is, a therapy which could be given to induce a state of ART-free remission - analogous to PTC or elite control. There are two main ways this could be achieved. The first is to reduce the reservoir size to a low enough level that viral rebound is improbable (if not impossible). This is supported by the observation that individuals with smaller HIV reservoir size have prolonged time to viral rebound [220–225]. The second is that an immunologic intervention could augment anti-HIV immune responses such that long-term immunologic control without ART could be achieved. Therapeutic approaches to achieve both of these goals are introduced in the subsequent sections.

1.7.2 Major approaches towards the development of an HIV cure

Attempts to replicate the success of the Berlin patient have studied HIV-infected individuals requiring alloSCT for malignancies. Two further case studies, known as the Boston patients, experienced delayed but eventual viral rebound following alloSCT from CCR5 wild-type donors [279]. Several other cases of individuals who received alloSCT from donors with CCR5Δ32 mutations have shown reductions in reservoir size in some individuals, but also highlighted the high-mortality associated with this intervention [304–308]. The potential for viral rebound with a CXCR4 tropic virus has also been shown [305, 309]. A European consortium has identified a number of individuals who, post alloSCT, have undetectable HIV reservoir size [310]. In the absence of a TI study, it is unknown whether these individuals could be considered "cured". Even if it can induce durable remission in some individuals,

the toxicity of transplantation approaches mean that this will not be a widely utilisable approach for HIV cure.

Gene therapy has also been explored for HIV eradication - via editing of CCR5 or the HIV provirus itself. Several early phase clinical trials are underway using genome editing to disrupt CCR5 in autologous CD4 T cells. Approaches to editing the HIV genome directly are also under investigation with the idea that the provirus, if damaged, could be prevented from rebounding. Both of these gene editing approaches (reviewed in [311]) are limited by difficulties in ensuring delivery of gene editing technology to all target cells, as well as the scalability of these interventions.

A key approach to HIV cure has been termed "kick and kill". The rationale behind this strategy is to induce viral transcription through the use of a latency reversing agent (LRA). This "kick" would make latently infected cells antigenic and thus susceptible to immune mediated clearance (the "kill"). Under protective ART, to prevent further reservoir seeding, this approach could result in reduction in HIV reservoir size [312]. A number of agents with the ability to disrupt latency *in vitro* have been identified including histone deacetylase inhibitors (HDACis), protein kinase C (PKC) agonists and disulfiram [313–315]. Several HDACis, such as vorinostat and romidepsin, have been shown to induce viral transcription *in vivo* but have not resulted in decreases in HIV reservoir size in clinical trials [221, 316–320]. Even with maximal cellular activation (for example, through CD3/CD28 stimulation) not all latent proviruses are able to be reactivated *ex vivo* [202]. The magnitude of latency reversal observed with LRAs, even in combination, is lower again [315, 321], suggesting that more specific targeting of mechanisms that regulate latency may be required to get adequate disruption. Strategies using HDACis to reverse latency are limited not only by the modest viral reactivation observed, but of the negative effects these drugs may exert on CD8 T cell and NK cell functionality [322, 323]. Furthermore, when LRA-treated CD4 T cells were co-cultured *ex vivo* with autologous CD8 T cells, reductions in total HIV DNA were not associated with reductions in replication competent virus [324]. This suggests that cells harbouring replication competent virus may have additional barriers to

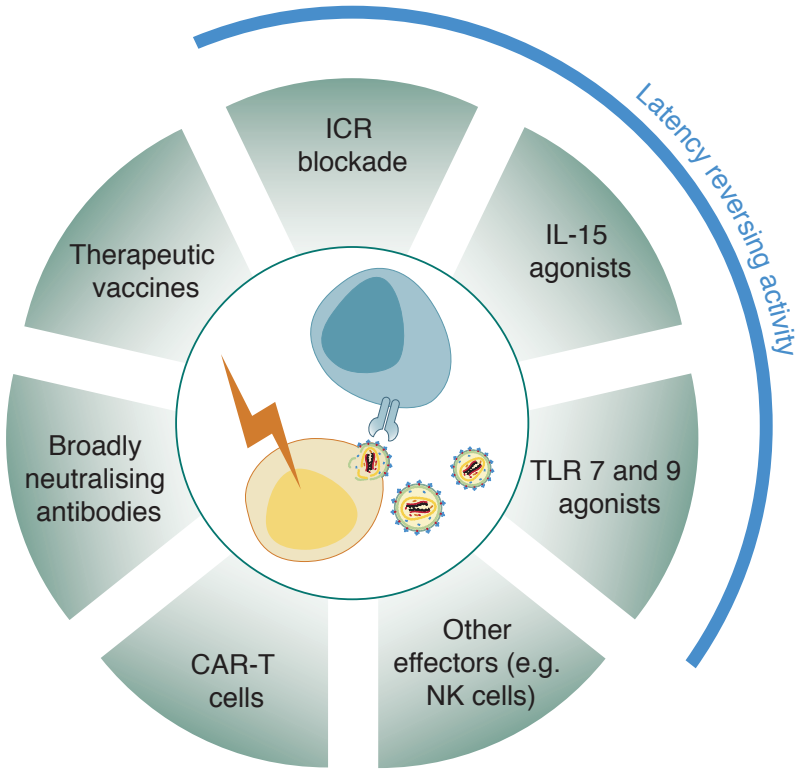


Figure 1.6: Potential strategies to augment anti-HIV immunity as part of HIV curative interventions.

immune-mediated clearance as part of a "kick and kill" strategy [324]. Overall, the success of latency reversal to date has been modest. Either with, or without this "kick", it is becoming increasingly clear that T cell augmentation strategies will be needed to clear residual virus in any HIV curative intervention.

1.7.3 The central role of anti-HIV immunity in developing HIV curative interventions – moving beyond "kick and kill"

Effective anti-HIV immune responses are likely to play a critical role in induction and maintenance of state of remission. Diverse strategies to improve T cell responses have been developed and are being trialled - here, these strategies will be briefly introduced and are summarised in Figure 1.6.

In addition to a role in preventing HIV acquisition, vaccines have been investigated as part of a therapeutic strategy for HIV (reviewed in [213, 325, 326]).

One of the most promising vaccine candidates identified in simian models uses a CMV vectored vaccine contains inserts for the SIV proteins Gag, Rev/Tat/Nef, Env and Pol (RhCMV/SIV). When administered prior to infection, this RhCMV/SIV vaccine did not prevent acquisition of SIV infection, but resulted in striking durable viral control [327] and eventual eradication of the reservoir [328] in a subset of vaccinated animals. This control was linked to effector memory CD8 T cell responses elicited by the vaccine [327]. In an attempt to address if this vaccine would have the same effect once infection was established, animals who had commenced ART shortly after infection were vaccinated and underwent TI; early ART initiation was chosen to ensure that animals had a small reservoir size (similar to the experiments where this vaccine was used prior to acquisition) [184]. In all of these animals viral rebound occurred rapidly and without subsequent control of plasma virus or reservoirs, despite eliciting similar SIV-specific immune responses [184]. These differing results suggest that ideal features of a preventative vaccine may not be the same as those desired in therapeutic vaccination.

In the context of HIV cure, therapeutic vaccines have been developed and trialled along with LRAs as part of a "kick and kill" approach. Three clinical trials combining latency reversal (using an HDACi) with a therapeutic vaccine have now been conducted [297, 329–331]. The REDUC trial[1] showed modest decreases in reservoir size following vaccination and romidepsin treatment, but rapid viral rebound was observed following TI [329]. In contrast, in both other trials (BCN02[2] and RIVER[3]) no reduction in HIV reservoir size was observed; latency disruption measured by low copy viral load assays or CA-usRNA have not yet been reported [297, 331]. Preliminary results from BCN02 suggest that some individuals may have delayed time to viral rebound [297], but without a control group this is difficult to interpret [294]. Overall, whilst all these therapeutic vaccines

[1]Vacc4x with recombinant human granulocyte-macrophage stimulating-factor with the HDACi romidepsin

[2]MVA.HIVconsv in individuals who had been previously given ChAd.HIVconsv and MVA.HIVconsv prime/boost vaccination, with the HDACi romidepsin

[3]ChAdV63.HIVconsv prime and MVA.HIVconsv boost vaccines prime/boost vaccination, with the HDACi vorinostat

have been shown to be immunogenic [297, 330, 331], results of these trials have been disappointing and further work is needed to identify the ideal characteristics of a therapeutic vaccine for HIV cure.

The IL-15 superagonist ALT-803 has a number of desirable features as a therapeutic agent in HIV cure. This molecule has been shown to reverse latency *ex vivo* [332] and improve NK cell responses in HIV-infected humanised mice [333]. In SIV-infected macaques, it was also recently shown to facilitate trafficking of SIV-specific CD8 T cells into B cell follicles [334], a major sanctuary site [253]. A phase one trial of this agent in HIV infection is underway (NCT02191098). Another class of molecules that can potential reverse latency as well as augment immune responses are toll-like receptor (TLR) agonists. Both TLR-7 and TLR-9 agonists have been shown to reverse HIV latency and augment CD8 T cell and/or NK cell responses *ex vivo* and *in vivo* [335–338].

As markers of effector T cell dysfunction and also of HIV reservoir size, ICRs are of high interest in the context of HIV cure. Anti-PD-1 and CTLA-4 antibodies may disrupt HIV latency *in vivo* [261, 262]. Combined with the role of ICR blockade in improving T cell immune responses, it is possible that ICR blockade could provide both the "kick" and "kill" needed for curative interventions. Results from immune checkpoint blockade in simian models have been promising with reports of improved CD8 T cell responses [339, 340], improved viral control [339–341] and reduced immune activation [342] following *in vivo* treatment. Several cases have been reported of individuals infected with HIV who are treated with ICR blocking antibodies as part of treatment for malignancy (discussed in section 1.5.1). As this field moves forward, larger observational cohort and interventional studies are needed to assess the viability of this approach; several such studies are underway in individuals with and without concomitant malignancy (NCT03239899, NCT03367754, NCT03354936, NCT02408861, NCT03304093). Unfortunately, one human trial with an anti-PD-L1 Antibody (BMS-936559) was ended early due to concerns of ocular toxicity observed in non-human primate studies [264]. In this study, improvements in HIV-specific T cell responses were noted in 2 of 6

individuals treated [264]. Further work is needed to evaluate the safety and efficacy of these drugs for HIV immunotherapy.

Chimeric antigen receptor (CAR)-T cells are cytotoxic T cells which have an engineered (antibody-like) receptor to direct these towards a particular antigenic target and induce MHC-independent T cell responses. They have shown significant efficacy in the context of haematological malignancy and HIV-specific CAR-T cells have been developed and are in clinical trials (reviewed in [343, 344]). If efficacious, safety and scalability remain barriers that will need to be overcome with the use of CAR-T cells [344].

T cell trafficking has also been implicated in HIV curative strategies. The integrin α4β7 is expressed on a subset of CD4 T cells and mediates homing into gut mucosa [345]; it also interacts with HIV gp120 and may play a direct role in susceptibility to HIV infection of cells that express it [345]. A study of SIV-infected macaques treated with a monoclonal antibody against α4β7 showed a remarkable reduction in SIV reservoirs, and durable viral control in treated animals following TI [346]. The mechanisms for this control were unclear, and other investigators have been unable to replicate these striking findings [347]. Preliminary results of a single-arm study of the humanised α4β7 antibody vedolizumab (NCT02788175) showed no difference in viral rebound compared with historic controls [348]. Investigation of the relevance of this pathway is ongoing.

Another area of promise is the use of broadly neutralising antibodies (bNAbs). These antibodies are produced by a subset of HIV-infected individuals and have the ability to neutralise a broad range of viruses. With *in vivo* parenteral administration, these bNAbs have been shown to suppress viral replication [349–351] and delay time to viral rebound [295, 296] but only for the duration the antibodies are still circulating. In general, resistance occurs with monotherapy [295, 296, 349–351] and multiple bNAbs will likely be needed. Intriguingly, in one study of SIV macaques early bNAb administration was able to induce a durable state of viral control [352]. The reasons for this are unclear, but it has been hypothesised that the formation of immune complexes could aid the development of appropriate T cell

responses [352]. An alternative possibility is that the lowering of viral replication or shift in the location of this allows for the development of T cell responses in a more favourable milieu. The possibility that bNAb use could help inducing HIV-specific immune responses for longer-term immunologic control means these are of key interest for HIV cure strategies.

Finally, whilst the T cell response is considered to play a key role in immune mediate control of HIV, other immune effectors may also be important in HIV curative approaches. For example, NK cells have been linked to elite controller and PTC phenotypes [353, 354], as well as changes in reservoir size following *in vivo* treatment with panobinostat (an HDACi) [355]; as such, these are another plausible target for immunotherapeutic strategies towards an HIV cure.

1.8 Conclusion

The early establishment of the HIV reservoir, and the inefficacy of HIV-specific T cell responses in clearing this are two major barriers to HIV eradication. HIV cure strategies to date have been limited in their success, but have provided insight into a number of the reasons for this. This thesis aims to examine the impact of ART initiation during PHI on a number of aspects of T cell immunity which are pertinent to HIV cure approaches: how we measure efficacy of these interventions (Chapter 2), the resolution of T cell activation and ICR expression (Chapter 3) and what influences reservoir size itself (Chapters 4 and 5).

2

The impact of antiretroviral therapy initiated during primary HIV infection on viral remission following treatment interruption

Work presented in this chapter has been published in part in the below articles:

Martin GE & Frater J Post-treatment and spontaneous HIV control. *Current Opinions in HIV/AIDS*, **13**(5), pp. 402-407 (2018)

Martin GE, Gossez M, Williams JP *et al*, Post-treatment control or treated controllers? Viral remission in treated and untreated primary HIV infection. *AIDS*, **31**, pp. 477–484 (2017)

Contents

2.1 Context 38
2.2 Aims 39
2.3 Hypothesis 39
2.4 Results 40
2.4.1 Participants and study design 40
2.4.2 Transient control of viraemia (remission) is evident in untreated primary HIV infection 41
2.4.3 Duration of remission in treated and untreated controllers 43
2.4.4 Controllers have more favourable baseline clinical characteristics than non-controllers 46

2.4.5 Spontaneous controllers have lower baseline VL than those who received >12 weeks ART 46
2.4.6 Similar demographics and immunological characteristics in ART-receiving and spontaneous controllers 49
2.4.7 Comparison of the frequency of post-treatment remission and control in the literature 49
2.5 Discussion 50
2.5.1 Spontaneous remission 51
2.5.2 Comparing post-treatment and spontaneous remission . 52
2.5.3 Measuring post-treatment control and remission 53
2.5.4 Limitations of this work 55
2.5.5 Implications for treatment interruption trial design . . . 56
2.6 Conclusion 57

2.1 Context

Interventions aiming to achieve an HIV cure by depletion of the HIV reservoir are entering clinical trials. In the absence of a validated biomarker to prove cure, a key outcome measure in these studies is the time to detection of viral RNA, or "viral rebound" following TI [294–298].

Understanding that viral rebound occurs in a matter of weeks post-TI comes largely from studies of patients who commenced ART during chronic infection [356–358]. That PTC is observed almost exclusively in patients who commenced ART during PHI suggests that viral control in this period may differ from chronic infection. Despite this, the normal viral dynamics during untreated PHI are not well characterised and it is possible that sustained periods of viral suppression post-TI might actually reflect natural history rather than an effect of ART or another intervention. As many cure trials are focused on individuals who commence ART during PHI, an understanding of the normal viral dynamics in treated and untreated PHI will be critical in the evaluation of these interventions.

This chapter sets out to explore VL dynamics within the SPARTAC (Short Pulse Antiretroviral Therapy at HIV Seroconversion) trial, to determine if there are individuals who experience transient viral control during untreated PHI, and if so, how this compares with post-ART remission.

There are no studies that directly compare the frequency and duration of viral remission between treated and untreated patients infected with HIV. With international guidelines now advocating commencement of ART as early as possible (regardless of CD4 T cell count) [15], trials with a "no treatment" arm will not be able to be undertaken in the future. As a randomised control trial of short course ART during PHI, SPARTAC provides a unique opportunity to explore the frequency of viral remission in both treated and untreated PHI. In addition, with frequent VL sampling following TI, the trial allows for characterisation of the shorter periods of viral control that are likely to be observed in cure trials. This is critical for understanding if reports of virological remission following an intervention might be conflated by natural transient delays to detectable viraemia amongst individuals with treated PHI.

2.2 Aims

Specifically, the aims of this chapter are:

- **Aim 1** To quantify viral remission in untreated PHI (spontaneous remission) and following treated PHI (post-treatment remission);
- **Aim 2** To compare demographic and immunological characteristics of individuals with spontaneous and post-treatment remission.

2.3 Hypothesis

During PHI, some untreated individuals experience transient periods of viral remission. When viral remission is measured following interruption of ART initiated during PHI, this is more frequent than remission during untreated PHI.

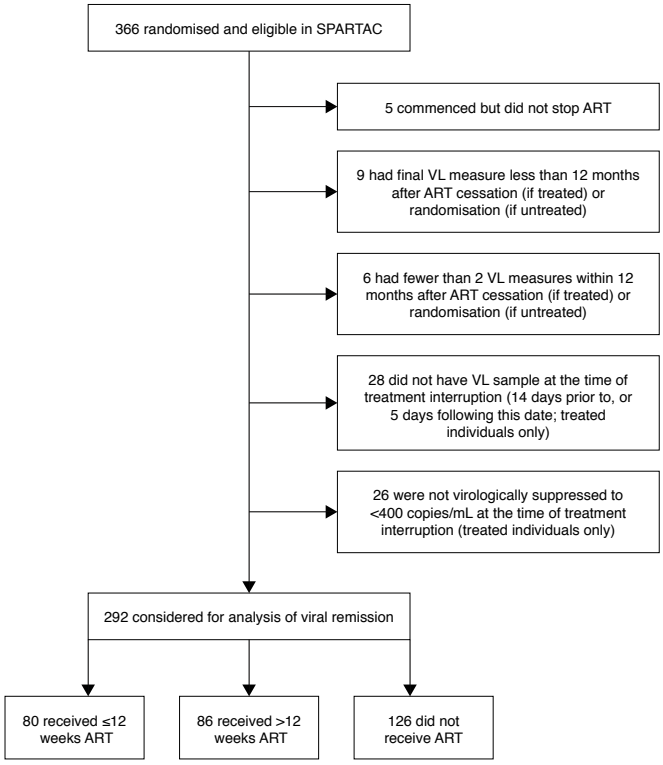


Figure 2.1: Individuals eligible for inclusion in analysis of viral remission in SPARTAC

2.4 Results

2.4.1 Participants and study design

SPARTAC was a multi-centre randomised controlled trial of short-course ART (12 or 48 weeks ART, versus no immediate ART) initiated during PHI. Details of this trial are in section 7.2)[359]. This analysis included participants recruited to the SPARTAC trial who had sufficient VL sampling and, if treated, were virologically suppressed prior to TI. Of 366 participants, 74 were excluded because they did not undergo TI, had insufficient VL sampling to assess for remission or for viral suppression at TI, or because they were not virally suppressed at the time of TI (Figure 2.1). With these exclusions, there were 292 individuals included in this analysis. Time on ART is analysed "as received" rather than according to randomisation arm, and stratified as 0, $\leq$12 or >12 weeks ART. This same 12 week cut-off was used in a previous "as received" analysis of SPARTAC [270].

Within this "at risk" group controllers were identified who experienced a period of remission which was defined for all as VL <400 copies/mL, on two measurements at least 16 weeks apart, with the period of remission starting within one year of randomisation or ART cessation (untreated and treated groups, respectively). This definition allowed for individuals with an initial high viral peak or rebound and subsequent control to be included (discussed further in section 2.5.3). Participants who experienced a viral blip of any magnitude at a single time point were included. Throughout this analysis, VL measurements <400 copies/mL were considered "suppressed" as this was the lower limit of detection for assays conducted at South African and Ugandan trial sites. As such, this was the lowest VL threshold that could be applied across all samples. Time of viral rebound was the first of at least two consecutive measurements >400 copies/mL. For all analyses presented, baseline refers to the date of randomisation. This chapter explored viral control which encompasses both durable PTC and remission. For clarity, the term remission is used to refer to periods of viral control which were less than 2 years.

2.4.2 Transient control of viraemia (remission) is evident in untreated primary HIV infection

Considering these participants, regardless of ART use, 35 of 292 (12.0%) experienced a period of suppressed viraemia (VL <400 copies/mL) of at least 16 weeks while off therapy and are termed "controllers" for this report. Of the 126 participants who did not receive immediate ART, 10 (7.9%) experienced a period of spontaneous viral control within one year of randomisation. Among individuals who received short course ART and underwent treatment interruption, 25 (15.1%) experienced viral remission in the subsequent year. When split by ART treatment duration, this equated to 9/80 (11.3%) who had received ≤12 weeks and 16/86 (18.6%) who had received >12 weeks ART.

To provide a visual illustration of the different VL patterns observed in this study, Figure 2.2 shows the longitudinal viral load measurements in different groups: those with rapid viral rebound (A) and who controlled following ART (B and C),

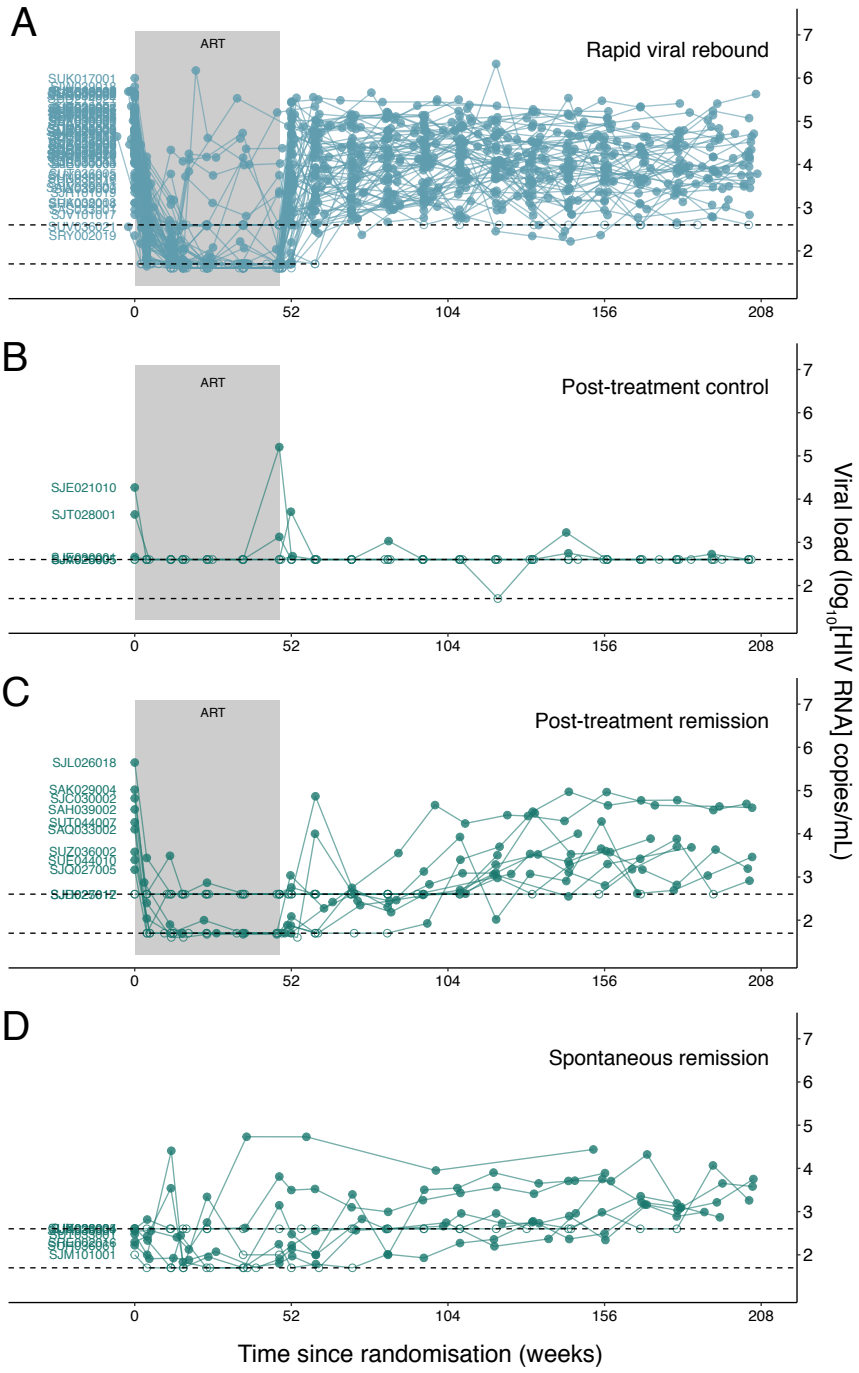


Figure 2.2: Different patterns of viral load dynamics observed in SPARTAC: (A) rapid viral rebound following treatment interruption, (B) post-treatment control, (C) post-treatment remission and (D) spontaneous remission. Panels A-C include all individuals included in this analysis who received >12 weeks ART (A n=70, B n=5, C n=11); Panel D includes all untreated individuals in this analysis who had a period of viral remission with eventual rebound (n=8). Shaded areas represent time on short-course ART. Viral load values following the commencement on long-term ART are not shown. Values lower than the limit of detection are shown as open circles. Dashed lines are shown 50 and 400 copies/mL.

as well as those who controlled spontaneously (D). For clarity, those individuals who received ≤12 weeks of ART are not shown. In this Figure, controllers who had received >12 weeks ART are split into two groups based on the duration of control. Here, post-treatment controllers are defined as those who had not rebounded by the end of follow up (B) with shorter periods of time classed as remission (C).

Post-treatment controllers have been almost exclusively identified among individuals who initiated ART during PHI, suggesting an impact of early ART on long term viral control [269, 271, 272, 275]. Here, there was some evidence of greater frequency of control in individuals who had received >12 weeks ART, when compared across all three groups, although this was not statistically significant (p=0.06; Table 2.1). In the best characterised cohort of PTCs to date (VISCONTI), patients received a median of three years ART prior to TI [271]. Twelve weeks of ART is likely to be too short to induce durable PTC, and it is possible that the participants who received ≤12 weeks ART in this analysis were more similar to untreated controllers than those who had received >12 weeks ART (this was also suggested by the primary outcome analysis of SPARTAC, which was based on clinical progression [359]). Accordingly, all comparisons were performed across the three groups rather than combining the two ART arms. Of note, if the ≤12 week group was excluded from the analysis of control there were significantly more controllers following ART compared with no treatment (18.6% versus 7.9%; p=0.03). In a previous analysis of time to viral rebound in only the treated participants in SPARTAC, longer treatment duration was significantly associated with slower viral rebound within 12 weeks of stopping ART, consistent with these findings [270].

2.4.3 Duration of remission in treated and untreated controllers

Whether the duration of viral control varied between controllers who did or did not receive ART was then explored. There were more participants with over 1 year of remission among those receiving >12 weeks ART compared with ≤12 weeks or no ART (13 (15.1%) versus 3 (3.8%) versus 8 (6.3%), respectively [Table 2.1]). Eight

	Total (n=292)	**≤12 weeks ART** (n=80)	**>12 weeks ART** (n=86)	**No ART** (n=126)	**p-value**
No. of controllers (% total participants)	35 (12.0)	9 (11.3)	16 (18.6)	10 (7.9)	0.06
Duration of short course ART [weeks; median (IQR)]	-	11.9 (11.8-12.0)	47.8 (47.3-47.9)	-	-
Interval between estimated seroconversion and randomisation [days; median (IQR)]	91.0 (61.0-116)	92.0 (64.0-106)	97.5 (58.0-125)	95.5 (76.8-116)	0.64
Viral subtype					0.28
B	13	2	6	5	
C	19	5	10	4	
Other (A1, B/F and D)	3	2	0	1	
Country[a]					0.38
South Africa/Uganda	20	6	10	4	
United Kingdom	11	3	3	5	
Other (Australia/Brazil)	4	0	3	1	
Sex					1
Male	13	3	6	4	
Female	22	6	10	6	
Age [years; median (IQR)]	31.0 (24.0-44.0)	40.0 (25.0-47.5)	27.5 (21.3-46.5)	32 (26.0-35.5)	0.33
HLA alleles[b]					
≥1 protective class I allele	11	1	7	3	0.44
≥1 disease-susceptible class I allele	11	5	5	1	0.04
B*35:01 allele	2	0	2	0	-

	Total (n=292)	**≤12 weeks ART** (n=80)	**>12 weeks ART** (n=86)	**No ART** (n=126)	**p-value**
Duration of remission (weeks)					-
<26	1	0	0	1	
26-52	10	6	3	1	
52-104	8	0	7	1	
>104	16	3	6	7	
No. without viral rebound at end of follow-up (% total participants)	8 (2.7)	1 (1.3)	5 (5.8)	2 (1.6)	-

Table 2.1: Characteristics of controllers identified in SPARTAC. Statistical tests were performed across all three groups. Categorical variables, including number of controllers, were compared using $\chi 2$ test or Fisher-Freeman-Halton exact test as appropriate; continuous variables were compared using Kruskal-Wallis test. IQR stands for interquartile range. Duration of remission was calculated between date of randomisation (untreated arm) or ART cessation (treated arms) and viral rebound.
[a]No controllers were identified from Ireland, Spain or Italy
[b]Analysis performed for participants with subtype B or C virus only. Protective class I alleles were defined as B*27:05, B*57:01 for subtype B and B*57:02, B*57:03, B*81:01, B*58:01 for subtype C. Disease-susceptible class I alleles were defined as B*35:01, B*07:02 for subtype B and B*58:02, B*18:01 for subtype C [73, 360, 361].

controllers (five of whom had received >12 weeks ART) experienced undetectable VL until the end of follow up (median 192 weeks [interquartile range (IQR) 165-202]). There was, however, no statistically significant difference between the duration of remission between the three groups when including the full duration of follow-up (p=0.22; log rank test on Kaplan Meier survival curves). Interestingly, when just considering the controllers, untreated participants were more likely to experience sustained control >104 weeks (7/10) compared with the treated controllers for whom rebound was more evenly distributed over the assessment period.

2.4.4 Controllers have more favourable baseline clinical characteristics than non-controllers

In comparison with the non-controllers (regardless of treatment group), future controllers had more favourable baseline clinical characteristics with higher CD4 T cell counts (median 700 versus 557 cell/µL), lower plasma VL (median 2.70 versus 4.59 $\log_{10}$ copies/mL), higher CD4 to CD8 ratio (median 0.77 versus 0.52) and lower total HIV DNA (mean 3.35 versus 3.85 $\log_{10}$ copies/10^6 CD4 T cells) [Figure 2.3 A-D; Table 2.2]. These findings are consistent with previous studies of viral control during PHI with [269, 362–364] and without [365, 366] treatment.

2.4.5 Spontaneous controllers have lower baseline VL than those who received >12 weeks ART

When focusing on just the controllers, untreated participants had similar baseline CD4 counts, CD4:CD8 ratios and HIV DNA levels to those who controlled following TI, but had significantly lower baseline VL than those who had received >12 weeks ART (median 2.30 versus 3.82 $\log_{10}$ copies/mL respectively [p=0.002; Figure 2.3 B; Table 2.2]). The interval between seroconversion and baseline was similar between treatment groups (Table 2.1) and did not explain this finding. This difference in baseline VL supports an additional impact of ART in inducing viral remission in some individuals who otherwise may not control viral replication, providing evidence for post-treatment control as a distinct phenomenon.

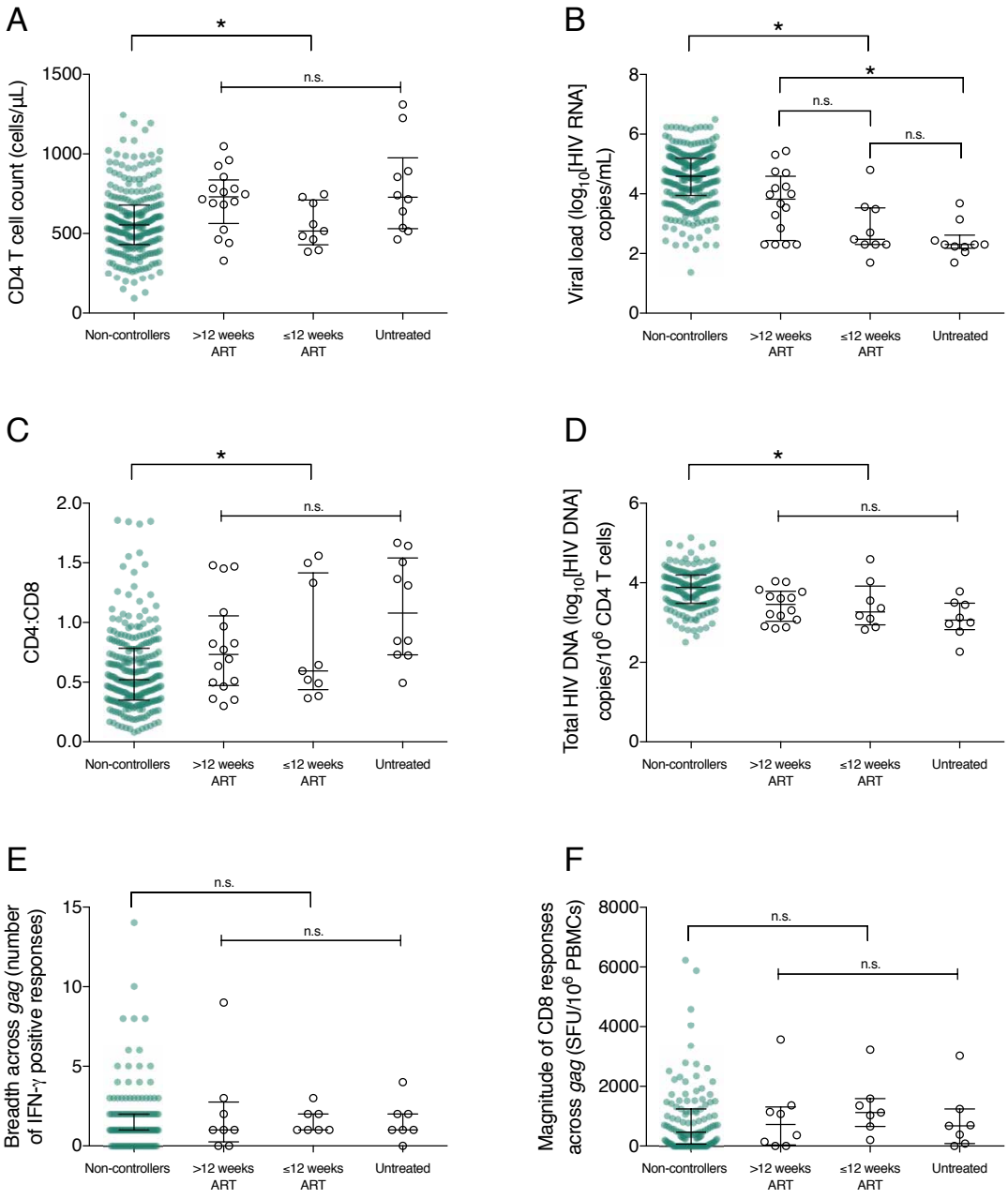


Figure 2.3: Baseline clinical variables of controllers (three groups shown with open circles) and non-controllers (green, shaded circles) identified in SPARTAC. Bars shown indicate the mean (standard deviation) for total HIV DNA (D) and median (interquartile range) for all other parameters (A-C, E, F). These values are shown in Table 2.2. CD4 count (A), viral load (B), CD4 to CD8 ratio (C; all total n=292), as well as breadth (E) and magnitude (F; both total n=145) of CD8 responses across *gag* were compared between non-controllers and combined controller groups using the Mann-Whitney test. Total HIV DNA (D; total n=200) was compared between these two groups using Student's t-test. Comparisons between three controller groups were made using Kruskal-Wallis (A-C, E, F) and ANOVA (D) tests. For viral load this was significantly different (p=0.006) and pairwise comparisons shown (B) were made between groups using the Mann-Whitney test. * indicates $p<0.05$.

	Non-controllers	**Controllers (combined)**	**>12 weeks ART** (controllers)	**≤12 weeks ART** (controllers)	**No ART** (controllers)
CD4 T cell count (cells/μL)	557 [434-681]	700 [515-783]	731 [564-837]	515 [429-710]	728 [531-976]
Viral load ($\log_{10}$[HIV RNA] copies/mL)	4.59 [3.95-5.19]	2.70 [2.30-3.98]	3.82 [2.44-4.59]	2.47 [2.30-3.53]	2.30 [2.18-2.62]
CD4:CD8	0.52 [0.35-0.78]	0.77 [0.50-1.36]	0.73 [0.47-1.06]	0.60 [0.44-1.42]	1.08 [0.73-1.54]
Total HIV DNA ($\log_{10}$[HIV DNA] copies/10^6 CD4 T cells)	3.85 (0.49)	3.35 (0.49)	3.43 (0.42)	3.44 (0.61)	3.11 (0.47)
Breadth of CD8 T cell ELISpot responses across *gag* (number of IFN-γresponses)	1.0 [1.0-2.0]	1.0 [1.0-2.0]	1.0 [0.3-2.8]	1.0 [1.0-2.0]	1.0 [1.0-2.0]
Magnitude of CD8 T cell ELISpot responses across *gag* (SFU/10^6 PBMCs)	466 [60.0-1240]	862 [190-1361]	722 [35.0-1310]	1120 [654-1593]	676 [86.0-1240]

Table 2.2: Baseline immunological and virological characteristics of non-controllers and controllers. Values for Total HIV DNA are shown as mean (standard deviation). For all other parameters the values shown are median [interquartile range]. Comparisons of these groups are shown in Figure 2.3. Abbreviations used: IFN-γ, interferon gamma; SFU, spot-forming units.

2.4.6 Similar demographics and immunological characteristics in ART-receiving and spontaneous controllers

There was no evidence for demographic differences between untreated and treated controllers in terms of sex, viral subtype, country of origin and age (Table 2.1). Because CD8 T cell responses are associated with clinical progression [367] and drive durable spontaneous (or "elite") control, the presence of protective HLA class I alleles amongst controllers identified in this study was assessed. The proportion of controllers with protective or disease-susceptible HLA class I alleles was similar between treatment groups (Table 2.1). Two controllers carried HLA B*35 alleles, which have been observed amongst PTCs in the VISCONTI case series [271, 276]. As a measure of CD8 recognition of HIV, CD8 T cell responses to HIV peptides were measured by interferon gamma (IFN-γ) enzyme linked ImmunoSpot (ELISpot). Responses across HIV *gag* did not differ between treated and untreated controllers and were similar in breadth (Figure 2.3 E) and magnitude (Figure 2.3 F; Table 2.1) to those measured in non-controllers. The percentage of CD4 and CD8 T cells expressing markers of exhaustion (PD-1, Tim-3 and Lag-3) and activation (HLA-DR, CD69, CD25 and CD38) at baseline also did not differ between controllers identified in different treatment groups (Table 2.3).

2.4.7 Comparison of the frequency of post-treatment remission and control in the literature

The frequency of viral control observed in this work was compared with other reports from the literature. Figure 2.4 shows studies that have measured the frequency of PTC (here defined as >2 years; green) and remission (>16 weeks; red) and plots these against the duration of control observed. The findings from this chapter (marked on the plot as Martin 2017 [277]) have been split into these two categories and are highlighted in bold. Overall, it can be observed that the frequencies of both PTC and remission measured here fall in the middle of the ranges reported by others. It is unsurprising that the frequency reported in studies that have measured remission is higher than those that have measured PTC. There are also two notable

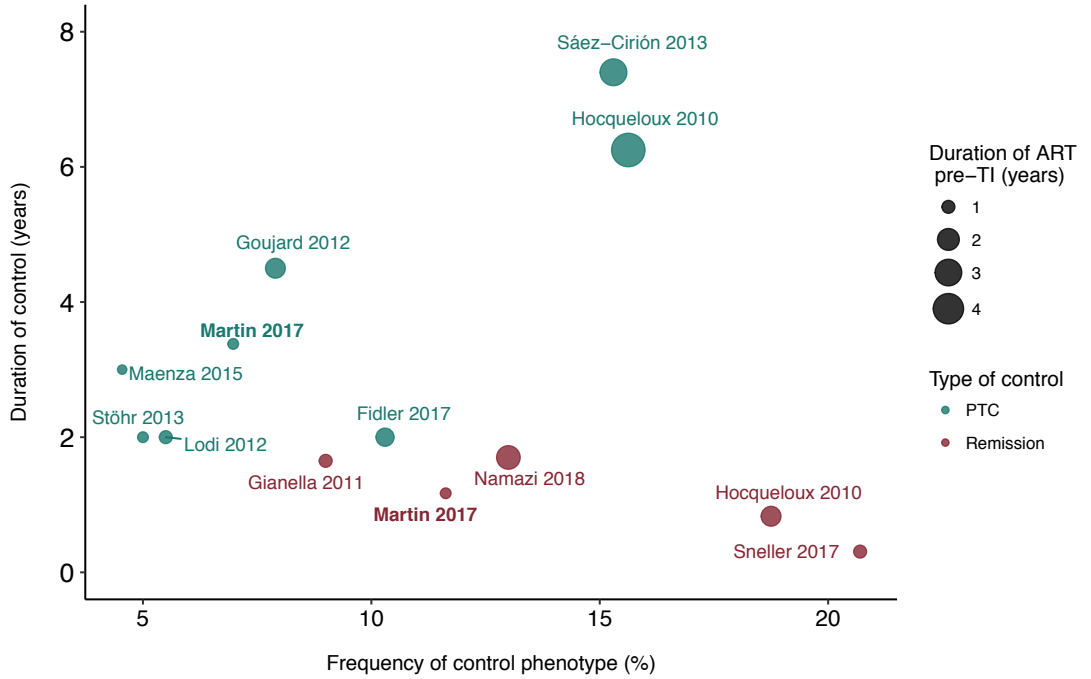


Figure 2.4: Estimates of post-treatment control and remission frequency in the literature. Each data point represents an individual study which has measured the frequency of post-treatment control or remission following TI amongst individuals who commenced ART during PHI. Included are analyses of the following studies: CASCADE [272, 274], ANRS Primo [269], VISCONTI [271, 292], SPARTAC [270, 277], CHAMP [288], ZHPI [209], SeaPIP [275] and NCT01859325 [294]. Those which define post-treatment control (>24 months following TI) are coloured green, those defining remission (>4 months following TI) are shown in red; where a study explored both phenotypes these are listed twice. The duration of control is the time between TI and viral rebound, or the end of follow-up, and is plotted at the median value amongst controllers. The size of the point corresponds to the median duration of ART prior to TI amongst controllers. Where a study did not report either of these values, the minimum value for inclusion in the study is used instead. Martin 2017 [277] refers to the data presented in this chapter and shows only those individuals with >12 weeks ART.

outliers which report a much higher frequency of post-treatment control; these are the studies by Sáez-Cirión 2013 [271] and Hocqueloux 2010 [292], both of which report findings from the VISCONTI cohort.

2.5 Discussion

This analysis has demonstrated long periods of transient viral remission in a substantial proportion of untreated individuals after PHI; if unrecognised, this may conflate data from those who transiently control after ART interruption. It has

		≤12 weeks ART (n=6)	**>12 weeks ART** (n=14)	**No ART** (n=6)	**p-value**
		Immune checkpoint receptors			
CD8	PD-1	32.1 [26.7-40.0]	26.2 [23.3-35.5]	25.7 [25.2-31.7]	0.60
	Tim-3	10.2 [8.0-15.3]	7.2 [4.1-12.4]	6.9 [6.1-8.4]	0.19
	Lag-3	0.90 [0.26-2.1]	0.35 [0.19-1.1]	0.50 [0.20-1.1]	0.71
CD4	PD-1	12.6 [8.7-15.9]	19.4 [12.3-26.2]	15.8 [9.9-22.2]	0.36
	Tim-3	4.8 [3.1-6.0]	3.1 [1.6-7.3]	5.0 [3.7-6.4]	0.80
	Lag-3	0.50 [0.23-0.74]	0.42 [0.15-1.3]	0.49 [0.25-0.68]	0.98
		Activation markers			
CD8	CD38	76.8 [59.5-80.2]	75.2 [67.5-77.0]	58.4 [51.7-61.8]	0.16
	HLA-DR	26.7 [26.7-34.5]	14.6 [9.6-21.5]	14.2 [13.1-17.7]	0.36
	CD69	1.4 [1.1-1.9]	2.1 [1.2-2.6]	1.6 [0.92-2.8]	0.73
	CD25	0.73 [0.46-1.9]	0.62 [0.36-1.1]	0.99 [0.72-1.9]	0.38
CD4	CD38	57.9 [55.6-69.0]	59.8 [52.5-61.8]	56.1 [54.2-56.7]	0.75
	HLA-DR	3.5 [3.0-4.7]	5.1 [2.1-7.2]	3.8 [3.0-4.2]	0.39
	CD69	0.53 [0.31-0.78]	0.53 [0.33-0.82]	0.31 [0.25-0.76]	0.54
	CD25	24.0 [22.1-32.4]	21.7 [16.2-24.6]	24.3 [10.8-31.2]	0.30

Table 2.3: Immune checkpoint receptor and activation marker expression on CD4 and CD8 T cells in controllers, stratified by duration of ART received. For all three groups, these were measured at baseline. Values shown are median [interquartile range] Comparisons were performed across all three groups using Kruskal-Wallis tests.

also confirmed previous reports of beneficial baseline characteristics associated with future virological control, and supports an additional impact of ART during PHI.

2.5.1 Spontaneous remission

Here, periods of spontaneous remission were observed in 7.9% of untreated recent seroconverters. Previous studies which have aimed to identify spontaneous remission in untreated PHI have estimated this at 8.5% [365] and 6.7% [366] (defined as two undetectable VL measurements <500 copies/mL whilst not taking ART). Whilst there are substantial differences in how remission was defined between these studies, these all support the idea that this is not a rare phenomenon. Of note, these two prior studies [365, 366] were performed in observational databases and as such, the

intervals between VL sampling were not consistent and were much longer than in SPARTAC. A key strength of the analysis presented here is the regularity and frequency of VL sampling undertaken post-TI in SPARTAC, which has allowed the dynamics of spontaneous remission to be explored in higher resolution.

Following the results of the START trial, which provided clear evidence of clinical benefit in starting ART irrespective of CD4 count [12], untreated controls cannot be included in future HIV trial protocols. The use of uncontrolled TI studies to measure the success of potentially curative strategies means that modest delays in viral rebound may be attributed to an intervention (including early initiation of ART). The findings presented here highlight that periods of viral suppression occur during the natural history of PHI. Accordingly, consideration of spontaneous remission in PHI will be critical to avoid overestimating the effect size of interventions used in TI studies.

2.5.2 Comparing post-treatment and spontaneous remission

A strength of this analysis is the ability to directly compare viral remission among treated and untreated individuals with PHI in the same well-characterised and frequently sampled randomised study (Figure 2.2 C-D). The identification of spontaneous remission amongst recent seroconverters raises the question of whether early ART is able to induce virologic control, or merely delays this natural history (potentially resulting in an apparent effect of ART). Several studies of ART initiated during PHI have demonstrated the presence of individuals who transiently control viral replication post-TI [269, 272, 273, 362, 363, 368]. None of these previous studies included an untreated arm, thus limiting their ability to evaluate the added impact of ART on the presence of transient viral control. An analysis of the Quest study (in which participants underwent TI following at least 72 weeks of ART initiated during PHI) [368] used data from untreated individuals from a separate PHI cohort (CASCADE) as controls. That analysis showed no significant difference in the frequency of transient viral control between the two studies [369],

although a different VL cut-off (1000 copies/mL) and duration of analysis were used. In this analysis, an increased frequency of remission was observed in individuals who received >12 weeks ART compared with untreated controls, providing direct evidence that early ART may improve virologic control post-TI in some individuals. That early ART can influence future viral remission is further supported by the observation made here that individuals with spontaneous remission have lower baseline VL than those who had remission following >12 weeks ART. Importantly, this analysis is the first to provide evidence of an effect of early ART on post-treatment remission by directly comparing treated and untreated seroconverters.

2.5.3 Measuring post-treatment control and remission

Identifying PTC and viral remission presents a number of challenges. Firstly, some individuals who control viral replication following TI may have controlled spontaneously had treatment not been started, and so it is difficult to distinguish these "treated controllers" from PTCs. This will have increasing relevance in the era of "test and treat", as spontaneous controllers may not be identified prior to ART initiation. In this analysis, there was no distinction between individuals with spontaneous and post-treatment remission on the basis of most clinical and immunological characteristics measured. This supports the idea that some of those who experienced post-treatment remission may have had a period of remission regardless of whether or not they were treated.

A further challenge, also identified here, is that the natural history of infection for some individuals includes a period of transient virological remission. In this analysis, 7.9% of untreated individuals had a period of remission after seroconversion, a frequency not dissimilar to that reported in some studies of ART-induced control (Figure 2.4). Therefore, interventional studies that use time to viral rebound after TI as an outcome measure may need to consider both the impact of ART alone as well as the potential for brief periods of spontaneous control as part of the natural history of disease in some individuals.

It has been reported, but not widely recognised, that some individuals treated during PHI have a high initial viral rebound following TI followed by a period of remission or PTC [269]. To allow for the inclusion of these individuals, periods of remission were permitted to commence any time within 12 months of ART cessation or randomisation. This was observed for a number of individuals in SPARTAC, including some who went on to exhibit durable post-treatment control (Figure 2.2 B). Notably, VL sampling in SPARTAC (with the first measurement 4 weeks following TI) is likely not frequent enough to capture an initial viral rebound for all individuals who exhibited it. This initial viral rebound followed by remission was also recently reported by Sneller *et al.* in individuals who underwent a TI in a randomised trial of a therapeutic vaccine [294]. This dynamic – which mirrors that of untreated primary infection – is of particular interest following a study in which SIV-infected rhesus macaques were treated with a monoclonal antibody against the integrin $\alpha 4\beta 7$, followed by a TI [346]. During TI, animals in the therapy, but not placebo arm, exhibited durable sustained aviraemia but only after a high VL peak [346]. It has since been suggested that TI protocols that restart ART as soon as plasma virus is detected may miss some individuals who, following a high initial VL peak, would subsequently go on to control [288]. The implications of this are discussed below (section 2.5.5).

As introduced earlier (section 1.6.3), estimates of PTC in the literature have varied substantially from 0-15% [269–272, 274, 275, 287, 292]. Here this has been visually represented in Figure 2.4. This overall pattern shown is consistent with the idea that inter-individual variation in time to viral rebound falls on a spectrum - and highlights the importance of clear and consistent definitions in studying these phenomena.

Whilst most studies measuring durable PTC estimate a frequency of between 0-10%, Figure 2.4 demonstrates that the estimates of this phenotype from the VISCONTI cohort are substantially higher. Of note, individuals in this cohort had a relatively longer period of viral suppression prior to TI [269–272, 275, 287] which is a potential explanation for this. Additionally, in both these studies, PTCs

were identified first and the denominator used to estimate the frequency of this phenotype was calculated retrospectively in observational databases. It is also possible that this method for calculating the denominator has introduced bias which could result in an overestimation of the frequency of PTC.

This chapter is not the first analysis to study viral rebound in SPARTAC. Work by Stöhr *et al.* [270] (shown in Figure 2.4) also looked at time to viral rebound in this trial. The analysis presented here has two key differences: the inclusion of individuals from the untreated arm, and the acceptability of viral rebound prior to the beginning of the control period. These differences were chosen specifically to study remission in the context of interpreting TI studies.

2.5.4 Limitations of this work

One of the uncertainties of this analysis was the relevance of the ≤12 week group. It is difficult to know how to interpret these participants, as phenotypically they may be closer to untreated participants than those who received >12 weeks ART. However, as this remains unclear they have been presented as a discrete group rather than being combined with one of the other arms, or excluded completely. If anything, the inclusion of this additional group represents a conservative approach to the analysis and suggests that the significant findings regarding clinical baseline characteristics are robust.

This work also includes SPARTAC participants from a number of different recruitment sites. There are demographic differences between those recruited in different countries; individuals from South Africa and Uganda were more likely than those from other sites to be female, and to be infected with subtype C viruses (Gossez M, Martin GE *et al.* (submitted)). Both of these factors have been associated with favourable disease outcomes [370] (reviewed in [371, 372]) and could conceivably impact on the frequency of viral remission - although the size of our study limits the ability to formally test this. Importantly, there was no significant difference in the frequency of controllers identified by country (Table 2.1). Further suggesting the robustness of these findings, if the analysis is repeated

when excluding individuals from South Africa and Uganda the major findings of the analysis are unchanged (data not shown).

2.5.5 Implications for treatment interruption trial design

This analysis was conducted with the interpretation of TI studies in mind, and has several implications for the measurement of viral remission in these studies.

The finding that some individuals who experience viral remission have a high viral rebound first has led to discussion in the field about whether ART in TI studies should be resumed immediately following detectable viraemia, or what an acceptable period of viraemia off ART might be [288, 294, 346]. Any TI study that allows individuals to remain off ART despite viral rebound must first consider patient safety. In making this evaluation, there is little evidence on the duration of viraemia after TI that might be considered safe, although it could be hypothesised that any period of durable viral replication may be harmful. Attempting to address these concerns, a recent analysis of ten individuals undergoing TI as part of a VRC01 (a broadly neutralising antibody) clinical trial explored the impact of this TI on virological and immunological parameters [373]. Following resumption of ART, the overall size and composition of the HIV reservoir returned to pre-TI levels, and increases in T cell activation were similarly transient [373]. Several studies have similarly shown no difference in levels of total HIV DNA [118, 374, 375], integrated HIV DNA [118, 376] or inducible viral transcripts or virions [118, 374]. Of note, in most of these studies ART was resumed if VL rebounded to >1000 copies/mL on one or two measurements [118, 373, 374]. It remains to be seen if such findings would similarly apply if less stringent criteria for re-initiation of ART were used.

The analysis presented here highlights the importance of appropriately matched control cohorts to avoid overestimating the effect size of an intervention (here being early ART). A challenge for TI studies is the limited applicability of historical control cohorts. Modern ART, with more potent drugs (particularly integrase inhibitors) will plausibly be associated with better tissue penetration, lower reservoirs and/or inflammation-associated immunological damage – potentially impacting rates of

remission. There is little evidence of the impact of integrase inhibitor use on reservoir size, although one recent case series that measured HIV DNA longitudinally in six individuals commencing tenofovir/emtricitabine/elvitegravir/cobicistat during PHI showed a rapid decay in this parameter, consistent with the rapid declines in plasma viraemia observed with integrase inhibitor use [377]. Contemporary cohorts may also differ from historical cohorts in terms of viral rebound dynamics following TI. Directly demonstrating the importance of this, Sneller *et al.* compared remission in the placebo arm of their vaccine study to viral remission rates reported in a recent romidepsin/vaccine clinical trial which had interpreted their findings in the context of historical control groups [294, 297]. They observed similar rates of remission between the two groups, even though when compared to historical controls, remission was more common following romidepsin/vaccine administration [294]. The inclusion of matched control groups is a key consideration studies of viral remission following TI.

2.6 Conclusion

This work aimed to quantify spontaneous and post-treatment remission in individuals identified during PHI, and to compare the characteristics of these two groups. In doing this, it has demonstrated that transient viral remission is not a rare phenomenon amongst individuals with PHI, and occurred in 12% of recent seroconverters in SPARTAC. There is evidence that early ART increases the frequency of this in some individuals, although remission was also observed in individuals with untreated PHI - both of these observations support my hypothesis. Whilst evidence exists that PTC and spontaneous control are mechanistically distinct here similar clinical and immunologic characteristics in individuals experiencing post-treatment and spontaneous viral remission were observed. It is likely that both duration and mechanisms of viral control following TI are spectra, and clear and consistent definitions are needed in order to better characterise these.

3

Characterisation of activation and T cell immune checkpoint receptor expression during treated primary HIV infection

An analysis of some of the data presented in this work has been published in:

> Hoffmann M*, Pantazis N*, Martin GE*, *et al*, Exhaustion of Activated CD8 T cells Predicts Disease Progression in Primary HIV-1 Infection. *PLoS Pathogens*, **2**(7), e1005661 (2016).

Contents

3.1 Context 60
3.2 Aims 61
3.3 Hypothesis 62
3.4 Results 62
3.4.1 Clinical characteristics of the HEATHER cohort 62
3.4.2 Immunologic changes during primary HIV infection . . 65
3.4.3 Biomarkers of T cell exhaustion 72
3.4.4 Incomplete resolution of immune parameters following ART initiated during primary HIV infection 78
3.4.5 Immunologic changes during primary HIV infection are linked to markers of clinical progression 86
3.5 Discussion 89
3.5.1 T cell differentiation 90
3.5.2 T cell activation and Tim-3 expression 93
3.5.3 ICR expression and co-expression 96
3.5.4 Partial but incomplete restoration of T cell parameters with early initiation of ART 98

3.5.5 CD39 as a biomarker of T cell exhaustion 98
3.5.6 Soluble immune checkpoint receptors 100
3.5.7 Strengths and limitations of this work 103
3.6 Conclusion 103
3.6.1 Next steps 104

3.1 Context

In the development of HIV cure strategies, individuals who commence therapy during PHI are of particular interest because a smaller HIV reservoir size [36, 116, 117, 206–212] may make targeting this pool of cells a more achievable goal. Following therapeutic success in the treatment of several malignancies, the use of immune checkpoint blockade is being investigated as part of future treatment strategies for HIV [130, 213, 302]. ICRs are perturbed during primary and chronic infection, where they are associated with altered T cell effector function (section 1.4.2). During PHI, the expression of ICRs has been linked to subsequent CD4 T cell decline [134], and time to viral rebound following treatment interruption [255] - suggesting that these markers are clinically relevant during the early stages of infection. Interestingly, there is evidence that the expression of ICRs differs between primary and chronic infection. PD-1 and TIGIT expression, as well as ICR co-expression, have been reported to increase as the infection progresses from primary to chronic stages [135, 136, 139, 146]. In one study, the proliferative defects associated with PD-1 expression were only observed in chronic infection, but not PHI [140], suggesting a temporally distinct role for this marker. Few studies have directly compared the resolution of perturbations in ICR expression between ART initiation in primary and chronic infection, but those that have suggest similar levels of reduction of ICR expression regardless of the timing of therapy [115, 135, 139]. Further work is needed to determine whether elevated ICR expression is maintained following suppressive ART initiated during PHI. Understanding this will be critical for designing appropriately timed and targeted therapeutic interventions involving immune checkpoint blockade.

It is now recognised that early initiation of ART (not guided by CD4 count) is associated with improved HIV disease outcomes [12, 108–110]. Additionally, some immunological parameters improve when ART is initiated in PHI compared with later during chronic infection [98, 108, 112–114, 116, 378]. Interestingly, both soluble and cellular measures of immune activation may not normalise despite early ART initiation [116, 212, 379, 380]. With chronic immune activation a major driver of HIV-related morbidity, even during successful ART [9], there is significant interest in whether early initiation of therapy can normalise this and other immunological parameters.

Here, a large analysis was performed of immune parameters during primary HIV infection, both prior to and following ART - measuring memory differentiation, transcription factors, ICR expression/co-expression and T cell activation. Immune checkpoint receptor expression is complex - with increasing recognition of heterogeneity within exhausted populations [170–172], and close links to activation and memory development (section 1.4.2). By studying these parameters on different memory subsets, and co-expression of multiple markers, the immunological changes observed during PHI and following ART can be clearly represented. To do this, individuals were studied from the HIV Reservoir Targeting with Early Antiretroviral Therapy (HEATHER) cohort, a prospective observational cohort of treated PHI.

3.2 Aims

Specifically, the aims of this chapter are:

- **Aim 1** To characterise T cell activation, immune checkpoint receptor expression and memory composition during primary HIV infection;
- **Aim 2** To establish if these aspects of T cell immunity have normalised relative to healthy controls following a year of ART initiated during primary HIV infection.

3.3 Hypothesis

Immunological perturbations observed during primary HIV infection are not fully resolved following one year of ART initiated at this time.

3.4 Results

3.4.1 Clinical characteristics of the HEATHER cohort

HEATHER is a longitudinally studied observational cohort of more than 300 individuals who commenced ART during PHI. Details of this study are in section 7.2.2. This chapter and Chapter 4 will focus on a subset of 66 individuals enrolled in the HEATHER study whose demographics are reflective of the entire HEATHER cohort. The clinical and demographic details of these individuals are listed in Table 3.1. Individuals in this study were all male with a median age of 34 (IQR 28 - 41) years at the time of ART start. For comparison, 10 healthy controls are included in this work (100% male; median age 35 [IQR 31 - 43] years). HIV-infected individuals commenced ART a median of 29 (IQR 14 - 45) days following a confirmed HIV diagnosis, equating to a median of 52 (IQR 34 - 98) days following estimated seroconversion.

Individuals in this cohort had a high median baseline VL (5.4 $\log_{10}$ copies/mL; IQR 4.4 - 6.4), with the decrease following ART initiation shown in Figure 3.1 A. 63 (95%) of these individuals were virologically suppressed to <50 copies/mL by one year following ART initiation. The dynamics of CD4 and CD8 count, as well as CD4 to CD8 ratio following ART initiation are shown in Figure 3.1 B-D.

A number of different methods for diagnosing PHI, as listed in Table 3.1, were used in this study. Where an individual met multiple of these definitions, they were assigned the method with the highest accuracy in dating recent infection (Table 7.1 and Figure 3.2 show the order or priority used). 26 individuals (39%) in this study were antigen positive without detectable antibodies, meaning they were diagnosed during Fiebig stages I or II.

Sex	
male	66 (100%)
Age (years; median [IQR])	34 [28 - 41]
Time between date of confirmed HIV+ test and ART initiation (days; median [IQR])	29 [14 - 45]
Time between estimated date of seroconversion and ART initiation (days; median [IQR])	52 [34 - 98]
Time between ART initiation and first VL <50 copies/mL (days; median [IQR])[1]	133 [87 - 238]
Baseline HIV RNA (log_{10} copies/mL; median [IQR])	5.4 [4.4 - 6.4]
Baseline CD4 T cell count (cells/µL; median [IQR])[2]	530 [406 - 652]
Baseline CD8 T cell count (cells/µL; median [IQR])[2]	1028 [825 - 1334]
Baseline CD4 to CD8 ratio (median [IQR])[2]	0.52 [0.36 - 0.79]
Method for diagnosing primary HIV infection	
antigen positive (p24 or PCR) but antibody negative	26 (39%)
rising antibody titre	1 (2%)
negative test with 6 months of positive test	31 (47%)
recent incidence testing algorithm	8 (12%)
Mode of acquisition	
MSM	59 (89%)
MSW	1 (2%)
unknown/unrecorded	6 (9%)
Clade	
B	35 (53%)
C	1 (2%)
CRF02_AG	3 (5%)
CRF02_AG/B	3 (5%)
other recombinant form	10 (15%)
unknown/unrecorded	14 (21%)
Initial ART regimen	
unknown/unrecorded	3 (5%)
Backbone	
tenofovir containing	58 (88%)
abacavir containing	5 (8%)
Additional agent(s)	
protease inhibitor	38 (58%)
NNRTI	11 (17%)
integrase inhibitor	13 (20%)
protease inhibitor & integrase inhibitor	1 (2%)

Table 3.1: Baseline clinical parameters for the subset of individuals in the HEATHER cohort included in this work. Abbreviations: CRF, circulating recombinant form; IQR, interquartile range; MSM, men who have sex with men; MSW men who have sex with women; NNRTI, non-nucleoside reverse-transcriptase inhibitor.
[1] 63 of 66 individuals were virologically suppressed to <50 copies/mL by 1 year
[2] Data available for 65 out of 66 individuals

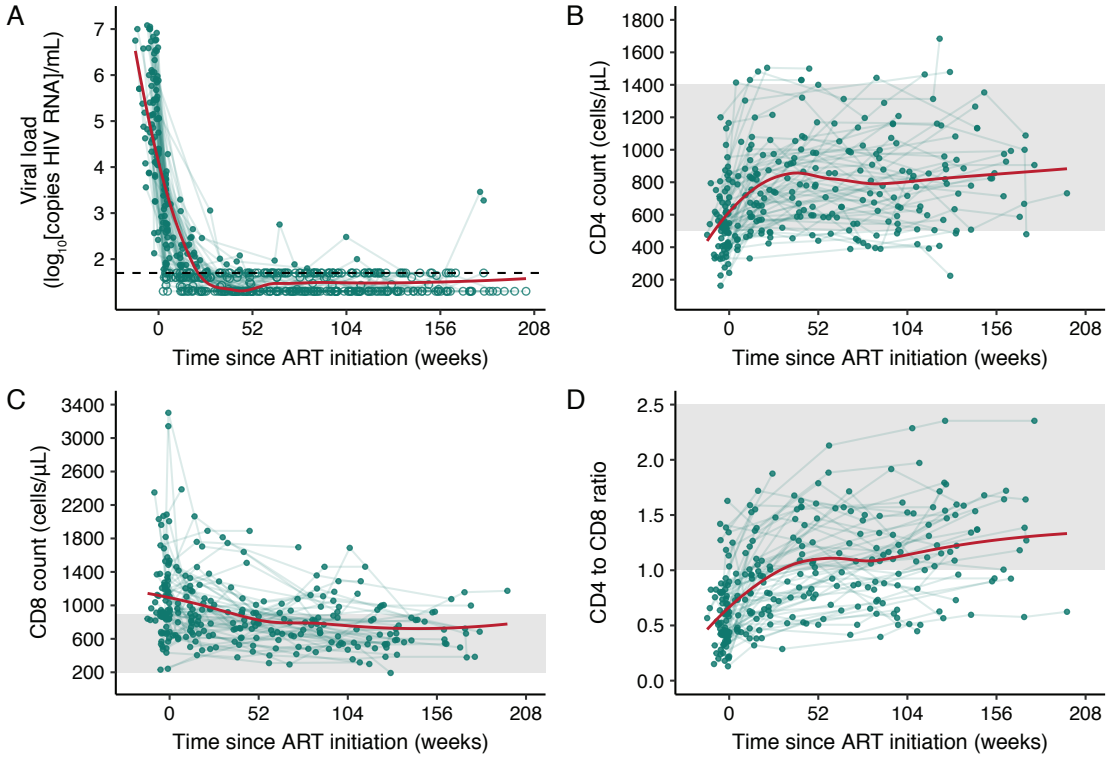


Figure 3.1: Changes in immunological and virological parameters following ART initiation in the HEATHER cohort. This figure shows the (A) viral load (B) CD4 count (C) CD8 count and (D) CD4 to CD8 ratio for these individuals in the 4 years following ART initiation. A trend line (shown in red) has been fitted using local polynomial regression fitting (LOESS) smoothing with an α value of 0.75. In (A) exact values are shown as closed circles, and those below the limit of detection are shown as open circles. The black dashed line indicates 50 copies/mL. In (B-D) the shaded region shows the normal range for these parameters. This figure includes a subset of 66 individuals who are the focus of this chapter; one individual has no baseline CD4 or CD8 count data available and only subsequent measures are shown in panels B-D.

There was a relationship between the baseline VL and the method used to diagnose PHI. Figure 3.2 A plots the baseline VL against the time since estimated seroconversion that this was measured. Individual points have been coloured based on the method used for diagnosing PHI and Figure 3.2 B shows the baseline VL for each of these groups. Here you can observe that baseline VL was higher for individuals for whom this was measured close to estimated seroconversion (r_s=-0.60, p<0.0001; Figure 3.2 A). This data has been superimposed over known VL dynamics during untreated PHI which suggests that when baseline VL has been measured close to seroconversion this may be more likely to coincide with peak VL, whereas

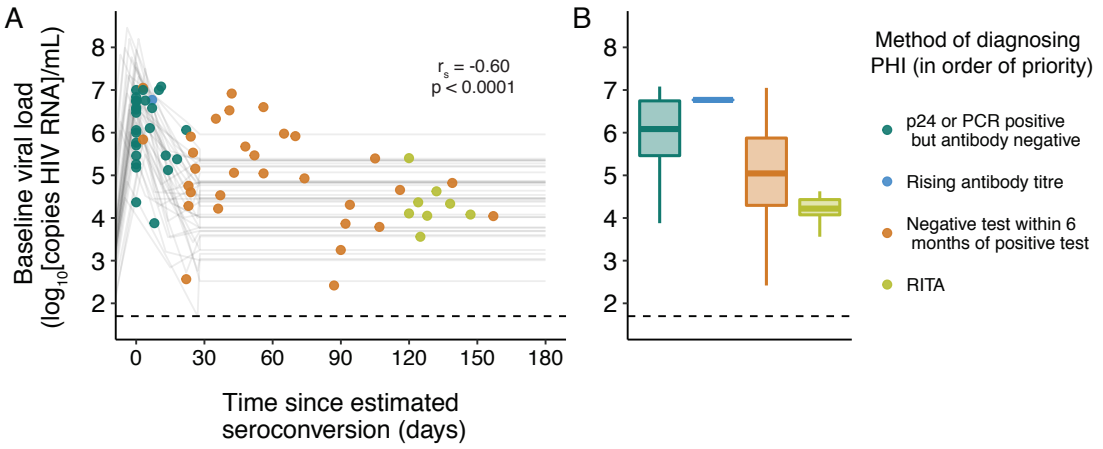


Figure 3.2: Relationship between baseline VL and method of diagnosing PHI for individuals in HEATHER. (A) Plots the baseline VL relative to the number of days this was measured after estimated seroconversion; individuals (n=66) are represented by closed circles and coloured by the method used to diagnose PHI. The relationship was assessed using a Spearman's correlation. Data are superimposed over published VL summary data from individuals in a prospective acute infection cohort (RV 217; n=37) [54] and are represented as grey lines showing peak, nadir and set point VL. This is to show the HEATHER baseline VL measurements relative to known VL dynamics in acute HIV infection. These data were plotted so that the mean day of first enzyme immunoassay positivity in the RV 217 cohort is plotted at 0 on the x-axis. (B) shows these same data as histograms stratified by method of diagnosing PHI. If individuals met multiple diagnostic criteria, they are plotted as the criterion with the most reliability in estimating date of seroconversion; these are shown in the legend in the order of priority used.

when it has been measured later this may represent the set point.

3.4.2 Immunologic changes during primary HIV infection

3.4.2.1 T cell memory expansion and CD8 T cell activation during primary HIV infection

During PHI, there are marked changes in the T cell pool including an expansion in the absolute CD8 count and decrease in CD4 count to outside of the normal range (both evident in Figure 3.1 B-C). Characterisation of the composition of CD4 and CD8 T cell pools at this time was performed. The division of CD8 T cells into naïve, CM, EM and terminally differentiated (T_{EMRA}) subsets was performed based on the expression of CD45RA and CCR7 as shown in Figure 3.3 A (the gating strategy to define CD4 and CD8 T cells is shown in Figure B.1). For CD4 T cells, shown in Figure 3.3 B, CD27 was used to additionally define transitional memory (TM)

cells. During PHI, there was an change in both CD8 and CD4 T cells towards more differentiated memory subsets. Compared with healthy controls (shown in green), individuals during PHI (shown in red) exhibited a decrease in naïve and CM CD8 T cells, and a marked expansion of EM cells (Figure 3.3 C). Similarly, in the CD4 T cell compartment there was an expansion of EM and T_{EMRA} cells (Figure 3.3 D), with a reciprocal decrease in naïve and CM cells that did not reach statistical significance.

Accompanying this was a dramatic increase in CD8 T cell activation (measured here by CD38 expression). Figure 3.3 E shows the expression of CD38 on CD8 T cells in healthy individuals and during PHI (left panel) and a representative plot from one individual in each group (right panel). In contrast, on CD4 T cells (Figure 3.3 F) there was no difference in CD38 expression between these two groups.

3.4.2.2 Increased T cell expression of immune checkpoint receptors during primary HIV infection

Figure 3.4 shows the expression of four ICRs (PD-1, Tim-3, TIGIT and CD39) on different CD8 and CD4 memory subsets during PHI. Representative gating of these ICRs is shown in Figure 3.4 I. There were marked differences in the expression of these four ICRs between memory subsets. On both CD4 and CD8 T cells, the expression of all these markers was lowest on naïve cells. For CD8 T cells, the highest expression of all four ICRs was observed on EM cells (panels A, C, E and G). This contrasts with CD4 T cells where different ICRs had distinct patterns of expression. For PD-1 (panel B), the pattern of expression on CD4 T cells resembled that of CD8 T cells, with the highest expression of TM and EM subsets. For both Tim-3 and TIGIT (panels D and F), expression on EM CD4 T cells was lower than that of TM cells and in the case of TIGIT, markedly decreased compared with T_{EMRA} cells. CD39 expression was markedly elevated on TM CD4 T cells compared with all other memory subsets (panel H). Similar patterns of differential ICR expression between memory subsets were also observed following 1 year of ART and in healthy controls (data not shown).

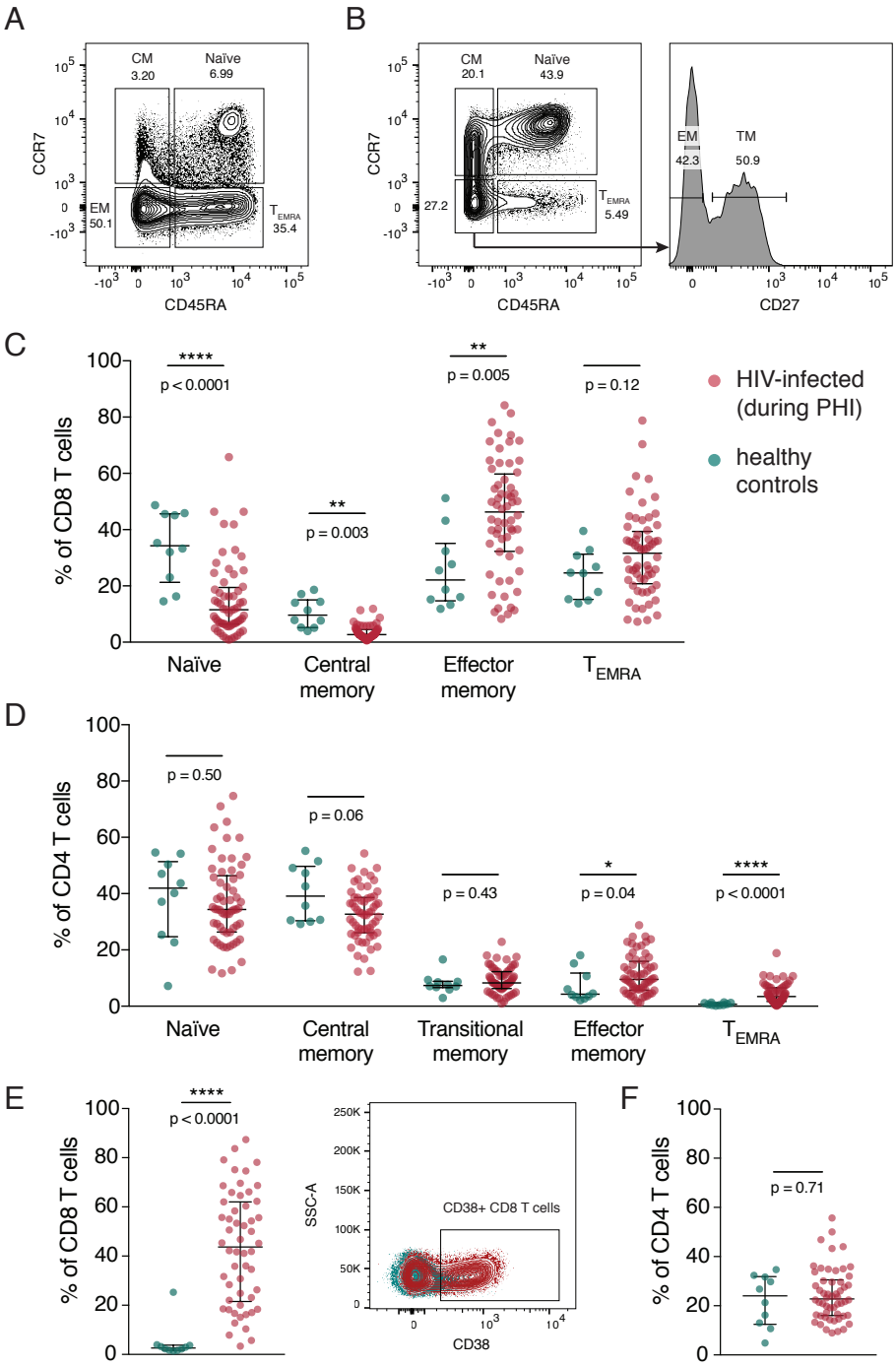


Figure 3.3: T cell memory expansion and activation during PHI. (A) Representative gating of CD8 T cell memory subsets. (B) Representative gating of CD4 T cell memory subsets. The percentage of T cells comprising each memory subset is shown in (C; CD8 T cells) and (D; CD4 T cells) for healthy individuals (n=10; green) and HIV-infected individuals during PHI (n=60; red). (E) Expression of CD38 on CD8 T cells (n=54 PHI; n=10 healthy) with a representative plot overlaying one donor from each group. (F) Expression of CD38 on CD4 T cells (n=54 PHI; n=10 healthy). Groups were compared using a Mann-Whitney test. Bars indicate median and interquartile range. * indicates $p<0.05$; ** indicates $p<0.01$; **** indicates $p<0.0001$.

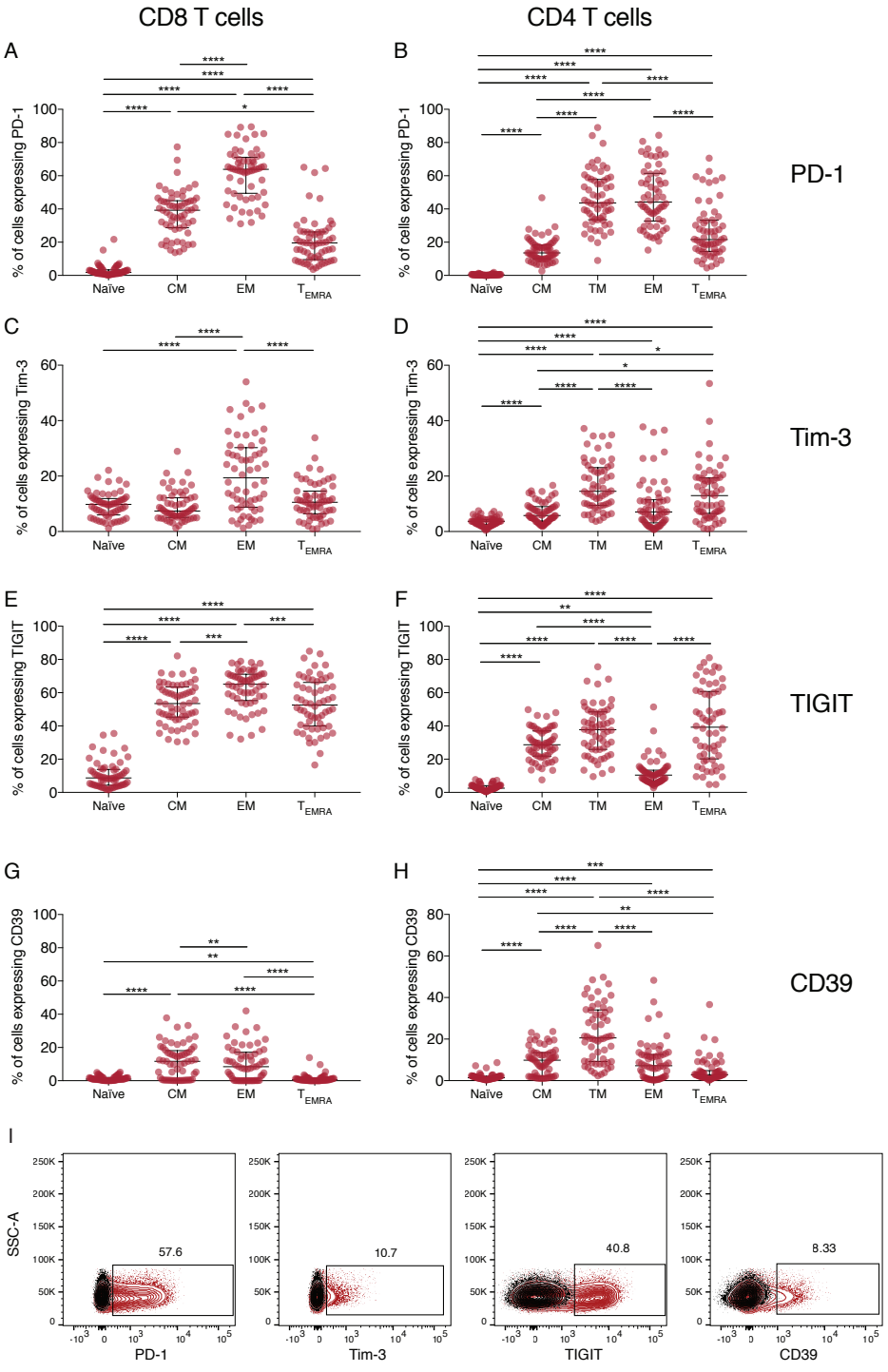


Figure 3.4: ICR expression on CD8 T cell memory subsets during PHI. The expression of PD-1 (A-B), Tim-3 (C-D), TIGIT (E-F) and CD39 (G-H) is shown. Panels A, C, E and G show ICR expression on CD8 T cells and panels B, D, F, H show the same on CD4 T cells. Groups were compared using a Friedman test (overall $p<0.05$ for all cases), with subsequent pairwise comparison with Dunn's test corrected for multiple comparisons. Representative gating of ICRs is shown in panel I. These plots are gated on CD8 EM cells and show staining from one individual during PHI (red) overlaid over gating control (black). Bars indicate median and interquartile range. * indicates $p<0.05$; ** indicates $p<0.01$; *** indicates $p<0.01$; **** indicates $p<0.001$.

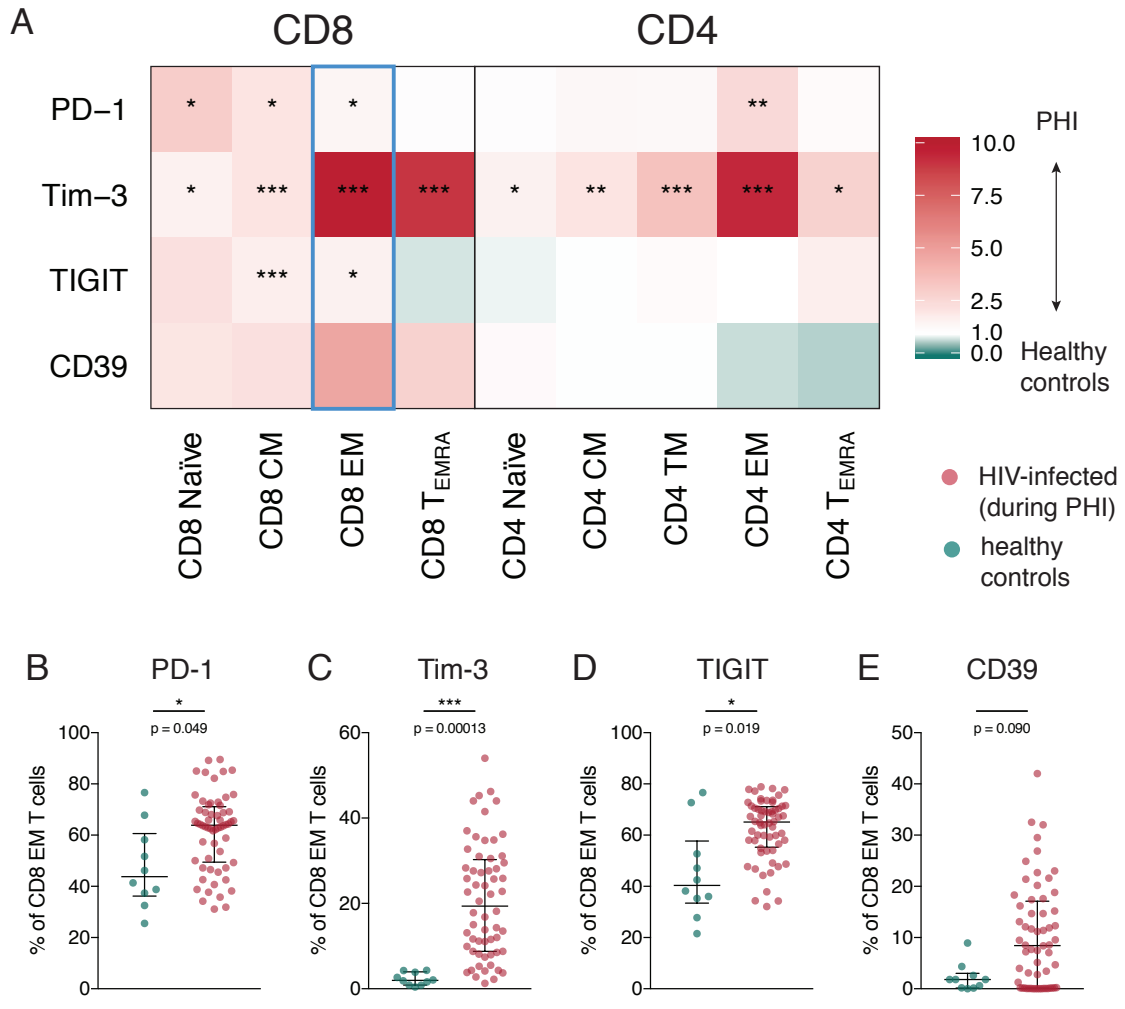


Figure 3.5: Increases in ICR expression during PHI. Comparisons of ICR expression between healthy controls (n=10) and individuals during PHI (n=60) are summarised in (A). Blocks, each corresponding to an ICR measured on a CD4 or CD8 T cell subset, are shaded according to the fold change in PHI relative to healthy controls. Groups were compared using Mann-Whitney tests and adjustment of p-values for multiple comparisons was performed across all comparisons presented here to control the false discovery rate. (B-E) show the data for CD8 EM cells, as indicated by the blue box in (A). Asterisks and listed p-values correspond to the adjusted p-value. Bars indicate median and interquartile range. * indicates $p<0.05$; ** indicates $p<0.01$; *** indicates $p<0.001$; **** indicates $p<0.0001$.

Elevated ICR expression has been previously reported during PHI and chronic infection where it reflects T cell exhaustion (section 1.4.2). Given that more differentiated CD4 and CD8 T cells were expanded during PHI, and that ICRs were expressed at higher levels on these differentiated subsets, it is possible that any changes in T cell ICR expression with HIV infection (or treatment) could actually reflect shifts in the memory distribution. For this reason, further analyses will consider the expression of these ICRs separately on each memory subset.

Figure 3.5 shows that the expression of ICRs was increased on memory CD4 and CD8 T cells during PHI. For each marker, the expression on each memory subset amongst individuals with PHI was compared with healthy controls. Figure 3.5 A shows the summary of these comparisons, with each box shaded to reflect the median fold change in the PHI group compared with the healthy controls, and asterisks to indicate the significance level of this difference after correction for multiple comparisons (the full results of each of these tests are listed in Table B.1). Here it can be observed that the ICR with the highest fold increase during PHI is Tim-3, which was increased on all memory subsets. PD-1 and TIGIT were also increased during PHI on CM and EM CD8 T cell subsets, and in the case of PD-1 also on EM CD4 T cells. Figure 3.5 B-E show the individual comparisons between healthy controls and individuals with PHI for each of these ICRs on CD8 EM cells (marked with a blue box in panel A). Whilst CD39 had a moderate fold increase on CD8 EM cells this did not reach statistical significance, due to the large number of individuals expression negligible amounts of CD39. This observation will be expanded upon in section 3.4.3.1.

This phenotyping was performed on bulk T cells and, whilst it was not possible to characterise the HIV-specific T cell responses for all of these individuals, tetramer staining from a subgroup of individuals during PHI provides insight into the dynamics of HIV-specific CD8 T cells during PHI. In Figure 3.6 the memory phenotype and PD-1 expression of HIV-specific CD8 T cell populations is shown for 9 individuals during PHI, and compared with tetramer specific cells to other viral infections (EBV and influenza). During PHI, almost all HIV-specific CD8 T cells

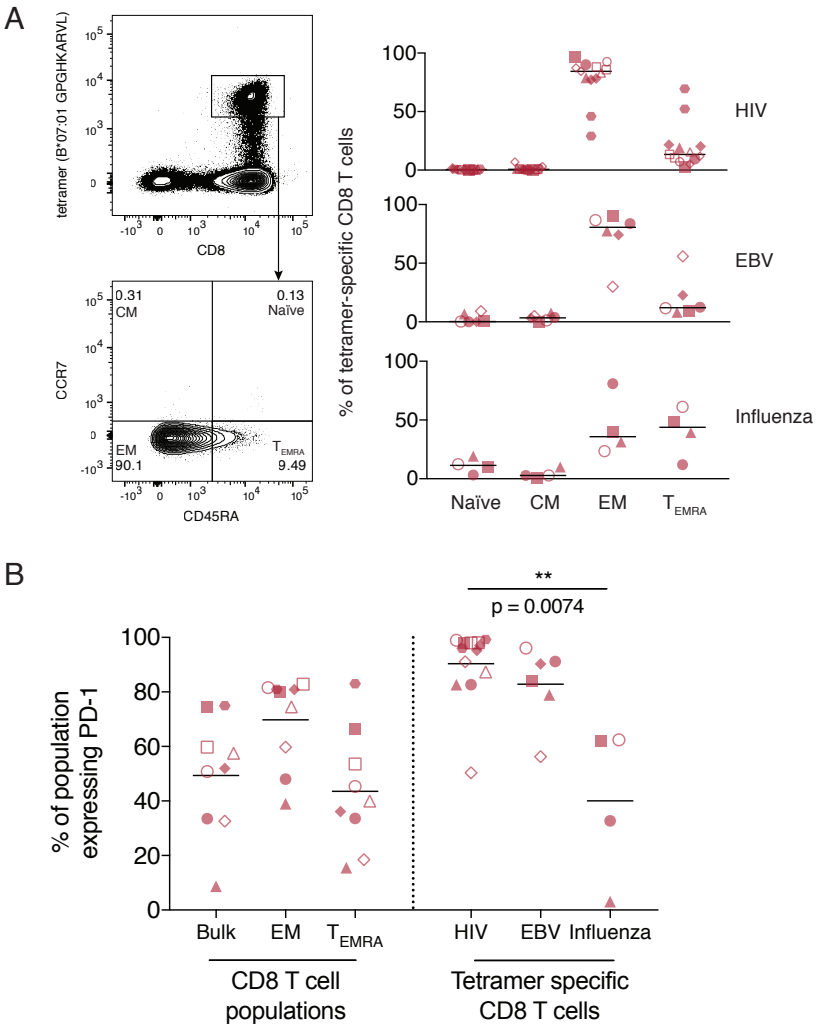


Figure 3.6: Memory phenotype and PD-1 expression on tetramer-specific CD8 T cells during PHI. (A) Memory phenotype of HIV, EBV and influenza-specific CD8 T cells from individuals (n=9) during PHI. The panel on the left shows representative gating. (B) PD-1 expression on bulk CD8 T cell populations, as well as tetramer specific CD8 T cells. Tetramer specific CD8 T cells were compared using a Kruskal-Wallis test (overall p = 0.0088) with subsequent pairwise comparisons using Dunn's test. Symbol shapes indicate tetramers from the same individual. EBV and influenza tetramers were not available for all individuals; for some individuals multiple different HIV tetramers were used and these are shown as separate data points. Bars indicate median. ** indicates p<0.01.

had an EM phenotype (Figure 3.6), which was similarly observed for EBV-specific cells but differed from influenza-specific cells where an approximately equal split was observed between EM and T_{EMRA} cells; representative tetramer staining and memory phenotype for one individual is also shown (the full gating strategy of these population is shown in Figure B.2). HIV-specific CD8 T cells during PHI expressed very high levels of PD-1 when compared with other tetramer-specific cells, and bulk memory populations (Figure 3.6 B). PD-1 on HIV specific T cells decreased following ART initiation (Figure B.3 A shows a trend towards this decrease) but remained unchanged on CD8 T cells specific for EBV or influenza, or if ART was not started (Figure B.3 B).

3.4.3 Biomarkers of T cell exhaustion

3.4.3.1 Negligible expression of CD39 on T cells from some individuals

In Figure 3.5 E it appears that some individuals express negligible levels of CD39. Figure 3.7 A plots the expression of CD39 on CD8 T cells during PHI against this same parameter following 1 year of ART; histograms showing the distribution of expression at each time point have been added to the axes. Here it can be appreciated that there were a substantial proportion of individuals with near-zero expression of CD39, and that this was observed for the same individuals at both time points. This does not appear to be artefactual as this phenotype is stable within an individual over time (Figure 3.7 A), and consistent when different flow cytometry panels are used (data not shown).

These individuals were divided into two groups based on the CD8 T cell expression of CD39 - here termed “non-expressors” and “expressors”. The cut-off value has been defined based on this plot as 1% during PHI and 0.3% following ART treatment, and is shown with a dashed line in Figure 3.7 A and B. Using this definition, there was no difference in the proportion of individuals classified as a CD39 non-expressor between the HIV-infected cohort and healthy controls (31% vs 30% respectively; $p>0.99$, Fisher’s exact test). When the expression of CD39 on CD4 T cells was compared between the two groups, there was significantly higher

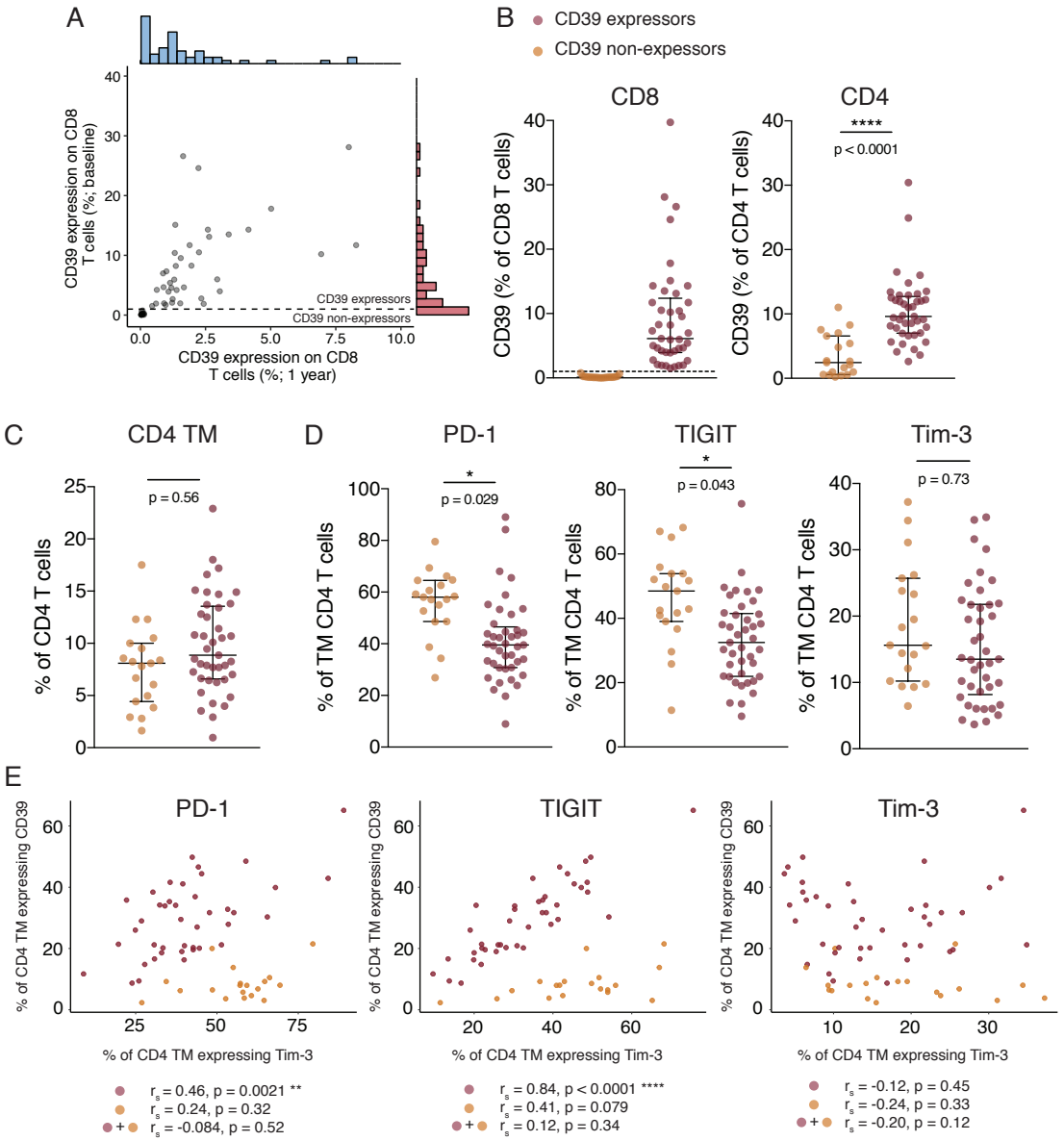


Figure 3.7: Inter-individual variation in CD39 expression. (A) Correlation between CD39 expression on CD8 T cells at baseline and at 1 year (n=54), with histograms showing distribution of values on each axis. For both A and B the dashed line indicates the 1% cut-off used to divide individuals into expressors and non-expressors. Comparison of immunological parameters between expressors (n=41) and non-expressors (n=19) is shown in B-D. (B) CD39 expression on CD8 and CD4 T cells. (C) Frequency of CD4 T cells with a transitional memory (TM) phenotype. (D) PD-1, TIGIT and Tim-3 expression on CD4 TM T cells. Groups were compared using Mann-Whitney tests. For C and D the full list of comparisons is shown in Table B.2 and adjustment of p-values for multiple comparisons was performed; asterisks and listed p-values correspond to the adjusted p-value. (E) Spearman correlations between CD39 expression and expression of PD-1, TIGIT and Tim-3 on CD4 TM T cells, stratified by CD39 expressor status. Bars indicate median and interquartile range. * indicates $p<0.05$; ** indicates $p<0.01$; *** indicates $p<0.001$; **** indicates $p<0.0001$.

CD39 expression in the expressor group (Figure 3.7 B), although non-expressors have considerably more CD39 on CD4 T cells than was observed for the CD8 T cells (that is, non-expressor CD4 T cells are capable of producing the protein).

All measured clinical and immunological variables were compared between CD39 expressors and non-expressors; full results of these tests are shown in Table B.2. Importantly, when corrected for multiple comparisons, there was no difference in baseline markers of clinical progression (CD4 count, VL, CD4 to CD8 ratio) between these two groups. The only two variables to significantly differ were the expression of PD-1 and TIGIT on CD4 TM cells. In Figure 3.4 H, it was observed that the TM subset expressed significantly higher levels of CD39 compared to all other memory subsets. Whilst there was no difference in the frequency of CD4 TM cells between CD39 expressors and non-expressors (Figure 3.7 C), CD39 non-expressing individuals had increased levels of the ICRs PD-1 and TIGIT (but not Tim-3) on CD4 TM cells (Figure 3.7 D). This result would be expected if there was a negative correlation between CD39 expression and PD-1 or TIGIT expression on CD4 TM cells. In Figure 3.7 E it can be observed that this is not the case - there was, in fact, a strong positive correlation between CD39 expression and that of PD-1 and TIGIT on CD4 TM cells, although only amongst individuals classified as CD39 expressors. When this analysis was performed on the overall cohort, or restricted to CD39 non-expressors, there was no significant relationship. CD39 and Tim-3 expression on these cells was unrelated to one another.

There are several single nucleotide polymorphisms (SNPs) which have been associated with CD39 expression. These SNPs and the potential implications of the findings presented here will be discussed in section 3.5.5. For subsequent results presented in this work (including clustering and co-expression analyses) CD39 was not included as the marked difference between CD39 expressors and non-expressors limited interpretability of these results. In the absence of genotype information on which to split individuals, a stratified analysis was not performed. There is no evidence, however, other than for the CD4 TM subset, that these two groups differ in the immunological or clinical variables presented here.

3.4.3.2 Soluble PD-1 and Tim-3 as novel biomarkers

In addition to their surface bound forms, soluble forms of both PD-1 and Tim-3 exist. The plasma levels of soluble PD-1 (sPD-1) and Tim-3 (sTim-3) were measured in a subset of 48 individuals during PHI and following one year of ART, and in healthy controls. The levels of these markers in these three groups are shown Figure 3.8 A (PD-1) and B (Tim-3). For both sPD-1 and sTim-3, levels were elevated during PHI (shown in red) relative to healthy controls (green), but reduced to levels comparable to healthy controls following a year of ART (blue).

The relationship of sPD-1 and sTim-3 to their surface counterparts was explored in Figure 3.8 C. This plot shows the summary of Spearman correlations between each soluble ICR, and the expression of the equivalent marker on each CD4 and CD8 T cell subset. Blocks are coloured according the correlation coefficient (r_s), and asterisks indicate the significance level of this relationship following correction for multiple comparisons (the full results of each of these tests are listed in Table B.3). For each marker, the top row represents measures taken during PHI, and the bottom row following 1 year of ART. In addition to memory CD8 T cells, PD-1 was also measured on subsets of CD8 T cells defined by their expression of the transcription factors T-bet and Eomes (which are described in detail in section 3.4.4.2). Throughout, sPD-1 and sTim-3 levels were positively correlated with surface expression of the same marker however sPD-1 and sTim-3 show different relationships with their surface forms. sTim-3 correlated with Tim-3 expression on bulk and EM CD8 T cells (Figure 3.8 D) during PHI but this relationship did not persist following the initiation of ART. In contrast, sPD-1 correlated with the expression of PD-1 on differentiated CD4 (EM and T_{EMRA} [Figure 3.8 E]) and CD8 (T_{EMRA}, T-bet^{high}Eomes^{low} and T-bet^{low}Eomes^{Eomes}) subsets, but only following 1 year of ART.

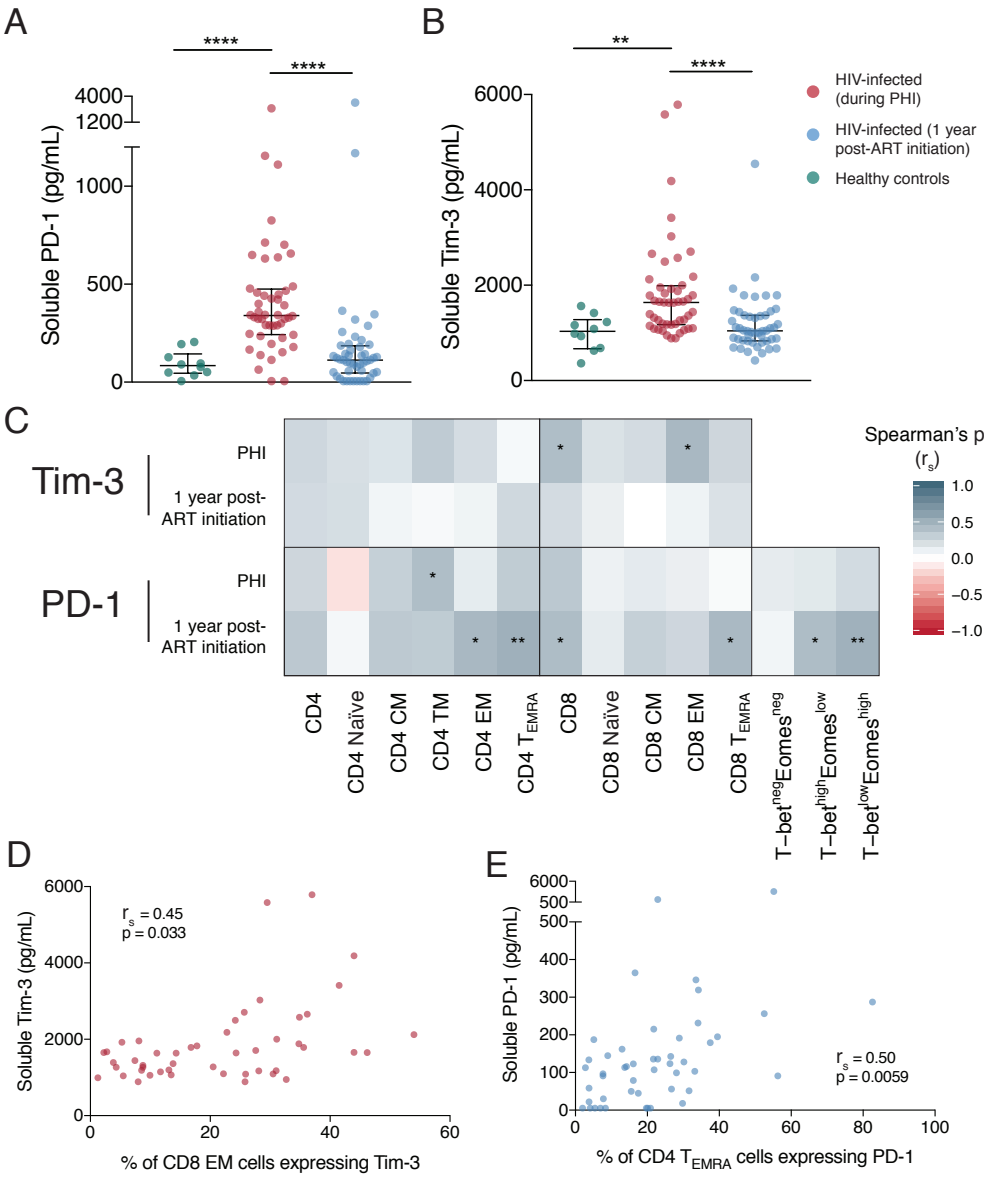


Figure 3.8: Soluble PD-1 and Tim-3 during PHI. (A) Plasma levels of soluble PD-1 are shown from healthy controls (green; n=10), during PHI (red; n=48) and 1 year post-ART initiation (blue; n=48). (B) Plasma levels of soluble Tim-3 in the same three groups. Groups were compared using a Kruskal-Wallis test with pairwise comparisons performed with Dunn's test. (C) Summary of Spearman correlations between soluble PD-1 and Tim-3, and the expression of the same markers on T cell subsets during PHI (top row for each marker) and 1 year following ART initiation (bottom row for each marker); adjustment of p-values for multiple comparisons was performed across all comparisons for a given marker to control the false discovery rate. Each box represents a correlation and is shaded according the correlation coefficient (r_s). (D) Correlation between soluble Tim-3 and Tim-3 expression of CD8 EM cells during PHI. (E) Correlation between soluble PD-1 and PD-1 expression on CD4 T_{EMRA} cells following 1 year of ART. Asterisks and listed p-values correspond to the adjusted p-value. The full results of each of these tests are listed in Table B.3. Bars indicate median and interquartile range. * indicates $p<0.05$; ** indicates $p<0.01$; *** indicates $p<0.001$; **** indicates $p<0.0001$.

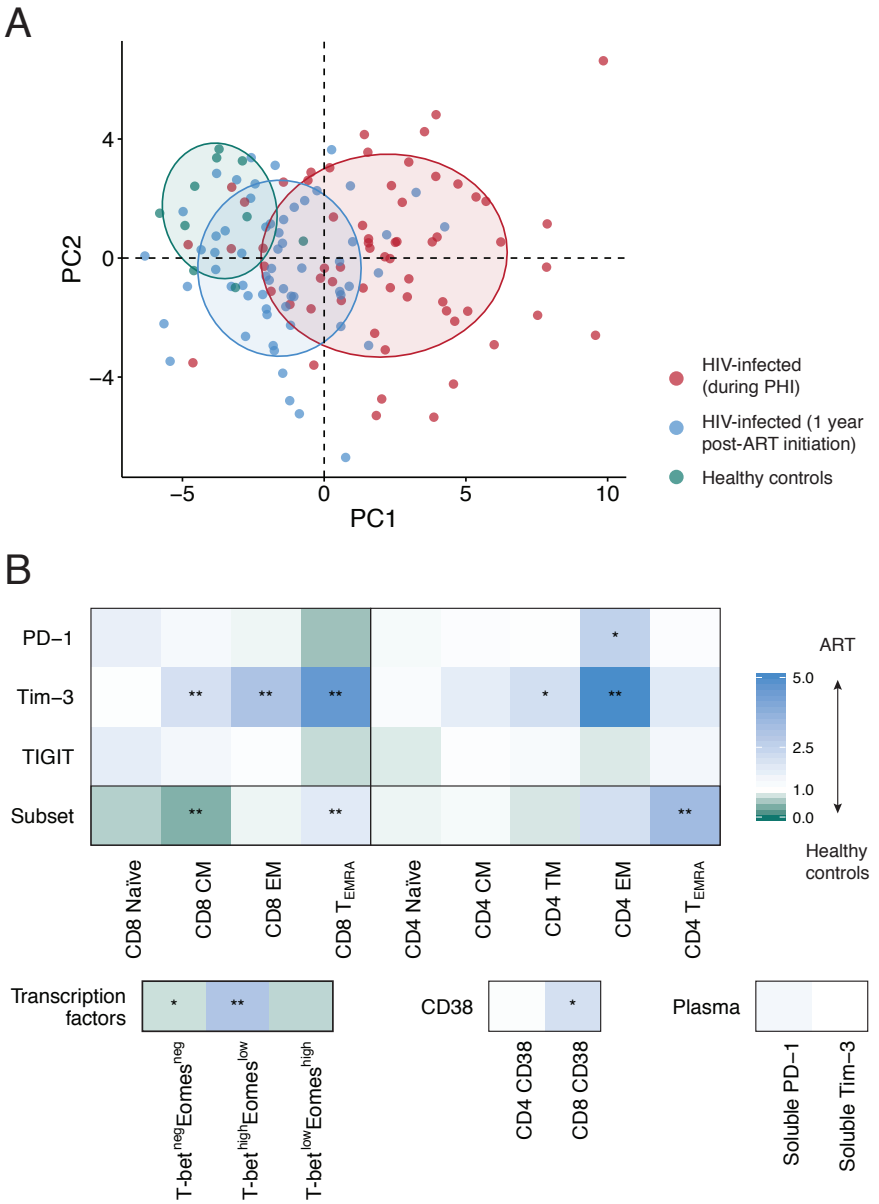


Figure 3.9: Immune parameters are incompletely resolved following 1 year of ART. (A) Principle component analysis of all immune parameters measured here; plotted are the first two principle components (PC1 against PC2). Each point represents an individual from one of the following groups: healthy controls (green), primary HIV infection (red) and 1-year following ART initiation (blue). Ellipses have been added to aid in visual comparison and encompass 60% of values for each group. Comparisons of ICR expression between healthy controls and individuals following 1 year of ART are summarised in (B). Blocks, each corresponding to an immune parameter, are shaded according to the fold difference between ART-treated individuals relative to healthy controls. Groups were compared using Mann-Whitney tests and adjustment of p-values for multiple comparisons was performed across all comparisons presented here to control the false discovery rate. The full results of each of these tests are listed in Table B.4. Asterisks and listed p-values correspond to the adjusted p-value. * indicates $p<0.05$; ** indicates $p<0.01$; *** indicates $p<0.001$; **** indicates $p<0.0001$.

3.4.4 Incomplete resolution of immune parameters following ART initiated during primary HIV infection

This work has described T cell activation, memory expansion and increases in ICR expression during PHI. To explore if these had normalised following a year of ART, a principle component analysis (PCA) was performed. PCA is a technique used for high dimensional data which converts information in highly correlated variables into a smaller number of uncorrelated principle components. Figure 3.9 A shows the results of the PCA performed using all the immune parameters described in this chapter: the proportion of CD4 and CD8 memory subsets and CD8 T cells with different combinations of T-bet and Eomes, CD38 expression, the expression of ICRs on each CD4 and CD8 subset, and plasma levels of sPD-1 and sTim-3. Here it is evident that whilst individuals during PHI (shown in red) and healthy controls (green) form distinct clouds, the same individuals following 1 year of ART (blue) overlap these two other groups. This suggests partial, but incomplete resolution of immune parameters towards levels seen in healthy controls following 1 year of ART.

To further characterise which parameters remained different to healthy controls, the levels of each of these markers in individuals following 1 year of ART was compared with healthy controls. Figure 3.9 B shows the summary of these comparisons (the full results of each of these tests are listed in Table B.4). Similar to previous plots, each box is shaded to reflect the median fold difference in the ART treated group compared with the healthy controls, and asterisks to indicate the significance level of this difference after correction for multiple comparisons. Persistent differences in CD4 and CD8 memory differentiation, CD8 T cell activation and ICR expression were all evident and will be expanded upon in the following sections.

3.4.4.1 Expansion of terminally differentiated T cells

During untreated PHI a marked expansion in CD8 EM cells was evident, with reciprocal decline in naïve and CM pools. Figure 3.10 A shows that following 1 year of ART (blue) restoration of the proportion of naïve and EM CD8 T cells had occurred although further expansion of the T_{EMRA} subset was evident. This shift

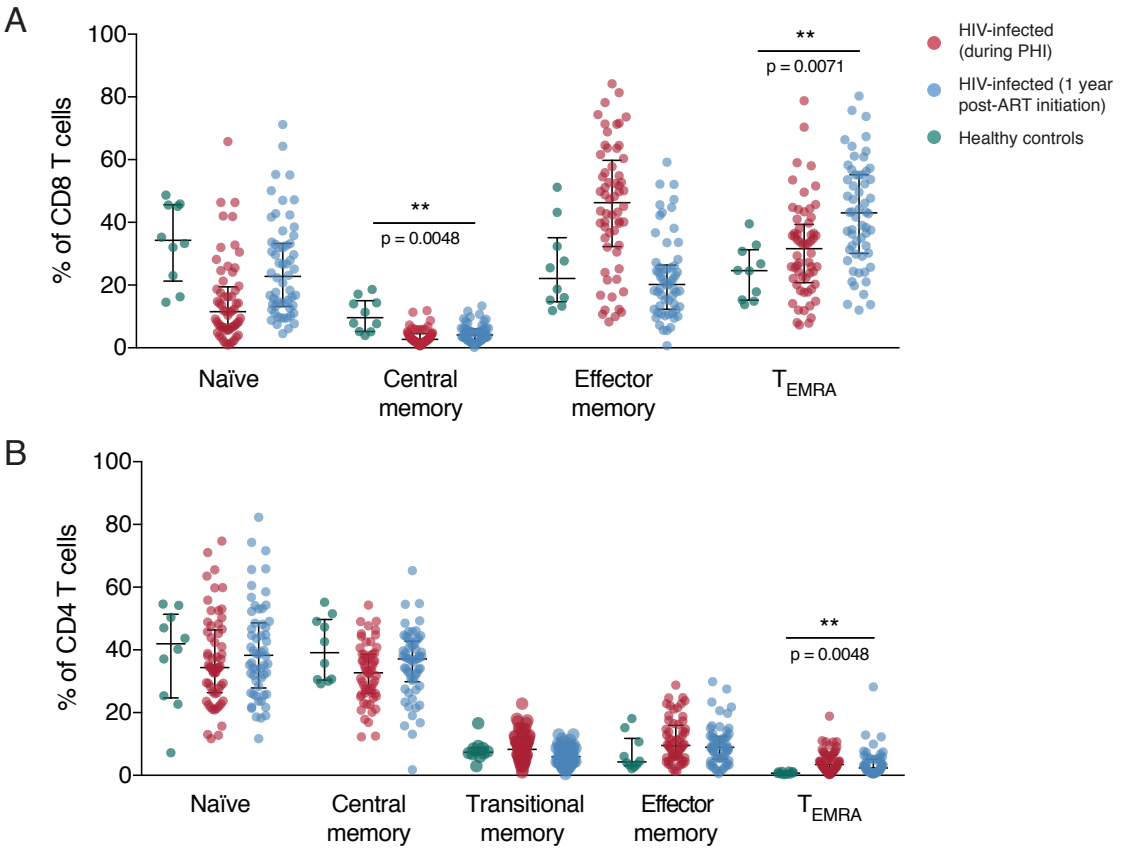


Figure 3.10: Changes in T cell memory subsets following 1 year of ART. The percentage of T cells comprising each memory subset is shown in (A; CD8 T cells) and (B; CD4 T cells) for healthy individuals (n=10; green), HIV-infected individuals during PHI (n=60; red) and following 1 year of ART (n=58; blue). Comparisons shown are those performed as in Figure 3.9 between healthy controls and ART treated individuals. The HIV-infected group during PHI is shown for visual comparison only and was formally compared to healthy controls in Figure 3.3. Asterisks and listed p-values correspond to the adjusted p-value. ** indicates $p<0.01$.

not only occurred in the bulk CD8 T cell pool, but also in HIV-specific CD8 T cells (Figure B.4 A) where this progression was seen even if ART was not started (Figure B.4 B). These changes were less marked for CD4 T cells (Figure 3.10 B), however it can also be observed that the proportion of T_{EMRA} cells, but not EM, were still elevated relative to healthy controls. Overall, these changes demonstrate that following 1 year of ART, expanded effector T cell subsets have declined to levels comparable to healthy controls but that persistent or further expansion of terminally differentiated T cells can be observed.

3.4.4.2 Expansion of CD8 T cells expressing T-bet and Eomes

CD8 T cells can also be divided into subpopulations based on their expression of T-bet and Eomes (introduced in section 1.4.2). Figure 3.11 A shows the representative gating of three populations: T-bet^{neg}Eomes^{neg}, T-bet^{high}Eomes^{low} and T-bet^{low}Eomes^{high}. The proportion of these three populations is shown in Figure 3.11 B in healthy controls (shown in green), during PHI (red) and following 1 year of ART (blue). During PHI, a decrease in T-bet^{neg}Eomes^{neg} occurred, with reciprocal expansion of the T-bet^{high}Eomes^{low} population. Following ART initiation, partial restoration of the T-bet^{neg}Eomes^{neg} population occurred although the T-bet^{high}Eomes^{low} population remained elevated. At this point a decline in the frequency of the more terminally differentiated T-bet^{low}Eomes^{high} was also seen. The proportion of T-bet^{neg}Eomes^{neg} cells correlated very highly with the frequency of naïve CD8 T cells during PHI (shown in Figure 3.11 C); the same pattern was seen following 1 year of ART and in healthy controls (data not shown).

The ICRs PD-1 and Tim-3, as well as CD38, were differentially expressed between these populations of CD8 T cells (Figure 3.11 D-I). During PHI, T-bet^{low}Eomes^{high} CD8 T cell expressed the highest levels of PD-1 and CD38 (Figure 3.11 D, E, H, I). For PD-1, this was also true following ART initiation (Figure 3.11 D), but differed from CD38; following ART initiation activation of this population markedly declined on all subsets, with the highest CD38 expression observed on CD8 T-bet^{high}Eomes^{low} (Figure 3.11 I). Tim-3 expression, in contrast, was lowest on the T-bet^{low}Eomes^{high} CD8 T cells during PHI and following ART initiation (Figure 3.11 F, G).

One of the most striking observations during PHI was the elevated CD38 expression on CD8 T cells. The results presented in Figure 3.9 B show that following 1 year of ART this was not completely restored to the level of healthy controls. CD38 expression on CD8 T cells in healthy controls, during PHI and following ART is shown in Figure 3.12 A, and shows that whilst CD38 expression remains persistently elevated, it has decreased substantially from the levels seen during PHI.

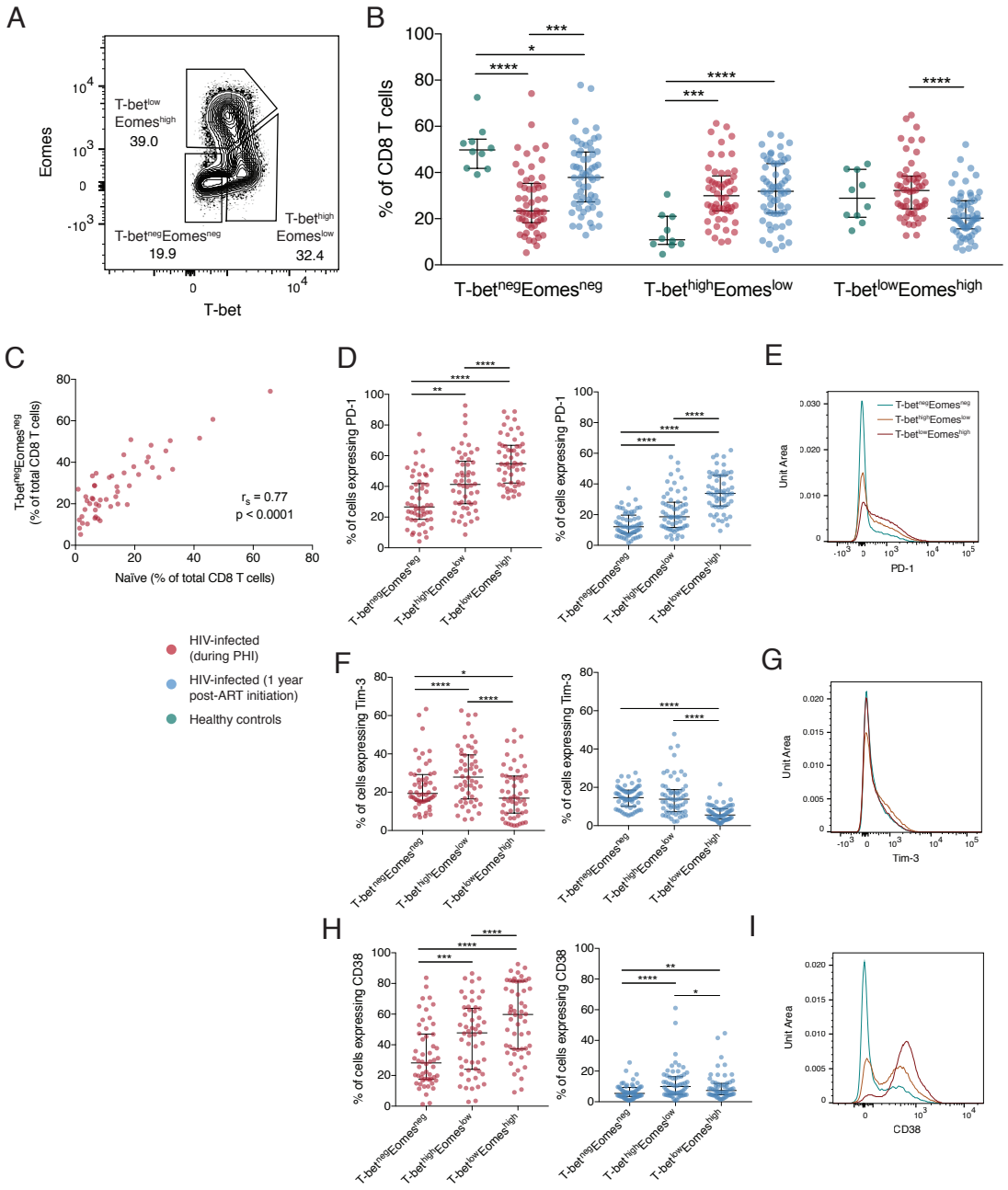


Figure 3.11: Subsets of CD8 T cells expressing combinations of the transcription factors T-bet and Eomes. (A) Representative gating from one donor during PHI shows the division of CD8 T cells into 3 populations: T-bet^{neg}Eomes^{neg}, T-bet^{high}Eomes^{low} and T-bet^{low}Eomes^{high}. (B) The frequency of each of these populations in healthy controls (green; n=10), during PHI (red; n=54) and 1 year post-ART initiation (blue; n=60) is shown. Groups were compared with a Kruskal-Wallis test (overall p for all tests <0.001) with subsequent pairwise comparisons performed with Dunn's test.

Figure 3.11: *continued.* (C) The frequency of T-bet^{neg}Eomes^{neg} and naïve CD8 T cells are plotted (n=51); data were tested using a Spearman correlation. The expression of PD-1, Tim-3 and CD38 on these subsets is shown in D-I. Representative flow plots from each subset are overlaid from one donor during PHI for PD-1 (E), Tim-3 (G) and CD38 (I). The percentage of each subset expressing these markers is shown during PHI (red, left panel) and following 1 year of ART (blue, right panel) for PD-1 (D), Tim-3 (F) and CD38 (G). Groups were compared using a Friedman test (overall p for all tests <0.001) with subsequent pairwise comparisons performed with Dunn's test. Bars indicate median and interquartile range. * indicates p<0.05; ** indicates p<0.01; *** indicates p<0.001; **** indicates p<0.0001.

Figure 3.12 B shows the co-expression of CD38, PD-1 and Tim-3 on T-bet^{high}Eomes^{low} and T-bet^{low}Eomes^{high} CD8 T cells (similar plots for all three subsets are shown in Figure B.5). In healthy controls (left column), the co-expression of these markers was seen in a very small proportion of these populations. Unsurprisingly, the increased expression of these markers during PHI (middle column) was also accompanied by an increase in co-expression. Next, the proportion of T-bet^{high}Eomes^{low} and T-bet^{low}Eomes^{high} CD8 T cells co-expressing different combinations of CD38, PD-1 and Tim-3 was compared between ART treated individuals and healthy controls. Co-expression combinations which were persistently different in ART treated individuals (right column) are marked on the corresponding segments with asterisks to indicate the significance of this test following correction for multiple comparisons. Here it can be observed that following a year of ART, co-expressing combinations of these markers were persistently elevated relative to healthy controls following 1 year of ART, although the overall proportion of cells expressing one or more of these markers did not differ. A direct comparison of this is shown in Figure 3.12 C (for T-bet^{high}Eomes^{low} cells) and D (for T-bet^{low}Eomes^{high} cells).

3.4.4.3 Persistently elevated immune checkpoint receptor co-expression

Co-expression of ICRs was assessed on CD4 and CD8 T cell memory subsets. Compared with healthy controls, an increased proportion of CD8 EM cells during PHI (Figure 3.13 A) expressed any of the ICRs PD-1, Tim-3 or TIGIT. The proportion of all CD8 T cell memory subsets co-expressing different combinations of the ICRs PD-1, Tim-3 and TIGIT was compared between ART treated individuals

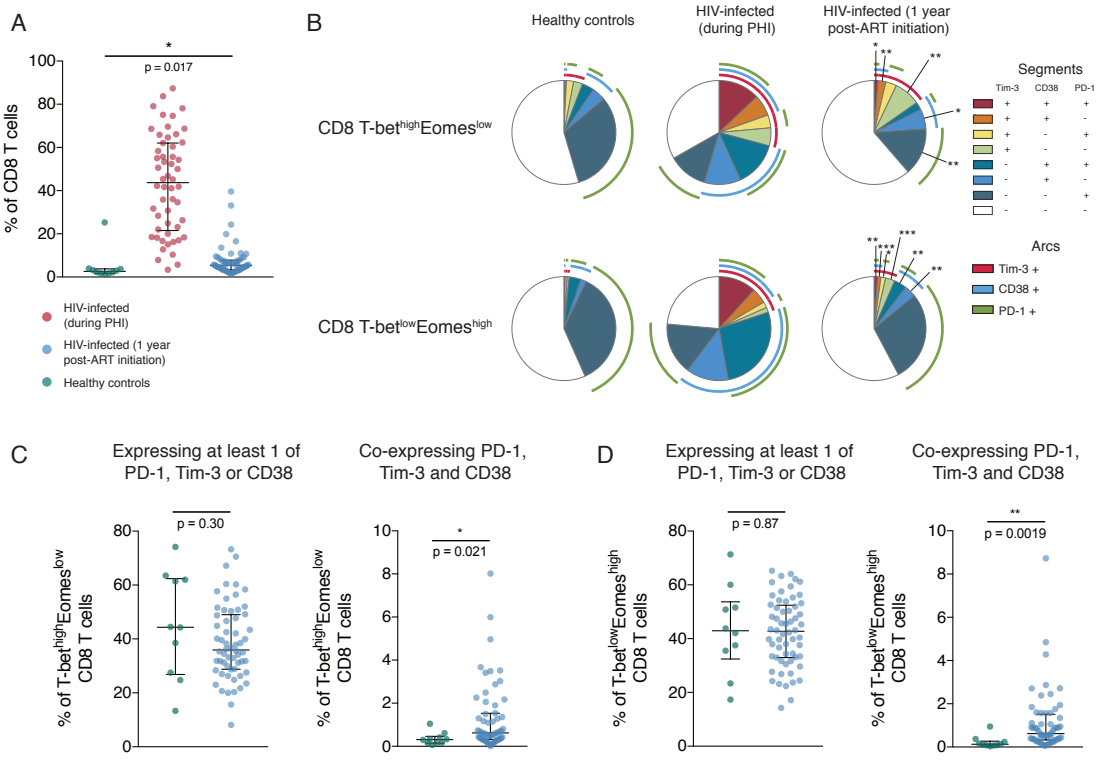


Figure 3.12: Co-expression of CD38, Tim-3 and PD-1 remains elevated on CD8 T cells following 1 year of ART. (A) Expression of CD38 on CD8 T cells for healthy individuals (n=10; green), HIV-infected individuals during PHI (n=54; red) and following 1 year of ART (n=60; blue). Comparisons shown are those performed as in Figure 3.9 between healthy controls and ART treated individuals. The HIV-infected group during PHI is shown for visual comparison only and was formally compared to healthy controls in Figure 3.3. (B) Co-expression of these markers on CD8 subsets in the same three groups. Each segment represents the proportion of cells (median) with a different co-expression combination; arcs indicate which markers are in that combination. Co-expressing combinations were compared between healthy controls and ART treated individuals using a Mann-Whitney test; p-values were adjusted to control the false-discovery rate. Segments marked with an asterisk are significantly different between healthy controls and ART-treated individuals. The percentage of CD8 T-bet^{high}Eomes^{low} (C) and T-bet^{low}Eomes^{high} (D) cells which express at least 1 of PD-1, Tim-3 or CD38 (left panel) or all three markers (right panel) was compared between healthy controls (green) and ART-treated individuals (blue). Bars indicate median and interquartile range. Asterisks and listed p-values correspond to the adjusted p-value. * indicates $p<0.05$; ** indicates $p<0.01$; *** indicates $p<0.001$.

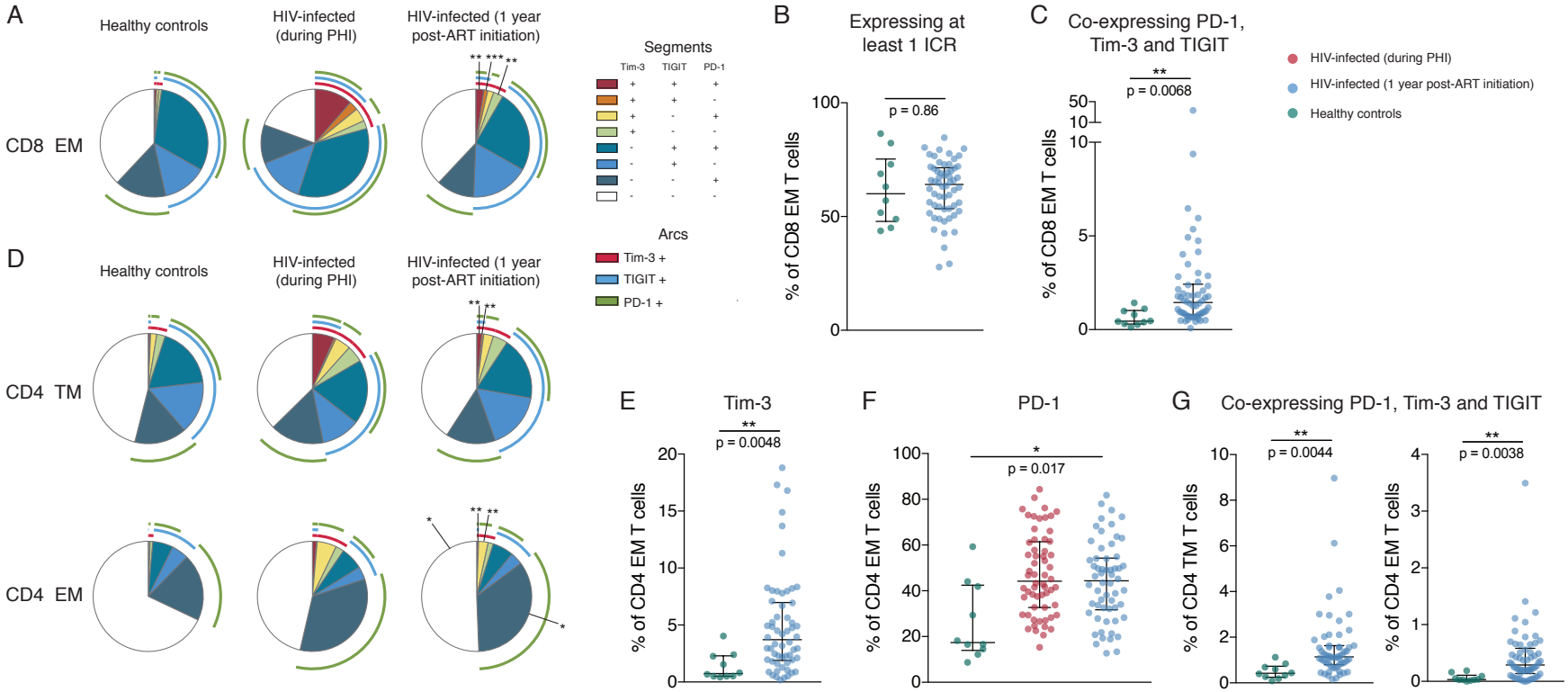


Figure 3.13: Co-expression of ICRs remains elevated following 1 year of ART. (A) Co-expression of ICRs on CD8 EM cells from healthy controls (n=10), during PHI (n=60) and following 1 year of ART (n=58). (D) Co-expression of ICRs on TM and EM cells from healthy controls. In (A) and (D) each segment represents the proportion of cells (median) with a different co-expression combination; arcs indicate which markers are in that combination. Co-expressing combinations (on all CD4 and CD8 memory subsets) were compared between healthy controls and ART treated individuals using a Mann-Whitney test; p-values were adjusted (separately for CD4 and CD8 cells) to control the false-discovery rate. Segments marked with an asterisk are significantly different between healthy controls and ART-treated individuals. *continued.*

Figure 3.13: *continued.* The percentage of CD8 EM cells which express at least 1 ICR (PD-1 or Tim-3 or TIGIT) (B) or all three ICRs (C) was compared between healthy controls (green) and ART-treated individuals (blue). Similar comparisons are shown for percentage CD4 EM cells which express Tim-3 (E) or PD-1 (F). In (F), the HIV-infected group during PHI has been added for visual comparison. (G) Comparison of the percentage of CD4 TM (left panel) and EM cells (right panel) which co-express all three ICRs between healthy controls and following 1 year of ART. Bars indicate median and interquartile range. Asterisks and listed p-values correspond to the adjusted p-value. * indicates $p<0.05$; ** indicates $p<0.01$; *** indicates $p<0.001$.

and healthy controls as described in section 3.4.4.2. Again, asterisks are used to indicate which segments remained persistently different between these two groups. Here it can be observed that following 1 year of ART the overall proportion of CD8 EM cells expressing at least one ICR did not differ from healthy controls (Figure 3.13 B). Despite this, the co-expression of ICRs was significantly increased (Figure 3.13 A, C). Similar patterns of co-expressed ICR elevation were also observed on CD8 CM and T_{EMRA} cells (plots for all of these subsets are shown in Figure B.6). Of note, persistent elevation of Tim-3 on memory CD8 T cells following 1 year of ART is shown in Figure 3.9 B, and all elevated co-expressing combinations in Figure 3.13 A contained Tim-3, suggesting Tim-3 marker underlies this finding.

A similar analysis was performed for CD4 T cells. Figure 3.13 D shows the co-expression on ICRs on TM and EM CD4 T cells (equivalent plots for naïve, CM and T_{EMRA} cells are in Figure B.7). On TM CD4 T cells following 1 year of ART there was persistent elevation of co-expressing combinations which include Tim-3 and TIGIT (Figure 3.13 D, G). A different pattern was seen in the EM CD4 T cells. Here, there was a persistent elevation in the proportion of cells which express at least one ICR (shown by the decrease in the white segment; Figure 3.13 D). In addition, co-expressing combinations that contained Tim-3 and PD-1, or PD-1 alone were persistently elevated compared with healthy controls. Consistent with this observation from the co-expression data, in the single expression analysis presented Figure 3.9 B, Tim-3 and PD-1 were elevated on CD4 EM cells compared with healthy controls. These data are shown in Figure 3.13 E (Tim-3) and F (PD-1). The PHI group are also shown in panel F because, unlike most measured variables

which partially return towards the level of healthy controls with ART, PD-1 on EM CD4 T cells appears unchanged with ART. In summary, co-expression of ICRs on CD4 and CD8 memory T cells remained elevated following 1 year of ART initiated during PHI, with co-expressing combinations that differ composed of the same markers that were elevated when each are measured separately.

3.4.5 Immunologic changes during primary HIV infection are linked to markers of clinical progression

One hypothesis is that immune parameters which had not normalised following a year of ART may be related to pre-therapy markers of disease progression (such as CD4 count and VL). To test this, correlation coefficients were calculated between all variables in Figure 3.9 B which remain significantly different from healthy controls, and the following baseline clinical variables: CD4 count, CD8 count, CD4 to CD8 ratio, VL, age, time from estimated seroconversion to ART start and time to VL suppression. Interestingly, there was no evidence to support any relationship between these clinical and immunological variables (results in Table B.5).

A similar analysis performed with those variables that were perturbed during PHI reveals a very different picture. Here, there was a high level of correlation between baseline markers of clinical progression and CD8 differentiation and activation (full results in Table B.6). Figure 3.14 shows these relationships for the expression of CD38 on CD8 T cells, and the proportion of CD8 T cells with an EM phenotype - the two immunological measures most highly correlated with clinical parameters. Baseline VL was correlated with CD8 CD38 expression (panel A) and as well as the EM subset (panel B); with inverse relationships of both to the CD4 to CD8 ratio (panels C and D respectively). Both of these were also correlated with time to viral load suppression following ART initiation (Figure 3.14 E, F). Indeed, these clinical measures appear to be independently related to CD8 T cell CD38 expression and EM phenotype. If all three (baseline VL, CD4 to CD8 ratio and time to viral suppression) are included in a multivariable linear regression model, baseline VL and time to viral suppression are independently associated with CD38

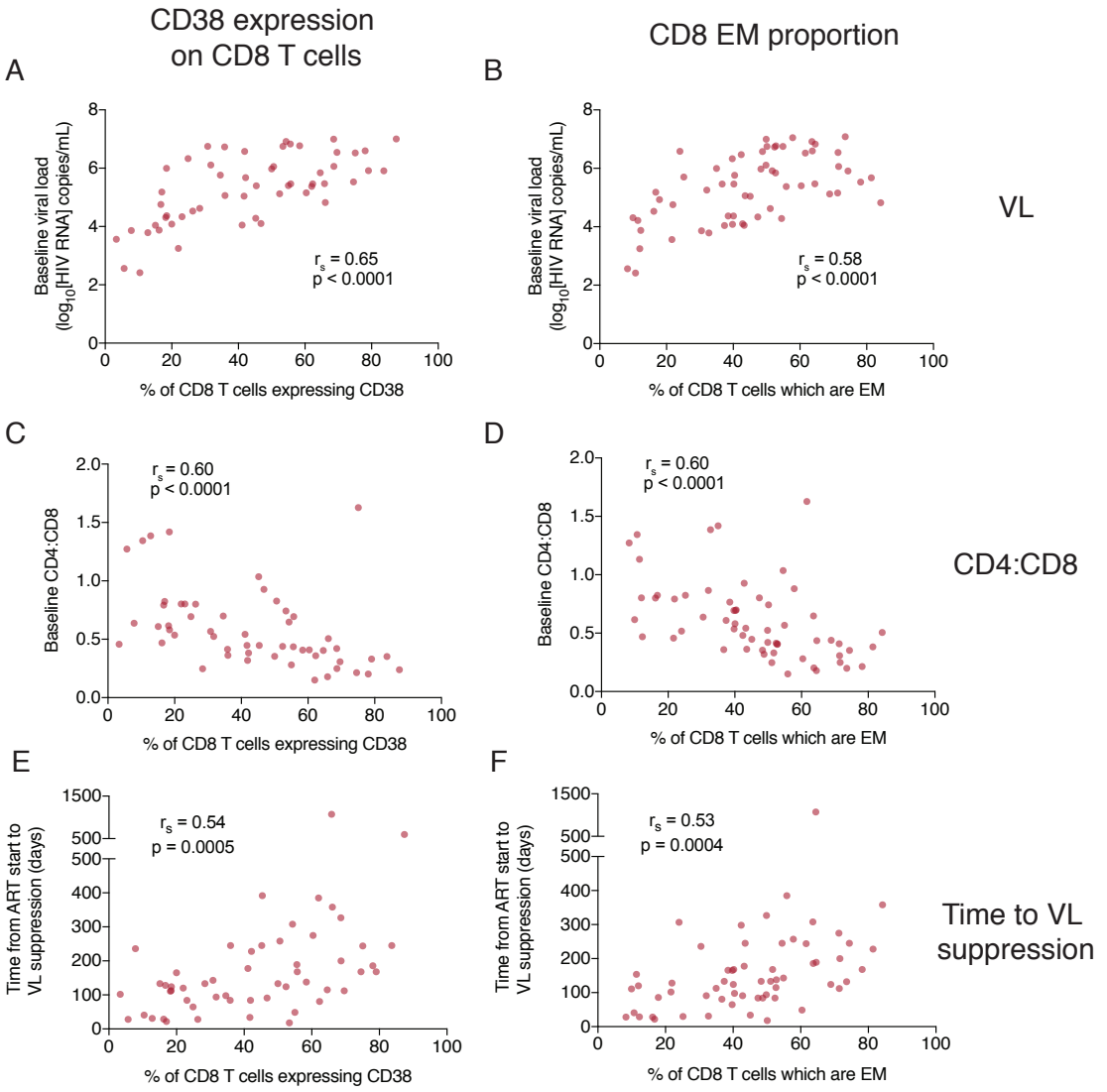


Figure 3.14: Immunological changes during PHI correlate with measures of clinical progression. Relationship between baseline VL (A-B), CD4 to CD8 ratio (C-D) and time to viral load suppression (E-F) and CD38 expression on CD8 T cells (A, C, E, n=54) and the proportion of CD8 T cells which are EM (B, F, n=60; D, n=59). Spearman correlations between were performed between combinations of immunological and clinical measures during PHI (as listed in Table B.6); adjustment of p-values for multiple comparisons was performed across all comparisons for a given marker to control the false discovery rate. Listed p-values correspond to the adjusted p-value.

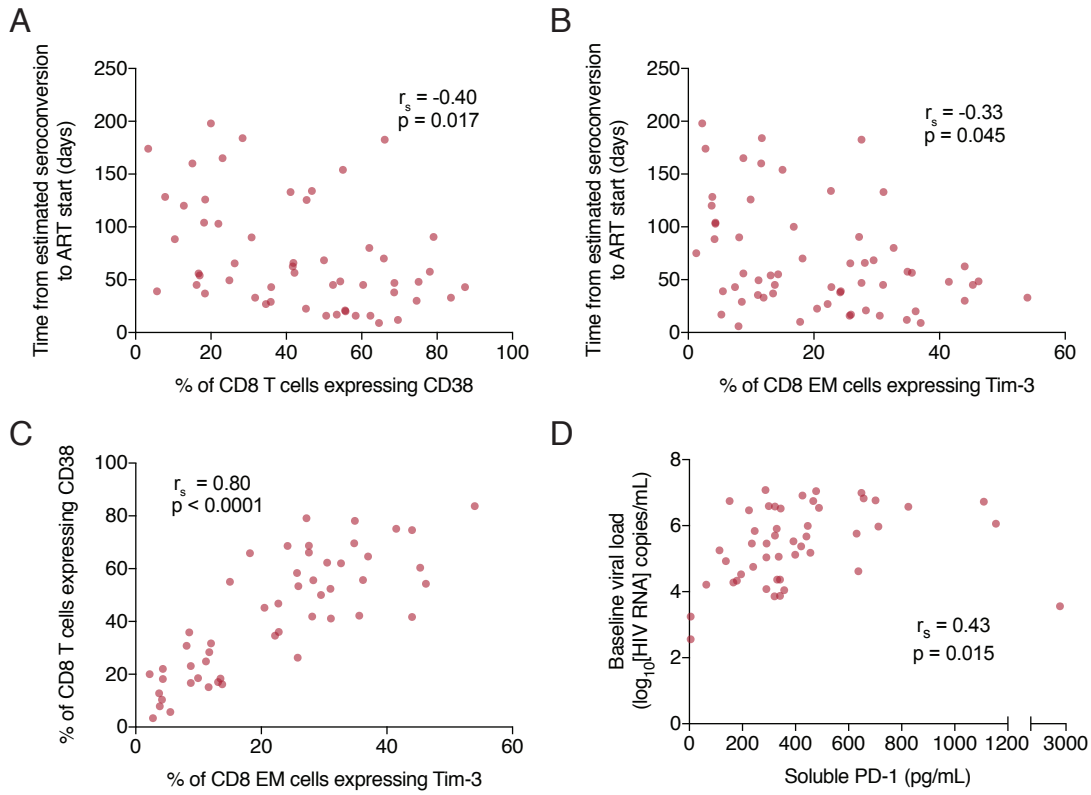


Figure 3.15: Additional relationships between immunological changes during PHI. Relationship between time from estimated seroconversion to ART start and CD38 expression on CD8 T cells (A, n=54) and the proportion of CD8 T cells which are EM (B, n=60). (C) Shows the relationship between these two variables (n=57). (D) Relationship between baseline VL and soluble PD-1 (n=48). Spearman correlations between these pairs were performed. For A, B and D these are listed in Table B.6; adjustment of p-values for multiple comparisons was performed across all comparisons for a given marker to control the false discovery rate. Listed p-values correspond to the adjusted p-value.

expression, and all three are associated with the EM phenotype (Table B.7). The inter-relatedness of these variables is explored further in the context of HIV reservoir size in Chapter 4. Although levels of CD38 were not elevated on CD4 T cells during PHI (Figure 3.3 F), and as such are not shown in Table B.6, a modest correlation was observed between CD4 T cell expression of CD38 (r_s=-0.346, p = 0.010, n=54) but not with VL or CD4 to CD8 ratio.

Early initiation of ART is thought to be associated with improved immunological outcomes. The cohort presented here all begin ART during PHI but there was a small amount of variation in the time from estimated seroconversion to ART

start (median 52, range 6 - 198 days). Within this range there was little evidence of a relationship between time to ART start and immunological parameters, with only two of these (CD8 CD38 expression, and Tim-3 expression on EM CD8 T cells; Figure 3.15 A, B) significantly related to this time interval. Most individuals commenced ART on the same day or shortly after their baseline visit, meaning that the time interval from seroconversion to ART start was almost identical to the time from seroconversion to baseline study visit (r_s=0.95, p<0.0001, n=66). As such, these results also reflect that levels of CD38 and Tim-3 expression were lower when measured further after seroconversion. Interestingly, these were the same two variables with the greatest fold increase during PHI (Figures 3.3 E and 3.5 A, C). The expression of CD38 on CD8 T cells, and Tim-3 expression on EM CD8 T cells were also highly correlated with one another (Figure 3.15 C; also seen following 1 year, not shown).

Whilst CD8 differentiation and activation were highly related to baseline markers of clinical progression, few ICRs were. The only ICR expressed on the cell surface with a relationship to baseline clinical parameters was Tim-3. The only other ICR related to clinical variables was PD-1 in its soluble form, which correlated positively with baseline VL (Figure 3.15 D), and inversely with the CD4 count and CD4 to CD8 ratio.

In summary, T cell differentiation and activation during PHI were closely linked to markers of clinical progression at this time. Aspects of these processes which had not normalised following 1 year of ART do not appear to be related to these baseline clinical measures.

3.5 Discussion

This work has described a number of immunological perturbations during PHI and explored the impact of ART initiation on the restoration of these. During PHI, T cell differentiation and activation both occur, and ICR expression is increased. The major finding of this chapter was that following 1 year of ART started in

PHI, persistent immune activation and elevated ICR expression/co-expression were observed. Whilst some of these changes have been very well described, others add a new level of detail to our understanding of immune processes at this early time. Importantly, these results demonstrate that elevation of ICRs during PHI occurs mostly on memory CD4 and CD8 T cells, and is not merely a result of shifting memory populations. Striking was the marked increase of Tim-3 during PHI and the failure of this to resolve after a year of suppressive ART. As an observational cohort study, this work cannot define the mechanisms responsible for these persistent changes - for example, it is unclear if the persistent Tim-3 elevation observed reflects residual immune activation or marks cells with a functional deficit. As a detailed descriptive study, however, these results can be used as a basis to focus future studies on how ART can be used to maximise immunologic recovery.

3.5.1 T cell differentiation

This chapter demonstrated the expansion of EM CD8 T cells and high baseline CD8 T cell counts that have long been recognised to characterise early HIV infection (section 1.3), and have been described in several PHI cohort studies [54, 88, 89, 140, 378]. A largely EM phenotype of HIV-specific T cells during early untreated infection was confirmed [51]. The shifts observed here in the CD4 T cell department have also been described during PHI [140]. Following ART initiation, the T_{EMRA} populations (both CD4 and CD8) continued to expand. This has been described following early ART initiation [117, 139], but also occurs in the transition from primary to chronic infection [88, 139, 140] presumedly as previously activated cells are being driven towards terminal differentiation. In the case of ART initiation, this is further amplified by the relative shrinkage of the EM pool in the absence of ongoing antigen. In the CD8 compartment, the frequency of EM cells was closely linked with baseline markers of clinical progression: VL, CD4 to CD8 ratio and time to viral load suppression.

Despite many years of study it is still debated how much of the marked CD8 T cell expansion is HIV-specific and how much is a bystander effect. The extent of CD8

EM expansion observed here (median 46% of the EM pool) and by others [54, 88, 89, 140, 378] is at odds with studies that have demonstrated narrow, low magnitude viral-specific responses during early infection [82, 381–383] - suggesting the presence of bystander activation. A potential explanation for this comes from the fact that many studies of the magnitude and quality of this response have used IFN-γ readouts to identify HIV-specific T cells [82, 101, 381–385]. This may underestimate the HIV-specific response as, even during early infection, not all viral-specific cells produce IFN-γ [85, 386]. More recent work has shown that during acute infection a highly activated, proliferating phenotype (Ki-67+Bcl-^{low} or CD38+HLA-DR+) was found in HIV-, but not EBV-, influenza- or CMV-specific cells [85, 86]. As this phenotype accounted for a large amount of the bulk EM expansion, the authors suggest that this is likely almost entirely HIV-specific [85, 86]. Of note this is in contrast to other reports of EBV- and CMV-specific cells with a similar, activated phenotype during early HIV infection [94, 387]. Providing more recent evidence for bystander activation, higher levels of TCR diversity have been observed in the expanded EM pool than would be expected if this was due to clonal expansion of HIV-specific cells [388]. Furthermore, memory CD8 T cells specific for CMV and influenza, as well as HIV, show increased cycling and granzyme B expression in chronic HIV infection [388]. Suggesting a mechanism, this same phenotype can be induced by IL-15 treatment *in vitro* [388], levels of which are increased in tissues during HIV infection [388, 389]. Further work is needed to confirm the degree of HIV-specific versus bystander CD8 T cell activation during early HIV infection.

The balance of the transcription factors T-bet and Eomes are linked to CD8 T cell fate. Here, a close correlation was observed between the frequency of T-bet^{neg}Eomes^{neg} and naïve CD8 T cells. Indeed, early induction of T-bet expression following TCR stimulation is critical for the development of effector and memory functions (reviewed in [40]), and it is likely that this population indeed corresponds to antigen inexperienced (naïve) cells.

In murine models, T-bet^{low}Eomes^{high} CD8 T cells are considered to be a terminally exhausted subset. These cells are characterised by very high PD-1

expression, poor responsiveness to PD-1 blockade and limited capacity to self-renew [167, 168], instead developing in the setting of persistent antigen from T-bet^{high}Eomes^{low} cells [167]. Indeed, these phenotypes appear to be applicable to chronic HIV infection with the T-bet^{low}Eomes^{high} subset reported to express low levels of perforin [88] and be poorly polyfunctional [169]. Further suggesting the relevance of this functional division, elevated T-bet expression has been associated with cytotoxic capacity in elite controllers [390] whilst persistently elevated Eomes expression was associated with a high degree of functional exhaustion in a recent high-dimensional analysis [171]. Here, the highest levels of PD-1 expression were observed on the T-bet^{low}Eomes^{high} subset, as has been previously reported [169]. These cells were also very highly activated (measured by CD38 expression) in PHI, but not following treatment. Tim-3 expression in contrast, was highest on the T-bet^{low}Eomes^{high} progenitor subset, consistent with prior findings of elevated T-bet in Tim-3 expressing CD8 T cells [127, 141].

CD8 T cell memory subsets and T-bet/Eomes were measured separately so cannot be directly compared. T-bet^{low}Eomes^{high} cells have been reported to have a CD45RO+CCR7-CD27+ phenotype [169], which represents a subset of the EM population defined here. The vast majority of HIV-specific CD8 T cells during chronic infection have been shown to be T-bet^{low}Eomes^{high} [169]. The frequency of these T-bet^{low}Eomes^{high} cells has been shown to increase from primary to chronic infection if ART is not started [88]. This population declined following a year of ART, similar to what has been shown when ART is started during chronic infection [169]. This supports the notion that this population cannot self-renew and, in the absence of antigen, is not being replenished from progenitor populations. Compared with healthy controls, however, the T-bet^{high}Eomes^{low} pool was markedly elevated during PHI and maintained at similar levels following ART. Given that the upregulation of T-bet is so closely linked to TCR stimulation [40], it is possible that a substantial portion of these cells are HIV-specific, although this was not directly measured; bystander activation of already antigen-experienced cells remains a possibility. T-bet^{high}Eomes^{low} CD8 T cells could represent an antigen-experienced

population that does not yet have the terminally exhausted T-bet^{low}Eomes^{high} phenotype but persists or is preserved on ART when started during PHI - and could be a therapeutic target. It remains to be seen if T-bet^{high}Eomes^{low} cells from HIV-infected individuals can proliferate in response to PD-1 blockade, as has been observed in mice [167], and further investigation of this population is needed.

3.5.2 T cell activation and Tim-3 expression

Upregulation of CD38 on CD8 T cells has been well described in both chronic and primary HIV infection, where it is linked to long-term clinical outcomes [90–93] - and was a key finding here. This activation had largely, but incompletely resolved following 1 year of ART. The possibility that one year of ART is too short to fully resolve this activation and that, if sampled at a later time, this may have normalised is discussed below in section 3.5.4. Consistent with other reports [90, 391, 392], the level of CD38 expression at baseline was closely related to markers of disease progression including the baseline VL and CD4 to CD8 ratio. There was also a negative relationship between the time to ART initiation and CD38 expression on CD8 T cells. This reflects the fact that individuals who commenced ART further after seroconversion also had their immunophenotyping performed at this point. CD8 T cell activation peaks with VL (section 1.4.1) and the relationship observed here between time from seroconversion and CD38 expression mirrors that seen with VL (Figures 3.2 A and 3.15 A) - both likely reflect the decline from VL peak. This decline in VL and CD8 CD38 expression over time have both been reported in PHI cohorts [87–90, 97]. A relationship was observed between CD38 expression on CD8 T cells and to time to viral load suppression; this may be due to limitations in the utility of the baseline VL measurement in this cohort and is discussed further in Chapter 4 (section 4.5.2).

It is interesting that CD38 expression on CD4 T cells was not elevated as it was hypothesised that this compartment would also show marked activation. Most studies have used multiple markers of CD4 T cell activation, and increased HLA-DR/CD38 co-expression has indeed been shown on CD4 T cells during untreated

HIV infection [391, 393–395]. The findings presented here, however, are consistent with other reports of relatively stable CD38 expression on CD4 T cells during progression of untreated infection and following ART initiation [90, 387, 393]. One possible explanation for this is that CD38 is expressed at very high levels on circulating naïve CD4 T cells [393, 396], making the naïve compartment a likely source of the measured CD38. Together, these suggest that CD38 alone may be a less sensitive marker of activation on bulk CD4 compared with CD8 T cells.

Tim-3 featured prominently in the results and was highly elevated on all memory subsets during PHI, an increase which had incompletely resolved during ART. In addition, this was the only ICR with correlations at baseline to clinical parameters. Elevation of Tim-3 on bulk CD4 and CD8 T cells during primary infection has been previously reported where, as here, it was linked to VL and CD4 count [127]. In this initial report, Tim-3 expression on CD8 T cells was highly correlated with CD38 [127]. Indeed the expression of Tim-3 here was also closely related to that of CD38, shown by the correlation between Tim-3 and CD38 on CD8 T cells and co-expression of these markers at baseline. These findings contrast with what was observed in SPARTAC where CD8 T cell expression of Tim-3 did not correlate with VL or CD38 expression [134]; this study did, however, show that CD38/Tim-3 co-expression was linked to VL [134], supporting the connection between Tim-3 and CD38 observed here. Levels of both Tim-3 and CD38 remained elevated following ART. Persistent elevation of Tim-3 with suppressive ART has previously been shown during chronic infection where residual Tim-3 was linked to CD38 expression but not CD4 count or VL [127]. There were some differences in the pattern of Tim-3/CD38 co-expression between the two time points. During PHI Tim-3 was largely co-expressed with CD38 on both T-bet^{high}Eomes^{low} and T-bet^{low}Eomes^{high} CD8 T cells, consistent with previous findings [127]. Following 1 year of ART, the co-expression of these was elevated but there was also an elevation of populations that expressed one, but not the other of these markers. This divergence of expression raises the possibility of distinct roles in different stages of infection.

In a recent large-scale analysis of exhaustion-specific genes Tim-3 was not included because, like CD38, it was also highly expressed in effector as well as exhausted CD8 T cell transcriptomic signatures [171]. The close links consistently observed between CD38 and Tim-3 expression raise the question - is Tim-3 a marker of activation during early infection? Initial work by Jones *et al.* identified a role for Tim-3 in T cell exhaustion during HIV infection. In this study Tim-3^{high} cells had demonstrated defects in IFN-γ, TNF-α and CD107a expression which were evident during primary infection [127]. Defects in proliferation, cytotoxicity and the ability to rescue functionality via Tim-3 blockade, however, have only been assessed during the chronic phases of infection [127, 141]. The latter of these are effector functions which are largely lost in the progression from primary to chronic infection (section 1.4) and it is possible that during PHI Tim-3 marks a population of activated but not yet terminally exhausted cells; this hypothesis has not been investigated. The possibility that Tim-3 has activating roles has been previously raised [397] and is supported by recent findings that signalling through Tim-3 enhances TCR signalling and plays an activating role in LCMV infection models [398]. In this murine work, Tim-3 was involved in the generation of short-lived effector CD8 T cells - the authors speculate that Tim-3 may have more similarity to other co-stimulatory, rather than co-inhibitory receptors [398]. Tim-3 mediated expansion of short-lived effectors was associated with low Eomes expression [398] - consistent with observations here that the highest level of Tim-3 was on T-bet^{high}Eomes^{low} CD8 T cells and not on the terminally exhausted T-bet^{low}Eomes^{high} cells. In the SPARTAC trial, high Tim-3 expression was associated with slower disease progression, but only in individuals in whom this was measured within 12 weeks of seroconversion [134]. The reasons for this finding were unclear, as elevated levels of the other ICRs measured (Lag-3 and PD-1) were associated with faster CD4 T cell decline [134]. It could be hypothesised that high Tim-3 expression early during infection is associated with effector CD8 function - and could explain these results. The role of Tim-3 at different stages of HIV infection needs further investigation before this is used as an immunotherapeutic target.

3.5.3 ICR expression and co-expression

There were distinct patterns of ICR marker expression between different memory subsets of both CD4 and CD8 T cells. On CD8 T cells the highest levels of PD-1, Tim-3, CD39 and TIGIT during PHI were observed on EM CD8 T cells. For CD4 T cells, the TM subset expressed the highest levels of CD39, Tim-3 and TIGIT, with TM and EM CD4 T cells both having high PD-1 levels. In general, these were similar to what has been previously described [115, 133, 135–137, 147, 151, 156, 236, 242].

Reports of elevated PD-1 expression on bulk CD8 T cells in untreated HIV infection [131, 132, 147] are likely driven by both increases in EM CD8 T cells and changes in PD-1 expression. Consistent with several other reports [131, 132, 142, 147, 156], PD-1 expression was very high on HIV-specific CD8 T cells. During PHI PD-1 expression was elevated on naïve, CM and EM CD8 T cell subsets, but not on T_{EMRA} cells. This upregulation of PD-1 on less differentiated CD8 T cells, has been previously observed during PHI [140]. Persistent elevation of PD-1 on differentiated CD8 T cell subsets has been observed following ART initiated during in chronic infection [140] and, if untreated, PD-1 expression on memory subsets increases from primary to chronic infection [135, 140]. In contrast, following 1 year of ART PD-1 expression on CD8 T cells was no different from healthy controls suggesting that ART during PHI may abrogate these further increases in PD-1 levels.

Amongst CD4 T cells PD-1 was increased only on EM cells, and this did not resolve (indeed, this barely changed) following a year of ART. The subset-specificity of this elevation has been previously noted [135], as has the inability of early ART to reduce PD-1 expression on these cells [135, 140]. Classically, CM and TM CD4 T cells subsets are considered to be the most enriched for proviral DNA in the periphery [36, 206, 231, 234, 235], although EM cells also contribute to the HIV reservoir. Interestingly, although PD-1 expressing CD4 T cells are considered to be enriched for HIV DNA, this has only been shown for TM and CM subsets (the latter not quite reaching statistical significance), but not for EM cells [242]. This

suggests the persistent elevation of PD-1 on EM CD4 T cells may not be marking an enriched reservoir, and the functional implications of this requires further research.

Here, TIGIT expression was elevated on CD8 CM and EM T cells during PHI, but there were no changes in the CD4 T cell compartment. Previous reports have shown significantly elevated levels of TIGIT expression on bulk CD4 and CD8 T cells during chronic, but not primary infection [136, 137]. It appears that measuring this marker on memory subsets has allowed for detection of elevated expression at this earlier stage of infection and, if untreated, TIGIT levels may further increase on these cells. Indeed, following a year of therapy, TIGIT expression on all memory subsets was no different from healthy controls. This contrasts with findings from Tauriainen *et al.* who showed that TIGIT levels on bulk CD8 T cells continued to increase even if ART was started during PHI [137]. The reasons for this discrepancy are not clear, but one plausible explanation is the measurement of TIGIT on bulk versus memory CD8 T cells. Following treatment, TIGIT expression decreased on EM CD8 T cells such that there was a trend towards this being most highly expressed on T_{EMRA} cells. Thus, the drive towards more differentiated memory subsets observed following ART may increase the TIGIT measurements on bulk CD8 T cells.

This work is the first to report on the co-expression of PD-1, Tim-3 and TIGIT. Here, TIGIT was very commonly co-expressed with PD-1 on all memory subsets, a co-expression pattern that has been observed on productively infected CD4 T cells from viraemic individuals [250]. On both CD4 and CD8 T cells ICR co-expression was persistently elevated following ART. In general, however, the co-expression patterns observed here reflect what was shown for the individual ICRs. For example, persistent elevation of Tim-3 on EM CD8 T cells following a year of ART is reflected in the elevation of co-expressing combinations that all contain this marker. On CD4 EM T cells, where PD-1 expression was persistently elevated, all co-expressing subsets that remain elevated relative to healthy controls contain PD-1. On TM CD4 T cells, where Tim-3 was the only marker to remain abnormally high, Tim-3 and TIGIT co-expression was shown to be elevated relative to healthy controls. Most

of these co-expression patterns are driven by a single ICR, and the measurement of these combinations does not add substantially to these findings.

3.5.4 Partial but incomplete restoration of T cell parameters with early initiation of ART

Here there was partial but incomplete restoration of T cell parameters with early initiation of ART. This was characterised by persistent elevation of Tim-3, CD38 and PD-1 on EM CD4 T cells. One possibility is that one year of ART may not be sufficient to normalise all immunological parameters and, if measured at a later time point these may have resolved. There is, however, evidence that immune activation persists even after longer periods of ART started during early infection [116, 212, 379, 380] and it is conceivable that this is a long-lasting immunologic change. In one such study, levels of CD38/HLA-DR co-expression on CD8 T cells remained elevated relative to healthy controls after 96 weeks of ART initiated during PHI [380], but these levels reached a steady state 48 weeks after ART initiation. Similarly, levels of multiple ICRs (including PD-1 and TIGIT) have been shown to decrease markedly over the first year of ART initiated in early infection, but then plateau [135, 139]. Similar findings have been seen for chronic infection. In a very large study of soluble biomarkers of immune activation and inflammation were measured longitudinally; whilst many of these decreased over the first year of ART, further declines were not noted [399]. These studies all suggest that the initial declines in T cell activation and ICR expression noted may not continue or slow substantially over subsequent periods of time. It appears that events over the first year of ART are critical and supports the appropriateness of an initial one year time point. Nevertheless, consideration of whether the elevated Tim-3 expression observed here persists with longer periods of ART is an area for future research.

3.5.5 CD39 as a biomarker of T cell exhaustion

There was substantial variation in CD39 expression levels, with CD8 T cells from ~30% of individuals expressing negligible levels of this protein. Supporting the

observations made here, a number of SNPs associated with CD39 expression have been identified. In two largest GWAS studies of immune cell phenotypes, a large number of SNPs in or near the *ENTPD1* (CD39 encoding gene) locus were identified as being related to the surface expression of CD39 on both CD4 and CD8 T cells [400, 401]. In both datasets, CD39 was expression was the largest genetically-linked source of phenotypic variation observed. The associated difference in expression with this SNP remains stable over time within an individual, consistent with the findings presented here, and has been confirmed at mRNA, protein and functional levels [402, 403]. In one study the estimated population frequency of the low-expressing variant was 30% [404] - the same as the frequency of "non-expressors" defined here based on CD39 protein expression levels.

On CD4 T cells CD39 was expressed almost exclusively by T_{reg} cells and CD39 mediated catalysis of adenosine tri/diphosphate (ATP/ADP) to adenosine is one of the ways in which these cells exert their suppressive function [403, 405]. CD39 expression associated with one of these SNPs (rs10748643) has been directly linked to the suppressive capacity of T_{reg} cells, whereby individuals with a lower CD39 expressing genotype have less T_{reg} mediated suppression [403]. Another study failed to replicate this difference in suppressive capacity, but rather demonstrated a role for CD39 in driving effector CD4 T cell fate - linking the low expressing genotype with improved vaccine responses [404]. Both of these demonstrate CD39 expression on CD4 T cells to have a suppressive role on immune responses. A different CD39 SNP, rs11188513 (also identified in the GWAS above [400]), has been associated with progression to AIDS in several clinical cohorts such that individuals with a lower-expressing variant exhibited slower disease progression [406], consistent with its role in suppressing immune function.

The highest expression of CD39 was measured on CD4 TM cells. Of note, no specific markers of T_{reg} lineage (for example Foxp3 or CD25) were measured so it is not clear if the CD39 expression observed here is attributable to these cells. Based on descriptions in the literature, however, this is likely. Expression of PD-1 and TIGIT, but not Tim-3, was also elevated on CD4 TM T cells from individuals

with a low-expressing CD39 phenotype. This suggests that CD39 on these cells is playing a functional role, and that PD-1 and TIGIT may be compensating for its absence. In HIV-infected and uninfected individuals Tim-3 is not co-expressed with CD25 (a defining marker of classical T_{reg} cells) [127] - providing a potential explanation for this observation, and highlighting the different roles of these ICRs.

Whilst the reported association between HIV disease progression and CD39 was attributed to T_{reg} function [406], this thesis has shown that the phenotype is consistent between CD4 and CD8 T cells. Indeed, both the SNPs discussed above are linked with expression of CD39 on CD8, as well as CD4, T cells [400]. On CD8 T cells, CD39 has been identified as a specific marker of T cell exhaustion which may be more specifically up-regulated on exhausted CD8 T cells than PD-1 [129]. It is plausible, that the connection between the identified CD39 SNP and HIV disease progression could be mediated via CD8 T cell exhaustion. Of note, in this work there were no significant differences in baseline markers of disease progression (CD4 count, VL, CD4 to CD8 ratio) between individuals with different CD39-expressing status that would support this. A major limitation of this analysis is that CD39 genotyping was not performed, which would have confirmed a genetic basis for the phenotype observed, and allowed for analyses to be stratified by genotype.

Whilst the phenotypic differences observed with this genotype are stark, low-expressing variants remain common in the population, and few disease associations have been described; this suggests some redundancy in the role of CD39. Previously reported elevation of CD39 on CD8 T cells during HIV infection was confirmed [129]. The high level of genetic control of its expression, however, does have implications for the use of CD39 as a biomarker in population studies, potentially limiting its utility in this context and certainly highlighting the need to consider CD39 genotype.

3.5.6 Soluble immune checkpoint receptors

In large-scale studies, several soluble markers of inflammation and coagulation (including C-reactive protein, CRP and D-dimer) have been identified as predictors of mortality in individuals living with HIV [407, 408]. In part this has been possible

because soluble plasma markers are cheaper and simpler to measure in large numbers of samples than cell-based measures of immune function. Soluble forms of several ICRs including PD-1, Tim-3 and Lag-3 have been identified, but have not been widely studied in the context of HIV infection.

Soluble ICRs may interact with ICR pathways in two main ways. Soluble receptors may be biologically active by themselves, either by inducing signalling upon binding to their ligands, or competing with the surface form for that ligand. Soluble PD-1 is thought to be produced by alternative mRNA splicing [409, 410], and evidence from the study of rheumatoid arthritis suggests that sPD-1 can directly antagonise surface PD-1 function [409, 411]. Another mechanism for soluble ICR production is by cleavage from the cell surface. This may reduce signalling on the cell which originally expressed that molecule - this has been identified as the method of production of sTim-3 during HIV infection [412].

There are several lines of evidence that sPD-1 and sTim-3 have biological activity *in vivo*. Plasma levels of sPD-1 and sTim-3 are elevated in a number of autoimmune conditions where they have been linked to disease activity [409, 411, 413–417]. In chronic HBV infection high levels of both sPD-1 and sTim-3 are associated with the risk of development of hepatocellular carcinoma, independently of the viral load [418–420]. Whilst no prior work has characterised the expression of sPD-1 in HIV infection, treatment of CD4 and CD8 T cells from SIV-infected macaques has been shown to improve proliferative responses to peptide stimulation, and cytokine production [421, 422], similar to the results of blocking the PD-1 pathway with monoclonal antibodies. sTim-3 has been shown to be elevated in acute, primary and chronic HIV infection where it is correlated with markers of disease progression [412].

Here an exploratory analysis of the expression of sPD-1 and sTim-3 during PHI was performed, and showed that both markers are elevated relative to healthy controls. The finding of raised sTim-3 during early infection is consistent with previous observations [412], and is the first report to demonstrate similarly increased sPD-1 levels during HIV infection. Both markers had normalised to the levels seen in healthy controls following 1 year of ART. This work is also the first to report

the relationship between the surface expression of both PD-1 and Tim-3 to their soluble forms. Particularly interesting is the different patterns observed for both markers. Plasma Tim-3 correlated most closely with the expression of this marker on CD8 EM cells (also the subset with the highest fold elevation of this marker; Figure 3.5) and this was only observed prior to ART initiation. Here, the levels of sTim-3 mirror those of the surface protein and sTim-3 appears to act like an acute-phase reactant. Unlike Clayton *et al.* there was not a significant correlation of sTim-3 with VL (following correction for multiple comparisons), although the effect size observed was similar to the modest correlation they report [412].

In contrast, levels of sPD-1 correlated with PD-1 expression on differentiated subsets of CD4 and CD8 T cells, and only after 1 year of ART initiation. On these subsets PD-1 expression is likely to represent functional exhaustion. Prior to ART initiation, the only cell-surface ICR with any relationship to baseline markers of clinical progression was Tim-3 (PD-1 did not correlate with these). sPD-1 was also related to VL, CD4 count and CD4 to CD8 ratio - meaning this was more closely related to markers of disease progression than surface PD-1 at this time. These intriguing results suggest the possibility that sPD-1 could serve as a useful biomarker of T cell exhaustion during treated HIV infection, although this would need to be investigated further. Whilst perturbations in PD-1 expression during HIV infection have been well studied, few have considered other molecules that interact with this signalling. In addition to sPD-1, included here, the measurement of PD-1 ligands PD-L1 and PD-L2 and their soluble forms is also possible. If PD-1 blockade continues to be explored as a therapeutic option for HIV infection, consideration of these other aspects of the signalling pathways may help to improve stratification of who will benefit from this therapy. Furthermore, the measurement of sPD-1 could be a cost-effective and accessible means of measuring T cell exhaustion in the context of HIV infection - allowing this to be assessed in large scale studies.

3.5.7 Strengths and limitations of this work

In the era of "test and treat" more people living with HIV will commence ART early and an understanding of persistent immune deficits following early ART initiation will be critical. This well-characterised cohort of individuals treated during PHI was recruited as part of conventional clinical care in the United Kingdom and represent a "real-world" snapshot of what is likely to be achievable. This work has captured individuals from very early through to later in primary infection, and demonstrated some differences over these time periods; Fiebig staging was not performed as part of HEATHER and as such these analyses have not been stratified by time since infection. As a cohort study, one limitation is the variation, albeit small, observed in the time intervals between measurement of markers of clinical progression (which were collected as per routine clinical care), the baseline study visit and time of ART initiation.

Whilst this work has made an effort to characterise a large number of aspects of T cell activation, memory differentiation and ICR expression it is limited by the fact that it largely focuses on bulk, rather than HIV-specific T cells and does not contain any measures of T cell function. Effort has been made to measure ICR expression on memory subsets to delineate the differences between these two processes. The analysis, however, is limited by the choice of markers used to distinguish memory subtypes. There are high levels of heterogeneity within T cell populations and further division of these population (for example by CD28 expression, or CD27 on CD8 T cells) would be possible.

Finally, as discussed in section 3.5.4, the final time point studied here was 1 year following ART initiation and further longitudinal follow up would provide insight into the permanence of some of these observations.

3.6 Conclusion

This work aimed to characterise the immunologic changes during PHI and to examine whether ART initiated at this time results in normalisation of these. It has confirmed

that early HIV infection is characterised by major shifts in the differentiation of bulk CD4 and CD8 T cells, in particular by the expansion of activated, CD8 T cells with an EM phenotype. Following 1 year of ART, relative expansion of the T_{EMRA} T cells occurs, along with a decline in the terminally exhausted T-bet^{low}Eomes^{high} population. Overall, these suggest a permanent alteration in the T cell pool or the persistence of the driver of this change despite early ART initiation.

There were two key findings with relevance to biomarkers in cohort studies of HIV infection. The first is that CD39 may have limited utility in such contexts, due to near-zero expression in a substantial proportion of individuals. The second is the possibility of using soluble ICRs, particularly sPD-1, as measures of T cell exhaustion pathways.

Increased expression of the ICRs PD-1, Tim-3, TIGIT and CD39 on memory T cells was also seen - and in the case of PD-1 on EM CD4 T cells this elevation remained unchanged following ART initiation. Tim-3 expression was closely coupled with CD8 T cell activation, both parameters which partially but incompletely resolved after a year of ART - supporting the hypothesis put forward at the beginning of the chapter.

3.6.1 Next steps

This work was largely exploratory and has generated a number of interesting questions to be studied in the future including whether incomplete resolution of T cell activation, PD-1 expression and Tim-3 expression persists with more durable periods of ART. In addition, these findings suggest close links in early infection between CD8 T cell activation and Tim-3 expression; further work which looks at the function of this marker over the evolution of the HIV response is needed.

The increased expression of ICRs during primary HIV infection observed here has been linked to time to viral rebound following treatment interruption [255], a phenomenon which is also predicted by the size of the HIV reservoir [220]. The changes in T cell activation and memory differentiation observed here could also

plausibly be linked to reservoir size. To define this relationship further Chapter 4 explores whether the activation, memory differentiation and ICR expression of T cells relates to the size of the HIV reservoir.

4

The relationship between T cells and the CD4 T cell HIV reservoir during treated primary HIV infection

Contents

4.1 Context 108
4.2 Aims 109
4.3 Hypothesis 109
4.4 Results 110
4.4.1 HIV reservoir size following 1 year of ART is closely related to pre-ART reservoir size 110
4.4.2 Reservoir size is related to HLA class I alleles 110
4.4.3 Immunological and clinical variables associated with HIV reservoir size are highly correlated 112
4.4.4 Reservoir size at baseline is related to CD8 T cell activation and memory expansion 114
4.4.5 Reservoir size at baseline is the best predictor of reservoir size once stabilised on ART 117
4.4.6 Immunological variables at 1 year do not have a statistically independent relationship with HIV reservoir size . 118
4.5 Discussion 120
4.5.1 Proviral burden is set during early infection 120
4.5.2 Limitations of viral load during as a predictor of reservoir size 121
4.5.3 Activation, ICR expression and memory expansion . . . 123
4.5.4 Model selection - advantages and disadvantages 125
4.5.5 Strengths and limitations of this work 126
4.6 Conclusion 128

4.1 Context

Little is known about the immunological events that influence reservoir size. It is highly plausible that T cell immune responses, with their known role in mediating viral replication (see section 1.4.1), could limit seeding or facilitate decay of the HIV reservoir. Whilst there are very few studies that look longitudinally to define the formation of the HIV reservoir, there is some evidence that this may be the case. In the SPARTAC trial, both CD4 and CD8 T cell responses, as well as protective HLA class I alleles, were linked with lower levels of HIV DNA prior to ART initiation [255]. Adding to this, recent work from a cohort treated during acute infection showed that HIV-specific T cell responses could reduce VL, and limit reservoir seeding, when ART was initiated at peak viraemia [86]. Both of these suggest a role for T cell immunity during early infection in limiting initial reservoir size.

T cell activation is well-established as a mediator of disease progression in untreated individuals, and of non-AIDS co-morbidities during treated infection [9, 90–93, 233]. Many cross-sectional studies have also demonstrated a relationship between HIV reservoir size during ART and contemporaneous levels of both CD4 and CD8 T cell activation [117, 229, 255, 256, 423, 424]. Two recent longitudinal studies aimed to clarify this relationship. In individuals who initiated ART during chronic infection, no link between pre-ART inflammation/activation was observed with reservoir size over time [425]. Contrasting with this, in acute infection several soluble biomarkers linked to interferon-α (IFN-α) signalling were identified as correlates of subsequent reservoir size [426]. Further interrogation of these relationships is warranted.

There is also substantial evidence linking ICR expression to the size of the HIV reservoir (discussed in section 1.5.1). One of the limitations of many of these studies is that ICR expression has often been measured on bulk T cells. The HIV reservoir is preferentially found in memory subsets [36, 206, 231, 234, 235] which also express

higher levels of ICRs (demonstrated in Chapter 3). As such, ICR expression on bulk T cell subsets could be a surrogate for altered memory distribution and is recognised as an obvious confounder [138, 427]. Furthermore, many of these relationships were demonstrated for a single marker, even though the expression of many ICRs is closely related to one another - and also to T cell activation [127, 133–135, 137, 147–149, 153, 156, 171]. As such, the exact relationship of reservoir size with T cell subset distribution, activation and ICR expression remains to be defined.

As a prospective study of individuals commencing ART during PHI, HEATHER provides the opportunity to study reservoir dynamics over time. This work is the first longitudinal analysis of the potential influence of T cell activation and ICR expression on eventual HIV reservoir size. This chapter aims to define the relationship of several immunological and clinical parameters to the size of the HIV reservoir once stabilised on ART and provide insight into potential mechanisms and immunologic events which influence the reservoir.

4.2 Aims

Specifically, the aims of this chapter are:

- **Aim 1** To determine if HIV reservoir size on ART is related to T cell differentiation, activation and/or ICR expression;
- **Aim 2** If so, to explore if such relationships are independent of markers of clinical progression;
- **Aim 3** To establish if these relationships exist prior to the initiation of ART, once stabilised on ART or both.

4.3 Hypothesis

Pre-therapy viral burden and ICR expression on memory CD4 T cells is related to HIV reservoir size in individuals who commence ART during PHI.

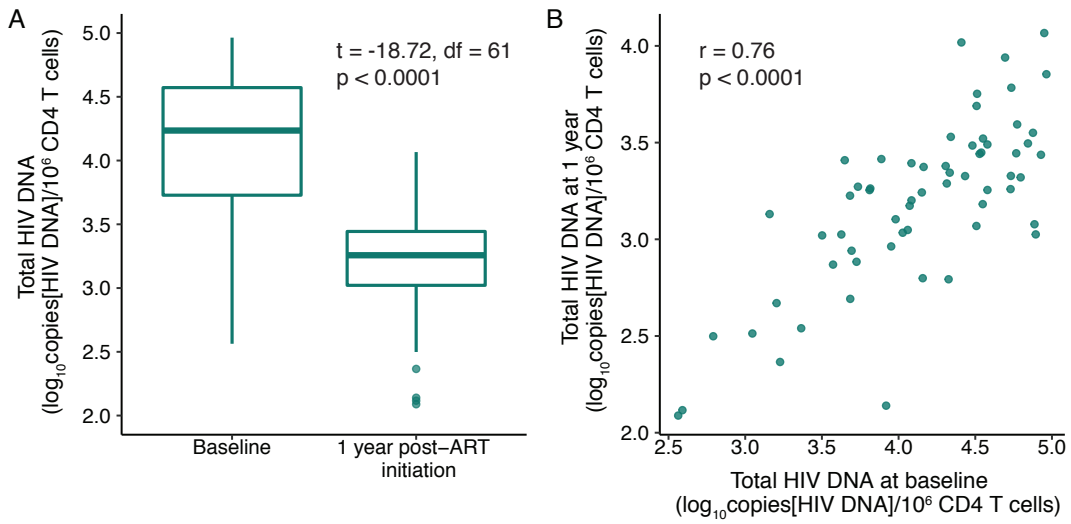


Figure 4.1: Relationship between total HIV DNA measured at baseline and 1 year following ART initiation. Data is shown for individuals with measures available at both time points (n=62). For (A) comparison was made using a paired t-test and in (B) a Pearson's correlation was performed.

4.4 Results

4.4.1 HIV reservoir size following 1 year of ART is closely related to pre-ART reservoir size

In this work, reservoir size was measured as total HIV DNA copies per 10^6 CD4 T cells. Results presented here are from 63 of 66 individuals described in Table 3.1 for whom a measurement of reservoir size at 1 year following ART initiation was available; the remaining 3 individuals did not attend study visits at 1 year. Compared with pre-ART levels, total HIV DNA decreased a mean of 0.9 $\log_{10}$ copies following 1 year of ART (Figure 4.1 A; p <0.0001). Levels of total HIV DNA pre-therapy and following 1 year of ART were highly correlated (Figure 4.1 B; r=0.76, p<0.0001).

4.4.2 Reservoir size is related to HLA class I alleles

HLA class I alleles have a well-characterised relationship with viral control during HIV infection; this analysis was performed to assess if there was also link with reservoir size. Figure 4.2 shows the relationship between HLA class I alleles and total HIV DNA at 1 year in the 61 individuals in this analysis for whom HLA type

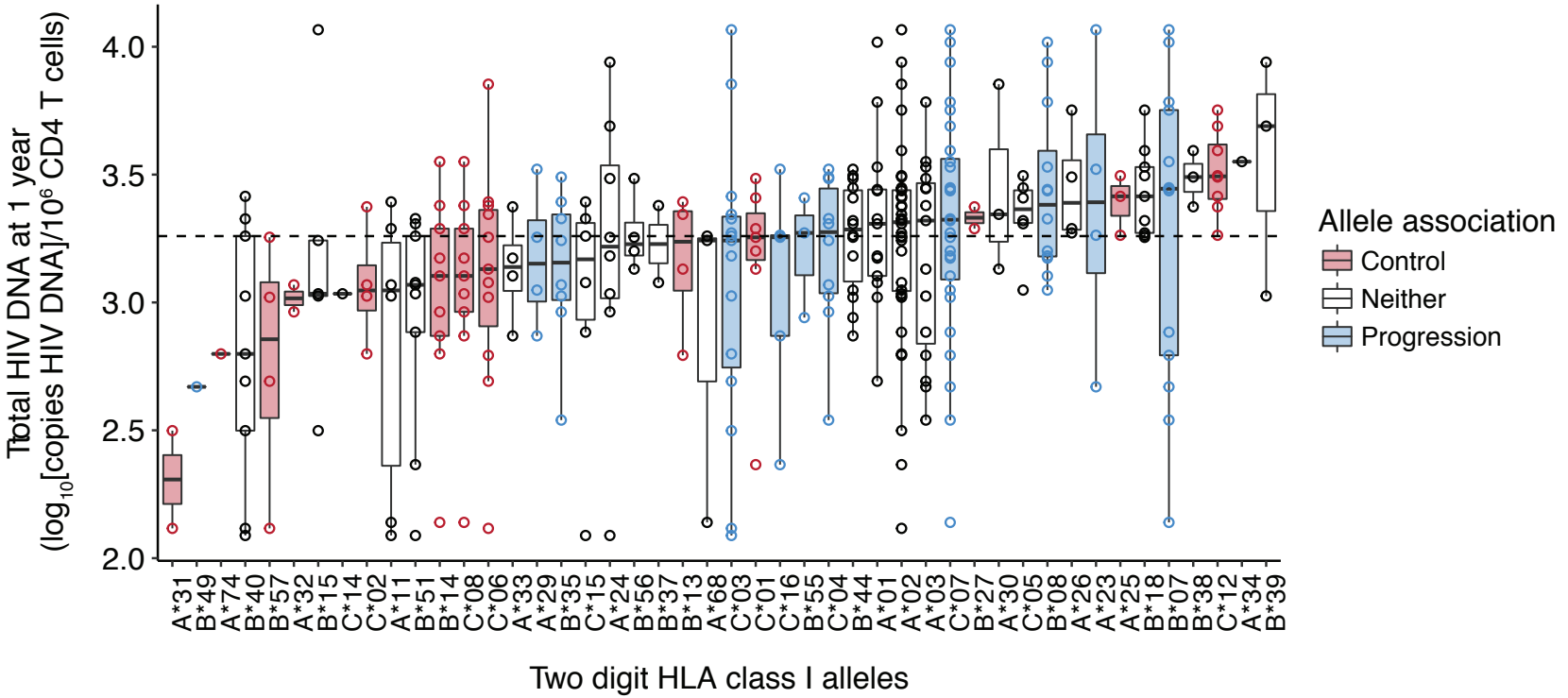


Figure 4.2: Relationship between HLA class I alleles and total HIV DNA at 1 year post-ART initiation. Alleles, shown on the x-axis, are ordered based on the median value of total HIV DNA for all individuals possessing that allele. Boxplots show the distribution of total HIV DNA in amongst individuals possessing that allele, and each observation is shown as an open circle. Data is shown for 61 individuals and a total of 333 alleles. For one individual only B alleles were available and are included here; similarly for another individual only A and C alleles were available. Where individuals were homozygous for a given allele, this is only shown once. The dashed line shows the median value of total HIV DNA for the entire cohort. Alleles were classified as being associated with disease progression (blue) or control (red), or neither (white), based on those identified in the International HIV Controllers Study at a significance level of 0.05 [73].

was available. In this figure, HIV DNA is shown for each allele represented in the cohort, with these alleles ordered by the median value of total HIV DNA amongst individuals possessing that allele. Alleles have been coloured as associated with viral control (red), progression (blue) or neither. An overall trend is apparent whereby the median total HIV DNA for alleles associated with viral control was lower, shown by a clustering of these alleles towards the left hand side of the plot. The converse is seen for alleles associated with progression. Unsurprisingly, this same relationship was observed with baseline HIV DNA (data not shown). This analysis was performed at two digit resolution, because the relatively small number of individuals in this cohort limited the interpretability of this plot when performed to four digit resolution.

4.4.3 Immunological and clinical variables associated with HIV reservoir size are highly correlated

Chapter 3 described a number of immunological and clinical parameters in the HEATHER cohort. Here, the relationship of these with the size of the HIV reservoir was assessed. Included in this analysis were the following: baseline clinical variables (CD4 count, CD8 count, VL, CD4:CD8, time to ART start and time to VL suppression on ART), the proportion of CD4 and CD8 memory subsets, the expression of ICRs (PD-1, TIGIT and Tim-3) on memory CD4 and CD8 T cells, soluble ICRs (sPD-1 and sTim-3), CD38 expression on CD4 and CD8 T cells and the proportion of T-bet/Eomes expressing CD8 populations. Several of these immunological and clinical parameters measured were highly correlated with HIV reservoir size at 1 year. Figure 4.3 A shows the relationship of reservoir size with all of the variables measured prior to the initiation of ART (baseline). Here, each row or column represents a different variable, and these are ordered by the strength of the correlation with reservoir size at 1 year (marked with an arrow). The presence of a circle indicates a significant correlation (at $p<0.05$), and the size and intensity of the coloured circle corresponds to the magnitude of the correlation coefficient. Variables with a significant relationship with reservoir size at 1 year are marked by a green square. Here, a couple of important observations can be made. First, the



Figure 4.3: Correlations between clinical/immunological variables and HIV reservoir size.

Figure 4.3: *continued.* Corrplots showing the relationship between HIV reservoir size at 1 year (log10totalDNA) and immunological/clinical variables (n=63) measured at baseline (A) or following 1 year of ART (B). Reservoir size at 1 year (log10totalDNA) is shown in the top left corner and is marked with an arrow. For both A and B, variables have been ranked based on the magnitude of absolute correlation coefficient with log10totalDNA in decreasing order from the top left hand corner. The size and colour of each circle corresponds to the correlation coefficient between any two variables. Correlation coefficients were calculated using the Spearman method with pairwise complete observations; only correlations significant at a 0.05 level are shown (other boxes are left blank). Green boxes enclose variables which have a significant correlation with log10totalDNA at a 0.05 level.

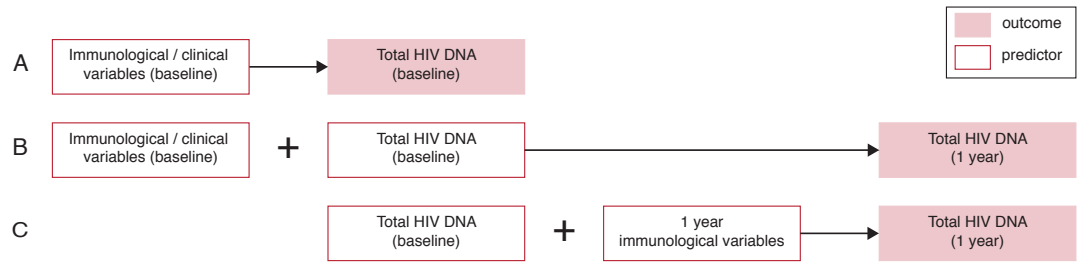


Figure 4.4: Stages of analysis to look at reservoir size

variable with the strongest correlation with HIV reservoir size at 1 year was reservoir size when measured at baseline. It can also be observed that the variables which were most closely related to reservoir size, in the top left hand corner, were also highly correlated with one another. Figure 4.3 B shows the same results for variables measured at the same time as HIV reservoir size (1 year post-ART initiation). Here, substantially fewer immunological variables were correlated with HIV reservoir size when measured at this time compared with at baseline.

4.4.4 Reservoir size at baseline is related to CD8 T cell activation and memory expansion

To further assess which variables were most closely related to HIV reservoir size, and the independence of these, regression models were fitted to the data. Correlative analyses suggested an important role for baseline total HIV DNA in determining reservoir size at one year. For this reason, the models were fitted as shown in Figure 4.4. Model A asks which variables are related to baseline total HIV DNA. Model B asks which variables when measured at baseline are related to reservoir size at 1

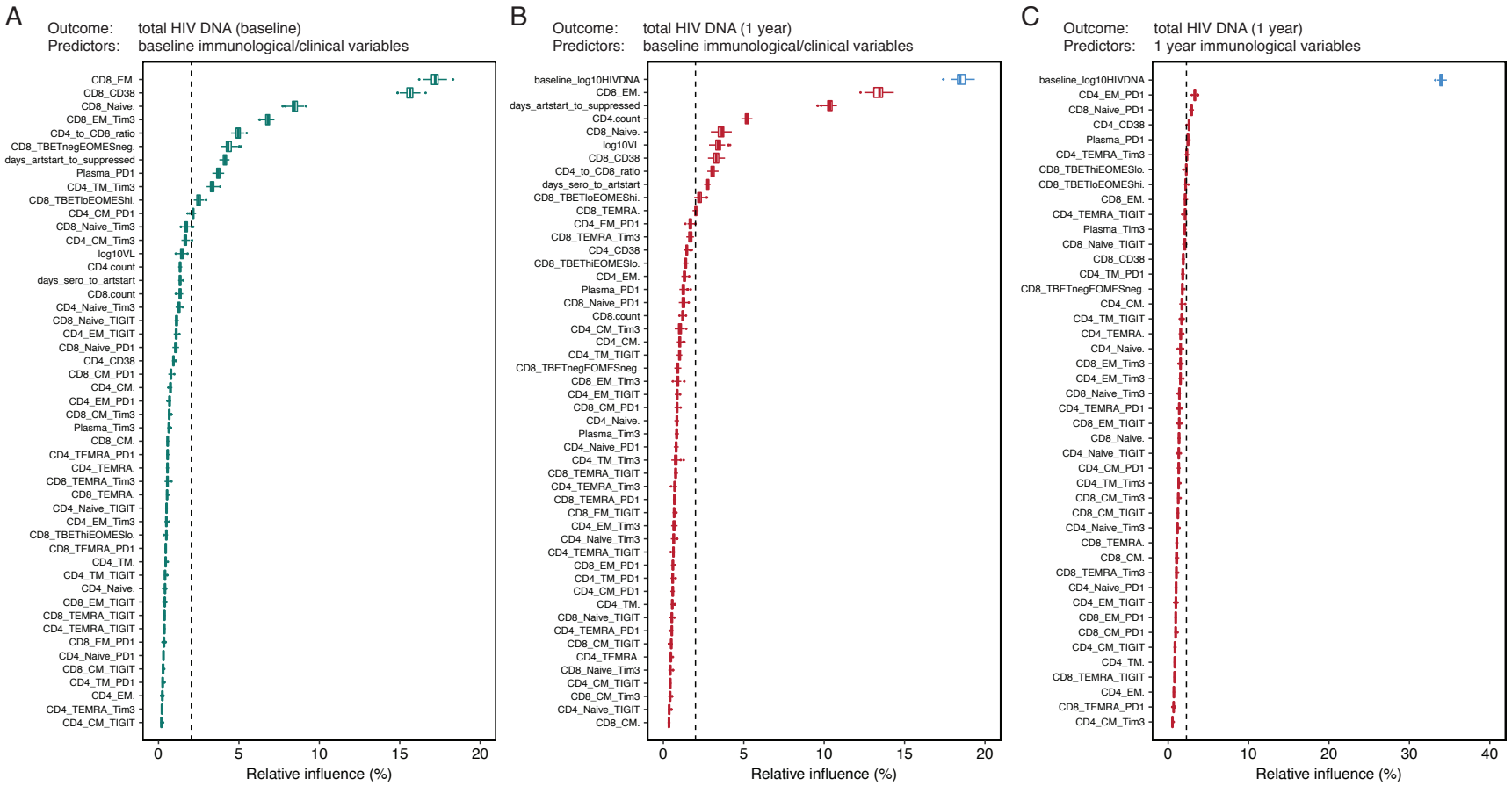


Figure 4.5: Boosted regression tree models to assess predictors of reservoir size. Outcomes of three different models are shown; each shows the summary results of 100 model runs as a box plot. Model A was constructed using baseline total HIV DNA as the outcome (49 predictors, n=62). B (50 predictors, n=63) and C (44 predictors, n=63) were constructed using total HIV DNA at 1 year as the outcome. In both B and C, total HIV DNA at baseline was included as a predictor and is highlighted in blue. Influential predictors were defined as those whose relative contribution was greater than 100 divided by the total number of covariates, this value is indicated by the dashed vertical line.

year (and includes baseline total HIV DNA, thus asking if these are independent of baseline total HIV DNA). Model C asks which variables are related to reservoir size at 1 year when measured contemporaneously and are independent of baseline total HIV DNA. For all three of these, two different types of regression were used: boosted regression tree (BRT) and least absolute shrinkage and selection operator (LASSO). Results for Model A (both BRT and LASSO) will first be presented along with a brief discussion of these techniques, then the results will turn to Models B and C.

This dataset poses several challenges in the fitting of multivariable regression models, most notably with missing data. Overall, 8.4% of observations are missing for this dataset. The most common reasons for this were unavailable samples, poor sample viability or low cell count. The pattern of missing data is shown in Appendix B (Figure B.8) and was $\leq$10% for each of the subsets of the data used to construct models A-C. In addition to missing data, the large number of parameters measured relative to observations, as well as the strong correlations between many of these variables are also problematic. To ensure the robustness of any conclusions drawn, two different types of model, both of which have different ways of dealing with these problems, were fitted to the data and their output compared. The relative merits of these two, BRT and LASSO, are discussed in detail in section 4.5.4.

BRT models are a machine learning approach that builds a series of regression trees, with each subsequent tree aiming to improve the fit of observations which were most poorly explained by the existing set of trees. Importantly, this approach can handle missing data so no imputation was required. Figure 4.5 A shows the relative importance of each predictor in a BRT model fitted with baseline total HIV DNA as the outcome, and all other baseline variables as predictors (model A in Figure 4.4). The relative influence of each variable can be estimated based on the number of times that variables is selected for splitting and the improvement to the model as a result of that split averaged across all trees; a higher number indicates a greater effect of the variable. Here the dashed line shows the expected relative influence if all of the variables had no relationship to the outcome. It shows that 10 of the 62 predictors had a consistent influence in predicting baseline reservoir size.

Notably, CD8 memory subsets (the proportion of EM and naïve cells), as well as CD8 CD38 expression were the variables with the highest relative influence.

LASSO is a type of multivariable regression which is designed to cope with multicollinearity and large numbers of predictors. It does this by adding a penalty to the coefficient of each term and is able to penalise coefficients to zero, thus performing variable selection. Linear LASSO models were fitted to the data and the results are shown in Table 4.1. As with other linear regression, models cannot be fitted with missing data. As such, two different models were fitted: one where the analysis was limited to only those observations with no missing data (complete) and one in which the missing values were imputed using a random forest based method of multiple imputation[1]. For model A, LASSO selected a subset of 6 variables with non-zero coefficients which were predictive of baseline total HIV DNA; all of these were also selected by the BRT model. The model constructed using the imputed and complete datasets selected the same variables, although the model constructed on the imputed dataset selected more variables than that restricted to only complete observations.

The variables with influence on baseline total HIV DNA size related to CD8 memory expansion (the proportion of naïve and EM, as well as T-bet^{neg}Eomes^{neg} CD8 T cells) and CD4 memory ICR expression (PD-1 on TM and Tim-3 on CM CD4 T cells), as well as CD38 expression on CD8 T cells; these are shown in the first two columns of Table 4.1. These findings are summarised diagrammatically in Figure 4.6 and indicate that when measured at baseline, CD8 memory expansion and activation as well as CD4 memory ICR expression had a relationship with the reservoir size at this time.

4.4.5 Reservoir size at baseline is the best predictor of reservoir size once stabilised on ART

Having established which variables were related to baseline reservoir size, models were then fitted to explore if any of the clinical or immunological variables had

[1]Values were not imputed for n=3 at baseline (Figure B.8 A, row F) and n=2 at 1 year (Figure B.8 B, row D) who had no immunological measures available at that time point.

Model	A	A	B	B	C	C
Outcome	HIV DNA (baseline)		HIV DNA (1 year)		HIV DNA (1 year)	
Predictors	baseline variables		baseline variables		1 year variables	
Data	complete	imputed	complete	imputed	complete	imputed
(Intercept)	4.14	3.94	1.96	1.72	2.13	1.91
CD8_Naive.	-0.0157	-0.0122	-	-	-	-
CD8_EM.	-	0.000999	-	-	-	-
CD8_CD38	0.00620	0.00743	-	-	-	-
CD8_TBETnegEOMESneg.	-	-0.00245	-	-	-	-
CD4_TM_Tim3	0.00242	0.00472	-	-	-	-
CD4_CM_PD1	-	0.00115	-	-	-	-
baseline_log10HIVDNA	-	-	0.271	0.339	0.248	0.311
days_artstart_to_suppressed	-	-	0.000458	0.000342	-	-
n	39	59	39	60	46	61
Deviance explained	0.64	0.67	0.51	0.58	0.42	0.47

Table 4.1: LASSO outputs for regression of immunological/clinical variables with reservoir size. Only variables with non-zero regression co-efficients are shown. Results are shown for three different models as defined in Figure 4.4. Model A was constructed using baseline total HIV DNA as the outcome (49 predictors). B (50 predictors) and C (44 predictors) were constructed using total HIV DNA at 1 year as the outcome. For each model, two different result are shown: one containing only complete cases of data, and the other where missing values were imputed.

additional, independent relationships with reservoir size at 1 year. Models B and C assessed the predictors of reservoir size at 1 year, and both included baseline total HIV DNA. In the BRT models (Figure 4.5 B-C), reservoir size at baseline was the most influential variable when combined with other pre-ART (model B) or 1 year (model C) variables. This was confirmed by the corresponding LASSO models (Table 4.1) with baseline HIV DNA being selected in both complete and imputed models.

4.4.6 Immunological variables at 1 year do not have a statistically independent relationship with HIV reservoir size

Having determined that baseline total HIV DNA is the best predictor of reservoir size at 1 year, models were then used to assess whether any of the immunological or clinical variables measured had an effect on reservoir size, independently of the

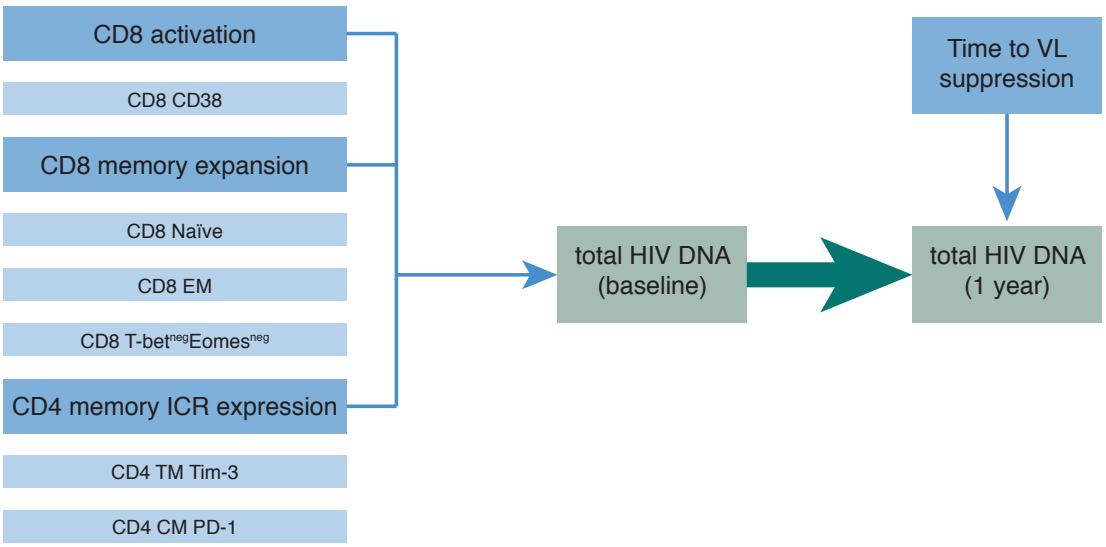


Figure 4.6: Model for factors which influence reservoir size in treated PHI from the results presented in this chapter.

baseline reservoir size. Figure 4.5 B shows the BRT model output when other baseline variables are included in the model and shows that several of these in addition to baseline total HIV DNA have influence in predicting reservoir size. Confirming this, LASSO models (Table 4.1) selected the time from ART start to VL suppression, in addition to baseline total HIV DNA as a variable with influence.

In contrast to what was observed at baseline, when the immunological variables measured at 1 year were included in the models (Figure 4.5 C; Table 4.1) none of these had influence on reservoir size at 1 year, independently of total HIV DNA measured at baseline. This is consistent with the modest correlations observed in Figure 4.3 B.

Variables that were influential in determining HIV reservoir size at 1 year are summarised in Figure 4.6. This shows that the best predictor of HIV reservoir at 1 year was reservoir size at baseline, which was linked to a number of immunological parameters at this time. Time to viral load suppression also had an influence on reservoir size, but no immunological parameters measured at 1 year had an independent relationship with reservoir size.

4.5 Discussion

This work has analysed the relationship of clinical and immunological parameters with the size of the HIV reservoir in individuals who commence ART during PHI. Overall, it has demonstrated the importance of immunological events during PHI in influencing eventual reservoir size. Here, the level of HIV DNA prior to ART initiation was the most important predictor of reservoir size following 1 year of ART, suggesting that reservoir size may be "set" during early infection. Interestingly, the level of HIV DNA pre-ART was more closely related to CD8 T cell activation, memory expansion and CD4 ICR expression than any of the clinical parameters measured.

This study adds significantly to understanding of the factors that influence eventual reservoir size. Importantly, this is the first study to show the relationship between T cell activation, memory expansion and ICR expression to eventual reservoir size. As a longitudinal study, it has been able to demonstrate that this relationship is mediated via the pre-therapy reservoir size - providing insight into the importance of this time point. Additionally, by including markers of memory differentiation, activation and ICR expression the relatedness of these phenomena during PHI has been demonstrated (discussed in section 4.5.3).

4.5.1 Proviral burden is set during early infection

One of the key findings of this analysis is that the HIV DNA level prior to ART initiation was the most influential predictor of subsequent reservoir size. This is similar to a recent analysis of treated chronic infection where pre-therapy HIV DNA levels correlated with the same at 1, 4 and >6 years on ART [425] and has been observed in several other studies [428–430]. These findings support previous research suggesting that set point HIV DNA levels in untreated individuals are reached shortly after peak VL [431], and extends this to show that this is true even if ART is started early.

A recent study of soluble biomarkers during acute infection demonstrated that several of these were related to HIV reservoir size (also measured by total HIV DNA) prior to and following 96 weeks of ART, independently of VL [426]. The soluble biomarkers identified can all be produced by myeloid cells in response to IFN-α/γ signalling; the authors speculate this could indirectly reflect innate and/or T cell responses to viral replication [426]. The analysis presented here supports these findings, and demonstrates a link between T cell activation and reservoir size. Of note, these results clearly show that the influence of these T cell parameters is mediated via the initial proviral burden; this is the first such analysis to demonstrate this relationship.

It remains unclear if these same relationships would exist during chronic infection. Gandhi *et al.* observed a relationship between T cell activation during chronic infection and HIV DNA in individuals commencing treatment at this time [425]. Unlike in both early infection studies ([145] and this analysis), this relationship did not persist following adjustment for baseline VL - suggesting time-dependent differences in the relative influence of baseline VL and T cell activation as predictors. It is possible that the influence of activation/inflammation on HIV reservoir size is strongest during early infection, and further longitudinal studies are need to confirm this.

4.5.2 Limitations of viral load during as a predictor of reservoir size

It is interesting to note that the viral load was only modestly correlated with baseline HIV DNA, as it had been hypothesised that these would be closely linked. Indeed, VL was not a significant predictor in either model fitted. Several studies have demonstrated a relationship between pre-therapy VL and HIV DNA [425, 429, 430, 432–435]. Notably, many of these studies included individuals treated during chronic infection, where the VL will have reached set point. In contrast, during PHI the viral load is substantially more labile. Within this cohort there was a link between baseline VL and the time after estimated seroconversion that this was

measured (Figure 3.2) whereby individuals with more recent seroconversion had a higher VL. This was also observed in another PHI cohort with similar time since infection [97] and suggests that VL measures taken over this time capture the decline from peak, rather than a steady state. Within HEATHER there is some variation in the time interval between when baseline VL and HIV DNA were measured (median 16 days; range 0-82 days). Both of these factors may contribute to the relatively weak relationship between VL and baseline HIV DNA observed here.

Two findings suggest an influence of viral burden on overall reservoir size. The first is the previously reported relationship between HLA class I alleles and HIV reservoir size [255], which was confirmed here. The well-characterised relationship between HLA class I alleles and VL is mediated via CD8 T cell killing of virally infected cells; stronger CD8 responses could result in smaller HIV reservoir size by both limiting seeding (via VL reduction) and contributing to decay of the pool of infected cells. The second relevant finding is the observation that time to viral load suppression had a influence on reservoir size independently of baseline HIV DNA level. This may be because individuals with longer time to VL suppression may have a window following ART initiation for reservoir seeding to continue. Alternatively, slower time to viral suppression may reflect higher pre-therapy viral burden not captured in the baseline VL measurement. Whilst most individuals commenced ART at or shortly after their baseline visit (median 0 days, 82% within 1 week), a small proportion had a larger interval between these (maximum 48 days) providing additional time for reservoir seeding not captured in the baseline HIV DNA measurement.

It is also possible that the overall pre-ART viral burden (both duration and magnitude of viraemia) influences HIV reservoir size, and is poorly captured by a single measurement during PHI. Indeed, the consistent observation that earlier ART limits reservoir size, even over the short time periods between the first three Fiebig stages [86, 428] implies a role for the total pre-therapy viral burden. Recent work from the FRESH cohort has shown CD8 T cell responses in acute infection are very closely linked to viraemia copy days, a measure of the cumulative viral

burden [436]. Within this subset of the HEATHER cohort, most individuals only had a single VL measurement prior to the initiation of ART. The calculation of cumulative viraemia was so significantly influenced by this value that it did not alter to the findings presented here (analysis not shown).

4.5.3 Activation, ICR expression and memory expansion

In addition to the finding that proviral burden appears to be set during PHI, there were also shown several relationships of immunological parameters to reservoir size. CD8 T cell activation (measured by CD38 expression) and differentiation (a decrease in naïve and T-bet^{neg}Eomes^{neg}, and increase in EM cells) were both associated with reservoir size. CD8 T cell memory expansion is an immunological hallmark of early HIV infection and associated with initial viral control (section 1.3), so it is not surprising that these same mechanisms may limit proviral burden during PHI. No relationships were observed with initial reservoir size and CD4 count or CD4 to CD8 ratio, although these have been previously reported [36, 242, 425, 429, 430, 432, 433, 435, 437]. This appears to be due to the close correlation of both of these parameters to the proportion of CD8 memory subsets, which did persist in the LASSO models (Figure 4.3 A). Overall, there was evidence for a significant link between the differentiation of CD8 T cells and reservoir size.

Higher levels of initial T cell activation were associated with increased reservoir size. This is consistent with the SPARTAC study where CD38 expression at baseline was significantly associated with total HIV DNA at that time [255]. It is possible that this is driven by higher initial viral burden (see section 4.5.2); it could also reflect poorer CD8 effector function suggesting that activation and dysfunction may already be coupled during PHI. Cross-sectional studies of primary and chronic HIV infection have shown relationships between contemporaneous HIV DNA and CD8 T cell activation during ART [117, 229, 233, 423, 424], although this has not been consistently demonstrated [430, 438, 439]. Such a link between CD8 activation following ART and HIV DNA levels was not observed here. Of note, in this work CD38 expression was used to define activation and most prior studies have

used HLA-DR/CD38 co-expression. Work from Cockerham *et al.* suggests that HIV DNA was only related to HLA-DR and not CD38 expression [423]. Notably, although no variables measured at 1 year predicted reservoir size independently of the baseline level, the variable most correlated with reservoir size at this time was the proportion of EM CD8 T cells. It is possible that this has captured residual immune activation not reflected in CD38 expression.

It is notable that the two measures of ICR expression which related to reservoir size were measured on TM and CM CD4 T cells, the subsets that most enriched for proviral DNA In the periphery [36, 206, 231, 234, 235]. Several cross-sectional studies have shown a relationship between PD-1 expression on bulk CD4 T cells during ART and overall reservoir size [229, 242, 256]; CM and TM CD4 T cells expressing PD-1 are also enriched for proviral DNA [36, 242]. The findings presented here demonstrate a relationship between PD-1 expression on CM CD4 T cells supporting these prior observations and showing that this relationship exists during untreated PHI. Contrasting with prior work, here this relationship did not continue during ART. The proportion of CD4 T cells with a CM phenotype did correlate with HIV DNA during ART (Figure 4.3 B), but was not independent of the baseline total HIV DNA. It is possible that previous studies, which have measured PD-1 on bulk T cells [229, 242, 256], are actually capturing this shift in memory proportions; this discrepancy could also be due to differences between individuals who commence ART in primary, compared with chronic, infection.

It is not known why ICR expressing cells on ART are enriched for proviral DNA. The results presented here suggest that this relationship is established in early infection. One possibility is that ICR expression is up-regulated on activated cells (which are more likely to be infected). Subsequent ICR-mediated modulation of cellular activation may also increase the possibility of that infection becoming latent [130]. Further supporting the role of these markers in early infection, expression of ICRs PD-1 and Tim-3 on bulk CD4 T cells in the SPARTAC study was predictive of viral rebound following TI, but only when measured prior to ART initiation [255]. Interestingly, whilst a link was demonstrated between PD-1 and Tim-3 with

reservoir size, these markers predicted viral rebound even when adjustment for total HIV DNA was performed [255] - suggesting multiple mechanisms in which ICR blockade may be beneficial in HIV cure strategies.

Overall, the nexus of T cell activation, memory expansion and viral replication during PHI seems to be closely linked to reservoir size. Does higher immune activation facilitate increased viral replication and therefore reservoir size? Or does this activation and memory expansion occur in response to a larger viral burden? The high level of correlation observed between these parameters makes it difficult to define what is driving this. These results suggest that targeting of host or viral factors which lead to early viral expansion and T cell activation may be a way of limiting HIV reservoir size.

4.5.4 Model selection - advantages and disadvantages

Datasets with large numbers of measured parameters relative to observations are becoming common in the biological sciences, with newer experimental techniques producing high-dimensional datasets. Here, two contemporary approaches to regression modelling which are able to address this problem have been employed.

In this chapter, fitted models have been structured around the baseline HIV DNA and look at each time point separately. This approach was appropriate because of the central role of baseline total HIV DNA in determining reservoir size at one year, and has produced highly interpretable models that clearly demonstrate the importance of variables measured at baseline but not at 1 year. This approach was also used in a recent analysis of soluble biomarkers which predict reservoir size [426].

The use of BRT models for this dataset has several advantages. In particular, this approach is able to handle missing data, does not make assumptions about the effect of predictor variables and can handle high-dimensional interactions [440]. The complexity of the BRT models fitted make it difficult to interpret the relationships between variables and the response. In contrast, the coefficient of the LASSO indicates whether a relationship with the outcome is positive (e.g.

CD38 expression on CD8 T cells) or negative (e.g. the percentage of naïve CD8 T cells). Whilst the penalisation applied by LASSO is able to manage multicollinearity and large numbers of predictors, these models have all of the challenges of fitting conventional generalised linear models: the need to specify model structure, assumptions about the distribution of residuals, and a need for datasets without missing data. These limitations may mean that decisions made during the fitting process have a substantial influence on the model outcome. In the results presented here, the fact that both models selected the same variables supports the robustness of the results presented. Furthermore, the LASSO models constructed on complete and imputed datasets was almost identical, with the exception of model A where more variables were selected in the imputed dataset, likely due to the increased power of the larger number of observations. This suggests that the imputation process has not introduced bias into the dataset.

In these results, the biggest difference in the output from the two models is that the LASSO models have selected fewer influential variables. This appears to be due to the way that these models handle correlated predictors which are present in this data. In the BRT models, the relative influence of two predictors which are highly correlated will be split between these predictors and as such this will select a larger number of variables that are important in explaining variation in the outcome. In the same situation the LASSO model, in contrast, will select only the variable with the strongest relationship with the outcome.

4.5.5 Strengths and limitations of this work

Several of the associations with reservoir size presented here have been observed previously - but almost always in isolation. Additionally, by measuring a number of these together the interrelatedness of these can be explored. By measuring ICR expression on memory T cell subsets the impacts of memory differentiation and ICR expression have been isolated - factors which are confounded in studies that measure this markers on bulk T cells. Whilst a comprehensive analysis of ICR, activation and T cell differentiation was performed, one limitation of this work

is that reservoir size was only measured using total HIV DNA. This measure is clinically relevant as lower levels have been associated with delayed viral rebound following TI [220–223]. Much of the HIV reservoir, however, is not replication competent [7, 188, 202, 216–218, 226]. Whilst total HIV DNA has been suggested to reflect replication-competent reservoir size in cohort studies [226], this work has not assessed if there is any impact of these immunological measures on the quality of proviruses comprising the reservoir.

A major strength of this study is its longitudinal design. It is possible, however, that 1 year of follow up is not sufficient time for ART to stabilise the HIV reservoir and that these results may not reflect the long-term reservoir. In two studies of chronic infection strong correlations were observed between HIV DNA levels at early time points and those much later (6-15 years) after ART initiation [425, 430, 441]. This is likely to also be true for individuals treated in PHI, as a more rapid initial decay of the reservoir compared with chronic infection has been observed and is attributed to less stable unintegrated DNA forms [210, 212, 432, 442]. This suggests the reservoir might be more stable by 1 year in individuals treated during PHI compared with chronic infection. Supporting this, in one study of treated PHI, measurements of total HIV DNA at 1 year were similar to the final time point available [116]. Despite these supportive observations, it remains possible that the relationships observed here may not be applicable at later time points.

Additionally, there are a number of immunological parameters which were not measured. In particular, without measuring T cell functionality it is not possible to define further the role of CD8 T cells in limiting initial reservoir. Work suggesting a role for soluble inflammatory markers suggested the importance of the myeloid compartment in early stages of HIV reservoir formation [426]. The innate and adaptive immune responses operate closely together, but here no aspects of innate immune function were measured. Finally, CD8 T cell activation emerged as a major influential factor, but only used a single marker was used to define T cell activation - it would be interesting to see if there are any difference between other measures

of activation, particularly given observations of a link between HLA-DR but not CD38 expression and reservoir size on ART [423].

4.6 Conclusion

This chapter aimed to define which of the immunological variables measured were related to reservoir size, if these were independent of clinical parameters and whether these relationships existed prior to or during ART initiated in PHI. This study adds to a growing body of evidence demonstrating the importance of events during early HIV infection and shows that reservoir size appears to be "set" during PHI. This work has shown that the magnitude of the early immunological insult, reflected in the CD8 T cell activation and memory expansion, is closely linked to initial HIV reservoir size. This immunological response, rather than the hypothesised viral burden, had the strongest link to reservoir size. This work has also confirmed findings that connect ICR expression on CD4 T cells with reservoir size, consistent with my hypothesis, and demonstrated that these exist even during untreated PHI. Overall, these suggest that PHI may be an appropriate time to target T cells to reduce HIV reservoir size.

5

CD32 as a marker of an enriched CD4 T cell HIV reservoir during treated primary HIV infection

Work presented in this chapter has been published in the below article:

> Martin GE*, Pace M*, Thornhill JP* *et al*, CD32 expressing CD4 T cells are phenotypically diverse and can contain proviral HIV DNA. *Frontiers in Immunology*, **8**(928) (2018).

Contents

5.1 Context 130
5.2 Aims 131
5.3 Hypothesis 131
5.4 Results 131
5.4.1 Depletion of CD32 expressing CD4 T cells by negative bead selection due to the expression of non-T cell markers 131
5.4.2 CD32 expressing CD3+CD4+ cells differ in their expression of immune checkpoint receptors and memory phenotype 135
5.4.3 $CD32^{high}$ CD3+CD4+ T cells are activated and express high levels of HIV co-receptors 136
5.4.4 HIV DNA in CD32 expressing CD3+CD4+ cell subsets 136
5.4.5 The frequency of CD32 expressing CD3+CD4+ cells is not related to the overall size of the HIV reservoir . . . 138
5.4.6 $CD32^{high}$CD4+ events are doublets which pass through a doublet exclusion gate 142
5.5 Discussion 142

5.5.1 Other studies of CD32 and the HIV reservoir have excluded the CD32^{high} population 144
5.5.2 The existence of B/T cell doublets can explain the observed phenotype of CD32^{high} events 145
5.5.3 Failure to reproduce a marked enrichment of HIV DNA in CD32-expressing cells 147
5.5.4 Associations of CD32-expression on CD4 T cells with activation and transcription 148
5.5.5 Lessons learnt and implications for future studies of markers of an enriched HIV reservoir 150
5.6 Conclusion 151

5.1 Context

Latently infected cells are extremely rare (0.0001 - 0.1% of CD4 T cells), complicating their study. Accordingly, there has been a research effort to identify cell surface markers that identify latently infected cells in order to facilitate their characterisation. A marker of an enriched HIV reservoir could also be used as a target in therapeutic interventions. CD32a (FcγRIIa) - a low affinity IgG receptor expressed on myeloid cells and granulocytes [443], has been proposed as a surface marker for latent HIV infection [245]. Whilst this finding is of extremely high interest, the expression of CD32 on CD4 T cells remains controversial and a role for low-affinity Fc receptors on these has not been well-established [444–446]. Although CD4 T cells are generally not considered to express CD32, expression may be induced by activation *in vitro* [447, 448]. Expression of CD32b on memory CD8 T cells in murine infection models is associated with reduced cytotoxicity and expansion, reversible on CD32b blockade [449]. This has interesting parallels with other co-inhibitory pathways, raising the possibility that CD32 isoforms may have a similar regulatory role on activated, antigen experienced CD4 T cells.

Here CD32 expression on CD3+CD4+ cells was studied and distinct populations that express this marker identified. CD32 expressing CD4 T cells in the blood of individuals treated during PHI were characterised, along with potential associations of these cells with overall reservoir size, cell phenotype and clinical progression.

Since the initial report of CD32a as a putative marker of an enriched HIV reservoir [245] there has been a considerable research effort to confirm, or refute, this finding [251, 450–455]. This work was conducted at that time and was one of the first studies in a growing body of evidence that CD32 does not mark a substantially enriched CD4 T cell reservoir. Importantly, this work identifies that CD32 expression on CD4 T cells unexpectedly occurs with a number of B cell markers - a key step in understanding the biological relevance of this population, and the implications of this marker for HIV cure strategies.

5.2 Aims

Specifically, the aims of this chapter are:

- **Aim 1** To investigate the phenotype of CD32-expressing CD4 T cells in healthy individuals and primary HIV infection;
- **Aim 2** To verify enrichment of HIV DNA in CD32+ CD4 T cells;
- **Aim 3** To explore the association between CD32 expressing CD4 T cells and measures of overall HIV reservoir size.

5.3 Hypothesis

CD32 is a marker of CD4 T cells enriched for HIV DNA in individuals treated during PHI.

5.4 Results

5.4.1 Depletion of CD32 expressing CD4 T cells by negative bead selection due to the expression of non-T cell markers

The experimental study of CD4 T cells frequently incorporates a commercial bead-based negative selection kit in the laboratory protocol to produce a purified

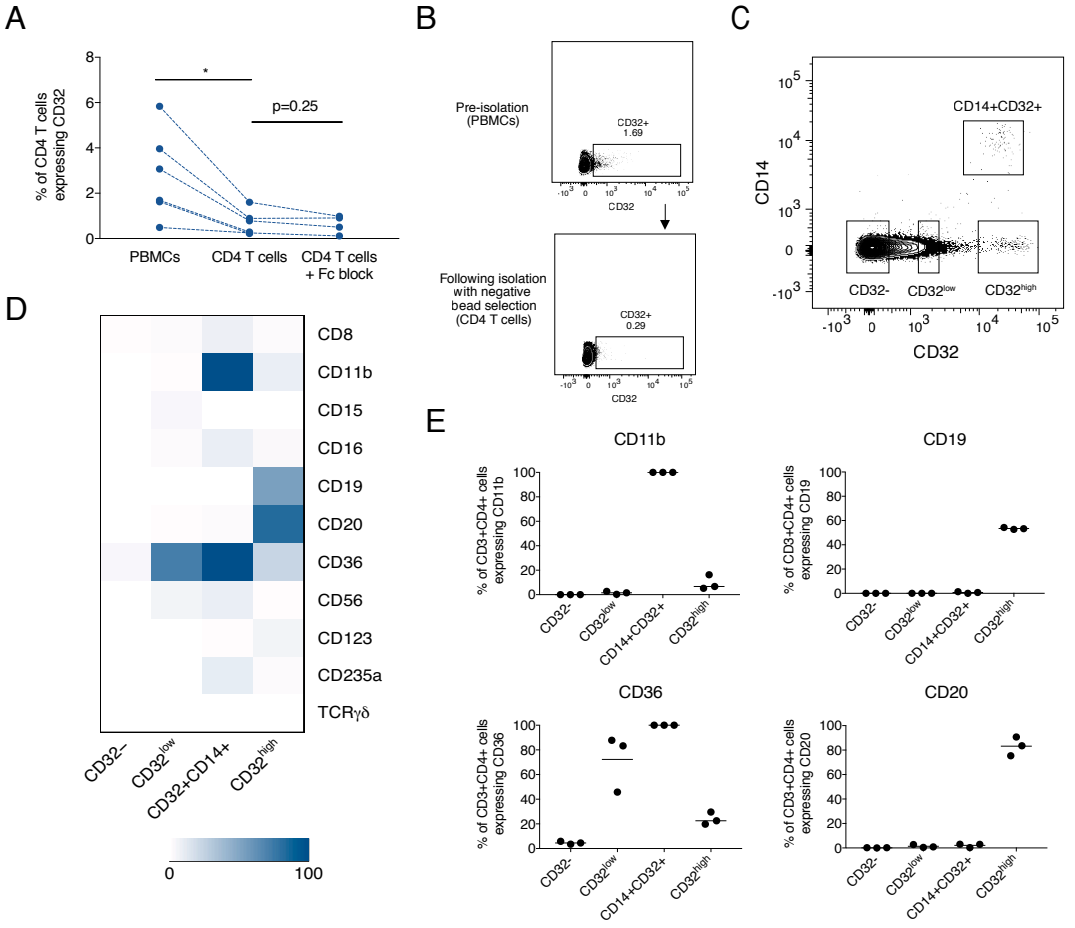


Figure 5.1: Depletion of diverse populations of CD32 expressing CD4 T cells by negative bead selection due to the expression of non-T cell markers. (A) The frequency of CD32+ CD3+CD4+ T cells when measured in PBMCs, or in CD4 T cells purified by negative bead selection, with and without Fc block prior. (B) Representative gating of data shown in A. (C) Gating of three CD32 expressing populations based on differing levels of expression and CD14: $CD32^{low}$, CD32+CD14+ and $CD32^{high}$. (D) Heat-map showing the percentage expression of markers used in CD4 negative bead isolation kits on subsets of CD3+CD4+ T cells (defined in C). Expression was measured by flow cytometry and values are shown as the mean of three individual donors. (E) Percentage expression of CD11b, CD19, CD36 and CD20 on CD3+CD4+ subpopulations as shown in D. Bar is shown at the mean.

population of CD4 T cells from bulk peripheral blood mononuclear cells (PBMCs). CD32 expression on purified CD4 T cells isolated by negative bead selection was noted to be consistently lower than in CD4 T cells in PBMCs. To test if the cell purification kits depleted CD32 expressing CD4 T cells, the frequencies of CD32+ CD4 T cells before and after negative selection were measured by flow cytometry. A significant decrease in CD32 expression after negative selection was observed (Figure 5.1 A and B) and this was not prevented by pre-treatment with an Fc blocking reagent to control for non-specific antibody binding (Figure 5.1 A).

As these data suggested that CD32+ CD4 T cells express other surface molecules specifically depleted by the negative selection kit (which does not contain anti-CD32 antibodies), the possibility that CD32 was co-expressed with other lineage-defining markers was tested. A panel of these markers was based on those included in CD4 T cell selection kits from several manufacturers. These were: CD8, CD11b, CD14, CD15, CD16, CD19, CD20, CD36, CD56, CD123, TCR$\gamma\delta$ and CD235a. The monocyte marker, CD14, distinguished a separate population of CD32+CD14+ cells. The remaining CD14-CD32+ cells could be divided into two distinct populations, $CD32^{low}$ and $CD32^{high}$ (Figure 5.1 C). Further characterisation was performed of lineage marker expression in these four populations: CD32-, $CD32^{low}$, $CD32^{high}$ and CD32+CD14+ and found clear phenotypic differences, consistent with four distinct cell populations (Figure 5.1 D). CD32- CD4 T cells did not express significant levels of any tested lineage markers. CD32+CD14+ cells all expressed CD11b (Figure 5.1 E) and were found almost entirely within a monocyte-rich FSC/SSC region (Figure B.9), consistent with these cells being monocytes despite high levels of CD3 expression. It is possible that these cells are monocytes which have acquired CD3 via trogocytosis. The $CD32^{low}$ population expressed high levels of CD36 (Figure 5.1 E), a scavenger receptor typically found on platelets and monocytes in blood but which has also been reported on CD4 T cells interacting with platelets [456]. The $CD32^{high}$ cells expressed high levels of CD19 and CD20, traditional markers of B cells (Figure 5.1 E).

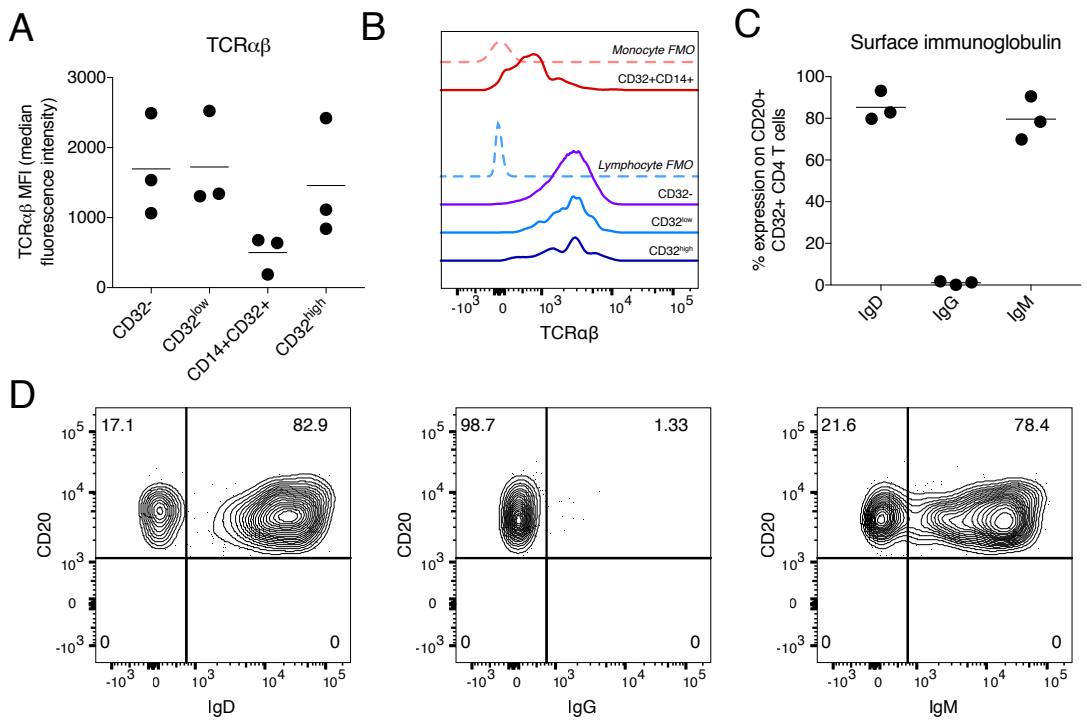


Figure 5.2: Characterisation of T cell receptor and immunoglobulin (Ig) expression on CD32^{high}CD3+CD4+ T cells. (A) Expression of TCRαβ on CD32 expressing CD3+CD4+ T cell populations was measured by flow cytometry and is shown here as median fluorescence intensity. Bar is shown at the mean. (B) Histogram showing TCRαβ staining on CD32 expressing CD3+CD4+ T cell populations of one sample shown in (A). Fluorescence minus one (FMO) controls are shown as dashed lines and individual populations as solid lines. (C) Percentage expression of Ig was measured on CD3+CD4+CD32^{high}CD20+ cells. Expression of IgD, IgG and IgM is shown. Expression was measured by flow cytometry and bar is shown at the mean. (D) Representative staining of data shown in (C).

As the CD32^{high} population has been reported to have the highest level of persistent HIV infection [245], further characterisation of this population was performed. These cells also expressed CD3, CD4, CD19 and CD20, whether these cells expressed other markers associated with B or T cell lineage and function was tested. To confirm that cells expressing CD3, CD4 and CD32 were T cells, staining was performed for TCRαβ expression. As would be expected for T cell populations, the CD32-, CD32^{low} and CD32^{high} populations all expressed similar levels of TCRαβ, while the CD32+CD14+ cells expressed very little, consistent with this subpopulation being monocytes (Figure 5.2 A-B). The expression of IgG, IgD, and IgM on the CD32^{high} cells was also examined. The CD32^{high} population,

which co-express CD20 and TCRαβ, expressed high levels of IgD and IgM, but not IgG, similar to a naïve B cell phenotype [457, 458] (Figure 5.2 C-D). These results, surprisingly, show that the CD32^{high} population express both T and B cell phenotypic markers.

Overall, these results have clear implications for those exploring the findings of Descours *et al.* [245] as negative bead isolation of CD4 T cells will not only reduce the overall number of CD32+ CD3+CD4+ cells but also affect the composition of the overall CD32 expressing population.

5.4.2 CD32 expressing CD3+CD4+ cells differ in their expression of immune checkpoint receptors and memory phenotype

The phenotype of CD32 expressing CD4+ populations was further characterised in individuals who commenced ART during PHI from the HEATHER cohort. Key demographic and clinical characteristics are shown in Table B.8. In these individuals both CD32^{low} and CD32^{high} CD3+CD4+ populations were studied without the use of cell enrichment kits (representative gating shown in Figure 5.3 A) and imposing a conservative lymphocyte gate to eliminate the CD32+CD14+ population (Figure B.9). In treated HIV+ individuals, the expression of PD-1, Tim-3 and TIGIT was elevated on CD32^{low} CD3+CD4+ cells compared with their CD32- and CD32^{high} counterparts (Figure 5.3 B-D).

The memory phenotype of CD32-, CD32^{low} and CD32^{high} CD3+CD4+ cell subsets was compared during treated PHI. CD32^{low} CD4 T cells had lower proportions of naïve and CM T cells than their CD32- counterparts. In contrast, TM, EM and T_{EMRA} cells made up a greater portion of the CD32^{low} CD4 T cell pool than for CD32- CD4 T cells (Figure 5.3 E), reflecting a more differentiated memory phenotype. In contrast, the CD32^{high} population largely consisted of cells which expressed CD45RA marking a naïve or T_{EMRA} phenotype. It is interesting that CM CD4 T cells, the memory subset with the highest level of proviral DNA [36, 236], were most common among CD32- cells and less frequent amongst both CD32^{low} and CD32^{high} cells.

The overall phenotype of these cells did not differ between participant groups. This same pattern of differential ICR expression was observed prior to ART initiation and in healthy controls, except for Tim-3 which was expressed at very low levels in CD4 T cells from controls; similarly, these cells had the same memory phenotype prior to ART initiation and in healthy controls (data not shown). The distinct phenotype of CD32-, CD32^{low} and CD32^{high} populations with regards to memory differentiation and ICR expression adds to the lineage marker evidence that these are distinct cellular populations, and are found in healthy as well as HIV-infected individuals.

5.4.3 CD32^{high} CD3+CD4+ T cells are activated and express high levels of HIV co-receptors

Amongst treated HIV-infected individuals (n=19, Table B.8) CD32^{high} CD3+CD4+ cells expressed markedly elevated levels of the activation marker HLA-DR compared to both other populations (Figure 5.3 F). In healthy controls, the expression of CCR5 and CXCR4, the co-receptors used by HIV for cellular entry, was increased on CD32^{high} CD4 T cells (Figure 5.3 G-H). For CCR5, this was also observed on the CD32^{low} population.

5.4.4 HIV DNA in CD32 expressing CD3+CD4+ cell subsets

Cells from participants treated during PHI (Table B.8) were sorted directly into the four CD3+CD4+ populations (CD32-, CD32^{low}, CD32+CD14+, and CD32^{high}; representative gating in Figure B.12) and HIV DNA measured by quantitative PCR (qPCR). HIV DNA was successfully quantified in sorted CD32-, CD32^{low}, CD32+CD14+, and CD32^{high} CD3+CD4+ T cells from most individuals (Figure 5.4). There was some degree of HIV DNA enrichment within CD32^{low} cells from most individuals, although this was generally of low magnitude. CD32+CD14+ cells also contained detectable HIV DNA in most individuals. HIV DNA was detectable in the CD32^{high} population from 7 of 9 individuals sorted, which was

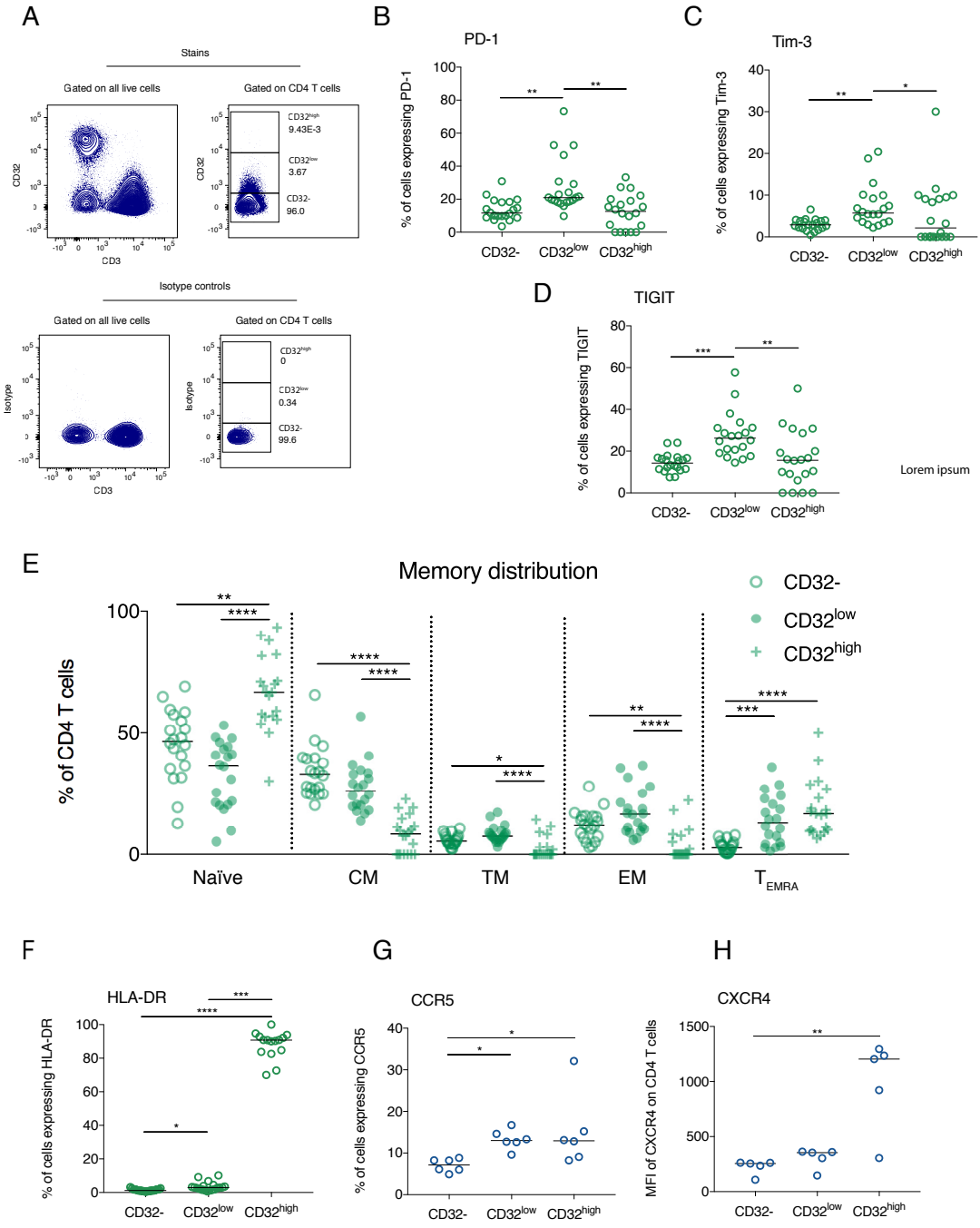


Figure 5.3: Further characterisation of CD32 expressing CD3+CD4+ cells. Representative gating of CD32 expressing populations on CD4 T cells from an HIV+ individual is shown (top panel) in (A), relative to isotype control (bottom panel). CD32-, CD32^{low} and CD32^{high} CD3+CD4+ T cell populations were compared with regards to their expression of PD-1 (B), Tim-3 (C), TIGIT (D; all n=20) and HLA-DR (F, n=19). For F, four samples were excluded from the analysis of the CD32^{high} population because there were 5 or fewer events.

Figure 5.3: *continued.*These same populations were compared with regards to their memory phenotype. The percentage of each population comprising naïve, central memory (CM), transitional memory (TM), effector memory (EM) and T_{EMRA} cells was quantified by flow cytometry and is shown in E (n=20). The comparisons are all shown in HIV+ individuals at 1 year following the initiation of antiretroviral therapy. The expression of HIV co-entry receptors CCR5 (G; n=6) and CXCR4 (H; n=5) was compared between CD32-, $CD32^{low}$ and $CD32^{high}$ CD3+CD4+ T cell populations in healthy individuals. Throughout, a Kruskal-Wallis test was used to compare all three groups; pairwise comparisons were performed on all combinations of groups only if the overall test p-value was <0.05. **** indicates p<0.0001, *** indicates p 0.0001-0.001, ** indicates p 0.001-0.01, * indicates p 0.01 – 0.05; for ease of interpretation if p≥0.05 for any comparison this is not shown on these plots.

enriched in four of these. The degree of enrichment varied substantially between individuals (Figure 5.4 B).

Extremely low cell inputs into the qPCR could result in over-estimation of both albumin and HIV DNA (Figure B.13), which would need to be considered when comparing different cell populations. To show that low inputs of HIV DNA did not give false positive signals, sorted CD32- HIV DNA was diluted such that each well contained <1 copy of HIV DNA. Under these conditions, there was no detectable signal in 21 wells (n=3 individuals, 2 or 3 triplicate dilutions per individual; from experiments in Figure B.13 B). Numbers of sorted cells from these experiments were sufficient to alleviate concerns regarding low input bias in the qPCR (Table B.9). These results show HIV DNA was detectable in all three populations of CD32 expressing CD4 T cells and that some enrichment in $CD32^{high}$ was observed in some individuals, although not in all. These experiments, however, have not been able to replicate the magnitude of enrichment or the inter-individual consistency reported by Descours *et al.* [245], despite starting with a similar number of PBMCs.

5.4.5 The frequency of CD32 expressing CD3+CD4+ cells is not related to the overall size of the HIV reservoir

To further explore the proposed association with CD32 expression and the HIV reservoir, additional individuals commencing ART during PHI from two clinical trials (SPARTAC and HEATHER) were studied. Key demographic and clinical

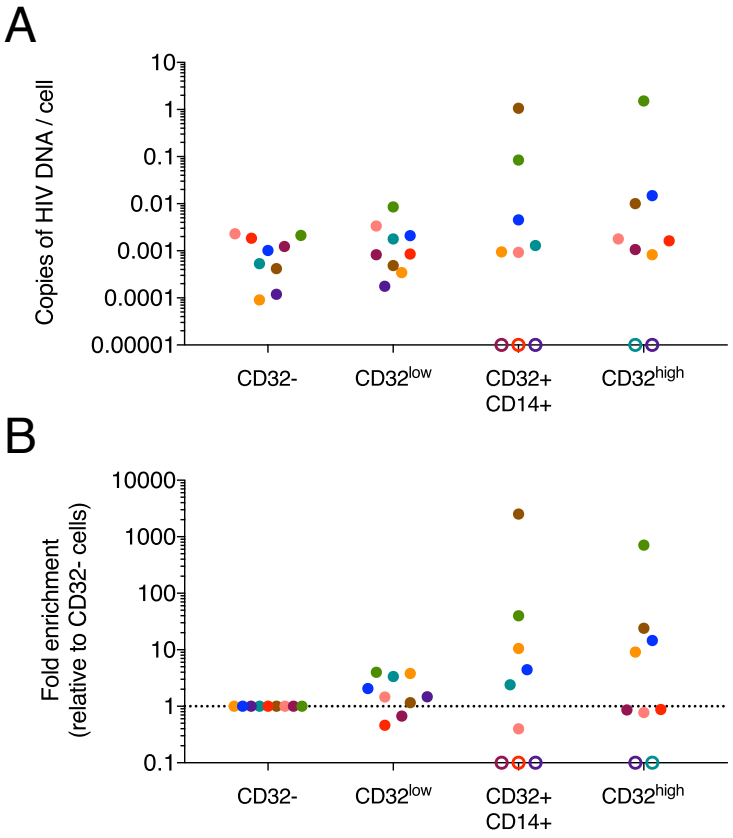


Figure 5.4: HIV DNA quantification in sorted CD32 expressing CD3+CD4+ T cell populations. HIV DNA was quantified in sorted CD32-, $CD32^{low}$, CD32+CD14+ and $CD32^{high}$ CD3+CD4+ T cell populations by qPCR (n=9). (A) Shows the absolute quantification of these data and (B) shows the fold change relative to the CD32- population. Copies of HIV-1 DNA were quantified and normalised to number of input cells (as determined by albumin PCR). PCR reactions for both albumin and total HIV were performed in triplicate for the CD32- population and in duplicate for the remaining three populations. Data shown are averages of the replicates. Data points are coloured by the individual from which the population was sorted. Where no signal was detectable for a given sorted population this is shown as an open circle on the axis. For all of these undetectable populations, it could not be determined if they were in fact negative for HIV DNA as the predicted level of infection (assuming equivalent level of infection to the CD32- fraction) was below the level of detection of our assay based on the available input cell equivalents.

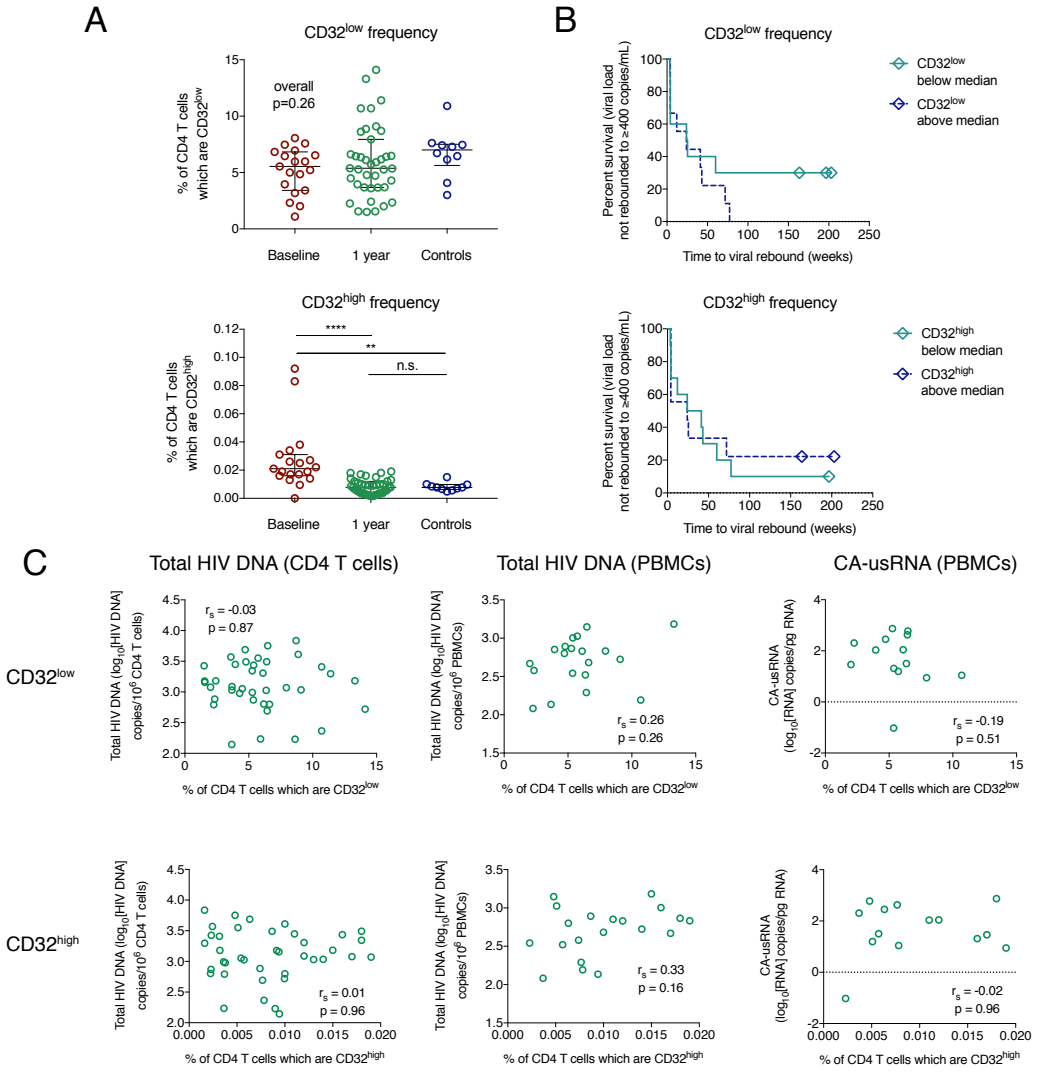


Figure 5.5: The frequency of CD32-expressing CD3+CD4+ cells does not correlate with the size of the HIV reservoir. The percentage of $CD32^{low}$ (top panel) and $CD32^{high}$ (bottom panel) CD3+CD4+ cell populations is shown in (A) for HIV+ individuals with primary HIV infection pre-therapy (baseline; n=19) and 1 year following ART initiation (n=39), as well as for controls (n=10); groups were compared using a Kruskal-Wallis test. Bars indicate the median with the interquartile range. Panel (B) shows survival curves (Kaplan-Meier) of time to viral rebound >400 copies/mL based on the frequency of $CD32^{low}$ (top panel) and $CD32^{high}$ (bottom panel) CD3+CD4+ cells stratified at the median (n=19). The relationship between measures of the HIV reservoir and percentage of $CD32^{low}$ (top panels) and $CD32^{high}$ (bottom panels) CD3+CD4+ cells in treated HIV+ individuals, shown in (C), was assessed using Spearman's rank correlation. Left column shows total HIV DNA measured in isolated CD4 T cells (n=39), the centre column is total HIV DNA measured in PBMCs (n=20) and the right column shows cell-associated unspliced HIV mRNA (n=14). **** indicates $p<0.0001$, ** indicates p 0.001-0.01, n.s. (not significant) indicates $p\geq0.05$.

characteristics are shown in Table B.8. The median time from estimated seroconversion to ART initiation was 74 days (IQR 36–114 days). Median baseline plasma VL was 4.94 $\log_{10}$ [copies/mL] (IQR 4.09–6.52) and CD4 T cell count was 545 cells/µL (IQR 453-696). Clinical, immunological and reservoir measures presented are at baseline (before the initiation of ART) and after 1 year of ART (median 48.1 weeks; IQR 47.9-52.9 weeks). Healthy controls (n=10; 100% male; median age 34.5 [IQR 30.5-42.5] years) were included for comparison.

For participants on ART, the median percentage of $CD32^{low}$ cells was 5.38 (range 1.51–14.1%) and the rarer $CD32^{high}$ population was 0.008% (range 0.002–0.02%). The frequency of $CD32^{low}$ cells did not differ from pre-therapy levels (median 5.55%, range 1.09-8.05%) or healthy controls (median 7.00%, range 3.00 – 10.9%; Figure 5.5 A; p=0.26). The frequency of $CD32^{high}$ cells was elevated during PHI relative to healthy controls (median 0.02%, range 0.01-0.09% versus median 0.007%, range 0.005-0.015%; p=0.0004), but had decreased to similar levels (p<0.0001) following 1 year of ART (Figure 5.5 A).

Whether the percentage of CD32 expressing CD3+CD4+ cells predicted time to VL rebound after TI was assessed in a subset of individuals after 48 weeks of suppressive ART (n=19). In Cox models, there was no evidence to support such an association for either $CD32^{low}$ or $CD32^{high}$ cells (Figure 5.5 B, Table B.10). Three individuals remained virologically suppressed at the end of follow up after TI (median 197 weeks), all of whom expressed levels of $CD32^{low}$ below the median (Figure 5.5 B). There was no correlation between the percentage of $CD32^{low}$ or $CD32^{high}$ cells and the overall size of the HIV reservoir on ART as measured by several assays: total HIV DNA in negatively selected CD4 T cells, total HIV DNA in PBMCs and the level of CA-usRNA in PBMCs (Figure 5.5 C). HIV DNA was also measured in CD4 T cells prior to ART initiation and again no correlation was observed between this and frequency of CD32 expressing populations (data not shown). In summary, there was no evidence that CD32 expression on CD4 T cells is a surrogate of the total reservoir size as measured by HIV DNA, CA-usRNA or time

to viral rebound. This is likely to be not just because CD32^{high} cells are rare but that, even if enriched, a large part of the HIV reservoir is contained in other cell types.

5.4.6 CD32^{high}CD4+ events are doublets which pass through a doublet exclusion gate

Other investigators noting CD3 and CD20 co-expression have attempted to determine if this finding might be artefactual and secondary to contamination, cell doublets, cryopreservation or cell separation techniques [459, 460]. To exclude the possibility that this phenotype was an artefact of density gradient separation or cryopreservation of PBMCs phenotyping was performed on fresh, whole blood from healthy donors and a similar pattern of CD32 and CD20 co-expression on CD3+CD4+ cells was observed (Figure B.10).

For all experiments, cells were tightly gated on singlets (as shown in Figure B.11 A), to minimise the possibility of a doublet artefact in our data. Of note, performing a second doublet exclusion step does not change the frequency or phenotype of these cells (Figure B.11 B). This gating approach, which is widely used, has been shown to permit some doublet events to pass through giving rise to rare populations expressing unusual combinations of markers [461]. To further investigate this, imaging cytometry was used to visualise the CD32^{high} cells. As with regular flow cytometry, this approach measures fluorescence information about each event, but also records microscopy images linked to events. CD32^{high} events (gated as previously) were examined from two different healthy donors. Figure 5.6 shows representative images from three CD32^{high} events. These show that CD3 and CD4 are co-expressed on a single cell, as are CD19 and CD32. The CD32^{high} event is composed of a doublet of a CD4 T cell and a B cell. Importantly, there were no clear singlet events that expressed CD3, CD4 and high levels of CD32.

5.5 Discussion

When measured by flow cytometry, CD3+CD4+CD32+ cells comprise several subpopulations with differing levels of CD32 expression and co-expression of other

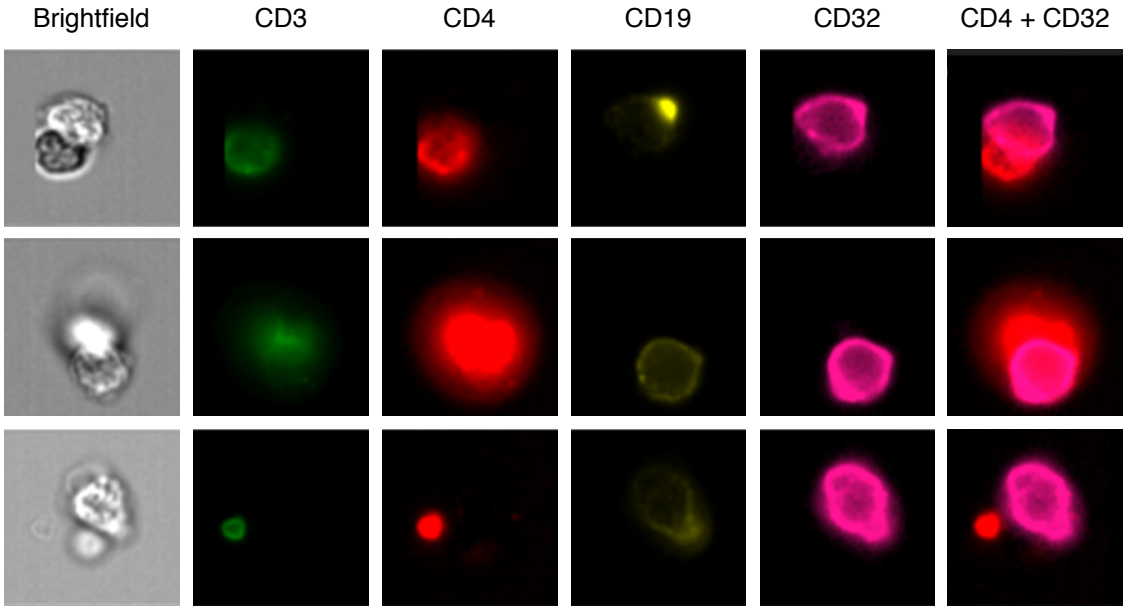


Figure 5.6: Imaging cytometry of CD32^{high} CD4+CD3+ cells. Three representative events from CD32^{high} gate are shown. Stains for CD3 (green), CD4 (red), CD19 (yellow), CD32 (pink) are shown. The last panel shows the overlay of CD4 and CD32.

markers. In particular, CD32^{high} events are largely doublets of CD4 T cells and B cells which can be detected despite stringent singlet gating. Here, there was no relationship between the frequency of CD32+ subpopulations and reservoir size by several measures including time to viral rebound following TI. By sorting CD32 expressing CD3+CD4+ events, a modest enrichment of HIV DNA was observed in some, but not all donors, and this was not of the magnitude that was initially described [245].

The original report of CD32a as a marker of a substantially enriched reservoir [245] was of significant interest within the field. This discussion will focus on some key technical aspects of the study of CD32 that are relevant to the interpretation of these findings, as well as this important paper. In their study, Descours *et al.* used an *in vitro* model of latent HIV infection that utilises the ability of the SIV accessory protein Vpx to overcome SAMHD1 restriction and allow integration of HIV into resting CD4 T cells [245]. The authors identified genes which were differentially expressed between latently infected and uninfected cells, some of which had corresponding surface proteins. These included *FCGR2A*, the gene

encoding CD32a; in this model, CD32 had the highest differential protein expression between latently infected and uninfected cells. Crucially, the authors then sorted CD32 expressing CD4 T cells from ART suppressed individuals and showed marked enriched in $CD32^{int}$ (equivalent to the $CD32^{low}$ gate described here) and $CD32^{high}$ CD4 T cells - an average of 633 and 1024 fold respectively [245].

5.5.1 Other studies of CD32 and the HIV reservoir have excluded the $CD32^{high}$ population

Given the heterogeneity described here, it is worth briefly mentioning how differences in flow cytometric gating strategies have impacted upon studies of CD32 and the HIV reservoir. Here, attempts were made to reproduce the gating strategy of Descours *et al.* who, for their *ex vivo* studies, did not gate out activated, naïve or lineage-marker expressing events [245]. As such, the existence of subpopulations within the CD3+CD4+CD32+ pool was clearly shown, and the division into $CD32^{low}$ and $CD32^{high}$ cells clearly reproduced. It is within the $CD32^{high}$ cells that the highest level (approximately 1000-fold) of enrichment was reported [245], and is the population of most interest. The results in this work demonstrate that this $CD32^{high}$ population consists of CD4 T cell/B cell doublets. Almost all other studies of the relevance of CD32 have used an additional gating step excluding either naïve (CD45RA+) [450, 453], HLA-DR+ [450] or CD14/CD19+ [452, 454] cells for their characterisation of *ex vivo* samples. These approaches represent a conservative approach to focusing on cells of interest in the study of the HIV reservoir. In doing so, however, all of these papers will have excluded the $CD32^{high}$ population reported to be most enriched by Descours *et al.* [245], as B cells express high levels of CD45RA [458], HLA-DR [458] and CD19. These reports thus examine populations which likely correspond to the $CD32^{low}$ or a combination of the $CD32^{low}$ and CD32+CD14+ populations characterised here.

Several isoforms of CD32 exist, of which CD32a (FcγRIIa) and CD32b (FcγRIIb) are the most widely expressed. These two isoforms have an almost identical extracellular domain, but different intracellular signalling domains such that signalling

through CD32b on antigen presenting cells is activating, but inhibitory through CD32a [443, 462]. In the *in vitro* model used to identify CD32 as a marker of the reservoir, Descours *et al.* note that *FCGR2A*, the gene encoding the CD32a isoform was specifically up-regulated, but not that of other isoforms [245]. Experiments extending this finding to HIV-infected individuals used the anti-CD32 antibody clone FUN-2, which does not distinguish between different CD32 isoforms. In the work presented here this same antibody clone was used, as for most other studies following up the original work [251, 262, 450, 453–455, 463]. CD32b, but not CD32a, is highly expressed on B cells [445]; the good staining of B cells with this FUN-2 clone observed here indicates that it binds to this CD32 isoform. Aware of this, Coindre *et al.* used a CD32a-specific antibody for their mass-cytometry characterisation of CD19-CD4+CD32a+ cells from infected individuals [451]. The CD32 measured on the $CD32^{high}$ population here and by Descours *et al.* likely comes from the CD32b isoform expressed on B cells.

Overall, due to either gating approaches or antibody choice, other studies exploring the relationship between CD32 and the HIV reservoir have characterised different subpopulations of the CD32+ cells described here - and have likely excluded the $CD32^{high}$ cells described to be most enriched by Descours *et al.*.

5.5.2 The existence of B/T cell doublets can explain the observed phenotype of $CD32^{high}$ events

The observation that $CD32^{high}$ events expressed a number of B and T cell markers was surprising. Whilst rare, CD20-expressing T cells populations have been described in healthy individuals and in a number of non-malignant disease states [459, 460, 464–467]. Of note, the cells described here differ from these reports which generally expressed CD20 but not CD19. The expression of CD19 on $CD32^{high}$ CD4 T cells was also recently confirmed by another group [455]. Subsequent imaging cytometry revealed that these events were, in fact, doublets of B and CD4 T cells. Unpublished work from Osuna *et al.* has also shown the presence of B/T cell doublets using a similar technique [468]. This group also reported some events which were CD4 T

cells which appeared to have acquired B cell markers by trogocytosis - shown by segments of the cell membrane staining for B cell markers [468]. In all CD32^{high} events examined non were found with this phenotype.

Gating of singlets using forward and side scatter characteristics is a conventional and well-accepted means of excluding doublet events. The existence of doublets not excluded using this strategy, however, has been previous reported [461]. In this study, CD3 and CD34 co-expressing singlet events were sorted using a similar approach to that described here; when the sorted cells were re-examined, they were found to be either CD3+ or CD34+ with no co-expression [461]. Doublets appeared to be creating an artefactual, rare population and were broken apart in the sorting process. Such events could theoretically arise when doublets fall through the laser beam on a particular angle, such that the second cell is completely hidden behind the first (i.e. in line with the laser beam) thus mimicking the height and area characteristics of a singlet. This is a potential cause of any rare population expressing unusual combinations of surface markers.

That these events are doublets explains a number of the aspects of CD32^{high} phenotype reported in this chapter. B cells express high levels of CD45RA [469], meaning that these events appear to have a naïve or T_{EMRA} phenotype. Furthermore, high levels of CXCR4 and HLA-DR are expressed on B cell circulating in the periphery [458], consistent with the phenotype observed here.

It is interesting that no difference in the frequency or phenotype of the CD32^{high} cells was observed between freshly phenotyped cells compared with those following density gradient separation and cryopreservation. This suggests that these doublets may exist *in vivo*. The B cells that comprise the doublets had a very consistent surface Ig pattern, with IgM and IgD but not IgG. This is consistent the phenotype of naïve circulating B cells (which have not yet undergone class-switching) [457, 458]. One possibility is that these represent functional interactions between TFH cell and B cells, which have exited germinal centres into the peripheral circulation at low frequencies. Indeed, Noto *et al.* (who did not gate out CD19+ events) showed that in lymph node, CD32 enriches for cells with a TFH phenotype, most markedly

in viraemic individuals [453]. In both the periphery and GALT, $CD32^{high}$ but not $CD32^{low}$ events have high levels of CXCR5 and Bcl6, key markers of TFH cell phenotype (Thornhill JP*, Martin GE*, Pace M* *et al.* [Submitted]). An important consideration here is that circulating B cells express CXCR5 [458] and could also be a source of this expression. In contrast, whilst Bcl6 is also expressed by B cells it is not generally found on naïve, circulating B cells and is only up-regulated at a protein level following B cell receptor engagement [470], supporting the idea that these doublets may contain TFH cells.

CD4 T cell/B cell interactions occur mostly in lymphoid tissue and would be unexpected in the periphery. If these observed doublets represent physiologically relevant events, they would be expected to occur more frequently in tissue sites. It could also be hypothesised that they would occur at elevated frequency in viraemic individuals, when antigenic stimulation of antibody production is occurring. Here, an increased frequency of peripheral $CD32^{high}$ events was observed during PHI compared with healthy controls and following ART initiation. Our group has also observed an elevated frequency of $CD32^{high}$ events in GALT and tonsil (Thornhill JP*, Martin GE*, Pace M* *et al.* [Submitted]). This increased expression in lymphoid tissue was also reported by Noto *et al.* who demonstrated more frequent CD32+CD4+ cells in lymph node than in the periphery in both HIV-infected and uninfected individuals [453]. Whilst this has not been directly demonstrated, these results are supportive that these events may be functionally relevant.

5.5.3 Failure to reproduce a marked enrichment of HIV DNA in CD32-expressing cells

These doublets would be of further interest if the component CD4 T cells were a substantial component of the HIV reservoir. Here, there was no observed relationship between the frequency of $CD32^{low}$ or $CD32^{high}$ events and the overall size of the HIV reservoir, a finding consistent with other recent reports [450, 452]. Reservoir size was measured in several ways - as total HIV DNA in both isolated CD4 T cells and PBMCs, CA-usRNA in PBMCs and time to viral rebound following TI.

Whilst some enrichment of HIV DNA in CD32^{low} and CD32^{high} events was seen for some individuals, this was modest and had a high degree of inter-individual variation. Certainly, these results did not demonstrate the approximately 1000-fold enrichment, or the inter-individual consistency of enrichment in CD32^{high} events previously reported [245]. The number of groups which have not replicated the original findings of Descours *et al.* is growing. Other studies have similarly reported no, or low magnitude enrichment of HIV DNA or RNA in CD32+ CD4 T cells [450, 453, 454, 463], or no difference in stimulated viral outgrowth [455]; whilst most of these likely excluded CD32^{high} events, the remaining population of CD32+ cells was still originally reported to be >600 fold enriched. The reasons for this discrepancy remain unclear. Differences in patient demographics (including timing of ART initiation) are unlikely to be a driver of this stark difference, especially as groups with a range of different patient characteristics have now been studied [450, 453–455, 463]. CD32^{high} events are rare and the number of recoverable cells following cell sorting remains low. Very low cell input into qPCR assays can result in overestimation of the infection frequency. Similarly, over-quantification of infection frequency secondary to low cell input has been reported for the viral outgrowth assay that uses p24 as a readout [471]. Experiments presented here started with a similar PBMC input to Descours *et al.* (50-100 million PBMCs), and thus would be expected to have similar numbers of cells to input into qPCR assays. There remains, however, a possibility that the assay used in the original study may have caused an overestimation of this infected cell frequency.

5.5.4 Associations of CD32-expression on CD4 T cells with activation and transcription

In addition to the extremely high levels of HLA-DR on CD32^{high} events, levels of this activation marker were also elevated on CD32^{low} CD4 T cells. High expression of HLA-DR has been noted on *ex vivo* CD32+ cells in several studies (with various gating strategies) [450, 452–455, 463]. Up-regulation of CD32 expression on CD4 T cells in response to *in vitro* activation [447, 448, 450, 454] and *in vitro* infection

with HIV [251, 450, 454] have both been reported. This upregulation occurs on productively infected cells [251, 450] and, in one study, was confirmed at an mRNA level to specifically be the CD32a isoform [454]. CD32 expressing CD4 T cells in lymph node have been shown to express higher levels of HIV RNA by both flow cytometry [453] and using fluorescence in-situ hybridisation [450]; in the latter study staining was performed with a CD32a-specific antibody [450]. Overall, it appears that some of the CD32 expression on CD4 T cells is associated with activation, viral transcription and CD32a expression.

The above findings suggest that upregulation of CD32a associated with infection occurs with cellular activation and transcriptional activity, rather than latency. In the Descours *in vitro* model, the up-regulated *FCGR2A* transcript and CD32a protein were measured in a sorted, unactivated HLA-DR-/CD69- cellular fraction. The synergistic effects of cellular activation and infection on CD32a expression further suggest a role for the infecting event itself [251, 450, 454]. The possibility that it could also occur with the infection event itself (in the absence of activation) would be consistent with the identification of *FCGR2A* as being specifically up-regulated in latently infected cells using this model [245]. Supporting this, a similar study which used an *in vitro* model to try to identify biomarkers of the HIV reservoir also noted upregulation of *FCGR2A* in latently infected cells in the absence of activation marker expression [244].

As such, whilst there is evidence that infection may upregulate the expression of the CD32a isoform specifically, *ex vivo* sorting experiments in the paper by Descours *et al.* used the pan-isotypic antibody clone FUN-2. This chapter has demonstrated CD32 expression CD3+CD4+ cells comes from several non-T cell sources - CD32+CD14+ monocytes and $CD32^{high}$ T/B cell doublets. The CD32 expression measured *ex vivo* by Descours *et al.* may thus represent a mix of isoforms and cellular sources. Even if monocytes and B cells were specifically excluded, the consistent association of CD32 expression with HLA-DR expression, and with transcriptional activity, demonstrates that CD32 marks a population of cells beyond those identified using *in vitro* latency models limited to resting cells.

5.5.5 Lessons learnt and implications for future studies of markers of an enriched HIV reservoir

Whilst these results suggest that CD32 is not a specific marker of an enriched HIV reservoir, this work has implications for the study of future putative reservoir markers. Latently infected cells are so rare; in order to be useful and specific, any marker of the HIV reservoir would be expressed on a very small population of CD4 T cells. Furthermore it would need to be something not usually expressed on CD4 T cells. It is clear that conventional flow cytometry cannot completely exclude doublet events; in this case, a B/T cell doublet has given rise to the appearance of CD32 expression on CD4 T cells. This will be a pitfall applicable to any future HIV reservoir markers. Of note, sorting these events and performing RNA-seq or qPCR for CD32 transcripts could plausibly "confirm" expression at an mRNA level because of the inclusion of B cells in sorted populations. Care will need to be taken to prove the expression of these markers using techniques that do not rely on flow cytometric analysis or sorting. One such approach used by Hogan *et al.*, who recently proposed CD30 as a marker of an enriched reservoir, was to show the presence of CD30 and CD4 mRNA and the absence of CD80 mRNA (for B and some other non-lymphocyte cells) in sorted CD30+ CD4 T cells [463]. Whilst excluding B cell contamination, this does not account for all possible non-CD4 T cell sources of CD30 expression. Direct imaging of cells, such as the imaging cytometry performed here, would be an additional safeguard.

The other pitfall identified with studying the reservoir in rare cell populations is the potential to over-quantify proviral DNA, or induced p24 [471] as a mere consequence of low cell input. Future studies of this nature should clearly demonstrate that the cell input used has not impacted on the quantification of provirus or induced virus in the specific assay employed.

Attempts to replicate previous findings should carefully consider the impact of any experimental decisions made. The results presented here indicate that the choice to gate out naïve, HLA-DR+, CD14+ or CD19+ events made by

several groups [450, 452–454] will have altered the composition of the CD32-expressing CD4 T cells studied from that of Descours *et al.*, adding complexity to the interpretation of the discrepant results.

The rapid turn around of results relating to CD32 expression has meant that results have become outdated almost as soon as they are published. Indeed, the analysis and interpretation of the experiments in this chapter has changed from the preprint version [472], the published version [473], and again to what is presented here. Novel models of scientific publishing which permit ongoing debate and discussion, whilst expediting the dissemination of results may be critical to improving the efficiency of global research efforts towards a HIV cure.

5.6 Conclusion

This chapter aimed to characterise CD32-expressing CD4 T cells and establish the relationship of these to the HIV reservoir. CD32-expressing CD3+CD4+ cells from healthy and HIV-infected individuals *ex vivo* represent a heterogeneous population and include CD32 expression from non-T cell sources: $CD32^{high}$ events are CD4 T/B cell doublets and CD32+CD14+ cells appear to be monocytes that have acquired CD3 expression. $CD32^{low}$ and $CD32^{high}$ events from some, but not all, individuals were enriched for HIV DNA, although this was generally of low-magnitude. This was in contrast to my initial hypothesis that these would be markedly enriched. This work adds to a growing body of evidence that CD32 is not a specific marker of an enriched CD4 T cell reservoir.

6

General discussion and conclusions

With a critical role in mediating initial antiviral control, T cell responses are of key importance to HIV curative interventions. This work has examined broad aspects of effector CD8 T cell responses and the CD4 T cell reservoir during treated PHI which are relevant to cure interventions.

The key findings of this work are:

- The occurrence of transient viral remission amongst a substantial proportion of individuals during PHI, which may conflate findings of curative intervention trials using TI to measure efficacy;
- Transient remission occurs at an increased frequency when ART is commenced during PHI, suggesting a role of early ART in inducing this phenotype in some individuals;
- PHI is associated with increased differentiation of bulk CD4 and CD8 T cells which persists despite early ART initiation;
- T cell activation, measured by CD38 expression, and Tim-3 expression are markedly elevated during PHI and incompletely resolved following 1 year of ART;

- Several ICRs (PD-1, TIGIT and CD39) are elevated on memory CD8 T cells during untreated PHI. PD-1 expression on EM CD4 T cells is elevated during PHI, and remains unchanged following a year of ART;
- HIV reservoir size appears to be determined during PHI in individuals who commence ART at this time;
- T cell activation and memory expansion, as well as viral burden are linked to HIV reservoir size, suggesting the importance of the initial host-viral interplay;
- CD32, a candidate biomarker of the HIV reservoir, does not specifically mark latently infected cells or relate to overall reservoir size in individuals treated during PHI;
- Circulating $CD32^{high}$ CD4 T cells in both healthy and HIV-infected individuals are B/CD4 T cell doublets.

Studies of extremely early (acute or hyperacute) HIV infection are useful for understanding the pathophysiology of this virus, particularly around viral load peak when the development of the immune response plays a determining role. The diagnosis of HIV infection at this extremely early stage is challenging and whilst several cohorts have been set up to do this [53, 54], this targeted approach to diagnosis is not feasible on a large scale. Much of the work in this thesis was conducted within HEATHER, an observational cohort of treated PHI with over 300 individuals enrolled. One of its strengths is that these individuals are diagnosed with HIV infection through routine clinical testing. As such, findings from this cohort demonstrate what is achievable in the clinical setting, and may represent a "best-case" scenario for widespread early ART initiation. One limitation of this work is the lack of a comparator group who began ART during chronic infection, where immune dysfunction has been largely described [88, 98, 99, 101–107]. As such, this work describes the immunologic status of individuals who begin ART early, but cannot compare if this differs from chronic infection. Arguably, as "test and treat" [15] is widely rolled out this comparison will become less relevant and

defining the new status quo of persistent immune dysfunction (as has been the focus here) is an increasingly relevant goal.

The works presented here have been conducted within large, well-characterised cohorts. This adds robustness to the findings presented, and has allowed for a comprehensive characterisation. Despite this, one of the limitations of this work is the lack of functional characterisation, meaning that the mechanistic conclusions that can be drawn are limited.

One of the key goals of this work was to try to unify some of the previous findings in the literature. As an example, elevated expression of PD-1, Tim-3, TIGIT, CD39 and CD38 during HIV infection have all been previously reported (section 1.4.2) - but largely in isolation. By measuring these together, this work has uncovered similarities and differences between these markers. Whilst the expression of these markers largely mirrors one another, subtle differences in the distribution of expression and resolution following ART were observed - these may actually reflect relevant functional differences. There may also, however, be some redundancy in these pathways both biologically and as potential biomarkers. Indeed, the results from Chapter 4 suggest that previously observed relationships between ICRs and reservoir size or viral rebound may reflect CD8 T cell activation and EM expansion - well characterised hallmarks of early HIV infection.

6.1 Early ART for curative interventions

Early ART has been considered as part of HIV curative interventions for two main reasons: limited seeding of the reservoir [36, 116, 117, 206–212] and preservation of effector immune functions [98, 112–115]. Recent evidence has shown that even ART initiation within weeks of infection, however, does not prevent reservoir establishment and is still associated with persistent immune activation [86, 118, 379, 474]. Early ART, practically speaking, will not be able to cure any individuals in whom infection has been established. This raises the question: is there still a role for early ART initiation in designing an HIV cure?

This thesis has focused on the impact of early ART on diverse aspects of clinical and immunological phenotypes that are relevant to HIV cure. The model put forward here is that early ART is able to "pause" pathological processes associated with progressive HIV infection, but not to alter their course if ART is stopped. This was evidenced in Chapter 2 where, in some individuals, ART appeared to delay transient viral remission. Furthermore, the high initial viral rebound observed here, as well as by others [294], resembles a deferred or second primary infection - the continuation of natural history as the "pause" is taken off. Chapter 3 demonstrated improvement, but not resolution, of immune activation, ICR expression and memory phenotype with early ART initiation. It is likely that if treatment was interrupted, these would continue to progress from this already HIV-experienced state.

What does this mean for HIV curative interventions? There are two main implications. Firstly, early ART can be conceptualised as a way to "buy time" during which to redirect or shape an immune response in a favourable direction. The inefficacy of the immune response to HIV appears to be due to both the high viral burden and the associated immunologic milieu. Under ART, the immune system could be primed during a more favourable systemic state to induce responses capable of long-lived viral control. Efforts to do this to date, including by therapeutic vaccination and structured treatment interruption [297, 329, 359] have not been successful. In part this is because, despite many years of studying HIV infection, our knowledge of what constitutes an ideal immune response is still incomplete; whilst T cells have been widely studied, NK cell responses and humoural immunity are an increasing research focus. Importantly, the inefficacy of these strategies to date does not necessarily signal future failure. Several approaches have shown to induce long-term immunovirological control in animal models including bNAb administration [352], CMV-vectored vaccine administration [327, 328] and TLR agonism [337]. It remains to be seen if these will also be useful in humans. It is likely, however, that as future strategies to direct the HIV immune response are developed, the ability to control the milieu will be critical to their success. In doing this, ART will likely play an important role in any immunotherapeutic

strategies. The demonstration in this thesis of a connection between host immunity and reservoir size during PHI is also important. This suggests that at this time there is still an ability of host immune responses to substantially impact on viral control. As such, PHI might be an important window of opportunity for immunologic interventions - and a good time to push "pause".

The second implication is that even a cure may not result in normal health. It is well-established that viral replication is not the only driver of pathology in HIV infection, evidenced by persistent chronic inflammation in elite controllers [391, 475–477] and during suppressive ART [9, 116, 212, 379, 380], as well as the risks of non-AIDS co-morbidities associated with this [9, 476, 477]. Indeed, this thesis has provided further evidence that immunological perturbations persist even with early ART initiation. It is not clear how HIV infection, in the absence of viral replication, exerts its pro-inflammatory effects. One possibility is that the infection itself irreversibly changes the immune response by kick-starting an ongoing inflammatory driver - mechanisms such as microbial translocation and CMV reactivation have been proposed and widely studied as such potential drivers [478, 479]. An alternative possibility for the long-term risks associated with HIV infection is that the magnitude and duration of this initial immunological insult are the driver of ongoing risk. This could be thought of as analogous to the concept of "pack-years" amongst individuals who smoke, where despite cessation there is a persistent health risk which is proportional to the lifetime exposure to smoke. This work has highlighted the importance of the magnitude of host-viral interplay in early infection in "setting" the size of the viral reservoir. Further work could explore if this initial response can similarly "set" disease outcomes on ART. Importantly, in both of these models, even complete eradication of the virus may not result in elimination of the inflammatory risk associated with HIV infection.

The reasons to aspire for an HIV cure extend beyond that of improving health; social and personal benefits of no longer being HIV-infected have emerged as additional motivating factors for the development of a cure [480–483]. These motivations are important and reflect the ongoing stigma around HIV infection.

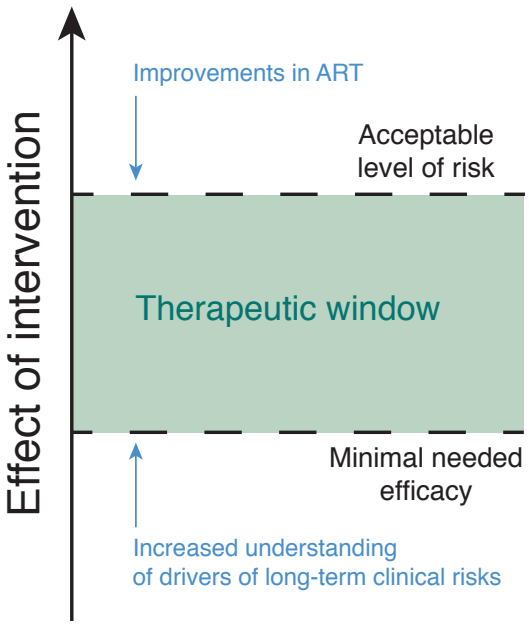


Figure 6.1: Shrinking therapeutic window for HIV curative interventions. Drugs are evaluated for their therapeutic window - the gap between the minimal concentration required for clinical efficacy and that which causes toxicity. Here, an analogy is drawn between this pharmacological concept and a hypothetical HIV curative intervention. Research advances may be shrinking the "therapeutic window" for HIV cure.

Safety and feasibility, however, must remain key considerations in the discussions around HIV cure. As ART improves, becoming safer, simpler and cheaper, the acceptable risk for curative interventions becomes lower. If, as suggested above, a cure cannot fully restore health then curative interventions will need to have a larger effect to make a meaningful clinical impact. These two factors may be shrinking the ideal "therapeutic window" of any hypothetical curative strategy from both directions (Figure 6.1).

6.2 Shifting the goalposts for HIV cure

The case study of Timothy Ray Brown provided hope that eradication of viral reservoirs could be a means of curing HIV. Whilst theoretically even a single intact provirus could give rise to recrudescent infection, modelling has suggested that substantial decreases in the reservoir may induce durable remission in many people [196, 484]. Growing evidence suggests that even in individuals with very low or

undetectable reservoir size, viral rebound usually occurs rapidly [118, 279, 282, 303]. This suggests that complete eradication of the reservoir, rather than a large reduction, will be needed for HIV cure. With this widespread and early seeding of the viral reservoir it seems unlikely that any intervention (pharmacological or immunological) will be able to target all of these proviruses. Whilst reduction in HIV reservoir size has been a goal of curative interventions for several years now, it is possible that it is time to shift the goalposts. If eradication of the viral reservoir is impossible, then interventions to induce a durable state of immunologic control may represent a better aspiration for the development of future curative strategies.

Another goal of HIV cure research has been the identification of a marker which can uniquely discriminate between latently infected and uninfected cells. The story of CD32, which the work described in Chapter 5 forms a part of, demonstrates the hype and some of the challenges around doing this. In particular, it has demonstrated a need for prudence when studying cell populations with unexpected phenotypes - an inevitable aspect of searching for a phenotype associated with latent infection. The complexity of the distribution of the HIV reservoir is staggering, with further diversity in cellular and anatomical composition of this being continually uncovered (Figure 1.5). Additional complexity comes from the fact that latency itself represents a spectrum from absolute suppression of viral transcription to low level viral production on ART. With this diversity it seems increasingly unlikely that latent infection will induce a single phenotypic marker (or marker combination) on all relevant reservoir cells. The identification of a marker which can enrich for latently infected cells, even if the magnitude is substantial, is of limited utility if any proviruses outside this pool can still give rise to viral rebound. Studies of CD32 differed in what they consider part of a "plausible" reservoir - with some excluding activated, naïve or non-lymphoid cells [450, 452–454]. These definitions of the reservoir reflect consensus about which cells the majority of proviruses persist in during long-term ART. It is, however, possible that cells not classically considered part of the reservoir (for example these naïve, activated or non-lymphoid cells) could contain intact proviral sequences. Given an increased understanding of the

need to target all residual proviruses, a broadening of the cells considered is needed such that rare or minor reservoirs are also considered.

6.3 Future directions

A key question with early ART initiation is whether or not effector functions are preserved so that they could be targeted therapeutically. Suggesting this may be possible, this work has shown preservation of a pool of T-bet^{high}Eomes^{low} cells which in murine models have proliferative and functional potential. It has not, however, characterised the functional capacity of these cells on ART. Whether early ART preserves the functional potential of HIV-specific T cells is being investigated in ongoing experiments. To do this, epigenetic changes in HIV-specific CD8 T cells have been measured before and after the initiation of ART, to look at whether the epigenetic program of these cells is poised for exhaustion or future functionality.

As ICR blockade for HIV therapy is being investigated, further work is needed to characterise the context-specific functions of these pathways. In particular, whether the expression of these molecules during early infection is indicative of future dysfunction, or a marker of cellular activation. If ICR blockade is able to induce functional T cell responses, the quality and durability of these is of key interest - as long-term immune surveillance is likely to be a requirement of successful HIV immunotherapeutic approaches.

The dynamics of normal, early viral control have been clearly defined in this thesis, but the mechanisms behind this are still incompletely characterised. Understanding the drivers of spontaneous control and part of early ART which modify this will be a crucial aspect of devising effective interventions. Closely linked with this is the identification of predictors of viral control/rebound. This is an important goal not only as this may provide such mechanistic insights, but could also be used to measure the efficacy of therapeutic interventions without the need to interrupt ART.

6.4 Conclusion

Primary HIV infection is characterised by the expansion of activated, effector memory CD8 T cells as well as the upregulation of ICRs (PD-1, Tim-3, TIGIT, CD39) on CD4 and CD8 T cells. At this time, transient virologic control is not uncommon - presumedly as the host immune response is initially able to control viral replication. The size of the HIV reservoir once established on ART is determined prior to ART initiation and is linked to this early host-viral interplay. Following the initiation of ART, immune activation and ICR expression decrease but do not completely normalise. Further work is needed to determine if the HIV-specific immune response on ART retains functional potential that can be redirected as part of HIV cure approaches.

7

Materials and Methods

Contents

7.1 Ethics Statement 164
7.2 Clinical cohorts 165
7.2.1 SPARTAC 165
7.2.2 HEATHER 166
7.3 Media and buffer composition 168
7.4 General techniques for working with *ex vivo* samples . 169
7.4.1 Cryopreservation of blood components 169
7.4.2 Thawing and handling of primary cells 169
7.4.3 T cell isolation 170
7.5 Flow cytometry 170
7.5.1 Surface staining 170
7.5.2 Intracellular staining 176
7.5.3 Acquisition of flow cytometry data 177
7.5.4 Analysis of flow cytometry data 178
7.5.5 Technical considerations 178
7.6 Cell sorting 179
7.6.1 Sorting of CD32 expressing CD4 T cells 179
7.6.2 Staining of HIV-specific CD8 T cells 180
7.7 HLA typing 182
7.7.1 DNA extraction 182
7.7.2 HLA typing by sequence specific primers 182
7.8 CD8 ELISpot assays 182
7.9 ELISA 184
7.10 HIV reservoir quantification 185
7.10.1 Nucleic acid extraction 185
7.10.2 Total HIV DNA quantification 185
7.10.3 Cell-associated unspliced RNA quantification 186
7.11 Determination of viral clade 189

7.12 Statistical analyses 189
7.12.1 Missing data 189
7.12.2 Group comparisons 191
7.12.3 Correlative analyses 191
7.12.4 Survival analyses 191
7.12.5 Principle component analysis 191
7.12.6 Regression analyses 192

7.1 Ethics Statement

The SPARTAC trial was approved by the following authorities: the Medicines and Healthcare products Regulatory Agency (UK), the Ministry of Health (Brazil), the Irish Medicines Board (Ireland), the Medicines Control Council (South Africa) and the Uganda National Council for Science and Technology (Uganda). It was also approved by the following ethics committees in the participating countries: the Central London Research Ethics Committee (UK), Hospital Universitário Clementino Fraga Filho Ethics in Research Committee (Brazil), the Clinical Research and Ethics Committee of Hospital Clinic in the province of Barcelona (Spain), the Adelaide and Meath Hospital Research Ethics Committee (Ireland), the University of Witwatersrand Human Research Ethics Committee, the University of Kwazulu-Natal Research Ethics Committee and the University of Cape Town Research Ethics Committee (South Africa), Uganda Virus Research Institute Science and Ethics Committee (Uganda), the Prince Charles Hospital Human Research Ethics Committee and St Vincent's Hospital Human Research Ethics Committee (Australia) and the National Institute for Infectious Diseases Lazzaro Spallanzani, Institute Hospital and the Medical Research Ethics Committee, and the ethical committee of the Central Foundation of San Raffaele, MonteTabor (Italy).

Recruitment for and studies within the HEATHER cohort were approved by the West Midlands—South Birmingham Research Ethics Committee (reference 14/WM/1104).

Recruitment of healthy individuals (used as comparison group to primary HIV infection cohort) was approved by the Sheffield Research Ethics Committee (reference 16/YH/0247). Leukocyte cones were obtained through anonymous donation to NHS Blood and Transplant (UK) after approval by NHS Blood and Transplant and the National Research Ethics Service Oxfordshire Research Ethics Committee. All participants have given informed consent for their participation in these studies.

7.2 Clinical cohorts

7.2.1 SPARTAC

SPARTAC was a multi-centre randomised controlled trial of short course antiretroviral therapy during PHI, which completed follow up in 2010. The full inclusion criteria and details of the trial are published elsewhere [359]. PHI (diagnosis within 6 months of acquisition) was defined as in Table 7.1. Participants were enrolled from 25 sites in Australia, Brazil, Ireland, Italy, South Africa, Spain, Uganda and the United Kingdom from August 2003 to July 2007. Eligible participants were randomised 1:1:1 to receive either 12 or 48 weeks of ART (followed by treatment interruption), or no treatment (standard of care). The primary trial endpoint was a composite of CD4 T cell count less than 350 cells/µL or the initiation of long term ART for any other reason. Study visits occurred at 0, 4, 12, 16, 24, 36, 48, 52 and 60 weeks, then every 12 weeks until the end of follow-up. Cryopreserved peripheral blood mononuclear cells (PBMCs) and plasma samples were collected at each study visit; CD4 count, CD8 count and VL were measured at each study visit.

The method for calculating estimated date of seroconversion (EDSC) is shown in Table 7.1. Time to viral rebound was assessed as time from treatment interruption to the first of two consecutive VL measurements >400 copies/mL (this was the limit of detection of the assay used at trial sites in South Africa and Uganda). Individuals who did not rebound were censored at the date of the last VL measurement. Data was collected and managed by the Medical Research Council Clinical Trials Unit (MRC CTU) who provided the clinical data used for analyses in this thesis.

For individuals from SPARTAC the baseline CD4 count was taken as the average of the counts measured at screening and baseline visit (Chapter 2), or the baseline visit value only when these analysis also included HEATHER participants (Chapter5). If the baseline VL was below the limit of detection this value was taken at the midpoint between the limit of detection and zero.

Whilst not designed for study of the HIV reservoir, the availability of longitudinal clinical samples and a treatment interruption mean that study has proven extremely valuable for studies of reservoir size and of viral rebound post ART cessation [220, 255, 270].

7.2.2 HEATHER

HEATHER is an observational cohort study of individuals who commenced ART during PHI. The cohort was established with the aim of studying the HIV reservoir during treated PHI, and the impact of immunological factors on the reservoir. Participants were either prospectively enrolled prior to ART initiation (HEATHER A) or identified as meeting these criteria retrospectively (HEATHER B). As such, individuals enrolled into HEATHER A have samples available prior to ART initiation. The definition of PHI used in HEATHER is very similar to that of SPARTAC (Table 7.1), allowing us to combine individuals from these two studies for some analyses. In order to be eligible for HEATHER, individuals need to meet the following criteria:

- Confirmed evidence of PHI (as defined in Table 7.1);
- Commence ART within 3 months of the date of HIV diagnosis;
- Remain on uninterrupted ART (HEATHER B), or are planned to start on suppressive ART for >1 year (HEATHER A).

In addition, if any of the following apply an individual is not eligible for enrolment in HEATHER:

- Unable or unwilling to give informed consent;
- Persistent anaemia (Hb level <10g/dL on two or more consecutive occasions);
- Current pregnancy;

SPARTAC	HEATHER
1. HIV positive antibody test within 6 months of a HIV negative antibody test 2. HIV antibody negative with positive RT-PCR assay for HIV-1 RNA 3. A low level of HIV antibodies (OD<0.6) according to a serologic testing algorithm for recent infection (subtype B strain only) 4. Equivocal HIV antibody test supported by a repeat test within 2 weeks showing a rising optical density 5. Having clinical manifestations of symptomatic HIV seroconversion illness supported by antigen positivity and <4 bands positive in western blot	1. As in SPARTAC 2. HIV antibody negative with positive RT-PCR assay for HIV-1 RNA (or positive p24 antigen or detectable viral load) 3. RITA assay result consistent with recent infection 4. As in SPARTAC 5. As in SPARTAC
EDSC calculated as: • Midpoint between the most recent negative or equivocal antibody test and the first positive test (criteria 1 or 4) • Date of the test (criteria 2, 3 if OD≤0.01 and 5) • Date of the test -[(OD×150)÷2] days (criterion 3 if OD>0.01)	*EDSC calculated as:* • Midpoint between the most recent negative antibody test and the first positive test (criterion 1) • Date of the test (criteria 2 and 5) • Date of the test -120 days (criterion 3)[1] • Date of equivocal test (criterion 4)

Table 7.1: Criteria used to define primary HIV infection used in SPARTAC and HEATHER. The method used to calculate EDSC or each criterion is also shown. Where individuals met multiple eligibility criteria the EDSC was taken from criteria in the following order of preference: 2, 4, 5, 1, 3. Abbreviations used: EDSC, estimated date of seroconversion; PCR, polymerase chain reaction; RITA, recent incident test algorithm; OD, optical density.
[1]120 days is the recency period of the RITA assay used (Serum/Plasma HIV LAg-Avidity EIA [Sedia Biosciences])[485, 486]

Name	Composition
R10	RPMI-1640 medium with 10% heat-inactivated FBS, 2mM L-glutamine, 100IU/mL penicillin and 0.1mg/mL streptomycin
FACS wash A	PBS with 5% FBS and 1mM EDTA
FACS wash B	PBS with 0.1% BSA and 0.01% sodium azide
PBA	PBS with 0.5% BSA and 0.1% sodium azide
FACS fixative	PBS with 2% formaldehyde
Isolation buffer	PBS with 2% FBS and 1 or 2mM EDTA

Table 7.2: Media and buffer composition. Abbreviations used: BSA, bovine serum albumin; EDTA, ethylenediaminetetraacetic acid; FACS, fluorescence activated cell sorting; FBS, fetal bovine serum; PBA, PBS/BSA/(sodium) azide buffer; PBS, phosphate buffered saline

- HBV and/or HCV co-infection at time of enrolment.

Study visits occurred at 0, 1 (HEATHER A only), 3 (HEATHER A only) and 6 months, then every 6 months until the end of follow-up. Cryopreserved PBMCs and plasma samples were collected at each study visit. CD4 count, CD8 count and VL were measured as part of routine clinical care and, as such, were measured less frequently than the study visits. Recruitment and follow-up are ongoing and are being conducted at Chelsea and Westminster Hospital, Guy's and St Thomas' and Imperial NHS Trusts (all in London, UK).

For individuals in HEATHER the baseline CD4 and CD8 counts were taken as the earliest value prior to the initiation of ART (or up to 14 days afterwards). Similarly, the baseline VL was taken as the earliest value prior to the initiation of ART (or up to 7 days afterwards). In both cases, usually only one value was available.

7.3 Media and buffer composition

Buffers or culture media were used throughout this work as listed in Table 7.2.

7.4 General techniques for working with *ex vivo* samples

7.4.1 Cryopreservation of blood components

Samples for SPARTAC were cryopreserved at the individual trial sites. For HEATHER, samples processed prior to March 2015 were processed at the Kings College London Infectious Diseases Biobank, after which all sample processing was moved to Oxford. Protocols may have differed between sites.

For samples processed in Oxford, acid-citrate-dextrose (ACD)-anticoagulated blood in collection tubes was centrifuged at 700-760xg for 10 minutes. Plasma was removed, aliquoted and stored at -80°C for future analysis.

Remaining blood was transferred to 50mL Falcon tubes (BD) and diluted to approximately original volume in phosphate buffered saline (PBS) and layered 2:1 over a cushion of Lymphoprep (Stemcell Technologies). Following density gradient separation by centrifugation (860-940xg for 20 minutes, no brake), peripheral PBMCs were removed to a separate tube and washed twice with R10. PBMCs were counted using a Muse Cell Analyser (Merck Millipore), which uses a fluorescent viability dye to exclude dead cells. Cells were resuspended at 1-2 x 10^7 cells/mL in 40% FBS, 50% RPM1-1640 and 10% dimethyl sulfoxide (DMSO) and aliquoted into CryoTube vials (Thermo). These were frozen overnight at -80°C in a Mr Frosty freezing container (Nalgene) prior to transfer to liquid nitrogen for long-term storage.

7.4.2 Thawing and handling of primary cells

Cryopreserved PBMCs were thawed in R10 media warmed to 37°C, at a ratio of 1-2 x 10^6 cells per mL media. If low cell viability was anticipated, 2.7 Kunitz units/mL of deoxyribonuclease (DNAse) (Qiagen) was added to this media. Cells were pelleted, before resuspension in appropriate volume of R10 or buffer for downstream applications.

Unless otherwise specified, centrifugation of primary cells in tubes was performed at approximately 700-760xg for 8-10 minutes; centrifugation of cells in 96 well plates were performed at 940xg for 3-5 minutes.

7.4.3 T cell isolation

CD4 and CD8 T cells were enriched from bulk PBMCs by negative magnetic selection as per kit instructions with volumes scaled directly for cell input and using Isolation buffer (as listed in Table 7.2). For SPARTAC samples this was performed using Dynabeads Untouched Human CD4 T cell enrichment kit (Invitrogen) with volumes scaled for 10^7 cells per test; for samples in HEATHER the EasySep Human CD4 Enrichment Kit (Stemcell Technologies) was used. CD8 T cells used for tetramer sorts (section 7.6.2) were enriched by negative magnetic selection MACS CD8+ T Cell Isolation Kit (Miltenyi).

7.5 Flow cytometry

7.5.1 Surface staining

Staining was performed in microcentrifuge tubes or 96-well V bottom plates. Cells were pelleted and resuspended in buffer (with antibodies added into this suspension), or a buffer/antibody mix. The antibody composition and buffer used for each panel is listed in Table 7.3 with details of the individual antibodies used in Table 7.4.

Staining volumes were directly scaled so that no more than 5 x 10^6 cells were stained per 50µL volume. When Live/Dead Near IR (Life Technologies) was used for exclusion of dead cells, this was used at a final 1:300 dilution and included in the antibody staining mix; where Fixable Viability Dye eFluor506 was used instead this was at a final dilution of 1:100.

Staining was performed for 30 minutes at 4°C after which cells were washed twice with buffer or PBS, fixed with 2% formaldehyde for 30 minutes, then washed twice and resuspended in PBS for acquisition.

Exceptions to this protocol were:

Panel	Sections	Buffer	Cytometer	Contains
A	Table 2.3	FACS Buffer B	MacsQuant Analyser (Miltenyi)	CD25 PE CD3 eFluor450 or VioBlue CD38 PE-Vio770 CD4 VioGreen CD69 FITC CD8 APC HLA-DR PerCP LiveDead Near IR
B	Table 2.3	FACS Buffer B	MacsQuant Analyser (Miltenyi)	CD3 eFluor450 or VioBlue CD4 VioGreen CD8 APC Lag-3 PerCP-eFluor710 Tim-3 PE LiveDead Near IR PD-1 PE-Cy7 (a)
C	Figures 3.3, 3.4, 3.5, 3.7, 3.9, 3.10, 3.13, 3.8, 3.14, 4.3, 4.5, B.1, B.6 & B.7. Tables 4.1, B.1, B.2, B.4, B.3, B.6 & B.5	BD Horizon Brilliant Stain Buffer (BD)	LSR II (BD)	CCR7 Pacific Blue CD27 AlexaFluor 700 CD3 BV570 CD39 APC CD4 BV605 CD45RA FITC CD8 BV650 Lag-3 PE-Cy7 LiveDead Near IR PD-1 PE-eFluor610 Tim-3 PE TIGIT PerCP-eFluor710
D	Figures 5.3 and 5.5	BD Horizon Brilliant Stain Buffer (BD)	LSR II (BD)	CCR7 Pacific Blue CD2 APC CD27 AlexaFluor 700 CD3 BV570 CD32 PE-Cy7 CD4 BV605 CD45RA FITC CD8 BV650 LiveDead Near IR PD-1 PE-eFluor610 Tim-3 PE TIGIT PerCP-eFluor710
E	Figure 5.5	FACS Buffer A	LSR II (BD)	CD3 FITC CD32 PE-Cy7 CD4 eFluor450 LiveDead Near IR PD-1 PE-eFluor610 TIGIT PerCP-eFluor710

Panel	Sections	Buffer	Cytometer	Contains
F	Figure 5.3	BD Horizon Brilliant Stain Buffer (BD)	LSR II (BD)	Bcl6 AlexaFluor488 CD3 BV570 CD32 PE CD4 BV605 CD8 BV650 CXCR5 Pacific Blue EPCAM APC-Vio770 HLA-DR AlexaFluor700 ICOS AlexaFluor647 LiveDead Near IR PD-1 PE-Cy7 (b) Tim-3 PE-CF594 (b) TIGIT PerCP-eFluor710
G	Figure 5.3	R10	LSR II (BD)	CCR5 PE or CXCR4 APC CD3 FITC CD32 PE-Cy7 CD4 eFluor450 LiveDead Near IR
H	Figures 5.1 and B.10	R10	LSR II (BD)	CD14 VioBlue CD3 AlexaFluor700 CD32 PE-Cy7 CD4 APC LiveDead Near IR One of: CD11b, CD16, CD18, CD20 (all FITC), CD123 or TCRγδ (both PE)
I	Figure 5.1	R10	LSR II (BD)	CD14 FITC CD3 AlexaFluor700 CD32 PE-Cy7 CD4 APC LiveDead Near IR One of: CD8 eFluor450, CD15 Pacific Blue or CD56 BV421
J	Figure 5.1	R10	LSR II (BD)	CD14 VioBlue CD235a APC-Cy7 CD3 FITC CD32 PE-Cy7 CD4 APC Fixable Viability Dye eFluor506
K	Figure 5.1	R10	LSR II (BD)	CD14 VioBlue CD3 FITC CD32 PE-Cy7 CD36 APC CD4 AlexaFluor700 LiveDead Near IR

Panel	Sections	Buffer	Cytometer	Contains
L	Figure 5.2	R10	LSR II (BD)	CD14 VioBlue CD20 FITC CD3 AlexaFluor700 CD32 PE-Cy7 CD4 APC LiveDead Near IR One of: IgD, IgG or IgM (all PE)
M	Figure 5.6	FACS buffer A	Imagestream MKII	CD14 VioBlue CD19 PE CD3 FITC CD32 PE-Cy7 CD4 APC LiveDead Near IR

Table 7.3: Flow cytometry panels used for surface staining experiments. Further details of antibodies listed are shown in Table 7.4

Antigen	Fluorochrome	Clone	Manufacturer	Staining conc. (µg/100µL)
Bcl6	AlexaFluor488	K122-91	BD	0.2
CCR5	PE	C57BL/6	BD	0.25
CCR7	Pacific Blue	G043H7	BioLegend	1.2-1.8
CCR7	PerCP-Cy5.5	G043H7	BioLegend	1.2
CD11b	FITC	M1/70.15.11.5	Miltenyi	0.066
CD123	PE	9F5	BD	0.0625
CD14	FITC	HCD14	BioLegend	0.8
CD14	VioBlue	TUK-4	Miltenyi	0.165
CD15	Pacific Blue	W6D3	BioLegend	0.8
CD16	FITC	CB16	eBioscience	0.0125
CD19	FITC	LT19	Miltenyi	0.066
CD19	PE	LT19	Miltenyi	0.044
CD2	APC	RPA-2.10	BioLegend	0.05
CD20	FITC	2H7	BioLegend	0.2
CD235a	APC-Cy7	HI264	BioLegend	0.3
CD25	PE	3G10	Miltenyi	0.088
CD27	AlexaFluor700	M-T271	BioLegend	0.4
CD3	AlexaFluor700	UCHT1	BioLegend	1
CD3	BV510	OKT-3	BioLegend	0.09
CD3	BV570	UCHT1	BioLegend	0.16
CD3	eFluor450	UCHT1	eBioscience	0.1
CD3	FITC	UCHT1	BioLegend	0.6
CD32	PE	FUN-2	BioLegend	0.1
CD32	PE-Cy7	FUN-2	BioLegend	0.4
CD36	APC	AC106	Miltenyi	0.11
CD38	AlexaFluor700	HB-7	BioLegend	0.1
CD38	PE-Vio770	IB6	Miltenyi	0.055
CD39	APC	A1	eBioscience	0.05
CD39	BV421	A1	BioLegend	0.1
CD4	AlexaFluor700	SK3	BioLegend	0.2
CD4	BV605	RPA-T4	BD	0.1
CD4	eFluor450	OKT4	eBioscience	0.05
CD4	APC	RPA-T4	BioLegend	0.1
CD4	VioGreen	VIT4	Miltenyi	0.22
CD45RA	FITC	HI100	eBioscience	0.4
CD45RA	BV785	HI100	BioLegend	0.24
CD56	BV421	HCD56	BioLegend	0.12
CD69	FITC	FN50	Miltenyi	0.22
CD8	APC	BW135/80	Miltenyi	0.011
CD8	eFluor450	OKT8	BioLegend	0.05
CD8	BV650	RPA-T8	BD	0.12
CD8a	BV711	RPA-T8	BioLegend	0.075
CD95 (Fas)	BV605	DX2	BioLegend	1.5
CXCR4	APC	12G5	BioLegend	0.4
CXCR5	Pacific Blue	J252D4	BioLegend	0.8
EPCAM	APC-Vio770	HEA-125	Miltenyi	0.25
Eomes	eFluor660	WD1928	eBioscience	0.024
HLA-DR	PerCP	AC122	Miltenyi	0.132
HLA-DR	AlexaFluor700	G46-6	BD	0.2
ICOS	AlexaFluor647	DX29	BD	0.048
IgD	PE	IA6-2	BioLegend	0.2

Antigen	Fluorochrome	Clone	Manufacturer	Staining conc. (µg/100µL)
IgG	PE	HP6017	BioLegend	0.4
IgM	PE	MHM-88	BioLegend	0.05
Lag-3	PE-Cy7	3D5223H	eBioscience	0.024
Lag-3	PerCP-eFluor710	3D5223H	eBioscience	0.024
PD-1	BV421	EH12.2H7	BioLegend	0.5
PD-1	PE-Cy7 (a)	eBioJ105	eBioscience	0.2
PD-1	PE-Cy7 (b)	EH12.2H7	BD	0.2
PD-1	PE-eFluor610	eBioJ105	eBioscience	0.2
T-bet	FITC	4B10	BioLegend	2
TCR$\alpha\beta$	PE-Cy7	IP26	BioLegend	0.1
TCR$\gamma\delta$	PE	11F2	Miltenyi	0.11
Tim-3	PE	344823	R&D	0.05
Tim-3	PE-CF594	7D3	BD	0.1
TIGIT	PerCP-eFluor710	MBSA43	eBioscience	0.05

Table 7.4: Antibodies used for flow cytometry experiments are listed here, with the final staining concentration.

- Samples for Panel F were stained at room temperature;

- Samples for HIV co-receptor stains (Panel G) were stained with LiveDead Near IR, CD32 PE-Cy7, CD3 FITC and CD4 eFluor450 as above. Following this, cells were incubated at 37°C for 20 minutes (for CCR5 PE) or at 4°C for 30 minutes (for CXCR4 APC).

Phenotyping of fresh lymphocytes (Figure B.10) was performed within 3 hours of blood collection using 1mL of ACD anticoagulated blood. Erythrocytes were lysed at 4°C for 10 minutes in 10mL of ammonium-chloride-potassium (ACK) buffer (Gibco) and washed prior to staining as above using Panel H (including anti-CD20; Table 7.3).

7.5.2 Intracellular staining

Staining was performed in microcentrifuge tubes or 96-well V bottom plates. Cells were pelleted and resuspended in buffer (with antibodies against surface epitopes added into this suspension), or a buffer/antibody mix. The antibody composition and buffer used for each panel is listed in Table 7.5 with details of the individual antibodies used in Table 7.4. Staining of surface epitopes was performed for 30 minutes at 4°C after which cells were washed twice with FACS buffer A prior to fixation and permeabilisation.

For Panel M, fixation and permeabilisation were performed with Foxp3 Buffer Set (BD) with reduced volumes (maximum volume 200/textmuL) to facilitate staining in 96-well plates. For Panel N, cells were permeabilised using FACS Permeabilising solution 2 (BD) as per the manufacturer's protocol. Cells were washed and resuspended in PBA containing antibodies against intracellular epitopes. Staining was performed at room temperature for 30 minutes after which cells were washed twice with PBA or PBS. Fixation was performed with 2% formaldehyde for 30 minutes, then cells were washed twice and resuspended in PBS for acquisition.

Panel	Sections	Buffer	Cytometer	Contains
N	Figures 3.3, 3.9, 3.11, 3.12, 3.8, 3.14, 4.3, 4.5 & B.5. Tables 4.1, B.2, B.4, B.3, B.6 & B.5	BD Horizon Brilliant Stain Buffer (BD)	LSR II (BD)	CD3 BV570 CD39 BV421 CD38 AlexaFluor 700 CD4 BV605 CD8 BV650 Lag-3 PE-Cy7 LiveDead Near IR PD-1 PE-eFluor610 Tim-3 PE Eomes eFluor660 (intracellular) T-bet FITC (intracellular)
O	Figure 5.2	R10	LSR II (BD)	CD14 VioBlue CD3 FITC CD32 PE CD4 APC LiveDead Near IR TCRαβ PE-Cy7 (intracellular)

Table 7.5: Flow cytometry panels used for intracellular staining experiments. Further details of antibodies listed are shown in Table 7.4

7.5.3 Acquisition of flow cytometry data

Samples were acquired on a LSR II (BD) or MacsQuant Analyser (Miltenyi) with standard laser configurations. Data were acquired on the day of or after sample preparation. Calibration of LSR II was performed daily using Cytometer Setup and Tracking (CS&T) beads (BD). Following this manual adjustment of voltages was performed. Standardisation of voltage adjustment between days was performed using 8-peak Rainbow Calibration Particles (BioLegend) to ensure comparability of data acquired over multiple days.

Samples for imaging cytometry were prepared as above acquired on an Amnis Imagestream MK II, with compensation performed using software provided with the machine. Data were analyses using IDEAS Software (Millipore).

Compensation controls were prepared using singly stained antibody or amine reactive dye capture beads as follows: BD Comp-Beads anti-mouse (BD), UltraComp

eBeads (eBioscience) or ArC amine reactive compensation beads (ThermoFisher). Unstained beads were also prepared. Compensation controls were prepared freshly and compensation performed on the days of each experiment.

7.5.4 Analysis of flow cytometry data

Data were analysed using FlowJo Version 10.0.7, 10.0.8r1 or 10.4 (Treestar).

Compensation was performed as part of the analysis process in FlowJo. The compensation matrix was applied to samples and visually checked against a fully stained sample by looking at each parameter plotted against one another (bivariate plots); if required, fine adjustment to the compensation parameters were applied at this point.

Specific gating approaches are described with individual experiments. The following general considerations were made when gating flow cytometry data:

- Doublet exclusion was performed based on forward scatter (FSC) area vs height characteristics;
- For samples acquired at the same time, gates were set on a single sample and applied to all other samples in the batch;
- All gates were visually checked to ensure their appropriate position;
- Gates for ICR marker positive populations were set on a partially stained anchor sample without the relevant antibody or fluorescence minus one (FMO) control such that approximately 0.1% of events were positive for the marker.

7.5.5 Technical considerations

7.5.5.1 Antibody titration

All antibodies using clones and colours not previously in use in our lab were titrated over at least 4 concentrations spanning approximately a 10-fold range to determine the concentration that best allowed for the discrimination of populations of interest.

For markers expressed at low levels in unactivated cells, antibodies were titrated in parallel on both unactivated cells and cells which had been activated overnight (16 hours) in R10 containing 5µg/mL concanavalin A (ConA) or 5µg/mL phytohaemagglutinin (PHA), after which the expression of these markers was up-regulated.

7.5.5.2 Considerations for cohort phenotyping

Efforts were made to minimise batch effect for experiments when phenotyping of cohorts was conducted over several days (Panels C, D, E, F and M). In particular the following were considered:

- Standardisation of cytometer setup as described in 7.5.3;
- Where possible, paired samples were analysed as part of the same batch;
- A number of aliquots of healthy PBMCs from leukocyte cones were cryopreserved and stored. Aliquots of the same sample were analysed with each batch and used to set gates. This was to maximise consistency of how gating was performed between batches.

7.6 Cell sorting

7.6.1 Sorting of CD32 expressing CD4 T cells

PBMCs or isolated CD4 T cells were stained in 15mL Falcon tubes. Cells were pelleted and resuspended at 1 x 10^8 cells/mL in R10 with antibodies as listed in Table 7.7; details of the individual antibodies used are shown in Table 7.4.

Staining was performed for 30 minutes at 4°C after which cells were washed twice with R10 and strained through 35µm nylon mesh prior to sorting. Cells were sorted directly into AL lysis buffer (Qiagen; for rare populations), R10 or PBS with 10% fetal bovine serum (FBS) prior to total HIV DNA quantification as described in section 7.10.

Panel name	Sections	Cytometer	Contains
CD32 sorts	Figures 5.4 and B.12	MoFlo XDP (Beckman Coulter)	CD14 VioBlue CD3 FITC CD32 PE-Cy7 CD4 APC LiveDead Near IR
Tetramer sorts	Figures 3.6, B.3 & B.4	FACSAria (BD)	CCR7 PerCP-Cy5.5 CD3 BV510 CD45RA BV785 CD8a BV711 CD95 (Fas) BV605 LiveDead Near IR PD-1 BV421 Tetramer 1 FITC Tetramer 2 PE Tetramer 3 APC

Table 7.7: Flow cytometry panels used for cell sorting experiments. Further details of antibodies listed are shown in Table 7.4

7.6.2 Staining of HIV-specific CD8 T cells

Cryopreserved PBMCs were thawed in R10 with 10mM HEPES and 0.001% β-mercaptoethanol, following which CD8 T cells were isolated as in section 7.4.3.

Staining of CD8 T cells was performed in two stages, with an initial tetramer staining and Fc blocking step followed by staining of surface epitopes. CD8 T cells were suspended at a concentration of 1 x 10^8 cells/mL in isolation buffer containing 10% Human TruStain FcX (Fc Receptor Blocking Solution; BioLegend) and appropriate MHC Class I/peptide multimers. HIV tetramers were included at a concentration of 30nM and EBV and influenza dextramers at 3.2nM; details of these reagents are provided in section 7.6.2.1. Staining/Fc block was performed at room temperature for 20 minutes.

Cells were washed and resuspended in isolation buffer containing 0.5X BD Horizon Brilliant Stain Buffer (BD) and antibodies as listed in Table 7.7. Surface staining was performed for 30 minutes at 4°C after which cells were washed twice with isolation buffer and strained through 30µm nylon mesh prior to acquisition and cell sorting (experiments on sorted populations are not included in this work).

Biotinylated monomers (ImmunAware)				
MHC Class I	*Peptide*	*Abbreviation*	*Organism*	*Antigen*
A*02:01	RLRPGGKKK	RK9	HIV	Gag p17
B*07:02	GPGHKARVL	GL9	HIV	Gag p24
B*57:01	KAFSPEVIPMF	KF11	HIV	Gag p24
B*57:01	TSTLQEQIAW	TW10	HIV	Gag p24
B*53:01	YPLTFGWCF	YF9	HIV	Nef
Dextramers (Immudex)				
B*08:01	RAKFKQLL	RL8	EBV	BZLF1
A*02:01	GILGFVFTL	GL9	Influenza A	M1 protein
A*02:01	CLGGLLTMV	CV9	EBV	LMP-2A
A*02:01	GLCTLVAML	GL9	EBV	BMLF1

Table 7.8: MHC Class I/peptide multimers.

7.6.2.1 MHC Class I/peptide multimers

Biotinylated monomers of MHC Class I/peptide complexes were custom produced for HIV peptides of interest by Anette Stryhn Buus (immunAware, Laboratory of Experimental Immunology, University of Copenhagen, Denmark), using previously published methods [487]. These are listed in Table 7.8. Tetramerisation was performed by the addition of Streptavidin-APC (Invitrogen), ExtrAvidin-PE or ExtrAvidin-FITC (both Sigma) to biotinylated monomers at a 1:4 molar ratio. The total volume of Streptavidin or ExtrAvidin conjugate was divided into at least 3 aliquots which were added sequentially at 4°C.

Individuals with HIV tetramer responses were identified either by testing PBMCs from individuals with known CD8 ELIspot responses (section 7.8) or by systematic screening of individuals with an appropriate HLA type. During screening, an HLA-mismatched tetramer was included as a negative control to confirm the specificity of tetramer responses identified.

For identification of EBV and influenza specific T cells, pre-conjugated MHC Class I dextramers [488] were purchased from Immudex (Copenhagen, Denmark) as listed in Table 7.8.

7.7 HLA typing

7.7.1 DNA extraction

DNA for HLA typing was extracted using a modification of the Puregene (Qiagen) system. Fresh or frozen granulocytes were suspended in 10mL red blood cell (RBC) Lysis Solution and incubated at room temperature for 5 minutes then spun at 2000*xg* for 5 minutes; this step was repeated if necessary. Cells were then suspended in 5mL Cell Lysis Solution and vortexed. 2.5mL Protein Precipitation Solution was added and mixture centrifuged at 4°C to remove precipitate. Supernatant was added into isopropanol to precipitate out DNA. Pelleted DNA was washed with 70% ethanol and air dried, before being resuspended in nuclease-free water. If no granulocytes were available, DNA was extracted from PBMCs as described in section 7.10.1. DNA was quantified using a NanoDrop (ThermoFisher).

7.7.2 HLA typing by sequence specific primers

The HLA type of the majority of SPARTAC participants had been determined prior to the commencement of this work [489]. For the remaining samples from SPARTAC, and those from HEATHER, HLA typing was performed to intermediate resolution using PCR with sequence specific primers (PCR-SSP) by the Transplant Immunology & Immunogenetics laboratory (Dr Martin Barnardo) at the Churchill Hospital (Oxford) or the Sequence Laboratory, MRC Human Immunology Unit, Weatherall Institute of Molecular Medicine (Tim Rostron; Oxford).

7.8 CD8 ELISpot assays

ELISpot)assays were performed using overlapping peptides (OLPs) in HIV-1 *gag*. For subtype C infected patients, a library of 66 18mers overlapping by 10 amino acids was used (sequences in Table C.1).

Cryopreserved PBMCs were thawed, counted and diluted to appropriate concentration (target 1.25-2.5 x 10^5 viable cells/mL depending on cell availability). Cells were rested overnight at 37°C prior to assay setup.

ELISpot plates were prepared by coating 96 well polyvinylidene difluoride plates (Merck Millipore) with 100µL of 0.5µg/mL anti-IFN-γ 1-D1K antibody (Mabtech AB) on the day prior to the assay and kept at 4°C until use. Wells were blocked to prevent non-specific binding by washing six times with PBS containing 1% FBS. To each well, R10, reconstituted peptides (test wells) or PHA (positive control wells) and PBMCs were added and plates incubated for 14-16 hours at 37°C with 5% CO_2. Final concentration per reaction was 2 µg/mL for peptide and 15.6 µg/mL for PHA containing wells. Four negative control and two positive control wells prepared per plate.

The following day, wells were washed six times with PBS then incubated at room temperature with 100µL of 0.5µg/mL biotinylated anti-IFN-γ 7-B6-1 antibody (Mabtech AB) for 90 minutes in the dark. Wells were washed as previously described and incubated with a streptavidin-alkaline phosphatase (ALP) conjugate (Mabtech AB) for 45 minutes in the dark. Following a further round of washing, plates were developed for 15-20 minutes under light using a chromogenic ALP substrate kit (BioRad) containing nitro-blue tetrazolium chloride (NBT) and 5-bromo-4-chloro-3-indoly phosphate (BCIP). Plates were washed with water to stop development reaction and left to dry overnight.

Plates were counted using an AID ELISpot plate reader (Autoimmun Diagnostika) with appropriate settings for the detection of IFN-γ. Similar assays for subtype B infected participants were performed by others [490] using 123 15mers overlapping by 11 amino acids (sequences in Table C.2) in *gag*, as well as optimal and variant epitopes in *gag*, *pol*, *nef* and *env*. For both subtype B and C analyses, background (calculated as the mean plus three standard deviations of the negative well counts) was subtracted and the number of responses normalised to spot forming units (SFU) per 10^6 cells. A response was considered positive if it was greater than 50 SFU.

	sPD-1	**sTim3**
Kit name	Human PD-1 (PDCD1) ELISA kit	Quantikine ELISA Human TIM-3 Immunoassay kit
Manufacturer	Thermo Scientific	R&D
Product code	EHPDCD1	DTIM30
Plasma dilution	1:2	1:5
Standards used (pg/mL)	2400 960 384 153.6 61.44 24.58	2000 1000 500 250 125 62.5 31.3

Table 7.9: ELISA kits used for the measurement of soluble (s) PD-1 and Tim-3.

7.9 ELISA

The concentration of sPD-1 and sTim-3 was measured in thawed plasma samples by enzyme linked immunosorbent assay (ELISA) with commercially available kits as shown in Table 7.9. Both kits were tested to determine the optimal dilution and range of standards to use, as well as testing for linearity of dilutions and compatibility with ACD plasma.

ELISA plates were read using a FLUOstar Omega (BMG Labtech) at 450nm with background measured at 540 or 550nm (sTim-3 and sPD-1 respectively) subtracted from these values.

Samples were measured in duplicate and standards in triplicate; the mean value of replicates was used. Standards were fitted with a 4-parameter logistic curve ([491] and as recommended by the manufacturer), which was used to calculate concentration of samples. The lower limit of detection (LLD) was defined as the greater of a) the lower asymptote of the standard curve or b) the mean value of all blank wells + 1.96 x standard deviation (SD). Any values below this were taken at the LLD.

A coefficient of variation (CV) of 20% was used as a maximal limit of acceptable variation. Samples with CV>20%, were repeated and in all cases the CV of the

repeats was below this threshold. When possible, paired samples were measured on the same plate to minimise the impact of any plate to plate variation.

7.10 HIV reservoir quantification

7.10.1 Nucleic acid extraction

HIV DNA was extracted from CD4 T cells or PBMCs using the QiaAMP Blood Mini Kit (Qiagen) as per manufacturer's instructions, including protease treatment and elution of DNA into distilled water. For sorted CD4 T cell populations (where cell input was low) the QIAmp DNA Micro kit (Qiagen) was used instead (Figure 5.4). DNA was stored at 4°C with HIV DNA quantification performed within 1 week of DNA extraction.

RNA was isolated using the Qiagen AllPrep DNA/RNA Mini kit (Qiagen) using the manufacturer's instructions with the optional on-column DNAse digestion step performed twice to eliminate any potential HIV DNA; RNA was eluted into distilled water and stored at -80°C until CA-usRNA quantification was performed.

7.10.2 Total HIV DNA quantification

HIV DNA was quantified relative to cell number using qPCR as previously described [492]. Cell copy number was initially quantified using an albumin qPCR. Samples were quantified in triplicate at two dilutions and the mean value (adjusted for dilution) across all samples was used in calculations. If sufficient DNA was available, 25,000 cell equivalents (and no less than 10,000 cell equivalents; except as specified in Chapter 5) of DNA was then used in a total HIV DNA qPCR, performed in triplicate. The mean number of copies of DNA was normalised to cell number and expressed as copies/10^6 CD4 T cells.

For both albumin and HIV qPCR reactions a similar protocol was used. 10µL of DNA was added into final reaction volume of 25µL containing LightCycler 480 Probes Master Mix (Roche), fluorescein (FAM) and quencher (BHQ-1) conjugated probe and two primers (all Eurofins MWG Operon) as per Table 7.10. Reactions

were cycled using the following program on a Roche LightCycler: one cycle of 95°C for 10 minutes; 45 cycles of 95°C for 15 seconds and 60°C for 1 minute. Data were analysed using proprietary software supplied with the machine.

The standard curve for both qPCR reactions was constructed using serial dilutions of DNA extracted from the 8E5/LAI cell line (NIH AIDS reagent program) which are known to contain a single integrated copy of HIV DNA per cell [493]. Standards were prepared in bulk by extracting DNA from cultured 8E5/LAI cells (as in 7.10.1), diluted in water and stored at -20°C in single-use aliquots at the correct dilution for input into the assay. For SPARTAC samples, standards for both qPCRs were run in duplicate of 10-fold dilutions ranging from 10^5 to 10^0 copies of DNA per reaction. For HEATHER samples, standards were run in duplicate of 3-fold dilutions ranging from 10,935 to 45 copies of DNA per reaction for albumin quantification and 3,645 to 15 copies of DNA per reaction for HIV DNA quantification.

For assays performed in HEATHER, there were some instances in which the level of HIV DNA was very low (below 15 copies/well). These values were dealt with as follows. Any replicate values from 5-15 copies were extrapolated from the curve; this is because the limit of detection (defined here as the lower limit for which 95% of wells were detectable) was experimentally determined to be 5 copies of DNA/well. Any samples with a replicate value <5 copies were assigned 2.5 for that replicate (the mid-point of the limit of detection and zero). Any samples with a negative replicate were repeated if possible; if not possible or if some repeat replicates were also negative these replicates were assigned a value of 0.

7.10.3 Cell-associated unspliced RNA quantification

Measurement of CA-usRNA transcripts was performed using a semi-nested qPCR assay as previously described [255], which was based on protocols developed in the Pasternak and Lewin labs [494–496].

The HIV standard was generated by *in vitro* transcribing the plasmid Sp5-NL4.3 (provided by the lab of Damian Purcell) using the RiboMax Large Scale SP6 RNA

Primer or probe	*Sequence*	*Concentration in reaction*	*Position in HXB2*
Albumin qPCR			
Albumin probe	5'-FAM–CCTGTCATGCCCACACAAATCTCTCC–BHQ-1-3'	200nM	-
Albumin forward primer	5'-GCTGTCATCTCTTGTGGGCTGT-3'	250nM	-
Albumin reverse primer	5'AAACTCATGGGAGCTGCTGGTT-3'	250nM	-
HIV qPCR			
HIV probe	5'-FAM–AGTRGTGTGTGCCCGTCTGTTG–BHQ-1-3'	500nM	552-573
HIV LTR OS (forward) primer	5'-GRAACCCACTGCTTAASSCTCAA-3'	500nM	506-528
HIV LTR AS (reverse) primer	5'-TGTTCGGGCGCCACTGCTAGAGA-3'	500nM	626-648

Table 7.10: Sequences of primers and probes used in qPCR quantification of HIV DNA. R refers to a randomly inserted purine base (A or G), S refers to a randomly inserted C or G. For sequences used against HIV, the binding position is given relative to a subtype B reference viral genome (HXB2). The final concentration in the reaction volume is given. Abbreviations: FAM (fluorescein amidite), BHQ-1 (Black Hole Quencher 1).

production System (Promega). HIV RNA standards were diluted in 10ng/µL uninfected PBMC RNA, and treated the same way as clinical samples throughout.

Complementary DNA (cDNA) was synthesised from extracted RNA samples and RNA standards as follows. Up to 500ng of RNA in nuclease-free water was added into a final reaction volume of 13.5µL containing 0.74 nM deoxyribonucleotide triphosphates (dNTPs), 0.1µg/µL random hexamers and 18.5ng/µL Oligo$(dT)_{12\text{-}18}$ (Invitrogen). Annealing was performed at 65°C for 5 minutes and samples kept on ice until next step. An additional master mix was added to give a final volume of 20µL containing 1X First Strand buffer (Invitrogen), 5mM dithiothreitol (DTT), 20U RNAseOUT RNAse inhibitor (Invitrogen) and 200U Superscript III Reverse Transcriptase (RT; Invitrogen). This sample was held at 42°C for 45 minutes, then at 80°C for 15 minutes to allow for reverse transcription. A control without RT was prepared for all samples.

To improve sensitivity, an initial PCR was performed to amplify the cDNA template. 5µL of cDNA was added into final reaction volume of 50µL containing 2.5mM $MgCl_2$, 0.8mM dNTPs (0.2µM each of dATP, dCTP, dGTP and dTTP; ThermoScientific), 2U Platinum *Taq* Polymerase (Invitrogen), 1X PCR buffer (supplied with enzyme) and MH535 and SL20 primers (all Eurofins MWG Operon) as per Table 7.11. Reactions were cycled using the following program on a thermocycler: one cycle of 95°C for 10 minutes; 15 cycles of 94°C for 20 seconds, 55°C for 40 seconds and 72°C for 40 seconds.

A qPCR reaction was then performed to quantify HIV copies; this second PCR uses primers which are semi-nested in the initial PCR product. 2µL of PCR product was added into final a reaction volume of 20µL containing 1X LightCycler 480 Probes Master Mix, FAM and BHQ-1 conjugated probe and SL20 and 4F primers as listed in Table 7.11. Reactions were cycled using the following program on a Roche LightCycler: one cycle of 95°C for 10 minutes; 45 cycles of 95°C for 15 seconds and 60°C for 1 minute. Data were analysed using proprietary software supplied with the machine.

All samples and RT- controls were measured in triplicate; averages of replicates were taken to calculate the number of copies of CA-usRNA. Any background from wells without RT were subtracted from final measurements. HIV RNA copies were normalised to RNA weight measured via NanoDrop (ThermoFisher).

7.11 Determination of viral clade

Viral subtype was determined based on available sequence data using the Stanford REGA tool. For SPARTAC this was performed by the MRC CTU using previous versions of this tool [497, 498]; for any missing values and in HEATHER, REGA version 3.0 was used [499].

7.12 Statistical analyses

Analyses were performed using GraphPad Prism (GraphPad Software, La Jolla, California, USA) (v6.0f or v7.0b), or R (v3.2.2 or v3.4.3) [500]. Except where otherwise specified, p-values <0.05 were considered statistically significant. Figures were produced using GraphPad Prism, FlowJo, Adobe Illustrator 22.1, SPICE 6.0 [501] and the following R packages: ggplot2 (v2.2.1) [502], ggpubr (v0.1.6) [503], corrplot (v0.84) [504] or gplots (v3.0.1) [505].

Unless otherwise indicated, for all boxplots the central bar indicates the median and the two hinges mark the 1st and 3rd quartiles. The whiskers extend to the greater of the largest value or 1.5 times the IQR; outliers are shown as points.

7.12.1 Missing data

Where possible, statistical tests were performed such that missing data was omitted. For the regression analyses presented in Chapter 4 missing data were imputed using the package MissForest [506], which employs a random forest based method for multiple imputation and has been shown to be superior to other multiple imputation methods in biological datasets with missingness levels ranging from 10-30% [506, 507].

First round PCR amplification			
Primer or probe	*Sequence*	*Concentration in reaction*	*Position in HXB2*
MH535 (forward) primer	5'-AACTAGGGAACCCACTGCTTAAG-3'	400nM	500-522
SL20 (reverse) primer	5'-TCTCCTTCTAGCCTCCGCTAGTC-3'	400nM	764-786
HIV qPCR			
HIV probe	5'FAM–AGTRGTGTGTGCCCGTCTGTTG–BHQ-1-3'	330nM	552-573
4F (forward) primer	5'-TAAAGCTTGCCTTGAGTGCT-3'	330nM	529-548
SL20 (reverse) primer	5'-TCTCCTTCTAGCCTCCGCTAGTC-3'	330nM	764-786

Table 7.11: Sequences of primers and probes used in qPCR quantification of call-associated unspliced RNA. R refers to a randomly inserted purine base (A or G), S refers to a randomly inserted C or G. For sequences used against HIV, the binding position is given relative to a subtype B reference viral genome (HXB2). The final concentration in the reaction volume is given. Abbreviations: FAM (fluorescein amidite), BHQ-1 (Black Hole Quencher 1).

7.12.2 Group comparisons

Categorical variables were compared using χ^2 or Fisher-Freeman Halton exact test as appropriate. For continuous variables, where data was non-normal or sample size was too small to confidently determine that data was normally distributed, non-parametric techniques were chosen. Where appropriate, paired tests were used. Where two groups were compared a Mann-Whitney or Student's t-test was used. Continuous variables were compared across three or more groups using the Kruskal-Wallis test, ANOVA, or, where data were paired, a Friedman test. Pairwise comparisons were performed on all combinations of groups only if the overall test p-value was <0.05. For large numbers of group comparisons, p values were adjusted to control the false discovery rate (FDR) using the method of Benjamini and Hochberg [508].

7.12.3 Correlative analyses

Individual correlative analyses were performed using Spearman's rank correlation or Pearson's correlation depending on distribution of the data. Corrgrams were generated using the package corrplot (v0.84) [504]. Where some data were missing, pairwise complete observations were used to calculate the correlation coefficients.

7.12.4 Survival analyses

Survival analyses were visualised with Kaplan-Meier plots and curves compared using log rank test. Associations were also examined with Cox proportional hazard models using the package survival (v2.41-3) [509].

7.12.5 Principle component analysis

Principle component analyses were performed using the package FactoMineR (v1.39) [510] and visualised using factoextra (v1.0.5) [511].

7.12.6 Regression analyses

7.12.6.1 Boosted regression tree models

Boosted regression tree models were fitted with a Gaussian outcome using the package gbm3 (v2.2) [512], with tuning parameters adjusted based on guidance in Elith *et al.* (2008) and Ridgeway (2007) [440, 513]. Models were fitted with an interaction depth of 5 with a minimum of 5 observations in a terminal node. The shrinkage parameter was adjusted between 0.0001 - 0.001 to aim for optimal number of trees to fall in the range of 3000-10000. The optimal number of trees was determined using 10 fold cross-validation, with the number of trees which minimised cross-validation error chosen. To account for stochastisity in model fitting, all results presented are the pooled outcomes of 100 models.

7.12.6.2 Penalised regression

LASSO models [514] were fitted using the R package glmnet (v2.0-16) [515]. For the analyses presented in Chapter 4, Gaussian regression models were fitted with an additive linear model (no interactions). The tuning parameter λ was determined using 10-fold cross-validation, with the λ value used being that which minimised cross-validation error plus one standard error.

References

1. Gottlieb, M. S. *et al.* Pneumocystis carinii Pneumonia and Mucosal Candidiasis in Previously Healthy Homosexual Men. *New England Journal of Medicine* **305,** 1425–1431 (Dec. 1981).
2. Barré-Sinoussi, F. *et al.* Isolation of a T-lymphotropic retrovirus from a patient at risk for acquired immune deficiency syndrome (AIDS). *Science* **220,** 868–871 (May 1983).
3. Gallo, R. *et al.* Isolation of human T-cell leukemia virus in acquired immune deficiency syndrome (AIDS). *Science* **220,** 865–867 (May 1983).
4. Deeks, S. G., Overbaugh, J., Phillips, A. & Buchbinder, S. HIV infection. *Nature Reviews Disease Primers* **1,** 15035 (Oct. 2015).
5. Barré-Sinoussi, F., Ross, A. L. & Delfraissy, J.-F. Past, present and future: 30 years of HIV research. *Nature Reviews Microbiology* **11,** 877–883 (Oct. 2013).
6. Chun, T.-W. *et al.* In vivo fate of HIV-1-infected T cells: Quantitative analysis of the transition to stable latency. *Nature Medicine* **1,** 1284–1290 (Dec. 1995).
7. Chun, T.-W. *et al.* Quantification of latent tissue reservoirs and total body viral load in HIV-1 infection. *Nature* **387,** 183–188 (May 1997).
8. Finzi, D. *et al.* Identification of a reservoir for HIV-1 in patients on highly active antiretroviral therapy. *Science* **278,** 1295–1300 (Nov. 1997).
9. Hearps, A. C., **Martin, G. E.**, Rajasuriar, R. & Crowe, S. M. Inflammatory Co-morbidities in HIV+ Individuals: Learning Lessons from Healthy Ageing. *Current HIV/AIDS Reports* **11,** 20–34 (Jan. 2014).
10. Boswell, R., Foisy, M. M. & Hughes, C. A. Dolutegravir Dual Therapy as Maintenance Treatment in HIV-Infected Patients: A Review. *Annals of Pharmacotherapy* **52,** 681–689 (Feb. 2018).
11. Llibre, J. M. *et al.* Efficacy, safety, and tolerability of dolutegravir-rilpivirine for the maintenance of virological suppression in adults with HIV-1: phase 3, randomised, non-inferiority SWORD-1 and SWORD-2 studies. *The Lancet* **391,** 839–849 (Mar. 2018).
12. INSIGHT START Study Group. Initiation of Antiretroviral Therapy in Early Asymptomatic HIV Infection. *New England Journal of Medicine* **373,** 795–807 (Aug. 2015).
13. Cohen, M. S. *et al.* Antiretroviral Therapy for the Prevention of HIV-1 Transmission. *New England Journal of Medicine* **375,** 830–839 (Sept. 2016).
14. Rodger, A. J. *et al.* Sexual Activity Without Condoms and Risk of HIV Transmission in Serodifferent Couples When the HIV-Positive Partner Is Using Suppressive Antiretroviral Therapy. *JAMA* **316,** 171–181 (July 2016).

15. World Health Organisation. *Guideline on when to start antiretroviral therapy and on pre-exposure prophylaxis for HIV* (Sept. 2015).

16. Ford, N. *et al.* World Health Organization Guidelines on Postexposure Prophylaxis for HIV: Recommendations for a Public Health Approach. *Clinical Infectious Diseases* **60,** S161–S164 (May 2015).

17. Irvine, C. *et al.* Efficacy of HIV Postexposure Prophylaxis: Systematic Review and Meta-analysis of Nonhuman Primate Studies. *Clinical Infectious Diseases* **60,** S165–S169 (May 2015).

18. UNAIDS. *Fact sheet - Latest statistics on the status of the AIDS epidemic* `http://www.unaids.org/sites/default/files/media_asset/UNAIDS_FactSheet_en.pdf`. July 2018.

19. UNAIDS. *90-90-90 An ambitious treatment target to help end the AIDS epidemic* `http://www.unaids.org/sites/default/files/media_asset/90-90-90_en.pdf`. Oct. 2014.

20. Los Alamos National Laboratory. *Landmarks of the HIV genome* `https://www.hiv.lanl.gov/content/sequence/HIV/MAP/landmark.html`. Jan. 2017.

21. Nyamweya, S. *et al.* Comparing HIV-1 and HIV-2 infection: Lessons for viral immunopathogenesis. *Reviews in Medical Virology* **23,** 221–240 (Feb. 2013).

22. Freed, E. O. HIV-1 assembly, release and maturation. *Nature Reviews Microbiology* **13,** 484–496 (June 2015).

23. Karn, J. & Stoltzfus, C. M. Transcriptional and Posttranscriptional Regulation of HIV-1 Gene Expression. *Cold Spring Harbor Perspectives in Medicine* **2,** a006916–a006916 (Nov. 2011).

24. Janeway, C. A. & Medzhitov, R. Innate Immune Recognition. *Annual Review of Immunology* **20,** 197–216 (Apr. 2002).

25. Kurioka, A., Klenerman, P. & Willberg, C. B. Innate-like CD8+ T-cells and NK cells: converging functions and phenotypes. *Immunology* **154,** 547–556 (Apr. 2018).

26. Vermijlen, D. & Prinz, I. Ontogeny of Innate T Lymphocytes - Some Innate Lymphocytes are More Innate than Others. *Frontiers in Immunology* **5** (Oct. 2014).

27. Artis, D. & Spits, H. The biology of innate lymphoid cells. *Nature* **517,** 293–301 (Jan. 2015).

28. Iwasaki, A. & Medzhitov, R. Regulation of Adaptive Immunity by the Innate Immune System. *Science* **327,** 291–295 (Jan. 2010).

29. Masopust, D., Vezys, V., Wherry, E. J. & Ahmed, R. A brief history of CD8 T cells. *European Journal of Immunology* **37,** S103–S110 (Nov. 2007).

30. Zhang, N. & Bevan, M. CD8+ T Cells: Foot Soldiers of the Immune System. *Immunity* **35,** 161–168 (Aug. 2011).

31. Zhu, J. & Paul, W. E. CD4 T cells: fates, functions, and faults. *Blood* **112,** 1557–1569 (Aug. 2008).

32. Nikolich-Žugich, J., Slifka, M. K. & Messaoudi, I. The many important facets of T-cell repertoire diversity. *Nature Reviews Immunology* **4,** 123–132 (Feb. 2004).

33. Itano, A. A. & Jenkins, M. K. Antigen presentation to naive CD4 T cells in the lymph node. *Nature Immunology* **4,** 733–739 (Aug. 2003).

34. Chen, L. & Flies, D. B. Molecular mechanisms of T cell co-stimulation and co-inhibition. *Nature Reviews Immunology* **13,** 227–242 (Mar. 2013).

35. Fritsch, R. D. *et al.* Stepwise Differentiation of CD4 Memory T Cells Defined by Expression of CCR7 and CD27. *The Journal of Immunology* **175,** 6489–6497 (Nov. 2005).

36. Chomont, N. *et al.* HIV reservoir size and persistence are driven by T cell survival and homeostatic proliferation. *Nature Medicine* **15,** 893–900 (June 2009).

37. Champagne, P. *et al.* Skewed maturation of memory HIV-specific CD8 T lymphocytes. *Nature* **410,** 106–111 (Mar. 2001).

38. Farber, D. L., Yudanin, N. A. & Restifo, N. P. Human memory T cells: generation, compartmentalization and homeostasis. *Nature Reviews Immunology* **14,** 24–35 (Dec. 2013).

39. Kaech, S. M., Wherry, E. J. & Ahmed, R. Effector and memory T-cell differentiation: implications for vaccine development. *Nature Reviews Immunology* **2,** 251–262 (Apr. 2002).

40. Kaech, S. M. & Cui, W. Transcriptional control of effector and memory CD8+ T cell differentiation. *Nature Reviews Immunology* **12,** 749–761 (Oct. 2012).

41. Newell, E., Sigal, N., Bendall, S., Nolan, G. & Davis, M. Cytometry by Time-of-Flight Shows Combinatorial Cytokine Expression and Virus-Specific Cell Niches within a Continuum of CD8+ T Cell Phenotypes. *Immunity* **36,** 142–152 (Jan. 2012).

42. Akondy, R. S. *et al.* Origin and differentiation of human memory CD8 T cells after vaccination. *Nature* **552,** 362–367 (Dec. 2017).

43. Gattinoni, L., Speiser, D. E., Lichterfeld, M. & Bonini, C. T memory stem cells in health and disease. *Nature Medicine* **23,** 18–27 (Jan. 2017).

44. Afik, S. *et al.* Targeted reconstruction of T cell receptor sequence from single cell RNA-seq links CDR3 length to T cell differentiation state. *Nucleic Acids Research* **45,** e148–e148 (July 2017).

45. Michie, C. A., McLean, A., Alcock, C. & Beverley, P. C. L. Lifespan of human lymphocyte subsets defined by CD45 isoforms. *Nature* **360,** 264–265 (Nov. 1992).

46. Sallusto, F., Lenig, D., Förster, R., Lipp, M. & Lanzavecchia, A. Two subsets of memory T lymphocytes with distinct homing potentials and effector functions. *Nature* **401,** 708–712 (Oct. 1999).

47. Hamann, D. *et al.* Phenotypic and Functional Separation of Memory and Effector Human CD8+ T Cells. *Journal of Experimental Medicine* **186,** 1407–1418 (Nov. 1997).

48. Roos, M. L. *et al.* Changes in the Composition of Circulating CD8+ T Cell Subsets during Acute Epstein-Barr and Human Immunodeficiency Virus Infections in Humans. *The Journal of Infectious Diseases* **182,** 451–458 (Aug. 2000).

49. Romero, P. *et al.* Four Functionally Distinct Populations of Human Effector-Memory CD8+ T Lymphocytes. *The Journal of Immunology* **178,** 4112–4119 (Mar. 2007).

50. Rufer, N. Ex vivo characterization of human CD8+ T subsets with distinct replicative history and partial effector functions. *Blood* **102,** 1779–1787 (Sept. 2003).

51. Appay, V. *et al.* Memory CD8+ T cells vary in differentiation phenotype in different persistent virus infections. *Nature Medicine* **8,** 379–385 (Apr. 2002).

52. Ma, C. *et al.* A clinical microchip for evaluation of single immune cells reveals high functional heterogeneity in phenotypically similar T cells. *Nature Medicine* **17,** 738–743 (May 2011).

53. Dong, K. L. *et al.* Detection and treatment of Fiebig stage I HIV-1 infection in young at-risk women in South Africa: a prospective cohort study. *The Lancet HIV* **5,** e35–e44 (Jan. 2018).

54. Robb, M. L. *et al.* Prospective Study of Acute HIV-1 Infection in Adults in East Africa and Thailand. *New England Journal of Medicine* **374,** 2120–2130 (June 2016).

55. Kaufmann, G. *et al.* Patterns of Viral Dynamics during Primary Human Immunodeficiency Virus Type 1 Infection. *The Journal of Infectious Diseases* **178,** 1812–1815 (Dec. 1998).

56. Fiebig, E. *et al.* Dynamics of HIV viremia and antibody seroconversion in plasma donors: implications for diagnosis and staging of primary HIV infection. *AIDS* **17,** 1871–9 (Sept. 2003).

57. McMichael, A. J., Borrow, P., Tomaras, G. D., Goonetilleke, N. & Haynes, B. F. The immune response during acute HIV-1 infection: clues for vaccine development. *Nature Reviews Immunology* **10,** 11–23 (Dec. 2009).

58. Crowell, T. A. *et al.* Acute Retroviral Syndrome Is Associated With High Viral Burden, CD4 Depletion, and Immune Activation in Systemic and Tissue Compartments. *Clinical Infectious Diseases* **66,** 1540–1549 (Dec. 2017).

59. Brenchley, J. M. *et al.* Differential Th17 CD4 T-cell depletion in pathogenic and nonpathogenic lentiviral infections. *Blood* **112,** 2826–2835 (July 2008).

60. Deleage, C. *et al.* Impact of early cART in the gut during acute HIV infection. *JCI Insight* **1,** e87065 (July 2016).

61. Guadalupe, M. *et al.* Severe CD4+ T-cell depletion in gut lymphoid tissue during primary human immunodeficiency virus type 1 infection and substantial delay in restoration following highly active antiretroviral therapy. *Journal of Virology* **77,** 11708–11717 (Nov. 2003).

62. Schuetz, A. *et al.* Initiation of ART during Early Acute HIV Infection Preserves Mucosal Th17 Function and Reverses HIV-Related Immune Activation. *PLoS Pathogens* **10,** e1004543 (Dec. 2014).

63. Cohen, M. S., Gay, C. L., Busch, M. P. & Hecht, F. M. The detection of acute HIV infection. *The Journal of Infectious Diseases* **202,** S270–S277 (Oct. 2010).

64. Ananworanich, J. *et al.* A novel acute HIV infection staging system based on 4th generation immunoassay. *Retrovirology* **10,** 56 (2013).

65. Chowdhury, A. *et al.* Differential Impact of In Vivo CD8+ T Lymphocyte Depletion in Controller versus Progressor Simian Immunodeficiency Virus-Infected Macaques. *Journal of Virology* **89,** 8677–8686 (June 2015).

66. Jin, X. *et al.* Dramatic Rise in Plasma Viremia after CD8+ T Cell Depletion in Simian Immunodeficiency Virus–infected Macaques. *The Journal of Experimental Medicine* **189,** 991–998 (Mar. 1999).

67. Schmitz, J. E. *et al.* Control of viremia in simian immunodeficiency virus infection by CD8+ lymphocytes. *Science* **283,** 857–860 (Feb. 1999).

68. Matano, T. *et al.* Administration of an anti-CD8 monoclonal antibody interferes with the clearance of chimeric simian/human immunodeficiency virus during primary infections of rhesus macaques. *Journal of Virology* **72,** 164–169 (1 Jan. 1998).

69. Gaufin, T. *et al.* Experimental depletion of CD8+ cells in acutely SIVagm-Infected African Green Monkeys results in increased viral replication. *Retrovirology* **7,** 42 (2010).

70. Cartwright, E. *et al.* CD8+ Lymphocytes Are Required for Maintaining Viral Suppression in SIV-Infected Macaques Treated with Short-Term Antiretroviral Therapy. *Immunity* **45,** 656–668 (Sept. 2016).

71. Fellay, J. *et al.* A Whole-Genome Association Study of Major Determinants for Host Control of HIV-1. *Science* **317,** 944–947 (Aug. 2007).

72. Limou, S. *et al.* Genomewide Association Study of an AIDS-Nonprogression Cohort Emphasizes the Role Played byHLAGenes (ANRS Genomewide Association Study 02). *The Journal of Infectious Diseases* **199,** 419–426 (Feb. 2009).

73. International HIV Controllers Study *et al.* The Major Genetic Determinants of HIV-1 Control Affect HLA Class I Peptide Presentation. *Science* **330,** 1551–1557 (Nov. 2010).

74. Borrow, P. *et al.* Antiviral pressure exerted by HIV-l-specific cytotoxic T lymphocytes (CTLs) during primary infection demonstrated by rapid selection of CTL escape virus. *Nature Medicine* **3,** 205–211 (Feb. 1997).

75. Goulder, P. J. *et al.* Late escape from an immunodominant cytotoxic T-lymphocyte response associated with progression to AIDS. *Nature Medicine* **3,** 212–217 (Feb. 1997).

76. Goonetilleke, N. *et al.* The first T cell response to transmitted/founder virus contributes to the control of acute viremia in HIV-1 infection. *The Journal of Experimental Medicine* **206,** 1253–1272 (June 2009).

77. Goulder, P. J. R. & Watkins, D. I. HIV and SIV CTL escape: implications for vaccine design. *Nature Reviews Immunology* **4,** 630–640 (Aug. 2004).

78. Borrow, P., Lewicki, H., Hahn, B. H., Shaw, G. M. & Oldstone, M. B. Virus-specific CD8+ cytotoxic T-lymphocyte activity associated with control of viremia in primary human immunodeficiency virus type 1 infection. *Journal of Virology* **68,** 6103–6110 (Sept. 1994).

79. Koup, R. A. *et al.* Temporal association of cellular immune responses with the initial control of viremia in primary human immunodeficiency virus type 1 syndrome. *Journal of Virology* **68,** 4650–4655 (July 1994).

80. Freel, S. A. *et al.* Initial HIV-1 Antigen-Specific CD8+ T Cells in Acute HIV-1 Infection Inhibit Transmitted/Founder Virus Replication. *Journal of Virology* **86,** 6835–6846 (Apr. 2012).

81. Altfeld, M. *et al.* Cellular Immune Responses and Viral Diversity in Individuals Treated during Acute and Early HIV-1 Infection. *The Journal of Experimental Medicine* **193,** 169–180 (Jan. 2001).

82. Streeck, H. *et al.* Human Immunodeficiency Virus Type 1-Specific CD8+ T-Cell Responses during Primary Infection Are Major Determinants of the Viral Set Point and Loss of CD4+ T Cells. *Journal of Virology* **83,** 7641–7648 (May 2009).

83. Yang, H. *et al.* Antiviral Inhibitory Capacity of CD8+ T cells Predicts the Rate of CD4+ T-Cell Decline in HIV-1 Infection. *The Journal of Infectious Diseases* **206,** 552–561 (June 2012).

84. Burgers, W. A. *et al.* Association of HIV-Specific and Total CD8+ T Memory Phenotypes in Subtype C HIV-1 Infection with Viral Set Point. *The Journal of Immunology* **182,** 4751–4761 (Apr. 2009).

85. Ndhlovu, Z. *et al.* Magnitude and Kinetics of CD8+ T Cell Activation during Hyperacute HIV Infection Impact Viral Set Point. *Immunity* **43,** 591–604 (Sept. 2015).

86. Takata, H. *et al.* Delayed differentiation of potent effector CD8+ T cells reducing viremia and reservoir seeding in acute HIV infection. *Science Translational Medicine* **9,** eaag1809 (Feb. 2017).

87. Appay, V. *et al.* Dynamics of T Cell Responses in HIV Infection. *The Journal of Immunology* **168,** 3660–3666 (Apr. 2002).

88. Demers, K. R. *et al.* Temporal Dynamics of CD8+ T Cell Effector Responses during Primary HIV Infection. *PLoS Pathogens* **12,** e1005805 (Aug. 2016).

89. Pastor, L. *et al.* Dynamics of CD4 and CD8 T-Cell Subsets and Inflammatory Biomarkers during Early and Chronic HIV Infection in Mozambican Adults. *Frontiers in Immunology* **8,** 1925 (Jan. 2018).

90. Deeks, S. G. *et al.* Immune activation set point during early HIV infection predicts subsequent CD4+ T-cell changes independent of viral load. *Blood* **104,** 942–947 (Apr. 2004).

91. Giorgi, J. V. *et al.* Shorter survival in advanced human immunodeficiency virus type 1 infection is more closely associated with T lymphocyte activation than with plasma virus burden or virus chemokine coreceptor usage. *The Journal of Infectious Diseases* **179,** 859–870 (Apr. 1999).

92. Sousa, A. E., Carneiro, J., Meier-Schellersheim, M., Grossman, Z. & Victorino, R. M. M. CD4 T Cell Depletion Is Linked Directly to Immune Activation in the Pathogenesis of HIV-1 and HIV-2 but Only Indirectly to the Viral Load. *The Journal of Immunology* **169,** 3400–3406 (Sept. 2002).

93. Hazenberg, M. D. *et al.* Persistent immune activation in HIV-1 infection is associated with progression to AIDS. *AIDS* **17,** 1881–1888 (Sept. 2003).

94. Doisne, J.-M. *et al.* CD8+ T cells specific for EBV, cytomegalovirus, and influenza virus are activated during primary HIV infection. *Journal of Immunology* **173,** 2410–2418 (Aug. 2004).

95. Bangs, S., McMichael, A. & Xu, X. Bystander T cell activation–implications for HIV infection and other diseases. *Trends in Immunology* **27,** 518–24 (Nov. 2006).

96. Kaech, S. M. *et al.* Selective expression of the interleukin 7 receptor identifies effector CD8 T cells that give rise to long-lived memory cells. *Nature Immunology* **4,** 1191–1198 (Nov. 2003).

97. Trautmann, L. *et al.* Profound metabolic, functional, and cytolytic differences characterize HIV-specific CD8 T cells in primary and chronic HIV infection. *Blood* **120,** 3466–3477 (Sept. 2012).

98. Lichterfeld, M. *et al.* Loss of HIV-1-specific CD8+ T Cell Proliferation after Acute HIV-1 Infection and Restoration by Vaccine-induced HIV-1–specific CD4+ T Cells. *The Journal of Experimental Medicine* **200,** 701–712 (Sept. 2004).

99. Streeck, H. *et al.* Antigen Load and Viral Sequence Diversification Determine the Functional Profile of HIV-1-Specific CD8+ T Cells. *PLoS Medicine* **5,** e100 (May 2008).

100. Ribeiro-dos-Santos, P. *et al.* Chronic HIV infection affects the expression of the 2 transcription factors required for CD8 T-cell differentiation into cytolytic effectors. *Blood* **119,** 4928–4938 (Apr. 2012).

101. Migueles, S. A. *et al.* HIV-specific CD8+ T cell proliferation is coupled to perforin expression and is maintained in nonprogressors. *Nature Immunology* **3,** 1061–1068 (Oct. 2002).

102. Brenchley, J. M. Expression of CD57 defines replicative senescence and antigen-induced apoptotic death of CD8+ T cells. *Blood* **101,** 2711–2720 (Nov. 2002).

103. Kostense, S. *et al.* Persistent numbers of tetramer+ CD8(+) T cells, but loss of interferon-gamma+ HIV-specific T cells during progression to AIDS. *Blood* **99,** 2505–2511 (Apr. 2002).

104. Appay, V. *et al.* HIV-Specific CD8+ T Cells Produce Antiviral Cytokines but Are Impaired in Cytolytic Function. *The Journal of Experimental Medicine* **192,** 63–76 (July 2000).

105. Zhang, D. *et al.* Most antiviral CD8 T cells during chronic viral infection do not express high levels of perforin and are not directly cytotoxic. *Blood* **101,** 226–235 (Aug. 2002).

106. Shacklett, B. L. *et al.* Abundant Expression of Granzyme A, but Not Perforin, in Granules of CD8+ T Cells in GALT: Implications for Immune Control of HIV-1 Infection. *The Journal of Immunology* **173,** 641–648 (June 2004).

107. Shankar, P. *et al.* Impaired function of circulating HIV-specific CD8(+) T cells in chronic human immunodeficiency virus infection. *Blood* **96,** 3094–3101 (Nov. 2000).

108. Okulicz, J. F. *et al.* Influence of the Timing of Antiretroviral Therapy on the Potential for Normalization of Immune Status in Human Immunodeficiency Virus 1–Infected Individuals. *JAMA Internal Medicine* **175,** 88 (Jan. 2015).

109. Serrano-Villar, S. *et al.* HIV-Infected Individuals with Low CD4/CD8 Ratio despite Effective Antiretroviral Therapy Exhibit Altered T Cell Subsets, Heightened CD8+ T Cell Activation, and Increased Risk of Non-AIDS Morbidity and Mortality. *PLoS Pathogens* **10,** e1004078 (May 2014).

110. Le, T. *et al.* Enhanced CD4+ T-Cell Recovery with Earlier HIV-1 Antiretroviral Therapy. *New England Journal of Medicine* **368,** 218–230 (Jan. 2013).

111. Thornhill, J. *et al.* Enhanced normalisation of CD4/CD8 ratio with early antiretroviral therapy in primary HIV infection. *Journal of the International AIDS Society* **17,** 19480 (Nov. 2014).

112. Malhotra, U. *et al.* Effect of Combination Antiretroviral Therapy on T-Cell Immunity in Acute Human Immunodeficiency Virus Type 1 Infection. *The Journal of Infectious Diseases* **181,** 121–131 (Jan. 2000).

113. Oxenius, A. *et al.* Early highly active antiretroviral therapy for acute HIV-1 infection preserves immune function of CD8+ and CD4+ T lymphocytes. *Proceedings of the National Academy of Sciences* **97,** 3382–3387 (Mar. 2000).

114. Cellerai, C. *et al.* Early and Prolonged Antiretroviral Therapy Is Associated with an HIV-1-Specific T-Cell Profile Comparable to That of Long-Term Non-Progressors. *PLoS One* **6,** e18164 (Apr. 2011).

115. Jensen, S. S. *et al.* Initiation of Antiretroviral Therapy (ART) at Different Stages of HIV-1 Disease Is Not Associated with the Proportion of Exhausted CD8+ T Cells. *PLOS One* **10,** e0139573 (Oct. 2015).

116. Jain, V. *et al.* Antiretroviral Therapy Initiated Within 6 Months of HIV Infection Is Associated With Lower T-Cell Activation and Smaller HIV Reservoir Size. *The Journal of Infectious Diseases* **208,** 1202–1211 (July 2013).

117. Amu, S. *et al.* Dysfunctional phenotypes of CD4+ and CD8+ T cells are comparable in patients initiating ART during early or chronic HIV-1 infection. *Medicine* **95,** e3738 (June 2016).

118. Colby, D. J. *et al.* Rapid HIV RNA rebound after antiretroviral treatment interruption in persons durably suppressed in Fiebig I acute HIV infection. *Nature Medicine* (2018).

119. Streeck, H. & Nixon, D. T Cell Immunity in Acute HIV-1 Infection. *The Journal of Infectious Diseases* **202,** S302–S308 (Oct. 2010).

120. Walker, B. & McMichael, A. The T-Cell Response to HIV. *Cold Spring Harbor Perspectives in Medicine* **2,** a007054–a007054 (Sept. 2012).

121. Rosenberg, E. S. *et al.* Vigorous HIV-1-Specific CD4+ T Cell Responses Associated with Control of Viremia. *Science* **278,** 1447–1450 (Nov. 1997).

122. Wherry, E. J. & Kurachi, M. Molecular and cellular insights into T cell exhaustion. *Nature Reviews Immunology* **15,** 486–499 (Aug. 2015).

123. Zajac, A. J. *et al.* Viral Immune Evasion Due to Persistence of Activated T Cells Without Effector Function. *The Journal of Experimental Medicine* **188,** 2205–2213 (Dec. 1998).

124. Aubert, R. D. *et al.* Antigen-specific CD4 T-cell help rescues exhausted CD8 T cells during chronic viral infection. *Proceedings of the National Academy of Sciences* **108,** 21182–21187 (Dec. 2011).

125. Barber, D. L. *et al.* Restoring function in exhausted CD8 T cells during chronic viral infection. *Nature* **439,** 682–687 (Dec. 2005).

126. Khalil, D. N., Smith, E. L., Brentjens, R. J. & Wolchok, J. D. The future of cancer treatment: immunomodulation, CARs and combination immunotherapy. *Nature Reviews Clinical Oncology* **13,** 273–290 (Mar. 2016).

127. Jones, R. B. *et al.* Tim-3 expression defines a novel population of dysfunctional T cells with highly elevated frequencies in progressive HIV-1 infection. *The Journal of Experimental Medicine* **205,** 2763–2779 (Nov. 2008).

128. Johnston, R. *et al.* The Immunoreceptor TIGIT Regulates Antitumor and Antiviral CD8+ T Cell Effector Function. *Cancer Cell* **26,** 923–937 (Dec. 2014).

129. Gupta, P. K. *et al.* CD39 Expression Identifies Terminally Exhausted CD8+ T Cells. *PLoS Pathogens* **11,** e1005177 (Oct. 2015).

130. Wykes, M. N. & Lewin, S. R. Immune checkpoint blockade in infectious diseases. *Nature Reviews Immunology* **18,** 91–104 (Oct. 2017).

131. Day, C. L. *et al.* PD-1 expression on HIV-specific T cells is associated with T-cell exhaustion and disease progression. *Nature* **443,** 350–354 (Aug. 2006).

132. Trautmann, L. *et al.* Upregulation of PD-1 expression on HIV-specific CD8+ T cells leads to reversible immune dysfunction. *Nature Medicine* **12,** 1198–1202 (Aug. 2006).

133. Zhang, J.-Y. *et al.* PD-1 up-regulation is correlated with HIV-specific memory CD8+ T-cell exhaustion in typical progressors but not in long-term nonprogressors. *Blood* **109,** 4671–4678 (June 2007).

134. Hoffmann, M. *et al.* Exhaustion of Activated CD8 T Cells Predicts Disease Progression in Primary HIV-1 Infection. *PLoS Pathogens* **12,** e1005661 (July 2016).

135. Cockerham, L. R. *et al.* Programmed death-1 expression on CD4+ and CD8+ T cells in treated and untreated HIV disease. *AIDS* **28,** 1749–1758 (July 2014).

136. Chew, G. M. *et al.* TIGIT Marks Exhausted T Cells, Correlates with Disease Progression, and Serves as a Target for Immune Restoration in HIV and SIV Infection. *PLoS Pathogens* **12,** e1005349 (Jan. 2016).

137. Tauriainen, J. *et al.* Perturbed CD8+ T cell TIGIT/CD226/PVR axis despite early initiation of antiretroviral treatment in HIV infected individuals. *Scientific Reports* **7,** 40354 (Jan. 2017).

138. Pombo, C., Wherry, E. J., Gostick, E., Price, D. A. & Betts, M. R. Elevated Expression of CD160 and 2B4 Defines a Cytolytic HIV-Specific CD8+ T-Cell Population in Elite Controllers. *Journal of Infectious Diseases* **212,** 1376–1386 (Apr. 2015).

139. Rutishauser, R. L. *et al.* Early and Delayed Antiretroviral Therapy Results in Comparable Reductions in CD8+ T Cell Exhaustion Marker Expression. *AIDS Research and Human Retroviruses* **33,** 658–667 (July 2017).

140. Breton, G. *et al.* Programmed Death-1 Is a Marker for Abnormal Distribution of Naive/Memory T Cell Subsets in HIV-1 Infection. *The Journal of Immunology* **191,** 2194–2204 (Aug. 2013).

141. Sakhdari, A. *et al.* Tim-3 Negatively Regulates Cytotoxicity in Exhausted CD8+ T Cells in HIV Infection. *PLoS ONE* **7,** e40146 (July 2012).

142. Petrovas, C. *et al.* PD-1 is a regulator of virus-specific CD8+ T cell survival in HIV infection. *The Journal of Experimental Medicine* **203,** 2281–2292 (Sept. 2006).

143. Tian, X. *et al.* The Upregulation of LAG-3 on T Cells Defines a Subpopulation with Functional Exhaustion and Correlates with Disease Progression in HIV-Infected Subjects. *The Journal of Immunology* **194,** 3873–3882 (Mar. 2015).

144. Blackburn, S. D. *et al.* Coregulation of CD8+ T cell exhaustion by multiple inhibitory receptors during chronic viral infection. *Nature Immunology* **10,** 29–37 (Nov. 2008).

145. Teigler, J. E. *et al.* Differential Inhibitory Receptor Expression on T Cells Delineates Functional Capacities in Chronic Viral Infection. *Journal of Virology* **91,** e01263–17 (Sept. 2017).

146. Peretz, Y. *et al.* CD160 and PD-1 Co-Expression on HIV-Specific CD8 T Cells Defines a Subset with Advanced Dysfunction. *PLoS Pathogens* **8,** e1002840 (Aug. 2012).

147. Yamamoto, T. *et al.* Surface expression patterns of negative regulatory molecules identify determinants of virus-specific CD8+ T-cell exhaustion in HIV infection. *Blood* **117,** 4805–4815 (Mar. 2011).

148. Vollbrecht, T. *et al.* Impact of changes in antigen level on CD38/PD-1 co-expression on HIV-specific CD8 T cells in chronic, untreated HIV-1 infection. *Journal of Medical Virology* **82,** 358–370 (Mar. 2010).

149. Paris, R. M. *et al.* Selective Loss of Early Differentiated, Highly Functional PD1high CD4 T Cells with HIV Progression. *PLoS One* **10,** e0144767 (Dec. 2015).

150. Beyer, M. *et al.* Tumor-necrosis factor impairs CD4+ T cell-mediated immunological control in chronic viral infection. *Nature Immunology* **17,** 593–603 (Mar. 2016).

151. Porichis, F. *et al.* Responsiveness of HIV-specific CD4 T cells to PD-1 blockade. *Blood* **118,** 965–974 (June 2011).

152. Peña, J., Jones, N. G., Bousheri, S., Bangsberg, D. R. & Cao, H. Lymphocyte Activation Gene-3 Expression Defines a Discrete Subset of HIV-Specific CD8+ T Cells That Is Associated with Lower Viral Load. *AIDS Research and Human Retroviruses* **30,** 535–541 (June 2014).

153. Ravimohan, S. *et al.* Elevated Pre-Antiretroviral Therapy CD39+CD8+ T Cell Frequency Is Associated With Early Mortality in Advanced Human Immunodeficiency Virus/Tuberculosis Co-infection. *Clinical Infectious Diseases* **64,** 1453–1456 (Feb. 2017).

154. Kaufmann, D. E. *et al.* Upregulation of CTLA-4 by HIV-specific CD4+ T cells correlates with disease progression and defines a reversible immune dysfunction. *Nature Immunology* **8,** 1246–1254 (Sept. 2007).

155. D'Souza, M. *et al.* Programmed Death 1 Expression on HIV-Specific CD4+ T Cells Is Driven by Viral Replication and Associated with T Cell Dysfunction. *The Journal of Immunology* **179,** 1979–1987 (July 2007).

156. Sauce, D. *et al.* PD-1 expression on human CD8 T cells depends on both state of differentiation and activation status. *AIDS* **21,** 2005–2013 (Oct. 2007).

157. Janbazian, L. *et al.* Clonotype and Repertoire Changes Drive the Functional Improvement of HIV-Specific CD8 T Cell Populations under Conditions of Limited Antigenic Stimulation. *The Journal of Immunology* **188,** 1156–1167 (Dec. 2011).

158. Doering, T. *et al.* Network Analysis Reveals Centrally Connected Genes and Pathways Involved in CD8+ T Cell Exhaustion versus Memory. *Immunity* **37,** 1130–1144 (Dec. 2012).

159. Wherry, E. J. *et al.* Molecular Signature of CD8+ T Cell Exhaustion during Chronic Viral Infection. *Immunity* **27,** 670–684 (Oct. 2007).

160. Bengsch, B. *et al.* Bioenergetic Insufficiencies Due to Metabolic Alterations Regulated by the Inhibitory Receptor PD-1 Are an Early Driver of CD8+ T Cell Exhaustion. *Immunity* **45,** 358–373 (Aug. 2016).

161. Sen, D. R. *et al.* The epigenetic landscape of T cell exhaustion. *Science* **354,** 1165–1169 (Oct. 2016).

162. Pauken, K. E. *et al.* Epigenetic stability of exhausted T cells limits durability of reinvigoration by PD-1 blockade. *Science* **354,** 1160–1165 (Oct. 2016).

163. Koyama, S. *et al.* Adaptive resistance to therapeutic PD-1 blockade is associated with upregulation of alternative immune checkpoints. *Nature Communications* **7,** 10501 (Feb. 2016).

164. Youngblood, B. *et al.* Chronic Virus Infection Enforces Demethylation of the Locus that Encodes PD-1 in Antigen-Specific CD8+ T Cells. *Immunity* **35,** 400–412 (Sept. 2011).

165. Youngblood, B. *et al.* Cutting Edge: Prolonged Exposure to HIV Reinforces a Poised Epigenetic Program for PD-1 Expression in Virus-Specific CD8 T Cells. *The Journal of Immunology* **191,** 540–544 (June 2013).

166. Kao, C. *et al.* Transcription factor T-bet represses expression of the inhibitory receptor PD-1 and sustains virus-specific CD8+ T cell responses during chronic infection. *Nature Immunology* **12,** 663–671 (May 2011).

167. Paley, M. A. *et al.* Progenitor and Terminal Subsets of CD8+ T Cells Cooperate to Contain Chronic Viral Infection. *Science* **338,** 1220–1225 (Nov. 2012).

168. Blackburn, S. D., Shin, H., Freeman, G. J. & Wherry, E. J. Selective expansion of a subset of exhausted CD8 T cells by PD-L1 blockade. *Proceedings of the National Academy of Sciences* **105,** 15016–15021 (Sept. 2008).

169. Buggert, M. *et al.* T-bet and Eomes Are Differentially Linked to the Exhausted Phenotype of CD8+ T Cells in HIV Infection. *PLoS Pathogens* **10,** e1004251 (July 2014).

170. Utzschneider, D. T. *et al.* T Cell Factor 1-Expressing Memory-like CD8+ T Cells Sustain the Immune Response to Chronic Viral Infections. *Immunity* **45,** 415–427 (Aug. 2016).

171. Bengsch, B. *et al.* Epigenomic-Guided Mass Cytometry Profiling Reveals Disease-Specific Features of Exhausted CD8 T Cells. *Immunity* **48,** 1029–1045.e5 (May 2018).

172. Im, S. J. *et al.* Defining CD8+ T cells that provide the proliferative burst after PD-1 therapy. *Nature* **537,** 417–421 (Sept. 2016).

173. Rutishauser, R. L. *et al. TCF-1 expression is associated with HIV-specific CD8+ T cell proliferative capacity* in *Conference on Retroviruses and Opportunistic Infections (CROI)* Mar. 4–7, 2018 (Boston, United States, 2018).

174. Martinez, G. J. *et al.* The Transcription Factor NFAT Promotes Exhaustion of Activated CD8+ T Cells. *Immunity* **42,** 265–278 (Feb. 2015).

175. Man, K. *et al.* Transcription Factor IRF4 Promotes CD8+ T Cell Exhaustion and Limits the Development of Memory-like T Cells during Chronic Infection. *Immunity* **47,** 1129–1141.e5 (Dec. 2017).

176. Crawford, A. *et al.* Molecular and Transcriptional Basis of CD4+ T Cell Dysfunction during Chronic Infection. *Immunity* **40,** 289–302 (Feb. 2014).

177. Kassu, A. *et al.* Regulation of Virus-Specific CD4+T Cell Function by Multiple Costimulatory Receptors during Chronic HIV Infection. *The Journal of Immunology* **185,** 3007–3018 (July 2010).

178. Sharpe, A. H. & Pauken, K. E. The diverse functions of the PD1 inhibitory pathway. *Nature Reviews Immunology* **18,** 153–167 (Nov. 2017).

179. Duraiswamy, J. *et al.* Phenotype, Function, and Gene Expression Profiles of Programmed Death-1 hi CD8 T Cells in Healthy Human Adults. *The Journal of Immunology* **186,** 4200–4212 (Mar. 2011).

180. Hong, J. J., Amancha, P. K., Rogers, K., Ansari, A. A. & Villinger, F. Re-Evaluation of PD-1 Expression by T Cells as a Marker for Immune Exhaustion during SIV Infection. *PLoS ONE* **8,** e60186 (Mar. 2013).

181. Rivino, L. *et al.* Hepatitis B virus-specific T cells associate with viral control upon nucleos(t)ide-analogue therapy discontinuation. *Journal of Clinical Investigation* **128,** 668–681 (Jan. 2018).

182. Schlaphoff, V. *et al.* Dual Function of the NK Cell Receptor 2B4 (CD244) in the Regulation of HCV-Specific CD8+ T Cells. *PLoS Pathogens* **7,** e1002045 (May 2011).

183. Campbell, J. H., Hearps, A. C., **Martin, G. E.**, Williams, K. C. & Crowe, S. M. The importance of monocytes and macrophages in HIV pathogenesis, treatment, and cure. *AIDS* **28,** 2175–2187 (Sept. 2014).

184. Okoye, A. A. *et al.* Early antiretroviral therapy limits SIV reservoir establishment to delay or prevent post-treatment viral rebound. *Nature Medicine,* [Epub ahead of print] (Aug. 2018).

185. Whitney, J. B. *et al.* Rapid seeding of the viral reservoir prior to SIV viraemia in rhesus monkeys. *Nature* **512,** 74–77 (July 2014).

186. Kearney, M. F. *et al.* Origin of Rebound Plasma HIV Includes Cells with Identical Proviruses That Are Transcriptionally Active before Stopping of Antiretroviral Therapy. *Journal of Virology* **90,** 1369–1376 (Nov. 2015).

187. Wagner, T. A. *et al.* Proliferation of cells with HIV integrated into cancer genes contributes to persistent infection. *Science* **345,** 570–573 (July 2014).

188. Cohn, L. *et al.* HIV-1 Integration Landscape during Latent and Active Infection. *Cell* **160,** 420–432 (Jan. 2015).

189. Bui, J. K. *et al.* Proviruses with identical sequences comprise a large fraction of the replication-competent HIV reservoir. *PLOS Pathogens* **13,** e1006283 (Mar. 2017).

190. Lorenzo-Redondo, R. *et al.* Persistent HIV-1 replication maintains the tissue reservoir during therapy. *Nature* **530,** 51–56 (Jan. 2016).

191. Martinez-Picado, J. & Deeks, S. G. Persistent HIV-1 replication during antiretroviral therapy. *Current Opinion in HIV and AIDS* **11,** 417–423 (July 2016).

192. Kearney, M. F. *et al.* Ongoing HIV Replication During ART Reconsidered. *Open Forum Infectious Diseases* **4,** ofx173 (2017).

193. Siliciano, J. D. *et al.* Long-term follow-up studies confirm the stability of the latent reservoir for HIV-1 in resting CD4+ T cells. *Nature Medicine* **9,** 727–728 (May 2003).

194. Strain, M. C. *et al.* Heterogeneous clearance rates of long-lived lymphocytes infected with HIV: Intrinsic stability predicts lifelong persistence. *Proceedings of the National Academy of Sciences* **100,** 4819–4824 (Apr. 2003).

195. Archin, N. M. *et al.* Immediate antiviral therapy appears to restrict resting CD4+ cell HIV-1 infection without accelerating the decay of latent infection. *Proceedings of the National Academy of Sciences* **109,** 9523–9528 (May 2012).

196. Hill, A. L., Rosenbloom, D. I. S., Fu, F., Nowak, M. A. & Siliciano, R. F. Predicting the outcomes of treatment to eradicate the latent reservoir for HIV-1. *Proceedings of the National Academy of Sciences* **111,** 13475–13480 (Aug. 2014).

197. Finzi, D. *et al.* Latent infection of CD4+ T cells provides a mechanism for lifelong persistence of HIV-1, even in patients on effective combination therapy. *Nature Medicine* **5,** 512–517 (May 1999).

198. Perelson, A. S. *et al.* Decay characteristics of HIV-1-infected compartments during combination therapy. *Nature* **387,** 188–191 (May 1997).

199. Murray, J. M. *et al.* HIV DNA Subspecies Persist in both Activated and Resting Memory CD4+ T Cells during Antiretroviral Therapy. *Journal of Virology* **88,** 3516–3526 (Jan. 2014).

200. Chavez, L., Calvanese, V. & Verdin, E. HIV Latency Is Established Directly and Early in Both Resting and Activated Primary CD4 T Cells. *PLoS Pathogens* **11,** e1004955 (June 2015).

201. Chun, T.-W. *et al.* HIV-infected individuals receiving effective antiviral therapy for extended periods of time continually replenish their viral reservoir. *The Journal of Clinical Investigation* **115,** 3250–3255 (11 Nov. 2005).

202. Ho, Y.-C. *et al.* Replication-Competent Noninduced Proviruses in the Latent Reservoir Increase Barrier to HIV-1 Cure. *Cell* **155,** 540–551 (Oct. 2013).

203. Imamichi, H. *et al.* Defective HIV-1 proviruses produce novel protein-coding RNA species in HIV-infected patients on combination antiretroviral therapy. *Proceedings of the National Academy of Sciences* **113,** 8783–8788 (July 2016).

204. Pollack, R. A. *et al.* Defective HIV-1 Proviruses Are Expressed and Can Be Recognized by Cytotoxic T Lymphocytes, which Shape the Proviral Landscape. *Cell Host & Microbe* **21,** 494–506.e4 (Apr. 2017).

205. Thomas, A. S. *et al.* T-cell responses targeting HIV Nef uniquely correlate with infected cell frequencies after long-term antiretroviral therapy. *PLoS Pathogens* **13,** e1006629 (Sept. 2017).

206. Josefsson, L. *et al.* The HIV-1 reservoir in eight patients on long-term suppressive antiretroviral therapy is stable with few genetic changes over time. *Proceedings of the National Academy of Sciences* **110,** E4987–E4996 (Nov. 2013).

207. Strain, M. *et al.* Effect of Treatment, during Primary Infection, on Establishment and Clearance of Cellular Reservoirs of HIV-1. *The Journal of Infectious Diseases* **191,** 1410–1418 (May 2005).

208. Procopio, F. A. *et al.* A Novel Assay to Measure the Magnitude of the Inducible Viral Reservoir in HIV-infected Individuals. *EBioMedicine* **2,** 874–883 (Aug. 2015).

209. Gianella, S. *et al.* Effect of early antiretroviral therapy during primary HIV-1 infection on cell-associated HIV-1 DNA and plasma HIV-1 RNA. *Antiviral Therapy* **16,** 535–545 (2011).

210. Buzon, M. J. *et al.* HIV-1 persistence in CD4+ T cells with stem cell-like properties. *Nature Medicine* **20,** 139–142 (Jan. 2014).

211. Eriksson, S. *et al.* Comparative Analysis of Measures of Viral Reservoirs in HIV-1 Eradication Studies. *PLoS Pathogens* **9,** e1003174 (Feb. 2013).

212. Novelli, S. *et al.* Long-term Therapeutic Impact of the Timing of Antiretroviral Therapy in Patients Diagnosed With Primary Human Immunodeficiency Virus Type 1 Infection. *Clinical Infectious Diseases* **66,** 1519–1527 (Dec. 2017).

213. Pitman, M. C., Lau, J. S. Y., McMahon, J. H. & Lewin, S. R. Barriers and strategies to achieve a cure for HIV. *The Lancet HIV* **5,** e317–e328 (June 2018).

214. Bruner, K. M., Hosmane, N. N. & Siliciano, R. F. Towards an HIV-1 cure: measuring the latent reservoir. *Trends in Microbiology* **23,** 192–203 (Apr. 2015).

215. Rouzioux, C. & Richman, D. How to best measure HIV reservoirs? *Current Opinion in HIV and AIDS* **8,** 170–175 (May 2013).

216. Bruner, K. M. *et al.* Defective proviruses rapidly accumulate during acute HIV-1 infection. *Nature Medicine* **22,** 1043–1049 (Aug. 2016).

217. Hiener, B. *et al.* Identification of Genetically Intact HIV-1 Proviruses in Specific CD4+ T Cells from Effectively Treated Participants. *Cell Reports* **21,** 813–822 (Oct. 2017).

218. Lee, G. Q. *et al.* Clonal expansion of genome-intact HIV-1 in functionally polarized Th1 CD4+ T cells. *Journal of Clinical Investigation* **127,** 2689–2696 (June 2017).

219. Kiselinova, M. *et al.* Integrated and Total HIV-1 DNA Predict Ex Vivo Viral Outgrowth. *PLoS Pathogens* **12,** e1005472 (Mar. 2016).

220. Williams, J. P. *et al.* HIV-1 DNA predicts disease progression and post-treatment virological control. *eLife* **3,** e03821 (Sept. 2014).

221. Rasmussen, T. A. *et al.* Panobinostat, a histone deacetylase inhibitor, for latent-virus reactivation in HIV-infected patients on suppressive antiretroviral therapy: a phase 1/2, single group, clinical trial. *The Lancet HIV* **1,** e13–e21 (Oct. 2014).

222. Lafeuillade, A., Poggi, C., Hittinger, G., Counillon, E. & Emilie, D. Predictors of Plasma Human Immunodeficiency Virus Type 1 RNA Control after Discontinuation of Highly Active Antiretroviral Therapy Initiated at Acute Infection Combined with Structured Treatment Interruptions and Immune-Based Therapies. *The Journal of Infectious Diseases* **188,** 1426–1432 (Nov. 2003).

223. Assoumou, L. *et al.* A low HIV-DNA level in peripheral blood mononuclear cells at antiretroviral treatment interruption predicts a higher probability of maintaining viral control. *AIDS* **29,** 2003–2007 (Sept. 2015).

224. Li, J. Z. *et al.* The size of the expressed HIV reservoir predicts timing of viral rebound after treatment interruption. *AIDS* **28,** 343–353 (Nov. 2015).

225. Pasternak, A., Prins, J. & Berkhout, B. *Cell-associated HIV-1 unspliced RNA level predicts both time to virological suppression and duration of post-treatment virological control in patients treated with temporary early ART* in *AIDS 2016* July 18–22, 2016 (Durban, South Africa).

226. Sharaf, R. *et al.* HIV-1 proviral landscapes distinguish posttreatment controllers from noncontrollers. *Journal of Clinical Investigation,* [Epub ahead of print] (July 2018).

227. Lamers, S. L. *et al.* HIV DNA Is Frequently Present within Pathologic Tissues Evaluated at Autopsy from Combined Antiretroviral Therapy-Treated Patients with Undetectable Viral Loads. *Journal of Virology* **90,** 8968–8983 (July 2016).

228. Rothenberger, M. K. *et al.* Large number of rebounding/founder HIV variants emerge from multifocal infection in lymphatic tissues after treatment interruption. *Proceedings of the National Academy of Sciences* **112,** E1126–E1134 (Feb. 2015).

229. Khoury, G. *et al.* Human Immunodeficiency Virus Persistence and T-Cell Activation in Blood, Rectal, and Lymph Node Tissue in Human Immunodeficiency Virus-Infected Individuals Receiving Suppressive Antiretroviral Therapy. *The Journal of Infectious Diseases* **215,** 911–919 (Feb. 2017).

230. Banga, R. *et al.* PD-1+ and follicular helper T cells are responsible for persistent HIV-1 transcription in treated aviremic individuals. *Nature Medicine* **22,** 754–761 (May 2016).

231. Yukl, S. A. *et al.* The Distribution of HIV DNA and RNA in Cell Subsets Differs in Gut and Blood of HIV-Positive Patients on ART: Implications for Viral Persistence. *The Journal of Infectious Diseases* **208,** 1212–1220 (July 2013).

232. Chun, T.-W. *et al.* Persistence of HIV in Gut-Associated Lymphoid Tissue despite Long-Term Antiretroviral Therapy. *The Journal of Infectious Diseases* **197,** 714–720 (Mar. 2008).

233. Yukl, S. *et al.* Differences in HIV Burden and Immune Activation within the Gut of HIV-Positive Patients Receiving Suppressive Antiretroviral Therapy. *The Journal of Infectious Diseases* **202,** 1553–1561 (Nov. 2010).

234. Soriano-Sarabia, N. *et al.* Quantitation of Replication-Competent HIV-1 in Populations of Resting CD4+ T Cells. *Journal of Virology* **88,** 14070–14077 (Sept. 2014).

235. Brenchley, J. M. *et al.* T-cell subsets that harbor human immunodeficiency virus (HIV) in vivo: implications for HIV pathogenesis. *Journal of Virology* **78,** 1160–1168 (3 Feb. 2004).

236. Jaafoura, S. *et al.* Progressive contraction of the latent HIV reservoir around a core of less-differentiated CD4+ memory T Cells. *Nature Communications* **5,** 5407 (Nov. 2014).

237. Pallikkuth, S. *et al.* Peripheral T Follicular Helper Cells Are the Major HIV Reservoir within Central Memory CD4 T Cells in Peripheral Blood from Chronically HIV-Infected Individuals on Combination Antiretroviral Therapy. *Journal of Virology* **90,** 2718–2728 (Dec. 2015).

238. Tran, T.-A. *et al.* Resting Regulatory CD4 T Cells: A Site of HIV Persistence in Patients on Long-Term Effective Antiretroviral Therapy. *PLoS One* **3,** e3305 (Oct. 2008).

239. Jiao, Y.-M. *et al.* CD4+CD25+CD127 regulatory cells play multiple roles in maintaining HIV-1 p24 production in patients on long-term treatment: HIV-1 p24-producing cells and suppression of anti-HIV immunity. *International Journal of Infectious Diseases* **37,** 42–49 (Aug. 2015).

240. Douek, D. C. *et al.* HIV preferentially infects HIV-specific CD4+ T cells. *Nature* **417,** 95–98 (May 2002).

241. McGary, C. S. *et al.* CTLA-4+ PD-1 - Memory CD4 +T Cells Critically Contribute to Viral Persistence in Antiretroviral Therapy-Suppressed, SIV-Infected Rhesus Macaques. *Immunity* **47,** 776–788.e5 (Oct. 2017).

242. Fromentin, R. *et al.* CD4+ T Cells Expressing PD-1, TIGIT and LAG-3 Contribute to HIV Persistence during ART. *PLOS Pathogens* **12,** e1005761 (July 2016).

243. Khoury, G. *et al.* Persistence of integrated HIV DNA in CXCR3+CCR6+ memory CD4+ T cells in HIV-infected individuals on antiretroviral therapy. *AIDS* **30,** 1511–1520 (June 2016).

244. Iglesias-Ussel, M., Vandergeeten, C., Marchionni, L., Chomont, N. & Romerio, F. High Levels of CD2 Expression Identify HIV-1 Latently Infected Resting Memory CD4+ T Cells in Virally Suppressed Subjects. *Journal of Virology* **87,** 9148–9158 (June 2013).

245. Descours, B. *et al.* CD32a is a marker of a CD4 T-cell HIV reservoir harbouring replication-competent proviruses. *Nature* **543,** 564–567 (Mar. 2017).

246. Fletcher, C. V. *et al.* Persistent HIV-1 replication is associated with lower antiretroviral drug concentrations in lymphatic tissues. *Proceedings of the National Academy of Sciences* **111,** 2307–2312 (Jan. 2014).

247. Estes, J. D. *et al.* Defining total-body AIDS-virus burden with implications for curative strategies. *Nature Medicine* **23,** 1271–1276 (Oct. 2017).

248. Wong, J. K. & Yukl, S. A. Tissue reservoirs of HIV. *Current Opinion in HIV and AIDS* **11,** 362–370 (July 2016).

249. Churchill, M. J., Deeks, S. G., Margolis, D. M., Siliciano, R. F. & Swanstrom, R. HIV reservoirs: what, where and how to target them. *Nature Reviews Microbiology* **14,** 55–60 (Nov. 2015).

250. Baxter, A. E. *et al.* Single-Cell Characterization of Viral Translation-Competent Reservoirs in HIV-Infected Individuals. *Cell Host & Microbe* **20,** 368–380 (Sept. 2016).

251. Grau-Expósito, J. *et al.* A Novel Single-Cell FISH-Flow Assay Identifies Effector Memory CD4+ T cells as a Major Niche for HIV-1 Transcription in HIV-Infected Patients. *mBio* **8,** e00876–17 (July 2017).

252. Perreau, M. *et al.* Follicular helper T cells serve as the major CD4 T cell compartment for HIV-1 infection, replication, and production. *The Journal of Experimental Medicine* **210,** 143–156 (Dec. 2012).

253. Fukazawa, Y. *et al.* B cell follicle sanctuary permits persistent productive simian immunodeficiency virus infection in elite controllers. *Nature Medicine* **21,** 132–139 (Jan. 2015).

254. Thornhill, J. P., Fidler, S., Klenerman, P., Frater, J. & Phetsouphanh, C. The Role of CD4+ T Follicular Helper Cells in HIV Infection: From the Germinal Center to the Periphery. *Frontiers in Immunology* **8** (Jan. 2017).

255. Hurst, J. *et al.* Immunological biomarkers predict HIV-1 viral rebound after treatment interruption. *Nature Communications* **6,** 8495 (2015).

256. Hatano, H. *et al.* Cell-Based Measures of Viral Persistence Are Associated With Immune Activation and Programmed Cell Death Protein 1 (PD-1)-Expressing CD4+ T cells. *The Journal of Infectious Diseases* **208,** 50–56 (Oct. 2012).

257. El-Far, M. *et al.* Nef promotes evasion of human immunodeficiency virus type 1-infected cells from the CTLA-4-mediated inhibition of T-cell activation. *Journal of General Virology* **96,** 1463–1477 (June 2015).

258. Shan, L. *et al.* Transcriptional Reprogramming during Effector-to-Memory Transition Renders CD4+ T Cells Permissive for Latent HIV-1 Infection. *Immunity* **47,** 766–775.e3 (Oct. 2017).

259. Zack, J. A. *et al.* HIV-1 entry into quiescent primary lymphocytes: Molecular analysis reveals a labile, latent viral structure. *Cell* **61,** 213–222 (Apr. 1990).

260. Stevenson, M., Stanwick, T. L., Dempsey, M. P. & Lamonica, C. A. HIV-1 replication is controlled at the level of T cell activation and proviral integration. *The EMBO Journal* **9,** 1551–1560 (5 May 1990).

261. Evans, V. A. *et al.* Programmed cell death-1 contributes to the establishment and maintenance of HIV-1 latency. *AIDS* **32,** 1491–1497 (July 2018).

262. Wightman, F. *et al.* Effect of ipilimumab on the HIV reservoir in an HIV-infected individual with metastatic melanoma. *AIDS* **29,** 504–506 (Feb. 2015).

263. Guihot, A. *et al.* Drastic decrease of the HIV reservoir in a patient treated with nivolumab for lung cancer. *Annals of Oncology* **29,** 517–518 (Dec. 2017).

264. Gay, C. L. *et al.* Clinical Trial of the Anti-PD-L1 Antibody BMS-936559 in HIV-1 Infected Participants on Suppressive Antiretroviral Therapy. *The Journal of Infectious Diseases* **215,** 1725–1733 (Apr. 2017).

265. Garff, G. L. *et al.* Transient HIV-specific T cells increase and inflammation in an HIV-infected patient treated with nivolumab. *AIDS* **31,** 1048–1051 (Apr. 2017).

266. Deeks, S. G. & Walker, B. D. Human Immunodeficiency Virus Controllers: Mechanisms of Durable Virus Control in the Absence of Antiretroviral Therapy. *Immunity* **27,** 406–416 (Sept. 2007).

267. Walker, B. D. & Yu, X. G. Unravelling the mechanisms of durable control of HIV-1. *Nature Reviews Immunology* **13,** 487–498 (July 2013).

268. Goulder, P. J. R. & Watkins, D. I. Impact of MHC class I diversity on immune control of immunodeficiency virus replication. *Nature Reviews Immunology* **8,** 619–630 (Aug. 2008).

269. Goujard, C. *et al.* HIV-1 control after transient antiretroviral treatment initiated in primary infection: role of patient characteristics and effect of therapy. *Antiviral Therapy* **17,** 1001–1009 (2012).

270. Stöhr, W. *et al.* Duration of HIV-1 viral suppression on cessation of antiretroviral therapy in primary infection correlates with time on therapy. *PLoS One* **8,** e78287 (2013).

271. Sáez-Cirión, A. *et al.* Post-Treatment HIV-1 Controllers with a Long-Term Virological Remission after the Interruption of Early Initiated Antiretroviral Therapy ANRS VISCONTI Study. *PLoS Pathogens* **9,** e1003211 (Mar. 2013).

272. Lodi, S. *et al.* Immunovirologic Control 24 Months After Interruption of Antiretroviral Therapy Initiated Close to HIV Seroconversion. *Archives of Internal Medicine* **172,** 1252–1255 (Sept. 2012).

273. Rosenberg, E. S. *et al.* Immune control of HIV-1 after early treatment of acute infection. *Nature* **407,** 523–526 (Sept. 2000).

274. Fidler, S. *et al.* Virological Blips and Predictors of Post Treatment Viral Control After Stopping ART Started in Primary HIV Infection. *JAIDS Journal of Acquired Immune Deficiency Syndromes* **74,** 126–133 (Feb. 2017).

275. Maenza, J. *et al.* How often does treatment of primary HIV lead to post-treatment control? *Antiviral Therapy* **20,** 855–863 (2015).

276. Essat, A. *et al. Association between immunogenetic factors and post-treatment control of HIV-1 infection. ANRS VISCONTI and PRIMO studies* in *AIDS 2018* July 23–27, 2018 (Amsterdam, Netherlands).

277. **Martin, G. E.** *et al.* Post-treatment control or treated controllers? Viral remission in treated and untreated primary HIV infection. *AIDS* **31,** 477–484 (Feb. 2017).

278. Hütter, G. *et al.* Long-Term Control of HIV byCCR5Delta32/Delta32 Stem-Cell Transplantation. *New England Journal of Medicine* **360,** 692–698 (Feb. 2009).

279. Henrich, T. J. *et al.* Antiretroviral-Free HIV-1 Remission and Viral Rebound After Allogeneic Stem Cell Transplantation. *Annals of Internal Medicine* **161,** 319–327 (Sept. 2014).

280. Frange, P. *et al.* HIV-1 virological remission lasting more than 12 years after interruption of early antiretroviral therapy in a perinatally infected teenager enrolled in the French ANRS EPF-CO10 paediatric cohort: a case report. *The Lancet HIV* **3,** e49–e54 (Jan. 2016).

281. Persaud, D. *et al.* Absence of Detectable HIV-1 Viremia after Treatment Cessation in an Infant. *New England Journal of Medicine* **369,** 1828–1835 (Nov. 2013).

282. Henrich, T. J. *et al.* HIV-1 persistence following extremely early initiation of antiretroviral therapy (ART) during acute HIV-1 infection: An observational study. *PLoS Medicine* **14,** e1002417 (Nov. 2017).

283. Cummins, N. W. *et al.* Extensive virologic and immunologic characterization in an HIV-infected individual following allogeneic stem cell transplant and analytic cessation of antiretroviral therapy: A case study. *PLoS Medicine* **14,** e1002461 (Nov. 2017).

284. Chereau, F. *et al.* Impact of CD4 and CD8 dynamics and viral rebounds on loss of virological control in HIV controllers. *PLoS ONE* **12,** e0173893 (Apr. 2017).

285. Canouï, E. *et al.* A Subset of Extreme Human Immunodeficiency Virus (HIV) Controllers Is Characterized by a Small HIV Blood Reservoir and a Weak T-Cell Activation Level. *Open Forum Infectious Diseases* **4,** ofx064 (2017).

286. Hocqueloux, L. *et al. Intermittent viremia after treatment interruption increased risk of ART resumption in post-treatment HIV-1 controllers. ANRS VISCONTI study* in *AIDS 2018* July 23–27, 2018 (Amsterdam, Netherlands).

287. Gianella, S., Anderson, C. M., Richman, D. D., Smith, D. M. & Little, S. J. No evidence of posttreatment control after early initiation of antiretroviral therapy. *AIDS* **29,** 2093–2097 (Oct. 2015).

288. Namazi, G. *et al.* The Control of HIV after Antiretroviral Medication Pause (CHAMP) study: post-treatment controllers identified from 14 clinical studies. *The Journal of Infectious Diseases,* [Epub ahead of print] (Aug. 2018).

289. Gurdasani, D. *et al.* A systematic review of definitions of extreme phenotypes of HIV control and progression. *AIDS* **28,** 149–162 (Jan. 2014).

290. Olson, A. D. *et al.* An Evaluation of HIV Elite Controller Definitions within a Large Seroconverter Cohort Collaboration. *PLoS One* **9,** e86719 (Jan. 2014).

291. Tucker, J. D., Volberding, P. A., Margolis, D. M., Rennie, S. & Barré-Sinoussi, F. Words Matter. *JAIDS Journal of Acquired Immune Deficiency Syndromes* **67,** e110–e111 (Nov. 2014).

292. Hocqueloux, L. *et al.* Long-term immunovirologic control following antiretroviral therapy interruption in patients treated at the time of primary HIV-1 infection. *AIDS* **24,** 1598–1601 (June 2010).

293. Perkins, M. J. *et al.* Brief Report. *JAIDS Journal of Acquired Immune Deficiency Syndromes* **75,** 364–369 (July 2017).

294. Sneller, M. C. *et al.* A randomized controlled safety/efficacy trial of therapeutic vaccination in HIV-infected individuals who initiated antiretroviral therapy early in infection. *Science Translational Medicine* **9,** eaan8848 (Dec. 2017).

295. Bar, K. J. *et al.* Effect of HIV Antibody VRC01 on Viral Rebound after Treatment Interruption. *New England Journal of Medicine* **375,** 2037–2050 (Nov. 2016).

296. Scheid, J. F. *et al.* HIV-1 antibody 3BNC117 suppresses viral rebound in humans during treatment interruption. *Nature* **535,** 556–560 (June 2016).

297. Mothe, B. *et al. Viral control induced by HIVconsv Vaccines & romidepsin in early treated individuals* in *Conference on Retroviruses and Opportunistic Infections (CROI)* Mar. 4–7, 2018 (Boston, United States).

298. Sued, O. *et al.* Structured Treatment Interruptions and Low Doses of IL-2 in Patients with Primary HIV Infection. Inflammatory, Virological and Immunological Outcomes. *PLoS One* **10,** e0131651 (July 2015).

299. Jakobsen, J. C. *et al.* Direct-acting antivirals for chronic hepatitis C. *Cochrane Database of Systematic Reviews* **6,** CD012143 (Sept. 2017).

300. Doyle, J. S. *et al.* New hepatitis C antiviral treatments eliminate the virus. *The Lancet* **390,** 358–359 (July 2017).

301. Yukl, S. A. *et al.* Challenges in Detecting HIV Persistence during Potentially Curative Interventions: A Study of the Berlin Patient. *PLoS Pathogens* **9,** e1003347 (May 2013).

302. **Martin, G. E.**, Alcami, J., Spano, J.-P. & Ross, A. L. Converging roads: the latest science from the 2017 IAS HIV Cure and Cancer Forum. *Journal of Virus Eradication* **3,** 236–241 (4 Oct. 2017).

303. Luzuriaga, K. *et al.* Viremic Relapse after HIV-1 Remission in a Perinatally Infected Child. *New England Journal of Medicine* **372,** 786–788 (Feb. 2015).

304. Hütter, G. More on shift of HIV tropism in stem-cell transplantation with CCR5 delta32/delta32 mutation. *New England Journal of Medicine* **371,** 2437–2438 (25 Dec. 2014).

305. Kordelas, L., Verheyen, J. & Esser, S. Shift of HIV Tropism in Stem-Cell Transplantation with CCR5 Delta32 Mutation. *New England Journal of Medicine* **371,** 880–882 (Aug. 2014).

306. Rothenberger, M. *et al.* Transplantation of CCR5delta32 Homozygous Umbilical Cord Blood in a Child With Acute Lymphoblastic Leukemia and Perinatally Acquired HIV Infection. *Open Forum Infectious Diseases* **5,** ofy090 (May 2018).

307. Duarte, R. F. *et al.* CCR5 delta32 homozygous cord blood allogeneic transplantation in a patient with HIV: a case report. *The Lancet HIV* **2,** e236–e242 (6 June 2015).

308. Wensing, A. *et al. Dominant HIV DNA populations present in different T-cell subsets before stem cell transplantation persist in tissues early after transplantation with CCR5delta32 stem cells* in *AIDS 2018* July 23–27, 2018 (Amsterdam, Netherlands).

309. Verheyen, J. *et al.* Rapid rebound of a preexisting CXCR4-tropic HIV variant after allogeneic transplantation with CCR5 delta32 homozygous stem cells. *Clinical Infectious Diseases,* [Epub ahead of print] (July 2018).

310. Nijhuis, M. *Stem Cell Transplantations: ICISTEM* in *AIDS 2018* July 23–27, 2018 (Amsterdam, Netherlands).

311. Spragg, C., Feelixge, H. D. S. & Jerome, K. R. Cell and gene therapy strategies to eradicate HIV reservoirs. *Current Opinion in HIV and AIDS* **11,** 442–449 (July 2016).

312. Deeks, S. G. Shock and kill. *Nature* **487,** 439–440 (July 2012).

313. Rasmussen, T. A., Tolstrup, M. & Søgaard, O. S. Reversal of Latency as Part of a Cure for HIV-1. *Trends in Microbiology* **24,** 90–97 (Feb. 2016).

314. Spivak, A. M. & Planelles, V. Novel Latency Reversal Agents for HIV-1 Cure. *Annual Review of Medicine* **69,** 421–436 (Jan. 2018).

315. Laird, G. M. *et al.* Ex vivo analysis identifies effective HIV-1 latency–reversing drug combinations. *Journal of Clinical Investigation* **125,** 1901–1912 (Mar. 2015).

316. Archin, N. M. *et al.* Administration of vorinostat disrupts HIV-1 latency in patients on antiretroviral therapy. *Nature* **487,** 482–485 (July 2012).

317. Archin, N. M. *et al.* Interval dosing with the HDAC inhibitor vorinostat effectively reverses HIV latency. *Journal of Clinical Investigation* **127,** 3126–3135 (July 2017).

318. Archin, N. M. *et al.* HIV-1 Expression Within Resting CD4+ T Cells After Multiple Doses of Vorinostat. *Journal of Infectious Diseases* **210,** 728–735 (Mar. 2014).

319. Elliott, J. H. *et al.* Activation of HIV Transcription with Short-Course Vorinostat in HIV-Infected Patients on Suppressive Antiretroviral Therapy. *PLoS Pathogens* **10,** e1004473 (Nov. 2014).

320. Søgaard, O. S. *et al.* The Depsipeptide Romidepsin Reverses HIV-1 Latency In Vivo. *PLoS Pathogens* **11,** e1005142 (Sept. 2015).

321. Darcis, G. *et al.* An In-Depth Comparison of Latency-Reversing Agent Combinations in Various In Vitro and Ex Vivo HIV-1 Latency Models Identified Bryostatin-1+JQ1 and Ingenol-B+JQ1 to Potently Reactivate Viral Gene Expression. *PLoS Pathogens* **11,** e1005063 (July 2015).

322. Pace, M. *et al.* Histone Deacetylase Inhibitors Enhance CD4 T Cell Susceptibility to NK Cell Killing but Reduce NK Cell Function. *PLoS Pathogens* **12,** e1005782 (Aug. 2016).

323. Jones, R. B. *et al.* Histone Deacetylase Inhibitors Impair the Elimination of HIV-Infected Cells by Cytotoxic T-Lymphocytes. *PLoS Pathogens* **10,** e1004287 (Aug. 2014).

324. Huang, S.-H. *et al.* Latent HIV reservoirs exhibit inherent resistance to elimination by CD8+ T cells. *Journal of Clinical Investigation* **128,** 876–889 (Jan. 2018).

325. Gray, G. E., Laher, F., Lazarus, E., Ensoli, B. & Corey, L. Approaches to preventative and therapeutic HIV vaccines. *Current Opinion in Virology* **17,** 104–109 (Apr. 2016).

326. Stephenson, K. E. Therapeutic vaccination for HIV. *Current Opinion in HIV and AIDS* **13,** 408–415 (Sept. 2018).

327. Hansen, S. G. *et al.* Profound early control of highly pathogenic SIV by an effector memory T-cell vaccine. *Nature* **473,** 523–527 (May 2011).

328. Hansen, S. G. *et al.* Immune clearance of highly pathogenic SIV infection. *Nature* **502,** 100–104 (Sept. 2013).

329. Leth, S. *et al.* Combined effect of Vacc-4x, recombinant human granulocyte macrophage colony-stimulating factor vaccination, and romidepsin on the HIV-1 reservoir (REDUC): a single-arm, phase 1B/2A trial. *The Lancet HIV* **3,** e463–e472 (Oct. 2016).

330. Tapia, G. *et al.* Sequential Vacc-4x and romidepsin during combination antiretroviral therapy (cART): Immune responses to Vacc-4x regions on p24 and changes in HIV reservoirs. *Journal of Infection* **75,** 555–571 (Dec. 2017).

331. Fidler, S. *et al. A randomised controlled trial comparing the impact of antiretroviral therapy (ART) with a 'Kick-and-Kill' approach to ART alone on HIV reservoirs in individuals with primary HIV infection (PHI); RIVER trial* in *AIDS 2018* July 23–27, 2018 (Amsterdam, Netherlands).

332. Jones, R. B. *et al.* A Subset of Latency-Reversing Agents Expose HIV-Infected Resting CD4+ T-Cells to Recognition by Cytotoxic T-Lymphocytes. *PLOS Pathogens* **12,** e1005545 (Apr. 2016).

333. Seay, K. *et al.* In Vivo Activation of Human NK Cells by Treatment with an Interleukin-15 Superagonist Potently Inhibits Acute in vivo HIV-1 Infection in Humanized Mice. *Journal of Virology* **89,** 6264–6274 (Apr. 2015).

334. Webb, G. M. *et al.* The human IL-15 superagonist ALT-803 directs SIV-specific CD8+ T cells into B-cell follicles. *Blood Advances* **2,** 76–84 (Jan. 2018).

335. Offersen, R. *et al.* A Novel Toll-Like Receptor 9 Agonist, MGN1703, Enhances HIV-1 Transcription and NK Cell-Mediated Inhibition of HIV-1-Infected Autologous CD4+ T Cells. *Journal of Virology* **90,** 4441–4453 (Feb. 2016).

336. Tsai, A. *et al.* Toll-Like Receptor 7 Agonist GS-9620 Induces HIV Expression and HIV-Specific Immunity in Cells from HIV-Infected Individuals on Suppressive Antiretroviral Therapy. *Journal of Virology* **91,** e02166–16 (Feb. 2017).

337. Lim, S.-Y. *et al.* TLR7 agonists induce transient viremia and reduce the viral reservoir in SIV-infected rhesus macaques on antiretroviral therapy. *Science Translational Medicine* **10,** eaao4521 (May 2018).

338. Vibholm, L. *et al.* Short-Course Toll-Like Receptor 9 Agonist Treatment Impacts Innate Immunity and Plasma Viremia in Individuals With Human Immunodeficiency Virus Infection. *Clinical Infectious Diseases* **64,** 1686–1695 (Mar. 2017).

339. Velu, V. *et al.* Enhancing SIV-specific immunity in vivo by PD-1 blockade. *Nature* **458,** 206–210 (Dec. 2008).

340. Hryniewicz, A. *et al.* CTLA-4 blockade decreases TGF-beta, IDO, and viral RNA expression in tissues of SIVmac251-infected macaques. *Blood* **108,** 3834–3842 (Dec. 2006).

341. Gill, A. L. *et al.* Programed death-1/programed death-ligand 1 expression in lymph nodes of HIV infected patients. *AIDS* **30,** 2487–2493 (Oct. 2016).

342. Shetty, R. D. *et al.* PD-1 blockade during chronic SIV infection reduces hyperimmune activation and microbial translocation in rhesus macaques. *Journal of Clinical Investigation* **122,** 1712–1716 (May 2012).

343. Wagner, T. A. Quarter Century of Anti-HIV CAR T Cells. *Current HIV/AIDS Reports* **15,** 147–154 (Mar. 2018).

344. Kuhlmann, A.-S., Peterson, C. W. & Kiem, H.-P. Chimeric antigen receptor T-cell approaches to HIV cure. *Current Opinion in HIV and AIDS* **13,** 446–453 (Sept. 2018).

345. Arthos, J. *et al.* The Role of Integrin alpha4beta7 in HIV Pathogenesis and Treatment. *Current HIV/AIDS Reports* **15,** 127–135 (Feb. 2018).

346. Byrareddy, S. N. *et al.* Sustained virologic control in SIV+ macaques after antiretroviral and $\alpha 4\beta 7$ antibody therapy. *Science* **354,** 197–202 (Oct. 2016).

347. Di Mascio, M. *et al. Evaluation of an antibody to Alpha4Beta7 in the control of SIV infection* in *AIDS 2018* July 23–27, 2018 (Amsterdam, Netherlands).

348. Fauci, A. *Durable control of HIV infections in the absence of antiretroviral therapy: Opportunities and obstacles* in *AIDS 2018* July 23–27, 2018 (Amsterdam, Netherlands).

349. Lynch, R. M. *et al.* Virologic effects of broadly neutralizing antibody VRC01 administration during chronic HIV-1 infection. *Science Translational Medicine* **7,** 319ra206–319ra206 (Dec. 2015).

350. Caskey, M. *et al.* Viraemia suppressed in HIV-1-infected humans by broadly neutralizing antibody 3BNC117. *Nature* **522,** 487–491 (Apr. 2015).

351. Caskey, M. *et al.* Antibody 10-1074 suppresses viremia in HIV-1-infected individuals. *Nature Medicine* **23,** 185–191 (Jan. 2017).

352. Nishimura, Y. *et al.* Early antibody therapy can induce long-lasting immunity to SHIV. *Nature* **543,** 559–563 (Mar. 2017).

353. Berger, C. T. & Alter, G. Natural killer cells in spontaneous control of HIV infection. *Current Opinion in HIV and AIDS* **6,** 208–213 (May 2011).

354. Sáez-Cirión, A. *Insights on Mechanisms of Post-Treatment Control* in *AIDS 2018* July 23–27, 2018 (Amsterdam, Netherlands).

355. Olesen, R. *et al.* Innate Immune Activity Correlates with CD4 T Cell-Associated HIV-1 DNA Decline during Latency-Reversing Treatment with Panobinostat. *Journal of Virology* **89,** 10176–10189 (July 2015).

356. Davey, R. T. *et al.* HIV-1 and T cell dynamics after interruption of highly active antiretroviral therapy (HAART) in patients with a history of sustained viral suppression. *Proceedings of the National Academy of Sciences of the United States of America* **96,** 15109–15114 (26 Dec. 1999).

357. García, F. *et al.* Dynamics of viral load rebound and immunological changes after stopping effective antiretroviral therapy. *AIDS* **13,** F79–F86 (11 July 1999).

358. Harrigan, P. R., Whaley, M. & Montaner, J. S. Rate of HIV-1 RNA rebound upon stopping antiretroviral therapy. *AIDS* **13,** F59–F62 (8 May 1999).

359. SPARTAC Trial Investigators *et al.* Short-course antiretroviral therapy in primary HIV infection. *New England Journal of Medicine* **368,** 207–217 (2013).

360. Goulder, P. & Walker, B. HIV and HLA Class I: An Evolving Relationship. *Immunity* **37,** 426–440 (Sept. 2012).

361. Kiepiela, P. *et al.* Dominant influence of HLA-B in mediating the potential co-evolution of HIV and HLA. *Nature* **432,** 769–775 (Dec. 2004).

362. Volberding, P. *et al.* Antiretroviral therapy in acute and recent HIV infection: a prospective multicenter stratified trial of intentionally interrupted treatment. *AIDS* **23,** 1987–1995 (Sept. 2009).

363. Kaufmann, D. E. *et al.* Limited Durability of Viral Control following Treated Acute HIV Infection. *PLoS Medicine* **1,** e36 (Oct. 2004).

364. Bloch, M. T. *et al.* The Role of Hydroxyurea in Enhancing the Virologic Control Achieved Through Structured Treatment Interruption in Primary HIV Infection. *JAIDS Journal of Acquired Immune Deficiency Syndromes* **42,** 192–202 (June 2006).

365. Madec, Y., Boufassa, F., Rouzioux, C., Delfraissy, J.-F. & and, L. M. Undetectable Viremia without Antiretroviral Therapy in Patients with HIV Seroconversion: An Uncommon Phenomenon? *Clinical Infectious Diseases* **40,** 1350–1354 (May 2005).

366. Madec, Y., Boufassa, F., Porter, K., Meyer, L. & Collaboration, C. Spontaneous control of viral load and CD4 cell count progression among HIV-1 seroconverters. *AIDS* **19,** 2001–2007 (17 Nov. 2005).

367. Payne, R. *et al.* Impact of HLA-driven HIV adaptation on virulence in populations of high HIV seroprevalence. *Proceedings of the National Academy of Sciences* **111,** E5393–E5400 (Dec. 2014).

368. Kinloch–de Loes, S. *et al.* Impact of Therapeutic Immunization on HIV-1 Viremia after Discontinuation of Antiretroviral Therapy Initiated during Acute Infection. *The Journal of Infectious Diseases* **192,** 607–617 (Aug. 2005).

369. Lampe, F. C. *et al.* Effect of transient antiretroviral treatment during acute HIV infection: comparison of the Quest trial results with CASCADE natural history study. *Antiviral therapy* **12,** 189–193 (2 2007).

370. Venner, C. M. *et al.* Infecting HIV-1 Subtype Predicts Disease Progression in Women of Sub-Saharan Africa. *EBioMedicine* **13,** 305–314 (Nov. 2016).

371. Addo, M. M. & Altfeld, M. Sex-Based Differences in HIV Type 1 Pathogenesis. *Journal of Infectious Diseases* **209,** S86–S92 (June 2014).

372. Taylor, B. S., Sobieszczyk, M. E., McCutchan, F. E. & Hammer, S. M. The Challenge of HIV-1 Subtype Diversity. *New England Journal of Medicine* **358,** 1590–1602 (Apr. 2008).

373. Clarridge, K. E. *et al.* Effect of analytical treatment interruption and reinitiation of antiretroviral therapy on HIV reservoirs and immunologic parameters in infected individuals. *PLoS Pathogens* **14,** e1006792 (Jan. 2018).

374. Salantes, D. B. *et al.* HIV-1 latent reservoir size and diversity are stable following brief treatment interruption. *Journal of Clinical Investigation,* [Epub ahead of print] (June 2018).

375. Papasavvas, E. *et al.* Analytical antiretroviral therapy interruption does not irreversibly change preinterruption levels of cellular HIV. *AIDS* **32,** 1763–1772 (Aug. 2018).

376. Strongin, Z. *et al.* Effect of Short-Term Antiretroviral Therapy Interruption on Levels of Integrated HIV DNA. *Journal of Virology* **92,** e00285–18 (Mar. 2018).

377. Bell, E. C. N. *et al.* High decay of blood HIV reservoir when tenofovir/emtricitabine/elvitegravir/cobicistat is initiated during the acute primary HIV infection. *Journal of Antimicrobial Chemotherapy* **72,** 2681–2683 (June 2017).

378. Cao, W. *et al.* Early Initiation Rather Than Prolonged Duration of Antiretroviral Therapy in HIV Infection Contributes to the Normalization of CD8 T-Cell Counts. *Clinical Infectious Diseases* **62,** 250–257 (Sept. 2015).

379. Sereti, I. *et al.* Persistent, Albeit Reduced, Chronic Inflammation in Persons Starting Antiretroviral Therapy in Acute HIV Infection. *Clinical Infectious Diseases* **64,** 124–131 (Oct. 2016).

380. Vinikoor, M. J. *et al.* Antiretroviral Therapy Initiated During Acute HIV Infection Fails to Prevent Persistent T-Cell Activation. *JAIDS Journal of Acquired Immune Deficiency Syndromes* **62,** 505–508 (Apr. 2013).

381. Radebe, M. *et al.* Limited Immunogenicity of HIV CD8+ T-Cell Epitopes in Acute Clade C Virus Infection. *The Journal of Infectious Diseases* **204,** 768–776 (Sept. 2011).

382. Dalod, M. *et al.* Weak anti-HIV CD8+ T-cell effector activity in HIV primary infection. *Journal of Clinical Investigation* **104,** 1431–1439 (Nov. 1999).

383. Turnbull, E. L. *et al.* Kinetics of Expansion of Epitope-Specific T Cell Responses during Primary HIV-1 Infection. *The Journal of Immunology* **182,** 7131–7145 (May 2009).

384. Betts, M. R. *et al.* Analysis of Total Human Immunodeficiency Virus (HIV)-Specific CD4+ and CD8+ T-Cell Responses: Relationship to Viral Load in Untreated HIV Infection. *Journal of Virology* **75,** 11983–11991 (Dec. 2001).

385. Gea-Banacloche, J. C. *et al.* Maintenance of Large Numbers of Virus-Specific CD8+ T Cells in HIV-Infected Progressors and Long-Term Nonprogressors. *The Journal of Immunology* **165,** 1082–1092 (July 2000).

386. Radebe, M. *et al.* Broad and persistent Gag-specific CD8+ T-cell responses are associated with viral control but rarely drive viral escape during primary HIV-1 infection. *AIDS* **29,** 23–33 (Jan. 2015).

387. Papagno, L. *et al.* Immune Activation and CD8+ T-Cell Differentiation towards Senescence in HIV-1 Infection. *PLoS Biology* **2,** e20 (Feb. 2004).

388. Younes, S.-A. *et al.* IL-15 promotes activation and expansion of CD8+ T cells in HIV-1 infection. *Journal of Clinical Investigation* **126,** 2745–2756 (June 2016).

389. Biancotto, A. *et al.* Abnormal activation and cytokine spectra in lymph nodes of people chronically infected with HIV-1. *Blood* **109,** 4272–4279 (May 2007).

390. Hersperger, A. R. *et al.* Increased HIV-specific CD8+ T-cell cytotoxic potential in HIV elite controllers is associated with T-bet expression. *Blood* **117,** 3799–3808 (Feb. 2011).

391. Hunt, P. *et al.* Relationship between T Cell Activation and CD4+ T Cell Count in HIV-Seropositive Individuals with Undetectable Plasma HIV RNA Levels in the Absence of Therapy. *The Journal of Infectious Diseases* **197,** 126–133 (Jan. 2008).

392. Eggena, M. *et al.* T Cell Activation in HIV-Seropositive Ugandans: Differential Associations with Viral Load, CD4+ T Cell Depletion, and Coinfection. *The Journal of Infectious Diseases* **191,** 694–701 (Mar. 2005).

393. Kestens, L. *et al.* Selective increase of activation antigens HLA-DR and CD38 on CD45RO+ T lymphocytes during HIV-1 infection. *Clinical & Experimental Immunology* **95,** 436–441 (June 1994).

394. De Armas, L. R. *et al.* Reevaluation of immune activation in the era of cART and an aging HIV-infected population. *JCI Insight* **2,** 95726 (Oct. 2017).

395. Smith, M. Z., Bastidas, S., Karrer, U. & Oxenius, A. Impact of antigen specificity on CD4+ T cell activation in chronic HIV-1 infection. *BMC Infectious Diseases* **13** (Feb. 2013).

396. Dianzani, U. *et al.* Interaction between endothelium and CD4+CD45RA+ lymphocytes. Role of the human CD38 molecule. *Journal of Immunology* **153,** 952–959 (3 Aug. 1994).

397. Ferris, R. L., Lu, B. & Kane, L. P. Too Much of a Good Thing? Tim-3 and TCR Signaling in T Cell Exhaustion. *The Journal of Immunology* **193,** 1525–1530 (Aug. 2014).

398. Avery, L., Filderman, J., Szymczak-Workman, A. L. & Kane, L. P. Tim-3 co-stimulation promotes short-lived effector T cells, restricts memory precursors, and is dispensable for T cell exhaustion. *Proceedings of the National Academy of Sciences* **115,** 2455–2460 (Feb. 2018).

399. Wada, N. I. *et al.* The effect of HAART-induced HIV suppression on circulating markers of inflammation and immune activation. *AIDS* **29,** 463–471 (Feb. 2015).

400. Roederer, M. *et al.* The Genetic Architecture of the Human Immune System: A Bioresource for Autoimmunity and Disease Pathogenesis. *Cell* **161,** 387–403 (Apr. 2015).

401. Orrù, V. *et al.* Genetic Variants Regulating Immune Cell Levels in Health and Disease. *Cell* **155,** 242–256 (Sept. 2013).

402. Friedman, D. J. *et al.* CD39 deletion exacerbates experimental murine colitis and human polymorphisms increase susceptibility to inflammatory bowel disease. *Proceedings of the National Academy of Sciences* **106,** 16788–16793 (Sept. 2009).

403. Rissiek, A. *et al.* The expression of CD39 on regulatory T cells is genetically driven and further upregulated at sites of inflammation. *Journal of Autoimmunity* **58,** 12–20 (Apr. 2015).

404. Fang, F. *et al.* Expression of CD39 on Activated T Cells Impairs their Survival in Older Individuals. *Cell Reports* **14,** 1218–1231 (Feb. 2016).

405. Borsellino, G. *et al.* Expression of ectonucleotidase CD39 by Foxp3+ Treg cells: hydrolysis of extracellular ATP and immune suppression. *Blood* **110,** 1225–1232 (Aug. 2007).

406. Nikolova, M. *et al.* CD39/Adenosine Pathway Is Involved in AIDS Progression. *PLoS Pathogens* **7,** e1002110 (July 2011).

407. Boulware, D. R. *et al.* Higher Levels of CRP, D-dimer, IL-6, and Hyaluronic Acid Before Initiation of Antiretroviral Therapy (ART) Are Associated With Increased Risk of AIDS or Death. *The Journal of Infectious Diseases* **203,** 1637–1646 (June 2011).

408. Kuller, L. H. *et al.* Inflammatory and Coagulation Biomarkers and Mortality in Patients with HIV Infection. *PLoS Medicine* **5,** e203 (Oct. 2008).

409. Wan, B. *et al.* Aberrant Regulation of Synovial T Cell Activation by Soluble Costimulatory Molecules in Rheumatoid Arthritis. *The Journal of Immunology* **177,** 8844–8850 (Dec. 2006).

410. Nielsen, C., Ohm-Laursen, L., Barington, T., Husby, S. & Lillevang, S. T. Alternative splice variants of the human PD-1 gene. *Cellular Immunology* **235,** 109–116 (June 2005).

411. Liu, C. *et al.* Soluble PD-1 aggravates progression of collagen-induced arthritis through Th1 and Th17 pathways. *Arthritis Research & Therapy* **17,** 340 (Nov. 2015).

412. Clayton, K. L. *et al.* Soluble T Cell Immunoglobulin Mucin Domain 3 Is Shed from CD8+ T Cells by the Sheddase ADAM10, Is Increased in Plasma during Untreated HIV Infection, and Correlates with HIV Disease Progression. *Journal of Virology* **89,** 3723–3736 (Jan. 2015).

413. Hansen, J. A. *et al.* A Novel Soluble Form of Tim-3 Associated with Severe Graft-versus-Host Disease. *Biology of Blood and Marrow Transplantation* **19,** 1323–1330 (Sept. 2013).

414. Chiba, M., Yanaba, K., Hayashi, M., Yoshihara, Y. & Nakagawa, H. Clinical significance of serum soluble T-cell immunoglobulin and mucin domain 3 levels in systemic sclerosis: Association with disease severity. *The Journal of Dermatology* **44,** 194–197 (Sept. 2016).

415. Yanaba, K., Hayashi, M., Yoshihara, Y. & Nakagawa, H. Serum levels of soluble programmed death-1 and programmed death ligand-1 in systemic sclerosis: Association with extent of skin sclerosis. *The Journal of Dermatology* **43,** 954–957 (Mar. 2016).

416. Greisen, S. *et al.* Increased soluble programmed death-1 (sPD-1) is associated with disease activity and radiographic progression in early rheumatoid arthritis. *Scandinavian Journal of Rheumatology* **43,** 101–108 (Nov. 2013).

417. Aarslev, K. *et al.* Soluble programmed death-1 levels are associated with disease activity and treatment response in patients with autoimmune hepatitis. *Scandinavian Journal of Gastroenterology* **52,** 93–99 (Sept. 2016).

418. Li, N. *et al.* Circulating soluble programmed death-1 levels may differentiate immune-tolerant phase from other phases and hepatocellular carcinoma from other clinical diseases in chronic hepatitis B virus infection. *Oncotarget* **8,** 46020–46033 (May 2017).

419. Cheng, H.-Y. *et al.* Circulating Programmed Death-1 as a Marker for Sustained High Hepatitis B Viral Load and Risk of Hepatocellular Carcinoma. *PLoS ONE* **9,** e95870 (Nov. 2014).

420. Li, F. *et al.* Highly elevated soluble Tim-3 levels correlate with increased hepatocellular carcinoma risk and poor survival of hepatocellular carcinoma patients in chronic hepatitis B virus infection. *Cancer Management and Research* **10,** 941–951 (May 2018).

421. Onlamoon, N. *et al.* Soluble PD-1 rescues the proliferative response of simian immunodeficiency virus-specific CD4 and CD8 T cells during chronic infection. *Immunology* **124,** 277–293 (June 2008).

422. Amancha, P. K., Hong, J. J., Rogers, K., Ansari, A. A. & Villinger, F. In Vivo Blockade of the Programmed Cell Death-1 Pathway Using Soluble Recombinant PD-1-Fc Enhances CD4+ and CD8+ T Cell Responses but Has Limited Clinical Benefit. *The Journal of Immunology* **191,** 6060–6070 (Nov. 2013).

423. Cockerham, L. R. *et al.* CD4+ and CD8+ T Cell Activation Are Associated with HIV DNA in Resting CD4+ T Cells. *PLoS One* **9,** e110731 (Oct. 2014).

424. Ruggiero, A. *et al.* During Stably Suppressive Antiretroviral Therapy Integrated HIV-1 DNA Load in Peripheral Blood is Associated with the Frequency of CD8 Cells Expressing HLA-DR/DP/DQ. *EBioMedicine* **2,** 1153–1159 (Sept. 2015).

425. Gandhi, R. T. *et al.* Levels of HIV-1 persistence on antiretroviral therapy are not associated with markers of inflammation or activation. *PLoS Pathogens* **13,** e1006285 (Apr. 2017).

426. Teigler, J. E. *et al.* Distinct biomarker signatures in HIV acute infection associate with viral dynamics and reservoir size. *JCI Insight* **3,** 98420 (May 2018).

427. Olesen, R. *et al.* Immune checkpoints and the HIV-1 reservoir: proceed with caution. *Journal of Virus Eradication* **2,** 183–186 (3 July 2016).

428. Ananworanich, J. *et al.* Impact of Multi-Targeted Antiretroviral Treatment on Gut T Cell Depletion and HIV Reservoir Seeding during Acute HIV Infection. *PLoS ONE* **7,** e33948 (Mar. 2012).

429. Hoen, B. *et al.* Predictors of Virological Outcome and Safety in Primary HIV Type 1-Infected Patients Initiating Quadruple Antiretroviral Therapy: QUEST GW PROB3005. *Clinical Infectious Diseases* **45,** 381–390 (Aug. 2007).

430. Besson, G. J. *et al.* HIV-1 DNA Decay Dynamics in Blood During More Than a Decade of Suppressive Antiretroviral Therapy. *Clinical Infectious Diseases* **59,** 1312–1321 (July 2014).

431. Ananworanich, J. *et al.* HIV DNA Set Point is Rapidly Established in Acute HIV Infection and Dramatically Reduced by Early ART. *EBioMedicine* **11,** 68–72 (Sept. 2016).

432. Ngo-Giang-Huong, N. *et al.* Proviral HIV-1 DNA in subjects followed since primary HIV-1 infection who suppress plasma viral load after one year of highly active antiretroviral therapy. *AIDS* **15,** 665–673 (6 Apr. 2001).

433. Burgard, M. *et al.* Factors influencing peripheral blood mononuclear cell-associated HIV-1 DNA level after long-term suppressive antiretroviral therapy in 236 patients. *AIDS* **23,** 2165–2171 (Oct. 2009).

434. Lambert-Niclot, S. *et al.* Similar Evolution of Cellular HIV-1 DNA Level in Darunavir/Ritonavir Monotherapy versus Triple Therapy in MONOI-ANRS136 Trial over 96 Weeks. *PLoS One* **7,** e41390 (July 2012).

435. Fourati, S. *et al.* Factors associated with a low HIV reservoir in patients with prolonged suppressive antiretroviral therapy. *Journal of Antimicrobial Chemotherapy* **69,** 753–756 (Nov. 2013).

436. Ndhlovu, Z. *et al. CD8+ T cell responses in treated hyperacute infection limit HIV reservoir size* in *Conference on Retroviruses and Opportunistic Infections (CROI)* Mar. 4–7, 2018 (Boston, United States).

437. Chun, T.-W. *et al.* Relationship between the Size of the Human Immunodeficiency Virus Type 1 (HIV-1) Reservoir in Peripheral Blood CD4+ T Cells and CD4+:CD8+ T Cell Ratios in Aviremic HIV-1-Infected Individuals Receiving Long-Term Highly Active Antiretroviral Therapy. *The Journal of Infectious Diseases* **185,** 1672–1676 (June 2002).

438. Buzón, M. J. *et al.* HIV-1 replication and immune dynamics are affected by raltegravir intensification of HAART-suppressed subjects. *Nature Medicine* **16,** 460–465 (Mar. 2010).

439. Poizot-Martin, I. *et al.* Lack of correlation between the size of HIV proviral DNA reservoir and the level of immune activation in HIV-infected patients with a sustained undetectable HIV viral load for 10 years. *Journal of Clinical Virology* **57,** 351–355 (Aug. 2013).

440. Elith, J., Leathwick, J. R. & Hastie, T. A working guide to boosted regression trees. *Journal of Animal Ecology* **77,** 802–813 (July 2008).

441. Bosman, K. *et al. Remarkable stability in size and composition of the latent reservoir over two decades of ART* in *AIDS 2018* July 23–27, 2018 (Amsterdam, Netherlands).

442. Koelsch, K. *et al.* Dynamics of Total, Linear Nonintegrated, and Integrated HIV-1 DNA In Vivo and In Vitro. *The Journal of Infectious Diseases* **197,** 411–419 (Feb. 2008).

443. Hogarth, P. M. & Pietersz, G. A. Fc receptor-targeted therapies for the treatment of inflammation, cancer and beyond. *Nature Reviews Drug Discovery* **11,** 311–331 (Mar. 2012).

444. Sandor, M. & Lynch, R. G. Lymphocyte Fc receptors: the special case of T cells. *Immunology Today* **14,** 227–231 (May 1993).

445. Nimmerjahn, F. & Ravetch, J. V. Fcg receptors as regulators of immune responses. *Nature Reviews Immunology* **8,** 34–47 (Jan. 2008).

446. Chauhan, A. K. Human CD4+ T-Cells: A Role for Low-Affinity Fc Receptors. *Frontiers in Immunology* **7,** 215 (June 2016).

447. Sandilands, G. P. *et al.* Differential expression of CD32 isoforms following alloactivation of human T cells. *Immunology* **91,** 204–211 (2 June 1997).

448. Engelhardt, W., Matzke, J. & Schmidt, R. E. Activation-dependent expression of low affinity IgG receptors Fc gamma RII(CD32) and Fc gamma RIII(CD16) in subpopulations of human T lymphocytes. *Immunobiology* **192,** 297–320 (5 Apr. 1995).

449. Starbeck-Miller, G. R., Badovinac, V. P., Barber, D. L. & Harty, J. T. Cutting Edge: Expression of FcgRIIB Tempers Memory CD8 T Cell Function In Vivo. *The Journal of Immunology* **192,** 35–39 (Nov. 2013).

450. Abdel-Mohsen, M. *et al.* CD32 is expressed on cells with transcriptionally active HIV but does not enrich for HIV DNA in resting T cells. *Science Translational Medicine* **10,** eaar6759 (Apr. 2018).

451. Coindre, S. *et al.* Mass Cytometry Analysis Reveals the Landscape and Dynamics of CD32a+ CD4+ T Cells From Early HIV Infection to Effective cART. *Frontiers in Immunology* **9,** 1217 (June 2018).

452. Wittner, M. *et al.* CD32 Expression of Different Memory T Cell Subpopulations in the Blood and Lymph Nodal Tissue of HIV Patients and Healthy Controls Correlates With Immune Activation. *JAIDS Journal of Acquired Immune Deficiency Syndromes* **77,** 345–349 (Apr. 2018).

453. Noto, A. *et al.* CD32+ and PD-1+ Lymph Node CD4 T Cells Support Persistent HIV-1 Transcription in Treated Aviremic Individuals. *Journal of Virology,* JVI.00901–18 [Epub ahead of print] (July 2018).

454. Badia, R. *et al.* CD32 expression is associated to T-cell activation and is not a marker of the HIV-1 reservoir. *Nature Communications* **9,** 2739 (July 2018).

455. Dhummakupt, A. *et al.* The Latent HIV Reservoir Resides Primarily in CD32-CD4+ T Cells in Perinatally, HIV-Infected Adolescents with Long-Term Virologic Suppression. *The Journal of Infectious Diseases,* [Epub ahead of print] (July 2018).

456. Zamora, C. *et al.* Functional consequences of platelet binding to T lymphocytes in inflammation. *Journal of Leukocyte Biology* **94,** 521–529 (June 2013).

457. Tangye, S. G., Avery, D. T., Deenick, E. K. & Hodgkin, P. D. Intrinsic differences in the proliferation of naive and memory human B cells as a mechanism for enhanced secondary immune responses. *Journal of immunology* **170,** 686–694 (2 Jan. 2003).

458. Perez-Andres, M. *et al.* Human peripheral blood B-cell compartments: A crossroad in B-cell traffic. *Cytometry Part B: Clinical Cytometry* **78B,** S47–S60 (2010).

459. Wilk, E. *et al.* Depletion of functionally active CD20+ T cells by rituximab treatment. *Arthritis & Rheumatism* **60,** 3563–3571 (Dec. 2009).

460. Katopodis, O. *et al.* Expansion of CD8+ T cells that express low levels of the B cell-specific molecule CD20 in patients with multiple myeloma. *British Journal of Haematology* **120,** 478–481 (3 Feb. 2003).

461. Kudernatsch, R. F., Letsch, A., Stachelscheid, H., Volk, H.-D. & Scheibenbogen, C. Doublets pretending to be CD34+ T cells despite doublet exclusion. *Cytometry Part A* **83A,** 173–176 (Dec. 2012).

462. Woof, J. M. & Burton, D. R. Human antibody-Fc receptor interactions illuminated by crystal structures. *Nature Reviews Immunology* **4,** 89–99 (Feb. 2004).

463. Hogan, L. E. *et al.* Increased HIV-1 transcriptional activity and infectious burden in peripheral blood and gut-associated CD4+ T cells expressing CD30. *PLoS Pathogens* **14,** e1006856 (Feb. 2018).

464. Schuh, E. *et al.* Features of Human CD3+CD20+ T Cells. *The Journal of Immunology* **197,** 1111–1117 (July 2016).

465. Palanichamy, A. *et al.* Rituximab Efficiently Depletes Increased CD20-Expressing T Cells in Multiple Sclerosis Patients. *The Journal of Immunology* **193,** 580–586 (June 2014).

466. Niu, J. *et al.* Dissection of a circulating CD3+ CD20+ T cell subpopulation in patients with psoriasis. *Clinical & Experimental Immunology* **192,** 206–212 (Mar. 2018).

467. Eggleton, P. *et al.* Frequency of Th17 CD20+ cells in the peripheral blood of rheumatoid arthritis patients is higher compared to healthy subjects. *Arthritis Research & Therapy* **13,** R208 (2011).

468. Osuna, C. E. *et al. CD32 does not mark the HIV-1/SIV latent reservoir* in *Conference on Retroviruses and Opportunistic Infections (CROI)* Mar. 4–7, 2018 (Boston, United States).

469. Krzywinska, E. *et al.* CD45 Isoform Profile Identifies Natural Killer (NK) Subsets with Differential Activity. *PLoS One* **11,** e0150434 (Apr. 2016).

470. Basso, K. & Dalla-Favera, R. Roles of BCL6 in normal and transformed germinal center B cells. *Immunological Reviews* **247,** 172–183 (Apr. 2012).

471. Bertagnolli, L. *et al. Majority of the latent reservoir resides in CD32a negative CD4 T cells* in *Conference on Retroviruses and Opportunistic Infections (CROI)* Mar. 4–7, 2018 (Boston, United States).

472. **Martin, G. E.** *et al.* Enrichment of the HIV reservoir in CD32+ CD4 T cells occurs early in blood and tissue. *bioRxiv* (July 2017).

473. **Martin, G. E.** *et al.* CD32-Expressing CD4 T Cells Are Phenotypically Diverse and Can Contain Proviral HIV DNA. *Frontiers in Immunology* **9,** 928 (May 2018).

474. Crowell, T. A. *et al.* Initiation of antiretroviral therapy before detection of colonic infiltration by HIV reduces viral reservoirs, inflammation and immune activation. *Journal of the International AIDS Society* **19,** 21163 (Jan. 2016).

475. Krishnan, S. *et al.* Evidence for Innate Immune System Activation in HIV Type 1-Infected Elite Controllers. *The Journal of Infectious Diseases* **209,** 931–939 (Nov. 2013).

476. Pereyra, F. *et al.* Increased coronary atherosclerosis and immune activation in HIV-1 elite controllers. *AIDS* **26,** 2409–2412 (Nov. 2012).

477. Hsue, P. Y. *et al.* Role of viral replication, antiretroviral therapy, and immunodeficiency in HIV-associated atherosclerosis. *AIDS* **23,** 1059–1067 (June 2009).

478. Klatt, N. R., Funderburg, N. T. & Brenchley, J. M. Microbial translocation, immune activation, and HIV disease. *Trends in Microbiology* **21,** 6–13 (Jan. 2013).

479. Gianella, S. & Letendre, S. Cytomegalovirus and HIV: A Dangerous Pas de Deux. *Journal of Infectious Diseases* **214,** S67–S74 (Sept. 2016).

480. McMahon, J. H., Elliott, J. H., Roney, J., Hagenauer, M. & Lewin, S. R. Experiences and expectations of participants completing an HIV cure focused clinical trial. *AIDS* **29,** 248–250 (Jan. 2015).

481. Zhang, A. *et al.* What Would an HIV Cure Mean to You? Qualitative Analysis from a Crowdsourcing Contest in Guangzhou, China. *AIDS Research and Human Retroviruses* **34,** 80–87 (Jan. 2018).

482. Simmons, R. *et al.* A global survey of HIV-positive peoples attitudes towards cure research. *HIV Medicine* **18,** 73–79 (May 2016).

483. Sylla, L. *et al.* If We Build It, Will They Come? Perceptions of HIV Cure-Related Research by People Living with HIV in Four U.S. Cities: A Qualitative Focus Group Study. *AIDS Research and Human Retroviruses* **34,** 56–66 (Jan. 2018).

484. Pinkevych, M. *et al.* HIV Reactivation from Latency after Treatment Interruption Occurs on Average Every 5-8 Days—Implications for HIV Remission. *PLoS Pathogens* **11,** e1005000 (July 2015).

485. Serhir, B. *et al.* Performance of Bio-Rad and Limiting Antigen Avidity Assays in Detecting Recent HIV Infections Using the Quebec Primary HIV-1 Infection Cohort. *PLoS One* **11,** e0156023 (2016).

486. Sedia Biosciences Corporation. *Sedia™ HIV-1 LAg-Avidity EIA (for Serum or Plasma Specimens) Package Insert* tech. rep. (Sedia Biosciences Corporation, 2016).

487. Leisner, C. *et al.* One-Pot, Mix-and-Read Peptide-MHC Tetramers. *PLoS One* **3,** e1678 (Feb. 2008).

488. Batard, P. *et al.* Dextramers: New generation of fluorescent MHC class I/peptide multimers for visualization of antigen-specific CD8+ T cells. *Journal of Immunological Methods* **310,** 136–148 (Mar. 2006).

489. Duda, A. *et al.* HLA-associated clinical progression correlates with epitope reversion rates in early human immunodeficiency virus infection. *Journal of Virology* **83,** 1228–1239 (2009).

490. Frater, J. *et al.* HIV-1-specific CD4+ responses in primary HIV-1 infection predict disease progression. *AIDS* **28,** 699–708 (2014).

491. Karpinski, K., Hayward, S. & Tryphonas, H. Statistical considerations in the quantitation of serum immunoglobulin levels using the Enzyme-Linked Immunosorbent Assay (ELISA). *Journal of Immunological Methods* **103,** 189–194 (Nov. 1987).

492. Jones, M. *et al.* Low copy target detection by Droplet Digital PCR through application of a novel open access bioinformatic pipeline,'definetherain'. *Journal of Virological Methods* **202,** 46–53 (2014).

493. Folks, T. M. *et al.* Biological and biochemical characterization of a cloned Leu-3-cell surviving infection with the acquired immune deficiency syndrome retrovirus. *The Journal of Experimental Medicine* **164,** 280–290 (1986).

494. Saleh, S. *et al.* Expression and reactivation of HIV in a chemokine induced model of HIV latency in primary resting CD4+ T cells. *Retrovirology* **8,** 80 (2011).

495. Pasternak, A. O. *et al.* Highly Sensitive Methods Based on Seminested Real-Time Reverse Transcription-PCR for Quantitation of Human Immunodeficiency Virus Type 1 Unspliced and Multiply Spliced RNA and Proviral DNA. *Journal of Clinical Microbiology* **46,** 2206–2211 (2008).

496. Pasternak, A. O. *et al.* Cellular Levels of HIV Unspliced RNA from Patients on Combination Antiretroviral Therapy with Undetectable Plasma Viremia Predict the Therapy Outcome. *PLoS One* **4,** e8490 (2009).

497. De Oliveira, T. *et al.* An automated genotyping system for analysis of HIV-1 and other microbial sequences. *Bioinformatics* **21,** 3797–3800 (Aug. 2005).

498. Alcantara, L. C. J. *et al.* A standardized framework for accurate, high-throughput genotyping of recombinant and non-recombinant viral sequences. *Nucleic Acids Research* **37,** W634–W642 (May 2009).

499. Pineda-Peña, A.-C. *et al.* Automated subtyping of HIV-1 genetic sequences for clinical and surveillance purposes: Performance evaluation of the new REGA version 3 and seven other tools. *Infection, Genetics and Evolution* **19,** 337–348 (Oct. 2013).

500. R Core Team. *R: A Language and Environment for Statistical Computing* R Foundation for Statistical Computing (Vienna, Austria, 2017). `https://www.R-project.org/`.

501. Roederer, M., Nozzi, J. L. & Nason, M. C. SPICE: Exploration and analysis of post-cytometric complex multivariate datasets. *Cytometry Part A* **79A,** 167–174 (Jan. 2011).

502. Wickham, H. *ggplot2: Elegant Graphics for Data Analysis* Springer-Verlag New York (2009). `http://ggplot2.org`.

503. Kassambara, A. *ggpubr: 'ggplot2' Based Publication Ready Plots* R package version 0.1.6 (2017). `https://CRAN.R-project.org/package=ggpubr`.

504. Wei, T. & Simko, V. *R package "corrplot": Visualization of a Correlation Matrix* (Version 0.84) (2017). `https://github.com/taiyun/corrplot`.

505. Warnes, G. R. *et al. gplots: Various R Programming Tools for Plotting Data* R package version 3.0.1 (2016). `https://CRAN.R-project.org/package=gplots`.

506. Stekhoven, D. J. & Buhlmann, P. MissForest–non-parametric missing value imputation for mixed-type data. *Bioinformatics* **28,** 112–118 (Oct. 2011).

507. Waljee, A. K. *et al.* Comparison of imputation methods for missing laboratory data in medicine. *BMJ Open* **3,** e002847 (Aug. 2013).

508. Benjamini, Y. & Hochberg, Y. Controlling the False Discovery Rate: A Practical and Powerful Approach to Multiple Testing. *Journal of the Royal Statistical Society Series B (Methodological)* **57,** 289–300 (1995).

509. Therneau, T. M. *A Package for Survival Analysis in S* version 2.38 (2015). `https://CRAN.R-project.org/package=survival`.

510. Lê, S., Josse, J. & Husson, F. FactoMineR: AnRPackage for Multivariate Analysis. *Journal of Statistical Software* **25** (2008).

511. Kassambara, A. & Mundt, F. *factoextra: Extract and Visualize the Results of Multivariate Data Analyses* R package version 1.0.5 (2017). `https://CRAN.R-project.org/package=factoextra`.

512. Hickey, J. *et al. gbm3: Generalized Boosted Regression Models* R package version 2.2 (2016). `https://github.com/gbm-developers/gbm3`.

513. Ridgeway, G. *Generalised Boosted Models: A guide to the gbm package* (2007).

514. Tibshirani, R. Regression Shrinkage and Selection Via the Lasso. *Journal of the Royal Statistical Society, Series B* **58,** 267–288 (1994).

515. Friedman, J., Hastie, T. & Tibshirani, R. Regularization Paths for Generalized Linear Models via Coordinate Descent. *Journal of statistical software* **33,** 1–22 (1 2010).

Appendices

A

Study committees

A.1 SPARTAC trial investigators

The SPARTAC Trial Investigators: Trial Steering Committee: Independent Members - A Breckenridge (Chair), P Clayden, C Conlon, F Conradie, J Kaldor*, F Maggiolo, F Ssali, Country Principal Investigators- DA Cooper, P Kaleebu, G Ramjee, M Schechter, G Tambussi, JM Miro, J Weber. Trial Physician: S Fidler. Trial Statistician: A Babiker. Data and Safety Monitoring Committee (DSMC): T Peto (Chair), A McLaren (in memoriam), V Beral, G Chene, J Hakim. Co-ordinating Trial Centre: Medical Research Council Clinical Trials Unit, London (A Babiker, K Porter, M Thomason, F Ewings, M Gabriel, D Johnson, K Thompson, A Cursley*, K Donegan*, E Fossey*, P Kelleher*, K Lee*, B Murphy*, D Nock*). Central Immunology Laboratories and Repositories: The Peter Medawar Building for Pathogen Research, University of Oxford, UK (R Phillips, J Frater, L Ohm Laursen*, N Robinson, P Goulder, H Brown). Central Virology Laboratories and Repositories: Jefferiss Trust Laboratories, Imperial College, London, UK (M McClure, D Bonsall*, O Erlwein*, A Helander*, S Kaye, M Robinson, L Cook*, G Adcock*, P Ahmed*). Clinical Endpoint Review Committee: N Paton, S Fidler. Investigators and Staff at Participating Sites: Australia: St Vincents Hospital, Sydney (A Kelleher), Northside Clinic, Melbourne (R Moore), East Sydney Doctors, Sydney (R McFarlane), Prahran Market Clinic, Melbourne (N Roth), Taylor Square Private Clinic, Sydney (R Finlayson), The Centre Clinic, Melbourne (B Kiem Tee), Sexual Health Centre, Melbourne (T Read), AIDS Medical Unit, Brisbane (M Kelly), Burwood Rd Practice, Sydney (N Doong), Holdsworth House Medical Practice, Sydney (M Bloch), Aids Research Initiative, Sydney (C Workman). Coordinating Centre in Australia: Kirby Institute University of New South Wales, Sydney (P Grey, DA Cooper, A Kelleher, M Law). Brazil: Projeto Praca Onze, Hospital Escola Sao Francisco de Assis, Universidade federal do Rio de Janeiro, Rio de Janeiro (M Schechter, P Gama, M Mercon*, M Barbosa de Souza, C Beppu Yoshida, JR Grangeiro da Silva, A Sampaio Amaral, D Fernandes de Aguiar, M de Fatima Melo, R Quaresma Garrido). Italy: Ospedale San Raffaele, Milan (G Tambussi, S Nozza, M Pogliaghi, S Chiappetta, L Della Torre, E Gasparotto), Ospedale

Lazzaro Spallanzani, Roma (G DOffizi, C Vlassi, A Corpolongo). South Africa: Cape Town: Desmond Tutu HIV-1 Centre, Institute of Infectious Diseases, Cape Town (R Wood, J Pitt, C Orrell, F Cilliers, R Croxford, K Middelkoop, LG Bekker, C Heiberg, J Aploon, N Killa, E Fielder, T Buhler). Johannesburg: The Wits Reproductive Health and HIV-1 Institute, University of Witswatersrand, Hillbrow Health Precinct, Johannesburg (H Rees, F Venter, T Palanee), Contract Laboratory Services, Johannesburg Hospital, Johannesburg (W Stevens, C Ingram, M Majam, M Papathanasopoulos). Kwazulu-Natal: HIV-1 Prevention Unit, Medical Research Council, Durban (G Ramjee, S Gappoo, J Moodley, A Premrajh, L Zako). Uganda: Medical Research Council/Uganda Virus Research Institute, Entebbe (H Grosskurth, A Kamali, P Kaleebu, U Bahemuka, J Mugisha*, HF Njaj*). Spain: Hospital Clinic-IDIBAPS, University of Barcelona, Barcelona (JM Miro, M Lopez-Dieguez*, C Manzardo, J. Ambrosioni, D. Nicolas, JA Arnaiz, T Pumarola, M Plana, M Tuset, MC Ligero, MT Garca, T Gallart, JM Gatell). UK and Ireland: Royal Sussex County Hospital, Brighton (M Fisher, K Hobbs, N Perry, D Pao, D Maitland, L Heald), St James's Hospital, Dublin (F Mulcahy, G Courtney, S O'Dea, D Reidy), Regional Infectious Diseases Unit, Western General Hospital and Genitourinary Dept, Royal Infirmary of Edinburgh, Edinburgh (C Leen, G Scott, L Ellis, S Morris, P Simmonds), Chelsea and Westminster Hospital, London (B Gazzard, D Hawkins, C Higgs), Homerton Hospital, London (J Anderson, S Mguni), Mortimer Market Centre, London (I Williams, N De Esteban, P Pellegrino, A Arenas-Pinto, D Cornforth*, J Turner*), North Middlesex Hospital (J Ainsworth, A Waters), Royal Free Hospital, London (M Johnson, S Kinloch, A Carroll, P Byrne, Z Cuthbertson), Barts & the London NHS Trust, London (C Orkin, J Hand, C De Souza), St Marys Hospital, London (J Weber, S Fidler, E Hamlyn, E Thomson*, J Fox*, K Legg, S Mullaney*, A Winston, S Wilson, P Ambrose), Birmingham Heartlands Hospital, Birmingham (S Taylor, G Gilleran). Imperial College Trial Secretariat: S Keeling, A Becker. Imperial College DSMC Secretariat: C Boocock. (* Left the study team before the trial ended.)

A.2 CHERUB Steering Committee

Andrew Lever (University of Cambridge), Mark Wills (University of Cambridge), Jonathan Weber (Imperial College, London), Sarah Fidler (Imperial College, London), John Frater (University of Oxford), Lucy Dorrell (University of Oxford), Mike Malim (King's College, London), Julie Fox (King's College London), Ravi Gupta (University College London), Clare Jolly (University College London).

B

Additional figures and tables

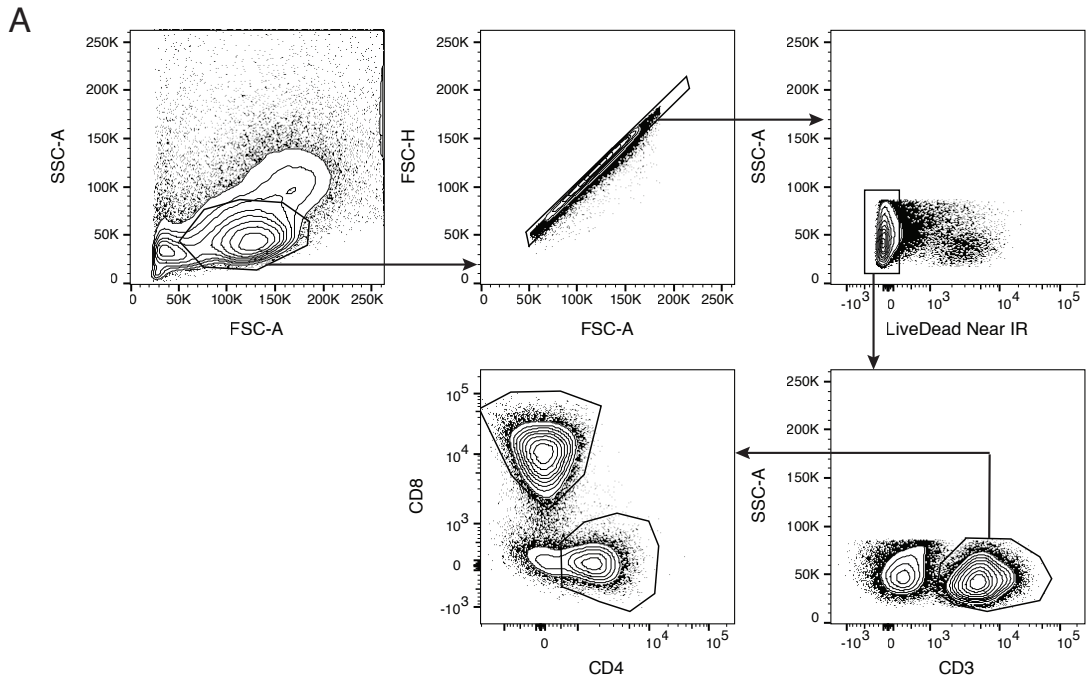


Figure B.1: Representative gating of CD4 and CD8 T cells. Cells were gated based on FSC-A vs SSC-A characteristics. Following doublet and dead cell exclusion, CD3 T cells were gated against SSC-A. CD4 and CD8 T cells were then gated based on the reciprocal expression of these markers.

T cell subset	Marker	Healthy (median [IQR])	PHI (median [IQR])	Diff.	U	n1	n2	p-value	p-value (adj.)
CD8_EM	**Tim-3**	2 [1.1-3.6]	19 [8.8-30]	9.8	23.5	10	60	3.61E-06	**0.000128**
CD8_EMRA	**Tim-3**	1.2 [0.84-3.3]	11 [7-15]	9	32	10	60	7.12E-06	**0.000128**
CD4_EM	**Tim-3**	0.75 [0.52-2.1]	7 [3.2-11]	9.4	47	10	60	2.26E-05	**0.000219**
CD4_TM	**Tim-3**	4.2 [3.2-6.3]	15 [9.4-23]	3.5	48	10	60	2.43E-05	**0.000219**
CD8_CM	**Tim-3**	3.5 [3.1-4.3]	7.4 [5.1-12]	2.1	62.5	10	60	6.95E-05	**0.000501**
CD8_CM	**TIGIT**	32 [29-44]	53 [46-63]	1.7	71	10	60	0.000125	**0.000753**
CD4_CM	**Tim-3**	2.8 [1.9-3.5]	5.8 [3.9-8.9]	2.1	81.5	10	60	0.000253	**0.0013**
CD4_EM	**PD-1**	17 [15-39]	44 [33-61]	2.5	117	10	60	0.00219	**0.00986**
CD8_CM	**PD-1**	19 [15-22]	39 [29-45]	2.1	120	10	60	0.00259	**0.0104**
CD4_EMRA	**Tim-3**	4.7 [3.8-6.8]	13 [6.8-19]	2.7	129.5	10	60	0.00433	**0.0156**
CD8_EM	**TIGIT**	40 [35-51]	65 [56-71]	1.6	135	10	60	0.00576	**0.0189**
CD8_Naive	**Tim-3**	6.1 [5.1-7]	9.8 [6.3-12]	1.6	142	10	60	0.0082	**0.0246**
CD8_Naive	**PD-1**	0.58 [0.33-1.6]	1.8 [1.1-3.3]	3.1	146.5	10	60	0.0102	**0.0283**
CD4_Naive	**Tim-3**	2.3 [1.4-2.7]	3.7 [2.5-4.3]	1.6	149.5	10	60	0.0118	**0.0304**
CD8_EM	**PD-1**	44 [38-57]	64 [50-70]	1.5	161.5	10	60	0.0205	**0.0493**
CD8_Naive	TIGIT	3.9 [2.8-9.3]	8.7 [4.6-14]	2.2	173	10	60	0.0337	0.0759
CD4_CM	PD-1	10 [7.2-13]	14 [10-18]	1.3	180	10	60	0.0448	0.0898
CD8_EM	CD39	1.8 [0.28-2.4]	8.5 [0.17-16]	4.7	180	10	60	0.0449	0.0898
CD8_EMRA	TIGIT	65 [58-73]	53 [40-65]	0.81	413	10	60	0.059	0.1
CD8_CM	CD39	5.4 [1-8.6]	12 [0.46-18]	2.1	187	10	60	0.059	0.1
CD8_EMRA	CD39	0.2 [0.062-0.48]	0.56 [0.18-1.4]	2.8	188	10	60	0.0613	0.1
CD4_TM	PD-1	34 [27-43]	44 [34-57]	1.3	188	10	60	0.0613	0.1
CD8_Naive	CD39	0.48 [0.26-0.85]	0.96 [0.34-1.9]	2	195	10	60	0.0794	0.124
CD4_EMRA	TIGIT	23 [16-35]	39 [21-61]	1.7	200.5	10	60	0.0966	0.145
CD4_EMRA	CD39	4.2 [2.9-6.3]	2.8 [1.7-4.8]	0.67	396.5	10	60	0.107	0.154
CD4_EMRA	PD-1	18 [12-25]	22 [15-33]	1.2	228	10	60	0.23	0.319
CD4_CM	TIGIT	27 [25-30]	29 [22-37]	1.1	256	10	60	0.465	0.62
CD4_TM	TIGIT	31 [28-41]	38 [26-48]	1.2	262.5	10	60	0.535	0.687
CD4_TM	CD39	21 [8.9-24]	21 [9.2-34]	0.99	267	10	60	0.585	0.716
CD4_EM	CD39	9.6 [3-14]	7.2 [1.5-13]	0.75	332	10	60	0.597	0.716
CD4_Naive	CD39	1.1 [1-1.7]	1.4 [0.91-2.1]	1.2	274	10	60	0.669	0.752
CD4_CM	CD39	9.9 [3.4-11]	9.9 [2.3-13]	0.99	274	10	60	0.669	0.752
CD4_EM	TIGIT	10 [8.5-14]	10 [6.7-13]	1	314.5	10	60	0.814	0.867
CD4_Naive	TIGIT	2.7 [2.3-3.4]	2.5 [1.8-4.1]	0.92	311.5	10	60	0.854	0.867
CD8_EMRA	PD-1	18 [8.7-30]	20 [9.7-26]	1.1	289	10	60	0.86	0.867
CD4_Naive	PD-1	0.3 [0.26-0.36]	0.34 [0.22-0.52]	1.1	289.5	10	60	0.867	0.867

Table B.1: Summary data for comparisons presented in Figure 3.5. Immune checkpoint receptor expression was compared between healthy controls (n=n1; 10) and individuals during primary HIV infection (n=n2; 60). Values shown are percentage expression and groups were compared using Mann-Whitney tests. Adjustment of p-values for multiple comparisons was performed across all comparisons presented here to control the false discovery rate. Abbreviations: IQR, interquatile range; PHI, primary HIV infection.

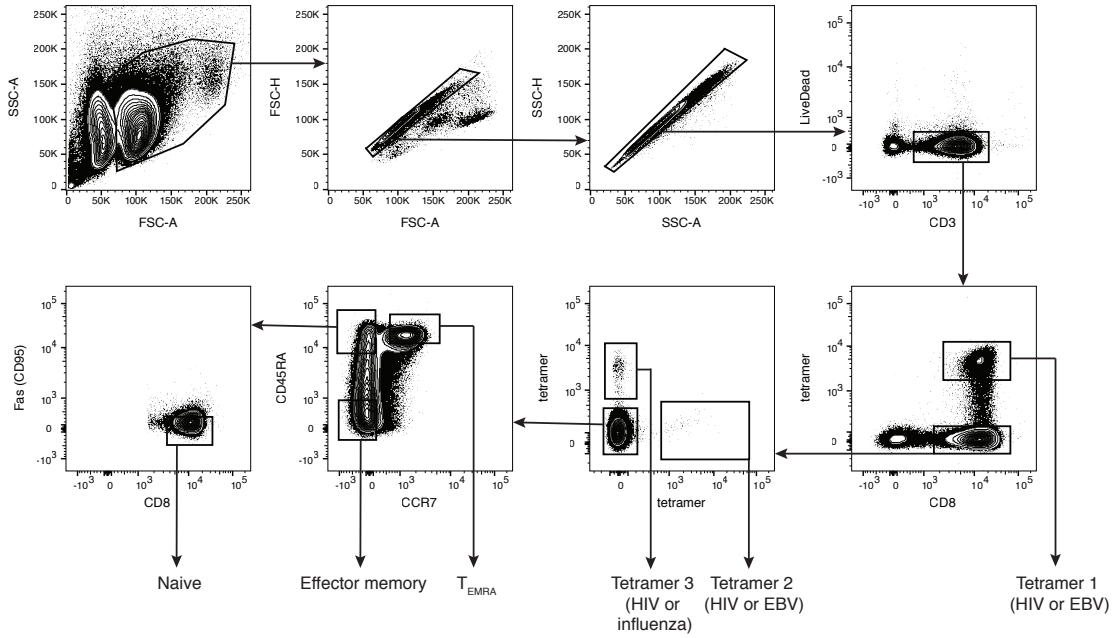


Figure B.2: Representative gating for tetramer stains. Data are shown from one experiment.

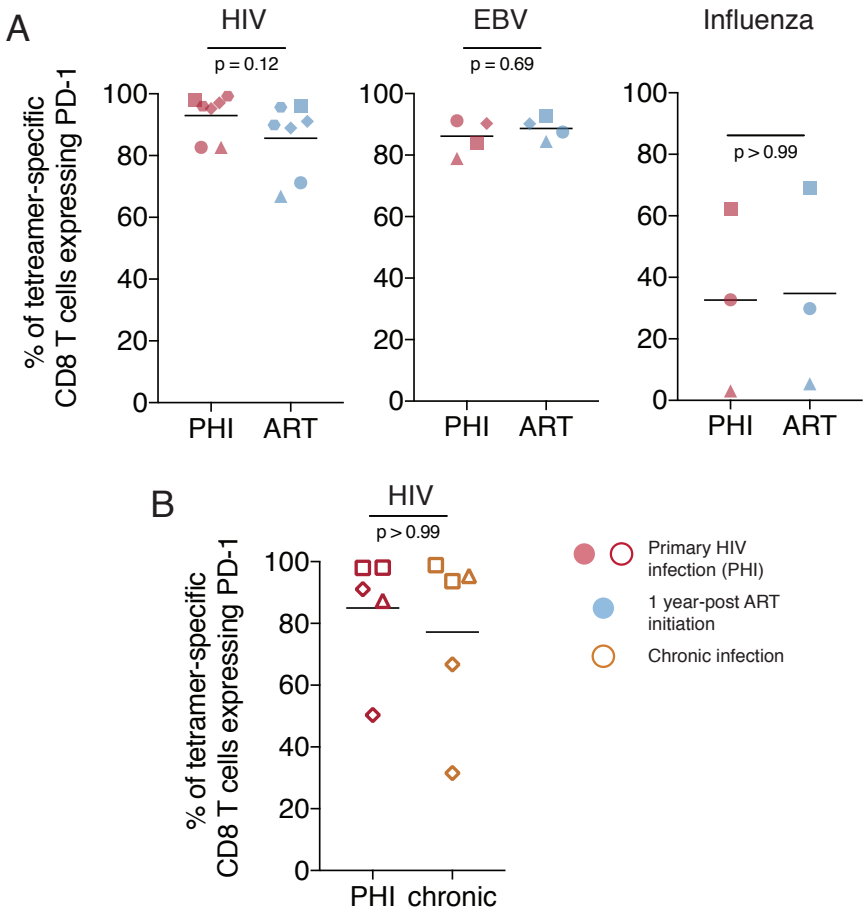


Figure B.3: Persistently high PD-1 expression on HIV-specific CD8 T cells with and without ART. (A) PD-1 expression on HIV, EBV and influenza specific CD8 T-cells during PHI and following 1 year of ART (n=5). EBV and influenza tetramers were not available for all individuals. (B) PD-1 expression on HIV-specific CD8 T cells in PHI and in chronic infection (n=3). Pairs were compared using a Mann-Whitney test. Throughout, symbol shapes indicate tetramers from the same individual. For some individuals multiple different HIV tetramers were used and these are shown as separate data points.

Variable	time point	n1	n2	U	p-value	p-value (adj.)
CD4_TM_PD1	**baseline**	41	19	162	0.000309	**0.0291**
CD4_TM_TIGIT	**baseline**	41	19	180.5	0.000922	**0.0433**
CD8_CD38	baseline	35	17	181	0.0226	0.455
CD4_CM_PD1	baseline	41	19	247.5	0.0245	0.455
CD4_CM_TIGIT	baseline	41	19	248.5	0.0255	0.455
CD4_TM.	12mo	41	17	476	0.0300	0.455
CD4_CM.	12mo	41	17	471	0.0363	0.455
CD4.count	baseline	44	19	556.5	0.0388	0.455
CD4_to_CD8_ratio	baseline	44	19	552	0.0449	0.465
CD8_Naive_PD1	12mo	41	17	464	0.0494	0.465
CD4_EM_TIGIT	baseline	41	19	271.5	0.0619	0.515
CD4_TEMRA_PD1	baseline	41	19	274	0.0676	0.515
CD4_Naive.	baseline	41	19	276	0.0725	0.515
CD8_EM_TIGIT	baseline	41	19	279.5	0.0818	0.515
CD4_EM_PD1	baseline	41	19	280	0.0832	0.515
CD8_Naive_TIGIT	12mo	41	17	449	0.0876	0.515
CD4_Naive.	12mo	41	17	253	0.105	0.563
CD4_TM.	baseline	41	19	491	0.108	0.563
CD4_EM_Tim3	baseline	41	19	289.5	0.114	0.563
CD4_TEMRA.	baseline	41	19	487.5	0.121	0.570
CD4_CD38	baseline	35	17	220.5	0.136	0.607
CD4_EM_PD1	12mo	41	17	263.5	0.149	0.636
CD8_TBET^{low}EOMES^{high}	12mo	41	17	431	0.161	0.659
CD4_TM_Tim3	baseline	41	19	306.5	0.190	0.734
CD4_TEMRA_Tim3	baseline	41	19	307.5	0.195	0.734
CD8_EM.	12mo	41	17	421	0.221	0.770
CD4_Naive_TIGIT	baseline	41	19	312	0.221	0.770
CD4_TM_PD1	12mo	41	17	280	0.245	0.786
CD8_TEMRA.	baseline	41	19	462.5	0.249	0.786
CD4_TEMRA_TIGIT	12mo	41	17	415	0.260	0.786
CD8_CM_TIGIT	baseline	41	19	318.5	0.263	0.786
baseline_log10HIVDNA	baseline	42	18	310	0.279	0.786
CD8_TEMRA_Tim3	baseline	41	19	323	0.294	0.786
CD4_CD38	12mo	41	17	287.5	0.301	0.786
CD8_EM_Tim3	baseline	41	19	324	0.302	0.786
CD4_Naive_Tim3	12mo	41	17	409	0.305	0.786
CD8_TEMRA_TIGIT	12mo	41	17	408.5	0.309	0.786
CD4_TEMRA.	12mo	41	17	406	0.330	0.796
CD4_TEMRA_Tim3	12mo	41	17	406	0.330	0.796
Plasma_PD1	baseline	34	14	196.5	0.352	0.817
CD8_CM_PD1	12mo	41	17	403	0.356	0.817
CD8_EM_TIGIT	12mo	41	17	399.5	0.388	0.829
days_sero_to_artstart	baseline	44	20	380.5	0.393	0.829
CD4_TEMRA_TIGIT	baseline	41	19	335	0.394	0.829
log10totalDNA	12mo	43	18	333	0.401	0.829
CD8_EM_PD1	12mo	41	17	397	0.412	0.829
CD8_CD38	12mo	41	17	301	0.422	0.829
CD4_EM.	baseline	41	19	439.5	0.431	0.829
CD4_TEMRA_PD1	12mo	41	17	302	0.432	0.829
CD8_Naive_Tim3	12mo	41	17	393	0.452	0.840
CD4_EM_Tim3	12mo	41	17	304	0.456	0.840

Variable	**time point**	**n1**	**n2**	**U**	**p-value**	**p-value (adj.)**
CD4_CM.	baseline	41	19	435	0.474	0.846
CD4_EM_TIGIT	12mo	41	17	308.5	0.500	0.846
CD8_CM_Tim3	baseline	41	19	347	0.504	0.846
CD8_Naive.	12mo	41	17	309	0.505	0.846
CD8_Naive.	baseline	41	19	348	0.515	0.846
CD4_CM_PD1	12mo	41	17	310	0.516	0.846
CD4_Naive_PD1	12mo	41	17	386	0.527	0.846
CD8_CM_TIGIT	12mo	41	17	385	0.539	0.846
days_artstart_to_suppressed	baseline	44	20	481	0.557	0.846
log10VL	baseline	44	20	399	0.560	0.846
Plasma_PD1	12mo	34	14	212	0.562	0.846
CD8_TEMRA_Tim3	12mo	41	17	382.5	0.567	0.846
CD4_Naive_PD1	baseline	41	19	354	0.578	0.846
CD8_CM.	12mo	41	17	380	0.596	0.846
CD4_CM_TIGIT	12mo	41	17	317.5	0.602	0.846
CD8_CM_PD1	baseline	41	19	356.5	0.605	0.846
CD8_TBET^{low}EOMES^{high}	baseline	35	17	271	0.612	0.846
Plasma_Tim3	baseline	34	14	216	0.630	0.858
Plasma_Tim3	12mo	34	14	258	0.658	0.884
CD8_Naive_TIGIT	baseline	41	19	415	0.691	0.895
CD8_Naive_Tim3	baseline	41	19	364.5	0.697	0.895
CD4_Naive_Tim3	baseline	41	19	365.5	0.709	0.895
CD8_TBET^{neg}EOMES^{neg}	baseline	35	17	316	0.725	0.895
CD8_EM.	baseline	41	19	368	0.741	0.895
CD8_TEMRA_PD1	12mo	41	17	368	0.746	0.895
CD8_CM.	baseline	41	19	369	0.751	0.895
CD8_EM_PD1	baseline	41	19	369	0.751	0.895
CD8.count	baseline	44	19	397	0.761	0.895
CD4_CM_Tim3	baseline	41	19	370.5	0.769	0.895
CD4_TM_Tim3	12mo	41	17	366	0.771	0.895
CD8_TBET^{high}EOMES^{low}	12mo	41	17	333	0.798	0.911
CD4_CM_Tim3	12mo	41	17	363.5	0.804	0.911
CD8_EM_Tim3	12mo	41	17	334.5	0.818	0.915
CD4_Naive_TIGIT	12mo	41	17	335.5	0.831	0.919
CD8_Naive_PD1	baseline	41	19	402	0.849	0.928
CD8_TEMRA_TIGIT	baseline	41	19	378.5	0.867	0.936
CD8_TBET^{high}EOMES^{low}	baseline	35	17	289	0.876	0.936
CD4_TM_TIGIT	12mo	41	17	341	0.905	0.938
CD8_CM_Tim3	12mo	41	17	356	0.905	0.938
CD8_TEMRA_PD1	baseline	41	19	382	0.911	0.938
CD8_TEMRA.	12mo	41	17	355	0.918	0.938
CD8_TBET^{neg}EOMES^{neg}	12mo	41	17	344.5	0.952	0.959
CD4_EM.	12mo	41	17	352	0.959	0.959

Table B.2: Summary data for comparisons presented in Figure 3.7. Expression of all immunological parameters was compared between CD39 expressors (n=n1) and non-expressors (n=n2) using Mann-Whitney tests. Adjustment of p-values for multiple comparisons was performed across all comparisons presented here to control the false discovery rate. Bolded variables are significant at a 0.05 level; variables are ranked based on the p-value. Abbreviations: 12mo, 1 year post-ART initiation.

T cell subset	Marker	time point	r_s	p-value	p-value (adj.)
CD4_TEMRA	PD1	12mo	0.5	0.000262	**0.00589**
CD8_TBET^{low}EOMES^{high}	PD1	12mo	0.49	0.000421	**0.00589**
CD4_EM	PD1	12mo	0.44	0.00154	**0.0122**
CD8_TEMRA	PD1	12mo	0.44	0.00174	**0.0122**
CD4_TM	PD1	baseline	0.41	0.00381	**0.0152**
CD8	PD1	12mo	0.42	0.00307	**0.0152**
CD8_TBET^{high}EOMES^{low}	PD1	12mo	0.42	0.00363	**0.0152**
CD8	PD1	baseline	0.35	0.0159	0.0538
CD4	PD1	12mo	0.34	0.0173	0.0538
CD4_CM	PD1	12mo	0.34	0.0196	0.055
CD4_TM	PD1	12mo	0.32	0.0243	0.0618
CD4_TEMRA	PD1	baseline	0.32	0.029	0.0676
CD4_CM	PD1	baseline	0.3	0.0404	0.0814
CD8_CM	PD1	12mo	0.3	0.0407	0.0814
CD4	PD1	baseline	0.26	0.0775	0.138
CD8_EM	PD1	12mo	0.26	0.079	0.138
CD8_TBETloEOMEShi	PD1	baseline	0.24	0.149	0.246
CD4_Naive	PD1	baseline	-0.14	0.348	0.465
CD4_EM	PD1	baseline	0.13	0.365	0.465
CD8_CM	PD1	baseline	0.14	0.337	0.465
CD8_TBEThiEOMESlo	PD1	baseline	0.15	0.352	0.465
CD8_Naive	PD1	12mo	0.14	0.355	0.465
CD8_TBETnegEOMESneg	PD1	baseline	0.14	0.411	0.501
CD8_EM	PD1	baseline	0.11	0.456	0.533
CD8_Naive	PD1	baseline	0.1	0.491	0.55
CD8_TBET^{neg}EOMES^{neg}	PD1	12mo	0.082	0.584	0.629
CD4_Naive	PD1	12mo	0.061	0.678	0.703
CD8_TEMRA	PD1	baseline	0.046	0.755	0.755
CD8_EM	Tim3	baseline	0.45	0.00149	**0.0328**
CD8	Tim3	baseline	0.41	0.00423	**0.0465**
CD4_TM	Tim3	baseline	0.33	0.0228	0.167
CD4	Tim3	baseline	0.25	0.0819	0.278
CD4_EM	Tim3	baseline	0.22	0.127	0.278
CD8_CM	Tim3	baseline	0.23	0.124	0.278
CD8_TEMRA	Tim3	baseline	0.26	0.0735	0.278
CD4	Tim3	12mo	0.24	0.102	0.278
CD4_Naive	Tim3	12mo	0.22	0.139	0.278
CD4_TEMRA	Tim3	12mo	0.25	0.088	0.278
CD8	Tim3	12mo	0.23	0.123	0.278
CD4_Naive	Tim3	baseline	0.21	0.158	0.29
CD8_Naive	Tim3	baseline	0.19	0.192	0.302
CD8_TEMRA	Tim3	12mo	0.19	0.188	0.302
CD4_CM	Tim3	baseline	0.18	0.224	0.328
CD8_Naive	Tim3	12mo	0.11	0.472	0.649
CD4_CM	Tim3	12mo	0.082	0.579	0.67
CD4_EM	Tim3	12mo	0.087	0.557	0.67
CD8_EM	Tim3	12mo	0.094	0.526	0.67
CD4_TEMRA	Tim3	baseline	0.056	0.706	0.777
CD4_TM	Tim3	12mo	0.048	0.747	0.782
CD8_CM	Tim3	12mo	-0.0011	0.994	0.994

Table B.3: Summary data for correlations presented in Figure 3.8. Spearman correlations between soluble PD-1 and Tim-3, and the expression of the same markers on T cell subsets during PHI (baseline) and 1 year following ART initiation (12mo); adjustment of p-values for multiple comparisons was performed across all comparisons for a given marker to control the false discovery rate. Adjustment of p-values for multiple comparisons was performed across all comparisons presented here to control the false discovery rate. Abbreviations: adj., adjusted; ART, antiretroviral therapy; PHI, primary HIV infection.

T cell subset	Marker	Healthy (median [IQR])	ART (median [IQR])	Diff.	U	n1	n2	p-value	p-value (adj.)
CD4_EMRA	**Subset**	0.7 [0.44-1.2]	2.3 [1.1-5.1]	3.3	90.5	10	58	0.000569	**0.00478**
CD8_CM	**Subset**	9.7 [5.8-14]	4.2 [2.6-6]	0.43	489.5	10	58	0.000569	**0.00478**
CD8_TBET^{high} EOMES^{low}	**Subset**	11 [9.1-19]	32 [22-44]	2.9	72	10	60	0.000134	**0.00478**
CD8_CM	**Tim-3**	3.5 [3.1-4.3]	7.2 [4.8-8.6]	2	93	10	58	0.000667	**0.00478**
CD8_EM	**Tim-3**	2 [1.1-3.6]	5.9 [3.5-10]	3	78	10	58	0.00025	**0.00478**
CD8_EMRA	**Tim-3**	1.2 [0.84-3.3]	5.3 [2.9-9.2]	4.6	91	10	58	0.000587	**0.00478**
CD8_EMRA	**Subset**	25 [16-30]	43 [30-55]	1.7	102.5	10	58	0.0012	**0.00708**
CD4_EM	**Tim-3**	0.75 [0.52-2.1]	3.7 [1.9-6.9]	5	104	10	58	0.00132	**0.00708**
CD4_EM	**PD-1**	17 [15-39]	44 [32-54]	2.5	123	10	58	0.00394	**0.0169**
CD8	**CD38**	2.6 [1.8-3.6]	5.4 [3.4-7.6]	2.1	127	10	60	0.00379	**0.0169**
CD8_TBET^{neg} EOMES^{neg}	**Subset**	50 [43-53]	38 [27-49]	0.76	452	10	60	0.011	**0.0394**
CD4_TM	**Tim-3**	4.2 [3.2-6.3]	8.9 [4.9-12]	2.1	141.5	10	58	0.0104	**0.0394**
CD4_CM	Tim-3	2.8 [1.9-3.5]	4.5 [2.7-5.8]	1.6	160	10	58	0.0249	0.0825
CD8_CM	TIGIT	32 [29-44]	43 [36-50]	1.3	164.5	10	58	0.0304	0.0931
CD8_EMRA	TIGIT	65 [58-73]	47 [37-63]	0.73	414	10	58	0.0325	0.0931
CD8_TBET^{low} EOMES^{high}	Subset	29 [21-40]	20 [16-28]	0.7	422	10	60	0.0414	0.111
CD8_Naive	Subset	34 [25-45]	23 [13-33]	0.66	406.5	10	58	0.0446	0.113
CD8_EMRA	PD-1	18 [8.7-30]	9.8 [5.2-14]	0.55	400	10	58	0.0579	0.138
CD4_EMRA	Tim-3	4.7 [3.8-6.8]	8.4 [4.4-16]	1.8	189	10	58	0.0818	0.185
CD4_TM	Subset	7.3 [6.9-8.7]	6 [4.2-8.2]	0.82	384	10	58	0.105	0.227
CD8_Naive	PD-1	0.58 [0.33-1.6]	0.92 [0.55-2.4]	1.6	201	10	58	0.125	0.249
CD8_Naive	TIGIT	3.9 [2.8-9.3]	6.5 [3.9-12]	1.7	201.5	10	58	0.128	0.249
CD4_EM	Subset	4.3 [3.4-9.5]	8.9 [5.4-12]	2.1	209.5	10	58	0.166	0.297
CD8_CM	PD-1	19 [15-22]	24 [18-32]	1.3	208.5	10	58	0.161	0.297
CD4_EMRA	TIGIT	23 [16-35]	30 [19-53]	1.3	218.5	10	58	0.219	0.376
CD4_CM	TIGIT	27 [25-30]	29 [23-35]	1.1	227.5	10	58	0.283	0.451
CD8_EM	PD-1	44 [38-57]	40 [30-51]	0.92	353	10	58	0.279	0.451
CD4_Naive	Tim-3	2.3 [1.4-2.7]	2.7 [1.5-4.1]	1.2	232	10	58	0.319	0.49
CD4_CM	Subset	39 [31-49]	37 [30-42]	0.95	345.5	10	58	0.341	0.505
Soluble	PD-1	84 [50-120]	110 [49-180]	1.3	196	10	48	0.37	0.53
CD4_Naive	TIGIT	2.7 [2.3-3.4]	2.3 [1.5-3.4]	0.85	338	10	58	0.411	0.535
CD4_EM	TIGIT	10 [8.5-14]	8.7 [6.5-14]	0.84	338.5	10	58	0.406	0.535
CD8_Naive	Tim-3	6.1 [5.1-7]	6.7 [4.6-9.8]	1.1	240	10	58	0.391	0.535
CD4_CM	PD-1	10 [7.2-13]	11 [8-15]	1.1	243.5	10	58	0.426	0.538
CD8_EM	Subset	22 [15-31]	20 [13-26]	0.91	334	10	58	0.451	0.554
CD4_TM	TIGIT	31 [28-41]	38 [26-46]	1.2	251	10	58	0.505	0.603
CD4_TM	PD-1	34 [27-43]	36 [31-46]	1.1	254	10	58	0.539	0.607
CD8_EM	TIGIT	40 [35-51]	45 [38-55]	1.1	255	10	58	0.55	0.607
Soluble	Tim-3	1000 [740-1200]	1000 [840-1400]	1	210	10	48	0.544	0.607
CD4_Naive	PD-1	0.3 [0.26-0.36]	0.29 [0.18-0.44]	0.95	322.5	10	58	0.579	0.623
CD4_EMRA	PD-1	18 [12-25]	20 [9.9-30]	1.1	271	10	58	0.749	0.785
CD4	CD38	24 [14-31]	24 [15-29]	0.98	285.5	10	60	0.814	0.834
CD4_Naive	Subset	42 [28-50]	38 [29-48]	0.91	300.5	10	58	0.863	0.863

Table B.4: Summary data for comparisons presented in Figure 3.9. Immune parameters wwere compared between healthy controls (n=n1) and individuals following 1 year of ART (n=n2). Values shown are percentage expression for all markers except soluble PD-1 and Tim-3 (pg/mL). Groups were compared using Mann-Whitney tests. Adjustment of p-values for multiple comparisons was performed across all comparisons presented here to control the false discovery rate. Abbreviations: Diff., fold-difference (median); adj., adjusted; IQR, interquartile range; ART, antiretroviral therapy; PHI, primary HIV infection.

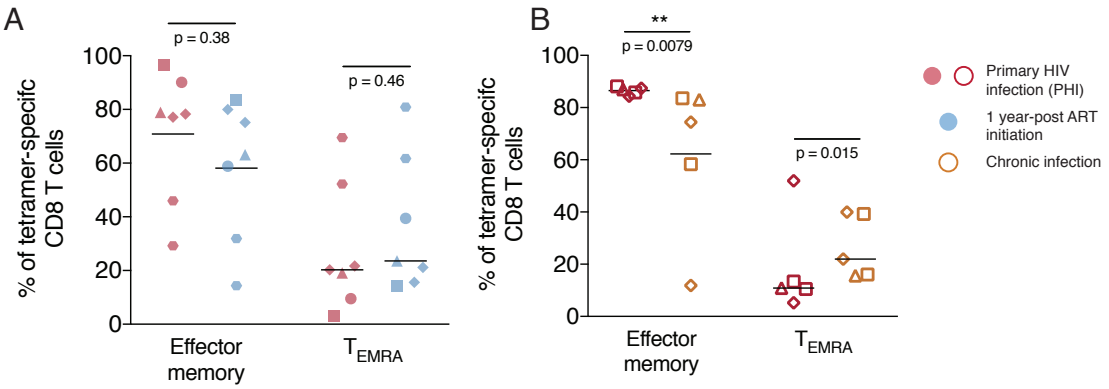


Figure B.4: Memory expansion of HIV-specific CD8 T cells with and without ART. (A) and (B) show the proportion of HIV-specific CD8 T cells made up of effector memory and T_{EMRA} cells. (A) Compares PHI with one year post-ART (n=5) whilst (B) compares PHI and chronic infection (n=3). Pairs were compared using a Mann-Whitney test. Throughout, symbol shapes indicate tetramers from the same individual. For some individuals multiple different HIV tetramers were used and these are shown as separate data points. ** indicates $p<0.01$.

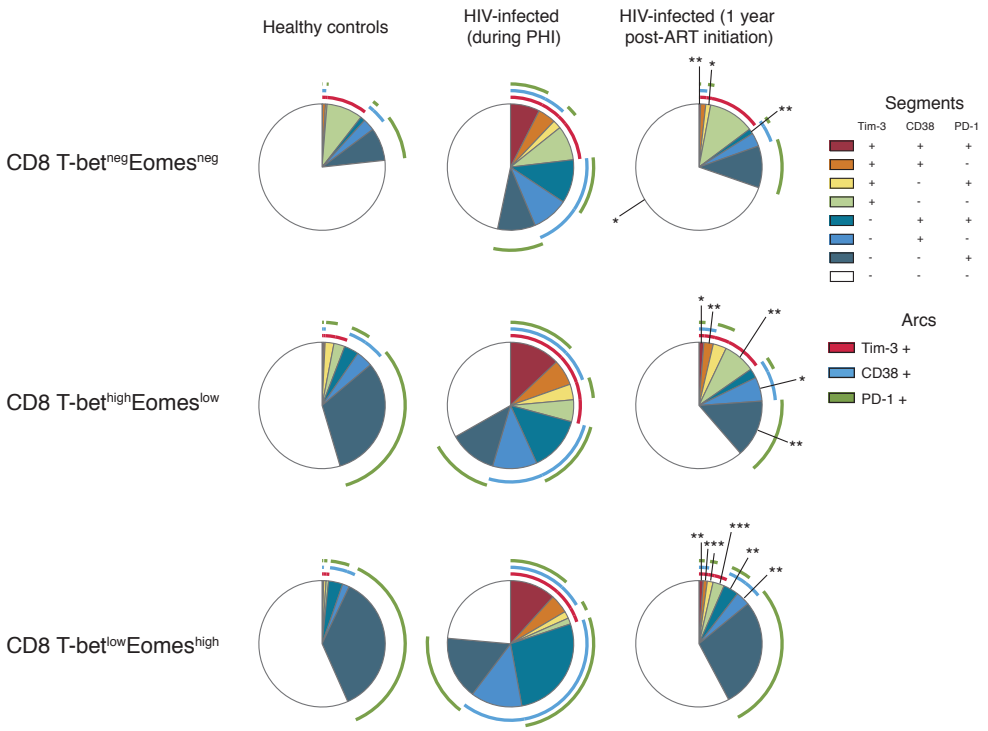


Figure B.5: Complete data for co-expression analysis presented in Figure 3.12. Co-expression of CD38, Tim-3 and PD-1 on CD8 subsets in healthy individuals (n=10), HIV infected individuals during PHI (n=54) and following 1 year of ART (n=60). Each segment represents the proportion of cells (median) with a different co-expression combination; arcs indicate which markers are in that combination. Co-expressing combinations were compared between healthy controls and ART treated individuals using a Mann-Whitney test; p-values were adjusted to control the false-discovery rate across all the comparisons shown here. Segments marked with an asterisk are significantly different between healthy controls and ART-treated individuals. Asterisks and listed p-values correspond to the adjusted p-value. * indicates $p<0.05$; ** indicates $p<0.01$; *** indicates $p<0.001$.

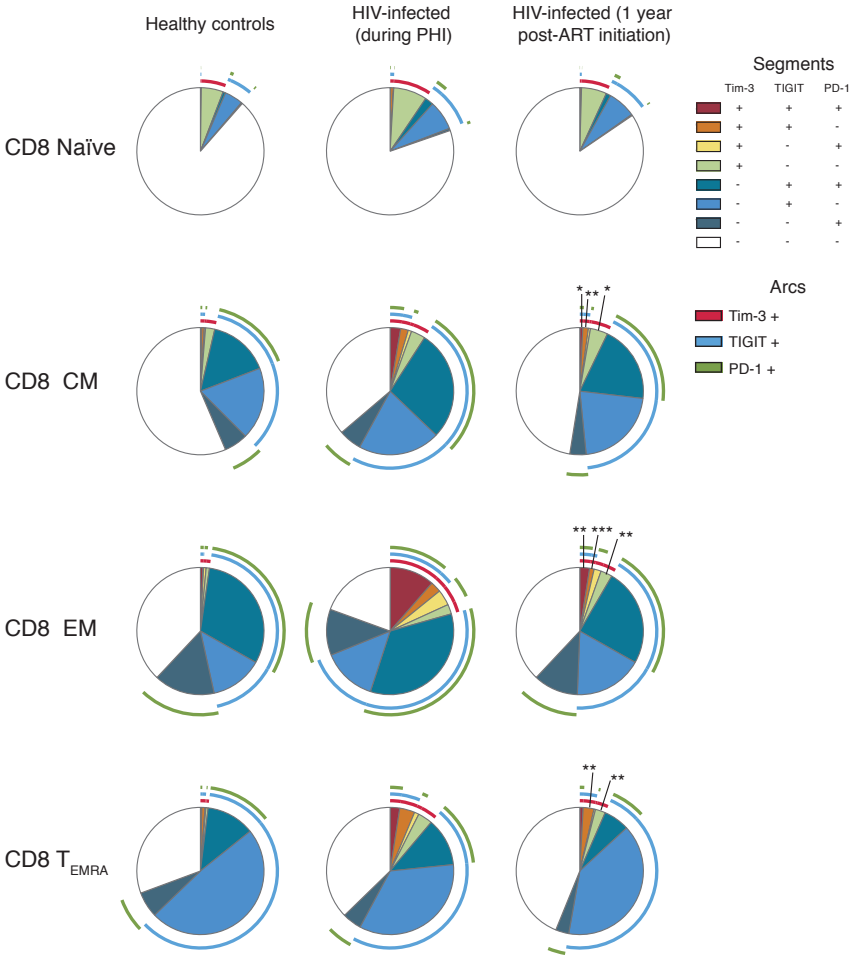


Figure B.6: Complete data for CD8 T cell co-expression analysis presented in Figure 3.13. Co-expression of ICRs on CD8 T cell subsets from healthy controls (n=10), during PHI (n=60) and following 1 year of ART (n=58). Each segment represents the proportion of cells (median) with a different co-expression combination; arcs indicate which markers are in that combination. Co-expressing combinations were compared between healthy controls and ART treated individuals using a Mann-Whitney test; p-values were adjusted to control the false-discovery rate across all the comparisons shown here. Segments marked with an asterisk are significantly different between healthy controls and ART-treated individuals. Asterisks and listed p-values correspond to the adjusted p-value. * indicates $p<0.05$; ** indicates $p<0.01$; *** indicates $p<0.001$.

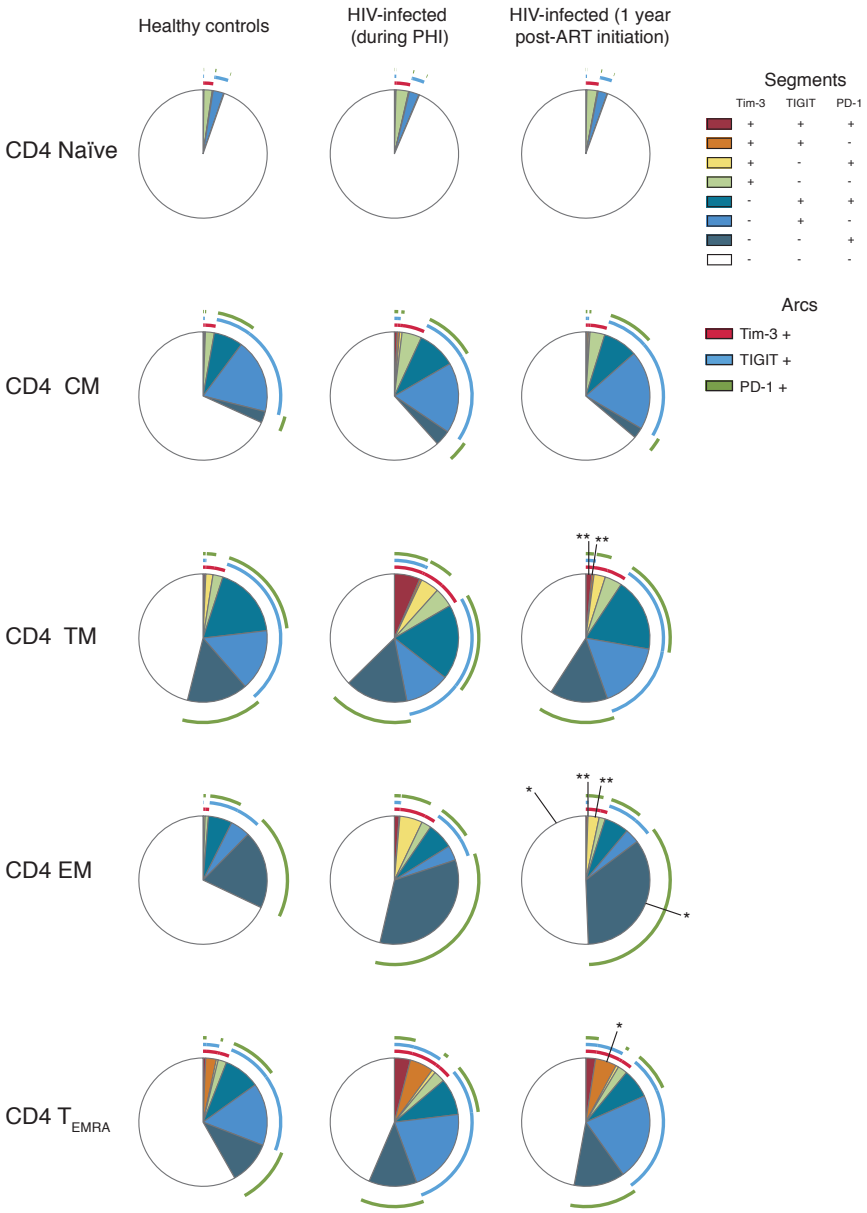


Figure B.7: Complete data for CD4 T cell co-expression analysis presented in Figure 3.13. Co-expression of ICRs on CD4 T cell subsets from healthy controls (n=10), during PHI (n=60) and following 1 year of ART (n=58). Each segment represents the proportion of cells (median) with a different co-expression combination; arcs indicate which markers are in that combination. Co-expressing combinations were compared between healthy controls and ART treated individuals using a Mann-Whitney test; p-values were adjusted to control the false-discovery rate across all the comparisons shown here. Segments marked with an asterisk are significantly different between healthy controls and ART-treated individuals. Asterisks and listed p-values correspond to the adjusted p-value. * indicates $p<0.05$; ** indicates $p<0.01$; *** indicates $p<0.001$.

Immunological variable	Clinical variable	n	r_s	p-value	p-value (adj.)
CD4_TM_Tim3	CD8.count	57	0.35	0.0074	0.329
CD8_TBET^{neg} EOMES^{neg}	CD4_to_CD8_ratio	59	0.34	0.00783	0.329
CD8_CM_Tim3	days_sero_to_artstart	58	0.27	0.0444	0.736
CD8_CM_Tim3	age_at_artstart	58	-0.26	0.0532	0.736
CD4_EM_Tim3	CD8.count	57	0.25	0.0616	0.736
CD8_TBET^{neg} EOMES^{neg}	CD8.count	59	-0.24	0.0704	0.736
CD8_EM_Tim3	age_at_artstart	58	-0.23	0.079	0.736
CD8_CD38	days_sero_to_artstart	60	-0.22	0.089	0.736
CD4_TM_Tim3	age_at_artstart	58	-0.22	0.0933	0.736
CD4_EM_Tim3	age_at_artstart	58	-0.22	0.0943	0.736
CD8_EM_Tim3	CD8.count	57	0.22	0.108	0.736
CD4_TM_Tim3	CD4_to_CD8_ratio	57	-0.21	0.114	0.736
CD8_CM.	log10VL	58	0.21	0.119	0.736
CD8_TEMRA_Tim3	CD8.count	57	0.19	0.155	0.736
CD4_EM_PD1	days_artstart_to_suppressed	58	-0.19	0.162	0.736
CD8_TEMRA_Tim3	age_at_artstart	58	-0.19	0.162	0.736
CD8_TBET^{neg} EOMES^{neg}	age_at_artstart	60	-0.18	0.163	0.736
CD4_TM_Tim3	CD4.count	57	0.18	0.17	0.736
CD8_CM_Tim3	log10VL	58	-0.18	0.17	0.736
CD8_CD38	CD4.count	59	0.18	0.175	0.736
CD4_EM_Tim3	CD4_to_CD8_ratio	57	-0.18	0.184	0.736
CD8_TEMRA_Tim3	CD4_to_CD8_ratio	57	-0.17	0.193	0.737
CD8_CM_Tim3	days_artstart_to_suppressed	58	-0.17	0.209	0.745
CD8_EM_Tim3	CD4_to_CD8_ratio	57	-0.17	0.213	0.745
CD4_TEMRA.	days_sero_to_artstart	58	0.16	0.229	0.77
CD8_CM.	age_at_artstart	58	0.16	0.238	0.77
CD8_CM.	days_artstart_to_suppressed	58	0.15	0.26	0.787
CD8_CD38	log10VL	60	0.15	0.262	0.787
CD8_CM.	days_sero_to_artstart	58	-0.14	0.306	0.877
CD4_EM_PD1	days_sero_to_artstart	58	-0.13	0.326	0.877
CD4_TM_Tim3	log10VL	58	-0.13	0.339	0.877
CD8_CD38	age_at_artstart	60	-0.12	0.347	0.877
CD8_TEMRA_Tim3	log10VL	58	0.12	0.363	0.877
CD8_TBET^{high} EOMES^{low}	CD4_to_CD8_ratio	59	-0.12	0.378	0.877
CD8_CM.	CD8.count	57	0.11	0.407	0.877
CD8_TBET^{high} EOMES^{low}	CD8.count	59	0.11	0.421	0.877
CD8_EM_Tim3	CD4.count	57	0.11	0.424	0.877
CD8_TBET^{high} EOMES^{low}	age_at_artstart	60	-0.1	0.427	0.877
CD4_EM_PD1	CD4_to_CD8_ratio	57	-0.1	0.439	0.877
CD8_EM_Tim3	days_sero_to_artstart	58	-0.1	0.451	0.877
CD8_TEMRA_Tim3	CD4.count	57	0.097	0.473	0.877
CD8_TBET^{neg} EOMES^{neg}	days_artstart_to_suppressed	60	-0.094	0.477	0.877
CD8_TEMRA.	CD8.count	57	0.095	0.483	0.877
CD4_TEMRA.	CD4_to_CD8_ratio	57	0.093	0.49	0.877

Immunological variable	**Clinical variable**	**n**	**r_s**	**p-value**	**p-value (adj.)**
CD8_TEMRA.	log10VL	58	-0.092	0.494	0.877
CD4_EM_Tim3	log10VL	58	-0.09	0.501	0.877
CD8_TBET^{high} EOMES^{low}	CD4.count	59	0.086	0.516	0.877
CD4_TEMRA.	log10VL	58	-0.087	0.517	0.877
CD8_TEMRA.	CD4_to_CD8_ratio	57	-0.087	0.519	0.877
CD4_EM_Tim3	CD4.count	57	0.085	0.531	0.877
CD4_TM_Tim3	days_sero_to_artstart	58	0.084	0.532	0.877
CD4_TEMRA.	CD4.count	57	0.082	0.545	0.88
CD8_TEMRA.	days_artstart_to_suppressed	58	-0.076	0.569	0.902
CD4_EM_PD1	CD8.count	57	0.073	0.59	0.917
CD8_TBET^{high} EOMES^{low}	days_sero_to_artstart	60	-0.065	0.623	0.944
CD8_TEMRA.	age_at_artstart	58	0.064	0.634	0.944
CD4_EM_PD1	age_at_artstart	58	-0.061	0.648	0.944
CD8_CD38	CD8.count	59	0.059	0.658	0.944
CD8_CM.	CD4_to_CD8_ratio	57	-0.056	0.68	0.944
CD4_TEMRA.	age_at_artstart	58	-0.055	0.68	0.944
CD8_TBET^{neg} EOMES^{neg}	days_sero_to_artstart	60	0.053	0.685	0.944
CD8_CM.	CD4.count	57	0.042	0.756	0.956
CD8_TBET^{neg} EOMES^{neg}	CD4.count	59	0.041	0.756	0.956
CD4_EM_Tim3	days_sero_to_artstart	58	0.041	0.758	0.956
CD8_TEMRA.	CD4.count	57	0.037	0.782	0.956
CD8_TEMRA_Tim3	days_artstart_to_suppressed	58	-0.037	0.785	0.956
CD4_EM_Tim3	days_artstart_to_suppressed	58	0.036	0.789	0.956
CD8_TBET^{neg} EOMES^{neg}	log10VL	60	-0.035	0.793	0.956
CD4_EM_PD1	log10VL	58	-0.03	0.823	0.956
CD8_EM_Tim3	days_artstart_to_suppressed	58	-0.03	0.825	0.956
CD8_TEMRA.	days_sero_to_artstart	58	0.026	0.845	0.956
CD8_CM_Tim3	CD8.count	57	-0.026	0.851	0.956
CD8_EM_Tim3	log10VL	58	-0.025	0.851	0.956
CD4_TEMRA.	CD8.count	57	-0.024	0.861	0.956
CD4_TEMRA.	days_artstart_to_suppressed	58	0.023	0.863	0.956
CD8_CD38	days_artstart_to_suppressed	60	-0.022	0.869	0.956
CD8_CM_Tim3	CD4.count	57	0.017	0.898	0.956
CD8_TBET^{high} EOMES^{low}	days_artstart_to_suppressed	60	-0.016	0.902	0.956
CD8_TEMRA_Tim3	days_sero_to_artstart	58	0.012	0.928	0.956
CD8_CD38	CD4_to_CD8_ratio	59	-0.012	0.929	0.956
CD8_TBET^{high} EOMES^{low}	log10VL	60	-0.011	0.933	0.956
CD4_TM_Tim3	days_artstart_to_suppressed	58	0.011	0.933	0.956
CD4_EM_PD1	CD4.count	57	0.0049	0.971	0.976
CD8_CM_Tim3	CD4_to_CD8_ratio	57	0.0041	0.976	0.976

Table B.5: Correlations of immunological variables following 1 year of ART with baseline clinical variables. Spearman correlations between were performed between combinations of immunological variables measured 1 year following ART initiation and baseline clinical measures (during PHI); adjustment of p-values for multiple comparisons was performed across all comparisons for a given marker to control the false discovery rate. Abbreviations: adj., adjusted.

Immunological variable	**Clinical variable**	**n**	**r_s**	**p-value**	**p-value (adj.)**
CD8_Naive.	CD4_to_CD8_ratio	59	0.68	4.44E-09	**7.77E-07**
CD8_CD38	log10VL	54	0.65	2.67E-07	**2.20E-05**
CD8_TBET^{neg} EOMES^{neg}	CD4_to_CD8_ratio	54	0.63	3.77E-07	**2.20E-05**
CD8_EM.	CD4_to_CD8_ratio	59	-0.6	7.39E-07	**3.23E-05**
CD8_EM.	log10VL	60	0.58	2.21E-06	**7.75E-05**
CD8_CD38	CD4_to_CD8_ratio	54	-0.6	3.30E-06	**9.61E-05**
CD4_TM_Tim3	CD4_to_CD8_ratio	59	-0.55	6.39E-06	**0.00016**
CD8_EM.	days_artstart_to_suppressed	60	0.53	1.61E-05	**0.000353**
CD8_CD38	days_artstart_to_suppressed	54	0.54	2.32E-05	**0.000451**
CD4_TEMRA_Tim3	CD4_to_CD8_ratio	59	-0.52	2.74E-05	**0.00048**
CD8_CM.	CD4_to_CD8_ratio	59	0.5	4.93E-05	**0.000784**
CD8_Naive.	CD8.count	59	-0.49	7.94E-05	**0.00116**
CD8_CM_Tim3	CD4_to_CD8_ratio	59	-0.48	0.000117	**0.00158**
CD8_Naive_Tim3	CD4_to_CD8_ratio	59	-0.48	0.000127	**0.00159**
CD8_EM_Tim3	CD4_to_CD8_ratio	59	-0.48	0.000142	**0.00166**
CD8_TBET^{neg} EOMES^{neg}	log10VL	54	-0.49	0.000162	**0.00177**
CD4_TM_Tim3	CD8.count	59	0.46	0.000257	**0.00257**
Plasma_Tim3	days_artstart_to_suppressed	48	0.5	0.000264	**0.00257**
CD8_Naive.	days_artstart_to_suppressed	60	-0.43	0.000572	**0.00527**
CD8_TBET^{neg} EOMES^{neg}	CD8.count	54	-0.45	0.000651	**0.00569**
CD8_Naive.	log10VL	60	-0.42	0.000846	**0.00705**
CD4_EM_Tim3	CD4_to_CD8_ratio	59	-0.42	0.000993	**0.0079**
CD8_EM_Tim3	log10VL	60	0.41	0.00105	**0.00797**
CD4_TM_Tim3	days_artstart_to_suppressed	60	0.4	0.00171	**0.0125**
CD8_EM.	CD4.count	59	-0.39	0.00215	**0.0149**
Plasma_PD1	log10VL	48	0.43	0.00222	**0.0149**
CD4_EM_Tim3	CD4.count	59	-0.39	0.0024	**0.0156**
CD8_TEMRA_Tim3	CD4_to_CD8_ratio	59	-0.39	0.00254	**0.0159**
CD8_CD38	days_sero_to_artstart	54	-0.4	0.00274	**0.0165**
CD8_EM_Tim3	CD8.count	59	0.37	0.00349	**0.0203**
Plasma_PD1	CD4.count	47	-0.41	0.0038	**0.0203**
CD4_EM_Tim3	days_artstart_to_suppressed	60	0.37	0.00383	**0.0203**
CD8_EM.	CD8.count	59	0.37	0.00384	**0.0203**
CD8_TEMRA_Tim3	log10VL	60	0.37	0.00394	**0.0203**
Plasma_PD1	CD4_to_CD8_ratio	47	-0.4	0.00552	**0.0266**
CD4_TEMRA_Tim3	CD4.count	59	-0.36	0.00555	**0.0266**
CD8_EM_Tim3	days_artstart_to_suppressed	60	0.35	0.00562	**0.0266**
CD8_CM.	CD4.count	59	0.35	0.0061	**0.0281**
CD4_Naive_Tim3	CD4_to_CD8_ratio	59	-0.35	0.00638	**0.0286**
CD8_CD38	CD4.count	54	-0.36	0.00842	**0.0368**
CD8_TBET^{neg} EOMES^{neg}	days_artstart_to_suppressed	54	-0.35	0.00994	**0.0424**
CD8_EM_Tim3	days_sero_to_artstart	60	-0.33	0.0107	**0.0445**
CD4_TEMRA_Tim3	CD8.count	59	0.33	0.0113	**0.0461**
CD8_CD38	CD8.count	54	0.34	0.0125	**0.0498**
CD8_Naive_PD1	age_at_artstart	60	0.32	0.0132	0.0515
CD8_TEMRA_Tim3	days_sero_to_artstart	60	-0.31	0.0143	0.0536
CD8_CM_Tim3	CD4.count	59	-0.32	0.015	0.0536

Immunological variable	Clinical variable	n	r_s	p-value	p-value (adj.)
CD4_CM_Tim3	CD4_to_CD8_ratio	59	-0.32	0.015	0.0536
Plasma_Tim3	CD4_to_CD8_ratio	47	-0.35	0.015	0.0536
CD8_Naive_Tim3	CD4.count	59	-0.31	0.0158	0.0554
CD8_TEMRA_Tim3	CD8.count	59	0.31	0.0171	0.0579
CD8_CM_Tim3	log10VL	60	0.31	0.0173	0.0579
CD8_Naive.	CD4.count	59	0.31	0.0175	0.0579
CD8_CM_Tim3	CD8.count	59	0.3	0.02	0.0649
CD4_Naive_Tim3	days_artstart_to_suppressed	60	0.3	0.0206	0.0656
Plasma_Tim3	age_at_artstart	48	0.33	0.0214	0.0667
CD8_Naive_Tim3	CD8.count	59	0.3	0.0233	0.0715
CD4_Naive_Tim3	CD8.count	59	0.29	0.0243	0.0735
CD8_Naive_Tim3	days_artstart_to_suppressed	60	0.29	0.0272	0.0806
Plasma_Tim3	CD8.count	47	0.32	0.0308	0.0896
CD4_TM_Tim3	log10VL	60	0.28	0.0312	0.0896
Plasma_Tim3	log10VL	48	0.31	0.0335	0.0944
CD8_TEMRA_Tim3	days_artstart_to_suppressed	60	0.27	0.0347	0.0965
CD8_Naive_Tim3	days_sero_to_artstart	60	-0.26	0.0448	0.122
CD8_CM.	CD8.count	59	-0.26	0.0452	0.122
CD8_TBET^{neg} EOMES^{neg}	CD4.count	54	0.27	0.0481	0.126
CD8_Naive_PD1	days_artstart_to_suppressed	60	0.26	0.0483	0.126
CD8_Naive_Tim3	log10VL	60	0.25	0.0562	0.145
CD8_Naive_PD1	CD8.count	59	0.25	0.0572	0.145
CD8_TBET^{high} EOMES^{low}	CD4_to_CD8_ratio	54	-0.26	0.0613	0.153
CD8_EM_Tim3	CD4.count	59	-0.24	0.0644	0.159
CD8_TEMRA_Tim3	CD4.count	59	-0.24	0.0674	0.164
CD4_TEMRA_Tim3	log10VL	60	0.24	0.0689	0.165
CD4_TM_Tim3	CD4.count	59	-0.24	0.0721	0.17
CD4_CM_Tim3	CD8.count	59	0.23	0.0738	0.172
CD4_EM_Tim3	log10VL	60	0.23	0.0751	0.173
CD8_TBET^{high} EOMES^{low}	CD8.count	54	0.24	0.077	0.175
CD4_CM_Tim3	days_artstart_to_suppressed	60	0.22	0.0857	0.192
CD4_EM.	days_sero_to_artstart	60	0.21	0.108	0.239
CD4_CM_Tim3	log10VL	60	0.21	0.112	0.244
CD4_EM_PD1	CD4_to_CD8_ratio	59	-0.2	0.124	0.268
CD4_EM.	CD4_to_CD8_ratio	59	-0.2	0.129	0.276
CD8_CM_Tim3	days_artstart_to_suppressed	60	0.2	0.132	0.277
CD8_CM_TIGIT	days_artstart_to_suppressed	60	0.2	0.133	0.277
CD8_CM.	days_artstart_to_suppressed	60	-0.18	0.168	0.346
CD4_EM_Tim3	CD8.count	59	0.17	0.186	0.378
CD8_Naive_PD1	CD4_to_CD8_ratio	59	-0.17	0.192	0.386
CD4_EM.	CD4.count	59	-0.17	0.202	0.4
CD8_TBET^{high} EOMES^{low}	log10VL	54	0.18	0.203	0.4
CD8_Naive_PD1	days_sero_to_artstart	60	-0.16	0.208	0.405
CD4_EM_PD1	days_artstart_to_suppressed	60	0.16	0.214	0.41
CD8_EM.	days_sero_to_artstart	60	-0.16	0.216	0.41
CD8_EM_TIGIT	days_artstart_to_suppressed	60	0.16	0.221	0.416
CD4_EM_PD1	CD4.count	59	-0.16	0.227	0.423

Immunological variable	**Clinical variable**	**n**	**r_s**	**p-value**	**p-value (adj.)**
CD8_TBET^{high} EOMES^{low}	CD4.count	54	-0.17	0.23	0.424
CD8_EM_TIGIT	CD4.count	59	-0.15	0.255	0.458
CD8_CM_PD1	days_sero_to_artstart	60	-0.15	0.259	0.458
CD4_TM_Tim3	days_sero_to_artstart	60	0.15	0.259	0.458
CD8_CM_PD1	days_artstart_to_suppressed	60	0.15	0.26	0.458
CD4_EM.	days_artstart_to_suppressed	60	0.15	0.262	0.458
Plasma_Tim3	days_sero_to_artstart	48	-0.16	0.268	0.464
CD8_EM_TIGIT	days_sero_to_artstart	60	0.14	0.274	0.471
CD4_TEMRA.	CD8.count	59	0.14	0.282	0.479
CD4_CM_Tim3	CD4.count	59	-0.14	0.286	0.482
CD8_Naive.	age_at_artstart	60	-0.14	0.299	0.498
CD8_CM.	log10VL	60	-0.13	0.304	0.502
CD8_CM_TIGIT	days_sero_to_artstart	60	-0.13	0.325	0.532
CD8_TEMRA_Tim3	age_at_artstart	60	0.12	0.365	0.592
CD8_EM_TIGIT	log10VL	60	-0.12	0.375	0.602
CD4_CM_Tim3	age_at_artstart	60	-0.11	0.386	0.614
CD4_Naive_Tim3	log10VL	60	0.11	0.396	0.624
CD4_TEMRA.	CD4_to_CD8_ratio	59	-0.11	0.41	0.635
CD8_CM.	age_at_artstart	60	0.11	0.41	0.635
CD4_TEMRA_Tim3	days_artstart_to_suppressed	60	0.11	0.418	0.642
Plasma_PD1	days_artstart_to_suppressed	48	0.11	0.441	0.669
CD8_CM_PD1	CD8.count	59	0.1	0.444	0.669
CD8_EM_PD1	CD4.count	59	-0.1	0.45	0.671
CD8_CM_TIGIT	CD4.count	59	-0.1	0.453	0.671
CD8_EM_PD1	CD8.count	59	-0.098	0.46	0.676
CD8_EM_PD1	log10VL	60	-0.095	0.468	0.679
CD8_CM_TIGIT	CD8.count	59	0.096	0.47	0.679
CD4_EM.	CD8.count	59	0.094	0.477	0.684
CD4_EM_PD1	age_at_artstart	60	0.09	0.492	0.699
CD8_CM_TIGIT	CD4_to_CD8_ratio	59	-0.091	0.495	0.699
CD8_CM_PD1	CD4_to_CD8_ratio	59	-0.089	0.501	0.701
CD8_TBET^{neg} EOMES^{neg}	days_sero_to_artstart	54	0.093	0.505	0.702
CD4_EM_PD1	CD8.count	59	0.084	0.526	0.717
Plasma_PD1	CD8.count	47	0.094	0.529	0.717
CD8_TBET^{high} EOMES^{low}	days_artstart_to_suppressed	54	0.088	0.529	0.717
CD4_TM_Tim3	age_at_artstart	60	-0.082	0.535	0.721
CD8_Naive.	days_sero_to_artstart	60	0.08	0.542	0.723
CD8_EM_PD1	CD4_to_CD8_ratio	59	0.079	0.55	0.724
Plasma_PD1	age_at_artstart	48	-0.088	0.552	0.724
CD8_EM_Tim3	age_at_artstart	60	0.076	0.562	0.724
CD8_TBET^{high} EOMES^{low}	age_at_artstart	54	-0.08	0.565	0.724
CD4_TEMRA.	days_artstart_to_suppressed	60	0.076	0.566	0.724
CD4_Naive_Tim3	CD4.count	59	-0.076	0.567	0.724
CD8_CM_TIGIT	log10VL	60	0.072	0.582	0.738
CD8_EM_TIGIT	CD4_to_CD8_ratio	59	-0.071	0.591	0.744
CD8_CM_TIGIT	age_at_artstart	60	-0.07	0.597	0.744
CD8_CM_PD1	CD4.count	59	-0.069	0.604	0.744
CD8_CM_Tim3	days_sero_to_artstart	60	-0.068	0.604	0.744

Immunological variable	Clinical variable	n	r_s	p-value	p-value (adj.)
CD4_TEMRA.	days_sero_to_artstart	60	0.067	0.61	0.746
CD4_TEMRA_Tim3	age_at_artstart	60	0.066	0.619	0.752
CD4_TEMRA.	age_at_artstart	60	-0.063	0.634	0.765
CD8_Naive_PD1	log10VL	60	0.061	0.646	0.774
CD8_Naive_Tim3	age_at_artstart	60	0.059	0.654	0.779
CD4_EM_Tim3	days_sero_to_artstart	60	0.055	0.676	0.799
CD8_Naive_PD1	CD4.count	59	0.053	0.692	0.813
CD8_TBET^{high} EOMES^{low}	days_sero_to_artstart	54	0.049	0.727	0.848
Plasma_Tim3	CD4.count	47	0.051	0.735	0.849
Plasma_PD1	days_sero_to_artstart	48	-0.05	0.738	0.849
CD4_EM_Tim3	age_at_artstart	60	-0.04	0.763	0.872
CD8_CM_PD1	age_at_artstart	60	-0.034	0.797	0.896
CD4_EM.	age_at_artstart	60	0.034	0.798	0.896
CD4_CM_Tim3	days_sero_to_artstart	60	0.033	0.8	0.896
CD4_EM_PD1	days_sero_to_artstart	60	0.033	0.804	0.896
CD8_EM_PD1	days_artstart_to_suppressed	60	0.03	0.818	0.906
CD8_EM_PD1	days_sero_to_artstart	60	-0.027	0.839	0.923
CD8_EM_TIGIT	CD8.count	59	-0.026	0.845	0.923
CD8_EM.	age_at_artstart	60	-0.025	0.849	0.923
CD8_EM_TIGIT	age_at_artstart	60	-0.023	0.86	0.929
CD8_CM_Tim3	age_at_artstart	60	-0.021	0.871	0.932
CD8_EM_PD1	age_at_artstart	60	-0.02	0.876	0.932
CD4_EM.	log10VL	60	0.02	0.879	0.932
CD4_Naive_Tim3	days_sero_to_artstart	60	-0.014	0.918	0.968
CD8_CM.	days_sero_to_artstart	60	-0.01	0.939	0.973
CD4_TEMRA.	CD4.count	59	0.0099	0.94	0.973
CD4_TEMRA_Tim3	days_sero_to_artstart	60	-0.0096	0.942	0.973
CD4_TEMRA.	log10VL	60	-0.0091	0.945	0.973
CD8_CD38	age_at_artstart	54	0.0079	0.955	0.974
CD8_TBET^{neg} EOMES^{neg}	age_at_artstart	54	0.0074	0.958	0.974
CD8_CM_PD1	log10VL	60	0.0052	0.969	0.976
CD4_Naive_Tim3	age_at_artstart	60	0.0048	0.971	0.976
CD4_EM_PD1	log10VL	60	-0.0034	0.979	0.979

Table B.6: Summary data for comparisons presented in Figure 3.14. Spearman correlations between were performed between combinations of immunological and clinical measures during PHI; adjustment of p-values for multiple comparisons was performed across all comparisons for a given marker to control the false discovery rate. Abbreviations: adj., adjusted.

	CD38 expression on CD8 T cells		CD8 EM proportion	
	β	p-value	β	p-value
log_{10}VL	10.5	$2.7x10^{-6}$ ****	7.37	$1.1x10^{-4}$ ***
CD4:CD8	-11.6	0.10	-16.3	0.013 *
Time to viral load suppression (days)	0.0377	0.0073 **	0.0293	0.033 *
R^2_{adj}		0.54		0.45
n		54		59

Table B.7: Multivariable regression for CD8 T cell CD38 expression and EM phenotype. Multivariable linear regression models were fitted on variables prior to the initiation of ART.

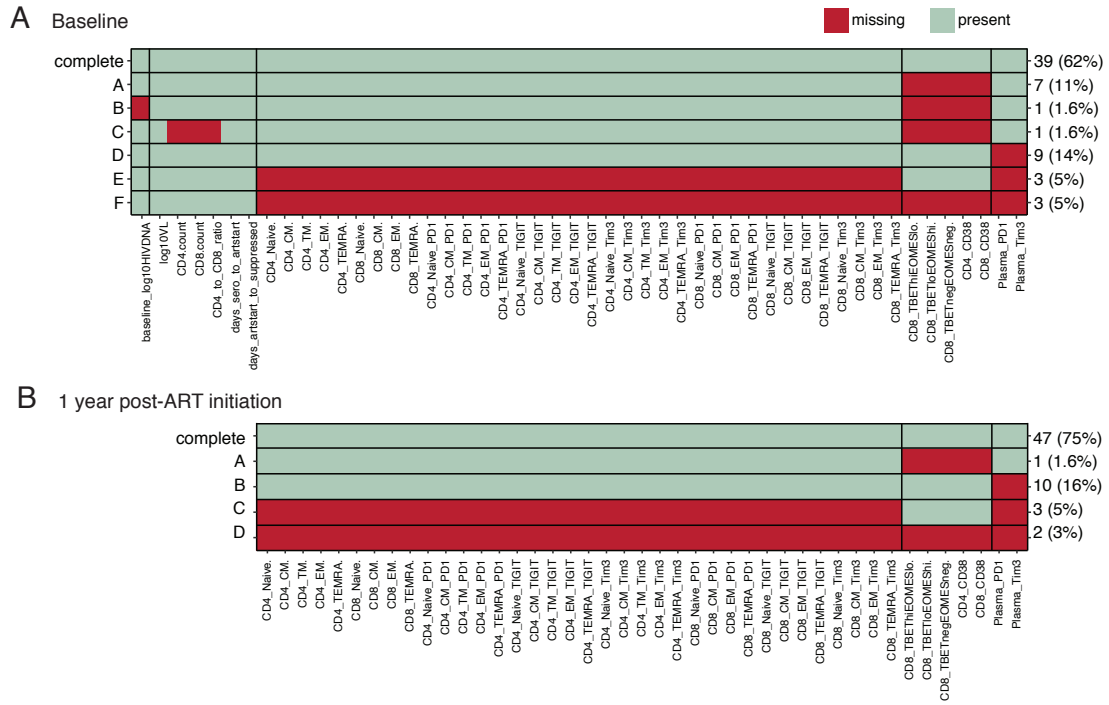


Figure B.8: Missing immunological and clinical data in HEATHER. This diagram shows the patterns of missing data at baseline (A) and following 1 year of ART (B) for the 63 individuals included in analysis of reservoir size in Chapter 4. Each row represents a pattern of data missingness and the right hand side shows how many individuals have this pattern. For some individuals there are no immunological observations available at a given time point. These are Pattern F (n=3) at baseline (all three samples had very low viability upon thawing and were not able to be included) and Pattern D (n=2) at 1 year (these individuals had not returned for 1 year visits at the time the assays were performed).

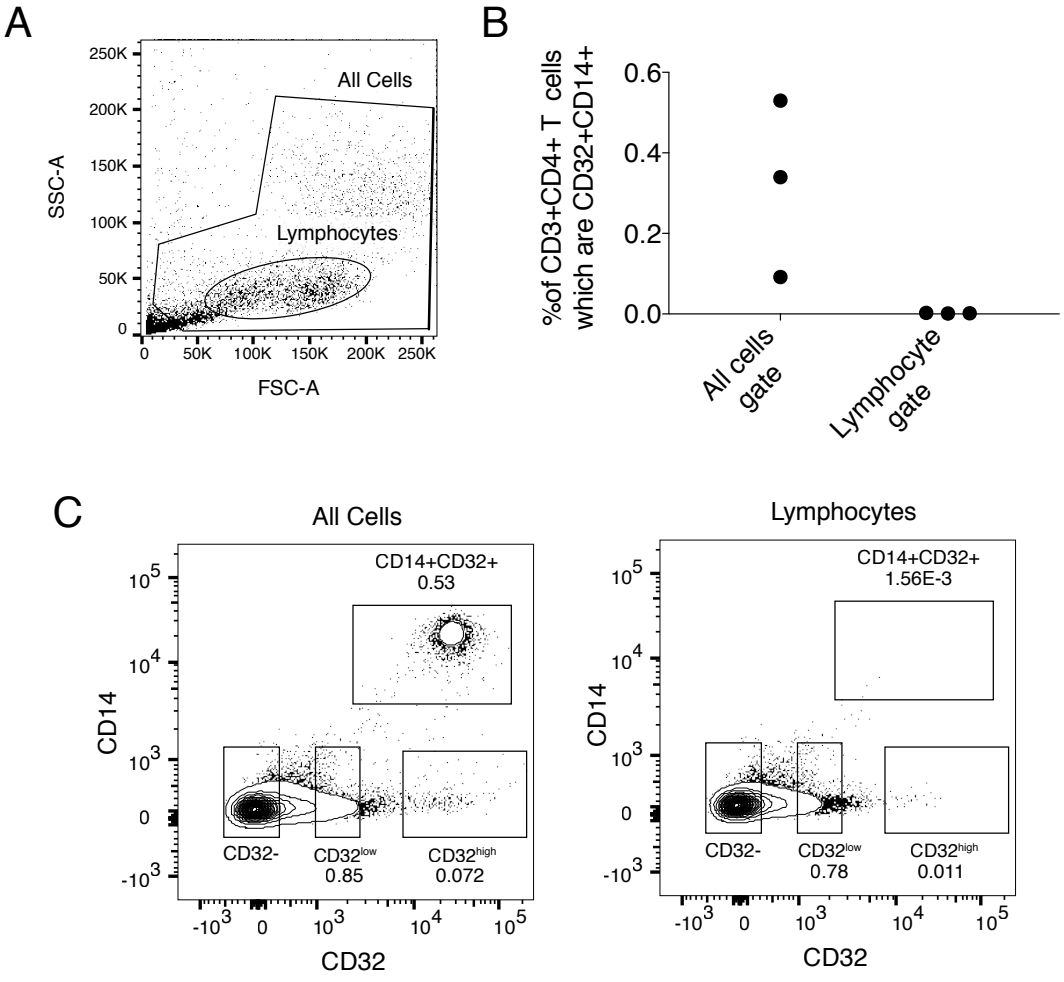


Figure B.9: CD14+CD32+ CD3+CD4+ cells have forward and side scatter characteristics which fall outside a conservative lymphocyte gate. CD32 expressing populations of CD3+CD4+ T cells are shown with different FSC-A and SSC-A gates. (A) Two different gates are shown based on FSC-A and SSC-A: Lymphocytes and All Cells. The All Cells gates includes the lymphocytes but also contains the monocyte population. (B) The percent of CD3+CD4+ T cells which are CD32+CD14+ when the same samples are gated these two different ways. Expression is shown from three individual donors. (C) Representative gating from one individual shown in B. Abbreviations: FSC-A (forward scatter, area), SSC-A (side scatter, area).

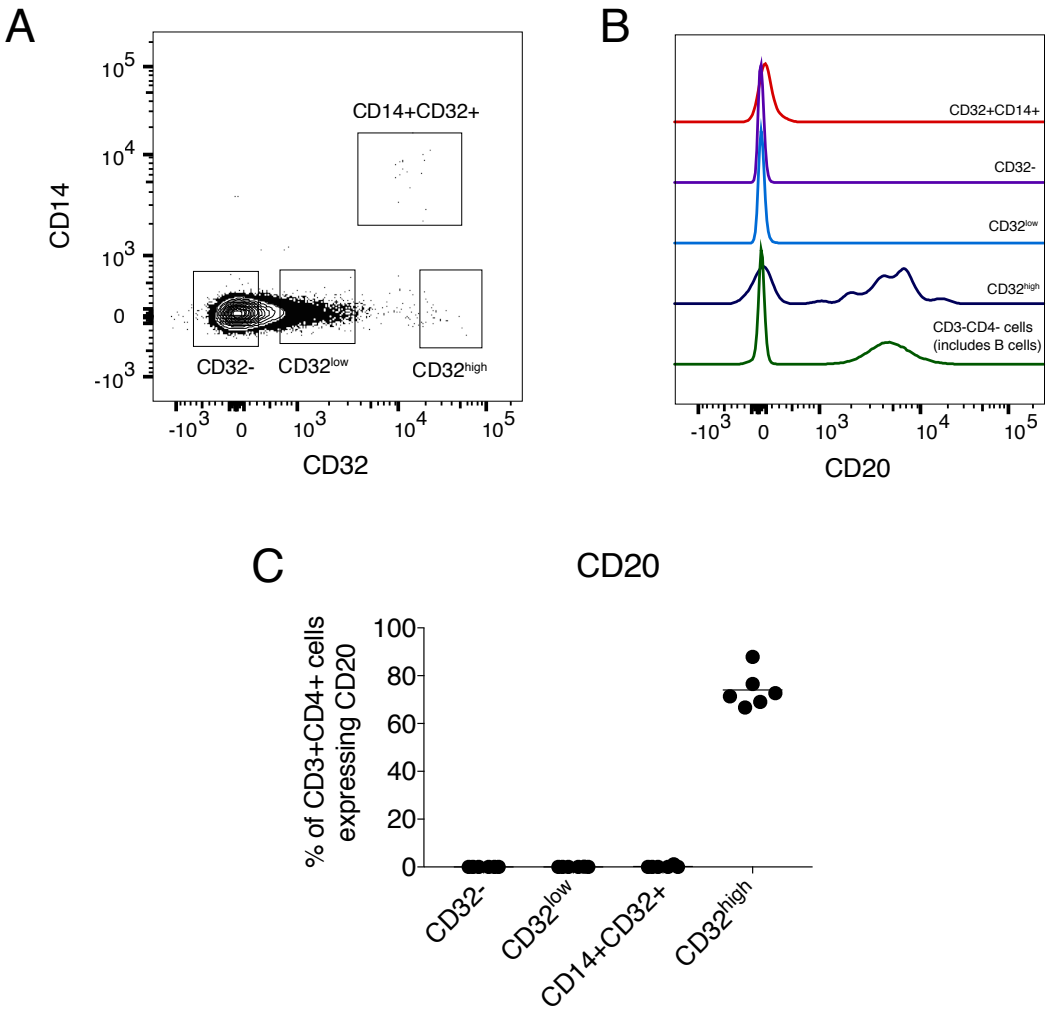


Figure B.10: CD32 expressing CD4 T cells from whole, fresh blood have a similar phenotype to those from cryopreserved PBMCs. Doublet exclusion strategy as used in phenotyping experiments. Phenotyping of CD32 expressing CD3+CD4+ T cells from whole, fresh blood (no cryopreservation or density gradient isolation of lymphocytes). (A) Gating of three CD32 expressing populations based on differing levels of expression and CD14: $CD32^{low}$, CD32+CD14+ and $CD32^{high}$. Plot shown from one representative donor. (B) Histogram showing CD20 staining on all CD32 expressing CD3+CD4+ T cell populations. Plot shown from one representative donor. (C) Percentage expression of CD20 on CD3+CD4+ subpopulations from 6 donors. Bar is shown at the mean.

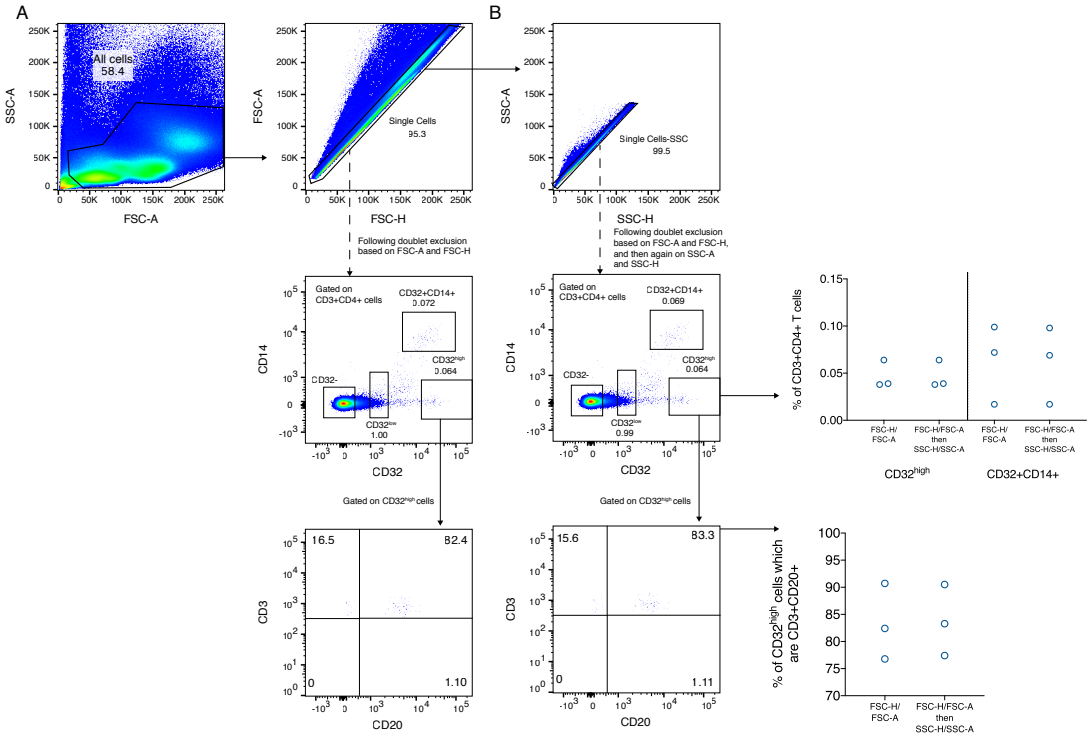


Figure B.11: Doublet exclusion strategy as used in phenotyping experiments. Representative doublet exclusion based on FSC-H and FSC-A for experiments presented in Figures 5.1, 5.2 and B.10. Below these gates are the phenotype of CD3+CD4+ T cells with regard to CD14 and CD32 expression, and CD20 expression. Shown in parallel in (B) are the same downstream gates if a second doublet exclusion step based on SSC-H and SSC-A is performed. The right hand side of this panel shows a quantification the frequency of these populations for n=3 donors for both the single and sequential doublet exclusion steps.

Group	HEATHER[1]	SPARTAC[2]	HEATHER[3]	HEATHER[4]
Sex				
Male	20 (100%)	5 (26%)	9 (100%)	19 (100%)
Age	33 (28 – 40.8)	27 (22 – 40)	30 (25 – 41)	34 (27 – 41)
Country				
United Kingdom	20 (100%)	4 (21%)	9 (100%)	19 (100%)
South Africa/Uganda	0	13 (68%)		
Other	0	2 (11%)		
Days between estimated date of seroconversion and ART initiation	41.5 (22.5 – 55.3)	109 (76 – 124)	38 (25.3 – 53.0)	61 (22.5 – 133)
Time of sampling (weeks since ART initiation)	52.5 (52.0 – 57.6)	47.9 (47.6 – 48.0)	119 (75.6 – 299)	51.4 (45 – 52.7)
Baseline CD4 T cell count (cells/µL)	514 (376 – 628)	634 (535 – 764)	587 (444 – 774)	563 (476 – 724)
Baseline HIV RNA ($\log_c$opies/mL)	6.32 (4.55 – 6.76)	4.32 (3.68 – 4.95)	6.67 (4.80 – 6.85)	4.82 (4.28 – 5.86)

Table B.8: Demographic and clinical characteristics of participants included in clinical studies. Values given represent n (%) for categorical variables and median (interquartile range) for continuous variables.
[1] Included in main phenotyping, Figures 5.3 A-E and 5.5 A, C.
[2] Figure 5.5 A, B and Table B.10.
[3] Included in quantification of HIV DNA in sorted CD32 expressing populations, Figure 5.4 and Table B.9.
[4] Included in the measurement of HLA-DR, Figure 5.3 F.

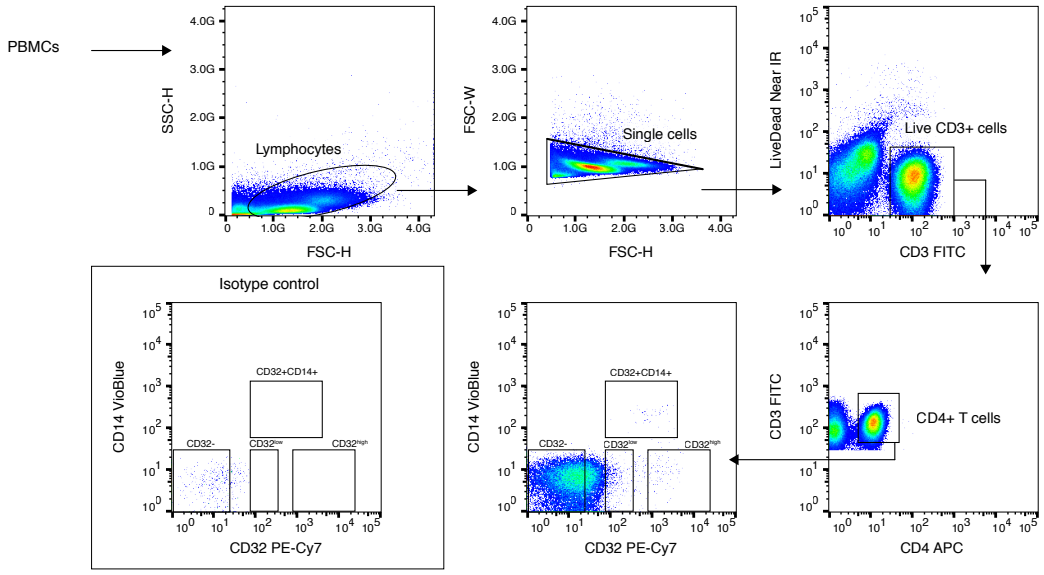


Figure B.12: Representative gating for sorts of CD3+CD4+ T cells based on CD32 expression. Sort strategy used for sorting of CD32-, $CD32^{low}$, CD32+CD14+ and $CD32^{high}$ populations.

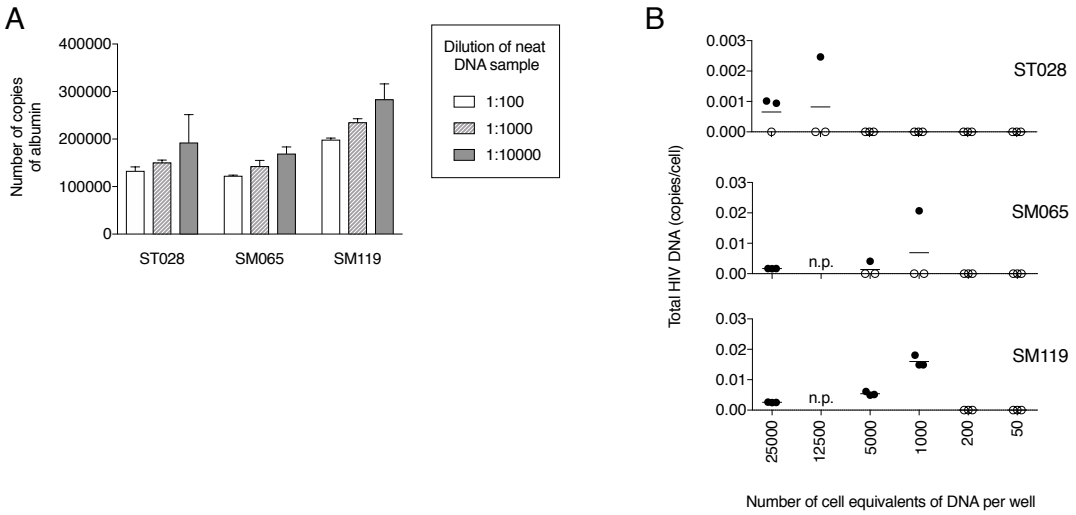


Figure B.13: Low cell input results in overestimation of HIV and albumin DNA by qPCR. Quantification of albumin and HIV DNA in serially diluted samples of DNA extracted from sorted CD32- CD4 T cells. (A) Quantification of number of copies of albumin DNA (used as a measure of cell equivalents of DNA) using qPCR when neat sample (153000, 242000, and 137000 cells per well for ST028, SM065 and SM119 respectively) was diluted 1:100, 1:1000 or 1:10000. Data are shown for three individuals (labelled on x-axis) and each dilution was performed in triplicate. Values shown are mean of replicates and error bars indicate the standard deviation. (B) Quantification of number of copies of HIV DNA via qPCR with decreasing cell equivalents of DNA used as input, starting with our usual assay input of 25000 cell equivalents per well. Data are shown for three individuals. Dilutions were performed in triplicate and each data point indicates an individual replicate; open circles indicate that the well was negative; n.p. indicates that a given dilution was not performed for that sample. Bar shows the mean of replicates.

Participant ID	Fold enrichment (relative to CD32- population)				Input number of cells per well				Number of wells positive for HIV DNA			
	CD32-	CD32^{low}	CD32+ CD14+	CD32^{high}	CD32-	CD32^{low}	CD32+ CD14+	CD32^{high}	CD32-	CD32^{low}	CD32+ CD14+	CD32^{high}
SM005	1	3.82	10.51	9.13	25000	9260	1280	842	2 of 3	2 of 2	2 of 2	1 of 2
ST344	1	1.16	2520.00	24.00	7890	1340	573	209	3 of 3	1 of 2	2 of 2	1 of 2
SM065	1	3.35	2.41	-	25000	14000	2040	1330	3 of 3	2 of 2	2 of 2	0 of 2
SM119	1	1.46	0.401	0.773	25000	8330	2420	7390	3 of 3	2 of 2	2 of 2	2 of 2
ST028	1	1.48	-	-	25000	25300	3110	4230	2 of 3	2 of 2	0 of 2	0 of 2
ST006	1	0.67	-	0.86	25000	7250	884	1230	3 of 3	2 of 2	0 of 2	1 of 2
ST414	1	2.06	4.45	14.6	10300	2190	320	243	3 of 3	2 of 2	1 of 2	1 of 2
ST420	1	4	40	712	25000	304	97	136	3 of 3	2 of 2	2 of 2	2 of 2
SM146	1	0.46	-	0.88	25000	40000	1240	973	3 of 3	2 of 2	0 of 2	1 of 2

Table B.9: qPCR detection of HIV DNA for CD3+CD4+ T cell populations sorted based on CD32 expression directly from PBMCs. The number of cell equivalents of DNA in each reaction was calculated by albumin qPCR. For each individual and cell population the table shows a) the fold enrichment of HIV DNA relative to CD32- population b) the input number of cell equivalents of DNA (calculated by albumin qPCR) for the HIV qPCR reaction in each well is shown and c) the number of wells that were positive. Where the level of HIV DNA was not detectable, fold enrichment could not be calculated and is shown as - .

Variable	**Time measured**	**Hazard ratio (95% confidence interval)**	**p-value**
Percentage of CD4 T cells which are $CD32^{low}$	48 weeks (treatment interruption)	1.0 (0.91 – 1.2)	0.53
Percentage of CD4 T cells which are $CD32^{high}$	48 weeks (treatment interruption)	6 x 10-19 (7 x 10-72 -5.2 x 10^{34})	0.50
CD4 T cell count (100 cells/µL)	Baseline	0.90 (0.64 – 1.3)	0.56
Viral load (log10[copies/mL])	Baseline	1.7 (0.99 - 2.9)	0.053
Total HIV DNA ($\log_{10}$[copies/10^6 CD4 T cells])	48 weeks (treatment interruption)	1.2 (0.29 – 4.8)	0.82

Table B.10: Univariable Cox proportional hazard models of variables listed and time to viral rebound >400 copies/mL. n=19 for all analyses. Hazard ratios correspond to a change of 100 cells/µL for CD4 T cell count or a log for viral load and total HIV DNA.

C

HIV-1 *gag* overlapping peptide sequences

OLP number	Sequence
1	MGARASILRGGKLDKWEK
2	RGGKLDKWEKIRLRPGGK
3	EKIRLRPGGKKHYMLKHL
4	GKKHYMLKHLVWASREL
5	KHLVWASRELERFAL
6	ASRELERFALNPGLL
7	ERFALNPGLLETSEGCK
8	GLLETSEGCKQIMKQL
9	EGCKQIMKQLQPALQTGT
10	QLQPALQTGTEELRSLY
11	TGTEELRSLYNTVATLY
12	SLYNTVATLYCVHAGIEV
13	LYCVHAGIEVRDTKEAL
14	IEVRDTKEALDKIEEEQNK
15	LDKIEEEQNKSQQKTQQA
16	NKSQQKTQQKAAADKGKV
17	KAAADKGKVSQNYPIV
18	GKVSQNYPIVQNLQGQMV
19	IVQNLQGQMVHQAISPR
20	QMVHQAISPRTLNAWVKV
21	PRTLNAWVKVIEEKAF
22	WVKVIEEKAFSPEVIPMF
23	AFSPEVIPMFTALSEGA
24	PMFTALSEGATPQDLNTM
25	GATPQDLNTMLNTVGGH
26	NTMLNTVGGHQAAMQMLK
27	GGHQAAMQMLKDTINEEA
28	LKDTINEEAAEWDRLHPV
29	AAEWDRLHPVHAGPIA
30	LHPVHAGPIAPGQMREPR
31	IAPGQMREPRGSDIA

OLP number	Sequence
32	MREPRGSDIAGTTSTL
33	SDIAGTTSTLQEQIAWM
34	STLQEQIAWMTSNPPVPV
35	WMTSNPPVPVGDIYKRWI
36	PVGDIYKRWIILGLNKIV
37	WIILGLNKIVRMYSPVSI
38	IVRMYSPVSILDIKQGPK
39	SILDIKQGPKEPFRDYV
40	GPKEPFRDYVDRFFKTLR
41	YVDRFFKTLRAEQATQDV
42	LRAEQATQDVKNWMTDTL
43	DVKNWMTDTLLVQNA
44	MTDTLLVQNANPDCKTIL
45	NANPDCKTILRALGPGA
46	TILRALGPGASLEEMMTA
47	GASLEEMMTACQGVGGPSH
48	ACQGVGGPSHKARVLAEA
49	SHKARVLAEAMSQANSA
50	AEAMSQANSAIMMQR
51	QANSAIMMQRSNFKGPKR
52	QRSNFKGPKRIVKCF
53	KGPKRIVKCFNCGKEGHI
54	CFNCGKEGHIARNCRAPR
55	HIARNCRAPRKKGCWK
56	RAPRKKGCWKCGKEGHQM
57	WKCGKEGHQMKDCTERQA
58	QMKDCTERQANFLGKIW
59	RQANFLGKIWPSHKGR
60	GKIWPSHKGRPGNFLQSR
61	GRPGNFLQSRPEPTA
62	FLQSRPEPTAPPAESFRF
63	TAPPAESFRFEETTPAPK
64	RFEETTPAPKQEPKDREPL
65	PKQEPKDREPLTSLK
66	KDREPLTSLKSLFGSDPLSQ

Table C.1: Sequences of overlapping peptides (OLPs) in *gag* used for CD8 ELISpot assays in subtype C infected patients.

OLP number	Sequence
1	MGARASVLSGGELDR
2	ASVLSGGELDRWEKI
3	SGGELDRWEKIRLRP
4	LDRWEKIRLRPGGKK
5	EKIRLRPGGKKKYKL
6	LRPGGKKKYKLKHIV
7	GKKKYKLKHIVWASR
8	YKLKHIVWASRELER
9	HIVWASRELERFAVN
10	ASRELERFAVNPGLL
11	LERFAVNPGLLETSE

OLP number	**Sequence**
12	AVNPGLLETSEGCRQ
13	GLLETSEGCRQILGQ
14	TSEGCRQILGQLQPS
15	CRQILGQLQPSLQTG
16	LGQLQPSLQTGSEEL
17	QPSLQTGSEELRSLY
18	QTGSEELRSLYNTVA
19	EELRSLYNTVATLYC
20	SLYNTVATLYCVHQR
21	TVATLYCVHQRIEVK
22	LYCVHQRIEVKDTKE
23	HQRIEVKDTKEALEK
24	EVKDTKEALEKIEEE
25	TKEALEKIEEEQNKS
26	LEKIEEEQNKSKKKA
27	EEEQNKSKKKAQQAA
28	NKSKKKAQQAAADTG
29	KKAQQAAADTGNSSQ
30	QAAADTGNSSQVSQN
31	DTGNSSQVSQNYPIV
32	SSQVSQNYPIVQNLQ
33	SQNYPIVQNLQGQMV
34	PIVQNLQGQMVHQAI
35	NLQGQMVHQAISPRT
36	QMVHQAISPRTLNAW
37	QAISPRTLNAWVKVV
38	PRTLNAWVKVVEEKA
39	NAWVKVVEEKAFSPE
40	KVVEEKAFSPEVIPM
41	EKAFSPEVIPMFSAL
42	SPEVIPMFSALSEGA
43	IPMFSALSEGATPQD
44	SALSEGATPQDLNTM
45	EGATPQDLNTMLNTV
46	PQDLNTMLNTVGGHQ
47	NTMLNTVGGHQAAMQ
48	NTVGGHQAAMQMLKE
49	GHQAAMQMLKETINE
50	AMQMLKETINEEAAE
51	LKETINEEAAEWDRL
52	INEEAAEWDRLHPVH
53	AAEWDRLHPVHAGPI
54	DRLHPVHAGPIAPGQ
55	PVHAGPIAPGQMREP
56	GPIAPGQMREPRGSD
57	PGQMREPRGSDIAGT
58	REPRGSDIAGTTSTL
59	GSDIAGTTSTLQEQI
60	AGTTSTLQEQIGWMT
61	STLQEQIGWMTNNPP
62	EQIGWMTNNPPIPVG
63	WMTNNPPIPVGEIYK
64	NPPIPVGEIYKRWII

OLP number	Sequence
65	PVGEIYKRWIILGLN
66	IYKRWIILGLNKIVR
67	WIILGLNKIVRMYSP
68	GLNKIVRMYSPTSIL
69	IVRMYSPTSILDIRQ
70	YSPTSILDIRQGPKE
71	SILDIRQGPKEPFRD
72	IRQGPKEPFRDYVDR
73	PKEPFRDYVDRFYKT
74	FRDYVDRFYKTLRAE
75	VDRFYKTLRAEQASQ
76	YKTLRAEQASQEVKN
77	RAEQASQEVKNWMTE
78	ASQEVKNWMTETLLV
79	VKNWMTETLLVQNAN
80	MTETLLVQNANPDCK
81	LLVQNANPDCKTILK
82	NANPDCKTILKALGP
83	DCKTILKALGPAATL
84	ILKALGPAATLEEMM
85	LGPAATLEEMMTACQ
86	ATLEEMMTACQGVGG
87	EMMTACQGVGGPGHK
88	ACQGVGGPGHKARVL
89	VGGPGHKARVLAEAM
90	GHKARVLAEAMSQVT
91	RVLAEAMSQVTNSAT
92	EAMSQVTNSATIMMQ
93	QVTNSATIMMQRGNF
94	SATIMMQRGNFRNQR
95	MMQRGNFRNQRKTVK
96	GNFRNQRKTVKCFNC
97	NQRKTVKCFNCGKEG
98	TVKCFNCGKEGHIAK
99	FNCGKEGHIAKNCRA
100	KEGHIAKNCRAPRKK
101	IAKNCRAPRKKGCWK
102	CRAPRKKGCWKCGKE
103	RKKGCWKCGKEGHQM
104	CWKCGKEGHQMKDCT
105	GKEGHQMKDCTERQA
106	HQMKDCTERQANFLG
107	DCTERQANFLGKIWP
108	RQANFLGKIWPSHKG
109	FLGKIWPSHKGRPGN
110	IWPSHKGRPGNFLQS
111	HKGRPGNFLQSRPEP
112	PGNFLQSRPEPTAPP
113	LQSRPEPTAPPEESF
114	PEPTAPPEESFRFGE
115	APPEESFRFGEETTT
116	ESFRFGEETTTPSQK
117	FGEETTTPSQKQEPI

OLP number	**Sequence**
118	TTTPSQKQEPIDKEL
119	SQKQEPIDKELYPLA
120	EPIDKELYPLASLRS
121	KELYPLASLRSLFGN
122	PLASLRSLFGNDPSS
123	LRSLFGNDPSSQ

Table C.2: Sequences of overlapping peptides (OLPs) in *gag* used for CD8 ELISpot assays in subtype B infected patients.

D
Publications

Publications which were directly reproduced in part in this thesis are shown here in published form. These have been reproduced with permission of the copyright holder or are avilable under an appropriate creative commons license (CC BY).

Chapter 2

Martin GE, Gossez M, Williams JP *et. al*, Post-treatment control or treated controllers? Viral remission in treated and untreated primary HIV infection. *AIDS*, **31**, pp. 477–484 (2017) - Page 268

Martin GE & Frater J Post-treatment and spontaneous HIV control. *Current Opinions in HIV/AIDS*, **13**(5), pp. 402-407 (2018)) - Page 277

Chapter 3

Hoffmann M*, Pantazis N*, Martin GE*, *et. al*, Exhaustion of Activated CD8 T cells Predicts Disease Progression in Primary HIV-1 Infection. *PLoS Pathogens*, **2**(7), e1005661 (2016). - Page 283

Chapter 5

Martin GE*, Pace M*, Thornhill JP* *et. al*, CD32 expressing CD4 T cells are phenotypically diverse and can contain proviral HIV DNA. *Frontiers in Immunology*, **8**(928) (2018). - Page 302

*indicates co-first authorship

The following publications were produced during my time as a DPhil student but do not appear in this thesis. These have been reproduced with permission of the copyright holder or are avilable under an appropriate creative commons license (CC BY).

Martin GE, Alcami J, Spano JP & Ross AL. Converging roads: the latest science from the 2017 IAS HIV Cure and Cancer Forum. *Journal of Virus Eradication*, **3** e1-e6 (2017). - Page 315

Martin GE, Pace M & Frater J Hidden menace: the key to curing HIV lies in eradicating the reservoir of viruses residing in quiescent immune cells. *The Scientist*, **29** 34-39 (2015). - Page 321

OPEN

CONCISE COMMUNICATION

Post-treatment control or treated controllers? Viral remission in treated and untreated primary HIV infection

Genevieve E. Martin[a], Morgane Gossez[a], James P. Williams[a], Wolfgang Stöhr[b], Jodi Meyerowitz[a], Ellen M. Leitman[c,d], Philip Goulder[c,e], Kholoud Porter[f], Sarah Fidler[g], John Frater[a,h,i], the SPARTAC Trial Investigators

See related paper on page 587

Objective(s): An HIV cure will impose aviraemia that is sustained following the withdrawal of antiretroviral therapy (ART). Understanding the efficacy of novel interventions aimed at curing HIV requires characterization of both natural viral control and the effect of ART on viral control after treatment interruption.

Design: Analysis of transient viral control in recent seroconverters in the Short Pulse AntiRetroviral Therapy at Acute Seroconversion trial.

Methods: We compared untreated and treated HIV seroconverters ($n = 292$) and identified periods of control (plasma HIV RNA < 400 copies/ml for ≥ 16 weeks off therapy) in 7.9% of ART-naive participants, and in 12.0% overall. HIV DNA was measured by qPCR, and HIV-specific $CD8^+$ responses were measured by enzyme-linked immunosorbent spot assay (ELISpot). T-cell activation and exhaustion were measured by flow cytometry.

Results: At baseline, future controllers had lower HIV DNA, lower plasma HIV RNA, higher $CD4^+ : CD8^+$ ratios (all $P < 0.001$) and higher $CD4^+$ cell counts ($P < 0.05$) than noncontrollers. Among controllers, the only difference between the untreated and those who received ART was higher baseline HIV RNA in the latter ($P = 0.003$), supporting an added ART effect.

Conclusion: Consideration of spontaneous remission in untreated individuals will be critical to avoid overestimating the effect size of new interventions used in HIV cure studies.
Copyright © 2017 Wolters Kluwer Health, Inc. All rights reserved.

AIDS 2017, **31**:477–484

Keywords: antiretroviral therapy, ELISpot, HIV, HIV DNA, natural history, post-treatment control, T lymphocytes

[a]Nuffield Department of Medicine, Peter Medawar Building for Pathogen Research, University of Oxford, Oxford, [b]MRC Clinical Trials Unit at University College London, London, [c]Department of Paediatrics, University of Oxford, Oxford, UK, [d]Harvard Medical School, Boston, Massachusetts, USA, [e]HIV Pathogenesis Programme, Doris Duke Medical Research Institute, University of KwaZulu-Natal, Durban, South Africa, [f]Research Department of Infection and Population Health, University College London, [g]Division of Medicine, Wright Fleming Institute, Imperial College, London, [h]The Oxford Martin School, and [i]Oxford National Institute of Health Research Biomedical Research Centre, Oxford, UK.

Correspondence to John Frater, Peter Medawar Building for Pathogen Research, Nuffield Department of Medicine, University of Oxford, Oxford OX1 3SY, UK.

E-mail: john.frater@ndm.ox.ac.uk
Received: 23 September 2016; revised: 9 November 2016; accepted: 30 November 2016.

DOI:10.1097/QAD.0000000000001382

ISSN 0269-9370 Copyright © 2017 The Author(s). Published by Wolters Kluwer Health, Inc. This is an open access article distributed under the Creative Commons Attribution License 4.0 (CCBY), which permits unrestricted use, distribution, and reproduction in any medium, provided the original work is properly cited.

Copyright © 2017 Wolters Kluwer Health, Inc. All rights reserved.

478 AIDS 2017, Vol 31 No 4

Introduction

Strategies to achieve an HIV cure by implementing interventions to deplete the HIV reservoir – a pool of latently infected cells containing transcriptionally repressed viral DNA – are entering clinical trials. In the absence of a validated biomarker to prove cure, a key outcome measure in these studies is the time to detection of viral RNA, or 'viral rebound', in plasma after stopping antiretroviral therapy (ART) in an analytic treatment interruption [1–5].

Patients with primary HIV infection (PHI) are of particular interest, as with lower reservoir sizes [6–9] and preserved immunity [6,10–13] with less immune escape [14–16], there may be increased prospect of achieving remission. ART alone, when initiated during PHI, may induce remission, as described for post-treatment controllers (PTCs) in the VISCONTI cohort [17]. However, to understand the impact of ART – or any other intervention – on remission requires characterization of the time from seroconversion to a detectable HIV plasma viral load in untreated patients. Treatment of PHI is now recommended in revised international clinical guidelines [18,19] meaning that randomized trials with a 'no treatment' arm cannot be undertaken. As such, we must turn to high-quality historical data to assist interpretation of treatment interruption studies.

The 'Short Pulse AntiRetroviral Therapy at Acute Seroconversion' (SPARTAC) trial [20,21] was a randomized controlled trial of 0, 12 or 48 weeks of ART initiated during PHI. The study design provided the unusual opportunity to compare viral load dynamics in treated and untreated seroconverters. We turned to SPARTAC to understand whether reports of PTC and virological remission following treatment interruption might be conflated by natural transient delays to detectable viraemia in untreated seroconverters.

Methods

Participants and trial design

SPARTAC (EudraCT number: 2004-000446-20) was a multicentre randomized controlled trial of short-course ART (12 or 48 weeks ART, vs no immediate ART) initiated during PHI [20]. For all analyses, baseline refers to the date of randomization. Of 366 participants, 74 were excluded for logistical reasons, leaving 292 participants who were included in this analysis. Participants were assessed according to whether they received 12 or less vs more than 12 weeks ART, compared with no immediate ART. This same 12 week cut-off was used in a previous 'as received' analysis of SPARTAC [22].

Within this 'at risk' group, we identified controllers who experienced a period of remission which was defined for all as HIV RNA less than 400 copies/ml, on two measurements at least 16 weeks apart, with the period of remission starting within 1 year of randomization or ART cessation (untreated and treated groups, respectively). We included participants who experienced a viral blip of any magnitude at a single time point. Time of viral rebound was the first of at least two consecutive measurements more than 400 copies/ml.

HIV DNA quantification

Total HIV DNA was quantified at baseline (where there were sufficient samples available; $n = 200$) by a previously described qPCR assay [21,23].

$CD8^+$ T-cell ELISpot assays

HIV Gag-specific $CD8^+$ T-cell responses were measured by IFN-γ ELISpot assays to overlapping peptides using methods described elsewhere [24,25].

Flow cytometry

The expression of exhaustion (PD-1, Tim-3 and Lag-3) and activation [CD25, CD38, CD69 and human leucocyte antigen (HLA) DR] markers on $CD4^+$ and $CD8^+$ T cells was measured on cryopreserved samples (refer to Supplemental Digital Content 1 for antibodies used, http://links.lww.com/QAD/B35). Data were acquired on a MacsQuant Analyser (Miltenyi, Bergisch Gladbach, Germany) and analysed using FlowJo Version 10.0.7 or 10.8.0r1 (Treestar, Ashland, Oregon, USA).

Statistical analyses

Categorical variables were compared using χ^2 or Fisher–Freeman–Halton exact test as appropriate. Continuous variables were compared across three groups using the Kruskal–Wallis test or analysis of variance (ANOVA). Pairwise comparisons were made using Mann–Whitney or Student's t test. Duration of viral control was assessed using Kaplan–Meier estimates. For all tests, P values less than 0.05 were considered statistically significant. Analyses were performed using R version 3.2.2. Plots were drawn using GraphPad Prism (GraphPad Software, La Jolla, California, USA) version 6.0f.

Results and Discussion

Transient control of viraemia is evident in untreated primary HIV infection

Most studies of virological control have focused on 'elite' and PTCs [17,26,27]. We set out to explore a different question – are there individuals who experience transient viral control during untreated PHI, and how does this compare with post-ART remission?

Our analysis included 292 of 366 participants recruited to the SPARTAC trial who had sufficient HIV RNA sampling and, if treated, were virologically suppressed prior to treatment interruption. Time on ART is analysed

Copyright © 2017 Wolters Kluwer Health, Inc. All rights reserved.

'as received' rather than according to randomization arm and stratified as 0, 12 or less or more than 12 weeks of ART. Throughout this analysis, HIV RNA measurements less than 400 copies/ml are considered 'suppressed' as this was the lower limit of detection for assays conducted at South African and Ugandan trial sites. As such, this was the lowest HIV RNA threshold that could be applied across all samples.

Considering these participants, regardless of ART use, 35 of 292 (12.0%) experienced a period of suppressed viraemia (HIV RNA < 400 copies/ml) of at least 16 weeks while off therapy and are termed 'controllers' for this report. Of the 126 participants who did not receive immediate ART, 10 (7.9%) experienced a period of spontaneous viral control within 1 year of randomization. Among individuals who received short-course ART ($n = 80 \leq 12$ weeks; $n = 86 > 12$ weeks) and underwent treatment interruption, 25 (15.1%) experienced viral remission in the subsequent year.

PTCs have been almost exclusively identified among individuals who initiated ART during PHI, suggesting an impact of early ART on long-term viral control [17]. We found some evidence of greater frequency of control in individuals who had received more than 12 weeks ART, when compared across all three groups, although this was not statistically significant ($P = 0.06$; Table 1). In the best characterized cohort of PTCs to date (VISCONTI), patients received a median of 3 years ART prior to treatment interruption [17]. Twelve weeks of ART is likely to be too short to induce durable PTC, and it is possible that the participants who received 12 weeks or less ART in this analysis were more similar to untreated controllers than those who received more than 12 weeks ART (as also indicated by the primary outcome analysis of SPARTAC, which was based on clinical progression [20]). Accordingly, we performed all comparisons across the three groups rather than combining the two ART arms. Of note, if the 12 week or less group was excluded from the analysis of control, there were significantly more controllers following ART compared with no treatment (18.6% vs 7.9%; $P = 0.03$). In our previous analysis of viral rebound in only the treated participants in SPARTAC, longer treatment duration was significantly associated with slower viral rebound within 12 weeks of stopping ART consistent with these findings [22].

A strength of this analysis is the ability to quantify viral remission among treated and untreated individuals with PHI in a well characterized and frequently sampled randomized study. Several studies of ART initiated during PHI have demonstrated the presence of individuals who transiently control viral replication post-treatment interruption [30–35]. None of these previous studies included an untreated arm, thus limiting their ability to evaluate the added impact of ART on the presence of transient viral control. An analysis of the Quest study (in which participants underwent treatment interruption following at least 72 weeks ART initiated during PHI) [32] used data from untreated individuals from a separate PHI cohort (CASCADE) as controls. That analysis showed no significant difference in the frequency of transient viral control between the two studies [36], although a different HIV RNA cut-off (1000 copies/ml) and duration of analysis were used.

Duration of remission in treated and untreated controllers

We next looked to see whether the duration of viral control varied between controllers who did or did not receive ART. There were more participants with over 1 year of remission among those receiving more than 12 weeks ART compared with 12 weeks or less or no ART [13 (15.1% of all participants) vs 3 (3.8%) vs 8 (6.3%), respectively (Table 1)]. Eight controllers (five of whom had received >12 weeks ART) experienced undetectable HIV RNA until the end of follow-up [median 192 weeks (interquartile range 165–202)]. There was, however, no statistically significant difference between the duration of remission between the three groups when including the full duration of follow-up ($P = 0.22$; log rank). Interestingly, when just considering the controllers, untreated participants were more likely to experience sustained control more than 104 weeks (7/10) compared with the treated controllers for whom rebound was more evenly distributed over the assessment period, and which may have implications for the underlying mechanisms.

Controllers have more favourable baseline clinical characteristics than noncontrollers

In comparison with the noncontrollers (regardless of treatment group), future controllers had more favourable baseline clinical characteristics with higher $CD4^+$ T-cell counts (median 700 vs 557 cells/μl), lower plasma HIV RNA (median 2.70 vs 4.59 $\log_{10}$ copies/ml), higher $CD4^+$-to-$CD8^+$ ratio (median 0.77 vs 0.52) and lower total HIV DNA [mean 3.35 vs 3.85 $\log_{10}$ copies/10^6 $CD4^+$ T cells (Fig. 1a–d; Table, Supplemental Digital Content 2 contains values, http://links.lww.com/QAD/B35)]. These findings are consistent with previous studies of viral control during PHI with [30,33,34,37] and without [38,39] treatment.

Spontaneous controllers have lower baseline HIV RNA than those who received more than 12 weeks antiretroviral therapy

When focusing on just the controllers, untreated participants had similar baseline $CD4^+$ cell counts, $CD4^+$: $CD8^+$ ratios and HIV DNA levels to those who controlled following treatment interruption, but had significantly lower baseline HIV RNA than those who had received more than 12 weeks ART [median 2.30 vs 3.82 $\log_{10}$ copies/ml, respectively ($P = 0.002$; Fig. 1b; Table, Supplemental Digital Content 2, http://links.lww.com/QAD/B35)]. The interval between

Copyright © 2017 Wolters Kluwer Health, Inc. All rights reserved.

Table 1. Characteristics of controllers identified in Short Pulse AntiRetroviral Therapy at Acute Seroconversion.

	Total, $n=292$	≤12 weeks ART, $n=80$	>12 weeks ART, $n=86$	No ART, $n=126$	*P* value
No. of controllers (% total participants)	35 (12.0)	9 (11.3)	16 (18.6)	10 (7.9)	0.06
Duration of short course ART [weeks; median (IQR)]	–	11.9 (11.8–12.0)	47.8 (47.3–47.9)	–	–
Interval between estimated serconversion and randomization [days; median (IQR)]	–	92.0 (64.0–106)	97.5 (58.0–125)	95.5 (76.8–116)	0.64
Viral subtype					0.16
B	13	2	6	5	
C	18	5	10	3	
Other (A1, B/C, B/F and D)	4	2	0	2	
Country[a]					0.38
South Africa/Uganda	20	6	10	4	
United Kingdom	11	3	3	5	
Other (Australia/Brazil)	4	0	3	1	
Sex					1
Male	13	3	6	4	
Female	22	6	10	6	
Age [years; median (IQR)]	–	40 (25–47.5)	27.5 (21.3–46.5)	32 (26–35.5)	0.33
HLA alleles [b]					
≥1 protective class I allele	11	1	7	3	0.54
≥1 disease-susceptible class I allele	11	5	5	1	0.08
B*35:01 allele	2	0	2	0	–
Duration of remission (weeks)					–
<26	1	0	0	1	
26–52	10	6	3	1	
52–104	8	0	7	1	
>104	16	3	6	7	
No. without viral rebound at end of follow-up	8 (2.7)	1 (1.3)	5 (5.8)	2 (1.6)	–

Statistical tests were performed across all three groups. Categorical variables, including number of controllers, were compared using χ^2 test or Fisher–Freeman–Halton exact test as appropriate; continuous variables were compared using Kruskal–Wallis test. IQR, interquartile range. Duration of remission was calculated between date of randomization (untreated arm) or ART cessation (treated arms) and viral rebound. ART, antiretroviral therapy. Protective class I alleles were defined as B*27:05, B*57:01 for subtype B and B*57:02, B*57:03, B*81:01, B*58:01 for subtype C. Disease-susceptible class I alleles were defined as B*35:01, B*07:02 for subtype B and B*58:02, B*18:01 for subtype C [24,28,29].
[a]No controllers were identified from Ireland, Spain or Italy.
[b]Analysis performed for participants with subtype B or C virus only.

seroconversion and baseline was similar between treatment groups and did not explain this finding (Table 1). This difference in baseline HIV RNA supports an additional impact of ART in inducing viral remission in some individuals who otherwise may not control viral replication, providing evidence for post-treatment control as a distinct phenomenon.

Similar demographics and immunological characteristics in antiretroviral therapy–receiving and spontaneous controllers.

Next, we compared the demographic and immunological characteristics of untreated and treated controllers ($n=35$). We found no evidence for demographic differences between untreated and treated controllers in terms of sex, viral subtype, country of origin and age (Table 1). Because $CD8^+$ T-cell responses are associated with clinical progression [40] and drive durable spontaneous (or 'elite') control, we looked for the presence of protective HLA Class I alleles amongst controllers identified in this study. The proportion of controllers with protective or disease-susceptible HLA Class I alleles was similar between treatment groups. Two controllers carried HLA B*35 alleles, which has been observed amongst PTCs in the VISCONTI case series [17]. As a measure of $CD8^+$ recognition of HIV, we measured $CD8^+$ T-cell responses to HIV peptides by Gamma Interferon ELISpot. We assessed responses across HIV Gag, which did not differ between treated and untreated controllers and were similar in breadth (Fig. 1e) and magnitude (Fig. 1f) to those measured in noncontrollers. The percentage of $CD4^+$ and $CD8^+$ T cells expressing markers of exhaustion (PD-1, Tim-3 and Lag-3) and activation (HLA-DR, CD69, CD25 and CD38) at baseline also did not differ between treatment groups (data not shown).

Conclusion

There are two key findings to this analysis. One is the demonstration of long periods of transient viral remission

Copyright © 2017 Wolters Kluwer Health, Inc. All rights reserved.

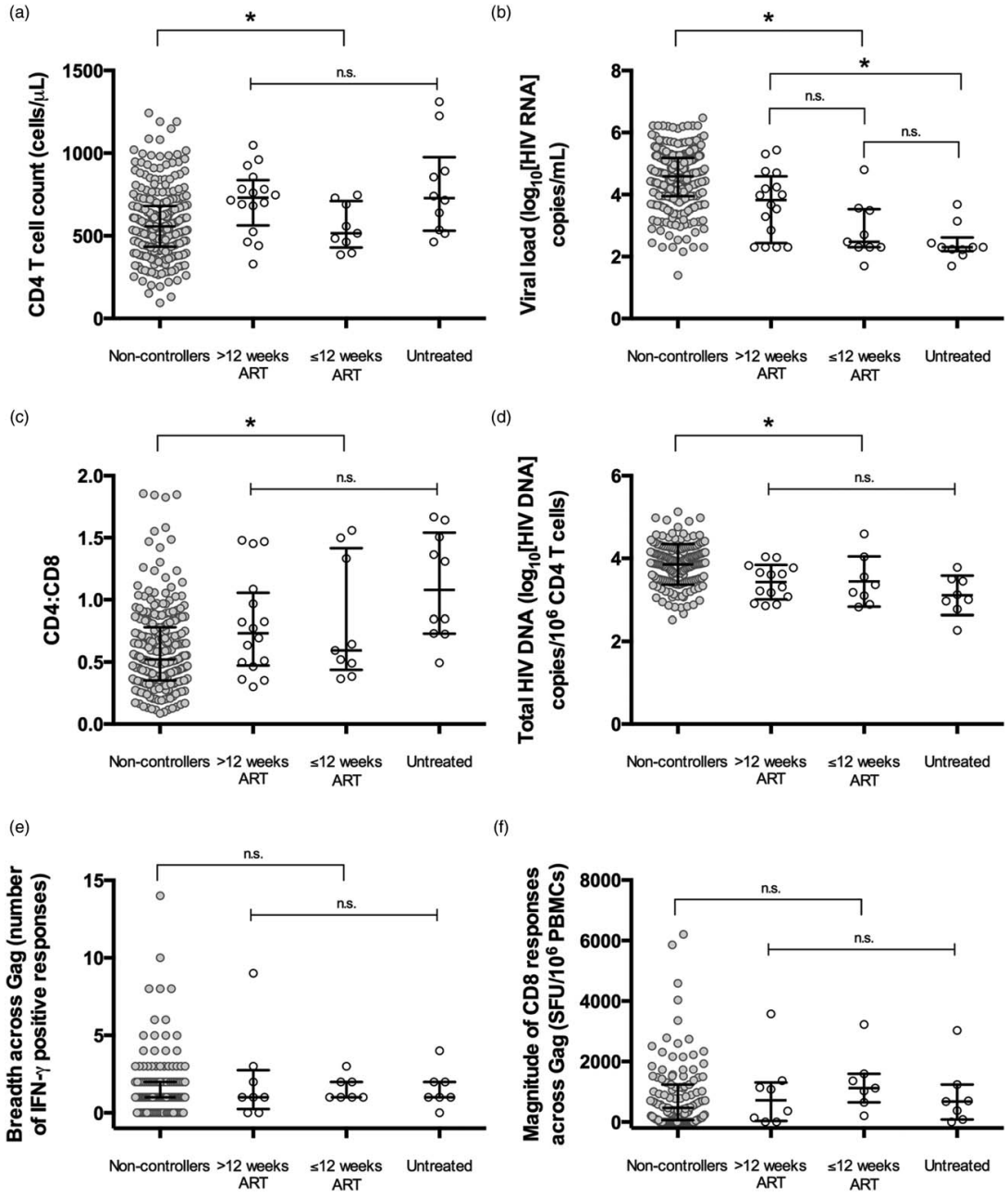


Fig. 1. Clinical characteristics of controllers identified in Short Pulse AntiRetroviral Therapy at Acute Seroconversion. Baseline clinical variables of controllers (three groups shown with open circles) and noncontrollers (green, shaded circles) identified in Short Pulse AntiRetroviral Therapy at Acute Seroconversion. Bars shown indicate the mean (SD) for total HIV DNA (d) and median (interquartile range) for all other parameters (a–c, e, f). $CD4^+$ cell count (a), viral load (b), $CD4^+$ to $CD8^+$ ratio [(C) all total $n = 292$], as well as breadth (e) and magnitude [(F) both total $n = 145$] of $CD8^+$ responses across Gag were compared between noncontrollers and combined controller groups using the Mann–Whitney test. Total HIV DNA [(d) total $n = 200$] was compared between these two groups using Student's t test. Comparisons between three controller groups were made using Kruskal–Wallis (a–c, e, f) and ANOVA (d) tests. For viral load, this was significantly different ($P = 0.006$), and pairwise comparisons shown (b) were made between groups using the Mann–Whitney test. $^*P < 0.05$.

Copyright © 2017 Wolters Kluwer Health, Inc. All rights reserved.

in a substantial proportion of untreated individuals after PHI, which may conflate data from those who transiently control after ART interruption. The second finding confirms previous reports of beneficial baseline characteristics associated with future virological control and supports an additional impact of ART during PHI.

Following the results of the START trial, which provided evidence of clear clinical benefit in starting ART irrespective of $CD4^+$ cell count [41], untreated controls cannot be included in future HIV trial protocols. The use of uncontrolled treatment interruption studies to measure the success of potentially curative strategies means that modest delays in viral rebound may be attributed to an intervention. Accordingly, consideration of spontaneous remission in PHI will be critical to avoid overestimating the effect size of interventions used in treatment interruption studies.

Acknowledgements

We thank the participants of SPARTAC. The SPARTAC Trial Investigators: Trial Steering Committee: Independent Members – A. Breckenridge (Chair), P. Clayden, C. Conlon, F. Conradie, J. Kaldor*, F. Maggiolo, F. Ssali, Country Principal Investigators – D.A. Cooper, P. Kaleebu, G. Ramjee, M. Schechter, G. Tambussi, J.M. Miro, J. Weber. Trial Physician: S. Fidler. Trial Statistician: A. Babiker. Data and Safety Monitoring Committee (DSMC): T. Peto (Chair), A. McLaren (in memoriam), V. Beral, G. Chene, J. Hakim. Co-ordinating Trial Centre: Medical Research Council Clinical Trials Unit, London (A. Babiker, K. Porter, M. Thomason, F. Ewings, M. Gabriel, D. Johnson, K. Thompson, A. Cursley*, K. Donegan*, E. Fossey*, P. Kelleher*, K. Lee*, B. Murphy*, D. Nock*). Central Immunology Laboratories and Repositories: The Peter Medawar Building for Pathogen Research, University of Oxford, UK (R. Phillips, J. Frater, L. Ohm Laursen*, N. Robinson, P. Goulder, H. Brown). Central Virology Laboratories and Repositories: Jefferiss Trust Laboratories, Imperial College, London, UK (M. McClure, D. Bonsall*, O. Erlwein*, A. Helander*, S. Kaye, M. Robinson, L. Cook*, G. Adcock*, P. Ahmed*). Clinical Endpoint Review Committee: N. Paton, S. Fidler. Investigators and Staff at Participating Sites: Australia: St Vincents Hospital, Sydney (A. Kelleher), Northside Clinic, Melbourne (R. Moore), East Sydney Doctors, Sydney (R. McFarlane), Prahran Market Clinic, Melbourne (N. Roth), Taylor Square Private Clinic, Sydney (R. Finlayson), The Centre Clinic, Melbourne (B. Kiem Tee), Sexual Health Centre, Melbourne (T. Read), AIDS Medical Unit, Brisbane (M. Kelly), Burwood Rd Practice, Sydney (N. Doong), Holdsworth House Medical Practice, Sydney (M. Bloch), Aids Research Initiative, Sydney (C. Workman). Coordinating Centre in Australia: Kirby Institute University of New South Wales, Sydney (P. Grey, D.A. Cooper, A. Kelleher, M. Law). Brazil: Projeto Praca Onze, Hospital Escola Sao Francisco de Assis, Universidade federal do Rio de Janeiro, Rio de Janeiro (M. Schechter, P. Gama, M. Mercon*, M. Barbosa de Souza, C. Beppu Yoshida, J.R. Grangeiro da Silva, A. Sampaio Amaral, D. Fernandes de Aguiar, M. de Fatima Melo, R. Quaresma Garrido). Italy: Ospedale San Raffaele, Milan (G. Tambussi, S. Nozza, M. Pogliaghi, S. Chiappetta, L. Della Torre, E. Gasparotto), Ospedale Lazzaro Spallanzani, Roma (G. DOffizi, C. Vlassi, A. Corpolongo). South Africa: Cape Town: Desmond Tutu HIV-1 Centre, Institute of Infectious Diseases, Cape Town (R. Wood, J. Pitt, C. Orrell, F. Cilliers, R. Croxford, K. Middelkoop, L.G. Bekker, C. Heiberg, J. Aploon, N. Killa, E. Fielder, T. Buhler). Johannesburg: The Wits Reproductive Health and HIV-1 Institute, University of Witswatersrand, Hillbrow Health Precinct, Johannesburg (H. Rees, F. Venter, T. Palanee), Contract Laboratory Services, Johannesburg Hospital, Johannesburg (W. Stevens, C. Ingram, M. Majam, M. Papathanasopoulos). Kwazulu-Natal: HIV-1 Prevention Unit, Medical Research Council, Durban (G. Ramjee, S. Gappoo, J. Moodley, A. Premrajh, L. Zako). Uganda: Medical Research Council/Uganda Virus Research Institute, Entebbe (H. Grosskurth, A. Kamali, P. Kaleebu, U. Bahemuka, J. Mugisha*, H.F. Njaj*). Spain: Hospital Clinic-IDIBAPS, University of Barcelona, Barcelona (J.M. Miro, M. Lopez-Dieguez*, C. Manzardo, J. Ambrosioni, D. Nicolas, J.A. Arnaiz, T. Pumarola, M. Plana, M. Tuset, M.C. Ligero, M.T. Garca, T. Gallart, J.M. Gatell). UK and Ireland: Royal Sussex County Hospital, Brighton (M. Fisher, K. Hobbs, N. Perry, D. Pao, D. Maitland, L. Heald), St James's Hospital, Dublin (F. Mulcahy, G. Courtney, S. O'Dea, D. Reidy), Regional Infectious Diseases Unit, Western General Hospital and Genitourinary Dept, Royal Infirmary of Edinburgh, Edinburgh (C. Leen, G. Scott, L. Ellis, S. Morris, P. Simmonds), Chelsea and Westminster Hospital, London (B. Gazzard, D. Hawkins, C. Higgs), Homerton Hospital, London (J. Anderson, S. Mguni), Mortimer Market Centre, London (I. Williams, N. De Esteban, P. Pellegrino, A. Arenas-Pinto, D. Cornforth*, J. Turner*), North Middlesex Hospital (J. Ainsworth, A. Waters), Royal Free Hospital, London (M. Johnson, S. Kinloch, A. Carroll, P. Byrne, Z. Cuthbertson), Barts & the London NHS Trust, London (C. Orkin, J. Hand, C. De Souza), St Marys Hospital, London (J. Weber, S. Fidler, E. Hamlyn, E. Thomson*, J. Fox*, K. Legg, S. Mullaney*, A. Winston, S. Wilson, P. Ambrose), Birmingham Heartlands Hospital, Birmingham (S. Taylor, G. Gilleran). Imperial College Trial Secretariat: S. Keeling, A. Becker. Imperial College DSMC Secretariat: C. Boocock. (* Left the study team before the trial ended.).

The SPARTAC Trial was funded by The Wellcome Trust (grant no. 069598/Z/02/Z), J.F. is funded by the Medical Research Council, G.M. is funded by the Nuffield Department of Medicine, the Clarendon Fund and the General Sir John Monash Foundation.

Copyright © 2017 Wolters Kluwer Health, Inc. All rights reserved.

Author contributions: Conceived and designed the experiments – G.M., W.S., K.P., S.F., J.F. Performed the experiments – G.M., M.G., J.W., J.M., E.L. Analysed the data – G.M., W.S., K.P., J.F. Contributed reagents/materials/analysis tools: P.G. Wrote the article: G.M., W.S., K.P., S.F., J.F.

Conflicts of interest

There are no conflicts of interest.

References

1. Tebas P, Stein D, Tang WW, Frank I, Wang SQ, Lee G, *et al.* **Gene editing of CCR5 in autologous CD4 T cells of persons infected with HIV.** *N Engl J Med* 2014; **370**:901–910.
2. Rasmussen TA, Tolstrup M, Brinkmann CR, Olesen R, Erikstrup C, Solomon A, *et al.* **Panobinostat, a histone deacetylase inhibitor, for latent-virus reactivation in HIV-infected patients on suppressive antiretroviral therapy: a phase 1/2, single group, clinical trial.** *Lancet HIV* 2014; **1**:e13–e21.
3. Sagot-Lerolle N, Lamine A, Chaix ML, Boufassa F, Aboulker JP, Costagliola D, *et al.* **Prolonged valproic acid treatment does not reduce the size of latent HIV reservoir.** *AIDS* 2008; **22**:1125–1129.
4. Bar KJ, Harrison LJ, Overton ET, Bardsley M, Messer M, Capparelli E, *et al.* ACTG 5340: The effect of VRC01 on viral kinetics after analytic treatment interruption. In: *Conference on Retroviruses and Opportunistic Infections (CROI)*. Boston; 2016.
5. Scheid JF, Horwitz JA, Bar-On Y, Kreider EF, Lu CL, Lorenzi JC, *et al.* **HIV-1 antibody 3BNC117 suppresses viral rebound in humans during treatment interruption.** *Nature* 2016; **535**:556–560.
6. Jain V, Hartogensis W, Bacchetti P, Hunt PW, Hatano H, Sinclair E, *et al.* **Antiretroviral therapy initiated within 6 months of HIV infection is associated with lower T-cell activation and smaller HIV reservoir size.** *J Infect Dis* 2013; **208**:1202–1211.
7. Buzon MJ, Martin-Gayo E, Pereyra F, Ouyang Z, Sun H, Li JZ, *et al.* **Long-term antiretroviral treatment initiated at primary HIV-1 infection affects the size, composition, and decay kinetics of the reservoir of HIV-1-infected CD4 T cells.** *J Virol* 2014; **88**:10056–10065.
8. Hocqueloux L, Avettand-Fenoel V, Jacquot S, Prazuck T, Legac E, Melard A, *et al.* **Long-term antiretroviral therapy initiated during primary HIV-1 infection is key to achieving both low HIV reservoirs and normal T cell counts.** *J Antimicrob Chemother* 2013; **68**:1169–1178.
9. Hey-Cunningham WJ, Murray JM, Natarajan V, Amin J, Moore CL, Emery S, *et al.* **Early antiretroviral therapy with raltegravir generates sustained reductions in HIV reservoirs but not lower T-cell activation levels.** *AIDS* 2015; **29**:911–919.
10. Oxenius A, Price DA, Easterbrook PJ, O'Callaghan CA, Kelleher AD, Whelan JA, *et al.* **Early highly active antiretroviral therapy for acute HIV-1 infection preserves immune function of CD8+ and CD4+ T lymphocytes.** *Proc Natl Acad Sci U S A* 2000; **97**:3382–3387.
11. Okulicz JF, Le TD, Agan BK, Camargo JF, Landrum ML, Wright E, *et al.* **Influence of the timing of antiretroviral therapy on the potential for normalization of immune status in human immunodeficiency virus 1-infected individuals.** *JAMA Intern Med* 2015; **175**:88–99.
12. Malhotra U, Berrey MM, Huang Y, Markee J, Brown DJ, Ap S, *et al.* **Effect of combination antiretroviral therapy on T-cell immunity in acute human immunodeficiency virus type 1 infection.** *J Infect Dis* 2000; **181**:121–131.
13. Le T, Wright EJ, Smith DM, He W, Catano G, Okulicz JF, *et al.* **Enhanced CD4+ T-cell recovery with earlier HIV-1 antiretroviral therapy.** *N Engl J Med* 2013; **368**:218–230.
14. Zimbwa P, Milicic A, Frater J, Scriba TJ, Willis A, Goulder PJ, *et al.* **Precise identification of a human immunodeficiency virus type 1 antigen processing mutant.** *J Virol* 2007; **81**:2031–2038.
15. Frater AJ, Edwards CT, McCarthy N, Fox J, Brown H, Milicic A, *et al.* **Passive sexual transmission of human immunodeficiency virus type 1 variants and adaptation in new hosts.** *J Virol* 2006; **80**:7226–7234.
16. Deng K, Pertea M, Rongvaux A, Wang L, Durand CM, Ghiaur G, *et al.* **Broad CTL response is required to clear latent HIV-1 due to dominance of escape mutations.** *Nature* 2015; **517**:381–385.
17. Saez-Cirion A, Bacchus C, Hocqueloux L, Avettand-Fenoel V, Girault I, Lecuroux C, *et al.* **Posttreatment HIV-1 controllers with a long-term virological remission after the interruption of early initiated antiretroviral therapy ANRS VISCONTI Study.** *PLoS Pathog* 2013; **9**:e1003211.
18. World Health Organisation. *Consolidated guidelines on the use of antiretroviral drugs for treating and preventing HIV infection: recommendations for a public health approach*. 2nd ed. Geneva: World Health Organisation; 2016.
19. Gunthard HF, Saag MS, Benson CA, del Rio C, Eron JJ, Gallant JE, *et al.* **Antiretroviral drugs for treatment and prevention of HIV infection in adults: 2016 recommendations of the International Antiviral Society-USA Panel.** *JAMA* 2016; **316**:191–210.
20. Fidler S, Porter K, Ewings F, Frater J, Ramjee G, Cooper D, *et al.*, SPARTAC Trial Investigators. **Short-course antiretroviral therapy in primary HIV infection.** *N Engl J Med* 2013; **368**:207–217.
21. Williams JP, Hurst J, Stohr W, Robinson N, Brown H, Fisher M, *et al.* **HIV-1 DNA predicts disease progression and posttreatment virological control.** *eLife* 2014; **3**:e03821.
22. Stohr W, Fidler S, McClure M, Weber J, Cooper D, Ramjee G, *et al.* **Duration of HIV-1 viral suppression on cessation of antiretroviral therapy in primary infection correlates with time on therapy.** *PLoS One* 2013; **8**:e78287.
23. Jones M, Williams J, Gartner K, Phillips R, Hurst J, Frater J. **Low copy target detection by Droplet Digital PCR through application of a novel open access bioinformatic pipeline, 'definetherain'.** *J Virol Methods* 2014; **202**:46–53.
24. Kiepiela P, Leslie AJ, Honeyborne I, Ramduth D, Thobakgale C, Chetty S, *et al.* **Dominant influence of HLA-B in mediating the potential co-evolution of HIV and HLA.** *Nature* 2004; **432**:769–775.
25. Frater J, Ewings F, Hurst J, Brown H, Robinson N, Fidler S, *et al.* **HIV-1-specific CD4(+) responses in primary HIV-1 infection predict disease progression.** *AIDS* 2014; **28**:699–708.
26. Okulicz JF, Lambotte O. **Epidemiology and clinical characteristics of elite controllers.** *Curr Opin HIV AIDS* 2011; **6**:163–168.
27. Migueles SA, Connors M. **Long-term nonprogressive disease among untreated HIV-infected individuals: clinical implications of understanding immune control of HIV.** *JAMA* 2010; **304**:194–201.
28. Pereyra F, Jia X, McLaren PJ, Telenti A, de Bakker PI, Walker BD, *et al.* **The major genetic determinants of HIV-1 control affect HLA class I peptide presentation.** *Science* 2010; **330**:1551–1557.
29. Goulder PJ, Walker BD. **HIV and HLA class I: an evolving relationship.** *Immunity* 2012; **37**:426–440.
30. Volberding P, Demeter L, Bosch RJ, Aga E, Pettinelli C, Hirsch M, *et al.* **Antiretroviral therapy in acute and recent HIV infection: a prospective multicenter stratified trial of intentionally interrupted treatment.** *AIDS* 2009; **23**:1987–1995.
31. Rosenberg ES, Altfeld M, Poon SH, Phillips MN, Wilkes BM, Eldridge RL, *et al.* **Immune control of HIV-1 after early treatment of acute infection.** *Nature* 2000; **407**:523–526.
32. Kinloch-de Loes S, Hoen B, Smith DE, Autran B, Lampe FC, Phillips AN, *et al.* **Impact of therapeutic immunization on HIV-1 viremia after discontinuation of antiretroviral therapy initiated during acute infection.** *J Infect Dis* 2005; **192**:607–617.
33. Kaufmann DE, Lichterfeld M, Altfeld M, Addo MM, Johnston MN, Lee PK, *et al.* **Limited durability of viral control following treated acute HIV infection.** *PLoS Med* 2004; **1**:e36.
34. Goujard C, Girault I, Rouzioux C, Lecuroux C, Deveau C, Chaix ML, *et al.* **HIV-1 control after transient antiretroviral treatment initiated in primary infection: role of patient characteristics and effect of therapy.** *Antivir Ther* 2012; **17**:1001–1009.
35. Lodi S, Meyer L, Kelleher AD, Rosinska M, Ghosn J, Sannes M, *et al.* **Immunovirologic control 24 months after interruption of antiretroviral therapy initiated close to HIV seroconversion.** *Arch Intern Med* 2012; **172**:1252–1255.
36. Lampe FC, Porter K, Kaldor J, Law M, Kinloch-de Loes S, Phillips AN, *et al.* **Effect of transient antiretroviral treatment during acute HIV infection: comparison of the Quest trial results with CASCADE natural history study.** *Antivir Ther* 2007; **12**:189–193.

Copyright © 2017 Wolters Kluwer Health, Inc. All rights reserved.

37. Bloch MT, Smith DE, Quan D, Kaldor JM, Zaunders JJ, Petoumenos K, *et al*. **The role of hydroxyurea in enhancing the virologic control achieved through structured treatment interruption in primary HIV infection: final results from a randomized clinical trial (pulse).** *J Acquir Immune Defic Syndr* 2006; **42**: 192–202.
38. Madec Y, Boufassa F, Rouzioux C, Delfraissy JF, Meyer L, Group SS. **Undetectable viremia without antiretroviral therapy in patients with HIV seroconversion: an uncommon phenomenon?** *Clin Infect Dis* 2005; **40**:1350–1354.
39. Madec Y, Boufassa F, Porter K, Meyer L, Collaboration C. **Spontaneous control of viral load and CD4 cell count progression among HIV-1 seroconverters.** *AIDS* 2005; **19**:2001–2007.
40. Payne R, Muenchhoff M, Mann J, Roberts HE, Matthews P, Adland E, *et al*. **Impact of HLA-driven HIV adaptation on virulence in populations of high HIV seroprevalence.** *Proc Natl Acad Sci U S A* 2014; **111**:E5393–5400.
41. Lundgren JD, Babiker AG, Gordin F, Emery S, Grund B, Sharma S, *et al*., Insight Start Study Group. **Initiation of antiretroviral therapy in early asymptomatic HIV infection.** *N Engl J Med* 2015; **373**:795–807.

Copyright © 2017 Wolters Kluwer Health, Inc. All rights reserved.

REVIEW

Post-treatment and spontaneous HIV control

Genevieve E. Martin[a] and John Frater[a,b]

Purpose of review
The aim of the current review is to explore the evidence around virological remission in ART-treated and untreated individuals living with HIV. With increasing evidence and interest in post-treatment control within the HIV-cure field, it is now increasingly important to agree on definitions to allow different 'controller' phenotypes to be clearly distinguished and mechanisms compared.

Recent findings
This review explores recent data on potential predictors and mechanisms driving spontaneous and post-treatment control. We explore data on the role of the reservoir as a determinant of control and the challenges associated with its study, including the safety of treatment interruption. We explore options around deriving a consensus on how to define different forms of control and the longer term utility of achieving remission.

Summary
Post-treatment control and remission following treatment interruption are becoming increasingly common measures of intervention efficacy in cure trials. As well as a need to show treatment interruption protocols are well tolerated and acceptable, for these measures to be robust and comparable between studies, clear and consensual definitions need to be agreed.

Keywords
post-treatment control, treatment interruption, viral remission

INTRODUCTION

Recent years have seen reports of individuals living with HIV who are able to control viral replication after stopping antiretroviral therapy (ART). Whereas spontaneous 'elite controllers' who maintain undetectable viraemia have been recognized from early in the HIV epidemic, such ART-induced control is a relatively new and unexpected phenotype. Described as 'post-treatment control' (PTC), it appears to be more frequent than spontaneous control in untreated individuals, and is particularly associated with ART initiation during primary HIV infection (PHI). Of particular interest in the development of HIV cure strategies, understanding the mechanisms driving PTC may inform interventions to induce long-term virological remission. This review will focus on the current evidence for virological control in the absence of ART, and explore recent findings on the underlying mechanisms.

POST-TREATMENT CONTROL IS DISTINCT FROM SPONTANEOUS VIRAL CONTROL

Studies of extreme phenotypes of HIV control have improved our understanding of HIV pathogenesis. Reports of HIV control prior to ART, here termed 'spontaneous control,' have included both control of viral replication (e.g. elite controllers) or an absence of CD4 count decline (e.g. long-term non-progressors; LTNPs). Here we focus our discussion on control of viral replication as this phenotype bears more similarity to PTC, and will allow us to highlight the parallels, and differences, between these two phenomena. Such sustained spontaneous control of viral replication is rare – occurring in less than 1% of infected individuals [1] – and has been associated with strong anti-HIV immunity (reviewed in [2,3]). This is evidenced particularly by associations with certain class I HLA alleles (such as B∗57 and B∗27), strong HIV-specific CD8 T-cell responses and is supported by GWAS studies linking control to the HLA class I locus in chromosome 6 [4].

[a]Nuffield Department of Medicine, Peter Medawar Building for Pathogen Research and [b]Oxford National Institute of Health Research Biomedical Research Centre, Oxford, UK

Correspondence to John Frater, FRCP, PhD, Nuffield Department of Medicine, Peter Medawar Building for Pathogen Research, Oxford, UK. E-mail: john.frater@ndm.ox.ac.uk

Curr Opin HIV AIDS 2018, 13:000–000
DOI:10.1097/COH.0000000000000488

1746-630X Copyright © 2018 Wolters Kluwer Health, Inc. All rights reserved.

Copyright © 2018 Wolters Kluwer Health, Inc. Unauthorized reproduction of this article is prohibited.

KEY POINTS

- Consistency is needed in the terminology and definitions used to describe post-treatment virological control.
- Following treatment interruption, some individuals treated during primary HIV infection experience a viral load peak before viral control – mirroring the dynamic in untreated early HIV infection.
- Low HIV reservoir size is associated with viral control following treatment interruption – but other host factors also play a critical role.
- Further work is needed to establish the safety of post-treatment control, and of treatment interruptions that permit viral rebound to high levels.

There is significant evidence that PTC is mechanistically distinct from spontaneous control. Although PTC is still rare amongst individuals who undergo treatment interruption, the estimated frequency appears to be substantially higher than that of spontaneous control [5–8]. Furthermore, PTC appears to be more frequent among individuals who initiate ART during primary HIV infection (PHI) [5–9], and who have a longer duration of therapy prior to treatment interruption [5,10]. PTCs have also been reported to have a small viral reservoir [6,8,9]. Together, this suggests a role for ART in inducing a control phenotype in some individuals who would otherwise have not been able to control viral replication. Importantly, the strong HIV-specific CD8 T-cell responses observed in elite controllers have not been seen in descriptions of PTC [6,8] – suggesting that the underlying mechanisms are not related to classical HLA Class I-mediated cytotoxic T-cell (CTL) control. Although the small numbers of PTC cohorts and case studies limit the power of analyses to identify associations with HLA class I, PTCs do not appear to be more likely than the broader population to possess protective alleles such as B*57 and B*27 [6,8,11]. In one of the earliest characterized PTC cohorts, VISCONTI, controllers were reported to have over-representation of HLA B*35, which is associated with rapid HIV progression [6], although this has not been consistently observed in other cohorts [11,12▪].

DEFINING AND MEASURING POST-TREATMENT CONTROL

As the number of reports of potential PTC increase, the need for a consistently applied definition becomes critical. Studies to identify post-treatment controllers have differed in the thresholds used to define an undetectable viral load, the duration of ART prior to interruption, whether or not viral blips are acceptable, and the duration of control [7,8,10,11,13–15]. This has parallels with the study of spontaneous viral control, where significant heterogeneity has been identified in both the terminology and clinical parameters used to identify controllers [16], which have been shown to lead to substantial variation in the estimated frequency of elite control [17]. As the duration of viral control following treatment interruption is now recognized to be a spectrum, it is likely that terminology and definitional differences will have similar effects on the measurement of PTC, highlighting the necessity of a consensus definition.

Ideally the definition of PTC would be mechanistic, particularly as these mechanisms may be distinct from spontaneous control. However, as data in this area are still lacking, definitions will need to focus on a clear phenotype. One option would be that the term PTC be reserved for the extreme of this type of viral control – that is, longstanding, sustained viral suppression (e.g. >5 years) to below the limit of detection of current best assays (e.g. 20 copies/ml). Such a definition would allow for more robust mechanistic studies. For those not fulfilling this extreme phenotype, we suggest the use of the term 'virological remission' to describe shorter periods of control, the duration of which should also be clearly described alongside the data. Whilst remission that persists could subsequently be re-termed PTC, the concept of remission also has utility as, drawing upon its meaning in the context of malignancy, it reflects the risk of viral rebound [18].

A key question that remains unanswered is whether transient remission is a step towards durable PTC, or merely a delay in viral rebound, consistent with normal inter-individual variation. Many HIV-cure studies use delayed time to viral rebound as a gold standard of efficacy [19▪▪,20–22]. This approach assumes that remission is a step towards PTC – and that progressive prolongation of the duration of remission will result in a PTC phenotype. There is, however, currently insufficient evidence that remission and durable PTC are mediated via the same processes.

In one of the best-characterized cohorts of PTC, VISCONTI, the estimated frequency of sustained control was 15% [6,23]. Other studies of early treated infection have estimated the frequency of individuals who controlled viral replication for more than 24 months following treatment interruption to be lower, ranging from 0 to 10% [5,7,8,10,11,15]. Figure 1 summarizes these studies (and others that have reported shorter periods of

Copyright © 2018 Wolters Kluwer Health, Inc. Unauthorized reproduction of this article is prohibited.

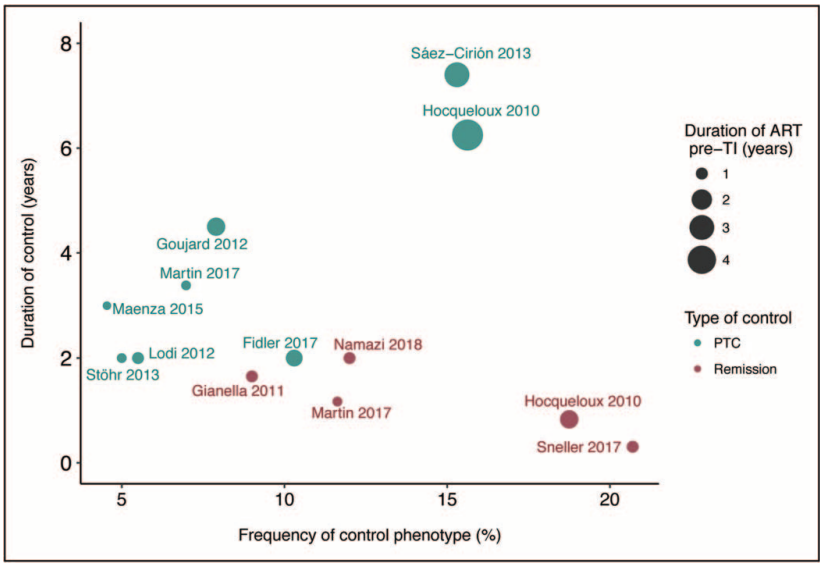


FIGURE 1. Estimates of the frequency of post-treatment control and remission. Each data point represents an individual study, which has measured the frequency of post-treatment control or remission following treatment interruption among individuals who commenced ART during PHI. Included are analyses of the following studies: CASCADE [7,10], ANRS Primo [8], VISCONTI [6,23], SPARTAC [5,12▪], CHAMP [13], ZHPI [24], SeaPIP [11] and NCT01859325 [19▪▪]. Those which define post-treatment control (here considered to be >24 months following treatment interruption) are coloured green, those defining remission (>4 months following treatment interruption) are shown in red. In some cases, a study explored both phenotypes; where possible these are disaggregated and listed twice, otherwise these are shown as remission. The duration of control is the time between treatment interruption and viral rebound, or the end of follow-up, and is plotted at the median value amongst controllers. The size of the point corresponds to the median duration of ART prior to treatment interruption amongst controllers. Where a study did not report either of these values, the minimum value for inclusion is used instead.

remission), and indicates an inverse correlation between frequency and duration of viral control. This suggests that definitions used to define control may have a large impact on reported frequency. There are several potential explanations for the variation in these estimates, including differences in the timing of ART initiation, the duration of ART prior to treatment interruption and the denominator used to calculate the frequency. Of note, individuals in the VISCONTI cohort ([6,23] in Fig. 1) had a relatively longer period of viral suppression prior to treatment interruption, which could in part explain why the frequency of PTC observed here is so much higher than other studies [5–8,11,15,23,24]. The frequency of PTC when ART is commenced during PHI has been reported to be higher than that observed following treatment interruption when ART is commenced during chronic infection [9], although there have been few studies that directly compare this. A recent report of PTC following treated chronic infection (for at least 6 months) estimated a frequency of 4% [25], within the range of that observed for PHI.

CHALLENGES IN STUDYING POST-TREATMENT CONTROL

Identifying PTC and viral remission presents a number of challenges. Firstly, some individuals who control viral replication following treatment interruption may have controlled spontaneously had treatment not been started, and it remains difficult to distinguish these 'treated controllers' from PTCs. This will have increasing relevance in the era of 'test and treat,' as spontaneous controllers may not be identified prior to ART initiation.

A further challenge is that the natural history of infection for some individuals includes a period of transient virological remission. An analysis of the SPARTAC trial looked at rates of remission (defined as viral load <400 copies/ml for at least 16 weeks) in individuals randomized to receive 12 or 48 weeks of ART, or no immediate therapy [12▪]. In the untreated arm of this trial, 7.9% of individuals had a period of remission after seroconversion, a frequency not dissimilar to that reported in some studies of ART-induced control. Therefore, studies using 'time to rebound after treatment interruption'

Copyright © 2018 Wolters Kluwer Health, Inc. Unauthorized reproduction of this article is prohibited.

as an outcome measure for an intervention may need to consider both the impact of ART alone as well as the potential for brief periods of spontaneous control in ART-naïve individuals.

As we start to look in more detail at viral rebound dynamics following treatment interruption, we can also observe that some individuals treated during PHI have a high initial viral rebound following treatment interruption followed by a period of remission or PTC. This was recently reported by Sneller *et al.* [19▪▪] in individuals who underwent a treatment interruption in a randomized trial of a therapeutic vaccine. This dynamic – which mirrors that of untreated primary infection – is of particular interest following a study in which SIV-infected rhesus macaques were treated with a monoclonal antibody against the integrin α4β7, followed by a treatment interruption [26▪▪]. During treatment interruption, animals in the therapy, but not placebo arm, exhibited durable sustained aviraemia but only after a high viral load peak [26▪▪]. It has since been suggested that treatment interruption protocols that restart ART as soon as plasma virus is detected may miss some individuals who, following a high initial viral load peak, would subsequently go on to control [13].

Any treatment interruption study that allow individuals to remain off ART despite viral rebound must first consider patient safety. There is little evidence on the duration of viraemia after treatment interruption that might be considered well tolerated, although it could be hypothesized that any period of durable viral replication may be harmful. Attempting to address these concerns, a recent analysis of 10 individuals undergoing treatment interruption as part of a VRC01 clinical trial explored the impact on virological and immunological parameters [27▪]. Following resumption of ART, the overall size and composition of the HIV reservoir returned to pretreatment interruption levels, and increases in T-cell activation were similarly transient. Of note, in this study, ART was resumed if viral load rebounded to more than 1000 copies/ml on two measurements at least 2 weeks apart [27▪]. Although reassuring, it remains to be seen if such findings would similarly apply if less stringent criteria for re-initiation of ART were used.

Finally, an additional challenge in studying PTC and remission is the limited applicability of historical control cohorts. Modern ART, with more potent drugs (particularly integrase inhibitors) will plausibly be associated with better tissue penetration, lower reservoirs and/or inflammation-associated immunological damage – potentially impacting rates of remission. There is little evidence of the impact of integrase inhibitor use on reservoir size, although one recent case series measured HIV DNA longitudinally in six individuals commencing tenofovir/emtricitabine/elvitegravir/cobicistat during PHI and showed a rapid decay in this parameter, consistent with more rapid declines in plasma viraemia [28]. It is also possible that contemporary cohorts will differ from historical cohorts in terms of viral rebound dynamics following treatment interruption. Directly demonstrating the importance of this, Sneller *et al.* [19▪▪] compared remission in the placebo arm of their vaccine study to viral remission rates reported in a recent romidepsin/vaccine clinical trial, which had interpreted their findings in the context of historical control groups [22]. They observed similar rates of remission between the two groups, even though when compared with historical controls, remission was more common following romidepsin/vaccine administration [19▪▪]. The inclusion of matched control groups is a key consideration study of viral remission following treatment interruption.

RESERVOIR SIZE, VIRAL BLIPS AND VIROLOGICAL CONTROL

A small HIV reservoir has been consistently linked to PTC. Initial evidence comes from case studies of individuals with very low HIV reservoirs either because of allogenic stem cell transplantation (alloSCT) [29,30] or extremely early ART initiation [31,32] who have experienced periods of PTC. Further evidence comes from the consistent observation that PTCs [6,8,9] and individuals with remission [12▪] have smaller HIV reservoir size (measured by HIV DNA) than noncontrollers. Reservoir size measured by HIV DNA has also shown to be predictive of time to viral rebound [33].

Several recent studies add to this body of evidence. Work presented by Sharaf *et al.* [34] confirms that individuals with virological remission post-treatment interruption have lower levels of total HIV DNA than noncontrollers. However, extending these findings, they show that the proportion of intact proviral sequences (i.e. those that could conceivably give rise to viral rebound) was similar between these two groups [34]. A large analysis of the CASCADE cohort aimed to identify factors associated with post-treatment interruption control in individuals treated during PHI [10]. They identified that a shorter interval between seroconversion and ART start, and a longer duration on ART, were both associated with viral control following treatment interruption [10]. Although reservoir size itself was not measured, these are both factors that could conceivably be acting by limiting initial reservoir size. Two further case studies describe individuals

Copyright © 2018 Wolters Kluwer Health, Inc. Unauthorized reproduction of this article is prohibited.

with extremely low/undetectable viral reservoir size, who following a period of viral remission experience eventual viral rebound [35▪,36▪]. One of these individuals had undergone alloSCT [36▪], and the other initiated ART at a very early stage following preexposure prophylaxis (PrEP) [35▪]. Viral rebound in these individuals occurred at 288 and 225 days, respectively, a time period remarkably similar to the duration of viral remission experienced by one of the Boston patients [30]. What is becoming clear, is that whilst low-reservoir size is a common feature of post-treatment interruption virological control, it is not on its own sufficient to confer this phenotype.

Atough the mechanisms driving PTC remain to be elucidated, studies of loss of spontaneous control can add to our understanding. A very large study of spontaneous controllers in the COHORE database explored factors that predicted loss of virological control [37]. They demonstrated that viral blips were predictive of subsequent loss of control [37], a factor that was also shown to predict loss of control following treatment interruption in CASCADE [10]. When compared with spontaneous controllers who experience viral blips, those who maintain consistently undetectable viral loads have been recently shown to have lower reservoir size and T-cell activation levels [38▪], suggesting that tighter control is associated with lower immune activation. This distinction between 'leaky' and strict virological control may also have utility in the study of PTC. It is possible in both models that immune activation may play a role in the loss of virological control. Demonstrating this in the context of spontaneous control, the COHERE study showed that increases in CD8 count and a decline in CD4 count preceded viral rebound [37].

IMMUNOLOGICAL DAMAGE DESPITE CONTROL OF VIRAL REPLICATION

Although viral replication has been the focus of the PTC phenotype, it is clear from the study of spontaneous control that deleterious effects can occur in the setting of virological suppression. Despite maintaining undetectable viral loads, elite controllers have been shown to have elevated levels of both T-cell activation and soluble inflammatory factors [39–42]. Furthermore, relative to uninfected controls, elite controllers have higher levels of inflammatory-related comorbidities including cardiovascular disease [41,42], suggesting persistent immunological damage despite control of viral replication. This has raised discussion about whether or not elite controllers should be treated with ART [43].

There have been studies of ART initiation in controller cohorts, which have shown reductions in immune activation. A small, pilot study showed that ART reduced low-level viral replication, which was associated with decreased T-cell activation [44]. Results of A5308, another prospective trial of treatment of HIV controllers were recently presented and supported these findings, showing reductions in activated CD8 T cells, as well as several immune checkpoint receptors (PD-1, TIGIT and CD160) in 28 treated spontaneous controllers [45].

If we are now in an era of treating elite control it raises the question – is PTC an appropriate goal for clinical research? If durable virological control without ART is not sufficient to prevent adverse outcomes, is PTC the best model for functional cure? There is currently insufficient evidence on inflammatory and clinical outcomes in long-term PTC, and these remain a research priority to determine if durable viral remission following treatment interruption is a well tolerated and ethical model for HIV cure.

CONCLUSION

Post-treatment control is potentially a very powerful model for understanding mechanisms for inducing and sustaining drug-free virological remission. To further understand this phenotype, detailed prospective mechanistic studies will be needed as well as consistency across the field in definitions and terminology. However, if proven to be a robust, well tolerated and inducible phenomenon the impact for the HIV cure field could be substantial.

Acknowledgements

J.F. is supported by the Medical Research Council (MR/L006588/1) and the National Institutes for Health Research Oxford Biomedical Research Centre.

Financial support and sponsorship

None.

Conflicts of interest

There are no conflicts of interest.

REFERENCES AND RECOMMENDED READING

Papers of particular interest, published within the annual period of review, have been highlighted as:
- ▪ of special interest
- ▪▪ of outstanding interest

1. Deeks SG, Walker BD. Human immunodeficiency virus controllers: mechanisms of durable virus control in the absence of antiretroviral therapy. Immunity 2007; 27:406–416.

Copyright © 2018 Wolters Kluwer Health, Inc. Unauthorized reproduction of this article is prohibited.

2. Walker BD, XG Yu. Unravelling the mechanisms of durable control of HIV-1. Nat Rev Immunol 2013; 13:487–498.
3. Goulder PJ, Watkins DI. Impact of MHC class I diversity on immune control of immunodeficiency virus replication. Nat Rev Immunol 2008; 8:619–630.
4. Fellay J, Shianna KV, Ge D, *et al.* A whole-genome association study of major determinants for host control of HIV-1. Science 2007; 317:944–947.
5. Stöhr W, Fidler S, McClure M, *et al.* Duration of HIV-1 viral suppression on cessation of antiretroviral therapy in primary infection correlates with time on therapy. PLoS One 2013; 8:e78287.
6. Sáez-Cirión A, Bacchus C, Hocqueloux L, *et al.* Post-treatment HIV-1 controllers with a long-term virological remission after the interruption of early initiated antiretroviral therapy ANRS VISCONTI Study. PLoS Pathog 2013; 9:e1003211.
7. Lodi S, Meyer L, Kelleher AD, *et al.* Immunovirologic control 24 months after interruption of antiretroviral therapy initiated close to HIV seroconversion. Arch Intern Med 2012; 172:1252–1255.
8. Goujard C, Girault I, Rouzioux C, *et al.,* ANRS CO6 PRIMO Study Group. HIV-1 control after transient antiretroviral treatment initiated in primary infection: role of patient characteristics and effect of therapy. Antivir Ther 2012; 17:1001–1009.
9. Assoumou L, Weiss L, Piketty C, *et al.,* ANRS 116 SALTO study group. A low HIV-DNA level in peripheral blood mononuclear cells at antiretroviral treatment interruption predicts a higher probability of maintaining viral control. AIDS 2015; 29:2003–2007.
10. Fidler S, Olson AD, Bucher HC, *et al.* Virological blips and predictors of post-treatment viral control after stopping ART started in Primary HIV Infection. J Acquir Immune Defic Syndr 2017; 74:126–133.
11. Maenza J, Tapia K, Holte S, *et al.* How often does treatment of primary HIV lead to post-treatment control? Antivir Ther 2015; 20:855–863.
12. ▪ Martin GE, Gossez M, Williams JP, *et al.,* SPARTAC Trial Investigators. Post-treatment control or treated controllers? Viral remission in treated and untreated primary HIV infection. AIDS 2017; 31:477–484.

This analysis within the SPARTAC trial quantified periods of viral remission during PHI and identified periods of remission, which resembled post-treatment remission, in individuals who did not receive immediate ART during PHI.

13. Namazi G, Fajnzylber JM, Aga E, *et al.* The CHAMP Cohort: Post-treatment controllers identified from 9 clinical studies [abstract number 231]. Presented at Conference on Retroviruses and Opportunistic Infections (CROI). 4–7 March, 2018, Boston.
14. Li JZ, Etemad B, Ahmed H, *et al.* The size of the expressed HIV reservoir predicts timing of viral rebound after treatment interruption. AIDS 2016; 30:343–353.
15. Gianella S, Anderson CM, Richman DD, *et al.* No evidence of post-treatment control after early initiation of antiretroviral therapy. AIDS 2015; 29: 2093–2097.
16. Gurdasani D, Iles L, Dillon DG, *et al.* A systematic review of definitions of extreme phenotypes of HIV control and progression. AIDS 2014; 28: 149–162.
17. Olson AD, Meyer L, Prins M, *et al.,* CASCADE Collaboration in EuroCoord. An evaluation of HIV elite controller definitions within a large seroconverter cohort collaboration. PLoS One 2014; 9:e86719.
18. Tucker JD, Volberding PA, Margolis DM, *et al.* Words matter: discussing research towards an HIV cure in research and clinical contexts. J Acquir Immune Defic Syndr 2014; 67:e110–e111.
19. ▪▪ Sneller MC, Justement JS, Gittens KR, *et al.* A randomized controlled safety/efficacy trial of therapeutic vaccination in HIV-infected individuals who initiated antiretroviral therapy early in infection. Sci Transl Med 2017; 9: pii: eaan8848.

This randomized control trial showed no efficacy of the intervention tested (therapeutic vaccine) in delaying time to viral rebound. Importantly, however, the authors describe similarities between the viral rebound dynamics in the placebo and interventional arm. The findings of this study highlight the importance of appropriately matched control groups in treatment interruption studies.

20. Bar KJ, Sneller MC, Harrison LJ, *et al.* Effect of HIV antibody VRC01 on viral rebound after treatment interruption. N Engl J Med 2016; 375:2037–2050.
21. Scheid JF, Horwitz JA, Bar-On Y, *et al.* HIV-1 antibody 3BNC117 suppresses viral rebound in humans during treatment interruption. Nature 2016; 535:556–560.
22. Mothe B, Moltó J, Manzardo C, *et al.* Viral control induced by HIVconsv vaccines & romidepsin in early treated individuals [abstract number 119LB]. Presented at Conference on Retroviruses and Opportunistic Infections (CROI). 13-16 February, 2017, Seattle.
23. Hocqueloux L, Prazuck T, Avettand-Fenoel V, *et al.* Long-term immunovirologic control following antiretroviral therapy interruption in patients treated at the time of primary HIV-1 infection. AIDS 2010; 24:1598–1601.
24. Gianella S, von Wyl V, Fischer M, *et al.,* Swiss HIV Cohort Study. Effect of early antiretroviral therapy during primary HIV-1 infection on cell-associated HIV-1 DNA and plasma HIV-1 RNA. Antivir Ther 2011; 16:535–545.
25. Perkins MJ, Bradley WP, Lalani T, *et al.* Brief report: prevalence of post-treatment controller phenotype is rare in HIV-infected persons after stopping antiretroviral therapy. J Acquir Immune Defic Syndr 2017; 75:364–369.
26. ▪▪ Byrareddy SN, Arthos J, Cicala C, *et al.* Sustained virologic control in SIV+ macaques after antiretroviral and alpha4beta7 antibody therapy. Science 2016; 354:197–202.

This interventional trial of a monoclonal antibody against the integrin $\alpha4\beta7$ in SIV-infected macaques showed a striking effect in inducing virological control in these animals. Interestingly, prior to controlling viral replication, many of these animals had a very high viral load peak.

27. ▪ Clarridge KE, Blazkova J, Einkauf K, *et al.* Effect of analytical treatment interruption and reinitiation of antiretroviral therapy on HIV reservoirs and immunologic parameters in infected individuals. PLoS Pathog 2018; 14:e1006792.

This study measured the size of the HIV reservoir and T-cell activation prior to and following treatment interruption performed as part of a clinical trial to test the efficacy of VRC01.

28. Ngo Bell EC, Vandenhende MA, Caldato S, *et al.* High decay of blood HIV reservoir when tenofovir/emtricitabine/elvitegravir/cobicistat is initiated during the acute primary HIV infection. J Antimicrob Chemother 2017; 72:2681–2683.
29. Hutter G, Nowak D, Mossner M, *et al.* Long-term control of HIV by CCR5 Delta32/Delta32 stem-cell transplantation. N Engl J Med 2009; 360:692–698.
30. Henrich TJ, Hanhauser E, Marty FM, *et al.* Antiretroviral-free HIV-1 remission and viral rebound after allogeneic stem cell transplantation: report of 2 cases. Ann Intern Med 2014; 161:319–327.
31. Persaud D, Gay H, Ziemniak C, *et al.* Absence of detectable HIV-1 viremia after treatment cessation in an infant. N Engl J Med 2013; 369: 1828–1835.
32. Frange P, Faye A, Avettand-Fenoel V, *et al.,* ANRS EPF-CO10 Pediatric Cohort and the ANRS EP47 VISCONTI study group. HIV-1 virological remission lasting more than 12 years after interruption of early antiretroviral therapy in a perinatally infected teenager enrolled in the French ANRS EPF-CO10 paediatric cohort: a case report. Lancet HIV 2016; 3:e49–e54.
33. Williams JP, Hurst J, Stohr W, *et al.,* SPARTAC Trial Investigators. HIV-1 DNA predicts disease progression and post-treatment virological control. Elife 2014; 3:e03821.
34. Sharaf R, Lee GQ, Sun X, *et al.* Proviral landscape in HIV-1 post-treatment controllers and noncontrollers [abstract number 364]. Presented at Conference on Retroviruses and Opportunistic Infections (CROI). 4–7 March, 2018, Boston.
35. ▪ Henrich TJ, Hatano H, Bacon O, *et al.* HIV-1 persistence following extremely early initiation of antiretroviral therapy (ART) during acute HIV-1 infection: an observational study. PLoS Med 2017; 14:e1002417.

This case report adds to the body of literature that extremely early initiation of ART is associated with subsequent post-treatment remission in some individuals.

36. ▪ Cummins NW, Rizza S, Litzow MR, *et al.* Extensive virologic and immunologic characterization in an HIV-infected individual following allogeneic stem cell transplant and analytic cessation of antiretroviral therapy: a case study. PLoS Med 2017; 14:e1002461.

This case report describes an individual with post-treatment remission following allogenic stem cell transplant.

37. Chereau F, Madec Y, Sabin C, *et al.,* HIV Controllers Project Working Group for the Collaboration of Observational HIV Epidemiological Research Europe (COHERE) in EuroCOORD. Impact of CD4 and CD8 dynamics and viral rebounds on loss of virological control in HIV controllers. PLoS One 2017; 12:e0173893.
38. ▪ Canoui E, Lecuroux C, Avettand-Fenoel V, *et al.,* ANRS CO21 CODEX Study Group. A subset of extreme human immunodeficiency virus (HIV) controllers is characterized by a small HIV blood reservoir and a weak T-cell activation level. Open Forum Infect Dis 2017; 4:ofx064.

This work identifies heterogeneity in spontaneous controller phenotype, in particular that stricter virological control (the absence of blips) was associated with lower T-cell activation and smaller HIV reservoir size.

39. Krishnan S, Wilson EM, Sheikh V, *et al.* Evidence for innate immune system activation in HIV type 1-infected elite controllers. J Infect Dis 2014; 209:931–939.
40. Hunt PW, Brenchley J, Sinclair E, *et al.* Relationship between T cell activation and CD4+ T cell count in HIV-seropositive individuals with undetectable plasma HIV RNA levels in the absence of therapy. J Infect Dis 2008; 197:126–133.
41. Pereyra F, Lo J, Triant VA, *et al.* Increased coronary atherosclerosis and immune activation in HIV-1 elite controllers. AIDS 2012; 26:2409–2412.
42. Hsue PY, Hunt PW, Schnell A, *et al.* Role of viral replication, antiretroviral therapy, and immunodeficiency in HIV-associated atherosclerosis. AIDS 2009; 23:1059–1067.
43. Crowell TA, Hatano H. Clinical outcomes and antiretroviral therapy in 'elite' controllers: a review of the literature. J Virus Erad 2015; 1:72–77.
44. Hatano H, Yukl SA, Ferre AL, *et al.* Prospective antiretroviral treatment of asymptomatic, HIV-1 infected controllers. PLoS Pathog 2013; 9:e1003691.
45. Li JZ, Segal FP, Bosch R, *et al.* ART reduces T cell activation and immune exhaustion markers in HIV controllers [abstract number 229]. Presented at Conference on Retroviruses and Opportunistic Infections (CROI), 4–7 March 2018, Boston.

Copyright © 2018 Wolters Kluwer Health, Inc. Unauthorized reproduction of this article is prohibited.

PLOS | PATHOGENS

RESEARCH ARTICLE

Exhaustion of Activated CD8 T Cells Predicts Disease Progression in Primary HIV-1 Infection

Matthias Hoffmann[1,2☯], Nikos Pantazis[3,4☯], Genevieve E. Martin[1☯], Stephen Hickling[1], Jacob Hurst[1,5], Jodi Meyerowitz[1], Christian B. Willberg[1,6], Nicola Robinson[1,6], Helen Brown[1,6], Martin Fisher[7†], Sabine Kinloch[8], Abdel Babiker[4], Jonathan Weber[9], Nneka Nwokolo[10], Julie Fox[11], Sarah Fidler[9‡], Rodney Phillips[1,5,6‡], John Frater[1,5,6‡*], SPARTAC and CHERUB Investigators[¶]

1 Peter Medawar Building for Pathogen Research, Nuffield Department of Medicine, Oxford, United Kingdom, **2** Division of Infectious Diseases and Hospital Epidemiology, Kantonsspital, St. Gallen, Switzerland, **3** Department of Hygiene, Epidemiology & Medical Statistics, Athens University Medical School, Athens, Greece, **4** MRC Clinical Trials Unit at UCL Institute of Clinical Trials & Methodology, London, United Kingdom, **5** The Oxford Martin School, Oxford, United Kingdom, **6** Oxford National Institute of Health Research Biomedical Research Centre, Oxford, United Kingdom, **7** Brighton and Sussex University Hospitals, Brighton, United Kingdom, **8** Division of Infection and Immunity, University College London, London, United Kingdom, **9** Division of Medicine, Wright Fleming Institute, Imperial College, London, United Kingdom, **10** Chelsea and Westminster Hospital, London, United Kingdom, **11** Department of Genitourinary Medicine and Infectious Disease, Guys and St Thomas' NHS Trust, London, United Kingdom

† Deceased.
☯ These authors contributed equally to this work.
‡ These authors also contributed equally to this work.
¶ Membership of the SPARTAC and CHERUB Investigators is provided in the Acknowledgments.
* john.frater@ndm.ox.ac.uk

CrossMark
click for updates

OPEN ACCESS

Citation: Hoffmann M, Pantazis N, Martin GE, Hickling S, Hurst J, Meyerowitz J, et al. (2016) Exhaustion of Activated CD8 T Cells Predicts Disease Progression in Primary HIV-1 Infection. PLoS Pathog 12(7): e1005661. doi:10.1371/journal.ppat.1005661

Editor: Ronald Swanstrom, University of North Carolina at Chapel Hill, UNITED STATES

Received: February 24, 2016

Accepted: May 5, 2016

Published: July 14, 2016

Copyright: © 2016 Hoffmann et al. This is an open access article distributed under the terms of the Creative Commons Attribution License, which permits unrestricted use, distribution, and reproduction in any medium, provided the original author and source are credited.

Data Availability Statement: Data are from the SPARTAC and HEATHER studies from which unrestricted release of data for public deposition would breach compliance with the protocol approved by the research ethics board. For SPARTAC, all trial data is maintained by the MRC Clinical Trials Unit, London, UK and can be accessed by contacting: m.gabriel@ucl.ac.uk. For HEATHER the contact is k.topping@imperial.ac.uk.

Funding: The study was funded by: Medical Research Council (JFr) (MR/L006588/1), Swiss National Science Foundation (MH) (PBBSB 116880),

Abstract

The rate at which HIV-1 infected individuals progress to AIDS is highly variable and impacted by T cell immunity. CD8 T cell inhibitory molecules are up-regulated in HIV-1 infection and associate with immune dysfunction. We evaluated participants (n = 122) recruited to the SPARTAC randomised clinical trial to determine whether CD8 T cell exhaustion markers PD-1, Lag-3 and Tim-3 were associated with immune activation and disease progression. Expression of PD-1, Tim-3, Lag-3 and CD38 on CD8 T cells from the closest pre-therapy time-point to seroconversion was measured by flow cytometry, and correlated with surrogate markers of HIV-1 disease (HIV-1 plasma viral load (pVL) and CD4 T cell count) and the trial endpoint (time to CD4 count <350 cells/μl or initiation of antiretroviral therapy). To explore the functional significance of these markers, co-expression of Eomes, T-bet and CD39 was assessed. Expression of PD-1 on CD8 and CD38 CD8 T cells correlated with pVL and CD4 count at baseline, and predicted time to the trial endpoint. Lag-3 expression was associated with pVL but not CD4 count. For all exhaustion markers, expression of CD38 on CD8 T cells increased the strength of associations. In Cox models, progression to the trial endpoint was most marked for PD-1/CD38 co-expressing cells, with evidence for a stronger effect within 12 weeks from confirmed diagnosis of PHI. The effect of PD-1 and Lag-3 expression on CD8 T cells retained statistical significance in Cox

PLOS | PATHOGENS

and Wellcome Trust (JW, RP, SF) (069598/Z/02/Z). The funders had no role in study design, data collection and analysis, decision to publish, or preparation of the manuscript.

Competing Interests: We were unable to contact Stephen Hickling, listed as an author of this paper, to confirm his involvement in the latest version. The corresponding author, John Frater, has therefore supplied the information regarding his contribution to the manuscript and his competing interests and it is correct to the best of his knowledge. The authors are not aware of any other potential conflict of interest associated with this manuscript.

proportional hazards models including antiretroviral therapy and CD4 count, but not pVL as co-variants. Expression of 'exhaustion' or 'immune checkpoint' markers in early HIV-1 infection is associated with clinical progression and is impacted by immune activation and the duration of infection. New markers to identify exhausted T cells and novel interventions to reverse exhaustion may inform the development of novel immunotherapeutic approaches.

Author Summary

After being infected with HIV, the pace of disease progression is highly variable between individuals. Some stay well with functioning immune systems for many years, whilst others progress to AIDS quickly. Understanding the factors that underpin these differences is important and may relate to factors such as viral adaptation and immune exhaustion. Recently, there has been interest in certain molecules—called 'exhaustion' or 'immune checkpoint' markers—which reflect how well the immune system functions. Recent trials show that therapies directed against these molecules can improve anti-cancer immunity. It is known from laboratory experiments that these markers are abundant in HIV infection suggesting that the human immune response to HIV is not fully effective. The relevance of these markers in patient cohorts remains unclear. This study measures three exhaustion markers—PD-1, Tim-3, Lag-3 –in individuals with HIV recruited to a randomised controlled trial of therapy in early HIV infection called SPARTAC. We find a complex picture in which these markers alone, together and in combination with other markers that reflect T cell activation (CD38) help predict the speed of clinical progression and immune decline, with differing effects dependent on the duration of infection. We propose that therapies directed against these markers could impact disease progression, vaccine efficacy or even newer curative strategies.

Introduction

Following infection with Human Immunodeficiency Virus Type 1 (HIV-1) the rate at which an individual develops AIDS is highly variable ranging from 'progressors' who, if untreated, experience rapid CD4 T cell decline in months to years to 'elite controllers', who spontaneously maintain undetectable plasma viraemia, often for decades. The tempo of HIV-1-associated disease progression might rest with particular characteristics of HLA class I molecules and the CD8 T cell immune responses which they dictate [1–5]. When a CD8 T cell encounters its cognate antigen, the up-regulation of T cell inhibitory molecules tightly controls the subsequent T cell activation [6–8], and inhibits autoimmunity [9–11]. However, the persistence of antigen can overcome homeostatic controls and lead to permanent CD8 T cell dysfunction or exhaustion [12–16]. In HIV-1 infection T cell exhaustion is associated with the up-regulation of surface molecules called immune checkpoint receptors (ICRs) such as PD-1, Tim-3 and Lag-3 [12,17–20], which have also been associated with the size of the HIV reservoir and time to viral rebound after therapy cessation[21,22].

We sought to determine whether, in primary HIV-1 infection (PHI), these indicators of CD8 T cell exhaustion would correlate with surrogate markers of disease (e.g. HIV-1 plasma viral load (pVL), CD4 T cell count) and actual time to progression within a strictly defined patient population enrolled into a randomized clinical trial of early antiretroviral therapy (ART). In particular, we wanted to study exhaustion in activated CD38 CD8 positive T cell

populations, as CD38 expression has also been correlated with disease progression. We found significant associations between ICR expression and both pVL and disease progression, and an enhanced effect when co-expressed on activated T cells.

Results

Analysis of baseline characteristics of SPARTAC participants

366 participants were enrolled into the SPARTAC trial[23]. Of 156 participants recruited at UK sites, 122 had adequate numbers of peripheral blood mononuclear cells (PBMCs) available for analysis at the pre-therapy 'baseline'–the closest documented visit to the estimated date of seroconversion. Patient characteristics are detailed in Table 1. The median (interquartile range, IQR) age at enrolment was 34 (28, 41) years. Only five participants were female, and the predominant mode for HIV-1 acquisition was sex between men (MSM) (93%). Of the 122, 41 were randomised to receive no immediate ART (SOC), 44 12 weeks ART (ART12) and 37 48 weeks ART (ART48). The median (IQR) time since the estimated date of seroconversion at randomisation was 77 (54, 98) days. The median (IQR) times for participants in 'early' ($\leq$12 weeks after seroconversion) and 'late' (>12 weeks after seroconversion) were 60 (42, 72) and 104 (93, 122) days, respectively. MSM were significantly over-represented in the early PHI group. The median (IQR) baseline CD4 T cell count and HIV-1 pVL were 550 (435, 675) cells/μl and 4.70 (4.0, 5.3) $\log_{10}$ RNA copies/ml, respectively, without significant differences in participants enrolled $\leq$ or > 12 weeks into PHI.

CD8 T cell exhaustion correlates with HIV-1 plasma viral load and CD4 T cell count

The expression of PD-1, Tim-3 and Lag-3 on the surface of CD8 T cells and the subset of activated CD8 T cells that co-expressed CD38 was determined by flow cytometry (Fig A in S1 Text) and was up-regulated in PHI compared with healthy controls ($P<0.01$ for all comparisons; Mann-Whitney)(Fig B in S1 Text). Expression of CD38 on CD8 T cells correlated with PD-1 expression (Spearman's rho 0.37; $p<0.001$) (Fig 1a) but not with Tim-3 or Lag-3 (Fig 1b and 1c). Table 2 shows the percentage of CD8 T cells expressing each of the three exhaustion

Table 1. Demographic and clinical characteristics of UK participants in the SPARTAC trial included in the analyses.

	Time from seroconversion to baseline measurement		Overall	
	≤12 weeks (n = 72; 59%)	>12 weeks (n = 50; 41%)	(N = 122; 100%)	P value
Sex				0.16
Male	71 (99)	46 (92)	117 (96)	
Female	1 (1)	4 (8)	5 (4)	
Risk Group				0.008
MSM	70 (97)	43 (86)	113 (93)	
Heterosexual	1 (1)	7 (14)	8 (7)	
Unknown	1 (1)	0 (0)	1 (1)	
Age *(years)*	34.5 (28.5, 40.0)	34.0 (27.0, 42.0)	34.0 (28.0, 41.0)	0.73
Baseline CD4 T cell count *(cells/μL)*	540 (433, 675)	560 (446, 675)	550 (435, 675)	0.85
Baseline HIV-1 RNA *(log_{10} copies/mL)*	5.0 (3.9, 5.5)	4.6 (4.2, 5.1)	4.7 (4.0, 5.3)	0.080
Days from seroconversion to randomization	60 (42, 73)	104 (93, 122)	77 (54, 98)	

Data are presented for the 122 participants overall, as well as for times from seroconversion estimated to be $\leq$ or > 12 weeks. Values are N (%) for categorical and median (interquartile range) for continuous variables. P-values determined by Fisher's exact and Mann-Whitney tests, respectively.

doi:10.1371/journal.ppat.1005661.t001

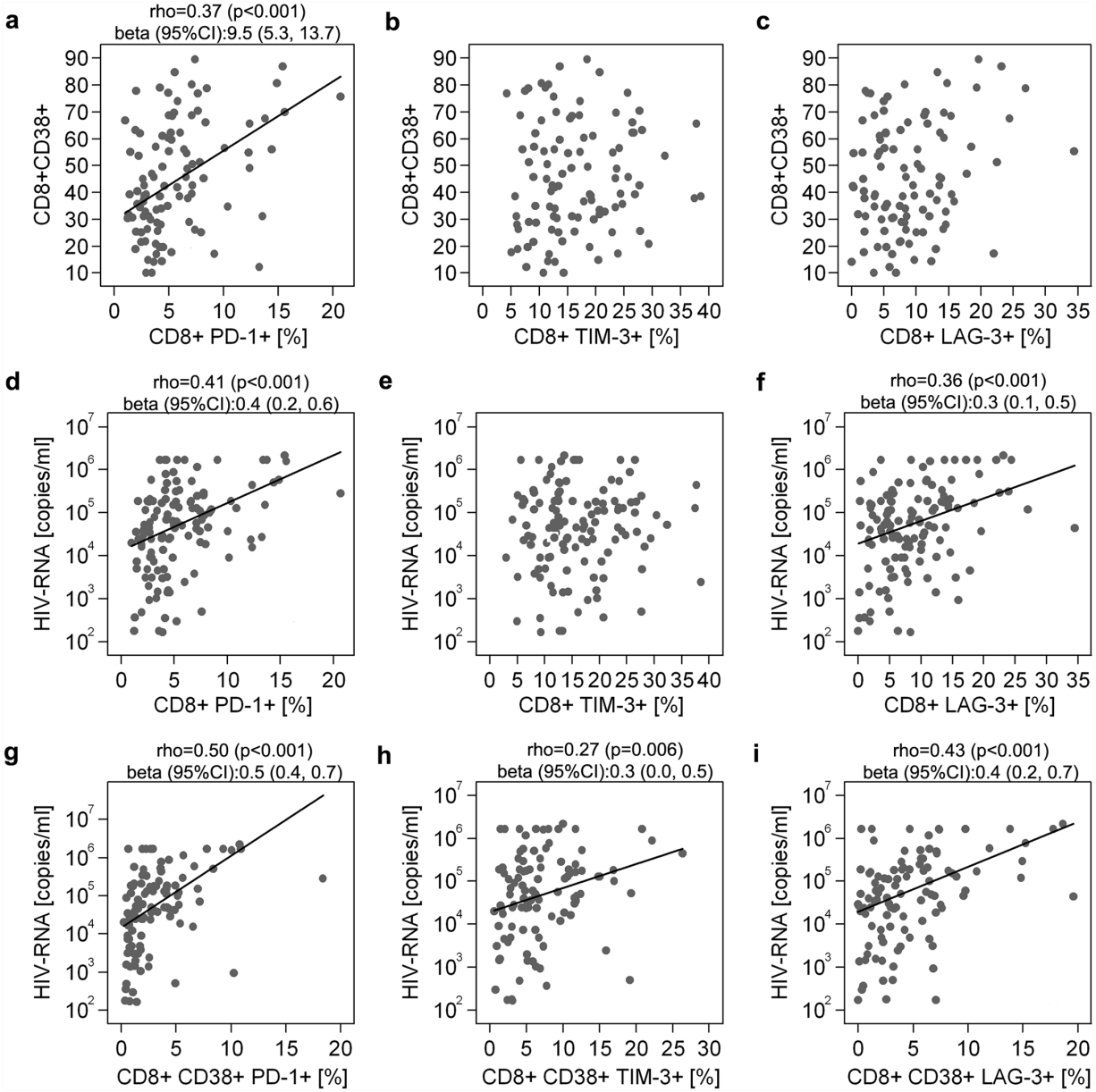


Fig 1. Association between PD-1, Tim-3 or Lag-3 expression on CD8 T cells with CD38 expression and HIV-1 plasma viral load. Expression of PD-1, Tim-3 and Lag-3 expression on CD8 T cells was compared with expression of CD38 on CD8 T cells (a-c). Expression of PD-1, Tim-3 and Lag-3 expression on both CD8 T cells (d-f) and CD8 CD38 T cells (g-i) was correlated with plasma viral load measured at the same time. Associations were evaluated using Spearman correlations. P values and Spearman's rho are presented. The fitted line, superimposed in the relevant scatterplots, was estimated through linear regression. For significant results, the value of beta (the estimated change in the vertical axis variables (log_{10} scale for HIV-1 RNA) per 1 SD increase in horizontal axis variables) and its confidence intervals (CI) are reported.

doi:10.1371/journal.ppat.1005661.g001

Table 2. Expression of exhaustion markers on CD8 and CD38 CD8 T cells by time from seroconversion to pre-therapy baseline measurement.

		Time between seroconversion and baseline		
	Overall	**< = 12 weeks**	**>12 weeks**	
	Median (IQR)	**Median (IQR)**	**Median (IQR)**	**P value[+]**
% CD8				
PD-1	4.5 (2.9, 7.2)	5.0 (3.2, 7.7)	4.2 (2.8, 6.9)	0.17
Tim-3	14.1 (11.1, 20.7)	15.3 (11.6, 20.6)	12.8 (9.3, 21.6)	0.38
Lag-3	8.0 (4.6, 12.5)	8.3 (4.8, 13.5)	7.7 (3.8, 11.3)	0.31
PD-1/Tim-3	0.7 (0.4, 1.3)	0.7 (0.4, 1.5)	0.6 (0.4, 1.1)	0.32
PD-1/Lag-3	0.7 (0.4, 1.1)	0.7 (0.4, 1.1)	0.6 (0.4, 1.0)	0.66
Lag-3/Tim-3	1.6 (0.9, 2.4)	1.6 (0.9, 2.4)	1.7 (0.9, 2.4)	0.99
% CD8 CD38				
PD-1	2.1 (1.1, 4.1)	2.7 (1.2, 4.5)	1.8 (0.9, 2.9)	0.054
Tim-3	6.1 (3.4, 10.0)	6.6 (4.6, 10.3)	4.7 (2.5, 9.3)	0.017
Lag-3	3.9 (1.7, 6.8)	4.8 (2.3, 7.2)	2.9 (1.1, 5.9)	0.006
PD-1/Tim-3	0.4 (0.2, 0.9)	0.5 (0.3, 1.1)	0.3 (0.2, 0.5)	0.057
PD-1/Lag-3	0.5 (0.2, 0.8)	0.6 (0.2, 0.9)	0.3 (0.1, 0.6)	0.012
Lag-3/Tim-3	1.0 (0.4, 1.6)	1.1 (0.7, 1.7)	0.8 (0.3, 1.4)	0.021

Percentage surface expression of PD-1, Tim-3 and Lag-3 either on their own or co-expressed. Cells analysed were CD8 T cells and activated CD38+ve CD8 T cells. For all data the denominator is total CD8 T Cells. Data are given as median values plus interquartile range (IQR). P-values were determined by Mann-Whitney tests.

[+] when corrected for multiple testing overall critical p = 0.004

doi:10.1371/journal.ppat.1005661.t002

markers at the pre-therapy baseline time-point; 4.5%, 14.1% and 8.0% of all CD8 T cells and 2.1%, 6.1% and 3.9% of CD38 CD8 T cells (denominator all CD8 T cells) expressed PD-1, Lag-3 and Tim-3, respectively (Table 2). When stratified by time since seroconversion ($\leq$12 weeks or >12 weeks), participants sampled earlier had (with the exception of PD-1 and PD-1/Tim-3 co-expression for which there was a trend) significantly higher percentages of expression of single and dual-expressed markers on CD8 CD38 T cells. The same was not observed for bulk CD8s (Table 2).

Correlations between the expression of ICRs on CD8 and CD38 CD8 T cells with CD4 T cell count, pVL and time since seroconversion were assessed (Table 3 and Fig 1d–1i). PD-1 and Lag-3 (Fig 1d and 1f), but not Tim-3 (Fig 1e), expression on CD8 T cells was associated with higher pVL ($p<0.001$ for both). Expression of ICRs on CD38 CD8 T cells was significantly and more strongly associated with higher pVL compared with on the bulk CD8 positive population ($p<0.01$ for all markers; Table 3, Fig 1g–1i). Co-expression on CD8 and CD38 CD8 T cells of either PD-1/Tim-3, PD-1/Lag-3 and Tim-3/Lag-3 was also positively associated with pVL (Table 3). PD-1 and PD-1/Lag-3 co-expression on CD8 T cells, and PD-1, PD-1/Tim-3 and PD-1/Lag-3 expression on CD38 CD8 T cells were significantly associated with lower baseline CD4 T cell counts (Table 3). These associations persisted after adjusting for multiple comparisons apart from that between CD4 T cell count and co-expression of PD-1/Lag-3 on CD38 CD4 T cells.

Association of exhaustion markers with clinical progression

Next we evaluated PD-1, Lag-3 and Tim-3 expression and progression to the SPARTAC trial primary endpoint (either CD4 T cell count <350 cells/μl or (re)initiation of ART). PD-1 expression at baseline on CD8 and CD38 CD8 T cells predicted clinical progression (log rank

Table 3. Correlation of PD-1, Tim-3 and Lag-3 expression on CD8 and CD38 CD8 T cells at baseline with CD4 T cell count, plasma HIV-1 RNA and time since seroconversion.

Marker	Baseline CD4 count	Baseline HIV-1 RNA	Time from seroconversion to baseline
CD8			
PD-1	-0.24 (0.008^{+})	0.41 (<0.001*)	-0.14 (0.13)
Tim-3	-0.02 (0.80)	0.05 (0.56)	-0.01 (0.89)
Lag-3	-0.03 (0.75)	0.36 (<0.001*)	-0.16 (0.074)
PD-1/Tim-3	-0.17 (0.072)	0.20 (0.033*)	-0.04 (0.67)
PD-1/Lag-3	-0.24 (0.010^{+})	0.37 (<0.001*)	-0.11 (0.26)
Tim-3/Lag-3	-0.08 (0.37)	0.28 (0.002*)	-0.08 (0.37)
CD8 CD38			
PD-1	-0.29 (0.002^{+})	0.50 (<0.001*)	-0.18 (0.061)
Tim-3	-0.16 (0.11)	0.27 (0.006*)	-0.17 (0.093)
Lag-3	-0.10 (0.30)	0.43 (<0.001*)	-0.31 (0.001†)
PD-1/Tim-3	-0.28 (0.004^{+})	0.43 (<0.001*)	-0.15 (0.13)
PD-1/Lag-3	-0.21 (0.036)	0.52 (<0.001*)	-0.28 (0.004†)
Tim-3/Lag-3	-0.15 (0.12)	0.43 (<0.001*)	-0.23 (0.017)

Percentage surface expression of PD-1, Tim-3 and Lag-3 either on their own or co-expressed. Cells analysed were CD8 T cells and activated CD38 positive CD8 T cells. Results of the correlations with CD4 T cell count, plasma HIV-1 RNA viral load and time since estimated date of seroconversion are given as Spearman's rho (P value). All values give to two decimal places, except for P values <0.1 (3 decimal places).

$^{+}$: significant at the 0.05 level after correction for testing multiple correlations with baseline CD4 T count (corrected overall critical p = 0.017)

*: significant at the 0.05 level after correction for testing multiple correlations with baseline HIV-1-RNA (corrected overall critical p = 0.046)

†: significant at the 0.05 level after correction for testing multiple correlations with time from seroconversion to baseline (corrected overall critical p = 0.008)

doi:10.1371/journal.ppat.1005661.t003

test, p = 0.049 and p = 0.014, respectively) (Fig 2a and 2d). This effect was most evident in patients recruited within 12 weeks of infection, when compared with those recruited after 12 weeks (Fig 2b and 2e vs 2c and 2f). Tim-3 and Lag-3 expression on CD8 (Fig 3) or CD38 CD8 (Fig C in S1 Text) T cells was not associated with clinical progression when the whole cohort was analysed although, surprisingly, there was evidence for slower disease progression in participants recruited ≤12 weeks from seroconversion with increased Tim-3 expression on CD8 T cells (log rank test, p = 0.01; Fig 3b). This could not be explained through a correlation with Tim-3 expression and PD-1 (or Lag-3) (Table C in S1 Text) and this advantage survived (P = 0.075) adjustment for PD-1, Lag-3, baseline CD4 count and therapy (Table D in S1 Text).

Cox proportional hazards models were used to explore further the association between baseline PD-1 expression on bulk CD8 T cells and clinical progression (Table 4). The association with PD-1 expression and clinical progression was preserved when ART alone (HR 1.75; p = 0.045) or ART and baseline CD4 T cell count (HR 1.76; p = 0.047) were included in the model, but not when accounting for pVL or following correction for multiple comparisons. In a model including time from seroconversion, ART and baseline CD4 T cell count there was a trend for an association between PD-1 expression and clinical progression (HR 1.72, 95% CI 0.98–3.03), but this was not significant when baseline pVL was included. When the magnitude of PD-1 expression was stratified into quartiles, there was evidence of a dose effect (HR: 1, 1.60, 1.71, 2.16 for each quartile, respectively) when ART and baseline CD4 T count were included in the model, but not when baseline pVL was included. We found no evidence to support a significant association with CD38 alone and time to the trial endpoint.

Cox models also demonstrated an effect of bulk CD8 T cell Lag-3 expression on progression when adjusted for ART initiation and CD4 T cell count (HR 1.46; p = 0.024), but not when including pVL (Table 4). As for PD-1 expression, there were significant associations with

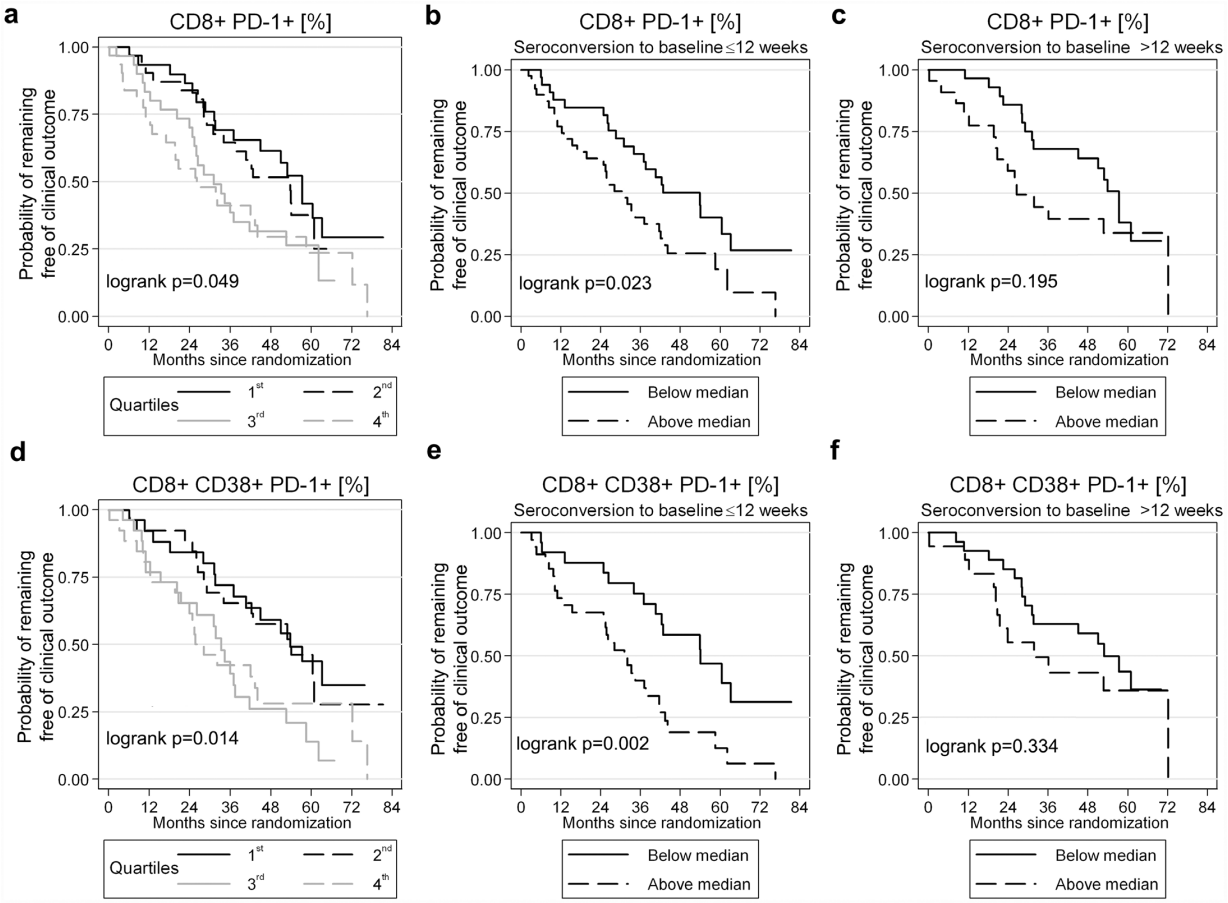


Fig 2. Impact of PD-1 expression on CD8 or CD38 CD8 T cells on clinical outcome. Survival analyses to show the effect of PD-1 expression on (a-c) CD8 and (d-f) CD38 CD8 cells on time to the primary end-point in the SPARTAC trial (CD4 T cell count <350 cells/μl or initiation of long-term ART). In panels a and d, percentage of PD-1 expression is stratifed into quartiles and significance is tested using a log rank test. Survival analyses show the impact of estimated time since seroconversion (reported as ≤12 weeks or >12 weeks) and PD-1 baseline expression on CD8 (b-c) and CD38 CD8 (e-f) T cells. Here, percentage PD-1 expression is stratifed at the median value.

doi:10.1371/journal.ppat.1005661.g002

clinical progression when including time since seroconversion, ART and baseline CD4 T cell count in the model (HR 1.45; p = 0.03) or when exploring dose effect when stratified into quartiles (HR 1, 1.43, 1.12, 2.17), but neither survived correction for baseline pVL. Tim-3 expression on bulk CD8 T cells did not predict progression.

Interestingly, on restricting the Cox models to CD38 CD8 T cells, all three markers were associated with disease progression in unadjusted models or when correcting for ART and CD4 T cell count although, again, not when adjusting for baseline pVL (Table 4).

Co-expression of T cell exhaustion markers and clinical progression

Having explored the impact of single exhaustion markers on clinical outcome, we next measured whether their co-expression would predict progression (Fig D in S1 Text and Table A in S1 Text). In survival analyses PD-1/Lag-3 co-expression on CD8 and CD38 CD8 T cells

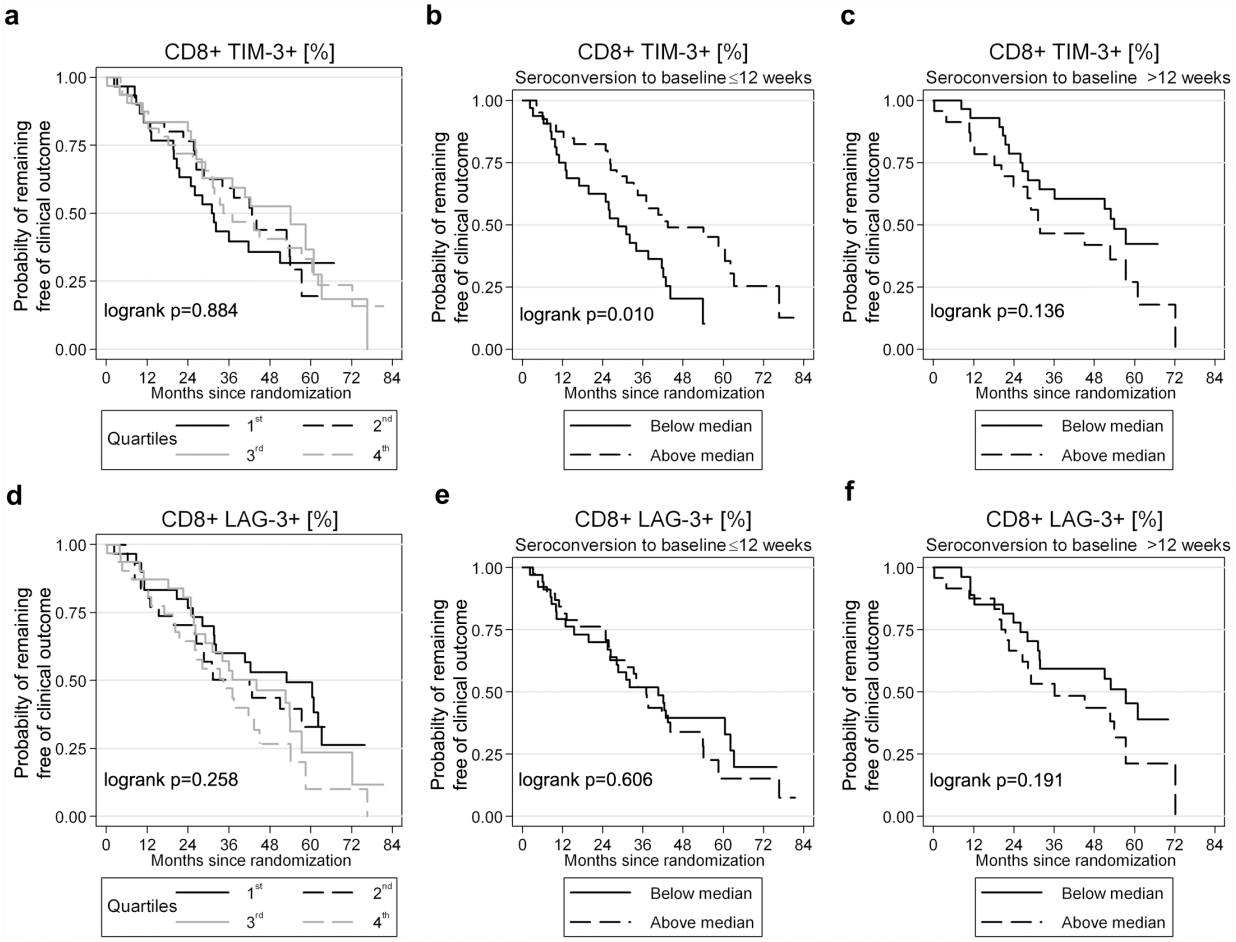


Fig 3. Impact of CD8 T cell Tim-3 and Lag-3 expression on clinical outcome. Survival analyses showing the effect of Tim-3 (a-c) and Lag-3 (d-f) expression on time to the primary end-point in the SPARTAC trial (CD4 T cell count <350 cells/μl or initiation of long-term ART). Percentage of marker expression is stratifed into quartiles (a, d) or, when tested in conjunction with the estimated time since seroconversion (reported as ≤12 weeks (b,e) or >12 weeks (c,f)), at the median value. Significance is tested using a log rank test.

doi:10.1371/journal.ppat.1005661.g003

(Fig Da and Dd in S1 Text; log-rank test, p = 0.012 and p = 0.027 respectively), and PD-1/Tim-3 co-expression on CD38 CD8 T cells (Fig Dj in S1 Text, p = 0.01) were associated with faster time to the trial primary endpoint, although not a better predictor than PD-1 alone. When considering time since seroconversion, the effects of PD-1/Lag-3 and PD-1/Tim-3 co-expression on bulk CD8s on clinical progression seemed more pronounced in patients recruited more than 12 weeks after seroconversion, compared with those recruited within 12 weeks (p = 0.030 and p = 0.024, respectively (Fig Dc and Di in S1 Text)). However, when restricting the analyses to activated CD38 CD8 T cells, PD-1/Lag-3 and PD-1/Tim-3 co-expression were, in contrast, associated with progression in individuals recruited within 12 weeks of seroconversion (p = 0.008, p = 0.008, respectively (Fig De and Dk in S1 Text)). There was no effect associated with Tim-3/Lag-3 co-expression.

Table 4. Cox proportional hazards models on disease progression and PD-1, Tim-3 and Lag-3 expression.

	Unadjusted HR (95% CI; P value[+])	Adjusted HR (95% CI; P value)		
		ART	ART CD4 T cell count	ART CD4 cell count HIV-1 RNA[‡]
CD8				
PD-1	1.68 (0.98, 2.86; 0.057)	1.75 (1.01, 3.01; 0.045)	1.76 (1.01, 3.09; 0.047)	0.99 (0.53, 1.83; 0.96)
Tim-3	0.99 (0.73, 1.33; 0.928)	0.98 (0.73, 1.31; 0.88)	1.00 (0.73, 1.35; 0.98)	0.91 (0.66, 1.25; 0.55)
Lag-3	1.30 (0.95, 1.77; 0.10)	1.35 (1.00, 1.84; 0.054)	1.46 (1.05, 2.04; 0.024[†])	1.07 (0.73, 1.58; 0.72)
CD38 CD8				
PD-1	2.43 (1.16, 5.12; 0.019)	2.71 (1.28, 5.74; 0.009*)	2.06 (0.96, 4.42; 0.064)	0.93 (0.37, 2.33; 0.88)
Tim-3	1.81 (1.14, 2.88; 0.012)	1.87 (1.17, 2.99; 0.009*)	2.05 (1.25, 3.34; 0.004[†])	1.55 (0.91, 2.65; 0.11)
Lag-3	1.62 (0.99, 2.66; 0.057)	1.84 (1.10, 3.09; 0.020*)	2.06 (1.17, 3.61; 0.012[†])	1.00 (0.49, 2.03; 1.00)

Cox proportional hazards model showing association with PD-1, Tim-3 and Lag-3 expression on CD8 and CD8 CD38 T cells with the SPARTAC trial primary endpoint. Data are presented unadjusted, and then in multivariable analyses including ART, CD4 T cell count and plasma viral load (HIV-1 RNA). Data are given as (HR (95% CI; p-value).

[+]: corrected for multiple testing overall critical p = 0.008

*: significant at the 0.05 level after correction for testing multiple markers (corrected overall critical p = 0.025)

[†]: significant at the 0.05 level after correction for testing multiple markers (corrected overall critical p = 0.025)

[‡]: corrected for multiple testing overall critical p = 0.008

doi:10.1371/journal.ppat.1005661.t004

In Cox proportional hazards models, there was a strong association with high PD-1/Tim-3 expression on CD8 T cells (above the median) with faster progression (HR 1.64 (95% CI 1.04. 2.60); p = 0.034), after adjusting for baseline CD4 T cell count, ART and pVL. The significant Kaplan-Meier analysis for PD-1/Lag-3 co-expression was not supported by Cox models when adjusting for baseline pVL.

Associations of PD-1, Tim-3 and Lag-3 with T cell memory subsets

Having determined associations between PD-1, Tim-3 and Lag-3 expression and clinical progression, we next identified the CD8 T cell memory subsets on which these markers were present (Fig E in S1 Text and Fig 4). We analysed samples from 16 participants of a second PHI cohort, HEATHER ('HIV Reservoir targeting with Early Antiretroviral Therapy'), with similar demographics and inclusion criteria to SPARTAC (Table B in S1 Text). Similar to previous reports in PHI we found that naïve, central memory (T_{CM}), effector memory (T_{EM}) and T_{EMRA} constituted 14.1, 4.4, 49.6 and 25.9% (median values) of the CD8 T cell population, respectively (Fig 4a). PD-1 and Lag-3 had similar distributions, with significantly higher expression in T_{EM} compared with all other T cell subsets. Although Tim-3 expression was highest amongst T_{EM}, there was relatively less expression on T_{CM} compared with PD-1 or Lag-3. Expression of all three markers on naïve cells was very low (especially for PD-1 and Tim-3).

Functional significance of PD-1, Tim-3 and Lag-3

To determine the functional significance of PD-1, Tim-3 and Lag-3 expression in PHI, we compared expression with the T-box transcription factor T-bet, eomesodermin (Eomes) and CD39. In HIV-1 infection, CD8 T cells which are T-bet^{dim}/Eomes^{hi} are associated with an exhausted functional phenotype with reduced polyfunctionality[24]. CD39 also identifies exhausted CD8 T cells in HIV-1 infection, and is associated with a transcriptional signature of T cell exhaustion[25]. We, therefore, explored whether these markers were co-expressed with Tim-3, Lag-3 and PD-1 in early HIV-1 infection in the HEATHER cohort. At the nearest available pre-therapy time-point to seroconversion T-bet^{dim}/Eomes^{hi} CD8 T cells had significantly

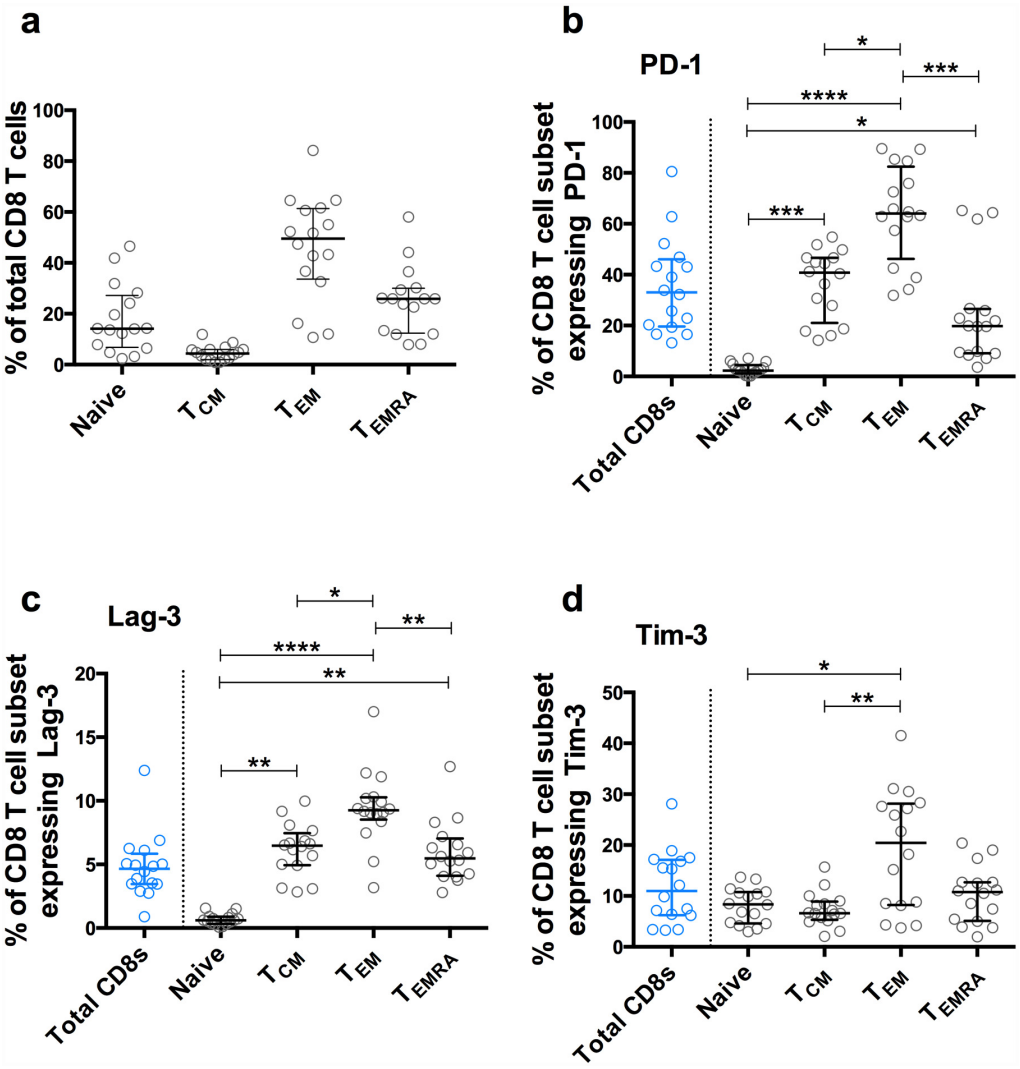


Fig 4. Distribution of PD-1, Lag-3 and Tim-3 expression according to CD8 T cell memory subsets. Overall distribution of naïve, central memory (T_{CM}), effector memory (T_{EM}) and T_{EMRA} CD8 T cells from pre-therapy baseline samples (a) and percentage expression on each of these subsets at the same time-point of PD-1 (b), Lag-3 (c) and Tim-3 (d). Markers represent medians and interquartile range. *p<0.05, **p<0.01, ***p<0.001, ****p<0.0001. Comparison of exhaustion marker expression across three or more groups was performed using Friedman's test (non-parametric, paired analysis of variance). Where a difference was found, subsequent pairwise comparisons between groups (Dunn's test) were performed with adjustment for multiple comparisons targeting on overall significance level of 0.05.

doi:10.1371/journal.ppat.1005661.g004

higher levels of expression of both PD-1 and Lag-3 (Fig 5). This population also expressed significantly higher levels of CD38 and CD39 but, interestingly, lower levels of Tim-3. We found the expression of CD39 to be bimodal with 50% of participants expressing <1% (Fig F in S1 Text), likely due to polymorphisms in CD39, as recently reported by Roederer et al [26]. There was no evidence for increased co-expression of Tim-3, Lag-3 and PD-1 in the CD39 'positive' (i.e. >1% expression) group compared with those expressing <1%. However, for those

PLOS | PATHOGENS

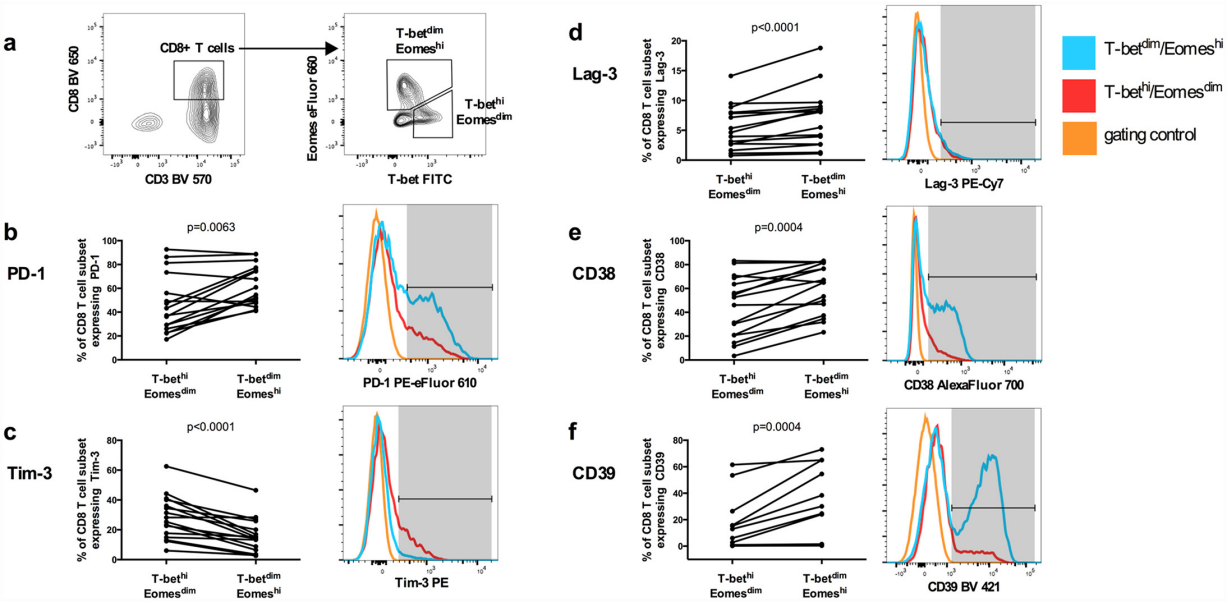


Fig 5. Association between PD-1, Tim-3 or Lag-3 expression on CD8 T cells with T-bet/Eomes and CD39 expression. The strategy for gating CD8 T cells based on T-bet and Eomes expression is shown in (a). Expression of PD-1 (b), Tim-3 (c), Lag-3 (d), CD38 (e) and CD39 (f) was compared between CD8 T cells staining T-bet^{hi}/Eomes^{dim} and T-bet^{dim}/Eomes^{hi} populations. The panels on the right show the expression of these markers from a single, representative sample with T-bet^{hi}/Eomes^{dim} (red line) and T-bet^{dim}/Eomes^{hi} (blue line) overlaid with gating control (orange line). The shaded area highlights cells that were considered positive for the marker. Expression of exhaustion markers between two subsets was compared using Wilcoxon matched-pairs signed rank test.

doi:10.1371/journal.ppat.1005661.g005

individuals with >1% CD39 expression, there was evidence for correlation between levels of CD39 and other exhaustion markers (Fig F in S1 Text).

Discussion

T cell immune exhaustion has been described as the loss of effector function as a result of repeated antigenic stimulation in persistent infections. Certain cell surface-expressed proteins —also called 'immune checkpoint receptors' (ICR)–have been associated with a continuous loss of T cell effector function [17,27], and have attracted much interest as mediators of T cell exhaustion and possible targets for cancer therapies [28–30]. Here, we evaluated the association of ICRs with clinical progression in early HIV-1 infection within the SPARTAC trial. Our results show that ICR expression at the time of enrolment into the study is linked with clinical progression, but that this relationship is highly complex with different ICR markers having a variable impact depending on their co-expression with other exhaustion and activation markers, and as well as the timing of diagnosis of PHI.

Expression of PD-1, Tim-3 and Lag-3 was increased in PHI compared with HIV-uninfected controls and was predominantly found on the CD8 T_{EM} subset. We found strong evidence to support an association between ICR expression and HIV-1 pVL, in line with previous observations [12,20], although not for Tim-3, which contrasts with reports in chronic HIV infection [18]. However, when gated on activated CD38 CD8 T cells, all ICRs correlated strongly with pVL. Expression of CD38 on CD8 T cells is a well-documented marker for HIV-1 disease progression [31] although, surprisingly, we found no evidence supporting this association in our

study of primary HIV-1 infection. The increased expression of ICR markers on T_{EM}, the association with pVL (and also with CD4 T cell count for PD-1) and the increased strength of the relationship when gated on activated cells are together supportive of a close relationship between exhausted HIV-specific T cell immunity and disease progression. To test this assertion, we turned to primary endpoint data from a randomised controlled trial exploring the impact of short-course ART in PHI on clinical outcomes.

In this sub-analysis of the SPARTAC RCT, there was evidence for PD-1, Lag-3 and Tim-3 predicting disease progression as determined by the time taken to reach the trial primary endpoint (either CD4 T cell count <350 cells/μl or (re)initiation of ART), but the strength of the association varied according to factors such as co-expression with another ICR marker, expression of CD38, and time since seroconversion. Although not evident in the survival analyses, in Cox models only PD-1/Tim-3 co-expression significantly predicted progression when adjusting for CD4 count, ART and pVL.

Despite correlating with pVL, neither Lag-3 nor Tim-3 alone were predictive of clinical progression. Lag-3 is a major histocompatibility complex (MHC) class II ligand that negatively interferes with the positive signal cascade derived from the TCR–MHC interaction. The role of Lag-3 in HIV-1 infection is not yet fully elucidated and data are conflicting[32][33,34]. Although we observed a clear correlation with pVL, sole Lag-3 expression on CD8 and CD38 CD8 T cells did not translate into an association with clinical disease progression.

Tim-3 expression showed distinct associations with clinical disease progression and may even be antagonistic to PD-1 early in HIV-1 infection; Tim-3 was associated with delayed progression in participants identified within 12 weeks of seroconversion, but no effect was seen for Tim-3/PD-1 co-expression. This protective Tim-3 effect was not seen for individuals recruited later than 12 weeks after seroconversion, for whom PD-1/Tim-3 co-expression was disadvantageous. The mechanism of the immuno-regulatory effect of Tim-3 is not clear [35], but this marker has been associated with dysfunction of HIV-1 specific CD8 T cells in chronically infected individuals [18]. Further evidence for the complex role of Tim-3 can be found in the LCMV model where it was only transiently up-regulated during acute infection [36], whereas in chronic infection PD-1/Tim-3 T cells were more exhausted with impaired proliferative capacities than PD-1 single positive T cells [36]. Tim-3 may be crucial in the early phases of HIV-1 infection to ensure the differentiation of antigen specific effector T cells whereas later in infection continuous Tim-3 signalling may lead to T cell exhaustion [35].

Our study has several limitations. First, we evaluated the expression of ICRs on CD8 and CD8 CD38 T cells irrespective of their restriction, although we showed that the majority of ICR expression was on the T_{EM} memory subset. Further in depth longitudinal analyses of these responses in HIV-1 specific T cell populations in conjunction with their activation status will be needed to confirm our findings. Secondly, other investigators have suggested that in acute HIV-1 infection PD-1 expression does not necessarily equate to exhaustion [37]. We could not evaluate the functionality of the immune responses to compare with exhaustion T cell status due to restricted sample availability. However, we demonstrated strong associations of these ICRs during PHI with the T-bet^{dim}/Eomes^{hi} CD8 population and CD39 expression. This provides evidence of functional exhaustion of these ICR-expression cells as T-bet^{dim}/Eomes^{hi} and CD39 expressing CD8 T cells have been shown to have reduced polyfunctionality, cytokine expression and exhausted transcriptional profiles [24,25,38]. Ideally, one would be able to tease out the overlap between T cell exhaustion and activation—which functionally appear to lie on a similar spectrum. However, the different pathways associated with each ICR marker, as well as their low levels of co-expression, might suggest that the phenotypes are mechanistically separate and that they are independent targets for future therapies and interventions.

The SPARTAC trial consisted of different ART durations and we were not able to show any differences between trial arms, rendering the impact of different ART durations in PHI on the expression of immune exhaustion markers unanswered. Nevertheless, we did correct for the various treatment arms in the multivariable Cox model, and still found significant correlations with exhaustion marker expression and markers of disease progression. Finally, due to the lack of remaining samples from SPARTAC, we turned to a second cohort of individuals sampled during PHI (HEATHER) to explore ICR expression on memory CD8 T cell subsets in conjunction with T-bet, Eomes and CD39. Different antibody clones and fluorochromes were used for these two cohorts and this will have an impact on measured levels of expression, particularly notable for PD-1. However, in none of our analyses do we combine data from the two cohorts and as these two PHI cohorts were very similar in terms of inclusion criteria and demographics, we would expect our findings to be closely related. Of note the characteristics of the HEATHER and SPARTAC participants were comparable, both largely MSM UK infected individuals with B clade virus identified with maximum of 6 months from a previous HIV negative test all starting immediate ART at PHI diagnosis.

In conclusion, our study is the first to show an association between ICR expression and clinical disease progression in a large cohort of 122 HIV-1 seroconverters. However, it is clear that the relationship between T cell immune activation, immune exhaustion, individual ICR markers and clinical outcomes is complex and further studies will be needed to clarify this. Our data suggest that interventions aimed at reversing T cell exhaustion and restoring T cell functionality may be most successful if applied shortly after HIV-1 acquisition, before an exhausted T cell phenotype is established. This may be also be pertinent for enhancing interventions which aim to reactivate the latent HIV reservoir to facilitate immune-directed killing in novel curative HIV strategies.

Materials and Methods

Ethics statement

The SPARTAC trial was approved by the following authorities: Medicines and Healthcare products Regulatory Agency (UK), Ministry of Health (Brazil), Irish Medicines Board (Ireland), Medicines Control Council (South Africa), and the Uganda National Council for Science and Technology (Uganda). It was also approved by the following ethics committees in the participating countries: Central London Research Ethics Committee (UK), Hospital Universitário Clementino Fraga Filho Ethics in Research Committee (Brazil), Clinical Research and Ethics Committee of Hospital Clinic in the province of Barcelona (Spain), The Adelaide and Meath Hospital Research Ethics Committee (Ireland), University of Witwatersrand Human Research Ethics Committee, University of Kwazulu-Natal Research Ethics Committee and University of Cape Town Research Ethics Committee (South Africa), Uganda Virus Research Institute Science and ethics committee (Uganda), The Prince Charles Hospital Human Research Ethics Committee and St Vincent's Hospital Human Research Ethics Committee (Australia), and the National Institute for Infectious Diseases Lazzaro Spallanzani, Institute Hospital and the Medical Research Ethics Committee, and the ethical committee Of the Central Foundation of San Raffaele, MonteTabor (Italy). HEATHER ('HIV Reservoir targeting with Early Antiretroviral Therapy') was approved by the West Midlands—South Birmingham Research Ethics Committee reference 14/WM/1104. Ethical approvals include use of samples for the studies described. All samples were analysed anonymously.

Participants and trial design

SPARTAC. Blood samples from participants of the SPARTAC trial (EudraCT Number: 2004-000446-20) recruited in the United Kingdom were used in this study. The design of the

trial is reported elsewhere [23]. In brief, SPARTAC was an open randomised controlled trial enrolling adults with PHI from 35 sites in Australia, Brazil, Ireland, Italy, South Africa, Spain, Uganda and the UK, from August 2003 to July 2007. Primary HIV-1 infection was defined as: a positive HIV-1 antibody test within 6 months after a negative test (criterion 1), a negative HIV-1 antibody test with a positive RT-PCR assay for HIV-1 RNA (criterion 2), a low level of HIV antibodies (optical density(OD) <0.6) according to a serologic testing algorithm for recent infection (subtype B strain only) (criterion 3), an equivocal HIV-1 antibody test with a repeat test within 2 weeks showing an increase in the level of HIV antibodies (criterion 4), or clinical manifestations of symptomatic HIV-1 seroconversion illness supported by antigen positivity and less than 4 positive bands on Western blot analysis (criterion 5). The time of seroconversion was estimated as the midpoint between the most recent negative or equivocal antibody test and the first positive test for patients who met criterion 1 or 4; as the date of the test for patients who met criterion 2, 3 (if OD ≤ 0.01) or 5; and as the date of the test $-[(OD\times150)\div2]$ days for patients who met criterion 3 (if OD >0.01). Participants were randomised to receive ART for 48 weeks (ART-48), 12 weeks (ART-12) or no therapy (standard of care, SOC). Where ART is included as a co-variate in subsequent analyses it is this duration of randomised therapy rather than the long-term ART commenced as part of the trial primary end-point to which we refer. 'Baseline' refers to date of randomisation. The trial primary end-point was a composite of either a CD4 T cell count <350 cells/μl (>3 months after randomisation and confirmed within 4 weeks) or initiation of long-term ART. We used 12 weeks as the cut-off for the 'early' and 'late' patients based on the original report which indicated this time-point to be a discriminator of progression rates.[23]

HEATHER. Sixteen PHI participants in the HEATHER ('HIV Reservoir targeting with Early Antiretroviral Therapy')(West Midlands—South Birmingham Research Ethics Committee reference 14/WM/1104) cohort were selected at random and based on sample availability (Table B in S1 Text). Inclusion criteria for HEATHER were: HIV-1 positive antibody test within 6 months of a HIV-1 negative antibody test, HIV-1 antibody negative with positive PCR (or positive p24 Ag or viral load detectable), RITA (recent incident assay test algorithm) assay result consistent with recent infection, equivocal HIV-1 antibody test supported by a repeat test within 2 weeks showing a rising optical density, having clinical manifestations of symptomatic HIV seroconversion illness supported by antigen positivity. The time of seroconversion was estimated as the midpoint between the most recent negative or equivocal test and the first positive test for those who met relevant criteria and as the date of test for all other participants. For each, the pre-therapy cryopreserved PBMC sample closest to seroconversion was used for analysis of co-expression of PD-1, Tim-3, Lag-3, Eomes, T-bet, CD39 and for CD8 T cell memory subset phenotyping.

Flow cytometry

Analyses associating markers with disease progression used cryopreserved PBMCs from SPARTAC samples taken at baseline (prior to any ART, if prescribed). Cell surface staining for flow cytometry was performed with: Live/Dead Pacific Blue 2ug/100ul (Invitrogen), CD19 Pacific Blue 0.4 μg/100μl (SJ25-C1), CD3 Pacific Orange 0.4 μg/100μl (UCHT1), CD8 PE-Cy5 PerCP 0.4 μg/100μl (SK1)[BD Bioscience], PD-1 APC 0.5 μg/100μl (MIH4)[eBioscience], Tim-3 PE 0.05 μg/100μl (344823)[R&D], Lag-3 FITC 2 μg/100μl (17B4)[LifeSpan Bioscience] and CD38 PE-Cy7 0.4 μg/100μl (HIT-2)[Biolegend]. The isotype controls for Lag-3 was IgG2a isotype FITC 0.4 μg/100μl (C45)[AdB serotech], for PD-1 was IgG1 isotype APC 0.4 μg/100μl (p3)[eBioscience] and for Tim-3 was IgG2a isotype PE 0.4 μg/100μl (R35-95)[BD Bioscience]. Cell population gating was performed based on mean fluorescence intensity "minus one" (FMO)

[39] and unstained controls (Fig A in S1 Text). Samples were acquired on a LSR II (BD) with standard laser configurations and analysed using FlowJo Version 8.7.7.

Analyses examining ICR expression on T cell memory subsets used cryopreserved PBMCs from the HEATHER cohort. Cells were stained in BD Horizon Brilliant Stain Buffer (BD) containing all antibodies and Live/Dead Near IR at 1 in 300 dilution (Life Technologies) in 96 well-V bottom plates at 4°C. PBMCs were stained with the following antibodies: CD3 Brilliant Violet (BV) 570 0.16 μg/100μl (UCHT1), CCR7 Pacific Blue 1.8 μg/100μl (G043H7)[BioLegend], CD4 BV 605 0.05 μg/100μl (RPA-T4), CD8 BV 650 0.012 μg/100μl (RPA-T8)[BD], PD-1 PE eFluor 610 0.2 μg/100μl (eBioJ105), Lag-3 PE-Cy7 0.024 μg/100μl (3D5223H), CD45RA FITC 0.4 μg/100μl (HI100)[eBioscience] and Tim-3 PE (as above).

For characterisation of T-bet/Eomes expression, PBMCs were stained as above in PBS with 5% fetal bovine serum and 1mM EDTA containing Live/Dead Near IR, anti-PD-1, anti-Tim-3, anti-Lag-3, along with antibodies to CD39 BV 421 0.1 μg/100μl (A1) and CD38 AlexaFluor 700 0.1 μg/100μl (HB-7)[BioLegend]. Fixation and permeabilisation were performed with Foxp3 Buffer Set (BD) as per manufacturer's instructions in reduced volumes to facilitate staining in 96-well plates. Staining of intracellular epitopes was performed at room temperature in PBS containing 0.5% BSA and 0.1% sodium azide with antibodies to CD3, CD4, CD8 (as above), and T-bet FITC 2 μg/100μl (4B10)[BioLegend] and Eomes eFluor660 0.024 μg/100μl (WD1928)[eBioscience]. All samples were acquired on a LSR II (BD). Data were analysed using FlowJo Version 10.8.0r1 (Treestar). Naïve T cells were defined as CD45RA+/CCR7+, T_{CM} as CD45RA-/CCR7+, T_{EM} defined as CD45RA-/CCR7- and T_{EMRA} as CD45RA+/CCR7-. (Fig Ea in S1 Text). CD8 T cells were divided into T-bet^{hi}/Eomes^{dim} and T-bet^{dim}Eomes^{hi} populations as described by Buggert et al [24](Fig 5a). Gates for exhaustion marker positive populations were set on a partially stained anchor sample without the relevant antibody such that <0.1% of events were positive for the marker (Fig Eb and Ec in S1 Text).

Statistical methods

Associations between T cell exhaustion markers on CD8 and CD38 CD8 positive cells and pVL or CD4 T cell count were evaluated using Spearman correlations. The fitted line, superimposed in the relevant scatterplots, was estimated through linear regression. When multiple markers were tested for correlations with other variables (e.g. baseline CD4 T cell count or HIV-1 RNA), the adjusted overall critical p-values were also reported. Adjustments were performed using the method of Simes [40] targeting on an overall false discovery rate of ≤0.05. Association of exhaustion markers with clinical progression (time to trial end-point) was assessed by Kaplan-Meier survival curves, log rank tests and Cox proportional hazards models. Covariables considered for all Cox models included ART treatment (as a time updated binary variable), baseline CD4 T cell count and pVL. Effects of the time interval between the estimated date of seroconversion and a baseline exhaustion marker's measurement (as a binary variable i.e. >12 or ≤12 weeks) and its first order interactions with the aforementioned covariates or the exhaustion markers under investigation were also assessed and, if significant, included in the final multivariable Cox model. Finally, we checked for any effects of the time gap between the last negative and first positive HIV tests used to estimate the seroconversion date. These analyses were performed using Stata 11 (Stata Corp., TX USA). P-values<0.05 were considered as statistically significant.

In the analyses from the HEATHER cohort, comparison of exhaustion marker expression across three or more groups was performed using Friedman's test (non-parametric, paired analysis of variance). Where a difference was found, subsequent pairwise comparisons between groups (Dunn's test) were performed with adjustment for multiple comparisons targeting on

overall significance level of 0.05. Expression of exhaustion markers between two T cell subsets was compared using Wilcoxon matched-pairs signed rank test. Statistical analyses were performed using GraphPad Prism 6.0f.

Supporting Information

S1 Text. Supporting information. Table A. Summary of log rank test results from Fig D in S1 Text. **Table B.** Demographic and clinical characteristics of participants in the HEATHER trial included in the analyses. **Table C.** Correlations of PD-1, Tim-3, Lag-3, PD1/Tim-3, PD1/Lag-3 and Tim-3/Lag-3. **Table D.** Cox Model adjusted for Tim-3, PD-1, Lag-3, baseline CD4 and ART. **Fig A.** Gating strategy: proportion of the total CD8 T cell population that express PD-1, Tim-3, Lag-3 or CD38. **Fig B.** Expression of PD-1, Tim-3 and Lag-3 on CD8 T cells in healthy controls and Primary HIV Infection. **Fig C.** Impact of Tim-3 and Lag-3 expression on CD38 CD8 T cells on clinical outcome. **Fig D.** Impact of co-expression at baseline on CD8 T cells of PD-1, Tim-3 and Lag-3 on clinical outcome. **Fig E.** Gating strategy used for the characterisation of PD-1, Tim-3 and Lag-3 on memory subsets. Fig F. Correlation of CD39 expression with PD-1, Lag-3 and Tim-3.
(DOCX)

Acknowledgments

We thank the participants of SPARTAC and HEATHER. The SPARTAC Trial Investigators: Trial Steering Committee: Independent Members- A Breckenridge (Chair), P Clayden, C Conlon, F Conradie, J Kaldor*, F Maggiolo, F Ssali, Country Principal Investigators- DA Cooper, P Kaleebu, G Ramjee, M Schechter, G Tambussi, JM Miro, J Weber. Trial Physician: S Fidler. Trial Statistician: A Babiker. Data and Safety Monitoring Committee (DSMC): T Peto (Chair), A McLaren (in memoriam), V Beral, G Chene, J Hakim. Co-ordinating Trial Centre: Medical Research Council Clinical Trials Unit, London (A Babiker, K Porter, M Thomason, F Ewings, M Gabriel, D Johnson, K Thompson, A Cursley*, K Donegan*, E Fossey*, P Kelleher*, K Lee*, B Murphy*, D Nock*). Central Immunology Laboratories and Repositories: The Peter Medawar Building for Pathogen Research, University of Oxford, UK (R Phillips, J Frater, L Ohm Laursen*, N Robinson, P Goulder, H Brown). Central Virology Laboratories and Repositories: Jefferiss Trust Laboratories, Imperial College, London, UK (M McClure, D Bonsall*, O Erlwein*, A Helander*, S Kaye, M Robinson, L Cook*, G Adcock*, P Ahmed*). Clinical Endpoint Review Committee: N Paton, S Fidler. Investigators and Staff at Participating Sites: Australia: St Vincents Hospital, Sydney (A Kelleher), Northside Clinic, Melbourne (R Moore), East Sydney Doctors, Sydney (R McFarlane), Prahran Market Clinic, Melbourne (N Roth), Taylor Square Private Clinic, Sydney (R Finlayson), The Centre Clinic, Melbourne (B Kiem Tee), Sexual Health Centre, Melbourne (T Read), AIDS Medical Unit, Brisbane (M Kelly), Burwood Rd Practice, Sydney (N Doong), Holdsworth House Medical Practice, Sydney (M Bloch), Aids Research Initiative, Sydney (C Workman). Coordinating Centre in Australia: Kirby Institute University of New South Wales, Sydney (P Grey, DA Cooper, A Kelleher, M Law). Brazil: Projeto Praca Onze, Hospital Escola Sao Francisco de Assis, Universidade federal do Rio de Janeiro, Rio de Janeiro (M Schechter, P Gama, M Mercon*, M Barbosa de Souza, C Beppu Yoshida, JR Grangeiro da Silva, A Sampaio Amaral, D Fernandes de Aguiar, M de Fatima Melo, R Quaresma Garrido). Italy: Ospedale San Raffaele, Milan (G Tambussi, S Nozza, M Pogliaghi, S Chiappetta, L Della Torre, E Gasparotto), Ospedale Lazzaro Spallanzani, Roma (G DOffizi, C Vlassi, A Corpolongo). South Africa: Cape Town: Desmond Tutu HIV-1 Centre, Institute of Infectious Diseases, Cape Town (R Wood, J Pitt, C Orrell, F Cilliers, R Croxford,

K Middelkoop, LG Bekker, C Heiberg, J Aploon, N Killa, E Fielder, T Buhler). Johannesburg: The Wits Reproductive Health and HIV-1 Institute, University of Witswatersrand, Hillbrow Health Precinct, Johannesburg (H Rees, F Venter, T Palanee), Contract Laboratory Services, Johannesburg Hospital, Johannesburg (W Stevens, C Ingram, M Majam, M Papathanasopoulos). Kwazulu-Natal: HIV-1 Prevention Unit, Medical Research Council, Durban (G Ramjee, S Gappoo, J Moodley, A Premrajh, L Zako). Uganda: Medical Research Council/Uganda Virus Research Institute, Entebbe (H Grosskurth, A Kamali, P Kaleebu, U Bahemuka, J Mugisha*, HF Njaj*). Spain: Hospital Clinic-IDIBAPS, University of Barcelona, Barcelona (JM Miro, M Lopez-Dieguez*, C Manzardo, JA Arnaiz, T Pumarola, M Plana, M Tuset, MC Ligero, MT Garca, T Gallart, JM Gatell). UK and Ireland: Royal Sussex County Hospital, Brighton (M Fisher, K Hobbs, N Perry, D Pao, D Maitland, L Heald), St James's Hospital, Dublin (F Mulcahy, G Courtney, S O'Dea, D Reidy), Regional Infectious Diseases Unit, Western General Hospital and Genitourinary Dept, Royal Infirmary of Edinburgh, Edinburgh (C Leen, G Scott, L Ellis, S Morris, P Simmonds), Chelsea and Westminster Hospital, London (B Gazzard, D Hawkins, C Higgs), Homerton Hospital, London (J Anderson, S Mguni), Mortimer Market Centre, London (I Williams, N De Esteban, P Pellegrino, A Arenas-Pinto, D Cornforth*, J Turner*), North Middlesex Hospital (J Ainsworth, A Waters), Royal Free Hospital, London (M Johnson, S Kinloch, A Carroll, P Byrne, Z Cuthbertson), Barts & the London NHS Trust, London (C Orkin, J Hand, C De Souza), St Marys Hospital, London (J Weber, S Fidler, E Hamlyn, E Thomson*, J Fox*, K Legg, S Mullaney*, A Winston, S Wilson, P Ambrose), Birmingham Heartlands Hospital, Birmingham (S Taylor, G Gilleran). Imperial College Trial Secretariat: S Keeling, A Becker. Imperial College DSMC Secretariat: C Boocock. (* Left the study team before the trial ended.).

The HEATHER study is conducted as part of the CHERUB (Collaborative HIV Eradication of Reservoirs: UK BRC) collaboration. (CHERUB Steering Committee: Andrew Lever (University of Cambridge), Mark Wills (University of Cambridge), Jonathan Weber (Imperial College, London), Sarah Fidler (Imperial College, London), John Frater (University of Oxford), Lucy Dorrell (University of Oxford), Mike Malim (King's College, London), Julie Fox (King's College London), Ravi Gupta (University College London), Clare Jolly (University College London). HEATHER Investigators: Julie Fox, Margaret-Anne Bevan, Philip Melling, Tammy Murray (St Thomas' Hospital, London), Sarah Fidler, John Thornhill, Kanta Mahay, Kristin Kuldanek (St Mary's Hospital, London), Nneka Nwokolo, Sathya Visvendra, Rhian Bull (Chelsea and Westminster Hospital, London), Jodi Meyerowitz, Emily Hopkins, Matthew Pace, Matthew Jones, Chan Phetsouphanh (University of Oxford). Additional CHERUB Program Liason Group members: Hanna Box, Caroline Foster (Imperial College, London), Abdel Babiker (MRC Clinical Trials Unit), John Cason (King's College, London)).

Author Contributions

Conceived and designed the experiments: MH NP GEM SH SF JW AB RP CBW JFr. Performed the experiments: GEM SH MH JM NR HB. Analyzed the data: NP JH MH JFr SH GEM. Contributed reagents/materials/analysis tools: NP JH. Wrote the paper: MH NP GEM SK NN JFr SF JFo. Recruited patients: MF JFo SF NN SK.

References

1. Feeney ME, Tang Y, Roosevelt KA, Leslie AJ, McIntosh K, Karthas N, et al. Immune escape precedes breakthrough human immunodeficiency virus type 1 viremia and broadening of the cytotoxic T-lymphocyte response in an HLA-B27-positive long-term-nonprogressing child. J Virol. 2004; 78: 8927–8930. PMID: 15280502

2. Frater AJ, Brown H, Oxenius A, Gunthard HF, Hirschel B, Robinson N, et al. Effective T-cell responses select human immunodeficiency virus mutants and slow disease progression. J Virol. 2007; 81: 6742–6751. PMID: 17409157
3. Goulder P, Price D, Nowak M, Rowland-Jones S, Phillips R, McMichael A. Co-evolution of human immunodeficiency virus and cytotoxic T-lymphocyte responses. Immunol Rev. 1997; 159: 17–29. PMID: 9416500
4. Kiepiela P, Leslie AJ, Honeyborne I, Ramduth D, Thobakgale C, Chetty S, et al. Dominant influence of HLA-B In mediating the potential co-evolution of HIV and HLA. Nature. 2004; 432: 769–774. PMID: 15592417
5. Leslie AJ, Pfafferott KJ, Chetty P, Draenert R, Addo MM, Feeney M, et al. HIV evolution: CTL escape mutation and reversion after transmission. Nat Med. 2004; 10: 282–289. PMID: 14770175
6. Grakoui A, Bromley SK, Sumen C, Davis MM, Shaw AS, Allen PM, et al. The immunological synapse: a molecular machine controlling T cell activation. Science. 1999; 285: 221–227. PMID: 10398592
7. Kalergis AM, Boucheron N, Doucey MA, Palmieri E, Goyarts EC, Vegh Z, et al. Efficient T cell activation requires an optimal dwell-time of interaction between the TCR and the pMHC complex. Nat Immunol. 2001; 2: 229–234. PMID: 11224522
8. Miceli MC, Parnes JR. Role of CD4 and CD8 in T cell activation and differentiation. Adv Immunol. 1993; 53: 59–122. PMID: 8512039
9. Brunet JF, Denizot F, Luciani MF, Roux-Dosseto M, Suzan M, Mattei MG, et al. A new member of the immunoglobulin superfamily—CTLA-4. Nature. 1987; 328: 267–270. PMID: 3496540
10. Lenschow DJ, Bluestone JA. T cell co-stimulation and in vivo tolerance. Curr Opin Immunol. 1993; 5: 747–752. PMID: 7694594
11. Chen L, Flies DB. Molecular mechanisms of T cell co-stimulation and co-inhibition. Nat Rev Immunol. 2013; 13: 227–242. doi: 10.1038/nri3405 PMID: 23470321
12. Day CL, Kaufmann DE, Kiepiela P, Brown JA, Moodley ES, Reddy S, et al. PD-1 expression on HIV-specific T cells is associated with T-cell exhaustion and disease progression. Nature. 2006; 443: 350–354. PMID: 16921384
13. Gruener NH, Lechner F, Jung MC, Diepolder H, Gerlach T, Lauer G, et al. Sustained dysfunction of antiviral CD8+ T lymphocytes after infection with hepatitis C virus. J Virol. 2001; 75: 5550–5558. PMID: 11356962
14. Lechner F, Sullivan J, Spiegel H, Nixon DF, Ferrari B, Davis A, et al. Why do cytotoxic T lymphocytes fail to eliminate hepatitis C virus? Lessons from studies using major histocompatibility complex class I peptide tetramers. Philos Trans R Soc Lond, B, Biol Sci. 2000; 355: 1085–1092. PMID: 11186310
15. Wherry EJ, Ha S-J, Kaech SM, Haining WN, Sarkar S, Kalia V, et al. Molecular signature of CD8+ T cell exhaustion during chronic viral infection. Immunity. 2007; 27: 670–684. PMID: 17950003
16. Zajac AJ, Blattman JN, Murali-Krishna K, Sourdive DJ, Suresh M, Altman JD, et al. Viral immune evasion due to persistence of activated T cells without effector function. J Exp Med. 1998; 188: 2205–2213. PMID: 9858507
17. Blackburn SD, Shin H, Haining WN, Zou T, Workman CJ, Polley A, et al. Coregulation of CD8+ T cell exhaustion by multiple inhibitory receptors during chronic viral infection. Nature Immunology. 2008; 10: 29–37. doi: 10.1038/ni.1679 PMID: 19043418
18. Jones RB, Ndhlovu LC, Barbour JD, Sheth PM, Jha AR, Long BR, et al. Tim-3 expression defines a novel population of dysfunctional T cells with highly elevated frequencies in progressive HIV-1 infection. Journal of Experimental Medicine. 2008; 205: 2763–2779. doi: 10.1084/jem.20081398 PMID: 19001139
19. Petrovas C, Price DA, Mattapallil J, Ambrozak DR, Geldmacher C, Cecchinato V, et al. SIV-specific CD8+ T cells express high levels of PD1 and cytokines but have impaired proliferative capacity in acute and chronic SIVmac251 infection. Blood. 2007; 110: 928–936. PMID: 17440051
20. Trautmann L, Janbazian L, Chomont N, Said EA, Gimmig S, Bessette B, et al. Upregulation of PD-1 expression on HIV-specific CD8+ T cells leads to reversible immune dysfunction. Nat Med. 2006; 12: 1198–1202. PMID: 16917489
21. Hurst J, Hoffmann M, Pace M, Williams JP, Thornhill J, Hamlyn E, et al. Immunological biomarkers predict HIV-1 viral rebound after treatment interruption. Nat Commun. 2015; 6: 8495. doi: 10.1038/ncomms9495 PMID: 26449164
22. Chomont N, Far El M, Ancuta P, Trautmann L, Procopio FA, Yassine-Diab B, et al. HIV reservoir size and persistence are driven by T cell survival and homeostatic proliferation. Nat Med. 2009; 15: 893–900. doi: 10.1038/nm.1972 PMID: 19543283

23. SPARTAC Trial Investigators, Fidler S, Porter K, Ewings F, Frater J, Ramjee G, et al. Short-course antiretroviral therapy in primary HIV infection. N Engl J Med. 2013 ed. 2013; 368: 207–217. doi: 10.1056/NEJMoa1110039 PMID: 23323897

24. Buggert M, Tauriainen J, Yamamoto T, Frederiksen J, Ivarsson MA, Michaëlsson J, et al. T-bet and Eomes are differentially linked to the exhausted phenotype of CD8+ T cells in HIV infection. PLoS Pathog. 2014; 10: e1004251. doi: 10.1371/journal.ppat.1004251 PMID: 25032686

25. Gupta PK, Godec J, Wolski D, Adland E, Yates K, Pauken KE, et al. CD39 Expression Identifies Terminally Exhausted CD8+ T Cells. PLoS Pathog. 2015; 11: e1005177. doi: 10.1371/journal.ppat.1005177 PMID: 26485519

26. Roederer M, Quaye L, Mangino M, Beddall MH, Mahnke Y, Chattopadhyay P, et al. The genetic architecture of the human immune system: a bioresource for autoimmunity and disease pathogenesis. Cell. 2015; 161: 387–403. doi: 10.1016/j.cell.2015.02.046 PMID: 25772697

27. Wei F, Zhong S, Ma Z, Kong H, Medvec A, Ahmed R, et al. Strength of PD-1 signaling differentially affects T-cell effector functions. Proceedings of the National Academy of Sciences of the United States of America. 2013; 110: E2480–E2489. doi: 10.1073/pnas.1305394110 PMID: 23610399

28. Sakuishi K, Jayaraman P, Behar SM, Anderson AC, Kuchroo VK. Emerging Tim-3 functions in antimicrobial and tumor immunity. Trends in Immunology. 2011; 32: 345–349. doi: 10.1016/j.it.2011.05.003 PMID: 21697013

29. Topalian SL, Hodi FS, Brahmer JR, Gettinger SN, Smith DC, McDermott DF, et al. Safety, Activity, and Immune Correlates of Anti–PD-1 Antibody in Cancer. N Engl J Med. 2012; 366: 2443–2454. doi: 10.1056/NEJMoa1200690 PMID: 22658127

30. Brahmer JR, Tykodi SS, Chow LQM, Hwu W-J, Topalian SL, Hwu P, et al. Safety and Activity of Anti–PD-L1 Antibody in Patients with Advanced Cancer. N Engl J Med. 2012; 366: 2455–2465. doi: 10.1056/NEJMoa1200694 PMID: 22658128

31. Giorgi JV, Hultin LE, McKeating JA, Johnson TD, Owens B, Jacobson L. P., et al. Shorter survival in advanced human immunodeficiency virus type 1 infection is more closely associated with T lymphocyte activation than with plasma virus burden or virus chemokine coreceptor usage. J Infect Dis. 1999; 179: 859–870. PMID: 10068581

32. Price P, Keane N, Gray L, Lee S, Gorry PR, French MA. Brief Report: CXCR4 or CCR5 tropism of human immunodeficiency virus type 1 isolates does not determine the immunological milieu in patients responding to antiretroviral therapy. Viral immunology. Mary Ann Liebert, Inc. 2 Madison Avenue Larchmont, NY 10538 USA; 2006; 19: 734–740.

33. Lim AY-F, Price P, Beilharz MW, French MA. Cell surface markers of regulatory T cells are not associated with increased forkhead box p3 expression in blood CD4+ T cells from HIV-infected patients responding to antiretroviral therapy. Immunology and Cell Biology. 2006; 84: 530–536. PMID: 16956389

34. Juno JA, Stalker AT, Waruk JL, Oyugi J, Kimani M, Plummer FA, et al. Elevated expression of LAG-3, but not PD-1, is associated with impaired iNKT cytokine production during chronic HIV-1 infection and treatment. Retrovirology. 2015; 12: 17. doi: 10.1186/s12977-015-0142-z PMID: 25810006

35. Ferris RL, Lu B, Kane LP. Too Much of a Good Thing? Tim-3 and TCR Signaling in T Cell Exhaustion. The Journal of Immunology. 2014; 193: 1525–1530. doi: 10.4049/jimmunol.1400557 PMID: 25086175

36. Jin H-T, Anderson AC, Tan WG, West EE, Ha S-J, Araki K, et al. Cooperation of Tim-3 and PD-1 in CD8 T-cell exhaustion during chronic viral infection. Proceedings of the National Academy of Sciences. 2010; 107: 14733–14738.

37. Youngblood B, Noto A, Porichis F, Akondy RS, Ndhlovu ZM, Austin JW, et al. Cutting edge: Prolonged exposure to HIV reinforces a poised epigenetic program for PD-1 expression in virus-specific CD8 T cells. J Immunol. 2013; 191: 540–544. doi: 10.4049/jimmunol.1203161 PMID: 23772031

38. Paley MA, Kroy DC, Odorizzi PM, Johnnidis JB, Dolfi DV, Barnett BE, et al. Progenitor and terminal subsets of CD8+ T cells cooperate to contain chronic viral infection. Science. 2012; 338: 1220–1225. doi: 10.1126/science.1229620 PMID: 23197535

39. Roederer M. Spectral compensation for flow cytometry: visualization artifacts, limitations, and caveats. Cytometry B Clin Cytom. 2001; 45: 194–205.

40. Simes RJ. An improved Bonferroni procedure for multiple tests of significance. Biometrica. 1986; 73: 751–754.

frontiers in Immunology

ORIGINAL RESEARCH
published: 04 May 2018
doi: 10.3389/fimmu.2018.00928

CD32-Expressing CD4 T Cells Are Phenotypically Diverse and Can Contain Proviral HIV DNA

Genevieve E. Martin[1†], Matthew Pace[1†], John P. Thornhill[1,2†], Chansavath Phetsouphanh[1], Jodi Meyerowitz[1], Morgane Gossez[1], Helen Brown[1], Natalia Olejniczak[1], Julianne Lwanga[3], Gita Ramjee[4], Pontiano Kaleebu[5], Kholoud Porter[6], Christian B. Willberg[1,7], Paul Klenerman[1,7], Nneka Nwokolo[8‡], Julie Fox[3‡], Sarah Fidler[2‡] and John Frater[1,7‡] On Behalf of the CHERUB Investigators*

[1] Peter Medawar Building for Pathogen Research, Nuffield Department of Medicine, University of Oxford, Oxford, United Kingdom, [2] Division of Medicine, Wright Fleming Institute, Imperial College, London, United Kingdom, [3] Department of Genitourinary Medicine and Infectious Disease, Guy's and St Thomas' NHS Foundation Trust, London, United Kingdom, [4] HIV Prevention Research Unit, South African Medical Research Council, Durban, South Africa, [5] Uganda Virus Research Institute (MRC), Entebbe, Uganda, [6] Research Department of Infection and Population Health, University College London, London, United Kingdom, [7] NIHR Biomedical Research Centre, University of Oxford, Oxford, United Kingdom, [8] Chelsea and Westminster Hospital, London, United Kingdom

OPEN ACCESS

Edited by:
Guido Poli,
Vita-Salute San Raffaele University, Italy

Reviewed by:
Mirko Paiardini,
Emory University School of Medicine, United States
Paul Urquhart Cameron,
University of Melbourne, Australia

***Correspondence:**
John Frater
john.frater@ndm.ox.ac.uk

[†]These authors have contributed equally to this work.

[‡]These authors have contributed equally as co-senior authors.

Specialty section:
This article was submitted to Viral Immunology, a section of the journal Frontiers in Immunology

Received: 01 March 2018
Accepted: 16 April 2018
Published: 04 May 2018

Citation:
Martin GE, Pace M, Thornhill JP, Phetsouphanh C, Meyerowitz J, Gossez M, Brown H, Olejniczak N, Lwanga J, Ramjee G, Kaleebu P, Porter K, Willberg CB, Klenerman P, Nwokolo N, Fox J, Fidler S and Frater J (2018) CD32-Expressing CD4 T Cells Are Phenotypically Diverse and Can Contain Proviral HIV DNA. Front. Immunol. 9:928. doi: 10.3389/fimmu.2018.00928

Efforts to both characterize and eradicate the HIV reservoir have been limited by the rarity of latently infected cells and the absence of a specific denoting biomarker. CD32a (FcγRIIa) has been proposed to be a marker for an enriched CD4 T cell HIV reservoir, but this finding remains controversial. Here, we explore the expression of CD32 on $CD3^+CD4^+$ cells in participants from two primary HIV infection studies and identify at least three distinct phenotypes ($CD32^{low}$, $CD32^+CD14^+$, and $CD32^{high}$). Of note, CD4 negative enrichment kits remove the majority of $CD4^+CD32^+$ T cells, potentially skewing subsequent analyses if used. $CD32^{high}$ CD4 T cells had higher levels of HLA-DR and HIV co-receptor expression than other subsets, compatible with their being more susceptible to infection. Surprisingly, they also expressed high levels of CD20, TCRαβ, IgD, and IgM (but not IgG), markers for both T cells and naïve B cells. Compared with other populations, $CD32^{low}$ cells had a more differentiated memory phenotype and high levels of immune checkpoint receptors, programmed death receptor-1 (PD-1), Tim-3, and TIGIT. Within all three $CD3^+CD4^+CD32^+$ phenotypes, cells could be identified in infected participants, which contained HIV DNA. CD32 expression on CD4 T cells did not correlate with HIV DNA or cell-associated HIV RNA (both surrogate measures of overall reservoir size) or predict time to rebound viremia following treatment interruption, suggesting that it is not a dominant biomarker for HIV persistence. Our data suggest that while $CD32^+$ T cells can be infected with HIV, CD32 is not a specific marker of the reservoir although it might identify a population of HIV enriched cells in certain situations.

Keywords: HIV, reservoir, CD32, primary HIV infection, HIV DNA

INTRODUCTION

A cure for HIV infection is contingent on targeting and neutralizing latently infected cells that persist despite effective antiretroviral therapy (ART). These cells are predominantly resting memory CD4 T cells containing transcriptionally silent, integrated proviral HIV DNA. Activation of these cells results in HIV production and disease progression in the absence of ART. Latently infected cells

are extremely rare (0.0001–0.1% of CD4 T cells), complicating their study. Accordingly, there has been a research effort to identify cell surface markers that identify latently infected cells to facilitate their characterization and targeting. For example, immune checkpoint receptors (ICRs) (1) such as programmed death receptor-1 (PD-1), T cell immunoglobulin (Ig) and mucin domain-containing molecule (Tim)-3, and T cell immunoreceptor with Ig and ITIM domains (TIGIT) are associated with an exhausted effector state (2–5), and their expression correlates with HIV disease progression and viral rebound following treatment interruption (TI) (4, 6, 7). ICRs have been reported to be highly expressed on cells comprising the HIV reservoir (8, 9), but are not discriminatory.

CD32a (FcγRIIa)—a low-affinity IgG receptor expressed on myeloid cells and granulocytes (10), has been proposed as a surface marker for latent HIV infection (11). While this finding is of extremely high interest, the expression of CD32 on CD4 T cells remains controversial, and a role for low-affinity Fc receptors on CD4 T cells has not been well-established (12–14). Although CD4 T cells are generally not considered to express CD32, expression may be induced by activation *in vitro* (15, 16). Expression of CD32b on memory CD8 T cells in murine infection models is associated with reduced cytotoxicity and expansion, reversible on CD32b blockade (17). This has interesting parallels with other co-inhibitory pathways, raising the possibility that CD32 isoforms may have a similar regulatory role on activated, antigen experienced CD4 T cells.

Here, we investigate CD32 expression on $CD3^+CD4^+$ cells and identify distinct populations that express this marker. We also characterize CD32-expressing CD4 T cells in the blood of individuals treated during primary HIV infection (PHI) [a group of interest due to an association with post treatment virological remission and a more labile reservoir (18–20)] and explore associations with overall reservoir size, cell phenotype, and clinical progression.

MATERIALS AND METHODS

Participants

Participants with PHI were recruited as part of the HEATHER (HIV Reservoir targeting with Early Antiretroviral Therapy) cohort. PHI was identified through one of the following criteria: (a) HIV-1 positive antibody test within 6 months of a HIV-1 negative antibody test, (b) HIV-1 antibody negative with positive PCR (or positive p24 Ag or viral load detectable), (c) RITA (recent incident assay test algorithm) assay result consistent with recent infection, (d) equivocal HIV-1 antibody test supported by a repeat test within 2 weeks showing a rising optical density, and (e) having clinical manifestations of symptomatic HIV seroconversion illness supported by antigen positivity. For inclusion in the cohort, participants with identified PHI commenced ART within 3 months of diagnosis and did not have co-infection with hepatitis B or C. Date of seroconversion was estimated as the midpoint of the dates of the most recent negative or equivocal test and positive test (criteria a and d above), the date of the test (b and e) or 120 days before the test date (c, the recency period of this assay). For our study, cryopreserved peripheral blood mononuclear cells (PBMCs) were used from the closest pre-therapy sample to seroconversion (baseline) and from a sample 9–15 months after commencement of ART (1 year).

Time to rebound analyses was conducted with a subset of participants from the SPARTAC (Short Pulse Antiretroviral Therapy at HIV Seroconversion) trial (EudraCT Number: 2004-000446-20). This was a multicenter, randomized controlled trial of short course ART during PHI, the full design of which is described elsewhere (21). The criteria used to define PHI in this trial are similar to above. In brief, this trial enrolled adults with PHI from 25 sites in Australia, Brazil, Ireland, Italy, South Africa, Spain, Uganda, and the UK. Participants with PHI were randomized to receive no immediate ART (standard of care), 12 or 48 weeks of ART, after which they underwent a TI. The primary trial endpoint was a composite of CD4 T cell count less than 350 cells/μL or the initiation of long-term ART for any reason. Cryopreserved PBMCs were used from participants who received 48 weeks of ART and were virologically suppressed to <400 copies/mL at the time of TI. Participants were included based on sample availability at the time of TI, and date of seroconversion was estimated as calculated previously (7).

Flow Cytometry and Cell Sorting

Cryopreserved PBMCs were thawed in RPMI-1640 medium supplemented with 10% FBS, L-glutamine, penicillin, and streptomycin (R10) containing 2.7 Kunitz units/mL of DNAse (Qiagen). For analysis of memory phenotype and ICR expression, cells were stained in BD Horizon Brilliant Stain Buffer (BD) containing all antibodies and Live/Dead Near IR at 1 in 300 dilution (Life Technologies) at 4°C for 30 min. PBMCs were stained with the following antibodies: CD32 PE-Cy7 (FUN-2), CD3 Brilliant Violet (BV) 570 (UCHT1), CCR7 Pacific Blue (G043H7), CD27 AlexaFluor700 (M-5271) (all BioLegend), CD4 BV605 (RPA-T4), CD8 BV650 (RPA-T8) (BD), PD-1 PE-eFluor 610 (eBioJ105), CD45RA FITC (HI100), TIGIT PerCP-eFluor710 (MBSA43) (all eBioscience), and Tim-3 PE (344823) (R&D). Isotype controls for CD32 were prepared using an irrelevant IgG2bκ antibody (MPC-11) (BioLegend). For time to rebound analyses, cells were stained as above in PBS with 5% FBS and 1 mM EDTA (FACS buffer) containing Live/Dead Near IR, CD32 PE-Cy7, PD-1 PE-eFluor610, TIGIT PerCP-eFluor710 as well as the following antibodies: CD3 FITC (UCHT1) (BioLegend) and CD4 eFluor450 (OKT4) (eBioscience). For measurement of HLA-DR expression, cells were stained for 20 min at room temperature with LiveDead Near IR and the following antibodies: CD3 BV570, CD4 BV605, CD8 BV650, CD32 PE (FUN-2) (BioLegend) and HLA-DR AlexaFluor700 (MAB) (BD). Samples for HIV co-receptor stains were stained with LiveDead Near IR, CD32 PE-Cy7, CD3 FITC, and CD4 eFluor450. Following this, cells were incubated at 37°C for 20 min with anti-CCR5 PE (C57BL/6) (BD) or at 4°C for 30 min with anti-CXCR4 APC (12G5) (Miltenyi).

For measurement of lineage marker expression on CD32-expressing CD4 T cells, PBMCs were stained as above in R10 with antibodies as listed in Panels 1–6 below. A CD32 isotype control was used as above, and gates for lineage markers were determined using a fluorescence minus one or the positive population from bulk PBMC.

Panel 1—CD11b, CD16, CD19, CD20, CD123, and TCRγδ staining. PBMCs were stained with LiveDead Near IR, CD3 AlexaFluor700 (UCHT1), CD4 APC (RPA-T4) (both BioLegend), CD32 PE-Cy7, CD14 VioBlue (TUK4) (Miltenyi), either CD11b FITC (M1/70.15.11.5) (Miltenyi), CD16 FITC (CB16) (eBioscience), CD19 FITC (LT19) (Miltenyi), CD20 FITC (2H7) (BioLegend), CD123 PE (9F5) (BD Bioscience) or TCRγδ PE (11F2) (Miltenyi).
Panel 2—CD8, CD15, CD56 staining. PBMCs were stained with LiveDead Near IR, CD3 AlexaFluor700, CD4 APC, CD32 PE-Cy7, and CD14 FITC (HCD14) (BioLegend) and CD8 eFluor450 (OKT8), CD15 Pacific Blue (W6D3), or CD56 BV421 (HCD56) (all BioLegend).
Panel 3—CD235a staining. PBMCs were stained with Fixable Viability Dye eFluor 506 (eBioscience), CD3 FITC, CD4 APC, CD32 PE-Cy7, CD14 VioBlue, and CD235a APC-Cy7 (HI264) (BioLegend).
Panel 4—CD36 staining. PBMCs were stained with LiveDead Near IR, CD3 FITC, CD32 PE-Cy7, CD4 AlexaFluor700 (SK3) (BioLegend), CD14 VioBlue, and CD36 APC (AC106) (Miltenyi).
Panel 5—TCR αβ staining. PBMCs were stained with LiveDead Near IR, CD3 FITC, CD4 APC, CD32 PE, and CD14 VioBlue. Cells were then permeabilized using BD FACS Permeabilizing solution 2 as per the manufacturer's protocol before washing and staining with TCR αβ PE-Cy7 (IP26) (BioLegend).
Panel 6—Ig staining. PBMCs were stained with LiveDead Near IR, CD3 AlexaFluor700, CD4 APC, CD32 PE-Cy7, CD14 VioBlue, CD20 FITC and IgD PE (IA6-2), IgG PE (HP6017), or IgM PE (MHM-88) (all BioLegend).

Phenotyping of fresh lymphocytes was performed within 3 h of blood collection using 1 mL of ACD anticoagulated blood. Erythrocytes were lysed at 4°C for 10 min in 10 mL of ammonium-chloride-potassium (ACK) buffer (Gibco) and washed before staining in FACS buffer as above using Panel 1.

All samples were acquired on an LSR II (BD). The same machine was used for all experiments with daily calibration with Cytometer Setup and Tracking beads (BD) to maximize comparability between days. Rainbow Calibration Particles (BioLegend) were also used for cohort phenotyping to minimize batch-to-batch variability. Data were analyzed using FlowJo Version 10.8.0r1 (Treestar). In some cases for the $CD32^{high}$ populations, cell numbers were very low. To ensure accuracy in the phenotyping of this population, any populations where there were five or fewer events were excluded from further phenotyping analyses. (Of note, the overall phenotype of this population did not change if this threshold was changed to fewer than 25 or 50 events.)

For sorting experiments, thawed PBMCs or tonsillar cells were stained in R10 at 4°C using Live/Dead Near IR, CD32 PE-Cy7, CD3 FITC and either (a) CD4 APC and CD14 VioBlue or (b) CD4 eFluor450. Cells were sorted using a Mo-Flo XDP into four $CD3^+CD4^+$ populations: $CD32^-$, $CD32^{low}$, $CD32^+CD14^+$, and $CD32^{high}$ cells.

CD4 Isolation Using EasySep Kit

Peripheral blood mononuclear cells were thawed as above. For Fc blocking experiments, this was split into two aliquots. One aliquot was treated for 10 min at room temperature with Human TruStain FcX (BioLegend) according to the manufacturer's protocol while the other was left untreated. A fraction of each aliquot was removed for CD32 staining. The remainder was used for CD4 enrichment *via* negative selection with the EasySep Human CD4 Enrichment Kit (StemCell) per the manufacturer's protocol. PBMCs or enriched CD4s were stained as above with Live/Dead Near IR, CD32 PE-Cy7, CD3 FITC, and CD4 eFluor450.

Measurement of HIV DNA

For measurement of HIV DNA in bulk CD4 T cells, CD4 T cells were enriched from cryopreserved PBMCs as above or using Dynabeads Untouched Human CD4 T Cell Enrichment kit (Invitrogen). DNA was extracted from PBMCs or enriched CD4 T cells (using QIAamp Blood Mini Kit, Qiagen) and sorted CD4 T cell subsets (using QIAamp DNA Micro Kit or Mini Kit, both Qiagen) for use as input for qPCR assays. Copies of HIV-1 DNA were quantified and normalized to number of input cells (as determined by albumin PCR), by a previously described assay (22, 23) with both qPCR assays performed in triplicate. For sorted populations, PCR reactions for both albumin and total HIV were performed in triplicate for the $CD32^-$ population and in duplicate for the remaining populations, except where otherwise noted. Negative sample wells were replaced with zeros when averaging replicate values.

Unspliced HIV-RNA Transcript Quantitation

RNA was isolated using the Qiagen AllPrep DNA/RNA Mini kit as per the manufacturer's recommendations with the addition of two on-column double DNase digestions. The RNA assay performed as previously described (6). Briefly, complementary DNA was subjected to two rounds of PCR using semi-nested primers. The first reaction was a 15-cycle endpoint reaction using MH535 (5′-AACTAGGGAACCCACTGCTTAAG-3′) and SL20 (5′-TCTCCTTCTAGCCTCCGCTAGTC-3′) primers at a concentration of 400 nM each. The second reaction was a 40-cycle quantitative reaction (forward primer 5′-TAAAGCTTGCCTTG AGTGCT, SL20 and the probe FAM—5′-AGTRGTGTGTG CCCGTCTGTTG-3′—BHQ-1; 330 nM each), performed using a Roche Lightcycler 480. The HIV standard was generated by *in vitro* transcribing the plasmid Sp5-NL4.3 (generously provided by the lab of D. Purcell) using the RiboMax Large Scale SP6 RNA production System (Promega). HIV RNA standards were diluted in 10 ng/μL uninfected PBMC RNA. Any background from wells without reverse transcriptase was subtracted from final measurements. HIV RNA copies were normalized to RNA weight measured *via* Nanodrop.

Statistical Analysis

Continuous variables were compared between groups using non-parametric tests throughout. Where three groups were compared, a Kruskal–Wallis test was used; pairwise comparisons were performed on all combinations of groups only if the overall test p-value was <0.05. Correlative analyses were performed using Spearman's rank correlation. Time to viral rebound was

assessed as time from TI to the first of two consecutive VL measurements >400 copies/mL (the limit of detection of the assay used at some trial sites). Individuals who did not rebound were censored at the date of the last VL measurement. Time to viral rebound was visualized with Kaplan–Meier curves stratified at the median and associations examined using Cox proportional hazard models. Analyses were performed using GraphPad Prism (GraphPad Software, La Jolla, CA, USA) version 6.0f or R version 3.2.2.

RESULTS AND DISCUSSION

Depletion of CD32-Expressing CD4 T Cells by Negative Bead Selection due to the Expression of Non-T Cell Markers

The experimental study of CD4 T cells frequently incorporates a commercial bead-based negative selection kit in the laboratory protocol to produce a purified population of CD4 T cells from

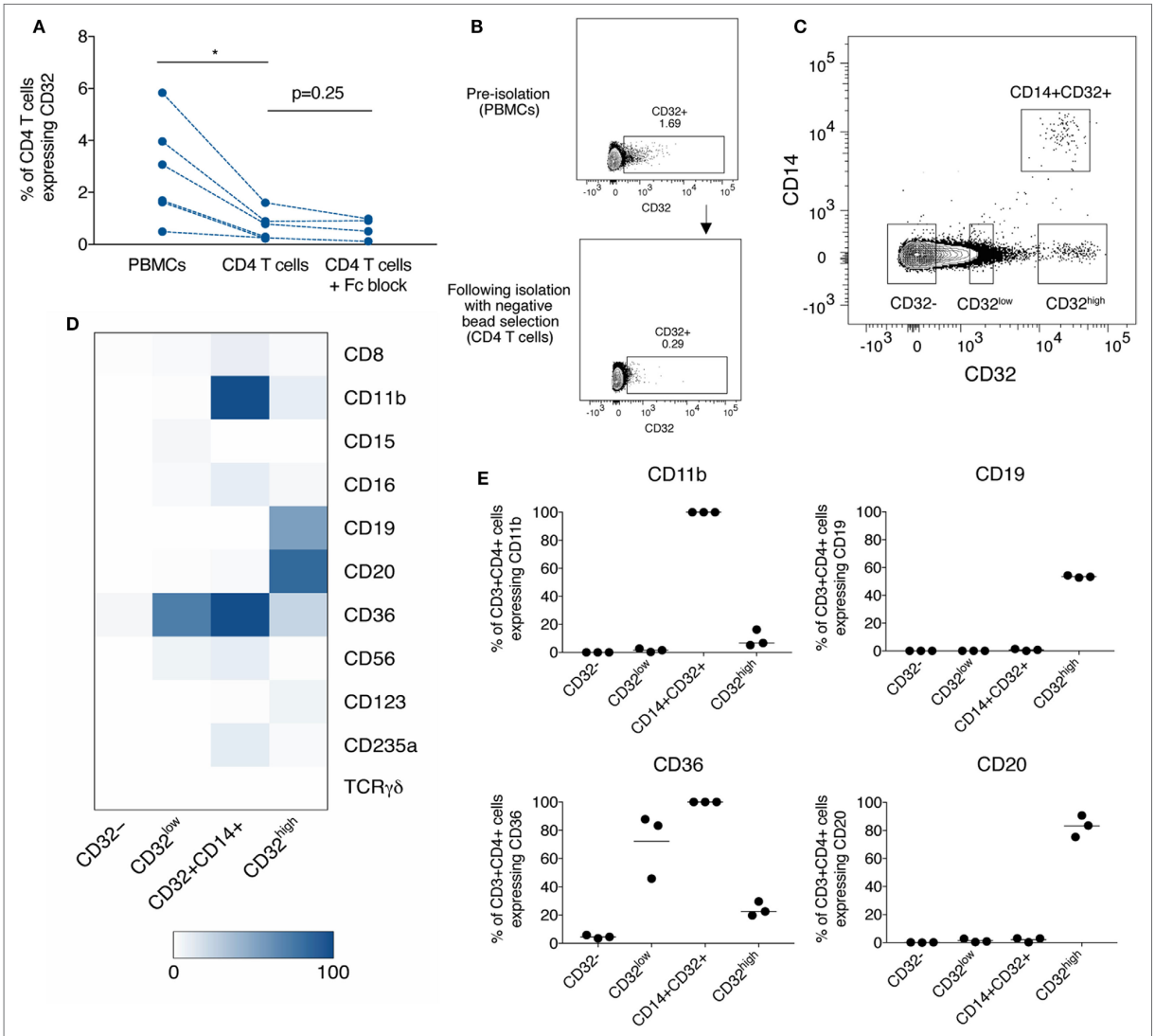


FIGURE 1 | Depletion of diverse populations of CD32-expressing CD4 T cells by negative bead selection due to the expression of non-T cell markers. **(A)** The frequency of $CD32^+CD3^+CD4^+$ T cells when measured in peripheral blood mononuclear cells (PBMCs), or in CD4 T cells purified by negative bead selection, with and without Fc block prior. **(B)** Representative gating of data shown in panel **(A)**. **(C)** Gating of three CD32-expressing populations based on differing levels of expression and CD14: $CD32^{low}$, $CD32^+CD14^+$, and $CD32^{high}$. **(D)** Heat-map showing the percentage expression of markers used in CD4 negative bead isolation kits on subsets of $CD3^+CD4^+$ T cells [defined in panel **(C)**]. Expression was measured by flow cytometry, and values are shown as the mean of three individual donors. **(E)** Percentage expression of CD11b, CD19, CD36, and CD20 on $CD3^+CD4^+$ subpopulations as shown in panel **(D)**. Bar is shown at the mean.

bulk PBMCs. We identified that CD32 expression on purified CD4 T cells isolated by negative bead selection was consistently lower than in CD4 T cells in PBMCs. To test if the cell purification kits depleted CD32-expressing CD4 T cells, we compared frequencies of CD32$^+$CD4 T cells before and after negative selection by flow cytometry. We found a significant decrease in CD32 expression after negative selection (**Figures 1A,B**), which was not prevented by pre-treatment with an Fc blocking reagent to control for non-specific antibody binding (**Figure 1A**).

As these data suggested that CD32$^+$CD4 T cells express other surface molecules specifically depleted by the negative selection kit (which does not contain anti-CD32 antibodies), we looked for co-expression with CD32 of a panel of lineage-defining markers used in CD4 T cell selection kits from several manufacturers. These were as follows: CD8, CD11b, CD14, CD15, CD16, CD19, CD20, CD36, CD56, CD123, TCRγδ, and CD235a.

The monocyte marker, CD14, distinguished a separate population of CD32$^+$CD14$^+$ cells. The remaining CD14$^-$CD32$^+$ cells could be divided into two distinct populations, CD32^{low} and CD32^{high} (**Figure 1C**). We therefore further characterized lineage marker expression in these four populations—CD32$^-$, CD32^{low}, CD32^{high}, and CD32$^+$CD14$^+$ and found clear phenotypic differences, consistent with four distinct cell populations (**Figure 1D**; Figure S1 in Supplementary Material). CD32$^-$CD4 T cells did not express significant levels of any tested lineage markers. CD32$^+$CD14$^+$ cells all expressed CD11b (**Figure 1E**) and were found almost entirely within a monocyte-rich FSC/SSC region (Figure S2 in Supplementary Material), consistent with these cells being monocytes despite high levels of CD3 expression. It is possible that these cells are monocytes which have acquired CD3 *via* trogocytosis. The CD32^{low} population expressed high levels of CD36 (**Figure 1E**), a scavenger receptor typically found on platelets and monocytes in blood but which has also been reported on CD4 T cells interacting with platelets (24). The CD32^{high} cells expressed high levels of CD19 and CD20, traditional markers of B cells (**Figure 1E**; representative staining in Figures S1B,C in Supplementary Material).

We focused on further characterization of the CD32^{high} population, which has been reported to have the highest level of persistent HIV infection (11). As these cells also expressed CD3, CD4, CD19, and CD20, we were interested to see whether these cells expressed other markers associated with B or T cell lineage and function. To confirm that cells expressing CD3, CD4, and CD32 were T cells, we stained for TCRαβ expression. As we would expect for T cell populations, the CD32$^-$, CD32^{low}, and CD32^{high} populations all expressed similar levels of TCRαβ, while the CD32$^+$CD14$^+$ cells expressed very little, consistent with this subpopulation being monocytes (**Figures 2A,B**). We examined the expression of IgG, IgD, and IgM on the CD32^{high} cells. We found the CD32^{high}

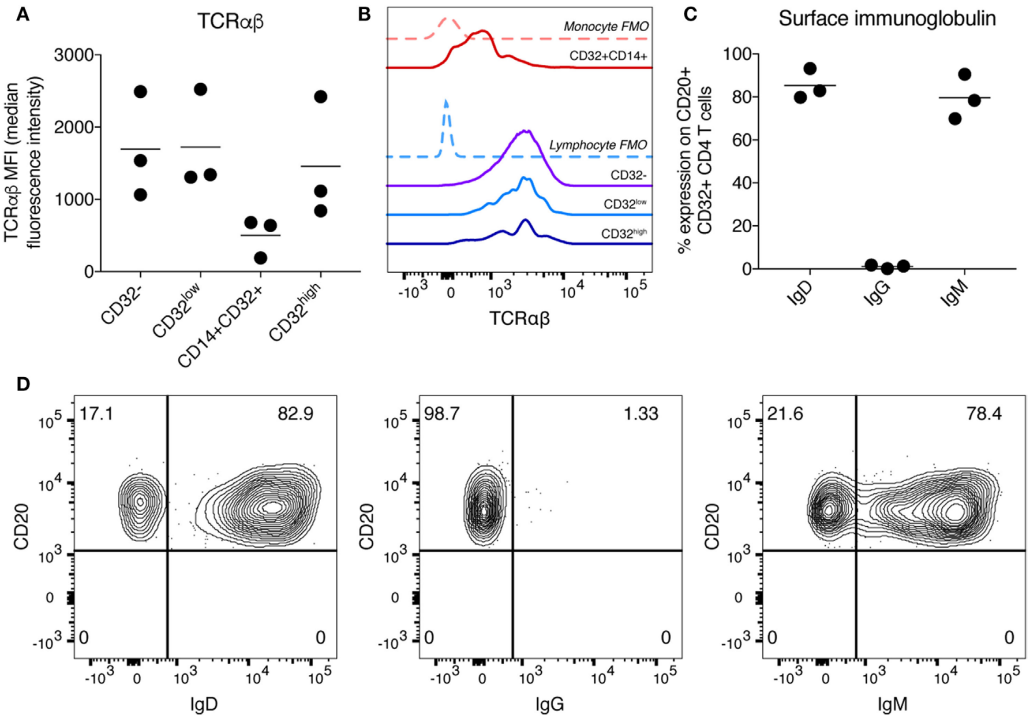


FIGURE 2 | Characterization of T cell receptor and immunoglobulin (Ig) expression on CD32^{high}CD3$^+$CD4$^+$ T cells. **(A)** Expression of TCRαβ on CD32-expressing CD3$^+$CD4$^+$ T cell populations was measured by flow cytometry and is shown here as median fluorescence intensity. Bar is shown at the mean. **(B)** Histogram showing TCRαβ staining on CD32-expressing CD3$^+$CD4$^+$ T cell populations of one sample shown in panel **(A)**. Fluorescence minus one (FMO) controls are shown as dashed lines and individual populations as solid lines. **(C)** Percentage expression of Ig was measured on CD3$^+$CD4$^+$CD32^{high}CD20$^+$ cells. Expression of IgD, IgG, and IgM is shown. Expression was measured by flow cytometry, and bar is shown at the mean. **(D)** Representative staining of data shown in panel **(C)**.

population, which co-express CD20 and TCRαβ, expressed high levels of IgD and IgM, but not IgG, similar to a naïve B cell phenotype (25) (**Figures 2C,D**). These results, surprisingly, show that the CD32^{high} population express both T and B cell phenotypic markers. While rare, CD20-expressing T cells populations have been described in healthy individuals and in a number of non-malignant disease states (26–31). Of note, the cells we described differ from these reports which generally expressed CD20 but not CD19.

Other investigators noting CD3 and CD20 co-expression have attempted to determine if this finding might be artefactual and secondary to contamination, cell doublets, cryopreservation or cell separation techniques (26, 31). Accordingly, for all experiments, cells were tightly gated on singlets (as shown in Figure S3A in Supplementary Material), to minimize the possibility of a doublet artefact in our data. Of note, performing a second doublet exclusion step does not change the frequency or phenotype of these cells (Figure S3B in Supplementary Material). To exclude the possibility that this phenotype was an artefact of density gradient separation or cryopreservation of PBMCs we stained fresh, whole blood from healthy donors and observed a similar pattern of CD32 and CD20 co-expression on CD3$^+$CD4$^+$ cells (Figure S4 in Supplementary Material).

Overall, these results have clear implications for those exploring the findings of Descours et al (11) as negative bead isolation of CD4 T cells will not only reduce the overall number of CD32$^+$CD3$^+$CD4$^+$ cells but also affect the composition of the overall CD32-expressing population.

TABLE 1 | Demographic and clinical characteristics of participants included in clinical studies.

	HEATHER (n = 20)[a]	SPARTAC (n = 19)[b]
Sex		
• Male	20 (100%)	5 (26%)
Age	33 (28–40.8)	27 (22–40)
Country		
• UK	20 (100%)	4 (21%)
• South Africa/Uganda	0	13 (68%)
• Other	0	2 (11%)
Time between estimated date of seroconversion and antiretroviral therapy (ART) initiation (days)	41.5 (22.5–55.3)	109 (76–124)
Time of sampling (weeks since ART initiation)	52.5 (52.0–57.6)	47.9 (47.6–48.0)
Baseline CD4 T cell count (cells/μL)	514 (376–628)	634 (535–764)
Baseline HIV RNA (log_{10} copies/mL)	6.32 (4.55–6.76)	4.32 (3.68–4.95)

Demographic and clinical characteristics of participants included in clinical studies. Values given represent n (%) for categorical variables and median (interquartile range) for continuous variables.

*[a]Data from these individuals contribute to **Figures 3A–E** and **5A,C** and Figures S5A–D, S6A, S9, and S10 in Supplementary Material.*

*[b]Data from these individuals contribute to **Figure 5** and Table S4 in Supplementary Material.*

CD32-Expressing CD3$^+$CD4$^+$ Cells Differ in Their Expression of ICRs and Memory Phenotype

We further explored the phenotype of CD32-expressing CD4$^+$ populations in individuals who commenced ART during PHI from the HEATHER (7) cohort. Key demographic and clinical characteristics are shown in **Table 1**. In these individuals, we studied both CD32^{low} and CD32^{high}CD3$^+$CD4$^+$ populations separately without using cell enrichment kits (representative gating shown in **Figure 3A**) and imposing a conservative lymphocyte gate to eliminate the CD32$^+$CD14$^+$ population (Figure S2 in Supplementary Material, with doublet exclusion as in Figure S3C in Supplementary Material).

The expression of the ICRs PD-1 and TIGIT has been reported to mark a population of CD3$^+$CD4$^+$ T cells enriched for HIV DNA, although the fold enrichment in HIV DNA is substantially lower than described for CD32 (8, 9, 11). We found that in treated HIV$^+$ individuals, the expression of PD-1, Tim-3, and TIGIT was elevated on CD32^{low} CD3$^+$CD4$^+$ cells compared with their CD32$^-$ and CD32^{high} counterparts (**Figures 3B–D**).

We compared the memory phenotype of CD32$^-$, CD32^{low}, and CD32^{high} CD3$^+$CD4$^+$ cell subsets during treated PHI. CD32^{low}CD4 T cells had lower proportions of naïve and central memory (T_{CM}) T cells than their CD32$^-$ counterparts. By contrast, transitional memory (T_{TM}), effector memory (T_{EM}), and T_{EMRA} cells comprised a greater portion of the CD32^{low} CD4 T cell pool than for CD32$^-$CD4 T cells (**Figure 3E**), reflecting a more differentiated memory phenotype. By contrast, the CD32^{high} population was largely comprised of cells which expressed CD45RA marking a naïve or T_{EMRA} phenotype. It is interesting that central memory cells—the memory subset with the highest level of proviral DNA (9, 32)—were most common among CD32$^-$ cells and less frequent among both CD32^{low} and CD32^{high} cells. Furthermore, CD32^{high} cells contained lower levels of PD-1, Tim-3, and TIGIT than CD32^{low} cells suggesting that this may be a distinct population of HIV-infected cells than those enriched ICR expressing populations (8, 9, 11).

The overall phenotype of these cells did not differ between participant groups. This same pattern of ICR expression was observed before ART initiation (Figures S5A–C in Supplementary Material) and in healthy controls (Figures S5E–G in Supplementary Material), except for Tim-3 which was expressed at very low levels in CD4 T cells from controls. Similarly, these cells had the same memory phenotype before ART initiation (Figure S6A in Supplementary Material) and in healthy controls (Figure S6B in Supplementary Material). The distinct phenotype of CD32$^-$, CD32^{low}, and CD32^{high} populations with regards to memory differentiation and ICR expression adds to the lineage marker evidence that these are distinct cellular populations and are found in healthy as well as HIV-infected individuals.

CD32^{high} CD3$^+$CD4$^+$ T Cells Are Activated and Express High Levels of HIV Co-Receptors

Among treated HIV-infected individuals (n = 19, Table S1 in Supplementary Material) CD32^{high} CD3$^+$CD4$^+$ cells expressed markedly elevated levels of the activation marker HLA-DR compared with both other populations (**Figure 3F**; also shown at baseline in Figure S5D in Supplementary Material). In healthy controls, the expression of CCR5 and CXCR4, the co-receptors

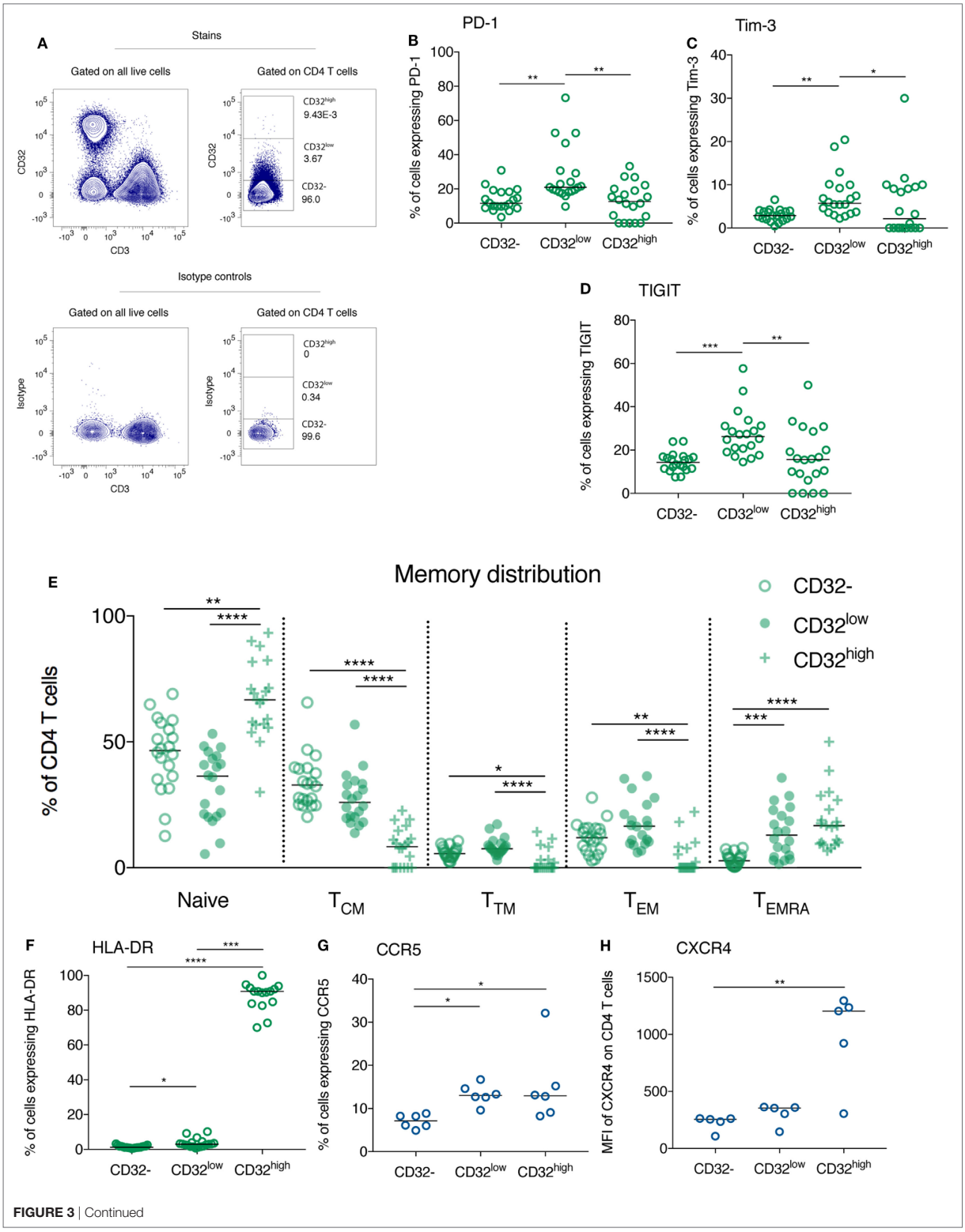


FIGURE 3 | Continued

FIGURE 3 | CD32-expressing $CD3^+CD4^+$ cells differ in their expression of immune checkpoint receptors, the activation marker HLA-DR and HIV co-receptors, as well as their memory phenotype. Representative gating of CD32-expressing populations on CD4 T cells from an HIV^+ individual is shown (top panel) in panel **(A)**, relative to isotype control (bottom panel). $CD32^-$, $CD32^{low}$, and $CD32^{high}CD3^+CD4^+$ T cell populations were compared with regards to their expression of programmed death receptor-1 (PD-1) **(B)**, Tim-3 **(C)**, TIGIT [**(D)**; all $n = 20$], and HLA-DR [**(F)**, $n = 19$]. For panel **(F)**, four samples were excluded from the analysis of the $CD32^{high}$ population because there were five or fewer events. These same populations were compared with regards to their memory phenotype. The percentage of each population composed of naïve ($CD45RA^+CCR7^+$), central memory (T_{CM}; $CD45RA^-CCR7^+$), transitional memory (T_{TM}; $CD45RA^-CCR7^-CD27^+$), effector memory (T_{EM}; $CD45RA^-CCR7^-CD27^-$), and T_{EMRA} cells ($CD45RA^+CCR7^-$) was quantified by flow cytometry and is shown in panel **(E)** ($n = 20$). The comparisons are all shown in HIV^+ individuals at 1 year following the initiation of antiretroviral therapy. The expression of HIV co-entry receptors CCR5 [**(G)**; $n = 6$] and CXCR4 [**(H)**; $n = 5$] was compared between $CD32^-$, $CD32^{low}$, and $CD32^{high}CD3^+CD4^+$ T cell populations in healthy individuals. Throughout, a Kruskal–Wallis test was used to compare all three groups; pairwise comparisons were performed on all combinations of groups only if the overall test p-value was < 0.05; $^{****}p < 0.0001$, $^{***}p = 0.0001$–0.001, $^{**}p = 0.001$–0.01, $^{*}p = 0.01$–0.05; for ease of interpretation if $p \geq 0.05$ for any comparison this is not shown on these plots.

used by HIV for cellular entry, was increased on $CD32^{high}CD4$ T cells (**Figures 3G,H**). For CCR5, this was also observed on the $CD32^{low}$ population.

The HIV reservoir is considered to be comprised of resting CD4 T cells (9, 33–35). The elevated expression of the activation marker HLA-DR on CD32-expressing CD4 T cells observed here is, therefore, potentially surprising. This finding is, however, consistent with two recent reports of elevated HLA-DR on bulk $CD32^+CD4$ T cells from HIV-infected individuals (36, 37). Upregulation of CD32 expression on CD4 T cells with *in vitro* activation has been previously reported (15, 16), and it is possible that CD32 expression might mark a more activated subpopulation of CD4 T cells. This, rather than upregulation upon viral integration, could explain the increased frequency of $CD32^{high}$ cells observed during PHI (**Figure 5A**). Activated CD4 T cells are preferentially infected with HIV but rapidly die; the HIV reservoir is thought to form from cells that are infected while activated and then transition to a resting state (35, 38, 39), or while undergoing this transition (40). It is possible that with high cellular activation and high co-receptor expression, $CD32^{high}$ cells might be more susceptible to infection with HIV. Whether these cells are able to persist and contribute to long-term latency remains unclear.

HIV DNA in CD32-Expressing $CD3^+CD4^+$ Cell Subsets

In initial experiments using negative selection beads, sorting CD4 T cells into $CD32^+$ and $CD32^-$ fractions revealed an enrichment of HIV DNA in $CD32^+$ cells from individuals who commenced ART during PHI (clinical characteristics in Table S1 in Supplementary Material; sort strategy in Figure S7A in Supplementary Material) (41). As well as concerns detailed above over the impact of the negative selection beads, we also determined that for individuals with extremely low yields of sorted $CD32^+CD3^+CD4^+$ cells, low cell inputs into the qPCR resulted in over-estimation of both albumin and HIV DNA (Figure S8 in Supplementary Material), which would need to be accounted for when comparing different cell populations. We, therefore, re-analyzed these data (Table S2 in Supplementary Material) accounting for assay cell input (which was lower for the $CD32^+$ compared with the $CD32^-$ populations) and the number of positive qPCR replicates, and found that HIV DNA could still be detected within $CD32^+CD4$ T cells, with some evidence for enrichment. All qPCR assays performed on sorted DNA included control wells without DNA template, which were consistently negative. To show that low inputs of HIV DNA did not give false positive signals, we diluted sorted $CD32^-$ HIV DNA such that each well contained <1 copy of HIV DNA and found no detectable signal in 21 wells ($n = 3$ individuals, 2 or 3 triplicate dilutions per individual; from experiments in Figure S8B in Supplementary Material).

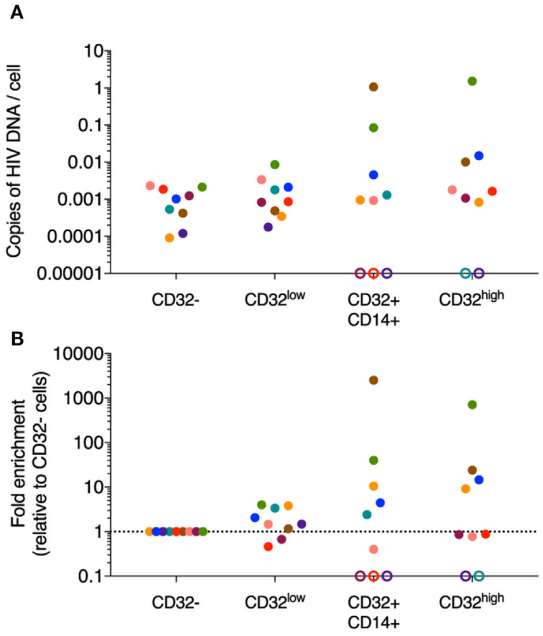


FIGURE 4 | HIV DNA quantification in sorted CD32-expressing $CD3^+CD4^+$ T cell populations. HIV DNA was quantified in sorted $CD32^-$, $CD32^{low}$, $CD32^+CD14^+$, and $CD32^{high}$ $CD3^+CD4^+$ T cell populations by qPCR ($n = 9$). **(A)** Shows the absolute quantification of these data and **(B)** shows the fold change relative to the $CD32^-$ population. Copies of HIV-1 DNA were quantified and normalized to number of input cells (as determined by albumin PCR). PCR reactions for both albumin and total HIV were performed in triplicate for the $CD32^-$ population and in duplicate for the remaining three populations. Data shown are averages of the replicates. Data points are colored by the individual from which the population was sorted. Where no signal was detectable for a given sorted population, this is shown as an open circle on the axis. For all of these undetectable populations, we could not determine if they were in fact negative for HIV DNA as the predicted level of infection (assuming equivalent level of infection to the $CD32^-$ fraction) was below the level of detection of our assay based on the available input cell equivalents.

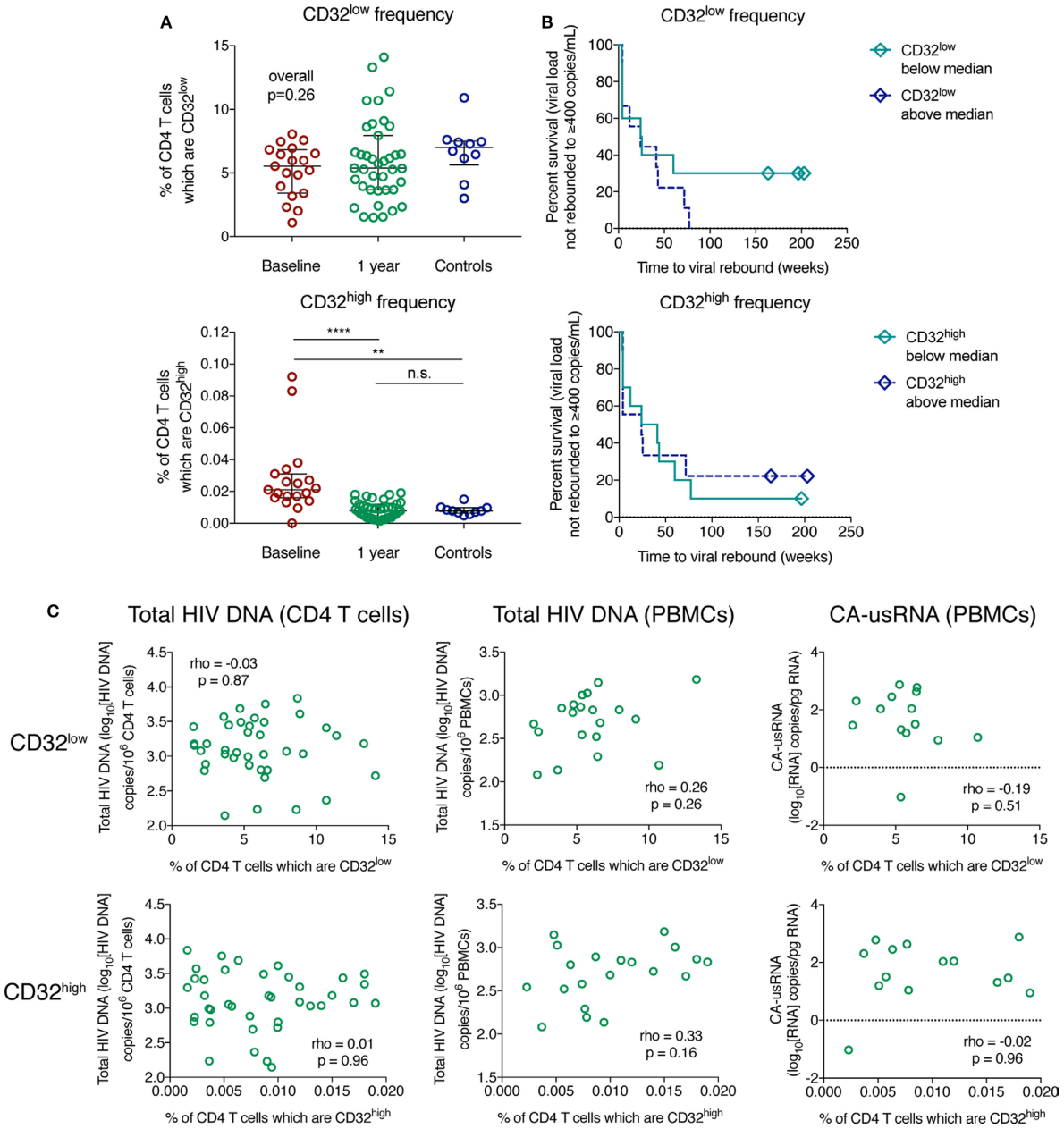


FIGURE 5 | The frequency of CD32-expressing CD3$^+$CD4$^+$ cells does not correlate with the size of the HIV reservoir. The percentage of CD32^{low} (top panel) and CD32^{high} (bottom panel) CD3$^+$CD4$^+$ cell populations is shown in panel **(A)** for HIV$^+$ individuals with primary HIV infection pre-therapy (baseline; $n = 19$) and 1 year following antiretroviral therapy initiation ($n = 39$), as well as for controls ($n = 10$); groups were compared using a Kruskal–Wallis test. Bars indicate the median with the interquartile range. Panel **(B)** shows survival curves (Kaplan–Meier) of time to viral rebound >400 copies/mL based on the frequency of CD32^{low} (top panel) and CD32^{high} (bottom panel) CD3$^+$CD4$^+$ cells stratified at the median ($n = 19$). The relationship between measures of the HIV reservoir and percentage of CD32^{low} (top panels) and CD32^{high} (bottom panels) CD3$^+$CD4$^+$ cells in treated HIV$^+$ individuals, shown in panel **(C)**, was assessed using Spearman's rank correlation. Left column shows total HIV DNA measured in isolated CD4 T cells ($n = 39$), the center column is total HIV DNA measured in peripheral blood mononuclear cells (PBMCs) ($n = 20$), and the right column shows cell-associated unspliced HIV RNA ($n = 14$); ****$p < 0.0001$, **$p = 0.001$–0.01, n.s. (not significant) indicates $p \geq 0.05$.

However, to negate the impact of negative selection beads on the CD32$^+$ CD4 T cell population, all experiments were repeated sorting directly from bulk PBMCs. Cells from participants treated during PHI (Table S1 in Supplementary Material) were sorted directly into the four CD3$^+$CD4$^+$ populations (CD32$^-$, CD32^{low}, CD32$^+$CD14$^+$, and CD32^{high}; Figure S7B in Supplementary Material) and HIV DNA quantified by qPCR. We were able to quantify HIV DNA in sorted CD32$^-$, CD32^{low}, CD32$^+$CD14$^+$, and CD32^{high} CD3$^+$CD4$^+$ T cells from most individuals (**Figure 4A**). As expected, numbers of sorted cells from these populations were higher than for previous experiments using CD4 negative selection kits alleviating concerns regarding low input bias in the qPCR (Table S3 in Supplementary Material). We observed some degree of HIV DNA enrichment within CD32^{low} cells from most individuals, although this was generally of low magnitude. CD32$^+$CD14$^+$ cells also contained detectable HIV DNA in most individuals. We also observed detectable HIV DNA in the CD32^{high} population from seven of nine individuals sorted, which was enriched in four of these. The degree of enrichment varied substantially between individuals (**Figure 4B**).

Despite the technical challenges detailed above, we were confident that HIV DNA was detectable in all three populations of CD32-expressing CD4 T cells and that some enrichment in CD32^{high} was observed in some individuals, although not in all. We have not, however, been able to replicate the magnitude of enrichment or the inter-individual consistency reported by Descours et al. (11), despite starting with a similar number of PBMCs. Importantly, our study population of participants with treated PHI also differs from this previous study which included greater heterogeneity in regards to timing of ART initiation.

The Frequency of CD32-Expressing CD3$^+$CD4$^+$ Cells Is Not Related to the Overall Size of the HIV Reservoir

To further explore the proposed association with CD32 expression and the HIV reservoir, we studied additional individuals commencing ART during PHI from two clinical trials [SPARTAC (21) and HEATHER (7)]. Key demographic and clinical characteristics are shown in **Table 1**. The median time from estimated seroconversion to ART initiation was 74 days (interquartile range, IQR 36–114 days). Median baseline plasma viral load (pVL) was 4.94 $\log_{10}$(copies/mL) (IQR 4.09–6.52), and CD4 T cell count was 545 cells/μL (IQR 453–696). Clinical, immunological, and reservoir measures presented are at baseline (before the initiation of ART) and after 1 year of ART (median 48.1 weeks; IQR 47.9–52.9 weeks). Healthy controls [$n = 10$; 100% male; median age 34.5 (IQR 30.5–42.5) years] were included for comparison.

For participants on ART, the median percentage of CD32^{low} cells was 5.38 (range 1.51–14.1%), and the rarer CD32^{high} population was 0.008% (range 0.002–0.02%). The frequency of CD32^{low} cells did not differ from pre-therapy levels (median 5.55%, range 1.09–8.05%) or healthy controls (median 7.00%, range 3.00–10.9%; **Figure 5A**; $p = 0.26$). Although unstimulated CD4 T cells are not generally expected to express CD32 (10), we are not the first to observe low-level expression of CD32 on CD4 T cells from healthy controls (42). The frequency of CD32^{high} cells was elevated during PHI relative to healthy controls (median 0.02%, range 0.01–0.09% versus median 0.007%, range 0.005–0.015%; $p = 0.0004$) but had decreased to similar levels ($p < 0.0001$) following 1 year of ART (**Figure 5A**).

Whether the percentage of CD32-expressing CD3$^+$CD4$^+$ cells predicted time to pVL rebound after ART TI was assessed in a subset of individuals after 48 weeks of suppressive ART ($n = 19$). In Cox models, we found no evidence to support such an association for either CD32^{low} or CD32^{high} cells (**Figure 5B**, Table S4 in Supplementary Material). Three individuals remained virologically suppressed at the end of follow-up after TI (median 197 weeks), all of whom expressed levels of CD32^{low} below the median (**Figure 5B**). We did not observe any correlation between the percentage of CD32^{low} or CD32^{high} cells and the overall size of the HIV reservoir on ART as measured by several assays: total HIV DNA in negatively selected CD4 T cells, total HIV DNA in PBMCs, and the level of cell-associated unspliced RNA (CA-usRNA) in PBMCs (**Figure 5C**; Figure S9 in Supplementary Material). We also measured HIV DNA in CD4 T cells before ART initiation and again observed no correlation between this and frequency of CD32-expressing populations (Figure S10 in Supplementary Material). In summary, we found no evidence that CD32 expression on CD4 T cells is a surrogate of the total reservoir size as measured by HIV DNA, CA-usRNA or time to viral rebound. This is likely to be not just because CD32^{high} cells are rare but that, even if enriched, a large part of the HIV reservoir is contained in other cell types.

CONCLUSION

We have identified three distinct populations of CD32-expressing CD3$^+$CD4$^+$ T cells that differ in regards to their expression of lineage markers, ICRs, HLA-DR, and their memory phenotype. Our findings have implications for others studying these cells—particularly our finding that negative bead isolation of CD4 T cells will deplete a major fraction of CD32-expressing cells due to their expression of non-T cell markers. We have also shown that some CD32-expressing CD3$^+$CD4$^+$ cells also express CD14 and have a phenotype that suggests that these cells are monocytes. Efforts to ensure that these are excluded from analyses (which can be achieved with stringent gating) will be necessary in future studies.

The CD32^{high} population is of particular interest because of the previously reported high level of HIV DNA enrichment. The surface co-expression of both B and T cell markers is unusual, but has been previously reported (26–31), and further study into the biology of this population is warranted. In the absence of this functional characterization we are cautious in drawing any conclusions about the origin of these cells. Possibilities include that this phenotype is the result of a functional interaction between B cells and CD4 T cells, or represents an unusual lymphocyte with the capability to express markers of both lineages. With high levels of activation and HIV co-receptor expression it is possible that this population may be preferentially infected with HIV,

although due to the rarity of this population we have not been able to directly test this.

We were able to identify HIV DNA in CD32^{-}, CD32^{low}, CD32^{+}CD14^{+}, and CD32^{high} cells. Although cautious about the conclusions that can be drawn from our data, we found evidence for some degree of enrichment of HIV DNA in CD32-expressing populations in some individuals, although we were not able to replicate the magnitude of enrichment previously reported. One possible explanation is that unlike Descours et al. (11), we studied only individuals who commenced ART during PHI, when the reservoir size is smaller (18, 19, 43, 44), and it is possible that the distribution and dynamics of reservoir formation and decay may also differ. We also highlight some of the technical challenges in quantifying exact levels of HIV DNA in rare cell populations which will need to be considered in future studies of the reservoir. Even if CD32-expressing CD4 T cells are enriched for HIV DNA in a given individual, it is likely that a large part of the reservoir is contained outside of this population. Supporting this, we found no evidence that CD32 expression on CD4 T cells is a surrogate of the total reservoir size as measured by HIV DNA, CA-usRNA or time to viral rebound. Overall, our data suggest that CD32 is not a specific marker of the reservoir but might identify a population of HIV enriched cells in a subset of patients.

DATA AVAILABILITY STATEMENT

The raw data supporting the conclusions of this manuscript will be made available by the authors on appropriate application. Data are from the SPARTAC and HEATHER studies from which unrestricted release of data for public deposition would breach compliance with the protocol approved by the research ethics boards. For SPARTAC, all trial data can be accessed by contacting hanna.box@imperial.ac.uk. For HEATHER, data can be accessed from the Collaborative HIV Eradication of Reservoirs: UK BRC steering committee by contacting john.frater@ndm.ox.ac.uk.

ETHICS STATEMENT

Recruitment for and studies within the HEATHER cohort were approved by the West Midlands—South Birmingham Research Ethics Committee (reference 14/WM/1104). Tonsil tissue was obtained from one HIV^{+} individual undergoing routine tonsillectomy, 2 months after acquiring HIV, through the Imperial College Communicable Disease Group Biobank. The SPARTAC trial was approved by the following authorities: the Medicines and Healthcare products Regulatory Agency (UK), the Ministry of Health (Brazil), the Irish Medicines Board (Ireland), the Medicines Control Council (South Africa), and the Uganda National Council for Science and Technology (Uganda). It was also approved by the following ethics committees in the participating countries: the Central London Research Ethics Committee (UK), Hospital Universitário Clementino Fraga Filho Ethics in Research Committee (Brazil), the Clinical Research and Ethics Committee of Hospital Clinic in the province of Barcelona (Spain) and the Adelaide and Meath Hospital Research Ethics Committee (Ireland), the University of Witwatersrand Human Research Ethics Committee, the University of Kwazulu-Natal Research Ethics Committee, and the University of Cape Town Research Ethics Committee (South Africa), Uganda Virus Research Institute Science and ethics committee (Uganda), the Prince Charles Hospital Human Research Ethics Committee and St Vincent's Hospital Human Research Ethics Committee (Australia), and the National Institute for Infectious Diseases Lazzaro Spallanzani, Institute Hospital and the Medical Research Ethics Committee, and the ethical committee of the Central Foundation of San Raffaele, MonteTabor (Italy). PBMCs used for characterisation of CD32-expressing CD3^{+}CD4^{+} cell populations (**Figures 1**, **2**, and **3G,H**; Figures S1 and S2 in Supplementary Material) used in this study were isolated from leukocyte cones obtained through anonymous donation to NHS Blood and Transplant (UK) after approval by NHS Blood and Transplant and the National Research Ethics Service Oxfordshire Research Ethics Committee. Recruitment of healthy individuals (used as comparison group to primary HIV infection cohort and for fresh blood phenotyping; **Figure 5A**; Figures S3, S4E–G, and S5B in Supplementary Material) was approved by the Sheffield Research Ethics Committee (reference 16/YH/0247). All participants have given written informed consent for their participation in these studies.

AUTHOR CONTRIBUTIONS

The experiments were conceived and designed by GM, MP, JT, CW, PKl, and JFr. Experiments were performed by GM, MP, JT, CP, MG, HB, and NO and data analyzed by GM, MP, JT, KP, and JFr. Design and recruitment of the trials was performed by JL, NN, JFo, SF, GR, PKa, and JFr, with trial management performed by JM. The paper was written by GM, MP, JT, and JFr with input from all authors.

ACKNOWLEDGMENTS

We thank the participants of SPARTAC and HEATHER. The HEATHER study is conducted as part of the CHERUB (Collaborative HIV Eradication of Reservoirs: UK BRC) collaboration. CHERUB Steering Committee: Andrew Lever (University of Cambridge), Mark Wills (University of Cambridge), Jonathan Weber (Imperial College, London), Sarah Fidler (Imperial College, London), John Frater (University of Oxford), Lucy Dorrell (University of Oxford), Mike Malim (King's College, London), Julie Fox (King's College London), Ravi Gupta (University College London), Clare Jolly (University College London). The SPARTAC Trial Investigators: Trial Steering Committee: Independent Members—A. Breckenridge (Chair), P. Clayden, C. Conlon, F. Conradie, J. Kaldor*, F. Maggiolo, and F. Ssali, Country Principal Investigators—D. A. Cooper, P. Kaleebu, G. Ramjee, M. Schechter, G. Tambussi, J. M. Miro, and J. Weber. Trial Physician: S. Fidler. Trial Statistician: A. Babiker. Data and Safety Monitoring Committee (DSMC): T. Peto (Chair), A. McLaren (in memoriam), V. Beral, G. Chene, and J. Hakim. Coordinating Trial Centre: Medical Research Council Clinical Trials Unit, London (A. Babiker, K. Porter, M. Thomason, F. Ewings, M. Gabriel,

D. Johnson, K. Thompson, A. Cursley*, K. Donegan*, E. Fossey*, P. Kelleher*, K. Lee*, B. Murphy*, and D. Nock*). Central Immunology Laboratories and Repositories: The Peter Medawar Building for Pathogen Research, University of Oxford, UK (R. Phillips, J. Frater, L. Ohm Laursen*, N. Robinson, P. Goulder, and H. Brown). Central Virology Laboratories and Repositories: Jefferiss Trust Laboratories, Imperial College, London, UK (M. McClure, D. Bonsall*, O. Erlwein*, A. Helander*, S. Kaye, M. Robinson, L. Cook*, G. Adcock*, and P. Ahmed*). Clinical Endpoint Review Committee: N. Paton and S. Fidler. Investigators and Staff at Participating Sites: Australia: St Vincent's Hospital, Sydney (A. Kelleher), Northside Clinic, Melbourne (R. Moore), East Sydney Doctors, Sydney (R. McFarlane), Prahran Market Clinic, Melbourne (N. Roth), Taylor Square Private Clinic, Sydney (R. Finlayson), The Centre Clinic, Melbourne (B. Kiem Tee), Sexual Health Centre, Melbourne (T. Read), AIDS Medical Unit, Brisbane (M. Kelly), Burwood Rd Practice, Sydney (N. Doong), Holdsworth House Medical Practice, Sydney (M. Bloch), Aids Research Initiative, Sydney (C. Workman). Coordinating Centre in Australia: Kirby Institute University of New South Wales, Sydney (P. Grey, D. A. Cooper, A. Kelleher, and M. Law). Brazil: Projeto Praca Onze, Hospital Escola Sao Francisco de Assis, Universidade federal do Rio de Janeiro, Rio de Janeiro (M. Schechter, P. Gama, M. Mercon*, M. Barbosa de Souza, C. Beppu Yoshida, J. R. Grangeiro da Silva, A. Sampaio Amaral, D. Fernandes de Aguiar, M. de Fatima Melo, and R. Quaresma Garrido). Italy: Ospedale San Raffaele, Milan (G. Tambussi, S. Nozza, M. Pogliaghi, S. Chiappetta, L. Della Torre, and E. Gasparotto), Ospedale Lazzaro Spallanzani, Roma (G. DOffizi, C. Vlassi, and A. Corpolongo). South Africa: Cape Town: Desmond Tutu HIV-1 Centre, Institute of Infectious Diseases, Cape Town (R. Wood, J. Pitt, C. Orrell, F. Cilliers, R. Croxford, K. Middelkoop, L. G. Bekker, C. Heiberg, J. Aploon, N. Killa, E. Fielder, and T. Buhler). Johannesburg: The Wits Reproductive Health and HIV-1 Institute, University of Witswatersrand, Hillbrow Health Precinct, Johannesburg (H. Rees, F. Venter, and T. Palanee), Contract Laboratory Services, Johannesburg Hospital, Johannesburg (W. Stevens, C. Ingram, M. Majam, and M. Papathanasopoulos). Kwazulu-Natal: HIV-1 Prevention Unit, Medical Research Council, Durban (G. Ramjee, S. Gappoo, J. Moodley, A. Premrajh, and L. Zako). Uganda: Medical Research Council/Uganda Virus Research Institute, Entebbe (H. Grosskurth, A. Kamali, P. Kaleebu, U. Bahemuka, J. Mugisha*, and H. F. Njaj*). Spain: Hospital Clinic-IDIBAPS, University of Barcelona, Barcelona (J. M. Miro, M. Lopez-Dieguez*, C. Manzardo, J. Ambrosioni, D. Nicolas, J. A. Arnaiz, T. Pumarola, M. Plana, M. Tuset, M. C. Ligero, M. T. Garca, T. Gallart, and J. M. Gatell). UK and Ireland: Royal Sussex County Hospital, Brighton (M. Fisher, K. Hobbs, N. Perry, D. Pao, D. Maitland, and L. Heald), St. James's Hospital, Dublin (F. Mulcahy, G. Courtney, S. O'Dea, and D. Reidy), Regional Infectious Diseases Unit, Western General Hospital and Genitourinary Department, Royal Infirmary of Edinburgh, Edinburgh (C. Leen, G. Scott, L. Ellis, S. Morris, and P. Simmonds), Chelsea and Westminster Hospital, London (B. Gazzard, D. Hawkins, and C. Higgs), Homerton Hospital, London (J. Anderson and S. Mguni), Mortimer Market Centre, London (I. Williams, N. De Esteban, P. Pellegrino, A. Arenas-Pinto, D. Cornforth*, and J. Turner*), North Middlesex Hospital (J. Ainsworth and A. Waters), Royal Free Hospital, London (M. Johnson, S. Kinloch, A. Carroll, P. Byrne, and Z. Cuthbertson), Barts and the London NHS Trust, London (C. Orkin, J. Hand, and C. De Souza), St Mary's Hospital, London (J. Weber, S. Fidler, E. Hamlyn, E. Thomson*, J. Fox*, K. Legg, S. Mullaney*, A. Winston, S. Wilson, and P. Ambrose), Birmingham Heartlands Hospital, Birmingham (S. Taylor and G. Gilleran). Imperial College Trial Secretariat: S. Keeling and A. Becker. Imperial College DSMC Secretariat: C. Boocock. (*Left the study team before the trial ended.)

FUNDING

JFr was supported by the Medical Research Council (Grant no. MR/L006588/1) and the National Institute of Health Research Oxford Biomedical Research Centre.

SUPPLEMENTARY MATERIAL

The Supplementary Material for this article can be found online at https://www.frontiersin.org/articles/10.3389/fimmu.2018.00928/full#supplementary-material.

REFERENCES

1. Wherry EJ, Kurachi M. Molecular and cellular insights into T cell exhaustion. *Nat Rev Immunol* (2015) 15(8):486–99. doi:10.1038/nri3862
2. Trautmann L, Janbazian L, Chomont N, Said EA, Gimmig S, Bessette B, et al. Upregulation of PD-1 expression on HIV-specific CD8$^+$ T cells leads to reversible immune dysfunction. *Nat Med* (2006) 12(10):1198–202. doi:10.1038/nm1106-1329b
3. Jones RB, Ndhlovu LC, Barbour JD, Sheth PM, Jha AR, Long BR, et al. Tim-3 expression defines a novel population of dysfunctional T cells with highly elevated frequencies in progressive HIV-1 infection. *J Exp Med* (2008) 205(12):2763–79. doi:10.1084/jem.20081398
4. Day CL, Kaufmann DE, Kiepiela P, Brown JA, Moodley ES, Reddy S, et al. PD-1 expression on HIV-specific T cells is associated with T-cell exhaustion and disease progression. *Nature* (2006) 443(7109):350–4. doi:10.1038/nature05115
5. Chew GM, Fujita T, Webb GM, Burwitz BJ, Wu HL, Reed JS, et al. TIGIT marks exhausted T cells, correlates with disease progression, and serves as a target for immune restoration in HIV and SIV infection. *PLoS Pathog* (2016) 12(1):e1005349. doi:10.1371/journal.ppat.1005349
6. Hurst J, Hoffmann M, Pace M, Williams JP, Thornhill J, Hamlyn E, et al. Immunological biomarkers predict HIV-1 viral rebound after treatment interruption. *Nat Commun* (2015) 6:8495. doi:10.1038/ncomms9495
7. Hoffmann M, Pantazis N, Martin GE, Hickling S, Hurst J, Meyerowitz J, et al. Exhaustion of activated CD8 T cells predicts disease progression in primary HIV-1 infection. *PLoS Pathog* (2016) 12(7):e1005661. doi:10.1371/journal.ppat.1005661
8. Fromentin R, Bakeman W, Lawani MB, Khoury G, Hartogensis W, DaFonseca S, et al. CD4$^+$ T cells expressing PD-1, TIGIT and LAG-3 contribute to HIV persistence during ART. *PLoS Pathog* (2016) 12(7):e1005761. doi:10.1371/journal.ppat.1005761
9. Chomont N, El-Far M, Ancuta P, Trautmann L, Procopio FA, Yassine-Diab B, et al. HIV reservoir size and persistence are driven by T cell survival and homeostatic proliferation. *Nat Med* (2009) 15(8):893–900. doi:10.1038/nm.1972
10. Hogarth PM, Pietersz GA. Fc receptor-targeted therapies for the treatment of inflammation, cancer and beyond. *Nat Rev Drug Discov* (2012) 11(4):311–31. doi:10.1038/nrd2909
11. Descours B, Petitjean G, Lopez-Zaragoza JL, Bruel T, Raffel R, Psomas C, et al. CD32a is a marker of a CD4 T-cell HIV reservoir harbouring

replication-competent proviruses. *Nature* (2017) 543(7646):564–7. doi:10.1038/nature21710
12. Sandor M, Lynch RG. Lymphocyte Fc receptors: the special case of T cells. *Immunol Today* (1993) 14(5):227–31. doi:10.1016/0167-5699(93)90168-K
13. Nimmerjahn F, Ravetch JV. Fcgamma receptors as regulators of immune responses. *Nat Rev Immunol* (2008) 8(1):34–47. doi:10.1038/nri2206
14. Chauhan AK. Human CD4(+) T-cells: a role for low-affinity Fc receptors. *Front Immunol* (2016) 7:215. doi:10.3389/fimmu.2016.00215
15. Sandilands GP, MacPherson SA, Burnett ER, Russell AJ, Downie I, MacSween RN. Differential expression of CD32 isoforms following alloactivation of human T cells. *Immunology* (1997) 91(2):204–11. doi:10.1046/j.1365-2567.1997.00241.x
16. Engelhardt W, Matzke J, Schmidt RE. Activation-dependent expression of low affinity IgG receptors Fc gamma RII(CD32) and Fc gamma RIII(CD16) in subpopulations of human T lymphocytes. *Immunobiology* (1995) 192(5):297–320. doi:10.1016/S0171-2985(11)80172-5
17. Starbeck-Miller GR, Badovinac VP, Barber DL, Harty JT. Cutting edge: expression of FcgammaRIIB tempers memory CD8 T cell function in vivo. *J Immunol* (2014) 192(1):35–9. doi:10.4049/jimmunol.1302232
18. Jain V, Hartogensis W, Bacchetti P, Hunt PW, Hatano H, Sinclair E, et al. Antiretroviral therapy initiated within 6 months of HIV infection is associated with lower T-cell activation and smaller HIV reservoir size. *J Infect Dis* (2013) 208(8):1202–11. doi:10.1093/infdis/jit311
19. Buzon MJ, Martin-Gayo E, Pereyra F, Ouyang Z, Sun H, Li JZ, et al. Long-term antiretroviral treatment initiated at primary HIV-1 infection affects the size, composition, and decay kinetics of the reservoir of HIV-1-infected CD4 T cells. *J Virol* (2014) 88(17):10056–65. doi:10.1128/JVI.01046-14
20. Ananworanich J, Schuetz A, Vandergeeten C, Sereti I, de Souza M, Rerknimitr R, et al. Impact of multi-targeted antiretroviral treatment on gut T cell depletion and HIV reservoir seeding during acute HIV infection. *PLoS One* (2012) 7(3):e33948. doi:10.1371/journal.pone.0033948
21. SPARTAC Trial Investigators, Fidler S, Porter K, Ewings F, Frater J, Ramjee G, et al. Short-course antiretroviral therapy in primary HIV infection. *N Engl J Med* (2013) 368(3):207–17. doi:10.1056/NEJMoa1110039
22. Williams JP, Hurst J, Stohr W, Robinson N, Brown H, Fisher M, et al. HIV-1 DNA predicts disease progression and post-treatment virological control. *Elife* (2014) 3:e03821. doi:10.7554/eLife.03821
23. Jones M, Williams J, Gartner K, Phillips R, Hurst J, Frater J. Low copy target detection by Droplet Digital PCR through application of a novel open access bioinformatic pipeline, 'definetherain'. *J Virol Methods* (2014) 202:46–53. doi:10.1016/j.jviromet.2014.02.020
24. Zamora C, Canto E, Nieto JC, Ortiz MA, Diaz-Torne C, Diaz-Lopez C, et al. Functional consequences of platelet binding to T lymphocytes in inflammation. *J Leukoc Biol* (2013) 94(3):521–9. doi:10.1189/jlb.0213074
25. Tangye SG, Avery DT, Deenick EK, Hodgkin PD. Intrinsic differences in the proliferation of naive and memory human B cells as a mechanism for enhanced secondary immune responses. *J Immunol* (2003) 170(2):686. doi:10.4049/jimmunol.170.2.686
26. Wilk E, Witte T, Marquardt N, Horvath T, Kalippke K, Scholz K, et al. Depletion of functionally active CD20+ T cells by rituximab treatment. *Arthritis Rheum* (2009) 60(12):3563–71. doi:10.1002/art.24998
27. Schuh E, Berer K, Mulazzani M, Feil K, Meinl I, Lahm H, et al. Features of human CD3+CD20+ T cells. *J Immunol* (2016) 197(4):1111–7. doi:10.4049/jimmunol.1600089
28. Palanichamy A, Jahn S, Nickles D, Derstine M, Abounasr A, Hauser SL, et al. Rituximab efficiently depletes increased CD20-expressing T cells in multiple sclerosis patients. *J Immunol* (2014) 193(2):580–6. doi:10.4049/jimmunol.1400118
29. Niu J, Zhai Z, Hao F, Zhang Y, Song Z, Zhong H. Dissection of a circulating CD3(+) CD20(+) T-cell subpopulation in patients with psoriasis. *Clin Exp Immunol* (2018) 192(2):206–12. doi:10.1111/cei.13106
30. Katopodis O, Liossis SN, Viglis V, Pouli A, Dimopoulos MA, Sfikakis PP. Expansion of CD8+ T cells that express low levels of the B cell-specific molecule CD20 in patients with multiple myeloma. *Br J Haematol* (2003) 120(3):478–81. doi:10.1046/j.1365-2141.2003.04087.x
31. Eggleton P, Bremer E, Tarr JM, de Bruyn M, Helfrich W, Kendall A, et al. Frequency of Th17 CD20+ cells in the peripheral blood of rheumatoid arthritis patients is higher compared to healthy subjects. *Arthritis Res Ther* (2011) 13(6):R208. doi:10.1186/ar3541
32. Jaafoura S, de Goer de Herve MG, Hernandez-Vargas EA, Hendel-Chavez H, Abdoh M, Mateo MC, et al. Progressive contraction of the latent HIV reservoir around a core of less-differentiated CD4(+) memory T cells. *Nat Commun* (2014) 5:5407. doi:10.1038/ncomms6407
33. Siliciano JD, Kajdas J, Finzi D, Quinn TC, Chadwick K, Margolick JB, et al. Long-term follow-up studies confirm the stability of the latent reservoir for HIV-1 in resting CD4+ T cells. *Nat Med* (2003) 9(6):727–8. doi:10.1038/nm880
34. Finzi D, Blankson J, Siliciano JD, Margolick JB, Chadwick K, Pierson T, et al. Latent infection of CD4+ T cells provides a mechanism for lifelong persistence of HIV-1, even in patients on effective combination therapy. *Nat Med* (1999) 5(5):512–7. doi:10.1038/8394
35. Chun TW, Carruth L, Finzi D, Shen X, DiGiuseppe JA, Taylor H, et al. Quantification of latent tissue reservoirs and total body viral load in HIV-1 infection. *Nature* (1997) 387(6629):183–8. doi:10.1038/387183a0
36. Wittner M, Dunay GA, Kummer S, Bockhorn M, Hufner A, Schmiedel S, et al. CD32 expression of different memory T cell subpopulations in the blood and lymph nodal tissue of HIV patients and healthy controls correlates with immune activation. *J Acquir Immune Defic Syndr* (2018) 77(4):345–9. doi:10.1097/QAI.0000000000001622
37. Grau-Exposito J, Serra-Peinado C, Miguel L, Navarro J, Curran A, Burgos J, et al. A novel single-cell FISH-flow assay identifies effector memory CD4(+) T cells as a major niche for HIV-1 transcription in HIV-infected patients. *mBio* (2017) 8(4):e00876–17. doi:10.1128/mBio.00876-17
38. Eisele E, Siliciano RF. Redefining the viral reservoirs that prevent HIV-1 eradication. *Immunity* (2012) 37(3):377–88. doi:10.1016/j.immuni.2012.08.010
39. Chun TW, Finzi D, Margolick J, Chadwick K, Schwartz D, Siliciano RF. In vivo fate of HIV-1-infected T cells: quantitative analysis of the transition to stable latency. *Nat Med* (1995) 1(12):1284–90. doi:10.1038/nm1295-1284
40. Shan L, Deng K, Gao H, Xing S, Capoferri AA, Durand CM, et al. Transcriptional reprogramming during effector-to-memory transition renders CD4(+) T cells permissive for latent HIV-1 infection. *Immunity* (2017) 47(4):766.e–75.e. doi:10.1016/j.immuni.2017.09.014
41. Martin G, Pace M, Thornhill J, Phetsouphanh C, Meyerowitz J, Gossez M, et al. Enrichment of the HIV reservoir in CD32+ CD4 T cells occurs early in blood and tissue. *bioRxiv* (2017) 169342. doi:10.1101/169342
42. Zandieh A, Izad M, Fakhri M, Amirifard H, Khazaeipour Z, Harirchian MH. Cytometric profiling in various clinical forms of multiple sclerosis with respect to CD21+, CD32+, and CD35+ B and T cells. *Transl Neurodegener* (2013) 2(1):14. doi:10.1186/2047-9158-2-14
43. Hocqueloux L, Avettand-Fenoel V, Jacquot S, Prazuck T, Legac E, Melard A, et al. Long-term antiretroviral therapy initiated during primary HIV-1 infection is key to achieving both low HIV reservoirs and normal T cell counts. *J Antimicrob Chemother* (2013) 68(5):1169–78. doi:10.1093/jac/dks533
44. Hey-Cunningham WJ, Murray JM, Natarajan V, Amin J, Moore CL, Emery S, et al. Early antiretroviral therapy with raltegravir generates sustained reductions in HIV reservoirs but not lower T-cell activation levels. *AIDS* (2015) 29(8):911–9. doi:10.1097/QAD.0000000000000625

Conflict of Interest Statement: The authors declare that the research was conducted in the absence of any commercial or financial relationships that could be construed as a potential conflict of interest.

Copyright © 2018 Martin, Pace, Thornhill, Phetsouphanh, Meyerowitz, Gossez, Brown, Olejniczak, Lwanga, Ramjee, Kaleebu, Porter, Willberg, Klenerman, Nwokolo, Fox, Fidler and Frater. This is an open-access article distributed under the terms of the Creative Commons Attribution License (CC BY). The use, distribution or reproduction in other forums is permitted, provided the original author(s) and the copyright owner are credited and that the original publication in this journal is cited, in accordance with accepted academic practice. No use, distribution or reproduction is permitted which does not comply with these terms.

Journal of Virus Eradication 2017; 3: e1–e6 CONFERENCE REPORT

Converging roads: the latest science from the 2017 IAS HIV Cure and Cancer Forum

Genevieve E Martin[1], José Alcami[2], Jean-Phillipe Spano[3] and Anna Laura Ross[4]

[1] Peter Medawar Building for Pathogen Research, Nuffield Department of Medicine, University of Oxford, Oxford, UK
[2] AIDS Immunopathogenesis Unit, Instituto de Salud Carlos III, Madrid, Spain
[3] Pitié-Salpêtrière Hospital, Pierre et Marie Curie University, INSERM-UMRS 1136, Paris, France
[4] International and Scientific Relations, ANRS, 101 rue de Tolbiac, 75013 Paris, France

Introduction

The 2017 IAS HIV Cure and Cancer Forum took place in Paris on 22–23 July. This year, the annual HIV cure meeting organised by the IAS had a change in format, with the forum specifically showcasing the interface between HIV cure or remission and cancer research. Symbolically, the meeting was held at the Institut Curie, an internationally renowned cancer research institute. The audience, limited to 200 to foster active interaction among the participants, included several oncologists and cancer researchers, in addition to members the HIV cure community.

The forum aimed to highlight the benefits of interdisciplinary research in the hope that this may lead to progress towards the goal of HIV remission. In part, this dialogue is of interest because people with HIV are living longer and as a consequence may go on to develop cancer. At this point the treatment options will have to take into account the presence of both diseases. A second point, which may prove to have even more pertinence, is that research into both HIV cure and cancer share many similarities, spanning basic science, diagnostics and innovative therapeutic approaches (Figure 1). The notion of identifying and quantifying the burden of disease is crucial in both areas, on the one side identifying HIV latently infected cells, and on the other, detecting cancerous cells. Equally relevant to the two areas is the understanding of the mechanisms responsible for re-shaping and affecting the immune response to prevent clearance of the diseased cells. Finally, many of the therapeutic strategies currently being investigated in the context of HIV cure and remission studies have also been used in cancer research, such as immune checkpoint blockers, cytokine therapy, modified T cell approaches and gene therapy.

Monsef Benkirane (CNRS, Montpellier, France), who delivered the keynote address, highlighted that the notions of persistence and resistance represent the barriers to cure in both HIV and several cancers. Both conditions can be regarded as residual diseases. Cancer stem cells retain similar characteristics to latently infected HIV cells and even though their molecular bases are very different, similar types of cure strategies are being developed. He then presented recently published work from his group that identified CD32a, a low-affinity IgG receptor, as a marker of a significantly enriched CD4 T cell reservoir [1]. This marker was identified using an *in vitro* model that uses SIV-derived *vpx* to overcome SAMHD1 restriction, thereby allowing infection of resting cells. To identify candidate genes that are differentially expressed between latently infected and uninfected cells, they compared the transcriptomic profiles of these two cell populations. CD32a expression on latently infected cells was confirmed in their model by flow cytometry. Cell sorting of patient samples demonstrated that CD32a is a marker of an enriched *in vivo* reservoir. CD4 T cells are not usually considered to express CD32a, making this finding unexpected. Finally, Benkirane spoke about how the chromatin spatial organisation can impact on HIV integration site selection. Recent advances have improved our ability to map interactions between genes and regulatory elements at distant DNA sites [2]. Using data obtained from previous studies mapping HIV integration sites [3,4], he showed that integration sites are enriched in the enhancer regions of specific clusters of genes that interact with one another (termed 3D clusters).

Corresponding author: Genevieve E Martin, Peter Medawar Building for Pathogen Research, University of Oxford, South Parks Road, OX1 3SY, Oxford, UK
Email: genevieve.martin@ndm.ox.ac.uk

© 2017 The Authors. Journal of Virus Eradication published by Mediscript Ltd
This is an open access article published under the terms of a Creative Commons License.

Characterising the reservoir

For both HIV and cancer, a major barrier to finding a cure is the persistence of a rare population of cells capable of giving rise to relapse (for malignancies) or viral rebound (in the case of HIV) during treatment (Figure 2). Identifying, quantifying and characterising these cells are critical issues for designing therapies in both cases. Work presented at this forum demonstrated a number of innovative approaches to improve the understanding of these two analogous and rare cell populations.

Looking to define the exact anatomical location of functional viral reservoirs, Francois Villinger (University of Louisiana at Lafayette, USA) talked about the use of immuno-PET with CT scan as a tool for *in vivo* imaging of viral replication [5]. Using ^{64}Cu-labelled antibodies targeted against HIV *env* (as well as a number of non-HIV targets including CD4, CD8 and $\alpha4\beta7$), he was able to non-invasively measure the anatomical distribution of cells of interest in SIV-infected macaques. This technique is a promising tool for studying viral rebound dynamics following treatment interruption and the impact of therapies. Villinger also presented preliminary results from SIV-infected macaques treated with anti-$\alpha4\beta7$ (a promising therapy that has been shown to induce sustained virological remission in macaques) [6], showing that the monoclonal antibody aided CD4 restoration in gut, spleen and lymph nodes.

Measuring the HIV reservoir, which is largely present in lymphoid tissue, requires direct sampling of latently infected cells. The ability to accurately quantify reservoir size in tissues, without invasive biopsies, would be a significant step towards HIV cure. Sarah-Jane Dawson (Peter MacCallum Cancer Centre, Australia) presented her work using cell-free circulating tumour DNA (ctDNA) in plasma to monitor tumour progression in tissues. The ctDNA is identified as coming from a tumour source on the basis of specific genomic changes; its presence and levels can be used to monitor how treatment is progressing as well as detecting minimal residual disease post therapy [7,8]. This elegant solution highlights the analogous challenges in assessing remission in HIV and cancer – two conditions in which tissue represents a site of residual disease.

Our ability to study and target HIV reservoirs has been limited by the rarity of latently infected cells in patients on ART and the absence of specific biomarkers. Following on from the recent work identifying CD32a as a marker of an enriched CD4+ reservoir [1], Genevieve Martin (University of Oxford) presented a characterisation of CD32-expressing CD4 T cells in a cohort of individuals treated during primary HIV infection. These results confirmed enrichment of HIV DNA in CD32+ CD4 T cells, which

Box 1. HIV and cancer research: the community perspective

As new advances in innovative therapeutic strategies for HIV cure and remission move closer to the clinic, community engagement and participation of people living with HIV is crucial. A round-table discussion on the design of, and participation in, clinical trials provided the community perspective; this was voiced by Michael Louella (defeatHIV Community Advisory Board) and Gilliosa Spurrier (Melanoma France). Current inclusion criteria in many clinical trials are quite stringent, excluding large numbers of potential participants. For HIV remission studies, the majority of ongoing trials include participants who control the virus with antiretrovirals and are doing well overall. However, those who may have the most to gain from a potential remission do not necessarily meet these inclusion criteria. When trying to understand the motivation behind clinical trial participation, it should be considered that current participants are often motivated by altruism and a desire to help move research forwards, even with the understanding that this research will not necessarily benefit them directly. Among the reasons limiting the involvement of people living with HIV in clinical research, the panel cited inadequate engagement and education. Misleading media reports, sometimes promoting false hope and unrealistic timelines for HIV cure, are also clouding the issue, making it harder to get potential participants involved. In the interface between HIV and cancer, people living with HIV are often excluded from cancer trials and *vice versa*. Louella concluded with a *vade mecum* for improving community involvement in research:

- Increased funding for community engagement
- Planning for early involvement and future access
- Supporting effective community response
- Redress the balance of power between researchers and participants

Finally, the panel stressed the importance of expanding the selection of population groups to include more female participants, children and adolescents, and importantly, to ensure that participants from resource-limited settings are included, even if access issues remain present.

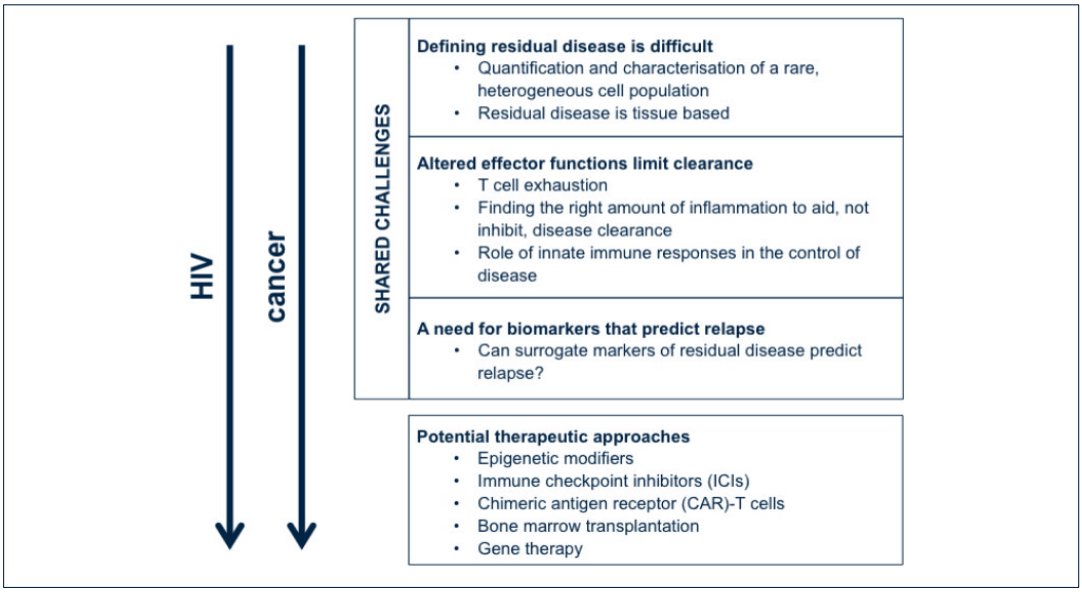


Figure 1. Parallels between HIV and cancer highlighted during the 2017 IAS Cure and Cancer Forum

also expressed high levels of immune checkpoint receptors PD-1, Tim-3 and TIGIT [9].

Epigenetic control

The broadening of our understanding of epigenetic control mechanisms was a key theme throughout the meeting. Jonathan Karn (Case Western Reserve University, Cleveland, USA) highlighted that epigenetic silencing is progressive and hierarchical – with histone deacetylation, as well as histone and DNA methylation all occurring to drive proviruses towards more permanent states of silencing. Histone deacetylase inhibitors (HDACis) have been investigated as latency-reversing agents (LRAs) in clinical trials [10-14]. Karn presented findings that showed several inhibitors of the histone methyltransferases EZH2 and EHMT2 were able to reverse latency *in vitro*, acting synergistically with vorinostat or IL-15 [15]. Looking then to DNA methylation around the provirus, Carine van Lint (Université Libre de Bruxelles, Belgium) presented work identifying UHRF1 as a factor which is recruited to the 5′ LTR and plays a role in DNA methylation-mediated silencing of viral expression. This molecule has not previously been linked to HIV latency, but as a potential therapeutic target for several malignancies, therefore inhibitors of UHRF1 could also play a role as LRAs [16].

The epigenetic work presented at the meeting not only focused around the regulation of proviral expression but also extended to include the epigenetics of effector cell fate. An initial example of this was described by Geneviève Almounzi (Institut Curie, France) who spoke about how the SUV39H1–H3K9me3–HP1α pathway, which is able to promote silencing of Th1 genes, ensures the stability of the Th2 lineage [17]. Using a *Listeria* infection model, Sebastian Amigorena (Institut Curie, France) also described a role for SUV39H1 in the silencing of genes that are involved in CD8 T cell memory differentiation. This work raises interesting possibilities about targeting the epigenome to augment anti-HIV or anti-tumour responses. Demonstrating that HIV infection itself can also induce epigenetic changes that impact on immunity, Stephanie Shiau (Columbia University, USA) presented a poster showing that early-treated HIV-infected children have DNA methylation dysregulation at a number of loci, including NLRC5, which regulates MHC class I expression [18].

Journal of Virus Eradication 2017; 3: e1–e6 CONFERENCE REPORT

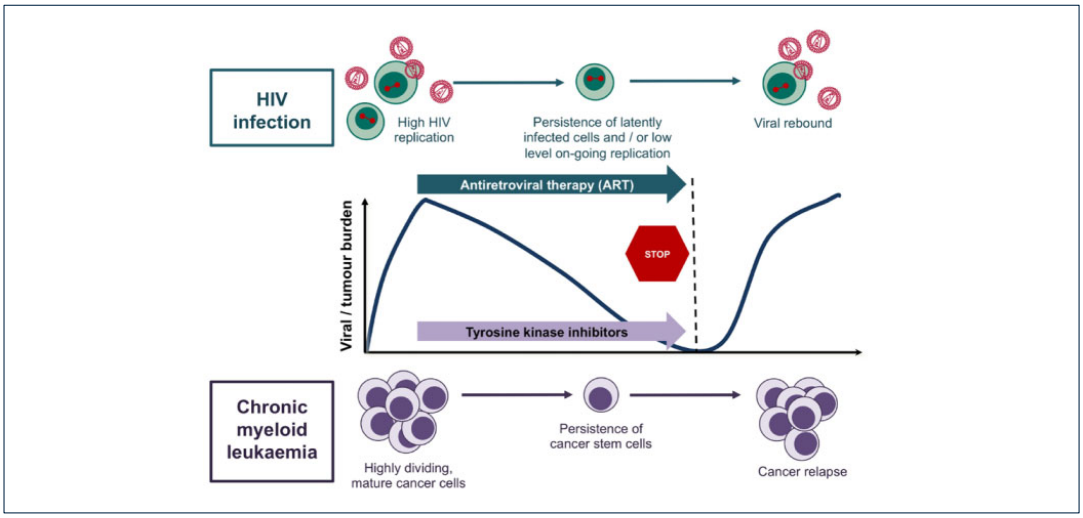


Figure 2. Residual disease in cancer and HIV infection is a common barrier to achieving cure. In HIV infection, antiretroviral therapy (ART) rapidly controls high viral replication in activated CD4 lymphocytes. However, latently infected lymphocytes are not targeted by ART and their persistence produces viral rebound upon treatment interruption. In chronic myeloid leukaemia, highly dividing mature cells are kept under control by tyrosine kinase inhibitors. Among the tumour population some cells are more resistant to treatment, but full remission can be achieved in the majority of patients. The persistence of cancer stem cells that are not eliminated with tyrosine kinase inhibitor treatment may give rise to relapse

Numerous therapeutic approaches to blocking or reactivating HIV were presented, targeting both the virus itself, as well as epigenetic pathways regulating its expression. Adam Capoferri (Johns Hopkins University School of Medicine, USA) presented data from AMC075, a Phase II study of conventional chemotherapy with or without vorinostat for individuals undergoing treatment for HIV-associated lymphoma. Consistent with another recent study using vorinostat [14], they did not observe any changes in HIV reservoir size (measured by quantitative viral outgrowth assay) with this therapy [19].

Several classes of licensed small-molecule drugs were described as either novel LRAs, or as possessing antiviral activity. Isa Muñoz-Arias (University of California San Francisco, USA) presented data showing that three small-molecule drugs used in cancer therapeutics (sunitinib, sorafenib and bortezomib) are able to reactivate latent virus from latently infected cell lines, as well as *ex vivo* from primary CD4 T cells. In patient samples, sunitinib was able to induce more cell-associated HIV RNA than either romidepsin or bryostatin [20]. A Jak inhibitor, baricitinib, was the focus of the work presented by Christina Gavegnano (Emory University, USA); this drug was shown to have antiviral activity and to prevent HIV reactivation in both lymphoid and myeloid cells [21]. Mayte Coiras (Instituto Carlos III, Spain) presented a poster demonstrating the antiviral and anti-proliferative activity of the tyrosine kinase inhibitors dasatinib and ponatinib, both of which are currently used in the treatment of chronic myeloid leukaemia (CML) [22]. The antiviral activity of these molecules was mediated through the inhibition of SAMHD1 phosphorylation and lymphocyte proliferation blocking [23].

Immunology and inflammation

Innate immunity revisited

The parallel evolution of innate and adaptive immune systems has allowed for both rapid responses to 'non-self', as well as targeted responses and the development of immunological memory. While the role of the adaptive immune system in targeting HIV has been extensively studied, recent work has underlined a major role of the innate immunity in the control of HIV infection and, particularly, with regard to the establishment of viral reservoirs. As with adaptive immune responses, there are parallels in the way innate immunity responds to infectious diseases and cancers. In particular, innate immune mechanisms, including interferon induction and natural-killer (NK) cell activity, are able to tackle both cancers and virally infected cells.

Michaela Müller-Trutwin (Institut Pasteur, France) compared the immune response in acute SIV infection between two non-human primate models, the African green monkeys (AGM) in which the infection is not pathogenic and the Asian macaques (AM), which develop AIDS. In both models there is high plasma viral load but new data presented at the meeting showed a decrease in SIV-RNA levels in lymph nodes in AGM but not in AM, particularly in B cell follicles. The control of viral load in lymph nodes was associated with the recruitment of a specific population of CXCR5+ NK cells to the follicles in AGM that was absent in AM. Redistribution of NK cells to the follicles was associated with high levels of membrane-bound IL-15 in follicular dendritic cells. Overall these findings unveil a new NK function in controlling viral replication specifically in lymph nodes, but not in other organs such as the gut-associated lymphoid tissue (GALT).

Mirko Paiardini (Emory University, USA) compared two groups of SIV-infected macaques treated with ART alone or in combination with IL-21 and IFNα. IL-21 was added with the aim of preserving Th17 cell activity and decreasing microbial translocation and inflammation. IFNα was introduced to improve natural immune responses and induce interferon stimulated genes (ISGs). Macaques treated with ART plus IL-21 and IFNα maintained lower levels of activation and had a reduced viral reservoir. In this group, viral rebound after treatment interruption was modestly delayed and reduced, probably in association with decreased activation and preservation of Th17 responses [24].

Further highlighting the role of interferons in HIV control, Paul Hertzog (Hudson Institute, Australia) gave an overview on the type I interferon (IFN) system. He presented original data on IFNε, which is expressed in the female genital tract and regulated by oestrogens

[25]. IFNε displays lower affinity for IFN receptors and lower specific activity than other members of type I IFNs, and is a good example of the functional diversity of type I IFNs. It displays antiviral activity, protecting from HSV-2 and chlamydia infections in murine models, as well as showing antiviral activity against HIV-1 *in vitro* [25,26]. Linking control mechanisms of viral infections and cancers, Hertzog presented data showing that IFNε also displays anti-tumoral activity, both through the regulation of anti-tumour immune cells and direct suppression of ovarian cancer development and dissemination. Linking type I interferons to the control and establishment of HIV reservoirs, Paul Cameron (Doherty Institute, University of Melbourne, Australia) presented a poster that extended previous observations [27] showing that treatment with IFNα and IFNβ prior to infection reduces the number of latently infected cells. However, once latency is established IFNα increases viral reactivation [28].

Overall, these studies suggest that innate immune mechanisms can play a major role not only in the establishment of the reservoirs in early infection, but also in their control during the chronic stage of infection.

Adaptive memory responses and the control of HIV reservoirs

Several presentations addressed the potential role of adaptive cellular responses in the control of HIV reservoirs. Ranjit Sivanandham (University of Pittsburg, USA) suggested a depletion of T regulatory cells (Tregs) as a means to decrease the size of the reservoir and enhance cytotoxic T lymphocyte (CTL) responses against HIV. This hypothesis is based on previous results showing that Tregs represent an important reservoir in SIV/HIV infections and contribute to the impairment of CTL responses [29]. Active depletion of Tregs using diphtheria immunotoxin coupled to CCR4 and IL-2 or low doses of cyclophosphamide (Cy) were assayed in SIV-infected macaques. Both immunotoxins were shown to be effective in depleting Tregs and inducing CTL responses, thus aiding in the control of viral replication [30].

Further investigations as to how we can augment the 'kill' needed to eradicate HIV were presented in the poster sessions. Victor Appay (Centre d'Immunologie et des Maladies Infectieuses, France) showed in a poster that it is possible to prime CD8 T cell responses against tumour antigens or HIV using stimulator of interferon gene (STING) ligands. In particular, cGAMP was extremely potent in inducing effector functions, including cytotoxic potential [31]. In a model of resting lymphocytes, Alba Ruiz (IrsiCaixa, Spain) measured HIV reactivation and cytotoxic T lymphocyte (CTL) killing driven by different combinations of LRAs. Cellular killing was directly related to both LRA potency but also the CTL activation state. Interestingly, besides its role as an LRA, bryostatin increased the activation status of CTLs, leading to enhanced cell killing [32].

Clinical approaches

A major focus of the forum was the recent developments in immunotherapy in the field of oncology, and the potential for this type of therapy to be applied to HIV. Aurélien Marabelle (Gustave Roussy Hospital, France) discussed the recent paradigm shift in cancer therapy, with therapies now targeting immune cells rather than the malignancy itself. This has been accomplished by using monoclonal antibodies against immune checkpoint molecules on T lymphocytes. Blockade of these pathways, which have been linked to T cell exhaustion, can restore effector function and generate a strong anti-tumour response. Immune checkpoint inhibitors (ICIs) targeting several molecules have been approved for clinical use; these include the anti-cytotoxic T lymphocyte antigen (CTLA-4) antibodies ipilimumab and tremelimumab, and the anti-programmed death-1 (PD-1) receptor antibodies nivolumab and pembrolizumab. Compared with conventional chemotherapy and radiation therapy, these drugs have dramatically improved the outcome of certain malignancies. They are remarkable in terms of the magnitude of clinical benefit seen, the broad range of cancers for which they have efficacy and a relatively durable response. These developments are heralding a new standard of care in the field of oncology.

Not all cancer patients, however, benefit clinically from immune checkpoint blockade and the identification of factors that can predict clinical response is needed. Moreover, there is significant associated toxicity – and caution needs to be exercised due to the predominantly autoimmune nature of this toxicity, which differs from conventional therapy. Pre-clinical work has already shown that combinations of ICIs might have increased efficacy, but combining these drugs is also likely to result in a worse safety profile. These drugs are expensive and the field needs to develop new clinical research methodology in order to identify the patients who will benefit most from them, and to refine their schedule and route of administration [33].

ICIs could potentially be used to augment anti-HIV immunity or act as LRAs, and this was a major theme of the work presented at the forum. The PD-1/PDL-1 axis has been shown to be a critical player in T cell exhaustion, a state of immune dysfunction encountered in cases of chronic infections and cancers [34]. Bulk CD4 and CD8 activated T cells also express high PD-1 levels during HIV infection [35] and PD-1 expression on HIV specific T cells is associated with T cell exhaustion and disease progression. PD-1 is significantly up-regulated on HIV-1 specific CD8 T cells, and some studies have already shown that blockade of the PD-1/PDL-1 pathway would increase HIV-specific CD4 and CD8 T cell function [36,37].

Sharon Lewin (Doherty Institute, University of Melbourne, Australia) presented work on the ability of ICIs to disrupt latency *in vitro*. In HIV-infected individuals on ART, the HIV reservoir is enriched in PD-1^{hi} cells and cells that express multiple immune checkpoint markers [38,39]. The work from her group aimed to address whether combinations of ICIs (including anti-PD-1) could be used to reverse latency, with the potential to be used as part of a strategy for cure. Lewin reported that when using an *in vitro* model, anti-PD-1 antibodies disrupt HIV latency in non-proliferating but not in proliferating T cells. In the non-proliferating cells latency reversal was possible only with the presence of T cell activation (with staphylococcal enterotoxin B, SEB) or with multiple ICIs. In proliferating cells latency reversal was only possible with multiple ICIs [40]. These findings suggest that co-expression of IC markers, especially of proliferating latently infected cells, may limit the potency of anti-PD-1 alone for latency reversal.

Thus far, ICI use in HIV-infected individuals has been limited, and initial studies have focused on HIV-infected individuals receiving immunotherapy for cancer [41,42]. Timothy Henrich (University of California San Francisco, USA) reported on three cART-suppressed individuals receiving multiple doses of anti-PD-1 therapy (nivolumab) for malignancies (head and neck, and cutaneous squamous cancer). Their results showed that anti-PD-1 treatment did not lead to sustained or consistent decreases in CD4 HIV-1 DNA or cell-associated RNA but was associated with a transient increase in CD8 T cell responses to HIV-1 [43]. Presenting further data on PD-1 blockade in HIV-infected individuals, Brigitte Autran (Hôpital Pitié-Salpêtrière, France) described a case series of 12 HIV-infected patients treated with nivolumab for non-small cell lung cancer (NSCLC) or melanoma [44]. Six of the 12 individuals had a partial tumour response or stable disease with nivolumab therapy, with the remainder having progressive disease.

Journal of Virus Eradication 2017; 3: e1–e6 CONFERENCE REPORT

Overall, therapy was well tolerated and all individuals had stable CD4 cell counts, and remained virologically suppressed, throughout nivolumab treatment. Two of these individuals were presented in more detail. In one, a transient increase in HIV DNA levels was observed, alongside an increase in HIV-specific CD8 T cells [41]. In the other, a three-fold decrease in HIV-DNA levels was observed and this coincided with a dramatic increase in HIV-specific T cells. In both individuals, a decreased expression of immune checkpoint receptors was also observed with nivolumab therapy. Taken together, these two studies suggest a potential effect of PD-1 blockade on anti-HIV CD8 responses. Changes in the HIV reservoir were observed in some, but not all, individual studies and further work is needed to establish whether PD-1 blockade has a consistent effect on HIV reservoir size.

The winner of the IAS-ANRS Dominique Dormont Prize, Maria Salgado (IrsiCaixa, Spain), presented her work in the IciStem consortium. She aimed to identify factors that relate to the reduction in the HIV reservoir size in HIV-infected individuals undergoing allogeneic stem cell transplant for malignancy. Five out of the six patients followed had undetectable HIV reservoirs following allogeneic transplant, and time to full donor chimerism and alloreactivity (graft-versus-host disease) were identified as factors that are potentially important for achieving this outcome [45].

Another novel strategy that is promising in targeting cancers, and potentially HIV, is the use of CAR-T cells (chimeric antigen receptor T cells). Some clinical data were presented by Lawrence Corey (Fred Hutchinson Cancer Research Center, USA) on the use of CD19-targeting CAR-T cells in haematological malignancy, with high response rates in refractory acute lymphoblastic leukaemia and non-Hodgkin's lymphoma. He highlighted that significant toxicities have been observed with CAR-T cells, in particular neurological side effects and cytokine release syndrome (CRS). Anti-HIV-1 CAR-T cells may have the potential to kill HIV-1-infected cells that have escaped endogenous immune responses. These cells have been shown to kill autologous virally infected cells *in vitro*. Corey suggested that CAR-T cells designed to target HIV will need to possess several characteristics in order to succeed *in vivo*. These include modifications to protect CAR-T cells from HIV-1 infection, access to immunological sanctuary sites (including germinal centres of B cell follicles) and long-term persistence.

Scientists working in HIV and cancer research share many challenges in the development of targeted and effective therapies for eradication. These parallel challenges mean that several therapeutic approaches developed in the cancer field are being investigated for HIV cure. The efficacy and safety of long-term ART means that there is, however, a significant difference in the acceptable level of toxicity between therapies for HIV cure and malignancies. Further work is needed to determine whether ICIs and CAR-T cell-based therapies are safe in the clinic before their use in attempting to cure HIV.

Conclusion

Specialists in the research fields of HIV and oncology came together in this one-and-a-half-day meeting in order to foster an exchange of ideas. The various sessions highlighted some of the similarities between the two areas (summarised in Figure 1). One area of particular interest was diagnostics, as it will be essential to characterise and quantify the rare cell population that is responsible for residual disease in both cancer and HIV. Ongoing collaboration between researchers in HIV and cancer will be important in the use of immunotherapy to manipulate the immune system to elicit adequate responses. While the scientific community remains cautious, conscious that effective therapies for cancer may not give the desired results for HIV cure or remission, data presented at the forum highlighted the fact that a synergistic approach will prove to be beneficial to both disciplines.

Acknowledgments

We acknowledge the contribution of Rebecca Allen (University of Oxford) who provided assistance in editing the manuscript.

References

1. Descours B, Petitjean G, Lopez-Zaragoza JL *et al.* CD32a is a marker of a CD4 T-cell HIV reservoir harbouring replication-competent proviruses. *Nature* 2017; **543**: 564–567.
2. Mifsud B, Tavares-Cadete F, Young AN *et al.* Mapping long-range promoter contacts in human cells with high-resolution capture Hi-C. *Nat Genet* 2015; **47**: 598–606.
3. Wagner TA, McLaughlin S, Garg K *et al.* HIV latency. Proliferation of cells with HIV integrated into cancer genes contributes to persistent infection. *Science* 2014; **345**: 570–573.
4. Maldarelli F, Wu X, Su L *et al.* HIV latency. Specific HIV integration sites are linked to clonal expansion and persistence of infected cells. *Science* 2014; **345**: 179–183.
5. Santangelo PJ, Rogers KA, Zurla C *et al.* Whole-body immunoPET reveals active SIV dynamics in viremic and antiretroviral therapy-treated macaques. *Nat Methods* 2015; **12**: 427–432.
6. Byrareddy SN, Arthos J, Cicala C *et al.* Sustained virologic control in SIV+ macaques after antiretroviral and alpha4beta7 antibody therapy. *Science* 2016; **354**: 197–202.
7. Yeh P, Hunter T, Sinha D *et al.* Circulating tumour DNA reflects treatment response and clonal evolution in chronic lymphocytic leukaemia. *Nat Commun* 2017; **8**: 14756.
8. Dawson SJ, Tsui DW, Murtaza M *et al.* Analysis of circulating tumor DNA to monitor metastatic breast cancer. *N Engl J Med* 2013; **368**: 1199–1209.
9. Martin GE, Pace M, Thornhill JP *et al.* 2017. Enrichment of the HIV reservoir in CD32+ CD4 T cells occurs early and is closely associated with immune checkpoint receptor expression (OA 1-2). *IAS HIV Cure & Cancer Forum.* 22nd and 23rd July. Paris, France.
10. Sogaard OS, Graversen ME, Leth S *et al.* The depsipeptide romidepsin reverses HIV-1 latency *in vivo*. *PLoS Pathog* 2015; **11**: e1005142.
11. Rasmussen TA, Tolstrup M, Brinkmann CR *et al.* Panobinostat, a histone deacetylase inhibitor, for latent-virus reactivation in HIV-infected patients on suppressive antiretroviral therapy: a phase 1/2, single group, clinical trial. *Lancet HIV* 2014; **1**: e13–21.
12. Elliott JH, Wightman F, Solomon A *et al.* Activation of HIV transcription with short-course vorinostat in HIV-infected patients on suppressive antiretroviral therapy. *PLoS Pathog* 2014; **10**: e1004473.
13. Archin NM, Liberty AL, Kashuba AD *et al.* Administration of vorinostat disrupts HIV-1 latency in patients on antiretroviral therapy. *Nature* 2012; **487**: 482–485.
14. Archin NM, Kirchherr JL, Sung JA *et al.* Interval dosing with the HDAC inhibitor vorinostat effectively reverses HIV latency. *J Clin Invest* 2017; **127**: 3126–3135.
15. Nguyen K, Das B, Dobrowolski C, Karn J. Multiple histone lysine methyltransferases are required for the establishment and maintenance of HIV-1 latency. *MBio* 2017; **8**.
16. Bouchat S, Verdikt R, Delacourt N *et al.* 2017. Identification of a new factor involved in DNA methylation-mediated repression of latent HIV-1 (OA 2-1). *IAS HIV Cure & Cancer Forum.* 22nd and 23rd July. Paris, France.
17. Allan RS, Zueva E, Cammas F *et al.* An epigenetic silencing pathway controlling T helper 2 cell lineage commitment. *Nature* 2012; **487**: 249–253.
18. Shiau S, Strehlau R, Wang S *et al.* 2017. Epigenetic dysregulation of the major histocompatibility complex (MHC) region in HIV-infected children on early antiretroviral therapy (P 6). *IAS HIV Cure & Cancer Forum.* July 2017. Paris, France.
19. Capoferri A, Ramos JC, Xu D *et al.* 2017. Impact of vorinostat treatment of non-Hodgkin's lymphoma on HIV-1 latent reservoir (OA 1-1). *IAS HIV Cure & Cancer Forum.* 22nd and 23rd July. Paris, France.
20. Munoz-Arias I, Hanhauser E, Hogan L *et al.* 2017. Small-molecule chemotherapeutic drugs reactivate HIV-1 via non-canonical pathways and modulate CD8 T cell response (OA 2-3). *IAS HIV Cure & Cancer Forum.* July 2017. Paris, France.
21. Gavegnano C, Montero C, Schinazi RF. 2017. Jak inhibitors employ novel mechanisms to block reservoir seeding and HIV persistence (OA 2-2). *IAS HIV Cure & Cancer Forum.* 22nd and 23rd July. Paris, France.
22. Bermejo M, Lopez-Huertas MR, Garcia-Perez J *et al.* Dasatinib inhibits HIV-1 replication through the interference of SAMHD1 phosphorylation in CD4+ T cells. *Biochem Pharmacol* 2016; **106**: 30–45.
23. Bermejo M, Ambrosioni J, Bautista G *et al.* 2017. Treatment with tyrosine kinase inhibitors make PBMCs from patients with chronic myeloid leukemia less susceptible to HIV-1 infection: control of CD4+ T cell activation to control HIV-1 replication (P 14). *IAS HIV Cure & Cancer Forum.* 22nd and 23rd July. Paris, France.
24. Micci L, Harper J, Paganini S *et al.* 2017. Combined IL-21 and IFNα treatment limits residual inflammation, viral persistence and delays viral rebound in SIV-infected rhesus macaques (OA 4-1). *IAS HIV Cure & Cancer Forum.* July 2017. Paris, France.
25. Fung KY, Mangan NE, Cumming H *et al.* Interferon-epsilon protects the female reproductive tract from viral and bacterial infection. *Science* 2013; **339**: 1088–1092.
26. Garcia-Minambres A, Eid SG, Mangan NE *et al.* Interferon epsilon promotes HIV restriction at multiple steps of viral replication. *Immunol Cell Biol* 2017; **95**: 478–483.
27. Evans VA, Kumar N, Filali A *et al.* Myeloid dendritic cells induce HIV-1 latency in non-proliferating CD4+ T cells. *PLoS Pathog* 2013; **9**: e1003799.

28. Van der Sluis RM, Mota T, Kumar NA *et al.* 2017. Plasmacytoid DCs control HIV latency in resting T cells by type I IFNα (P 32). *IAS HIV Cure & Cancer Forum.* July 2017. Paris, France.
29. Moreno-Fernandez ME, Presicce P, Chougnet CA. Homeostasis and function of regulatory T cells in HIV/SIV infection. *J Virol* 2012; **86**: 10262–10269.
30. Sivanandham R, Kleinman AJ, Policicchio BB *et al.* 2017. Evaluation of different Treg depletion approaches as strategies for improved SIV reactivation and clearance (OA 4-2). *IAS HIV Cure & Cancer Forum.* July 2017. Paris, France.
31. Papagno L, Nicoli F, Kuse N *et al.* 2017. Priming of tumour or HIV-specific human CD8+ T cells with superior functional properties using STING ligands (P 17). *IAS HIV Cure & Cancer Forum.* July 2017. Paris, France.
32. Ruiz A, Blanch-Lombarte O, Jimenez-Moyano E *et al.* 2017. Rapid CTL recognition of HIV-1 latently infected cells depends on the levels of inducible viral reactivation and CTL activation status (P 20). *IAS HIV Cure & Cancer Forum.* July 2017. Paris, France.
33. Postel-Vinay S, Aspeslagh S, Lanoy E *et al.* Challenges of phase 1 clinical trials evaluating immune checkpoint-targeted antibodies. *Ann Oncology* 2016; **27**: 214–224.
34. Wherry EJ. T cell exhaustion. *Nat Immunol* 2011; **12**: 492–499.
35. Cockerham LR, Jain V, Sinclair E *et al.* Programmed death-1 expression on CD4(+) and CD8(+) T cells in treated and untreated HIV disease. *AIDS* 2014; **28**: 1749–1758.
36. Katlama C, Deeks SG, Autran B *et al.* Barriers to a cure for HIV: new ways to target and eradicate HIV-1 reservoirs. *Lancet* 2013; **381**: 2109–2117.
37. Day CL, Kaufmann DE, Kiepiela P *et al.* PD-1 expression on HIV-specific T cells is associated with T-cell exhaustion and disease progression. *Nature* 2006; **443**: 350–354.
38. Fromentin R, Bakeman W, Lawani MB *et al.* CD4+ T Cells Expressing PD-1, TIGIT and LAG-3 Contribute to HIV Persistence during ART. *PLoS Pathog* 2016; **12**: e1005761.
39. Chomont N, El-Far M, Ancuta P *et al.* HIV reservoir size and persistence are driven by T cell survival and homeostatic proliferation. *Nat Med* 2009; **15**: 893–900.
40. Van der Sluis RM, Kumar NA, Evans VA *et al.* 2017. Anti-PD-1 disrupts HIV latency in non-proliferating but not in proliferating T cells (OA 3-3). *IAS HIV Cure & Cancer Forum.* July 2017. Paris, France.
41. Le Garff G, Samri A, Lambert-Niclot S *et al.* Transient HIV-specific T cells increase and inflammation in an HIV-infected patient treated with nivolumab. *AIDS* 2017; **31**: 1048–1051.
42. Wightman F, Solomon A, Kumar SS *et al.* Effect of ipilimumab on the HIV reservoir in an HIV-infected individual with metastatic melanoma. *AIDS* 2015; **29**: 504–506.
43. Scully E, Simoneau C, Delagrèverie H *et al.* 2017. HIV reservoir dynamics and immune responses after anti-PD-1 therapy (OA 3-1). *IAS HIV Cure & Cancer Forum.* July 2017. Paris, France.
44. Samri A, Lavolé A, Even S *et al.* 2017. PD-1 blockade in 12 HIV-infected patients with lung cancer (OA 3-2). *IAS HIV Cure & Cancer Forum.* July 2017. Paris, France.
45. Salgado M, Kwon M, Gálvez C *et al.* 2017. Achievement of full donor chimerism with episodes of alloreactivity contributes to reduce the HIV reservoir (OA 5-1). *IAS HIV Cure & Cancer Forum.* July 2017. Paris, France.



© JUSTIN GABBARD

Hidden Menace

Curing HIV means finding and eradicating viruses still lurking in the shadows.

BY GENEVIEVE MARTIN, MATTHEW PACE, AND JOHN FRATER

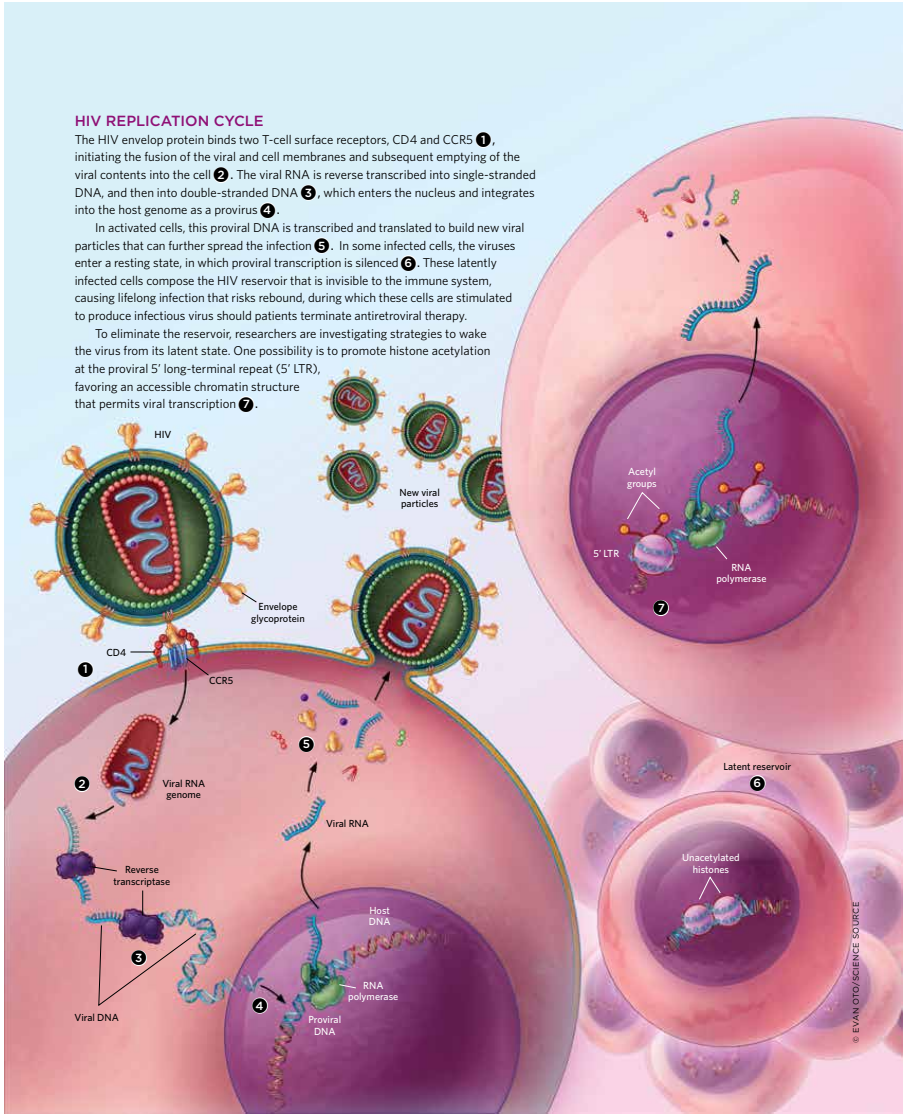
Since the early 1980s, when HIV was first identified, our knowledge of the virus—how it causes disease, how it interacts with our immune system, how it responds to drugs—has grown year by year. Drugs specifically designed to target HIV, and given as a cocktail of different agents—known as combination antiretroviral therapy (ART)—have decreased the mortality associated with HIV infection to the point where, for newly diagnosed individuals today, life expectancies are comparable to those who are HIV-negative.

But of the 35 million people currently living with HIV, the World Health Organization estimates that only around 40 percent use ART, partly because about half do not know they are infected. Providing ART to all who need it is a major challenge, and even when the drugs are available they are not a panacea. Regardless of treatment, there is increasing evidence that HIV-infected individuals may be at greater risk of non-AIDS comorbidities, for example, cardiovascular disease and dementia. Moreover, ART has to be taken for life: if the drugs are stopped, virus production quickly ramps up and the disease can progress, a phenomenon known as rebound.

Rebound occurs because HIV forms a reservoir in long-lived T cells that persists despite treatment. As with all retroviruses, a key aspect of the HIV replication cycle is the reverse transcription of the viral genome into DNA, followed by integration of this viral DNA, known as the provirus, into the host genome. (See illustration on page 36.) In activated cells, this proviral DNA can give rise to viral mRNA, proteins, and infectious viral particles. However, in some infected cells, the virus enters a resting state, termed latent infection, in which transcription or translation is restricted but integrated HIV is still present. These latently infected cells make up the HIV reservoir and, eventually, may be stimulated to produce infectious virus.

One challenge in targeting latently infected cells is that they do not produce HIV antigens and are therefore indistinguishable from uninfected cells.

The HIV reservoir consists largely of resting $CD4^+$ T cells, but other cells, such as macrophages, may also contribute. In patients who have been treated for many years with ART, these latently infected cells are rare, but still present. It has been estimated that the proportion of latently infected cells capable of giving rise to rebound virus production is approximately one in a million resting $CD4^+$ T cells in patients on ART.[1] However, the difficulty of reliably measuring the reservoir means this number could be significantly higher or lower. (See "Ethical Dilemmas" on page 38.) Regardless, the HIV reservoir is a major barrier to virus eradication, and its existence raises several questions for cure



strategies. Is it possible to completely eradicate latently infected cells from the body, or can we keep them silent to prevent viral rebound? Even more to the point, is it possible to prevent the reservoir from forming in the first place?

Different types of cure

Due to the assimilation of viral genetic elements into the host genome, researchers previously assumed that, once infection has taken hold, HIV can never be completely eliminated from the body. Yet in 2009, German clinicians announced the case of an apparent HIV cure in Timothy Ray Brown, also known as "the Berlin patient."[2] Brown underwent a bone marrow transplant following unsuccessful treatment for acute myeloid leukemia with conventional chemotherapy. The bone marrow donor selected by Brown's clinicians was homozygous for a mutation in the CCR5 gene, preventing the expression of the CCR5 HIV coreceptor on the surface of T cells and conferring a high degree of natural resistance to HIV infection. Following the transplant, Brown ceased taking ART, and the virus did not rebound. More than six years later, researchers have been unable to find evidence of replication-competent HIV in blood or tissues from this patient; it appears that any viral reservoir has been cleared.[3] Despite the exceptional circumstances surrounding this case, many believe that the Berlin patient serves as proof of concept that HIV can be cured.

Researchers have since attempted bone marrow transplants from donors carrying the same *CCR5* mutation in six other cases of HIV-positive patients. Unfortunately, all of these individuals died within a year from relapsed malignancy or transplantation complications.[4] In one of these individuals, rebound occurred after an HIV variant used an alternative T-cell coreceptor, CXCR4, suggesting a potential limitation to targeting only CCR5.[5]

These cases demonstrate the intrinsic dangers and difficulties of the Berlin patient strategy, which could never be realistically scaled up to help all those infected with HIV. Interestingly, when two patients in Boston underwent bone marrow transplants using tissue from a donor carrying wild-type *CCR5*, their viral levels dropped to undetectable levels, both in plasma and intracellularly, and these low levels endured for several years.[6] Unfortunately, viral rebound occurred within a few months of stopping ART, indicating that the *CCR5* mutation was indeed critical to the Berlin patient's cure.[7] This has led researchers to another strategy to eradicate HIV: using gene therapy to turn off *CCR5* expression. If successful, such a treatment could prevent additional cells from being infected with HIV, thwarting disease progression even in the presence of a viral reservoir. (See "Genome Editing Cuts Out HIV," *The Scientist*, July 21, 2014.)

In addition to preventing the spread of the virus to new cells within body, efforts to "cure" HIV have focused on reducing the size of the reservoir to achieve a remission or functional cure, in which patients could remain off therapy without rebounding, despite detectable HIV DNA in their bodies.

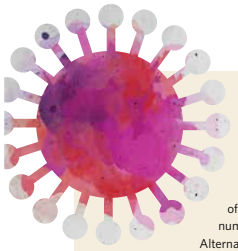
Early treatment, better control

While researchers have traditionally envisaged a "sterilizing cure," in which the virus is completely eliminated from the body, this may not be necessary for controlling the infection. In addition to preventing the spread of the virus to new cells within body, efforts to "cure" HIV have focused on reducing the size of the reservoir to achieve a remission or functional cure, in which patients could remain off therapy without rebounding, despite detectable HIV DNA in their bodies.

Serving as an example of functional cure, 14 patients across France known as the VISCONTI cohort have successfully stopped ART without return of virus production, some for many years. Unlike the Berlin patient, these patients still have detectable, although small, HIV reservoirs that could serve as a future source of viral reactivation.[8] Nevertheless, the fact that these patients have achieved long-term posttreatment control (PTC) could provide important clues for the development of an HIV cure.

A key factor with the VISCONTI cohort is that these individuals started treatment very soon after being infected. Although not all patients treated early are able to cease ART without rebound, several other cohorts that commenced ART during early stages of infection have also achieved varying levels of PTC. While viral rebound occurs rapidly in most individuals, between 5 percent and 15 percent of patients remain free of virus at 24 months after ART cessation.[8,9] In contrast, PTC is rarely, if ever, observed among patients who commenced ART only after their $CD4^+$ T cell counts declined below a cut-off point, suggesting that starting treatment during primary HIV infection appears to be important for controlling the virus. Further evidence for the potential of this strategy comes from the reported cure of an infant in Mississippi who, perinatally infected with HIV, commenced ART 30 hours after birth.[10] Treatment was discontinued at 18 months of life, and HIV levels remained undetectable for more than a year, until rebound occurred in July 2014.[11]

The SPARTAC (Short Pulse Antiretroviral Therapy at HIV Seroconversion) trial put early ART to the test in a large randomized trial that ran from 2003 to 2010 across eight countries. Adults testing positive for HIV received a short course of ART within 24 weeks of seroconversion, when an HIV-specific antibody becomes detectable in the blood, resulting in delayed $CD4^+$ T cell decline. The trial also showed that levels of HIV DNA correlated with this delay and predicted time to viral rebound, a finding that links early treatment with reduced reservoir size, possibly as a result of lim-

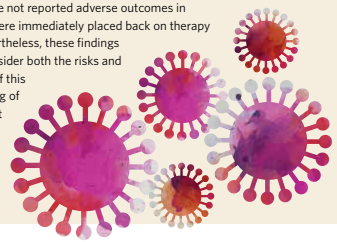


ETHICAL DILEMMAS

One problem researchers face in evaluating HIV cure strategies is measuring the size of the latent reservoir. Several assays exist to quantify the reservoir, each with significant limitations; it is likely that these assays either over- or underestimate its size. Estimates of the number of copies of proviral DNA, for example, include a large number of integrated viruses that appear to be nonfunctional. Alternatively, the assay used to measure only replication-competent copies of the virus may underestimate the true number because it cannot activate all such copies.

In the absence of robust methods for detecting latently infected cells, treatment interruption remains the sole way of testing HIV cure interventions. Ceasing therapy, however, risks resumption of HIV production and reseeding of the reservoir, which may impact disease progression and allows for transmission of the virus.

Evidence of adverse outcomes after treatment interruption comes from the SMART study, in which such interruption was associated with increased mortality, opportunistic infections, and major non-AIDS comorbidities in chronically infected patients (*N Engl J Med*, 355:2283-96, 2006). Importantly, the SMART study left patients untreated for long periods of time despite high levels of viremia. Researchers have not reported adverse outcomes in studies where patients were immediately placed back on therapy after viral rebound. Nevertheless, these findings highlight the need to consider both the risks and the ethical implications of this strategy. Close monitoring of patients during treatment interruption with clear plans for restarting ART need to be part of cure intervention trials.



iting the initial seeding of the reservoir.[12,13] Because it is almost certain that a cure will be easier to achieve in patients with lower numbers of latently infected cells, it seems that early treatment will be an important part of HIV eradication strategies.

Reversing latency

As most patients are not diagnosed with acute HIV infection and are unable to initiate ART early on, treatments are also needed to deplete the HIV reservoir once it is established. One challenge in targeting latently infected cells is that they do not produce HIV antigens and are therefore indistinguishable from uninfected cells. This transcriptional silence renders these cells invisible to immune surveillance and allows persistence of provirus over time. Although counterintuitive, waking the virus from its latent state may be the key to eradicating the reservoir, by rendering reservoir cells susceptible to immune clearance and other targeted treatments. Researchers are developing strategies combining drugs to reactivate latent virus and techniques to boost immune clearance of infected cells—a so-called kick-and-kill approach.

Transcription of proviral HIV DNA is dependent on the recruitment of appropriate transcription factors to the viral 5' long-terminal repeat (5' LTR). As with all genes, chromatin arrangement around the site of viral integration is an important regulator of transcriptional status. High histone acetylation at the 5' LTR is associated with an accessible chromatin structure, favoring transcription. Acetylation status is maintained by a balance between histone acetyltransferases, which act to promote acetylation, and histone deacetylases (HDACs), which decrease acetylation. HDAC inhibitors are drugs that promote nonspecific acetylation and activate cells latently infected with HIV both in vitro and in vivo.

Vorinostat is an HDAC inhibitor used to treat cutaneous T-cell lymphoma in humans. It has been shown to disrupt HIV latency in cellular models and in primary $CD4^+$ T cells from HIV-infected patients. Trial doses of vorinostat given to HIV-infected individuals with ART-suppressed viral replication caused increases in cellular acetylation and subsequent HIV transcription, but with no evidence of rebound.[14,15] In other words, the latent cell was activated enough to start the virus life cycle, but no new virions were detected. This could be due to posttranscriptional barriers to viral expression, such as mRNA degradation, or suboptimal dosing regimens. Although it is unclear what level of expression is needed to trigger immune clearance, it is presumed that at least protein expression, if not assembled virus, will be needed. Researchers at Aarhus University in Denmark have shown that two other HDAC inhibitors, panobinostat and romidepsin, have higher potency and can induce virus production in patients treated with ART.[16,17] Despite reactivation of latent viruses, however, neither of these drugs resulted in decreases in reservoir size. But given the short time period of these studies and the small number of patients, this is not altogether unexpected, and the results serve as evidence that it is possible to reactivate the reservoir in vivo.

Although HDAC inhibitors are the most widely studied class of HIV-activating drugs, several other candidates may also be able to reverse HIV latency. These include methyltransferase inhibitors, protein kinase C agonists (prostratin and bryostatin), the BET bromodomain-inhibiting molecule JQ1, and the zinc-chelating agent disulfiram. The distinct mechanisms of these agents mean that toxicities and efficacy will differ, and it is unclear which agents will be most suited for clinical use. Human trials using HDAC inhibitors and these other HIV-activating agents are exploring the effect of these drugs on viral transcription and translation, as well as the drugs' safety and tolerability.

Even if HIV-activating agents can provide the kick needed to disrupt HIV latency, there is no evidence that this will result in clearance of the reservoir by the immune system alone. As such, it is likely that these drugs will need to be used in combination with other strategies to promote immune clearance of these cells. The RIVER (Research in Viral Eradication of HIV Reservoirs) trial, for example, is combining vorinostat with vaccination in patients on ART in the U.K. A similar study in Denmark using the HDAC inhibitor romidepsin, and a different vaccine candidate is also underway.

© ISTOCK.COM/KOSTENKODESIGN/NIXKEN

Although counterintuitive, waking the virus from its latent state may be the key to eradicating the reservoir, by rendering reservoir cells susceptible to immune clearance and other targeted treatments.

Putting cure into context

Significant work remains to be done in the development of a potential cure for HIV. It is an exciting time in the field, with interventional trials running in parallel with continued basic research into the mechanisms of HIV infection and pathology. In addition, a number of large observational studies of the dynamics of reservoir size are underway to understand PTC, which may provide insights into factors that predict its occurrence, the mechanisms of reservoir formation and maintenance, and the probability of rebound.

Meanwhile, several different therapeutic approaches to an HIV cure are currently under investigation. In addition to gene therapy attempting to damage the CCR5 gene or block its expression, researchers are developing therapeutic HIV vaccines. (See "Defeating the Virus" on page 40.) Antibodies with broad HIV-neutralizing capability may have some in vivo activity against the virus, and transfusions of these are being trialled. Coupled with HIV-activating drugs, these immune augmentation strategies are important early steps towards a cure.

Of course, research into an HIV cure is only one of a multitude of approaches to solving the challenges posed by this virus. Prevention, testing, treatment, and managing comorbidities remain the cornerstone of HIV management and research worldwide. Curative interventions, while exciting, are still in very early stages of development; it is unlikely that these are going to play an important role in treatment of infected patients in the near future. Despite this, the prospect of an HIV cure remains a driving force for many, and a successful cure must, in some way, address the reservoir. In this rapidly progressing field, the next few years will be crucial in determining whether clearance of the reservoir may one day be possible.■

Genevieve Martin is a doctoral student in the Nuffield Department of Medicine at the University of Oxford, U.K. Matthew Pace is a postdoctoral researcher in the same department, as well as a James Martin Research Fellow at the Institute for Emerging Infections in the Oxford Martin School. John Frater holds positions at both institutions, as well as at the Oxford National Institute of Health Research Biomedical Research Centre, and is a clinician at the John Radcliffe Hospital in Oxford.

References

1. D. Finzi et al., "Latent infection of $CD4^+$ T cells provides a mechanism for lifelong persistence of HIV-1, even in patients on effective combination therapy," *Nat Med*, 5:512-17, 1999.
2. G. Hütter et al., "Long-term control of HIV by *CCR5* Delta32/Delta32 stem-cell transplantation," *N Engl J Med*, 360:692-98, 2009.
3. S.A. Yukl et al., "Challenges in detecting HIV persistence during potentially curative interventions: A study of the Berlin patient," *PLOS Pathog*, 9:e1003347, 2013.
4. G. Hütter et al., "More on shift of HIV tropism in stem-cell transplantation with *CCR5* delta32/delta32 mutation," *N Engl J Med*, 371:2437-38, 2014.
5. L. Kordelas et al., "Shift of HIV tropism in stem-cell transplantation with *CCR5* Delta32 mutation," *N Engl J Med*, 371:880-82, 2014.
6. T.J. Henrich et al., "Long-term reduction in peripheral blood HIV type 1 reservoirs following reduced-intensity conditioning allogeneic stem cell transplantation," *J Infect Dis*, 207:1694-702, 2013.
7. T.J. Henrich et al., "Antiretroviral-free HIV-1 remission and viral rebound after allogeneic stem cell transplantation: report of 2 cases," *Ann Intern Med*, 161:319-27, 2014.
8. L. Hocqueloux et al., "Long-term immunovirologic control following antiretroviral therapy interruption in patients treated at the time of primary HIV-1 infection," *AIDS*, 24:1598-601, 2010.
9. S. Lodi et al., "Immunovirologic control 24 months after interruption of antiretroviral therapy initiated close to HIV seroconversion," *Arch Intern Med*, 172:1252-55, 2012.
10. D. Persaud et al., "Absence of detectable HIV-1 viremia after treatment cessation in an infant," *N Engl J Med*, 369:1828-35, 2013.
11. K. Luzuriaga et al., "Viremic Relapse after HIV-1 Remission in a Perinatally Infected Child," *N Engl J Med*, 372:786-88, 2015.
12. SPARTAC Trial Investigators et al., "Short-course antiretroviral therapy in primary HIV infection," *N Engl J Med*, 368:207-17, 2013.
13. J.P. Williams et al., "HIV-1 DNA predicts disease progression and post-treatment virological control," *eLife*, 3:e03821, 2014.
14. J.H. Elliott et al., "Activation of HIV transcription with short-course vorinostat in HIV-infected patients on suppressive antiretroviral therapy," *PLOS Pathog*, 10:e1004473, 2014.
15. N.M. Archin et al., "Administration of vorinostat disrupts HIV-1 latency in patients on antiretroviral therapy," *Nature*, 487:482-85, 2012.
16. O.S. Søgaard et al., "The HDAC inhibitor romidepsin is safe and effectively reverses HIV-1 latency in vivo as measured by standard clinical assays," 20th International AIDS conference, Melbourne, Australia, July 20–25, 2014.
17. T.A. Rasmussen et al., "Panobinostat, a histone deacetylase inhibitor, for latent-virus reactivation in HIV-infected patients on suppressive antiretroviral therapy: a phase 1/2, single group, clinical trial," *Lancet HIV*, 1:e13-e21, 2014.